Springer Series on Touch and Haptic Systems

Thorsten A. Kern
Christian Hatzfeld
Alireza Abbasimoshaei *Editors*

Engineering Haptic Devices

Third Edition

EUROHAPTICS EHS

OPEN ACCESS

Springer

Springer Series on Touch and Haptic Systems

The Springer Series on Touch and Haptic Systems is published in collaboration with the EuroHaptics Society. It is focused on publishing new advances and developments in all aspects of haptics. Haptics is a multi-disciplinary field with researchers from Psychology, Physiology, Neurology, Engineering, and Computer Science (amongst others) contributing to a better understanding of the sense of touch, and researching into how to improve and reproduce Haptic interaction artificially in order to simulate real scenarios. The series includes monographs focused on specific topics, edited volumes covering general topics from different perspectives, and selected Ph.D. theses. Books in this series focus on Haptics or Haptic interfaces including:

- Neuroscience
- Perception & Psychophysics
- Haptic Rendering
- Devices and Technology
- Medical & Rehabilitation Applications
- Art & Design Applications
- Collaborative Haptics
- Mutimodal Interaction
- Tactile Display & Tactiles
- Sensing
- Haptic HCI (Interaction, Visualization)

Thorsten A. Kern · Christian Hatzfeld ·
Alireza Abbasimoshaei
Editors

Engineering Haptic Devices

Third Edition

Springer

Editors
Thorsten A. Kern
Institute for Mechatronics (M-4)
Hamburg University of Technology
Hamburg, Germany

Alireza Abbasimoshaei
Institute for Mechatronics (M-4)
Hamburg University of Technology
Hamburg, Germany

Christian Hatzfeld
Institut für Elektromechanische Konstruktionen
Technische Universität Darmstadt
Darmstadt, Hessen, Germany

ISSN 2192-2977 ISSN 2192-2985 (electronic)
Springer Series on Touch and Haptic Systems
ISBN 978-3-031-04535-6 ISBN 978-3-031-04536-3 (eBook)
https://doi.org/10.1007/978-3-031-04536-3

1st edition: Springer-Verlag Berlin Heidelberg 2009
2nd edition: Springer-Verlag London 2014

This Springer imprint is published by the registered company Springer Nature Switzerland AG
The registered company address is: Gewerbestrasse 11, 6330 Cham, Switzerland

'Series Editors' Foreword

This volume of the Springer Series on 'Touch and Haptic Systems', published as a collaboration between Springer and the EuroHaptics Society, is significant for several reasons. Engineering Haptic Devices marks a milestone in being the 20th volume in the series which saw its first volumes published in 2011. The volume is also significant for being the second open-access publication in the series. This will help it to reach the wider audience it justly deserves and the commercial sponsorship of Grewus GmbH is greatly appreciated. But most importantly, the volume is a major revision of an earlier edition. The new version is over 20% longer with many revised and new sections and now including many illustrations in colour. The changes will further reinforce the volume's position as the only comprehensive textbook approach to the topic of haptic devices which covers both the user and the technical design of haptic systems. The editors of Engineering Haptic Devices are Thorsten A. Kern, Christian Hatzfeld and Alireza Abbasimoshaei. We are saddened by the loss of Christian Hatzfeld deceased before the publication of this book. We suggest the book represents a fitting tribute to his work. All three editors contributed to writing of the chapters, joined by a number of authors with a wide range of experience in haptics. The book, which comprises 15 chapters plus appendices and glossary, is divided in two: Part I provides an introduction to the basics of haptics, and Part II covers most of the engineering aspects related to haptic devices. Chapter topics in Part I include motivation for the use of haptics, haptic as an interaction modality, user role in haptic systems and developing haptic systems. In Part II, topics include identification of requirements, haptic system structures, haptic system control, kinematics, actuators, sensors, interface, software, evaluation and case studies. Engineering Haptic Devices is written in a style that will be accessible to researchers, engineers and human factors practitioners already working in haptics and looking to use the work as a reference as well as to students attending advanced undergraduate and graduate courses and seeking a comprehensive grounding in this wide-ranging and important topic.

Madrid, Spain — Manuel Ferre
Ulm, Germany — Marc Ernst
Birmingham, UK — Alan Wing
March 2022

Note from the Book Editors

The idea for this book was born in 2003. Originally conceived as a supplement to Thorsten A. Kern's dissertation, it was intended to fill a gap: The regrettably small number of comprehensive, summary publications on haptics available to, for example, a technically interested person who is confronted for the first time with the task of designing a haptic device. In 2004, apart from a considerable number of conference proceedings, journals and dissertations, there was no document summarising the most important findings of this challenging topic.

The support of several colleagues, especially Prof. Dr.-Ing. Dr. med. Ronald Blechschmidt-Trapp and Dr.-Ing. Christoph Doerrer, helped to develop the idea further in the following years—and showed that this book had to become much more extensive than originally expected. With encouragement from Prof. Dr.-Ing. habil. Roland Werthschützky, the first edition was edited by Thorsten A. Kern during a Post-doc period. It was funded by the German Research Foundation (DFG, grant KE1456/1-1) with a special focus on consolidating the design methodology for haptic devices. Thanks to this funding, the financial basis for this task was guaranteed. The structure of the topic made it clear that the book would be significantly improved by contributions from specialists in different fields. In 2008, the German version *Entwicklung Haptischer Geräte* and in 2009 the English version *Engineering Haptic Devices* were published by Springer.

In 2010, the idea of a second edition of the book was born. With Kern's move from university to an industrial employer, attention also shifted from mainly kinaesthetic to tactile devices. This made severe gaps in the first edition eminent. In parallel, science made great strides in understanding the individual tactile modalities and blurring the boundaries between different conceptual approaches to the same perception. This now provided an opportunity to take an engineering approach to more than just vibrotactile perception. However, it took until 2013 for work to begin on the second edition. In that year, Christian Hatzfeld completed his doctoral thesis on the perception of vibrotactile forces. Also inspired by Prof. Dr.-Ing. habil. Roland Werthschützky, he took the lead in editing this second edition. Like the first edition, this work was also funded by the DFG (grant HA7164/1-1), which underlines the importance of an adapted design approach for haptic systems. In a fruitful collaboration between Springer and the series editors, the book was integrated into the *Springer Series on Touch and Haptic Systems* as we felt that the design of task-specific haptic interfaces would be well complemented by the other works in this series.

To our regret, our dear friend and editor of the second edition, Dr. Christian Hatzfeld, passed away in 2018 after a losing battle with cancer, leaving behind his wife and child. The third edition you hold in your hands still contains countless memories and influences from his work, and we are proud and honoured to have been able to continue his work.

In 2020, a new opportunity arose for this book when Kern returned to academia as a full-professor at Hamburg University of Technology. Despite a detour into the automotive world of visible displays, he returned to his scientific roots and picked up his work again on the design of haptic devices and actuators. This also prompted him to revise some of the content of this book with some distance, as he now not only sees more clearly how the global community has evolved and professionalised, but also notices which issues have remained. Dr. Alireza Abbasimoshaei, an experienced researcher who has made his mark in the field of rehabilitation robots, could be motivated to help with the editorial part of the work. Fortunately, we have also found a strong supporter of haptic research in Grewus GmbH, which focuses on the development of tactile system solutions, and with their help we have succeeded in making this edition of the book an open-access publication.

With the support of several former authors of the first and second editions, as well as some new authors who have taken on key roles in the structure of the book, we have been able to revise and update all sections to make the overall content more accessible and to better represent the current state of research. However, the biggest changes and strongest updates occurred in Chap. 12 with a sophisticated introduction to haptic and tactile rendering algorithms, taking into account the dynamic properties of haptic devices, and in Chap. 8 with finally a full introduction to serial and parallel kinematics and their specifics when it comes to force rendering and why haptics is so different from general robotics. Major updates have also been made to the control Sect. 7 explaining now in-depth concepts of impedance control for coupled systems and some real application examples. In addition, we took care to update each chapter and remove more bugs than we introduced while revising.

We thank all the authors who contributed to this book, as well as all the colleagues, students, and researchers in the haptics community who provided fruitful discussions, examples, and permission to include their work. We would also like to thank all the researchers around the world who have developed, used, and tested mechatronic devices and found amazing applications for them. This book would not be possible without these inspirations, and although we have tried to give a good overview, at the same time we are sure that we have overlooked excellent examples that we would have liked to include if only we had known about them. Our special thanks go to our student assistants whose work helped us with the final editing: Konika Narendra Khatri and Nis Willy Köpke. Last but not the least, we would like to single out one of the authors of this book, Fady Youssef, who was of great help to the editors with numerous discussions on content and practical actions. Especially in the very last phase, when we had to obtain open-access permissions for all illustrations that

were adopted and inspired by publications from the haptics community. Without the technical support of these people, such a work would probably not have reached this level of maturity.

We hope that this work will facilitate the work of students and engineers in the exciting and challenging development of haptic systems, and that it will serve as a useful resource for all developers, as the first and second editions have already done. In particular, we hope that the open-access approach of this edition will allow a wider community to critically discuss our work and perhaps gain some inspiration.

Of course, we would also like to express our condolences to Christian's family and hope that we prove worthy to continue his work.

Hamburg, Germany

Thorsten A. Kern
Alireza Abbasimoshaei

Preface

The term “haptics”, unlike the terms “optics” or “acoustics”, is not so familiar to most people, at least not in the meaning used in the scientific community: The words “haptics” and “haptic” refer to anything involving the sense of touch. “Haptic” is everything and everything is “haptic” because it describes not only the pure mechanical interaction but also includes thermal- and pain perception (nociception). The sense of touch enables humans and other living beings to perceive the “boundaries of their physical being”, i.e. to recognize where their own body begins and where it ends. While we perceive our wider environment through sight and hearing, the sense of touch covers our immediate surroundings: in the heat of a basketball game, a light touch on our back immediately alerts us to an attacking player we cannot see. We notice the intensity of the contact, the direction of the movement through a shear on our skin or a breeze moving our body hair—all without catching a glimpse of the opponent.

“Haptic systems” are divided into two classes. In engineering, there are three terms that are often used but have no clear meaning: System, Device and Component. Systems are—depending on the task of the designer—either a device or a component. A motor is a component of a car, but for the designer of the motor it is a device made of components (coils, magnets, encoders, ...).[1] There are the time-invariant systems (the keys on my keyboard) that produce a more or less unchanging haptic effect whether pressed today or a year from now. Structures such as surfaces, e.g. the wooden surface of my table, also belong to this group. These haptically interesting surfaces have the properties of “tactile textures” and are represented by a variety of dimensions, rough or smooth and soft or hard surfaces are just some of them. In addition to these temporally unchanging devices, there are *active, reconfigurable systems* that change their haptic properties partially or completely depending on a pre-selection—e.g. from a menu or due to an interaction with real or virtual environments.

[1] It can be helpful when reading a technical text to replace each of the above terms with the word “thing”. This suggestion is not entirely serious, but it surprisingly increases the comprehensibility of technical texts.

The focus of this book is on the technological design criteria for active reconfigurable systems that enable haptic coupling of user and object in a mainly mechanical understanding. Thermal and nociceptive perceptions are mentioned according to their importance, but not discussed in detail. This is also the case for passive haptic systems, although it must be emphasized that a careful understanding of passive haptic dimensions can be seen as key to the development of active haptic systems. Active haptic systems have been developed by research and industry in a wide variety and used for different purposes. They cover a wide range of applications, from low-cost interaction surfaces with tactile outputs to mid-priced devices in the consumer goods industry, mainly aimed at enhancing immersion in virtual worlds, to sophisticated general-purpose devices used in professional engineering or research applications. When confronted with this topic for the first time and seeing the variety of devices in a psychophysiological field that is not so commonplace, it is easy to get lost and fail to recognize the connections between the designs that are so different at first sight. Therefore, on the one hand, we believe in the need for a structured approach to the development of task-specific haptic systems and, on the other hand, in the need to know the different approaches to the components and structures of haptic systems. We would therefore like to offer guidance and the first point of orientation to avoid the most common pitfalls in understanding and to give some hints on the individual technical topics.

The fact that you have found this book shows that you are interested in haptics and its application in human-machine interaction. It also makes it very likely that you have already recognized some complexity in your design task. Perhaps you have already attempted to design a technical system that enables haptic human-machine interaction. Perhaps you are currently planning a project as part of your studies or a commercial product that will improve a particular manual control or introduce a new control concept. Maybe you are an engineer facing the task of using haptics in medical technology and training to improve patient safety, and trying to apply current advances to other interventions. Or maybe you are in component development and just need a quick reference for using actuators and exciters in your end-user application. If you belong to these groups, then we definitely want to help you.

Despite or precisely because of this great diversity of projects in industry and research dealing with haptic systems, the common understanding of "haptics" and the terms directly related to it, such as "kinaesthetic" and "tactile", are by no means as clear and uncontroversial as it should be. With this book, we would like to offer you some assistance to act more confidently in the development of designing haptic devices. We see this book as both a starting point for engineers and students who are new to haptics and the design of haptics and haptic interfaces as well as a reference for more experienced professionals. To make the book more usable and practical in this sense, we have added recommendations for further insights to most chapters.

The book begins by outlining the various areas that can benefit from the integration of haptics, including communication, interaction with virtual environments, and the most sophisticated applications of telepresence and teleoperation. Haptics as an interaction modality is discussed as a basis for the design of such systems. This includes various concepts of haptic perception and haptic interaction, as well as the main results from psychophysical studies that can and must be applied to the design of a task-specific haptic system. Please note that this book has been written by and is aimed at engineers from different disciplines. This means that psychophysical content in particular is sometimes simplified and abridged to give engineers working on a haptic device a basic insight into these topics. Again, you can find references if you want to dive deeper.

Next, the role of the user as a (mechanical) part of the haptic system is discussed in detail, as understanding the user as a very dynamic component of your technical device has a big impact on system properties such as stability and perceived haptic quality.

Part I of the book ends with an extension of the generally known development models for mechatronic systems to the specific design of haptic systems. This chapter places a special emphasis on the integration of perceptual properties and ergonomic aspects in this process. The authors believe that the systematic consideration of perceptual properties and features of the sensory apparatus based on the intended interaction can reduce critical requirements for haptic systems, which both reduces the effort and cost of development and leads to systems with higher perceived quality.

Part II of the book, an overview of technological solutions is given, such as the design of actuators, kinematics or complete systems including software and rendering solutions and the interfaces to simulation and virtual reality systems. This is done from two points of view. Firstly, the reader should be able to find the most important and widely used solutions for recurring problems such as actuator or sensor technology, including the necessary technical basis for their own designs and developments. Secondly, we wanted to give an overview of the large number of different principles used in haptic systems that might be a good solution for a new task-specific haptic system—or a remarkable experience of which solution not to try.

The authors of this book consider their task accomplished once this book helps to inspire more design engineers to develop haptic devices and thus accelerate the creation of more and better haptic systems on the market.

Hamburg, Germany
February 2022

Thorsten A. Kern
Christian Hatzfeld
Alireza Abbasimoshaei

Contents

Editors and Contributors

About the Editors

Thorsten A. Kern received his Dipl.-Ing. and Dr.-Ing. degrees from Darmstadt University of Technology (TUDA), Germany, in the fields of actuator and sensor development for medical human-machine interfaces (HMIs) in applications like minimally invasive surgery and catheterizations. He is currently the director at Hamburg University of Technology, Germany, of the Institute for Mechatronics in Mechanics. He previously worked in Automotive Industry at Continental as an R&D manager for interior components, leading a team of 300 engineers worldwide. He joined Continental in 2008 covering various functions with increasing range of responsibility in actuator development, motor development and active haptic device development before shifting toward R&D management and product management on Head-Up Displays. Between 2006 and 2008, he was working in parallel in a startup focusing on medical interventions and was the main editor of the first edition of "Engineering Haptic Devices". He joined Hamburg University in January 2019. His interests are specifically focused on all types of electromagnetic sensors and actuators and their system integration toward larger motor- or sensor-systems in high-dynamic applications. *t.kern@hapticdevices.eu*.

Christian Hatzfeld † joined the Institute of Electromechanical Design of Technische Universität Darmstadt as a research and teaching assistant in 2008 working in the group of Measurement and Sensor Technologies of Prof. Dr.-Ing. habil Roland Wertschützky. He received his doctoral degree in 2013 for a work about the perception of vibrotactile forces. Then he was the leader of the "Haptic Systems" group until his death in 2018. His research interests included development and design methods for task-specific haptic systems and the utilization of human perception properties to alleviate the technical design. He was the main editor of edition 2 of Engineering Haptic Devices and contributed significantly to a large number of chapters specifically focusing on psychophysical topics.

Alireza Abbasimoshaei is currently a researcher assistant at the Institute for Mechatronics in Mechanics at the Hamburg University of Technology in Germany. Before joining iMEK, he designed and built four robots and controlled them. The last one was at the Technical University of Braunschweig in Germany. He filed two patents for rehabilitation devices and sold a finger rehabilitation robot he developed to a hospital partner. He also developed a new control system for rehabilitation robots in the field of control. He is an expert in mechatronic system design with special emphasis on mechanical and control system design. *a.abbasimoshaei@hapticdevices.eu*.

Contributors

Abdulali Arsen received his Ph.D. degree in the Department of Computer Science and Engineering at Kyung Hee University, the Republic of Korea. His research focus lies in data-driven and physics-based modeling and rendering of non-linear object deformation and haptic textures in virtual and augmented environments. He is also interested in the design and control of soft robots, human-computer interaction and human-in-loop systems. Currently, he is a Research Associate at Bio-inspired Robotics Laboratory, University of Cambridge. *a.abdulali@hapticdevices.eu*.

Gölz Jacqueline is a Professor in Sensors, Actuators and Metrology at Ulm University of Applied Science. Earlier, she was with Roche Diabetes Care GmbH as a test design engineer for insulin delivering systems and as a lecturer at the Computer Science Department, Technische Universität Darmstadt. There she received her Ph.D. in Electrical Engineering in 2012, where she developed miniaturized piezoresistive strain sensing elements, among others, for robotic surgical systems in the field of minimally invasive surgery. *j.goelz@hapticdevices.eu*.

Reisinger Jörg is AE-Engineer and Enabling Technology Owner for haptics and haptic technologies, employed at Mercedes-Benz AG. Besides haptic specification and internal consulting, he is responsible for new haptic technologies and concepts, transferring and guiding them into serial production. Since 2008, he introduced a new haptic quality level, as well as new active haptic systems like in the Mercedes-Benz touchpads and the haptic touchscreens. His doctoral thesis dealt with the objective parameters of haptically perceived quality of control elements, for which he received the doctoral degree in mechanical engineering at TU Munich in 2009 in cooperation with Audi AG and Heilbronn University. *j.reisinger@hapticdevices.eu*.

Fady Youssef is currently working at the Institute for Mechatronics in Mechanics at the Hamburg University of Technology as a teaching and research assistant. His research is focused on remote haptics and robotics. He received his Master's degree in Mechatronics from the Hamburg University of Technology in 2020. He also received his Bachelor's degree from the German University in Cairo, Egypt. His special interests are in the area of haptic-enhanced telemanipulation and robotic design. *f.youssef@hapticdevices.eu*.

Further Contributions

Seokhee Jeon received his B.S. and Ph.D. degrees in computer science and engineering from the Pohang University of Science and Technology (POSTECH), in 2003 and 2010, respectively. He was a Postdoctoral Research Associate with the Computer Vision Laboratory, ETH Zurich. He joined the Department of Computer Engineering, Kyung Hee University, as an Assistant Professor, in 2012, and is now an Associate Professor. From 2021, he serves as a project director of the immersive media consortium university at Kyung Hee University. His research interests include data-driven haptic modeling and rendering, soft haptic actuators for medical applications and realistic multimodal feedback in virtual and augmented reality. *s.jeon@hapticdevices.eu*.

Sebastian Kassner received his doctoral degree (Dr.-Ing.) from Technische Universität Darmstadt in 2013 where his research was focused on haptic human-machine interfaces for robotic surgical systems in the field of minimally invasive surgery. His special interest is the application of the electromechanical network theory on the design process of haptic devices. He served as an expert in ISO's committee "Tactile and Haptic Interactions" (TC159/SC4/WG9). Since 2012, Sebastian has held different positions in the industry. He now works at Knorr-Bremse where he is a Specialist for Digital Strategy in the field of rail systems and transportation technologies. *s.kassner@hapticdevices.eu*.

Nataliya Koev received her doctoral degree (Dr.-Ing.) from Technische Universität Darmstadt in 2021. She joined the Department Measurements and Sensor Technology at the University of Darmstadt in 2013 as a teaching and research assistant. Her research was focused on sensor integration in medical guide wire for cardiac catheterization. Her special interest is the development of micro force sensors for medical applications. In 2020, she joined Wilhelm Büchner Hochschule as a research assistant. *n.koev@hapticdevices.eu*.

Thorsten Meiss received his doctoral degree (Dr.-Ing.) from Technische Universität Darmstadt in 2012. He joined the university's Institute of Electromechanical Design in 2004 as a teaching and research assistant. His research is focused on micro-electro-mechanical sensors, microfabrication and their application in medical and industrial systems. He founded the company EvoSense in 2013, supported and led research projects for medical microsensors, and developed and commercialized products from research to market. In 2018, he joined Mecatronix GmbH and Applied Materials Inc. and is manager in the field of new display manufacturing lines. *t.meiss@hapticdevices.eu*.

Dongkill Yu received his Master's degree (M.Sc.) from Korea University, Seoul, Korea, in 2001. He entered the Korea University in 1999 as a mechanical engineering bachelor's student. Since 2015, he focused on haptic function development of Central Information Display product for Vehicle. He is currently a professional engineer in Vehicle Component Solutions company of LG Electronics. Over 10 years, he developed a mechanical system of various Optical Disk Drives (mass production). *d.yu@hapticdevices.eu*.

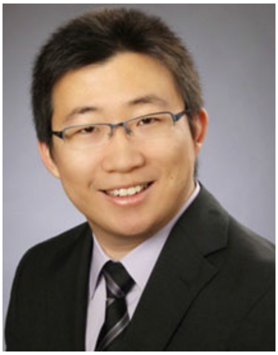

Wenliang Zhou is Engineer and Project Manager in User Interface Software development, employed at Mercedes-Benz AG. During 2011–2015, he developed and introduced novel measurement technology, framework for characterization of haptic displays. Using this new haptic measurement system, the new Mercedes Benz Touchpad and Touchscreen were introduced to the market for the first time with technically ensured high Haptical Feedback quality. *w.zhou@hapticdevices.eu*.

Authors of Editions 1 and 2

Former contributions to this book were made by

Dr.-Ing. Henry Haus
Dr.-Ing. Markus Jungmann
Dr.-Ing. Peter Lotz
Dr.-Ing. Marc Matysek
Dipl.-Ing. Oliver Meckel
Dr.-Ing. Carsten Neupert
Dr.-Ing. Thomas Opiz
Dr.-Ing. Alexander Rettig
Dr.-Ing. Tim Rossner
Dr.-Ing. Stephanie Sindlinger
Prof. Dr. rer. nat. Gerhard Weber
Dr.-Ing. Limin Zeng
Ingo Zoller, Ph.D.

Symbols

This list includes the most relevant symbols used throughout the book.

a	Sensory background noise (Weber's Law) (-)
a	Acceleration ($\frac{\mathrm{m}}{\mathrm{s}^2}$)
$\mathbf{a}$	Vector, summarizing actuator displacement and angles a_i (-)
A	Area, cross section (m^2)
$A(j\omega)$	Amplitude response Chap. 7 (dB)
A	Matrix of a linear system of equations (-)
α	Positive number (-)
α	Angle, Euler rotation (around the x-axis) (degree, radian)
α_{VK}	Coefficient of thermal expansion (K^{-1})
b	Wave impedance
B, B_0	Magnetic flux density (T)
B_r	Remanence flux density (T)
$\mathbf{B}$	Magnetic flux density (T)
$\mathbf{B}$	Matrix of a linear system of equations (-)
β	Angle, Euler rotation (around the y-axis) (degree, radian)
c_{index}	Arbitrary constant, further defined by index (-)
c	Spring constant (-)
c_θ	Threshold parameter of the psychometric function (-)
c_σ	Sensitivity parameter of the psychometric function (-)
c_λ	Decision criteria (Signal Detection Theory) (-)
C_{ijlm}	Elastic constants ($\frac{\mathrm{m}^2}{\mathrm{N}}$)
C, C_Q	Capacity ($\mathrm{F} = \frac{\mathrm{A \cdot s}}{\mathrm{V}}$)
C_b	Coupling capacity (at mechanical full-stop) (F)
C	Transmission elements, controller Chap. 7 (-)
$\mathbf{C}$	Matrix of a linear system of equations (-)
$\frac{\Delta C}{C_0}$	Capacity change (-)
$\mathbb{C}$	Complex numbers (-)
d	Damping/friction ($\frac{\mathrm{N}}{\mathrm{m \cdot s}}$)
d	Distance, deflection, diameter (m)

$d_{ij,k}$, d_{im}	Piezoelectric charge constant ($\frac{\text{V}}{\text{m}}$)
$\frac{d_t}{d'}$	Detectability (Signal Detection Theory) (-)
D	Density
D	Dielectric flux density (A sm^{-2})
$\mathbf{D}$	Dielectric displacement/electrical displacement density ($\frac{\text{C}}{\text{m}^2}$)
$\mathbf{D}$	(Transmission-) matrix of a linear system of equations (-)
ΔD	Position-discrete resolution (-)
δ	Phase difference (Sect. 10.5) (-)
e	Piezoelectric voltage coefficient ($\frac{\text{A}\cdot\text{s}}{\text{m}^2}$)
$\mathbf{e}_i$	Directional unit vector (-)
E	E-modulus, modulus of elasticity ($\frac{\text{N}}{\text{m}^2}$)
E	Electrical field strength ($\frac{\text{V}}{\text{m}}$)
$\underline{e}_T$	Absolute transparency error (Sect. 7.5.2) (-)
$\underline{e}'_T$	Relative transparency error (Sect. 7.5.2) (-)
E_{ref}	Reference field strength, with C_s of an ERF being given ($\frac{\text{V}}{\text{m}}$)
$\mathbf{E}$	Electrical field ($\frac{\text{V}}{\text{m}}$)
ε	Permittivity ($\varepsilon = \varepsilon_0 \cdot \varepsilon_r$) ($\frac{\text{A}\cdot\text{s}}{\text{V}\cdot\text{m}}$)
ε	Relative dielectric constant of piezoelectric material (at constant mechanical tension) ($\frac{\text{A}\cdot\text{s}}{\text{V}\cdot\text{m}}$)
ε	Remaining error (Chap. 7) (-)
ε_0	Electrical field constant ($\varepsilon_0 = 8,854 \cdot 10^{-12} \frac{\text{C}}{\text{V}\cdot\text{m}}$) ($\frac{\text{C}}{\text{V}\cdot\text{m}}$)
ε_r	Relative permittivity ($\varepsilon_r = \frac{E_0}{E}$) (-)
F	Mechanism DoF (-)
f	Frequency (Hz)
f_0, f_R	Resonance-frequency (Hz)
f_b, f_g	Border-frequency (Hz)
f_{tot}	Sum of all joint degrees-of-freedom of a mechanism (-)
$f_{i,\dots,g}$	Degree-of-freedom of the ith joint in a mechanism (-)
f_{id}	Sum of identical condition (-)
f_{id}	Sum of all identical links in a mechanism (-)
f_{ink}	Dynamics of the detection of all increments for positioning measurement (Hz)
$f(\cdot)$	Static non-linearity (-)
F	Bearing-/movement-DOF of a mechanism (-)
F	Force (-)
ΔF	Force-resolution (N)
Φ	Magnetic flux (Wb $=$ V $\cdot$ s)
$\phi(j\omega)$	Phase plot (degree)
ϕ	Roll angle, rotation (around z-axis) (degree, radian)
φ	Angle (degree)
φ_R	Phase margin (degree)
Φ	Stimulus (-)
Ψ	Subjective percept (-)
g	Number of joints in a mechanism (Chap. 8) (-)

g	Piezoelectric constant ($\frac{\mathrm{V \cdot m}}{\mathrm{N}}$)
$g(x,u,t)$	Transfer function (time domain)
$G(s)$, $\underline{G}$	Transfer function in Laplace domain (-)
g	Number of joints (-)
γ	Angle, Euler rotation (around the z-axis) (degrees, radians)
$\dot{\gamma}$	Shear-rate (s^{-1})
h	Height (m)
h	Viscous damping/friction (network theory; see Table 4.1) (-)
$h(t)$	Transfer function (-)
$\underline{h}$	Mobility $h = \frac{1}{Z}$ ($\frac{\mathrm{m}}{\mathrm{N \cdot s}}$)
h	Element of the complex hybrid matrix H (-)
H	Complex hybrid matrix (Chap. 7)(-)
H_c	Coercitive field strength ($\frac{\mathrm{A}}{\mathrm{m}}$)
$\mathbb{H}$	Hamilton numbers (-)
i, $\underline{i}$	(AC) current (A)
I	(DC) current (-)
I, **I'**	interaction path *intention* (Sect. 2.3) (-)
I_D	Index of difficulty (Sect. 13.2) (-)
I_p	Index of performance (Sect. 13.2) (-)
I	Moment of inertia (m^4)
j, i	Imaginary unit, $i = \sqrt{-1} \in \mathbb{C}$ (-)
J	Current density ($\frac{\mathrm{A}}{\mathrm{m}^2}$)
$\mathrm{J} = \frac{\partial \mathrm{x}}{\partial \mathrm{q}}$	JACOBIan matrix defined by the relation of actuator and TCP speeds (-)
k	Spring constant, mechanical stiffness, elasticity (Nm^{-1})
k	Geometrical design dependent constant of ERFs ($\mathrm{m} \cdot \mathrm{s}$)
k	Fill-factor of a coil (≥ 1) (-)
k	Coupling-factor or k-factor (Sect. 10.5) (-)
k	Number of chains in a mechanism (-)
k_M	Motor constant (-)
K_{krit}	Critical amplification
K_R	Amplification of a proportional controller
κ	Conditioning number of a mechanism (-)
l	Length (m)
L	Inductivity ($\mathrm{H} = \frac{\mathrm{V \cdot s}}{\mathrm{A}}$)
λ	Pole of a transfer function (-)
λ	Wavelength (m)
λ	Eigenvalue of a matrix (-)
λ	Spatial factor; 3 for 2D and 6 for 3D mechanisms (-)
L	Lagrangian function (J)
m	Mass (kg)
M	Torque (Nm)
μ	Movability of a charge-carrier ($\frac{\mathrm{m}^2}{\mathrm{V \cdot s}}$)
μ	frictional coefficient (-)

μ	Mean value (-)
μ	Magnetic permeability ($\mu = \mu_0 \cdot \mu_r$) ($\frac{\mathrm{V \cdot s}}{\mathrm{A \cdot m}}$)
μ_0	Magnetic field constant $\mu_0 = 4\pi \cdot 10^{-7} \frac{\mathrm{V \cdot s}}{\mathrm{A \cdot m}}$
μ_r	Relative permeability (-)
n, N	Number $\in \mathbb{N}$ (-)
n	Number of bodies (-)
$n = \frac{1}{k}$	Compliance (mN^{-1})
n_0, n_i	Refraction index (-)
$\mathbb{N}$	Natural numbers
ν	Global conditioning index (-)
$\omega = 2\pi f$	Angular frequency ($\mathrm{rad\,s}^{-1}$)
$\underline{\omega}, \underline{\Omega}$	Angular velocity ($\frac{\mathrm{rad}}{\mathrm{s}}$)
p	Tool center point pose (m, rad)
p	Pressure ($\frac{\mathrm{N}}{\mathrm{m}^2}$)
p	Probability (-)
p_L	Lapse rate of the psychometric function (-)
p_G	Guess rate of the psychometric function (-)
p_ψ	Psychometric function (-)
P	Dielectric polarization ($\frac{\mathrm{C}}{\mathrm{m}^2}$)
P	Power (-)
P_g	Degree of parallelism (-)
${}^iP_j$	Position vector of frame *j* relative to frame *i* (-)
P', **P'**	Interaction path *Perception* (Sect. 2.3) (-)
π	Piezoresistive coefficient ($\frac{\mathrm{m}^2}{\mathrm{N}}$)
π_l	Piezoresistive coefficient in longitudinal direction ($\frac{\mathrm{m}^2}{\mathrm{N}}$)
π_q	Piezoresistive coefficient in transversal direction ($\frac{\mathrm{m}^2}{\mathrm{N}}$)
ψ	Yaw angle, rotation around x-axis (degree, radian)
Ψ	Subjective percept (-)
q, Q	Electrical charge ($\mathrm{C} = \mathrm{A} \cdot \mathrm{s}$)
$q_i, i \in \mathbb{N}$	Driven joint i
q	Fluidic volume flow ($-\ \mathrm{m}^3\ \mathrm{s}^{-1}$)
$\mathbf{q}$	Vector of actor coordinates (-)
r	Distance, radius (m)
$r_i, i \in \mathbb{N}$	Active resistors ($\Omega = \frac{\mathrm{V}}{\mathrm{A}}$)
R	Electrical resistance (Ω)
R_m	Magnetic resistance/reluctance ($\frac{\mathrm{A}}{\mathrm{V \cdot s}}$)
$\mathbb{R}$	Real numbers (-)
$\Re$	Real part (-)
$\frac{dR}{R_0}$	Relative resistance change (-)
ΔR_{inch}	Position resolution given in dots-per-inch (dpi)
ΔR_{mm}	Position resolution given in millimeter (mm)
ρ	Density ($\frac{\mathrm{kg}}{\mathrm{m}^3}$)
ρ	Small number ≥ 0 (-)
ρ	Specific resistance/conductivity ($\Omega \cdot \mathrm{m}$)

${}^{i}R_{j}$	Rotation matrix of frame *j* relative to frame *i* (-)
$s(t)$, $\underline{S}$	Arbitrary signal in time and frequency domains (-)
s	Elasticity coefficient at a constant field strength ($\frac{\mathrm{m}^2}{\mathrm{N}}$)
s	LAPLACE operator, $s = \sigma + j\omega$ (-)
s	Sum of constraints (-)
S	Mechanical stress (mm^{-1})
S	Number of constraints in a mechanism (-)
σ	Conductivity, $\sigma = \frac{1}{\rho}$ ($\frac{\mathrm{S}}{\mathrm{m}} = \frac{\mathrm{A}}{\mathrm{V \cdot m}}$)
σ	Singular value of a matrix (-)
t	Time/point in time (s)
tr	Transmission ratio of a gear (-)
T	Mechanical tension ($\frac{\mathrm{N}}{\mathrm{m}^2}$)
T	Time constant, time delay (s)
τ	Shear force (Chap. 9) (N)
τ	Time constant of the step response of an electrical transmission system ($\tau = \frac{L}{R}$, $\tau = \frac{1}{RC}$) (s)
τ	Torque (Chap. 8) (Nm)
θ	Pitch angle, rotation about the *y*-axis (degree, radians)
$\boldsymbol{\Theta}$	Magnetomotive force (A)
iT_j	Transformation matrix of frame *j* relative to frame *i* (-)
ϑ	Temperature (K)
$u(t)$	(AC) voltage (V)
U	(DC) voltage (V)
u	Multidimensional input value of a linear system (-)
v	Velocity
V	Magnetic tension, magnetic voltage (A)
V	Volume (m^3)
V_x	LYAPUNOV function (Chap. 7) (-)
$V(x)$	Scalar nonlinear positive definite storage function of system states x
$\dot{V}$	Volume flow ($\frac{\mathrm{m}^3}{\mathrm{s}}$)
ΔV	Volume-element (m^3)
w	General value for in- and output values (-)
w	Unity vector (-)
W	Work, energy ($\mathrm{J} = \frac{\mathrm{kg \cdot m}^2}{\mathrm{s}^2}$)
x	Distance, displacement, translation, amplitude, elongation, position (m)
$\mathrm{x} = (x, y, z)$	Cartesian coordinates (-)
x	Inner states of a linear system (-)
x	Vector of TCP coordinates (position and orientation) (-)
Δx	Position resolution (m)
X	Transformation constant (-)
ξ	Displacement (m)
y	Control value (-)
y	Output (-)

y	Multidimensional output value of a linear system (-)
Y	Gyratoric transformation constant (-)
$\underline{Y}$	Mechanical admittance ($\frac{\mathrm{m}}{\mathrm{N \cdot s}}$)
z	Disturbance variable (-)
$\underline{Z}$	Mechanical impedance ($\frac{\mathrm{N \cdot s}}{\mathrm{m}}$)
$\underline{Z}$	Electrical impedance $\mathrm{V\ A^{-1}}$

Indices and Distinctions

The usage of the most relevant indices and distinctions used throughout the book is shown using the replacement character $\blacksquare$.

$\blacksquare_0$	Base or reference value
$\blacksquare_E$	Referring to the real or VR environment
$\blacksquare_H$	Referring to the master side of a teleoperator (probably derived from "handle")
$\blacksquare_M$	Referring to the master device of a haptic system
$\blacksquare_{max}$	Maximum value
$\blacksquare_{min}$	Minimum value
$\blacksquare_{rot}$	Referring to a rotational value
$\blacksquare_S$	Referring to the slave device of a haptic system
$\blacksquare_T$	Referring to the master side of a teleoperator
$\blacksquare^T$	Transformed vector or matrix
$\blacksquare_{trans}$	Referring to a translational value
$\blacksquare_{\text{user}}$	Referring to the user of a haptic system
$\delta\blacksquare$	Small change, differential
$\Delta\blacksquare$	Discretized element
$\blacksquare_\theta$	Referring to a psychophysical threshold
$\mathbf{X}$	Vector or matrix
$\blacksquare(t)$	Time-depending value
$\underline{\blacksquare}$	Complex value with amplitude/phase or real/imaginary part
$\dot{\blacksquare}$	Derivative with respect to time

Part I
Basics

Chapter 1
Motivation and Application of Haptic Systems

Thorsten A. Kern and Christian Hatzfeld

Abstract This chapter serves as an introduction and motivation for the field of haptic research. It provides an overview of the technical domains covered, but also introduces the philosophical and social aspects of human haptic sense. Various definitions of haptics as a perceptual and interaction modality are discussed to serve as a common ground for the rest of the book. Typical application areas such as telepresence, training, interaction with virtual environments and communication are introduced and typical haptic systems from these areas are discussed.

1.1 Research Disciplines

Haptics—in a non-scientific understanding, refers to the sense of touch and everything connected with it. If you think about it more carefully, you will realise that touch always requires interaction. Thus, the perception of touch cannot take place without contact, and consequently, without *something* being touched or being touched by. Following this basic concept, it is obvious that haptics requires interaction. A statement that sounds simple, but in terms of research and technical tasks it adds complexity to the subject. This is because, in contrast to vision and sound, haptics always has an impact on the touched object itself due to the interaction, and the classification of interactions varies depending on the physical properties of the body and object. If there is also awareness that the sense of touch is relevant to every mechanical part of the body that interacts with the environment, and in particular to

Christian Hatzfeld deceased before the publication of this book

T. A. Kern (✉)
Hamburg University of Technology, Eißendorfer Str. 38, 21073 Hamburg, Germany
e-mail: t.a.kern@tuhh.de

C. Hatzfeld
Technische Universität Darmstadt, Darmstadt, Germany

T. A. Kern et al. (eds.), *Engineering Haptic Devices*, Springer Series on Touch and Haptic Systems, https://doi.org/10.1007/978-3-031-04536-3_1

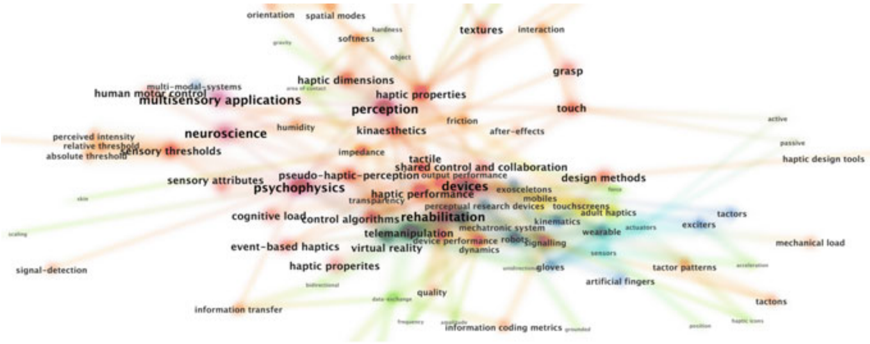

Fig. 1.1 Concept-Map on Haptic Disciplines, own visualization

every area covered with skin, each of them having different sensory capabilities, the challenges in this field should become clear.

Consequently with haptics-research still growing the field is restructured frequently. A snapshot of the core-disciplines is given in Fig. 1.1. Whereas 20 years ago haptic research areas were maybe eight or ten, the diversification of research changed drastically in the last decade due to increased understanding of interdependencies but also more specialization and specific needs of industry. One main direction can be found with the group of perception-based research covering psychophysical and neuroscience-related topics. This field has a strong influence on all the application-based research such as , or , which themselves again need several components and subsystems and are used in different applications.

The topic of this book is engineering haptic devices. So with regards to Fig. 1.1 we are in the blueish device and yellow application areas, but of course doing this the book does not ignore the interlinked areas and gives those details required to understand the influences from those interfaces.

1.2 Some Broad Scope on Haptics

But what is *haptics* in the first place? A common and general definition is given as

> **Definition** *Haptics* Haptics describes the sense of touch and movement and the (mechanical) interactions involving these.

but this will probably not suffice for the purpose of this book. This chapter will give some more detailed insight into the definition of haptics (Sect. 1.4) and will introduce four general classes of applications for haptic systems (Sect. 1.5) as the motivation for the design of haptic systems and—ultimately—for this book. Before that we will have a short summary of the philosophical and social aspects of this human sense (Sect. 1.3). These topics will not be addressed any further in this book, but should be kept in mind by every engineer working on haptics.

1.3 Philosophical and Social Aspects

An engineer tends to describe haptics primarily in terms of forces, elongations, frequencies, mechanical tensions and shear-forces. This of course makes sense and is important for the technical design process. However haptics starts before that. Haptic perception ranges from minor interactions in everyday life, e.g., drinking from a glass or writing this text, to a means of social communication, e.g. shaking hands or giving someone a pat on the shoulder, and very personal and private interpersonal experiences. Touch has a conscious, but also a very relevant unconscious component as demonstrated e.g. by a study of CRUSCO ET AL. [1] showing a tip to a waitress being on average 10% higher with the customer being slightly touched. This touch is known as the *Midas Touch* and is surprisingly independent of gender and age on both sides. This section looks at the spectrum and influence of haptics on humans beyond technological descriptions. It is also a hint for the development engineer to deal responsibly and consciously with the possibilities of outwitting the haptic sense.

1.3.1 Haptics as a Physical Being's Boundary

Haptics is derived from the Greek term "haptios" and describes "something which can be touched". In fact the consciousness about and understanding of the haptic sense has changed many times in the history of humanity. ARISTOTELES puts the sense of touch in the last place when naming the five senses:

1. sight
2. hearing
3. smell
4. taste
5. touch

Nevertheless he attests this sense a high importance concerning its indispensability as early as 350 B.C. [2]:

Some classes of animals have all the senses, some only certain of them, others only one, the most indispensable, touch.

The social estimation of the sense of touch experienced all imaginable phases. Frequently it was afflicted with the blemish of squalor, as lust is transmitted by it [3]:

Sight differs from touch by its virginity, such as hearing differs from smell and taste: and in the same way their lust-sensation differs

It was also called the sense of excess [4]. In a general subdivision between lower and higher senses, touch was almost constantly ranged within the lower class. In western civilization the church once stigmatized this sense as forbidden due to the pleasure which can be gained by it. However, in the 18th century the public opinion changed and KANT is cited with the following statement [5]:

This sense is the only one with an immediate exterior perception; due to this it is the most important and the most teaching one, but also the roughest. Without this sensing organ we would be able to grasp our physical shape, whose perception the other two first class senses (sight and hearing) have to be referred to, to generate some knowledge from experience.

KANT thus emphasizes the central function of the sense of touch. It is capable of teaching the spatial perception of our environment. Only touch enables us to feel and classify impressions collected with the help of other senses, put them into context and understand spatial concepts. Although stereoscopic vision and hearing develop early, the first-time interpretation of what we see and hear, requires the connection between both impressions perceived independently and information about distances between objects. This can only be provided by a sense, which can bridge the space between a being and an object. Such a sense is the sense of touch. The skin, being a part of this sense, covers a human's complete surface and defines his or her physical boundary, the physical being.

1.3.2 Formation of the Sense of Touch

As shown in the prior section, the sense of touch has numerous functions. The knowledge of these function enables the engineer to formulate demands on the technical system. It is helpful to consider the whole range of purposes the haptic sense serves. However, at this point we do not yet choose an approach by measuring its characteristics, but observe the properties of objects discriminated by it.

The sense of touch is not only specialized on the perception of the physical boundaries of the body, as said before, but also on the analysis of immediate surroundings including the contained objects and their properties. Human beings and their predecessors had to be able to discriminate e.g. the structure of fruits and leaves by touch, in order to identify their ripeness or whether they were eatable or not, like e.g. a furry berry among smooth ones. The haptic sense enables us to identify a potentially harming structure, like e.g. a spiny seed, and to be careful when touching it, in order to obtain its content despite its dangerous needles.

For this reason, the sense of touch has been optimized for the perception and discrimination of surface properties like e.g. roughness. Surface properties may range from smooth ceramic like or lacquered surfaces with structural widths in the area of some μm, to somewhat structured surfaces like coated tables and rough surfaces like coarsely woven cord textiles with mesh apertures in the range of several millimeters. Humans developed a very typical way how to interact with theses surfaces enabling

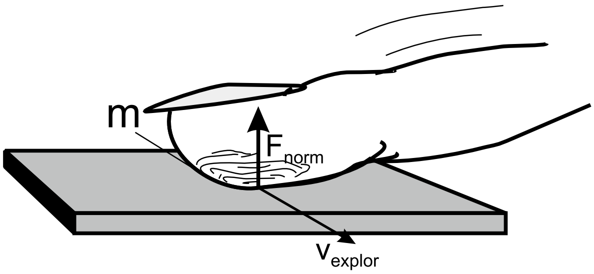

Fig. 1.2 Illustration for the interaction of movements, normal forces on the finger pad and frictional coupling

them to draw conclusions based on the underlying perception mechanism. A human being moves his or her finger along the surface (Fig. 1.2), allowing shear forces to be coupled to the skin. The level of the shear forces is dependent on the quality of the frictional coupling between the object surface and the skin. It is a summary of the tangential elasticity of the skin depending on the normal pre-load resulting from the touch F_{norm} and the velocity v_{explr} of the movement and the quality of the coupling factor μ.

Everyone who has ever designed a technical frictional coupling mechanism knows that without additional structures or adhesive materials viscous friction between two surfaces can hardly reach a factor of $\mu_r \geq 0.1$. Nevertheless nature, in order to be able to couple shear force more efficiently into the skin, has “invented” a special structure at the most important body-part for touching and exploration: the fingerprint. The epidermal ridges couple shearing forces efficiently to the skin, as by the bars a bending moment is transmitted into its upper layers. Additionally these bars allow form closures within structural widths of similar size, which means nothing else but canting between the object handled and the hand’s skin. At first glance this is a surprising function of this structure. When one looks again, it just reminds you of the fact that nature does not introduce any structure without a deeper purpose.

Two practical facts result from this knowledge: First of all the understanding of shear-forces’ coupling to the skin has come into focus of current research [6] and has resulted in an improvement of the design process of tactile devices. Secondly, this knowledge can be applied to improve the measuring accuracy of commercial force sensors by building ridge-like structures [7].

Another aspect of the haptic sense and probably a evolutionary advantage is the ability to use tools. Certain mechanoreceptors in the skin (see Sect. 2.1 for more details) detect high-frequency vibrations that occur when handling a (stiff) tool. Detection of this high-frequency vibrations allows to identify different surface properties and to detect contact situations and collisions [8].

1.3.3 Touchable Art and Haptic Aesthetics

Especially in the 20th century, art deals with the sense of touch and plays with its meaning. Drastically the furry-cup (Fig. 1.3) makes you aware of the significance of haptic texture for the perception of surfaces and surface structures. Whereas the general form of the cup remains visible and recognizable, the originally plane ceramic surface is covered by fur.

In 1968, the "Pad- and Touch-Cinema" (Fig. 1.4) allowed visitors to touch VALIE EXPORT's naked skin for 12 s through a box being covered by a curtain all the time. According to the artist this was the only valid approach to experience sexuality without the aspect of voyeurism [9]. These are just a few examples of how art and artists played with the various aspects of haptic perception.

As with virtual worlds and surroundings, also haptic interaction has characteristics of artistry. In 2004, ISHII from MIT Media Laboratory and IWATA from the University of Tsukuba demonstrate startling exhibits of "tangible user interfaces" based on bottles opened to "release" music.

And meanwhile, the human-triggered touch is extended to devices touching back. With MARC TEYSSIER exploring very actively the limits of what is socially acceptable or not in the unexplored field between art and robotics (Fig. 1.5).

Despite the artistic aspect of such installations, recent research evaluates new interaction possibilities for ↪ Human-Computer-Interaction (HCI)[1] based on such concepts:

Fig. 1.3 MERET OPPENHEIM: furry-cup, 1936 [9, 10], DIGITAL IMAGE ©2022, The Museum of Modern Art/Scala, Florence

[1] Please note that entries in the glossary and abbreviations are denoted by a ↪ throughout the book.

Fig. 1.4 VALIE EXPORT TAPP und TASTKINO, 1968, b/w—photography ©VALIE EXPORT, Bildrecht Wien, 2022, photo ©Werner Schulz, courtesy VALIE EXPORT, http://80.64.129.152:8080/share.cgi?ssid=0vdjJr7

Fig. 1.5 *MobiLimb* project with a device touching back [11], ©2022 MARC TEYSSIER, used with permission

- In [12], picture frames are used as tangible objects to initiate a video call to relatives and friends, when placed on a defined space on a special table cloth.
- With TOUCHÉ, *Disney Research* presents a capacitive sensing principle to use almost every object as a touch input device [13]. It is intended to push the development of immersive computers that disappear in objects.
- And even for everyday-objects touch-enhanced functions can be built-in and demonstrated, e.g. by the company *Playtronica* focusses on touch-enhancing everyday objects by an interpretation of capacitance into midi-signals and synth-music (Fig. 1.6).

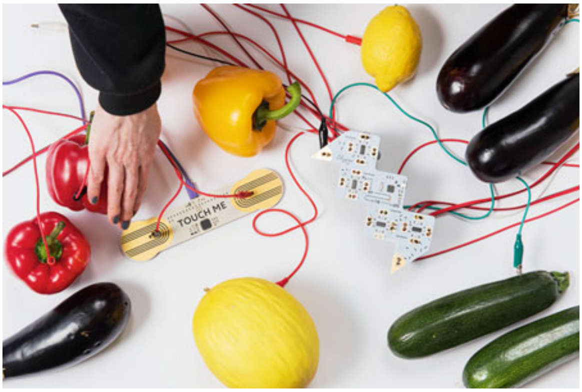

Fig. 1.6 PLAYTRONICA product *playtron* and *Touch ME* with capacitive measurement and midi-sound generation based on touch-intensity, ©2022 DARIA MALYSHEVA, used with permission

In technical applications, the personal feeling of haptic aesthetics is a distinguishing factor. Car manufactures work on objective quality schemes for the perceived quality of interfaces [14, 15] with the target to create a touchable brand identity, there are whole companies claiming to "*make percepts measurable*" [16] and designers provide toolkits to evaluate characteristics of knobs and switches [17, 18] and meanwhile even design-packages are proposed and commercialized to evaluate typical vibrational feedbacks [19]. However, the underlying mechanisms of the assessment of haptic aesthetics are not fully understood. While the general approach of all studies is basically the same, using multidimensional scaling and regression algorithms to combine subjective assessments and objective measurements [20], details on perceptional dimensions are subject to ongoing research [21] and sophisticated data-models [22].

CARBON AND JAKESCH published a comprehensive approach based on object properties and the assessment of familiarities [23]. This topic still remains a fascinating field of research for interdisciplinary teams from engineering and psychology and is applied to regular product design [24].

1.4 Technical Definitions of Haptics

To use the haptic sense in a technical manner, some agreements about terms and concepts have to be made. This section deals with some general definitions and classifications of haptic interactions and haptic perception and is the basis for the following Chap. 2, which will dig deeper into topics of perception and interaction.

1.4.1 Definitions of Haptic Interactions

The haptic system empowers humans to interact with real or virtual environments by means of mechanical, sensory, motor and cognitive abilities [25]. An interaction consists out of one or more operations, that can be generally classified into *motion control* and *perception* [26]. The operations in these classes are called *primitives*, since they cannot be divided and further classified.

The perception class includes the primitives *detection*, *discrimination*, *identification* and *scaling* of haptic information [27]. The analysis of these primitives is conducted by the scientific discipline called $\hookrightarrow$ psychophysics. To further describe the primitives of the description class, the term $\hookrightarrow$ stimulus has to be defined:

> **Definition** *Stimulus (pl. stimuli)* Excitation or signal that is used in a psychophysical procedure. It is normally denoted with the symbol Φ. The term is also used in other contexts, when a (haptic) signal without further specification is presented to a user.

Typical stimuli in haptics are forces, vibrations, stiffnesses, or objects with specific properties. With this definition, we can have a closer look at the perception primitives, since each single primitive can only be applied to certain haptic stimuli, as explained below.

Detection The detection primitive describes, how the presence of a stimulus is detected by a human respectively a user. Depending on the interaction conditions, stimuli can be detected or not detected. This depends not only on the sensory organs involved (see Sect. 2.1) but also on the neural processing. Only if a stimulus is detected, the other perception primitives can be applied.

Discrimination If more than one stimulus is present *and* detected, the primitive discrimination describes how information are perceived, that are included in different properties of the signal (like frequency or amplitude of a vibration) or an object (like hardness, texture, mass).

Identification As well as the discrimination primitive, also the identification primitive is based on more than one present and detected stimuli. These stimuli are however not compared to each other, but with practical or abstract knowledge to allow a classification of the information contained in the stimuli. An example for such a task is the identification of geometric properties of objects like size and global form.

Scaling Scaling is the fourth primitive of perception as generally described by psychophysicists. This primitive describes the behavior of scales when properties of stimuli and objects are rated [28]. While scaling is only of secondary meaning for the description of interactions, it can provide useful information about signal magnitudes in the design process.

The motor control class can be divided in different operations as well. In this class, the primitives *travel*, *selection* and *modification* exist [29]. They can be better explained, if they are linked to general interaction tasks [29, 30]:

Travel The movement or travel of limbs, the whole body or virtual substitutes (avatar) is used to search for or reach a destination or an object, to explore (unknown) environments or to change the position of oneself. Changing of a movement already in progress is included in this primitive.

Selection Especially in virtual environments, marking and/or selection of an object or a function is a vital primitive. It allows for a direct interaction in this environments in the first place.

Modification The modification primitive is based on a selection of a function or an object. It describes a change in orientation, position or other properties of an object as well as the combination of more than one object to a single one.

When using motor control primitives, not only the operation itself but the aim of the operation have to be considered for an accurate description of an interaction. If, for example, a computer is operated with a mouse as an input device and an icon on the screen is selected, this interaction could be described as a travel primitive or as a selection primitive. A closer look will probably reveal, that the travel primitive is used to reach an object on the screen. This object is selected in a following step. If this interaction should be executed with a new kind of haptic device, the travel primitive is probably considered subordinate to the selection primitive.

Based on these two classes of interaction primitives, SAMUR introduces a ↪ taxonomy of haptic interaction [31]. It is given in Fig. 1.7 and allows the classification of haptic interaction. A classification of a haptic interaction is useful for the design of new haptic systems: Requirements can be derived more easily (see Chap. 5), analogies can be identified and used in the design of system components and the evaluation is alleviated (see Chap. 13).

Next to the analysis of haptic interaction based on interaction primitives, some more psychophysically motivated approaches exist:

- LEDERMAN AND KLATZKY propose a classification of haptic interaction primitives in two operation classes: Identification (The *What-System*) and Localization (The *Where-System*) [32].
- HOLLINS proposes a distinction of primitives based on the spatial and temporal resolution of perception (and the combinations thereof) on the one side and and a class of "haptic" interactions on the other side [33]. Latter correspond roughly to the above mentioned motion control primitives.

The application of the taxonomy of haptic interactions as given in Fig. 1.7 to the development of task-specific haptic systems seems to be much more straightforward as the application of the approaches by LEDERMAN AND KLATZKY and HOLLINS as stated in the above listing. Therefore these are not pursued any further in this book.

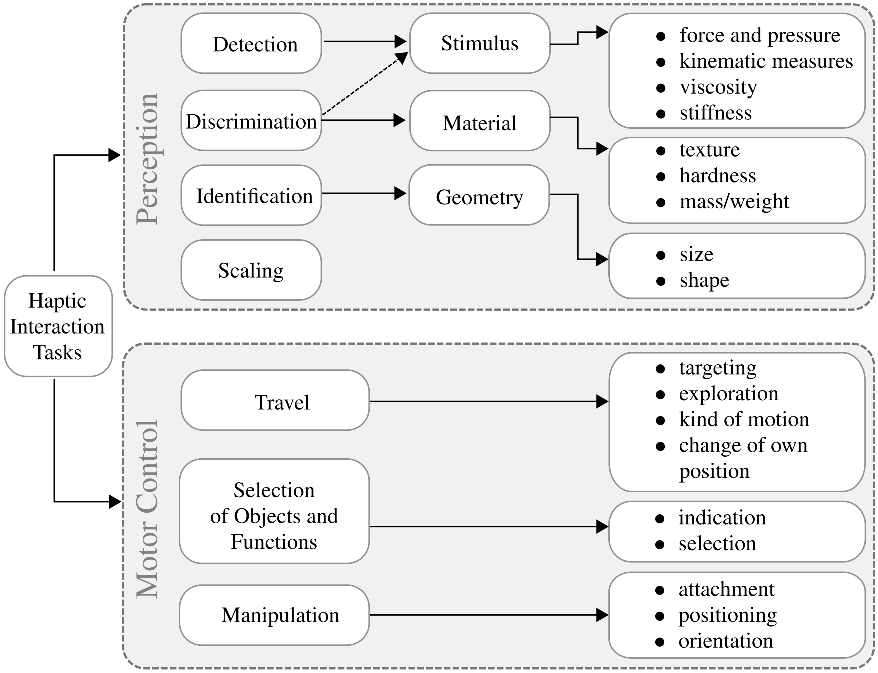

Fig. 1.7 Taxonomy of haptic interaction. Figure based on [27, 31]

Fig. 1.8 Taxonomy of haptic perception as defined in [30]

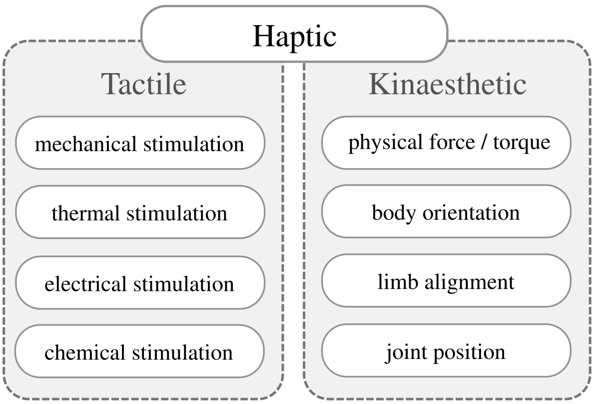

1.4.2 *Taxonomy of Haptic Perception*

Up till now, one of the main taxonomies in haptic literature has not been addressed: The classification based on ↪ kinaesthetic and ↪ tactile perception properties. It is physiological based and defines perception solely on the location of the sensory receptors. It is defined in the standard ISO 9241-910 [30] and given in Fig. 1.8.

With this definition, tactile perception is based on all ↪ cutaneous receptors. These include not only mechanical receptors, but also receptors for temperature, chemicals (i.e. taste) and pain. Compared to the perception of temperature and pain, mechanical interaction is on the one side much more feasible for task-specific haptic systems in terms of usability and generality, on the other side it is technically much more demanding because of the complexity of the mechanoreceptors and the inherited dynamics. Therefore this book will lay its focus on mechanical perception and interaction.

For processes leading to the perception pain the authors point to special literature [34] dealing with that topic, since an application of pain stimuli in a haptic system for everyday use seems not to be likely. The perception of temperature and possible applications are given for example in [35, 36]. Whereas some technical applications of thermal displays are known [37–39], these seem to be minor to mechanical interaction in terms of information transfer and dynamics. Therefore, temperature is primarily considered as an influencing factor on the mechanical perception capabilities and discussed more detailed in Sect. 2.1.2.

With the confinement on mechanical stimuli, we can define kinaesthetic and tactile perception as follows:

Definition *kinaesthetic* kinaesthetic perception describes the perception of the operational state of the human locomotor system, particularly joint positions, limb alignment, body orientation and muscle tension. For kinaesthetic perception, there are dedicated sensory receptors in muscles, tendons and joints as detailed in Sect. 2.1. Regarding the taxonomy of haptic interactions, kinaesthetic sensing is primarily involved the motion control primitives, since signals from kinaesthetic receptors are needed in the biological control loop for the positioning of limbs.

Definition *tactile* Tactile perception describes the perception based on sensory receptors located in the human skin. Compared to kinaesthetic receptors, they exhibit much larger dynamics and are primarily involved in the perception primitives of haptic interaction.

While originally the terms *tactile* and *kinaesthetic* are strictly defined by the location and the functions of the sensory receptors, they are used in a more general way recently. While the root of the word *kinesthesia* is linked to the description of movement, the term *kinaesthetic* is also used to describe static conditions nowadays [40]. Sometimes, kinaesthetic is only used for the perception of properties of limbs, while the term *proprioception* is used for properties regarding the whole body [41]. This differentiation is neglected further in this book because of its minor technical importance. The term *tactile* often describes any kind of sensor or actuator with a spatial resolution, regardless if it is used in an application addressing tactile perception as defined above. While these examples are only of minor importance for the design of haptic systems, the following usage of the terms is an important adaption of the definitions: Primarily based on the dynamic properties of tactile and kinaesthetic perception, the term definition is extended to haptic interactions in general nowadays. The reader may note that the following description is not accurate in terms of temporal sequence of the cited works, but focuses on the works with relevant contributions to the present use of the terms *kinaesthetic* and *tactile*.

Based on the works of SHIMOGA, the dynamics of kinaesthetic perception are set equal to the motion capabilities of the locomotor system [42]. The dynamics of tactile perception are bordered at about 1 ... 2 kHz for practical reasons. Higher frequencies can be perceived [43, 44], but it is questioned, whether they have significant contribution to perception [45, p. 3]. As further explained in Sect. 2.4.3, this limitation is technically reasonable and necessary for the design of the electromechanical parts of haptic systems. Figure 1.9 shows this dynamic consideration of haptic interaction based on characteristic values from [44, 46, 47].

To extend this dynamic model of perception to a more general definition of interactions, DANIEL AND MCAREE propose a bidirectional, asymmetric model with a low-frequency (<30 Hz) channel for the exchange of energy and a high-frequency channel for the exchange of information [48] with general implications on the design of haptic interfaces. The mapping based on dynamic properties is meaningful to a greater extend, since users can be considered as mechanical passive systems for frequencies above the dynamics of the active movement capabilities of the locomotion system [49]. This will be explained in more detail in Chap. 3. Altogether, these aspects (dynamics of perception and movement capabilities, exchange paths of energy and information and the modelling of the user as active and passive load to a system) lead to the nowadays widely accepted model for the partition of haptic interaction in low-frequency kinaesthetic interaction and high-frequency tactile perception.

Both taxonomies of haptic interaction as seen in Fig. 1.7 and haptic perception as seen in Fig. 1.8 and extended in Fig. 1.9 are relevant sources for standard vocabulary in haptic system design. This is needed in the design of haptic systems, since it will simplify and standardize descriptions of haptic interactions. These are necessary to describe the intended functions of a task-specific haptic system and will be described more detailed in Sect. 5.2. Further definitions and concepts about haptic interaction and perception are given in Chap. 2 in more detail. In the next part of this chapter, possible applications for haptic systems that will become part of the human haptic interaction with systems and environments are presented.

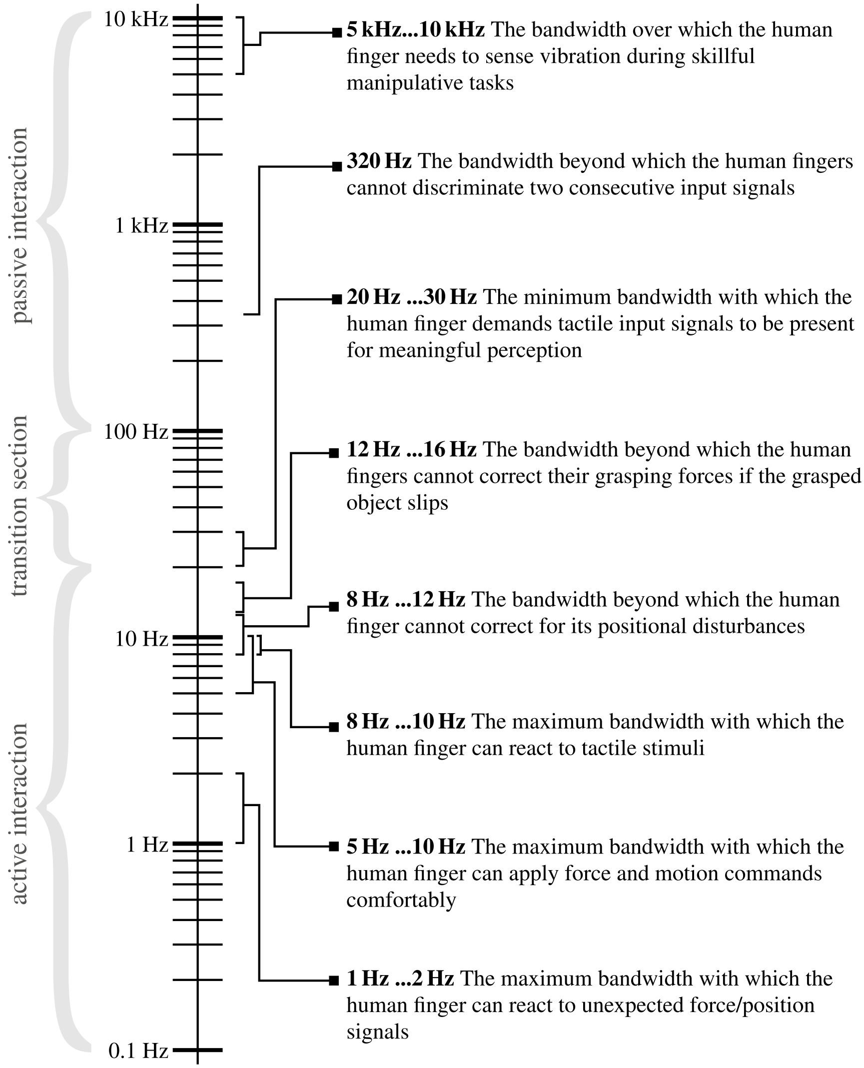

Fig. 1.9 Kinaesthetic and tactile haptic interaction. Figure is based on data from [44, 46, 47]

1.5 Application Areas of Haptic Systems

Haptic systems can be found in a multitude of applications. In this section, four general application areas are identified. Benefits and technical challenges of haptic systems in this areas are given. In the latter Sect. 2.3, these application areas are combined with a general model of human-system-environment interaction, leading to an interaction-based definition of basic system structures.

1.5.1 Telepresence, Teleaction and Assistive Systems

Did you ever think about touching a lion in a zoo's cage?

With a $\hookrightarrow$ telepresence and teleaction (TPTA)-system you could do just that without exposing yourself to risks, since they provide the possibility to interact mechanically with remote environments (We neglect the case of the lion feeling disturbed by the fondling...).

In a strict definition of TPTA-systems there is no direct mechanical coupling between operator and manipulated environment, but only via the TPTA-system. Thus the transmission of haptic signals is possible in the first place, since the mechanical interaction is converted to other domains (mainly electrical) and can be transmitted more easily. They are often equipped with additional multimodal features, mainly a one-directional visual channel displaying the environment to the operator of the TPTA-system.

Examples include systems for underwater-assembly, when visual cues are useless because of dispersed particles in the water [50], scaled support of micro- and nano-positioning [51, 52] and surgical applications [53, 54]. The use of TPTA-systems shortens task completion time, and minimizes errors and handling forces compared to systems without a haptic feedback [55]. In surgical applications new combinations of insofar incompatible techniques are possible, for example palpation in minimal invasive surgery. Studies also show an safety increase for patients [56]. In recent years especially the strong increase in band with in any networked application is driving imagination on what could be done. ANTONAKOGLOU ET AL. [57] did a very nice overview paper in the context of the availability of 5G. But despite aerial or space applications, the input-device stays in focus for an efficient operation [58].

Most TPTA-Systems knwon are used for research applications. Figure 1.10 shows an approach by *Quanser*, supplying a haptic interface and a robot manipulator arm. Based on this combination, versatile bilateral teleoperation scenarios can be designed, as for example NEUROARM, a teleoperation system for neurological interventions [59]. Example interventions include the removal of brain tumors, that require high position accuracy and real-time integration of $\hookrightarrow$ Magnetic Resonance Imaging (MRI) images.

The development of TPTA-systems is technically most challenging. This is caused by the unknown properties of the environment, having an influence on the system stability, the required high accuracy of sensors and actuators to present artifact-free haptic impressions and the data transmission over long distances with additional aspects of packeted transmission, (packet-)losses and latency.

A special type of TPTA-systems are so-called $\hookrightarrow$ comanipulators, that are mainly used in medical applications [53]. Despite the mechanical interaction over the TPTA-system, additional environment manipulation (and feedback) can be exerted by parts of the system (a detailed definition based on the description of the interaction can be found in Sect. 2.3). Examples for such comanipulators are INKOMAN and HAPCATH developed at the *Institute for Electromechanical Design*.

Fig. 1.10 Versatile teleoperation by *Quanser*: HD^2 haptic interface with 7 DoF of haptic feedback and *Denso* OPEN ARCHITECTURE robot with 6 DoF. Image courtesy by *Quanser*, Markham, Ontario, CA., used with permissions

The HAPCATH-system that adds haptic feedback to cardiovascular interventions is presented in detail as an example in Sect. 14.2. Figure 1.11 displays the INKOMAN instrument, which is the result of the joint research project SOMIT- FUSION funded by the German Ministry of Education and Research. It is an extension of a laparoscopic instrument with a parallel kinematic structure [60], that provides additional $\hookrightarrow$ degrees of freedom (DOF) of an universal tool platform [61]. This allows minimal invasive interventions at previously unreachable regions of the liver. By integrating a multi-component force sensor in the tool platform [62] interaction forces between instrument and liver can be displayed to the user [63]. This allows techniques like palpation to identify vessels or cancerous tissue. With the general form of a laparoscopic instrument, additional interaction forces can be exerted by the surgeon by moving the complete instrument, it is therefore classified as a comanipulation system.

TPTA systems are mainly focus of research activities, probably since there are only small markets with a high potential for this kind of systems. An exception are medical applications, where non-directly coupled instruments promise higher safety and efficient usage, for example by avoiding collisions between different instruments or lowering contact and grip forces [56, 64]. Also automated procedures like knot tying can be accelerated and conducted more reliable [65]. However, the distinction between a haptic TPTA-system and a robotic system for medical use is quite a thin line: The aforementioned functions do not require haptic feedback. This explains the large number of existing medical robotic systems in research and industry [66, 67], dominated by the well-known DA VINCI by *Intuitive Surgical Operations Inc.*. This system was developed for urological and gyneological interventions and incorporates a handling console with three-dimensional view of the operation area and a considerable number of instruments, that are directed by the surgeon on the console and actuated with cable drives [68]. There is no haptic feedback for this

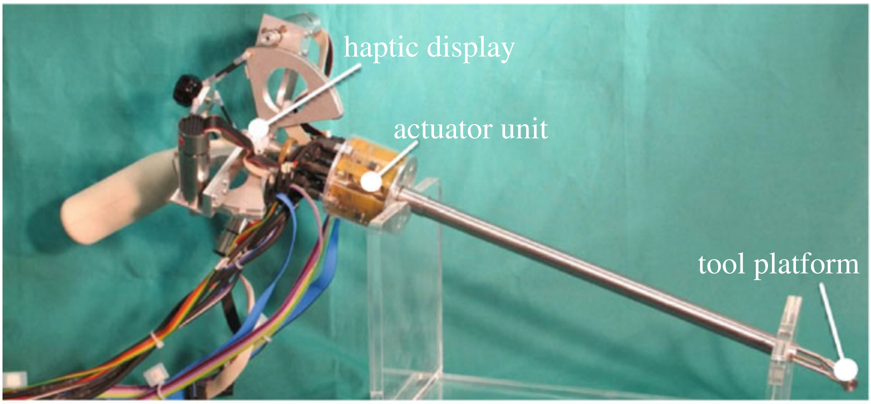

Fig. 1.11 INKOMAN—intracorporal manipulator for minimal invasive abdomen interventions with increased flexibility. The figure shows the handheld instrument with a haptic display based on a delta kinematic structure. The parallel kinematic structure used to move the tool platform is driven by ultrasonic traveling wave motors. Figure adapted from [63]

Fig. 1.12 DA VINCI SP surgical system for single port access, ©2022 *Intuitive Surgical Operations, Inc.*, used with permission

system preinstalled, although there are promising extensions available as discussed in Sect. 2.4.4. Just recently, the system is extended to single-port entry, which further reduces the liaisons of the intervention and allows a quick exchange of tools used during the procedure (Fig. 1.12).

For consumer application, *Holland Haptics* sold a product called FREBBLE intended to convey the feeling of holding someones hand over the internet. This was as well an interesting hardware concept as a low-cost teleoperation device.

Also practical magnetic resonance imaging studies into the hand neural control revealed significant progress, but the harsh MRI environments are a challenge for devices capable of delivering a large variety of stimuli. This work focused on presenting an fMRI-compatible haptic interface to find the neural mechanisms for precision grasp control. The interface is placed at the scanner bore, and it is controlled through a shielded electromagnetic actuation system. It is located at the scanner bed end and uses a high stiffness cable. Performance evaluation showed up to 94 N renderable forces and structural stiffness of 3.3 N/mm, and at least 19 Hz position control bandwidth.

In this system, two closed-loop cable transmissions actuate the two DOF, which are for each finger. It consists of aluminum profiles that hold redirection modules. Cables are passing through a length and tension adjustment mechanism. The guiding pulleys are combined with low friction polymer/glass ball bearings. They are fixed on an aluminum bar rigidly attached to the scanner bedside. Fixing the cables to the capstan prevents slippage. Due to the transmission friction, cable wear is important, and for making better interaction with operators, the cable should be easily exchangeable in a breakdown during an fMRI study.

1.5.2 Virtual Environments

The second main application area for haptic systems is interaction with virtual environments. Since this is quite a large field of applications, we will have a closer look on different areas, where interaction with generated situations is used in a wider extent.

Medical Training A large number of systems is designed to provide medical training without jeopardizing a real patient [69]. In addition to haptic feedback, this systems generally provide also visual and acoustic feedback to generate a realistic impression of the simulated procedure. You can find systems to train the diagnosis of joint lesions [70] and simulators for endoscopic, laparoscopic and intravascular interventions [31]. Figure 1.13 shows an example of such a surgical simulator. Surgeons trained on simulators show a better task performance in several studies [71, 72]. In addition simulators can be used very early in medical training, since they do not put patients at risk and have a higher availability.

Industrial Design In industrial design applications, virtual environments are used to simulate assembly operations and subjective evaluation of prototypes. Although there are much less applications than in medical training, this area pushes technology development: Some requirements can only be met with new concepts such as admittance systems and form displays. One of these is the *Haptic Strip*, that consists of a bend- and twistable surface that can be additionally positioned in 6 DoF in space [73]. It is shown in Fig. 1.14 and can be used to display large-scale forms of new designs without having to manufacture a prototype.

Multimodal Information Displays Since the haptic sense was developed to analyze objects and the environment, similar application with a high demand of intuitive access to information can be found in literature. Haptic systems are used to display large amount of information in biology and chemistry [74, Chap. 9] and are also used as means for the synthesis of complex molecules [75]. For this application, the human ability to detect patterns (in visual representations) is used for a coarse positioning of synthesis partners, whereas micro positioning is supported by haptic representation of the intermolecular forces.

Another example for multimodal display of information was recently presented by *Microsoft Research* [76]. The TouchMover is an actuated screen with haptic

Fig. 1.13 Laparoscopic simulator LAP MENTOR III The system was designed to simulate interventions in the abdomen. Picture courtesy of *Simbionix USA*, Cleveland, OH, USA., used with permission

feedback that can be used to display object and material properties or to intuitively access volumetric data like for example ↪ MRI scans. Figure 1.15 shows this application of the system. Annotations are marked visually and haptically with a detent, allowing for intuitive access and collaboration.

Consumer Electronics For the integration of haptic feedback in computer games, *Novint Technologies, Int.* presented the FALCON haptic interface in 2006. It is based on a delta parallel kinematic structure and distinguishes itself through a very competitive price tag at around 500$. This device is also used in several research projects like for example [77], because of the low price and the support in several ↪ application programming interface (API). Looking from the 202xth perspective, complex haptic enhanced input devices did not perform well in consumer electronics. The main area where they still persists are in gamepad or game-controller-applications but reduced to a function of pure *vibrotactile* feedback, *Sony*'s DUAL-SENSE TECHNOLOGY recently again increased the complexity and combined a vibration actuator with a motor-actuated and adaptable trigger. The future will show whether this is a revival of kinaesthetic feedback in consumer electronics.

But there are other areas. To provide a more intense gaming experience, haptic systems conveying low-frequency acoustic signals BUTT KICKER by *The Guitammer Company* exist (Fig. 1.16). The system delivers low-frequency signals increasing the immersion. To allow for the touch of fabric over the internet, the HAPTEX project developed rendering algorithms as well as interface hardware [78].

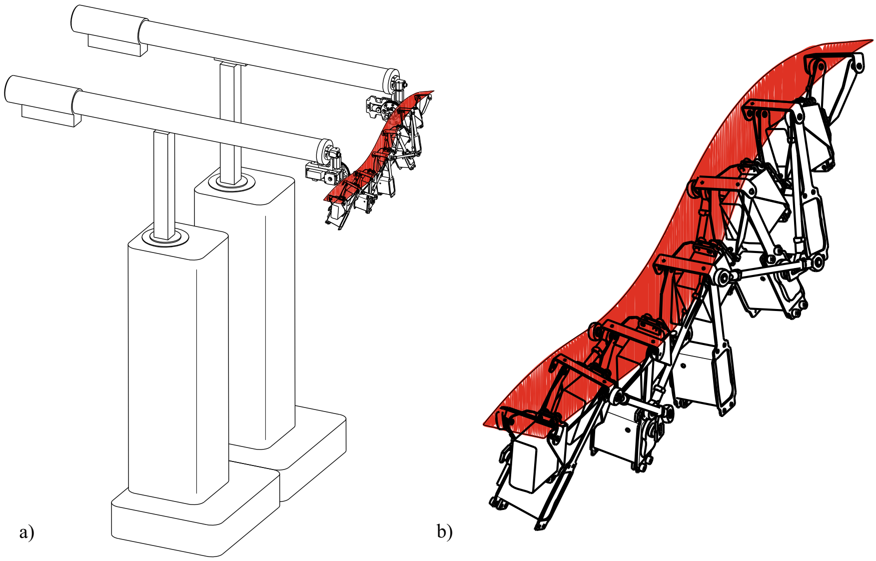

Fig. 1.14 The Haptic Strip system. The strip is mounted on two HAPTICMASTER admittance type interfaces. Capacitive sensors on the strip surface sense the user's touch. Figure is based on [73] © Springer Nature, all rights reserved

Fig. 1.15 TOUCHMOVER with user exploring MRI data. Picture courtesy of *Microsoft Research*, Redmond, WA, USA., used with permission

Compared to the design of TPTA-Systems the development of haptic interfaces for interactions with virtual environments seems to be slightly less complex, since more knowledge about the interaction environment is present in the design process. However, new aspects like derivation and allocation of the environment data arise with this applications. Because of the wider spread of such systems, cost efficiency has to be taken into account.

Fig. 1.16 Electrodynamic actuator BUTTKICKER for generating low-frequency oscillations on a gaming seat, ©2022 *The Guitammer Company*, used with permission

1.5.3 Non-invasive Medical Applications

Based on specific values of haptic perception diagnosis of certain illnesses and dysfunctions can be made. Certain types of eating disorders [79, 80] and diabetic neuropathy [38] are accompanied with diminished haptic perception capabilities. They can therefore be diagnosed with a measurement of perception or motor exertion parameters and comparison with the population mean. Next to diagnosis, haptic perception parameters can be used as a progress indicator in stroke [81] and limb [82] rehabilitation, too.

For these purposes cost-efficient systems with robust and efficient measurement protocols are needed. Because feedback from the user can be received with any means, development is easier than the development of TPTA- or VR-systems. These systems are foci of several research groups, up till now there is no system for comprehensive use in the market.

1.5.4 Communication

The fourth and by numbers largest application area of haptic systems is basic communications. The most prominent example is probably on your desk or in your pocket—the vibration function of your phone. Compared to communication based on visual and acoustic signals, haptics give the opportunity to convey information in a discrete way and offer the possibility of a spatial resolution. Communication via the haptic sense tends to be very intuitive, since feedback arises at the point the user is interacting with. A simple example is a switch, that will give a haptic feedback when pressed.

Therefore, haptics are an attractive communication channel in demanding environments, for example when driving a car. Several studies show that haptic communication tends to distract users less from critical operations than the use of other channels like vision or audition [83, 84]. Applications include assistive systems for navigation in military applications [85], a practical example for an adaptive haptic user interface for automotive use is given in Sect. 14.1. With the increasing number of steer-by-wire applications and the vision of autonomous driving vehicles, the haptic channel is identified as a possibility to raise awareness of the driver in possibly dangerous situations as investigated in [86].

More recently, the increasing use of consumer electronics with touch screens triggers a demand for technologies to add haptic feedback. It is intended to facilitate the use without recurring visual status inspection. Solutions for this applications include the usage of quite a lot different actuation principles, which will be the focus of Chap. 9.

Another application area are tactile interfaces for the blind and visual impaired [87, 88]. Despite displaying Braille characters, tactile interfaces offer navigation support (see for example the HAPTIMAP project providing toolkits for standard mobile terminals [89] or the tactile YOU-ARE-HERE-MAPS or interactions with graphic interfaces [90, 91]. Newer studies show even advantages on finger-rehabilitation for stroke-patients by vibrotactile actuation [92]. Figure 1.17 gives some examples of haptic systems used for communication applications.

Another type of haptic interface is the shape-changing interface. This interface type creates the information communication by altering its form. A usage of this haptic interface is navigation assistance by changing the shape and guiding the user to reach a point Fig. 1.18. This change is felt via the fingers of visually or hearing impaired, deafblind, and sighted pedestrians.

This shape-changing device is developed to implement the navigation guidance via a bi-directional expanding mechanism. It uses two similar parts to move away from the device central section. This shape change generates a sensation of variable volume. Inside of the system, one motor can be used for providing the rotational movement, and a rack and pinion can provide the translational movement. The top and bottom faces are designed to make the device easy to rest on the palm without pinching the user's skin.

Despite the analysis of energy-efficient actuation principles for mobile usage, scientific research in this area addresses the design of haptic icons for information transfer. Sometimes also called *tactons*, *hapticons* or *tactile icons*, the influence of rhythm, signal form, frequency and localization are investigated [94, 95]. Up till now, information transfer rates of 2 ... 12 bit per second were reported [96, 97], although the latter require a special haptic interface called the TACTUATOR designed for communication applications [98]. The exact bandwidth is still unclear yet. One application related study from SEO AND CHOI [99] reported 3.7 bits.

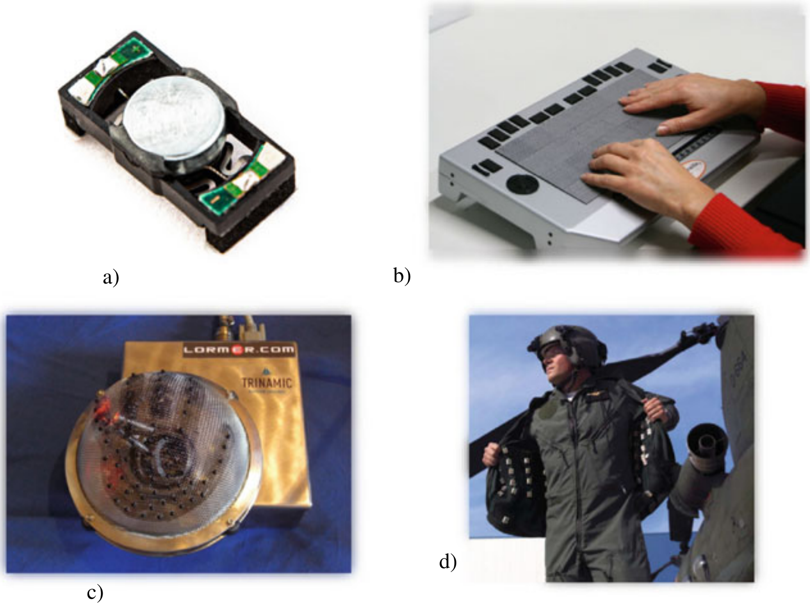

Fig. 1.17 Components and systems for communication via the haptic sense. **a** Exciter for touchpads and mobile devices—*Grewus* Exciter EXR4403L-01A). **b** HYPERBRAILLE-system for displaying graphic information for visual impaired users, image courtesy of *metec AG*, Stuttgart, Germany. **c** LORMER-system as machine-human-interface conveying text information using the lorm-alphabet on palm and hand of the user, image courtesy of THOMAS RUPP. **d** TACTILE TORSO DISPLAY, vest for displaying flight information on the pilots torso, image courtesy of *TNO*, Soesterberg, The Netherlands. All images used with permission

1.5.5 Completing the Picture

For completeness, also passive systems like a computer keyboard, trackballs and mice are part of this application area, since they will convey information given in form of a motion control operation to a (computer) system. Although there exists some kind of haptic feedback, it is not dependent on the interaction, but solely on the physical characteristics of the haptic system like inertia, damping or friction.

Another area inspired by haptic research and sometimes even used in haptic telepresence and telemanipulation scenarios is the area of robotic hands or limbs equipped with perception-inspired sensors. The whole area of tactile sensors was and is part of haptic research and referred to in chapter Chap. 10. Its main and fascinating application domain however is the area of robotics, especially when it comes to bionic-inspired systems [100]. A preliminary summit is reached by the micromechanical design of a fully dexterous robotic hand in combination with high-end combined capacitive pressure sensors (Fig. 1.19). But there is more to come, and not even limited to humanoid shapes.

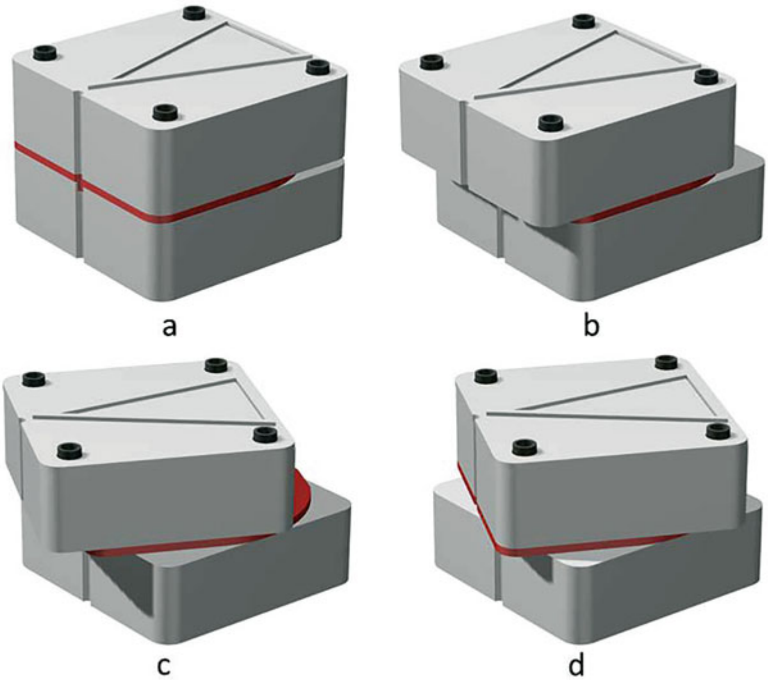

Fig. 1.18 Different shapes of the haptic interface for sending different commands [93], figures by AD SPIERS, used with permission

Fig. 1.19 Fully actuated robotic hand *Shadow Dexterous Hand* by *Shadow Robot Company* with integrated BIOTACS by *SynTouch* allowing manipulation with direct contact force- and direction measurement for each fingertip ©2022 *Shadow Robot Company*, used with permission

1.5.6 Why Use a Haptic System?

The reasons one might want to use a haptic system are quite numerous: Perhaps you want to improve the task performance or lower the error rate in a manipulation scenario, address a previously unused sensory channel to convey additional information or gain advantages over a competitor in an innovation driven market. This book will not answer the question if haptics is able to fulfil the wishes and intentions connected to this reasons, but will focus on the design of a specific haptic system for the intended application.

Although there are many guidelines on how to implement haptic and multimodal feedback for optimal task performance (they will be addressed in Sect. 5.1.2), there are only limited sources on how to decide whether a haptic feedback is usable for an application. ACKER provides some criteria for telepresence technologies in industrial applications [51], JONES gives guidelines on the usage of tactile systems [101].

1.6 Conclusions

Technical systems addressing the haptic sense cover a wide range of applications. Since this book focuses on the design process of task specific haptic interfaces, the following chapters will first focus on the deeper analysis of haptic interaction in Chap. 2 and the role of the user in a haptic system in Chap. 3, before a detailed analysis of the development and the structure of haptic systems is presented in Chaps. 4 and 6. This provides the basis for the second part of the book, that will deal with the actual design of a task-specific haptic system.

Recommended Background Reading

[102] Papetti, S. & Saitis, C.: **Musical Haptics**. Springer Nature, 2018
Inspirational between art and technology on haptics relevance for instruments.

[23] Carbon, C.-C. & Jakesch, M.: **A model for haptic aesthetic processing and its implications for design**. Proceedings of the IEEE, 101(9), pp. 2123–2133, 2013.
General model about the development of haptic aesthetics and the implications for the design of products.

[4] Grunwald, M.: **Human Haptic Perception: Basics and Applications**. Birkhäuser, Basel, CH, 2008.
General collection about the haptic sense with chapters about theory and history of haptics, neuro-physiological basics and psychological aspects of haptics.

References

1. Crusco AH, Wetzel CG (1984) The midas touch: the effects of interpersonal touch on restaurant tipping. Person Soc Psychol Bull 10(4):512–517. https://doi.org/10.1177/0146167284104003
2. Adams RJ (1999) Stable haptic interaction with virtual environments. PhD thesis. University of Washington, Washington
3. Wolf U (2007) Aristoteles' Nikomachische Ethik. Wiss, Buchges, Darmstadt. ISBN: 978-3-534-20824-13-534-20824-2
4. Grunwald M (2008) Human haptic perception: basics and applications. Birkhäuser. ISBN: 3764376112
5. Kant I (1983) Anthropologie in pragmatischer Hinsicht. Philosophische anthropologie; Charakter. Stuttgart: Reclam, p 389. ISBN: 3-15-007541-6
6. Gerling G, Thomas G (2005) The effect of fingertip microstructures on tactile edge perception. In: First joint eurohaptics conference and symposium on haptic interfaces for virtual environment and teleoperator systems, 2005. WHC 2005, pp 63–72. https://doi.org/10.1109/WHC.2005.129
7. Vasarhelyi G et al (2006) Effects of the elastic cover on tactile sensor arrays. Sens Actuat A Phys 132(1):245–251. https://doi.org/10.1016/j.sna.2006.01.009
8. Fiene J, Kuchenbecker KJ, Niemeyer G (2006) Event-based haptic tapping with grip force compensation. In: IEEE symposium on haptic interfaces for virtual environment and teleoperator systems. https://doi.org/10.1109/HAPTIC.2006.1627063
9. Getzinger G (2006) Haptik - Rekonstruktion eines Verlustes. Naturerkenntnis; Hautsinn. Profil, Wien, p 146. ISBN: 3-89019-521-0
10. Néret G (1998) Erotik in der Kunst des 20. Jahrhunderts. Erotik Motiv; Kunst; Geschichte 1900- 199213.1c. Tokyo: Taschen, p 200. ISBN: 3-8228-7853-7
11. Teyssier M et al, MobiLimb: augmenting mobile devices with a robotic limb. In: Proceedings of the 31st annual ACM symposium on user interface software and technology, vol 18. https://doi.org/10.1145/3242587. https://doi.org/10.1145/3242587.3242626
12. Wilde E et al (2013) Technisch vermitteltes soziales Handeln im Alter-ein Gestaltungsprozess. In: Lebensqualität im Wandel von Demografie und Technik (2013). https://doi.org/10.1007/s10278-011-9416-8
13. Sato M, Poupyrev I, Harrison C (2012) Touché: enhancing touch interaction on humans, screens, liquids, and everyday objects. In: Proceedings of the 2012 ACM annual conference on human factors in computing systems, pp 483–492. https://doi.org/10.1145/2207676.2207743
14. Anuguelov N (2009) Haptische und akustische Kenngrößen zur Objektivierung und Optimierung derWertanmutung von Schaltern und Bedienfeldern für den KFZ-Innenraum. Technische Dissertation Universität Dresden. http://d-nb.info/1007551739/
15. Reisinger J (2009) Parametrisierung der Haptik von handbetätigten Stellteilen. Dissertation. Technische Universität München. https://mediatum.ub.tum.de/doc/654165/654165.pdf
16. Battenberg Robotic GmbH & KG Co (2007) Wahrnehmungen messbar machen. Company Information. http://messrobotic.de/fileadmin/pdf/Produkte-MessroboticStandard-Wahrnehmungen.pdf
17. Gaspar J et al (2019) Push button design requirements and relations to button architecture elements. Int J Indust Ergonom 70:92–106. ISSN: 0169-8141. https://doi.org/10.1016/J.ERGON.2019.01.001
18. Jagodzinski R, Wintergerst G (2009) A toolkit for developing haptic interfaces - control dial based on electromagnetic brake. In: UIST. Victoria. http://www.acm.org/uist/archive/adjunct/2009/pdf/demos/paper184.pdf
19. Israr A et al (2019) Stereohaptics toolkit for dynamic tactile experiences. In: Lecture notes in computer science (including subseries lecture notes in artificial intelligence and lecture notes

in bioinformatics). LNCS, vol 11786, pp 217–232. ISSN: 16113349. https://doi.org/10.1007/978-3-030-30033-3_17. https://link.springer.com/chapter/10.1007/978-3-030-30033-3
20. Rösler F, Battenberg G, Schüttler F (2009) Subjektive Empfindungen und objektive Charakteristika von Bedienelementen. Automobiltechnische Zeitschrift 4:292–297. https://doi.org/10.1007/BF03222068
21. Okamoto S, Nagano H, Yamada Y (2013) Psychophysical dimensions of tactile perception of textures. IEEE Trans Hapt 6(1):81–93. ISSN: 19391412. https://doi.org/10.1109/TOH.2012.32
22. Culbertson H, Kuchenbecker KJ (2017) Importance of matching physical friction, hardness, and texture in creating realistic haptic virtual surfaces. IEEE Trans Hapt 10(1):63–74. ISSN: 19391412. https://doi.org/10.1109/TOH.2016.2598751
23. Carbon C-C, Jakesch M (2013) A model for haptic aesthetic processing and its implications for design. In: Proc IEEE 101(9):2123–2133. https://doi.org/10.1109/JPROC.2012.2219831
24. Breitschaft SJ, Carbon CC (2021) Function follows form: using the aesthetic association principle to enhance haptic interface design. In: Frontiers in psychology, vol 12, p 2619. ISSN: 16641078. https://doi.org/10.3389/FPSYG.2021.646986/BIBTEX
25. Jandura L, Srinivasan M (1994) Experiments on human performance in torque discrimination and control. In: Dynamic systems and control, ASME, DSC-55, vol 1, pp 369–375. http://www.rle.mit.edu/touchlab/publications/1994_002.pdf
26. Kirkpatrick A, Douglas S (2002) Application-based evaluation of haptic interfaces. In: 10th symposium on haptic interfaces for virtual environment and teleoperator systems. Orlando, pp 32–39. https://doi.org/10.1109/HAPTIC.2002.998938
27. Gall S, Beins B, Feldman J (2001) Psychophysics. In: The gale encyclopedia of psychology. Gale. ISBN: 978-0787603724
28. Stevens SS (1975) Psychophysics. Stevens G (ed). Transaction Books, Piscataway. ISBN: 978-0887386435
29. Bowman D, Hodges L (1999) Formalizing the design, evaluation, and application of interaction techniques for immersive virtual environments. J Vis Lang Comput 10(1):37–53. https://doi.org/10.1006/jvlc.1998.0111
30. ISO 9241: Ergonomics of Human System Interaction - Part 910: Framework for tactile and haptic interaction. ISO, 2011
31. Samur E (2012) Performance metrics for haptic interfaces. Springer. ISBN: 978-1447142249. https://doi.org/10.1007/978-1-4471-4225-6
32. Lederman SJ, Klatzky RL (2009) Haptic perception: a tutorial. In: Attent Percept Psychophys 71(7):1439. https://doi.org/10.3758/APP.71.7.1439
33. Hollins M (2002) Touch and haptics. In: Pashler H (ed) Steven's handbook of experimental psychology. Wiley, New York, pp 585–618. ISBN: 978-0471377771. https://doi.org/10.1002/0471214426.pas0114
34. Kruger L, Friedman MP, Carterette EC (eds) (1996) Pain and touch. Academic Press, Maryland Heights. ISBN: 978-0123992390
35. Darian-Smith I, Johnson K (1977) Thermal sensibility and thermoreceptors. J Investigat Dermatol 69(1):146–153. https://doi.org/10.1111/1523-1747.ep12497936
36. Jones L, Berris M (2002) The psychophysics of temperature perception and thermal interface design. In: 10th symposium on haptic interfaces for virtual environments and teleoperator systems. Orlando. https://doi.org/10.1109/HAPTIC.2002.998951
37. Ino S et al (1993) A tactile display for presenting quality of materials by changing the temperature of skin surface. In: IEEE international workshop on robot and human communication. https://doi.org/10.1109/ROMAN.1993.367718
38. Norrsell U et al (2001) Tactile directional sensibility and diabetic neuropathy. Muscle Nerve 24(11):1496–1502. https://doi.org/10.1002/mus.1174
39. Sato K, Maeno T (2012) Presentation of sudden temperature change using spatially divided warm and cool stimuli. In: Haptics: perception, devices, mobility, and communication. Springer, pp 457–468. https://doi.org/10.1007/978-3-642-31401-8_41

40. Clark F, Horch K (1986) Kinesthesia. In: Handbook of perception and human performance, Boff KR, Kaufman L, Thomas JP (eds). Wiley-Interscience, New York, pp 13.1–13.61. ISBN: 978-0471829577
41. Loomis JM, Lederman SJ (1986) Tactual perception. In: Handbook of perception and human performances vol 2, p. 2
42. Goertz REA (1964) Manipulator systems development at ANL. In: Proceedings of the 12th conference on remote systems technology, ANS, pp 117–136
43. Gault RH (1927) On the upper limit of vibrational frequency that can be recognized by touch. Sci New Ser 65(1686):403–404. https://doi.org/10.1126/science.65.1686.403
44. Shimoga K (1993) A survey of perceptual feedback issues in dexterous telemanipulation part II. Finger touch feedback. In: Proceedings of the IEEE virtual reality annual international symposium. Seattle, pp 271–279. https://doi.org/10.1109/VRAIS.1993.380769
45. Verrillo RT, Gescheider GA (1992) Perception via the sense of touch. In: Summers IR (ed) Tactile aids for the hearing impaired. Whurr, London, pp 1–36. ISBN: 978-1-870332-17-0
46. Brooks TL (1990) Telerobotic response requirements. In: IEEE international conference on systems, man and cybernetics. Los Angeles. https://doi.org/10.1109/ICSMC.1990.142071
47. Shimoga K (1993) A survey of perceptual feedback issues in dexterous telemanipulation part I. Finger force feedback. In: Proceedings of the IEEE virtual reality annual international symposium. Seattle, pp 263–270. https://doi.org/10.1109/VRAIS.1993.380770
48. Daniel R, McAree P (1998) Fundamental limits of performance for force reflecting teleoperation. Int J Robot Res 17(8):811–830. https://doi.org/10.1177/027836499801700801
49. Hogan N (1989) Controlling impedance at the man/machine interface. In: IEEE international conference on robotics and automation (ICRA). Scottsdale, pp 1626–1631. https://doi.org/10.1109/ROBOT.1989.100210
50. Dennerlein J, Millman P, Howe R (1997) Vibrotactile feedback for industrial telemanipulators. In: Sixth annual symposium on haptic interfaces for virtual environment and teleoperator systems. http://biorobotics.harvard.edu/pubs/1997/vibrotactile.pdf
51. Acker A (2011) Anwendungspotential von Telepräsenz-und Teleaktionssystemen für die Präzisionsmontage. Dissertation. Technische Universität München. http://mediatum.ub.tum.de/doc/1007163/1007163.pdf
52. Estevez P et al (2010) A haptic tele-operated system for microassembly. In: Ratchev S (ed) Precision assembly technologies and systems. Springer, Heidelberg, pp 13–20. https://doi.org/10.1007/978-3-642-11598-1_2
53. Vander Poorten EEB, Demeester E, Lammertse P (2012) Haptic feedback for medical applications, a survey. In: Actuator conference. Bremen. https://www.radhar.eu/publications/e.-vander-poorten-actuator12-haptic-feedback-for-medical-applications-a-survey
54. Westebring-van der Putten EP et al (2008) Haptics in minimally invasive surgery - a review. Minim Invas Therapy Allied Technol 17(1):3–16. https://doi.org/10.1080/13645700701820242
55. Nitsch V, Färber B (2012) A meta-analysis of the effects of haptic interfaces on task performance with teleoperation systems. IEEE Trans Hapt 6:387–398. https://doi.org/10.1109/ToH.2012.62
56. Wagner C, Stylopoulos N, Howe R (2002) The role of force feedback in surgery: analysis of blunt dissection. In: 10th symposium on haptic interfaces for virtual environment and teleoperator systems, vol 2002. https://doi.org/10.1109/HAPTIC.2002.998943
57. Antonakoglou K et al (2018) Toward haptic communications over the 5g tactile internet. In: IEEE Commun Surv Tutor 20.4 (Oct. 2018):3034–3039. ISSN:1553877X. https://doi.org/10.1109/COMST.2018.2851452
58. Young SN, Peschel JM (2020) Review of human-machine interfaces for small unmanned systems with robotic manipulators. In: IEEE Trans Human-Mach Syst 50(2):131–143. ISSN: 21682305. https://doi.org/10.1109/THMS.2020.2969380
59. Sutherland GR et al (2013) The evolution of neuroArm. Neurosurgery 72:A27–A32. https://doi.org/10.1227/NEU.0b013e318270da19

60. Röse A (2011) Parallelkinematische Mechanismen zum intrakoporalen Einsatz in der laparoskopischen Chirurgie. Dissertation. Technische Universität Darmstadt. http://tuprints.ulb.tu-darmstadt.de/2493/1/Dissertation_Roese_Druckversion.pdf
61. Schlaak HF et al (2008) A novel laparoscopic instrument with multiple degrees of freedom and intuitive control. In: Antwerpen B (ed) 4th European conference of the international federation for medical and biological engineering. https://doi.org/10.1007/978-3-540-89208-3_394
62. Rausch J (2012) Entwicklung und Anwendung miniaturisierter piezoresistiver Dehnungsmesselemente. Dissertation. Technische Universität Darmstadt. http://tuprints.ulb.tudarmstadt.de/3003/1/Dissertation-Rausch-online.pdf
63. Kassner S (2013) Haptische Mensch-Maschine-Schnittstelle für ein laparoskopisches Chirurgie-system. Dissertation. Technische Universität Darmstadt. http://tubiblio.ulb.tudarmstadt.de/63334/
64. King C-H et al (2009) Tactile feedback induces reduced grasping force in robot-assisted surgery. In: IEEE Trans Hapt 2(2):103–110. https://doi.org/10.1109/TOH.2009.4
65. Bauernschmitt R et al (2005) Towards robotic heart surgery: introduction of autonomous procedures into an experimental surgical telemanipulator system. Int J Medica Robot Comput Assist Surg 1(3):74–79. https://doi.org/10.1002/rcs.3010.1002/rcs.30
66. Pott P, Scharf H, Schwarz M (2005) Today's state of the art in surgical robotics. Comput Aided Surg 10(2):101–132. https://doi.org/10.1080/10929080500228753
67. Pott P, Schwarz M (2010) State of the art of medical robotics - areas of application. In: 44. Jahrestagung der DGBMT
68. Guthart G, Salisbury J Jr (2000) The intuitive telesurgery system: overview and application. In: IEEE international conference on robotics and automation (ICRA), vol 1. San Francisco, pp 618–621. https://doi.org/10.1109/ROBOT.2000.844121
69. Coles TR, Meglan D, John NW (2010) The role of haptics in medical training simulators: a survey of the state-of-the-art. IEEE Trans Hapt 4:51–66. https://doi.org/10.1109/TOH.2010.19
70. Riener R et al (2002) Orthopädischer Trainingssimulator mit haptischem Feedback. Automatisierungstechnik 50:296–301. https://doi.org/10.1524/auto.2002.50.6.296
71. Ahlberg G et al (2007) Proficiency-based virtual reality training significantly reduces the error rate for residents during their first 10 laparoscopic cholecystectomies. Am J Surg 193(6):797–804. https://doi.org/10.1016/j.amjsurg.2006.06.050
72. Bajka M et al (2009) Evaluation of a new virtual-reality training simulator for hysteroscopy. Surg Endosc 23(9):2026–2033. https://doi.org/10.1007/s00464-008-9927-7
73. Bordegoni M et al (2010) A force and touch sensitive self-deformable haptic strip for exploration and deformation of digital surfaces. In: Kappers AML, Bergmann-Tiest WM, van der Helm CT (eds) Haptics: generating and perceiving tangible sensations. LNCS, vol 6192. Proceedings of the eurohaptics conference, Amsterdam. Springer, Heidelberg, pp 65–72. https://doi.org/10.1007/978-3-642-14075-4_10
74. Burdea GC, Coiffet P (2003) Virtual reality Ed technology, Burdea GC, Coiffet P (eds). Wiley-Interscience, New York. ISBN: 978-0471360896
75. Brooks FP et al (1990) Project GROPE - haptic displays for scientific visualization. ACM SIGGRAPH Comput Graph 24:177–185. https://doi.org/10.1145/97880.97899
76. Sinclair M, Pahud M, Benko H 2013() TouchMover: actuated 3D touchscreen with haptic feedback. In: Proceedings of the 2013 ACM international conference on Interactive tabletops and surfaces. ACM, pp 287–296. https://doi.org/10.1145/2512349.2512805
77. Shah A et al (2010) How to build an inexpensive 5-DOF haptic device using two novint falcons. In: Kappers AML, Bergmann-Tiest WM, van der Helm FC (eds) Haptics: generating and perceiving tangible sensations, LNCS, vol 6191. Proceedings of the Eurohaptics conference, Amsterdam. Springer, Heidelberg, pp 136–143. https://doi.org/10.1007/978-3-642-14064-8_21
78. Haptex. Grant No. IST-6549, last visited 07.03.2012. European Union (2007). http://haptex.miralab.unige.ch/

79. Grunwald M et al (2001) Haptic perception in anorexia nervosa before and after weight gain. J Clin Exper Neuropsychol 23(4):520–529. https://doi.org/10.1076/jcen.23.4.520.1229
80. Grunwald M (2008) Haptic perception in anorexia nervosa. In: Grünwald M (ed) Human haptic perception: basics and applications. Birkhäuser, Basel. ISBN: 3764376112
81. Allin S, Matsuoka Y, Klatzky R (2002) Measuring just noticeable differences for haptic force feedback: implications for rehabilitation. In: Proceedings of the 10th symposium on haptic interfaces for virtual environments and teleoperator systems, Orlando. https://doi.org/10.1109/HAPTIC.2002.998972
82. Yang X et al (2007) Hand tele-rehabilitation in haptic virtual environment. In: Sanya C (ed) IEEE international conference on robotics and biomimetics (ROBIO), pp 145–149. https://doi.org/10.1109/ROBIO.2007.4522150
83. Ryu J et al (2010) Vibrotactile feedback for information delivery in the vehicle. In: IEEE Trans Hapt 3(2):138–149. https://doi.org/10.1109/TOH.2010.1
84. Spence C, Ho C (2008) Tactile and multisensory spatial warning signals for drivers. IEEE Trans Hapt 1:121–129. https://doi.org/10.1109/TOH.2008.14
85. Gilson R, Redden E, Elliott L (2007) Remote tactile displays for future soldiers. Technical report. U.S. Army Research Laboratory, Aberdeen Proving Ground. http://www.dtic.mil/cgi-bin/GetTRDoc?Location=U2&doc=GetTRDoc.pdf&AD=ADA468473
86. Liedecke C, Baumann G, Reuss H-C (2014) Potential of the foot as a haptic interface for future communication and vehicle controlling. In: 10th ITS European congress. Helsinki, FIN
87. Johansson G (2008) Haptics as a substitute for vision. In: Hersh MA, Johnson MA (eds) Assistive technology for visually impaired and blind people. Springer, Heidelberg, pp 135–166. ISBN: 978-1846288661
88. Summers I (ed) (1996) Tactile aids for the hearing impaired. Whurr, London, pp 978–1870332170
89. HaptiMap - haptic, audio and visual interfaces for maps and location based services. European Union Grant No. FP7-ICT-224675. www.haptimap.org
90. Asque C, Day A, Laycock S (2012) Cursor navigation using haptics for motion-impaired computer users. In: Haptics: perception, devices, mobility, and communication. Springer, Heidelberg, pp 13–24. https://doi.org/10.1007/978-3-642-31401-8_2
91. Prescher D, Weber G, Spindler M (2010) A tactile windowing system for blind users. In: Proceedings of the 12th international ACM SIGACCESS conference on computers and accessibility. ACM, Orlando, pp 91–98. https://doi.org/10.1145/1878803.1878821
92. Seim CE, Wolf SL, Starner TE (2021) Wearable vibrotactile stimulation for upper extremity rehabilitation in chronic stroke: clinical feasibility trial using the VTS Glove. J Neuro Eng Rehabilit 18(1):1–11. ISSN: 17430003. https://doi.org/10.1186/S12984-021-00813-7/FIGURES/6. arXiv:2007.09262. https://jneuroengrehab.biomedcentral.com/articles/10.1186/s12984-021-00813-7
93. Spiers AJ, Dollar AM (2016) Design and evaluation of shape-changing haptic interfaces for pedestrian navigation assistance. In: IEEE Trans Hapt 10(1):17–28
94. Brown L, Brewster S, Purchase H (2006) Multidimensional tactons for non-visual information presentation in mobile devices. In: Conference on human-computer interaction with mobile devices and services, pp 231–238. https://doi.org/10.1145/1152215.1152265
95. Enriquez M, MacLean K, Chita C (2006) Haptic phonemes: basic building blocks of haptic communication. In: Proceedings of the 8th international conference on multimodal interfaces (ICMI). ACM, Banff, pp 302–309. https://doi.org/10.1145/1180995.1181053
96. Cholewiak SA, Tan HZ, Ebert DS (2008) Haptic identification of stiffnes and force magnitude. In: Symposium on haptic interfaces for virtual environments and teleoperator systems. Reno. https://doi.org/10.1109/HAPTICS.2008.4479918
97. Tan H et al (2003) Temporal masking of multidimensional tactual stimuli. J Acoust Soc Am 116(9), Part 1:3295–3308. https://doi.org/10.1121/1.1623788
98. Tan H, Rabinowitz W (1996) A new multi-finger tactual display. J Acoust Soc Am 99(4):2477–2500. https://doi.org/10.1121/1.415560

99. Seo J, Choi S (2015) Edge flows: improving information transmission in mobile devices using two-dimensional vibrotactile flows. In: IEEE world haptics conference, WHC 2015, pp 25–30. https://doi.org/10.1109/WHC.2015.7177686
100. Bianchi M, Moscatelli A (2016) Human and robot hands. In: Springer series on touch and haptic systems. https://doi.org/10.1007/978-3-319-26706-7
101. Jones LA, Sarter NB (2008) Tactile displays: guidance for their design and application. In: Human factors 50(1):90–111. ISSN: 00187208. https://doi.org/10.1518/001872008X250638. https://journals.sagepub.com/doi/abs/10.1518/001872008x250638
102. Papetti S, Saitis C (2018) Musical haptics. In: Papetti S, Saitis C (eds) Springer series on touch and haptic systems. https://doi.org/10.1007/978-3-319-58316-7. http://link.springer.com/10.1007/978-3-319-58316-7

Chapter 2
Haptics as an Interaction Modality

Christian Hatzfeld and Thorsten A. Kern

Abstract This chapter focuses on the biological and behavioural basics of the haptic modality. On the one side, several concepts for describing interaction are presented in Sect. 2.2, on the other side, the physiological and psychophysical basis of haptic perception is discussed in Sect. 2.1. The goal of this chapter is to provide a common basis to describe interactions and to convey a basic understanding of perception and the description by psychophysical parameters. Both aspects are relevant for the formal description of the purpose of a haptic system and the derivation of requirements, further explained in Chap. 5. Several conclusions arising from the description of perception and interaction are given in Sect. 2.4.

2.1 Haptic Perception

This section will give a short summary of relevant topics from the scientific disciplines dealing with haptic perception. It is intended to reflect the current state of the art in a necessary extend for an engineer designing a haptic system. Physiologists and psychophysicists are therefore asked to forgive simplifications and impreciseness. For all engineers, Fig. 2.1 gives a general block diagram of haptic perception that forms a conscious ↪ percept from a ↪ stimulus.

Analysing each block of this diagram, the mechanical properties of the skin as stimulus' transmitting apparatus are dealt with in Chap. 3. Section 2.1.1 will deal with the characteristics of mechanoreceptors in skin and locomotion system, while

Christian Hatzfeld deceased before the publication of this book.

C. Hatzfeld (✉)
Technische Universität Darmstadt, Darmstadt, Germany

T. A. Kern (✉)
Hamburg University of Technology, Eißendorfer Str. 38, 21073 Hamburg, Germany
e-mail: t.a.kern@tuhh.de

T. A. Kern et al. (eds.), *Engineering Haptic Devices*, Springer Series on Touch and Haptic Systems, https://doi.org/10.1007/978-3-031-04536-3_2

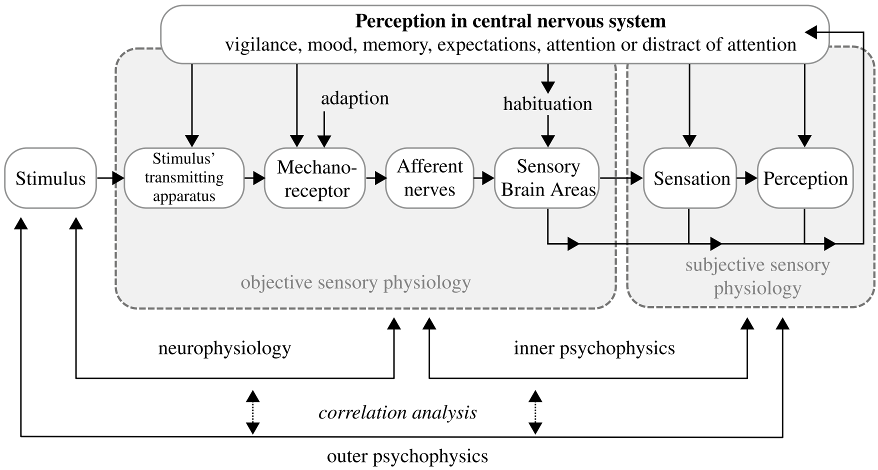

Fig. 2.1 Block diagram of haptic perception and the corresponding scientific areas investigating the relationships between single parts as defined in [1, 2]

Sect. 2.1.2 will introduce the psychophysical methods that are used to evaluate this characteristics. In Sects. 2.1.3 and 2.1.4 thresholds and super-threshold parameters of human haptic perception are presented.

2.1.1 Physiological Basis

This section deals with the physiological properties of the tactile and kinaesthetic receptors as defined in the previous chapter (Sect. 1.4.2). We will not cover neural activity in detail, but only look at a general model that is useful for a closer look on multimodal systems.

2.1.1.1 Tactile Receptors and Their Functions

From a histological view, there are four different sensory cell types in glabrous skin and two additional sensory cell types in hairy skin as well. They are located in the top 2 mm of the skin as shown in Fig. 2.2. The sensory cells in glabrous skin are named after their discoverers, while the additional cells in hairy skin have functional names [3]. Because of the complex mechanical transmission properties of the skin and other body parts like vessels and bone, compression and shear forces in the skin and—for high frequency stimuli—surface waves are expected in the skin as a reaction to external mechanical stimuli. These lead to various pressure and tension distributions in the skin, that are detected differently by the individual sensory cells. In general, sensory cells near the skin surface will react only to adjacently applied stimuli, while

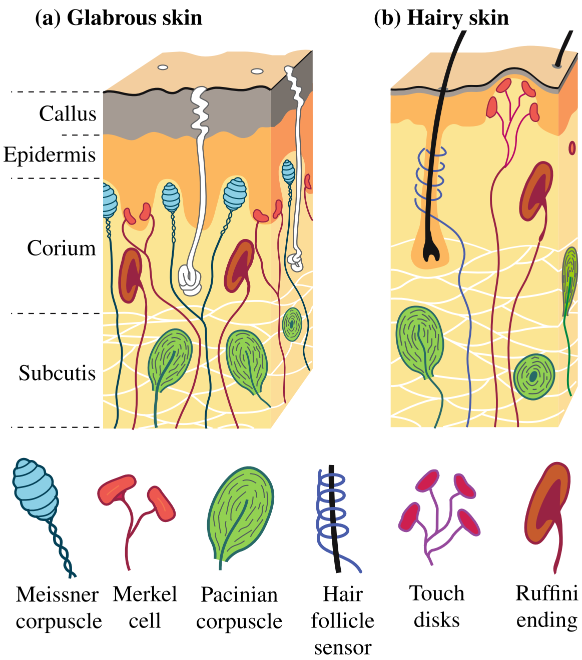

Fig. 2.2 Histology of tactile receptors in **a** glabrous and **b** hairy skin. Figure adapted from [4] © Springer Nature, all rights reserved

cells localized more deeply like the Ruffini endings and Pacinian corpuscles will react also to stimuli applied farther away. These differences are presented in the following for the well-researched receptors in glabrous skin. For hairy skin, less information is available. While tactile disks are assumed to exhibit similar properties as Merkel cells because of the same histology of the receptor, hair follicle receptors are attributed to detect movements on the skin surface. The following sections will concentrate on tactile receptor cells in glabrous skin because of the higher technical relevance of these areas.

To investigate the behavior of a individual sensory cell, a single nerve fiber is contacted with an electrode and electrical impulses in the fiber are recorded as shown in Fig. 2.3 [5]. The results of the following paragraphs are based on such measurements, that are very complicated to conduct on a living organism or a human test person.

From Sensory Cells to Mechanoreceptors and Channels

When reviewing literature about the physiology of haptic perception, several terms are used seemingly interchangeable with each other. Since microneurography often does not allow a distinct mapping of a sensory cell to the contacted nerve fiber, a formal separation between a single sensory cell as given in Fig. 2.2 and the term mechanoreceptor has been established [4]. A ↪ mechanoreceptor is defined as

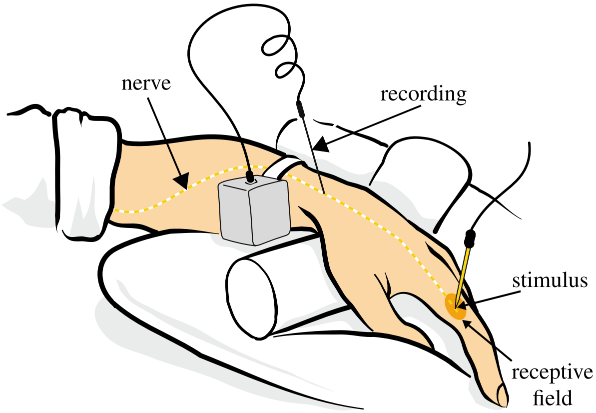

Fig. 2.3 Recording of electrical impulses of a single mechanoreceptor with microneurography. Figure adapted from [5] © Springer Nature, all rights reserved

Table 2.1 Receptive fields of the tactile mechanoreceptors in glabrous skin Table gives size and form of the receptive fields based on data from [4, 6–9]

Receptor type	Sensory cell	Size (mm^2)	Boundary
SA-I	Merkel disk	7–12	Distinct
SA-II	Ruffini endings	50–75	Diffuse
RA-I	Meissner corpuscle	7–19	Distinct
RA-II (PC)	Pacinian corpuscle	100–300	Diffuse

Definition *Mechanoreceptor* An entity consisting of one or more sensory cells, the corresponding nerve fibers and the connection to the central nervous system.

The classification of a mechanoreceptor is based on the size of the ↪ receptive fields and the adaptation behavior of the receptor when a constant pressure stimulus is applied. The receptive field denotes the area on the skin, in which an external mechanical stimulus will evoke a nervous impulse on a single nerve fiber. The size of the receptive field depends on the number of sensory cells that are connected to the investigated nerve fiber. Tactile mechanoreceptors exhibit either small (normally indicated with *I*) or large receptive fields (indicated with *II*). The adaptation behavior is classified as *slowly adapting (SA)* or *rapidly adapting (RA, sometimes also called fast adapting (FA))*. With these declarations, four mechanoreceptors can be defined, that are shown in Table 2.1. This nomenclature is based on a biological view. Next to this biological motivated terms, you will find the term *channel* in psychophysical literature to describe the connection between sensory cells and brain. A channel is defined as

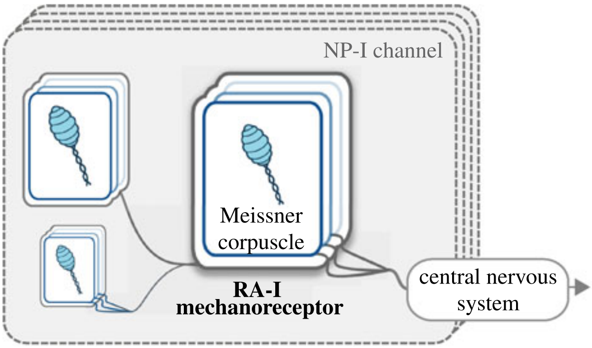

Fig. 2.4 Relation of the terms sensory cell, mechanoreceptor and channel using the NP-I channel as an example. The NP-I channel consists out of RA-I mechanoreceptors, that are based on Meissner corpuscles as sensory cells. NP-I and NP-III channels process signals of multiple sensory cells, while NP-II and PC channels are based on the signals of single sensory cells [11]

Definition *channel* Functional/structural pathway in which specific information about the external world is passed to some location in the brain where the perception of a particular sensory event occurs" *(Quote from* [10, p. 49]*)*

The difference to the definition of mechanoreceptors is the integration of functional processes like masking in the channel model. In general, the terms for channels and mechanoreceptors are used synonymously. The channels are named NP-I (RA-I receptor, NP standing for Non-Pacinian), NP-II (SA-II receptor), NP-III (SA-I receptor) and PC (RA-II receptor) [11]. There is experimental evidence for the presence and involvement of four channels in haptic perception in glabrous skin, but only three channels in hairy skin [12]. When using the channel model to describe haptic interaction one has to be aware, that certain aspects of interaction like surface properties and reactions to static stimuli cannot be explained fully by it [13, Chap. 4]. In this book, this discrepancy is not discussed in detail in favor of a primitive-based description of interactions that involves perception and motion control as well. An overview about the different terms for the description of tactile perception is given in Fig. 2.4.

Spatial Distribution of Mechanoreceptors

The spatial distribution of the different mechanoreceptors depends on the skin region considered. For the skin of the hand there is a varying distribution depending on the depth of the mechanoreceptors in the skin: near-surface receptors (RA-I, SA-) show a higher density in the finger tips than in the palm, deeper localized receptors show only a light dependency on the skin region. This is shown in Fig. 2.5.

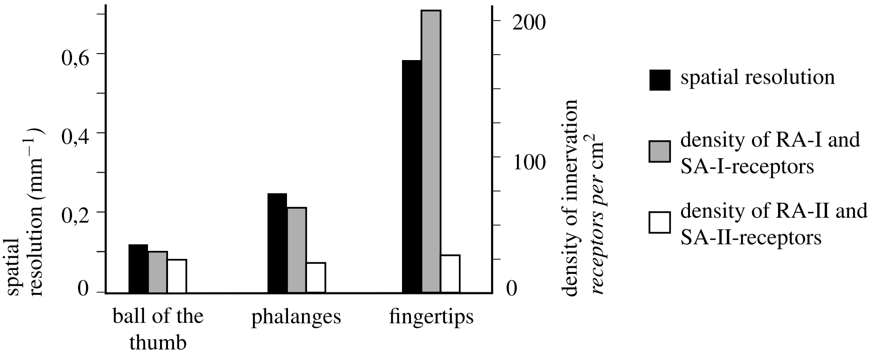

Fig. 2.5 Innervation density of mechanoreceptors near and far from the skin surface. The greater innervation density of Merkel and Meissner receptors leads to a higher spatial solution of quasi-static stimuli. Figure based on [4]

The highest density of receptors is found at the fingertips and adds up to 250 receptors/cm^2 [14] (primary source [15]). Thereof 60% are Meissner corpuscles, 60% are Merkel disks and 5% Ruffini endings and Pacinian corpuscles respectively [16]. Because of the high spatial density it can be assumed, that a mechanical stimulus will stimulate always several receptors of different type. However, not the density, but the absolute number of mechanoreceptors of different users are approximately the same [17]. Because of that, small hands are more sensitive than large hands. An inverse study was done by MILLER ET AL. [18] in which a simulated population of receptors was exposed to a virtual stress and the nervous signals were calculated and qualitatively compared to known neurological processes. The study was able to confirm a multitude of hypotheses from neurobiology and is a fascinating read.

Functions of Receptors and Channels

Next to the physiological and histological differences of the mechanoreceptors described above, channels differ in additional, functional properties [10, 11]:

Frequency Dependency Channels are sensitive in different frequency ranges. While NP-II and NP-III channels are sensitive to (quasi-)static and low-frequency stimuli (up to about 20–50 Hz), the PC channel becomes sensitive at about 50 Hz and detects stimuli up to a frequency of 10 KHz. The main reason for the frequency dependency lies in the biomechanical structure of the receptors [5, 19]. To investigate frequency dependence of channels, psychophysical measurements using masking schemes are used. This leads to different results for the sensitivity and frequency selectivity of the several channels depending on the measurement procedures.

Thresholds Each channel exhibits thresholds that are independent from the other channels. An aggregation of the information from different channels takes place in the central nervous system [10]. There is also no evidence of crosstalk between channels [20]. Recent studies find evidence for a linear behavior of the channels and the aggregation process (Sect. 2.1.4).

Summation Properties Summation describes the property of a channel, to consider more than one temporal or spatial contiguous stimuli as a single stimulus. The reasons for summation are given by the neural activities to conduct impulses through the nerve fibers [21]. There are also assumptions of summation mechanisms in the central nervous system to compensate for sensitivity differences of the different receptors in a channel [22, 23]. Studies show no spatial summation for (quasi-)static stimuli [24], but only for dynamic ones [25].

Temperature Dependency Thresholds and frequency dependency are influenced by temperature. A stronger dependency on temperature is attributed to NP-II and PC channels compared to NP-I and NP-III [11]. Other studies assess temperature induced threshold chances at the glabrous skin of the hand starting at a frequency of 125 Hz, but find no effect on the hairy skin of the forearm [26]. Next to this, also the mechanical properties of the skin exhibit a temperature dependency of the mechanical properties [27].

Table 2.2 gives an overview over the discussed properties for each channel. It also includes information about the coding of the channels referring to kinematic measures like deflection, velocity (change of deflection) and acceleration (change of velocity) [5, 6].

Based on this properties, functions of the different channels in perception and interaction can be identified [30–33].

NP-I (RA-I, Meissner corpuscle) Most sensory cells in human skin belong to the NP-I channel. They exhibit a lower spatial resolution than SA-I receptors, but have a higher sensibility and a slightly larger bandwidth. The corresponding sensory cells are called Meissner corpuscles and exhibit a biomechanical structure that makes them insensitive to quasi-static stimuli.

The RA-I receptors are sensitive to stimuli acting tangential to the skin surface. They are important for the detection of slip of hand held objects and the associated sensomotoric control of grip forces. Together with the PC channel they are relevant for the detection of frequencies of vibrations [34, 35].

The NP-I channel can detect bumps with a height of just 2 μm on a otherwise flat surface, if there is a relative movement between surface and skin. This movement leads to a deformation of the papillae on the skin by the object. Reaction forces and—deformations are located in a frequency bandwidth that will activate the RA-I receptors [36]. Similarly, filter properties of surface structures are used for the design of force sensors [37].

NP-II (SA-II, Ruffini ending) The SA-II receptors in this channel are sensitive to lateral elongation of the skin. They detect the direction of a external force, for example while holding a tool. The NP-II channel is more sensitive than the NP-III channel, but has a much lower spatial resolution.

This channel also transmits information about the position of limbs, when joint flexion induces skin elongation. The SA-II receptors are therefore also relevant

Table 2.2 Selection of relevant parameters of tactile sensory channels. Averaged values respectively common ranges are given, when more than one source is considered. For sizes of receptive fields see Table 2.1

Channel	Sensory cell	Receptor type	Sensitive bandwidth (Hz)	Spatial resolution (mm)	Coding	Summation properties	Temperature dependency
Sources	[11]	[11]	[6, 8, 10, 11, 28]	[29]	[5, 6]	[11, 13]	[11]
NP-I	Meissner corpuscle	RA-I	10 ... 50	3–5	Velocity	Spatial	Slightly
NP-II	Ruffini ending	SA-II	QS ... 50	10	Deflection	Temporal	Existent
NP-III	Merkel disc	SA-I	QS ... 20	0,5	Deflection, velocity	*Not known*	Slightly
PC	Pacinian corpuscle	RA-II	40 ... 1000	>20	Acceleration	Spatial and temporal	Existent

Used abbreviation: $\hookrightarrow$ quasi-static (QS) for kinaesthetic perception. With specific stimulation of the NP-II channel, an illusion about the position of limbs can be generated [38, 39].

NP-III (SA-I, Merkel disk) The NP-III channel with Merkel disks right under the skin surface is sensitive to strains in normal and shear directions. Because of the slow adaptation of the channel, the high density of sensory cells and the high spatial resolution (less than 0.5 mm although the receptive field is larger than that) it is used to detect elevations, corners and curvatures. It is therefore the basis for the detection of object properties like form and texture.

Because of the coding of intensity and intensity changes, this channel is responsible (together with the RA-I channel) for reading ↪ Braille. Studies also show an effect of the channel when wrist and elbow forces are to be controlled [40].

PC (RA-II, Pacinian corpuscle) The PC channel with rapidly adapting RA-II receptors exhibits the largest receptive fields and the largest sensitivity bandwidth. It is mainly used to detect vibrations arising in the usage of tools. These vibrations originate in the contact of the tool with the environment and are transmitted by the tool itself. They allow the identification of surface properties with a stiff tool, for example [41]. Because of the very high sensitivity (vibrational amplitudes of just a few nanometers can be detected by the PC channel [11]), also sensory cells located further away from the application of stimuli contribute to perception by reacting to surface wave propagation [3, 42]. To suppress the influence of dynamic forces arising in the movement of limbs on the perception of the PC channel, the Pacinian corpuscles exhibit a strong high-pass characteristic with slopes up to 60 dB per decade. This is realized by the biomechanical structure of the sensory cells.

In interactions, RA-II receptors signalize that something *is* happening, but do not necessarily contribute to the actual interaction. In addition, contributions of the PC channel to the detection of surface roughness and texture are assumed [7].

2.1.1.2 Kinaesthetic Receptors and Their Functions

For kinaesthetic perception there are two known receptor groups [29, 43, 44]. The so-called *neuromuscular spindles* consist out of muscle fibers with wound around nerve fibers that are placed parallel to the skeletal muscles. Because of that placement, strain of the skeletal muscles can be detected. Histological they consist out of two systems, the nuclear bag fibers and the nuclear chain fibers that react to intensity change and intensity [45].

The second group of receptors are *Golgi Tendon Organs*. These are located mechanically in series to the skeletal muscles and detect mechanical tension. They are used to control the force the muscle exerts as well as the maximum muscle tension. Special forms of the Golgi Organs exist in joints, where extreme joint position and ligament tension are detected [29]. They react mostly on intensity. Figure 2.6 shows these three types of receptors.

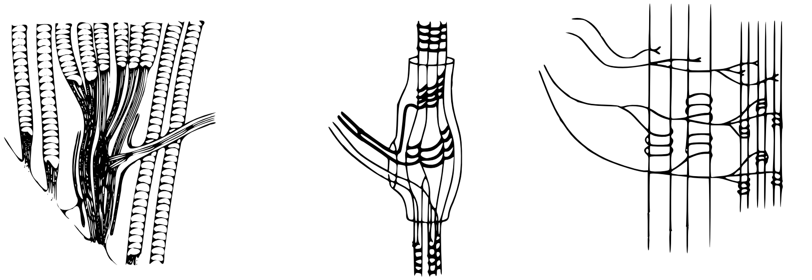

Fig. 2.6 Kinaesthetic Sensors for muscular tension (Golgi Tendon Organ) and strain (Bag and Chain Fibers). Figure adapted from [46] © Wiley, all rights reserved

The dynamic requirements on kinaesthetic sensors are lower compared to tactile sensors, since the extremities exhibit a low-pass behavior. The requirements with regard to relative resolution are comparable to the tactile system. Proximal joints exhibit a higher absolute resolution than distal joints. The hip joint can detect angle changes as low as 0.22°, while finger joint resolutions increases to 4.4° [43]. This is because of the greater influence of proximal joints on the position error of an extremity. The position accuracy increases with increasing movement velocity [44].

Kinaesthetic Perception is supported by information from the NP-II channel, from the vestibular organ responsible for body balance and from visual control by the eye. Different to the tactile system, the kinaesthetic system does not code intensities or their changes, but exhibits some sort of sense for the effort needed to perform a movement [47, 48]. For applications like for example rotary knobs this means, that a description based on movement energy with regard to rotary angle does correlate better with user ratings than the widespread description based on torques with regard to rotary angle.

2.1.1.3 Other Sensory Receptors

The skin also includes sensory receptors for thermal energy [49] as well as pain receptors. The latter are attributed a protection function, signaling pain when tissue is mechanically damaged [50]. Both aspects are not discussed in detail in this book because of the minor technical importance.

2.1.1.4 Neural Processing

Haptic information detected by the tactile and kinaesthetic mechanoreceptors are coded and transmitted by action potentials on the axons of the involved neurons to

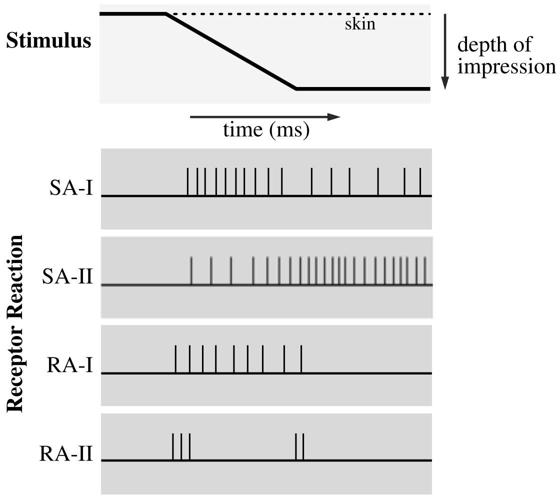

Fig. 2.7 Action potentials of sensory cells when a single stimulus is exerted on the skin. Figure adapted from [5]

the central nervous system. The coding of the information resembles the properties given in Table 2.2 and is illustrated in Fig. 2.7.

The biochemical processes taking place in the cells are responsible for the temporal summation (when several action potentials reach a dendrite of a neuron within a short interval) and the spatial summation (when action potentials of more than one receptor arrive at the same neuron) of mechanoreceptor signals. Each individual action potential would not be strong enough to evoke a relay of the signal through the neuron [51]. For the rest of this book, further neurophysiological considerations are of minor importance, but can be assessed in a standard physiology or neurophysiology textbook.

A more interesting question for the design of haptic systems is the synthesis of different information from haptic, visual and acoustic senses to a unconscious or conscious ↪ percept and a resulting action. While the neural processes are investigated in depth [52], there is no comprehensively confirmed theory about the processing in the central nervous system (spinal cord and brain).

Current research favors a Bayesian framework, that also incorporates former experiences when assessing information [53, 54]. Figure 2.8 gives a schematic description of this process, that is confirmed by current studies [55, 56].

2.1.2 *Psychophysical Description of Perception*

The investigation of perception processes, that is the link between an objectively measurable ↪ stimulus and a subjective ↪ percept, is the task of psychophysics, a section of experimental psychology. It was established by G. T. Fechner in the late mid of the 19th century [58]. As shown in Fig. 2.1, there are a several parts

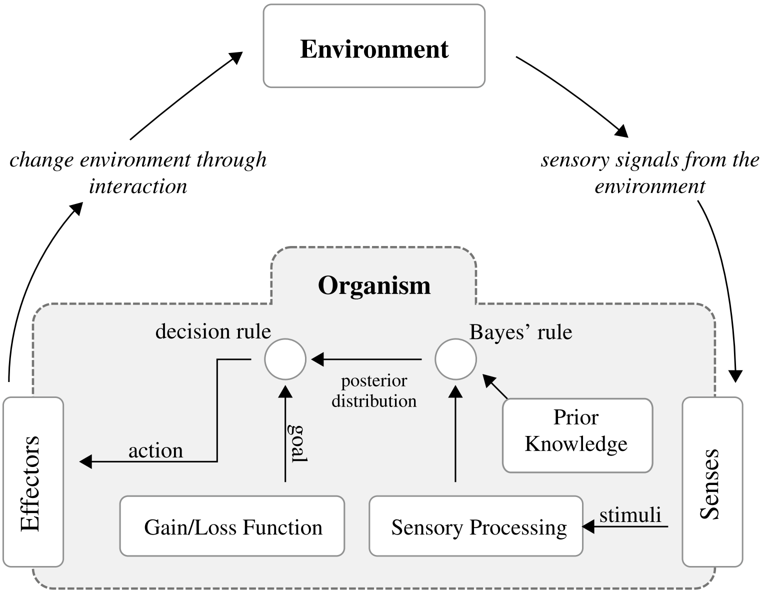

Fig. 2.8 Sensory integration according to HELBIG [57]. Prior knowledge is combined with current sensory impressions to a percept of the situation. Based on a gain/loss analysis, a decision is made and an interaction using the effectors (limbs, speech) is initiated

of psychophysical studies. *Inner psychophysics* deals with the connection of neural activity and the formation of percepts, while *outer psychophysics* will investigate the reactions to an outer stimulus. These parts were established already by FECHNER [1]. Nowadays, modern technologies also allow the investigation of neurophysiological problems linking outer stimuli with neural activity and the analysis of correlations between neurophysiology, inner psychophysics and outer psychophysics.

For the design of haptic systems we will concentrate on outer psychophysics, since only physical properties of stimuli and the corresponding subjective percepts will allow the derivation of design parameters and design goals. Therefore the remaining of this chapter will only deal with procedures and parameters from outer psychophysics. It will describe the main principles, that should be understand by each system engineer to interpret psychophysical studies correctly.

2.1.2.1 The Psychometric Function

Regardless of the kind of sense, the description of perception is not possible with the general engineering tools. Perception processes are whether non-linear nor stationary, because the perception process of inner psychophysics cannot be described that way. Looking at Fig. 2.8 this is obvious since weighting and decision processes and the risk assessment cannot be described in a universal way.

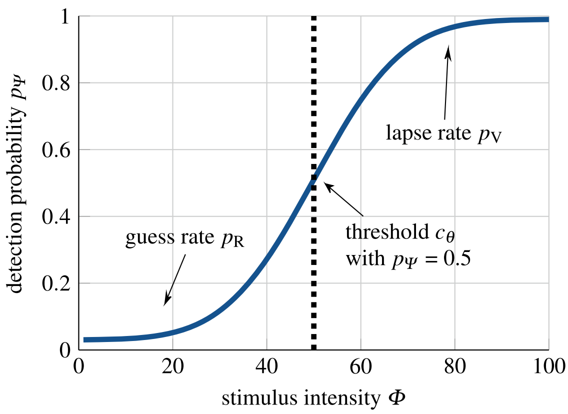

Fig. 2.9 Psychometric function based on a normal distribution with $c_\theta = 50$ stimulus units, guess rate p_G and lapse rate p_V

Because of that, perception processes in outer psychophysics are not described by specific values but by probability functions. From this functions, specific values can be extracted. Figure 2.9 gives an example of such a ↪ psychometric function. On the x-axis the intensity of an arbitrary stimulus Φ is plotted, while the y-axis gives the probability p for a test person detecting the stimulus with that intensity.

According to [59] the psychometric function p_Ψ has a general mathematical description according to Eq. (2.1).

$$p_\Psi(\Phi, c_\theta, c_\sigma, p_G, p_L) = p_G + (1 - p_G - p_L) \cdot f(\Phi, c_\theta, c_\sigma) \tag{2.1}$$

with a stimulus Φ and the following parameters:

Base Function f The base function determines the form of the psychometric function. In literature you can find different approaches for the base function. Often a cumulative normal distribution (Eq. (2.2)), sigmoid functions (Eq. (2.3)), and Weibull distributions (Eq. (2.4)) are used:

$$f_{\text{cdf}}(c_\theta, c_\sigma, \Phi) = \frac{1}{c_\sigma\sqrt{2\pi}} \int_{-\infty}^{\Phi} e^{\frac{-(t-c_\theta)^2}{2c_\sigma^2}}\,\mathrm{d}t \tag{2.2}$$

$$f_{\text{sig}}(c_\theta, c_\sigma, \Phi) = \frac{1}{1 + e^{-\frac{c_\sigma}{c_\theta}(\Phi - c_\theta)}} \tag{2.3}$$

$$f_{\text{wei}}(c_\theta, c_\sigma, \Phi) = 1 - e^{-(\frac{\Phi}{c_\theta})^{c_\sigma}} \tag{2.4}$$

Nowadays there is no computational limit for the calculation of functions and extracting values, therefore the choice of a base function of depends on prior experiences of the experimenter. When investigating the visual sense, a Weibull distribution will better fit data [60], when working with ↪ Signal Detection Theory (SDT), a normal distribution is assumed [61]. Sigmoid functions are often used in early simulation studies because of the low computational effort needed to calculate psychometric functions. The current state of the art in mathematics would allow for non model based description of the psychometric function. In psychophysics these approaches have not been seen very often up till now, whereas first studies show a comparable performance of these techniques compared to a model-based description [62].

Base Function Parameters $(c_\theta,\ c_\sigma)$ These two parameters can be treated demonstratively as the perception threshold and the sensitivity of the test person. c_θ will give the threshold, denoting the stimulus Φ with a detection probability of 0.5. The sensitivity parameter c_σ is given as the slope of the psychometric function at the threshold level. A high sensitivity will yield a large slope, a low sensitivity will yield a flatter curve, resulting in many false detections.

Guess Rate p_G The guess rate gives the portion of false positive answers for very low stimulus intensities that cannot be detected by the test person normally. Such false positive answers can arise in guessing, erroneous answers, or abstraction of the test person. In simulating psychometric functions, the guess rate is used to model force-choice answering paradigms.

Lapse Rate p_L The lapse rate models false negative answers, when a large stimulus intensity is not detected by a test person. The main reason for lapses is inattentiveness of the test person during a psychophysical procedure.

To find a psychometric function, psychophysics knows a bundle of procedures, that will be addressed in the next section. It has to be kept in mind, that all of the above and the following is not only valid for a stimulus with a changing intensity, but also for any other kind of changing signal parameter like frequency, energy and proportions between different signals.

2.1.2.2 Psychometric Procedures

The general goal of a psychometric procedure is the determination of a psychometric function p_Ψ as a whole or a single point $(\Phi|p_\Psi(\Phi))$ defined by a given probability p_Ψ. In general, each run of a psychometric procedure consists out of several trials, in which a stimulus is presented to a test person and a reaction is recorded in a predefined way. Figure 2.10 gives a general taxonomy to classify psychometric procedures.

Each procedure consists of a measuring method and an answering paradigm. The method determines the course of a psychometric experiment, particularly the start intensity of the stimulus and the changes during each run, the conditions to stop a trial and the calculation rule to obtain a psychometric function from the measured data. The answering paradigm defines the way, a test person is presented the stimulus and the available answering options. The choice of a suitable procedure is not topic of this book, but an interesting topic nevertheless. Further information about the simulation of procedures and the definition of suitable quality criteria can be found in [64, 65].

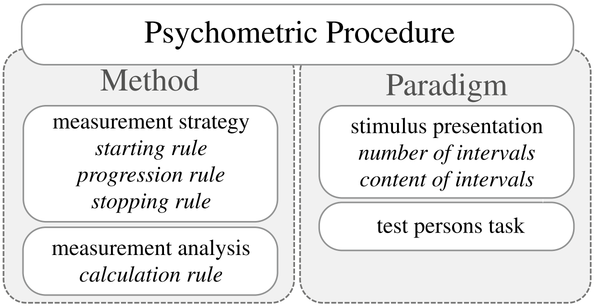

Fig. 2.10 Taxonomy of psychometric procedures. Figure is based on classifications in [63]

Methods

The first, nowadays called "classical", methods were developed back in the 19th century. The most familiar are called *Method of Constant Stimuli*, *Method of Limits* and *Method of Adjustment*. They have barely practical relevance in today's experiments, so they are not detailed here any further. Please refer to [66] for a more detailed explanation. Modern methods are derived from this classical methods, but are generally adaptive in a way, that the progression rule is depending on the answers of the test person in the course of the experiment [67]. They can be classified into heuristic and model based methods.

Heuristic Based Methods These methods are based on predetermined rules that are applied to the answers of the test person to change the stimulus intensity in the course of the psychophysical experiment (change of the progression rule). Stopping and starting rules are normally fixed (by the total number of trails for example) for each experiment beforehand. The most-widely spread heuristic method is the so-called *Staircase method*. It is based on the classic *Method of Limits* and tries to nest the investigated threshold with the intensities of the test stimulus. Figure 2.11 gives two examples of a staircase method with different progression rules. It becomes clear, that the name of this method originates in this kind of display of the test stimulus intensities over the test trails.

The definition of progression rules is based on the number of correct answers of the test person leading to a lower test stimulus and the number of false answers leading to a higher test stimulus. The original Staircase method, also called *Simple Up-Down Staircase* (upper part of Fig. 2.11), will change stimulus intensities after every trail, such converging at a threshold with a detection probability of 0.5 [68]. The request for other detection probabilities led to another form of the Staircase method, the so called *Transformed Up-Down Staircase Method*. For these methods, the progression rule is changed and needs for example more than one correct answer for a downward change of the test stimulus. Figure 2.11 gives an example of a 1up-3down progression rule, lowering the test stimulus after three correct answers and raising it for every false answer.

In [68], LEVITT calculates the convergence probability for several progression rules. Table 2.3 gives the convergence probabilities for common progression rules. To interpret studies about haptic perception incorporating experiments with staircase methods, the convergence probability has to be taken into account. However, newer studies cast some doubts on this interpretation of the progression rule [69], arguing that the amount of intensity change is much more relevant for the convergence of a staircase than the progression rule. For system design, one therefore has to resort to larger assessment factors in the interpretation of these kind of data. The calculation of a threshold is normally carried out as a mean of the last stimulus intensities leading to a reversal in the staircase direction. Typical values are for example 12 reversals for the calculation of the threshold and 16 reversals as a stopping criterion for the whole experiment run.

Another important heuristic method is so called *PEST—Parameter Estimation by Sequential Testing—Method* [70]. The heuristic keeps a given stimulus intensity until some assessment of the reliability of the answers can be made. The method was designed to yield a high accuracy with a small number of trails. One of the main disadvantages of this method is the calculation rule, that only considers the very last stimulus. However, several modern adaptations like *ZEST* and *QUEST* try to overcome some of these disadvantages [71].

Model Based Methods A model of the psychometric function is the basis of these methods, that measure or estimate the parameters of the function as given in Eq. (2.1). Most methods incorporate some kind of prior knowledge of the psychometric function from experience or previous experiments (Bayes' approach) and use different kinds of estimators (maximum likelihood, probit estimation). Examples for these methods are *ML-Test* [60], that uses a maximum likelihood estimator for the determination of the function parameter. The end of each experiment run is determined by the confidence interval of the estimated parameters. If the interval is smaller than a given value, the experiment run is stopped.

In 1999, KONTSEVICH AND TYLER introduced the *Ψ-Method* [72], combining promising elements from several other methods. This method is not very prominent in haptics research, but is considered the most sophisticated method in psychophysics in general [66, 73]. It is able to estimate a threshold in as little as about 30 trials and the sensitivity in about 300 trials.

One of the general advantages of a model based method is the calculation of a whole psychometric function, not only of a single threshold. Therefore, more than one psychometric parameter can be calculated from a single experiment. Adversely, one should have a slight confidence in the model used in the method for the investigated sense. As said above, data show a slightly advantage for Weibull-based models for the visual sense [60], while studies of the author of this chapter yield better results for a logistic function for the assessment of force perception thresholds [74].

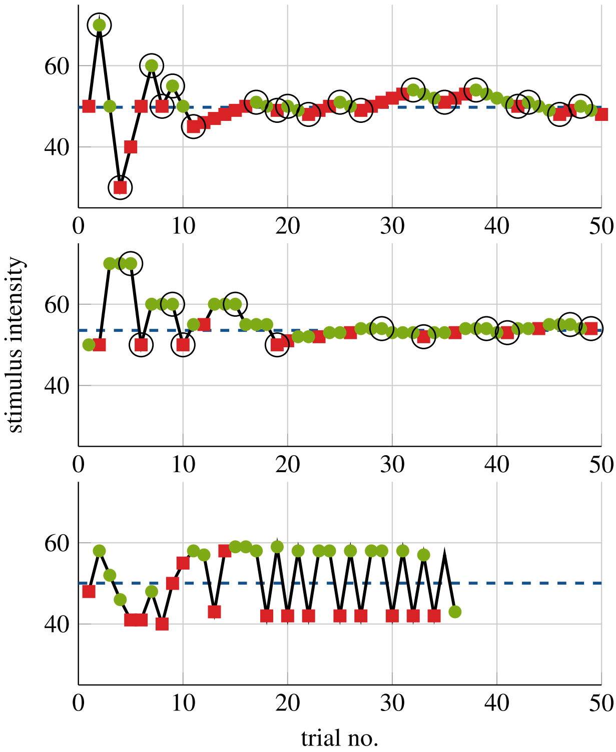

Fig. 2.11 Simulated runs of common psychometric methods. The upper graph shows a *simple up-down staircase*, theoretically converging at $c_\theta = 50$, the middle graph shows a *transformed up-down staircase* with a *1up-3down* progression rule and a theoretical convergence level of $c_\theta = 57.47$. The lower graph shows a run from a Ψ*-method*, also converging at $c_\theta = 50$. Simulated answers of the subject are shown in green circles (correct answer) and red squares (incorrect answer), staircase reversals are circled. The dotted line indicates the calculated threshold

Table 2.3 Probability of convergence of adaptive staircase methods with different progression rules. Table based on [68]

Progression rule	Number of false answers for raising stimulus intensity	Number of correct answers for lowering stimulus intensity	Number of convergence probability
1up-1down	1	1	$p(X) = 0.500$
1up-2down	1	2	$p(X) = 0.707$
2up-1down	2	1	$p(X) = 0.293$
1up-3down	1	3	$p(X) = 0.794$
1up-4down	1	4	$p(X) = 0.841$
4up-1down	4	1	$p(X) = 0.159$

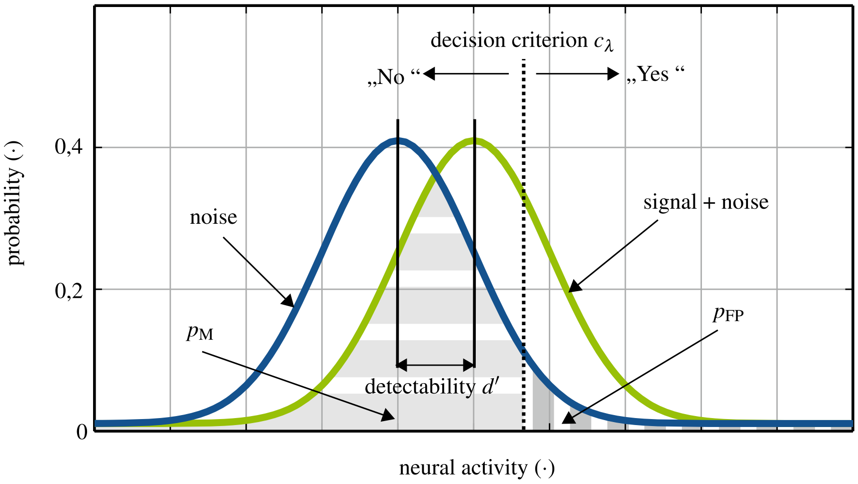

Fig. 2.12 Baseline model of the Signal Detection Theory (SDT). The model consists of two neural activity distributions for Noise and Signal + Noise. The noise distribution is always present and can be interpreted as sensory background noise. If an additional stimulus is presented, the whole distribution shifts upwards. The subject decides based on a decision criterion c_λ, whether a neural activity is based on a stimulus or not. The subject shown here exhibits a badly placed respectively conservative decision criterion: Many signals are missed (horizontal striped area p_M), but only a few false-positive answers are recorded (vertical striped area p_{FP}). The detectability d', defined as the span between the midpoints of both distributions, is independent from the decision criterion of the subject and can be used as an objective measure of the difficulty of a detection experiment

Paradigms

Answering paradigms describe the way a test person will give the answer to a stimulus in a way, that the procedure can react according to its inherent rules. The theoretical basis for answering paradigms is given in the $\hookrightarrow$ SDT, a statistical approach to describe arbitrary decision processes, that is often applied to sensory processes. It is based on the assumption, that not only stimuli, but also noise will contribute to perception. In the perception continuum, this is represented by a noise distribution (mainly Gaussian). If there is no stimulus present, the noise distribution will be present in neural activity and processing, if a stimulus is present, the noise distribution is added to the stimulus. Figure 2.12 shows this theoretical basis of $\hookrightarrow$ SDT.

Near the absolute detection threshold, both distributions will overlap. In this area on the perception continuum it is indistinguishable if a neural activity is coming from a stimulus or just from innate noise. To decide whether a stimulus is present or not, the test person will construct a decision criterion c_λ. If a input signal is greater than this criterion, a stimulus is identified, smaller inputs are neglected. Unfortunately, this decision criterion is varying with time and other external conditions. Therefore, one aim of $\hookrightarrow$ SDT is to investigate the behavior of a test person regarding this criterion. The detectability d' arising from the signal detection theory can be used to calculate comparable sensitivity parameters for different test persons and to compare studies with different psychometric procedures.

With these implementations, one can differentiate liberal (low decision criterion) from conservative (high decision criterion) test persons. For example, studies show that the consumption of alcohol will not change the sensitivity of a person, but will influence the decision criterion to become more liberal. This leads to a better detection of smaller stimuli, but will also produce more false-positive answers. Based on this stochastic approach of decision theory, answering paradigms can be defined, that are used to minimize the influence of varying decision criteria. The most common paradigms are described in the following.

Yes/No-Paradigm The easiest paradigm is the simple *Yes/No-Paradigm*. A test person will for example answer "yes" or "no" to the question, whether a stimuli was present or not. Obviously, a varying decision criterion will affect this answer. One has to trade this disadvantage for the shorter time this paradigm needs in presenting a stimulus compared to other paradigms.

Forced-Choice-Paradigm These paradigms arise directly from ↪ SDT to find an objective measure of a subjective assessment. To achieve this, each trial will include more than one alternative with a test stimulus and the test person is compelled to give a positive answer in every trial, for example which interval contained a stimulus or which stimulus hat the largest intensity. This paradigm can be combined with most of the methods mentioned above. In general, forced choice paradigms are denoted by *xAFC (x Alternative Forced-Choice)* or *xIFC (x Interval Forced Choice)*. The first abbreviation is used, when several alternatives are presented to a test person, while the term interval is used for a temporal sequence of the alternatives. x denotes the number of alternatives respectively intervals. Naturally, forced choice paradigms increase the guessing rate in the psychometric function with an additional probability of $\frac{1}{x}$. This has to be considered in the mapping of experimental results back to an psychometric function.

An example experiment setup would include five reference stimuli and one unknown test stimulus given to the test person. The test person would have do decide which reference stimulus corresponds to the test stimulus. If stimuli were miniature golf balls with different compliance, this experiment can be classified as a 5AFC paradigm.

Unforced-Choice-Paradigm In [75] KÄRNBACH describes an adaptive procedure, that does not require a forced choice, but also allows an "I don't know" answer. This procedure leads to more reliable results from test persons without extensive experience in simulations. Especially in experiments incorporating a comparison of different stimuli this answering paradigm could provide a more intuitive approach to the experiment for the test person and could therefore lead to more motivation and better results. Based on Fig. 2.10 this unforced-choice option belongs to the paradigm definition, but has to be incorporated in the method rules as well. Therefore this paradigm is only found in a limited number of studies, but finds also application in recent studies of haptic perception [76].

2.1.2.3 Psychometric Parameters

In most cases, not the whole psychometric function, but characteristic values are sufficient for the usage in the design of haptic systems. The most important parameters are described in this section.

Absolute Thresholds

These parameters describe the human ability, to detect a stimuli at all. They are defined as the stimulus intensity Φ with a detection probability of $p_\Psi = 0.5$ [77, Chap. 5]. However, since many psychometric procedures will not converge at this probability, most studies call their results threshold regardless of the convergence probability.

For the design of haptic systems, absolute thresholds will give absolute margins for sensors and actuators for noise- and otherwise induced errors: A vibration, that is "detected" by a sensor because of inherent noise in the sensor signal processing or displayed by an actuator is acceptable as long the user of a haptic system will not feel it. Therefore a reliable assessment of these thresholds is important to define suitable requirements. On the other hand, absolute thresholds define a lower limit in communication applications: Each coded information has to be at least as intense as the absolute threshold to be detectable, even if one probably will chose some considerably higher intensity level to ensure detection even in distracting environments.

Differential Thresholds

Differential thresholds describe the human ability to differentiate between two stimuli, that differ in only one property. The first differential thresholds were recorded by E. H. WEBER at the beginning of the last century [78]. He investigated the differential threshold of weight perception by placing a mass (reference stimulus Φ_0) of a test persons hand and adding additional mass $\Delta\Phi$ until the test person reported a higher weight. The additional mass needed to evoke this perception of a higher weight was called *Differenz Limen (DL)*.

Further studies showed that the quotient of $\Delta\Phi$ and Φ_0 would be constant in a wide range of reference stimulus intensities. This behavior is called *Weber's Law* and the *Weber fraction* given in Eq. (2.5) is also called ↪ Just Noticeable Difference (JND).

$$\text{JND} := \frac{\Delta\Phi}{\Phi_0 + a} \tag{2.5}$$

The ↪ JND is generally given in percent (%) or decibel (dB) with respect to the reference stimulus Φ_0. Since further studies of Weber's Law showed an increase in JNDs for low reference stimuli near the absolute threshold, the additional parameter a was introduced. It is generally interpreted as sensory background noise in the perception process [79, Chap. 1], which is a similarity to the basic assumption of the

$\hookrightarrow$ SDT. The resulting change of the JND near absolute thresholds is so large, that a consideration in the design of technical systems is advisable.

It is generally agreed, that the JND denotes the amount of stimulus change, that is detected as greater half the time. In literature one can find two different approaches to measure a JND in a psychophysical experiment. It has to be noted that these approaches do not necessarily measure the 50% point of the psychometric function:

- Direct comparison of a reference stimulus Φ_0 with a test stimulus $\Phi_0 + \Delta\Phi$. The stimulus controlled by the psychometric procedure is necessarily $\Delta\Phi$, tests persons have asses if the test stimulus is greater than the test stimulus. The JND is calculated according to the procedures calculation rule, the convergence probability has to be taken into account when interpreting and using the JND.
- According to [77, Chap. 5], the JND can also be determined by using two points of a psychometric function as given in Eq. (2.6)

$$\text{JND} := \Phi(p_\Psi = 0.75) - \Phi(p_\Psi = 0.25) \tag{2.6}$$

  This definition is useful, if one cannot control the stimulus intensity freely during the test and has to measure a complete psychometric function with fixed stimuli (for example real objects with defined texture, curvature or roughness) or with long adaptation times of the test person.

It has to be noted that both approaches do not necessarily lead to the same numerical value of a JND. For certain classes of experiments, special terms for the differential thresholds have been coined. They are briefly described in the following:

Point of Subjective Equality (PSE) In experiments with a fundamental difference between test and reference stimulus in addition to the stimulus change, the differential threshold with $p_\Psi = 0.5$ is also called *Point of Subjective Equality (PSE)*. At this stimulus configuration, the test person cannot discriminate the two stimuli. An example could be the assessment of the intensity of two vibrations that a coupled into the skin normally and laterally. The fundamental difference is the coupling direction and the intensities of both stimuli are adjusted in a way, that the intensity is perceived as equal by the test person.

Successiveness Limen (SL) If two stimuli are presented to a test person, they are only perceived as two different stimuli, if there is a certain time period in between them. This time period is called *Successiveness Limen (SL)*. For mechanical pulses, SL can be determined to about 5 ms, while direct stimulation of nerve fibers will exhibit a SL of about 50 ms [13, Chap. 4].

Two-point threshold The two-point threshold describes the distance between the application points of two stimuli that is needed to make this stimuli distinguishable from another. The smallest two-point thresholds can be found at tongue and lips (< 1 mm for static stimuli), at the fingertip thresholds of $1 \ldots 2$ mm can be found. Other body areas exhibit two-point thresholds of several centimeter as shown in Fig. 2.13 [5]. The *spatial resolution* is the reciprocal value of the two-point threshold.

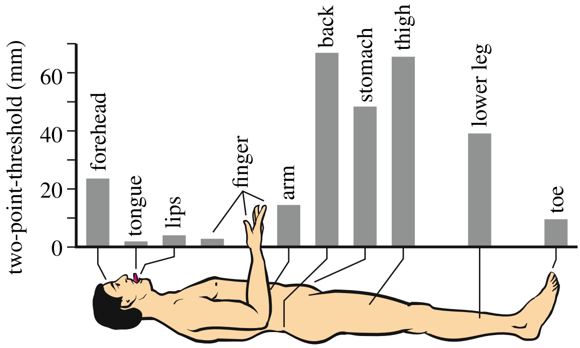

Fig. 2.13 Two-Point-Threshold at various locations, figure adapted from [5] © Springer Nature, all rights reserved

Just Tolerable Difference (JTD) The Just Tolerable Difference denotes the difference between two stimuli, that is differentiable, but still tolerable for the test subject. It is also termed the *Quality JND* and depends more on individual appraisal and judgment of the subjects than on the abilities of the sensory system. This measure can be used to determine system properties that are acceptable to a large number of users, as it is done in various other sensory modalities like taste [80] or vision [81].

The knowledge of differential thresholds has a major meaning. JNDs give the range of signals and stimuli that cannot be distinguished by the user, i.e. a limit for the reproducibility of a system. Proper consideration of JNDs in product design will yield systems with good user ratings and minimized technical requirements as shown for example in [82].

Description of Scaling Behavior

In the mid of the 19th century, FECHNER formulated a relation between objectively measurable stimulus Φ and the subjective percept Ψ based on *Weber's Law* in Eq. (2.5). He set the JND equal to a non-measurable increment of the subjective percept and integrated over several stimulus intensities defined by increments of the JND.[1] This leads to *Fechner's Law* as given in Eq. (2.7):

$$\Psi = c \log \Phi \tag{2.7}$$

In Eq. (2.7), c is a constant depending on the investigated sensory system. However, *Fechner's Law* is based on two assumptions that rendered invalid in further studies: The basis of a non-universal valid variant of *Weber's Law* and the assumption, that an increment as high as the current JND will evoke a increment in perception [79, Chap. 1]. In the mid of the 20th century, S. S. STEVENS proposed the *Power Law*, a new formulation of the relation of objective stimuli and subjective percepts, based on experimental data that could not be explained by *Fechner's Law*:

[1] An elaborate derivation can be found in [79, Chap. 1].

$$\Psi = c\Phi^a \tag{2.8}$$

In Eq. (2.8), c is a scaling parameter as well, that is often neglected in further analysis. The parameter a denotes the coupling between subjective perception and objective measurable stimuli and depends on the individual experiment. By logarithmization of Eq. (2.8), it can be calculated as the slope of the resulting straight line $\log \Psi = \log c + a \log \Phi$ [79, Chap. 13]. The *Power Law* can be summarized shortly as *"a constant percentage change in the stimulus produces a constant percentage change in the sensed effect"* [83, p. 16]. To analyze these changes particular psychometric procedures can be used, as for example found in [83]. Typical values in haptics include $a = 3.5$ for the intensity of electrical stimulation at the fingertip (a 20% increase will double the perceived intensity) and $a = 0.95$ for a vibration with a frequency of 60 Hz (i.e. a declining relation).

2.1.2.4 Factors Influencing Haptic Perception

From different studies of haptic perception, external influencing factors are known that affect absolute and differential thresholds. They originate in the properties of the different blocks given in Fig. 2.1. For the design of haptic systems they have to be considered as disturbance variables or can be used to purposeful manipulate the usage conditions. An example may be the design of a grip or the control of a minimum or maximum grip force at an end effector of a haptic system. The following list will give the technical relevant influencing factors.

Temperature Temperature will influence the mechanical properties of the skin [27]. Furthermore, perception channels exhibit a temperature dependance as given in Table 2.2. The absolute perception threshold is affected by temperature, the lowest thresholds are observed at about body temperature [84, 85]. This effect increases for higher frequencies [26, 86], denoting a higher temperature dependence of mechanoreceptors with greater receptive fields.

Age With increasing age the perception capabilities of high frequency vibration decrease. This is observed in different studies for finger and palm [87–92]. The change of form and spatial distribution of mechanoreceptors, especially of Pacinian Corpuscles, is deemed the cause for this effect.

Contact Area Because of the different receptive fields of the mechanoreceptors, the contact area is an important influencing parameter on haptic perception. With small contact areas, the thresholds for high frequency vibrations increase (higher intensities are needed for detection), while lowest thresholds can only be measured with large contact areas about the size of a finger tip or greater.

Furthermore, the absolute number and not the density of mechanoreceptors is approximately constant among test persons. Therefore the size of the hand is relevant for the perception capabilities, smaller hands will be more sensitive [17].

Since there is a (slight) correlation between sex and hand size, this is the reason for some contradictory studies about the dependency of haptic perception on the sex of the test person [89, 91, 93–95].

Other Factors Several other factors with influences on haptic perception thresholds like the menstrual cycle [85, 88, 96], diseases like *bulimia* or *anorexia nervosa* [97], skin moisture [98], and the influence of drinks and tobacco can be identified. In the design of haptic systems these factors cannot be incorporated in a meaningful way, since they can neither be controlled nor influenced in system design or usage.

2.1.2.5 What Do We Feel?

To investigate perception, an exact physical representation of the stimulus must be known. In auditory perception this is sound pressure, that will affect the eardrum and will be conducted via the middle ear to the nerve fibers in the cochlea and the organ of Corti. Visual perception is based on the detection of photons of a particular wavelength in the cones and rods in the retina.

In haptics, one will find different physical representations of stimuli, namely forces F and kinematic measures like acceleration a, velocity v or deflection d. The usage of a certain representation mainly depends on the purpose of the study or the system: forces are sometimes easier to describe and measure because of their characteristics as a flux coordinate defined at a single point. Kinematic measures exhibit characteristics of a differential coordinate, i.e. they can only be measured in relation to a prior defined reference. Many studies (especially of dynamic stimuli) are based on kinematic measures, since their definitions do not depend on the mechanical properties of the test person. Greenspan showed psychophysical measurements with less variation when stimuli were defined by kinematic measures compared to force [99].

However, there is evidence that humans do not only feel forces or kinematic measures. Perception is most likely based on the distribution of mechanical energy in the skin, where the mechanoreceptors are located. This distribution cannot be described with reasonable effort in detail (although there are some attempts for FE-modeling of the human skin [100–103]), furthermore it cannot be produced as a controlled stimuli for psychophysical experiments.

A common approach is to consider the human skin as a mechanical system, whose properties are not changed by haptic interaction. This is supported by studies conducted by Hogan, who showed that a human limb can be modeled as a passive mechanical impedance for frequencies higher that the maximum frequency of human motion capabilities. In that case, forces and kinematic measures coupled into the skin are related via the mechanical impedance $\underline{z}_{\text{user}}$ according to Eq. (2.9)

$$\frac{\underline{F}}{\underline{v}} = \underline{z}_{\text{user}} \tag{2.9}$$

with $v = \frac{\mathrm{d}d}{\mathrm{d}t} = \int a \,\mathrm{d}t$. Applied to perception this means, that each force perception threshold could be calculated from other thresholds defined by kinematic measures via the mechanical impedance of the test person. This relation is used in a couple of studies [104, 105] to calculate force perception thresholds from deflection-based measurements. Own studies of the author used force-based measurements to experimentally prove the relation given in Eq. (2.9) [106].

One can therefore conclude, that perception is based on the complex distribution of mechanical energy in the skin. For the design of haptic systems, a simplified consideration of the user as a source of mechanical energy with own mechanical parameters as given by the mechanical impedance $\underline{z}_{\text{user}}$ is applicable. Furthermore, this model is also valid for the description of perception, linking perception parameters by the mechanical impedance as well. Some important psychometric parameters are given in the next section of this chapter, a detailed view on the modeling of the user is given in Chap. 3. Meanwhile modern and fast imaging technologies revealed dynamical mechanical stimulations to reach much further than the area of interaction. Shao et al. showed that oscillations induced at the finger tip result in responses reaching almost as far as the wrist [107, 108]. The contribution and importance of such afferent vibrations to the overall perception is subject to ongoing research.

Hayward asked in [109]: *Is there a "plenhaptic" function?* A question unanswered still. But it is a tempting assumption that with the right understanding of perceptional dimensions we could translate the physical domain into a perceptional-domain in all temporal and macro- and micro-dynamics we know.

2.1.3 Characteristic Values of Haptic Perception

There are a vast number of studies investigating haptic perception. For the design process of haptic systems the focus does not lie on single biological receptors but rather on the human's combined perception resulting from the sum of all tactile and kinaesthetic mechanoreceptors. As outlined in the following chapters, a dedicated investigation of perception thresholds is probably advisable for the selected grip configuration of a haptic system. This section will give some results of the most important ones, but will fail in being complete. It is ordered according to the type of psychometric parameter. To interpret the results of the different studies correctly, Fig. 2.14 gives some explanation of the anatomical terms for skin location and skeleton parts.

2.1.3.1 Absolute Thresholds

One of the most advanced studies of haptic perception is carried out by the group of Gescheider et al. The probably most popular curve is the absolute perception threshold of vibrotactile stimuli defined by deflections of the skin at the thenar eminence as given in Fig. 2.15 [110]. Since the channel model arises in the work

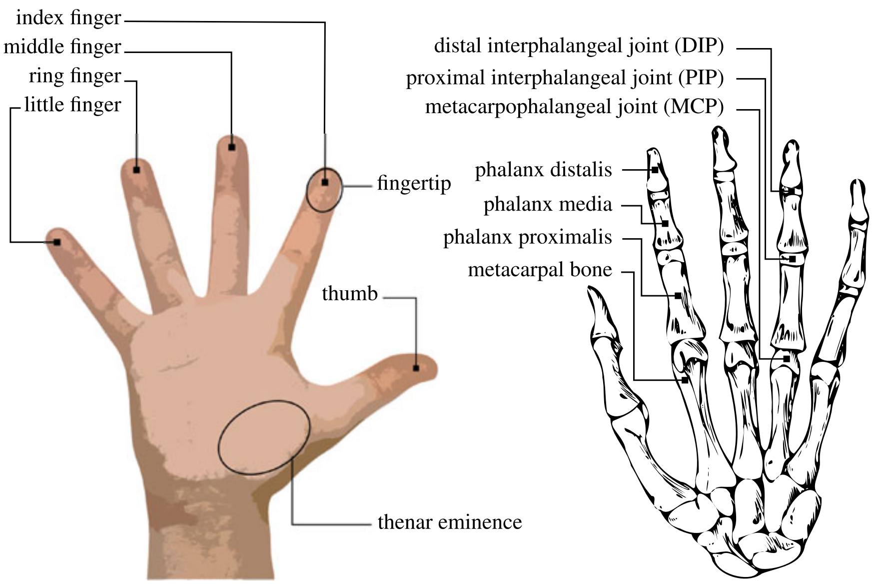

Fig. 2.14 Anatomical terms for skin areas and skeleton parts of the human hand

of this group, a lot of their studies deal with these channels and their properties. In Fig. 2.15 some properties of this model can be seen: The thresholds are influenced by the receptive fields, the highly sensitive RA-II-receptors are only exited with large contact areas, in addition, the most sensitive channel will be responsible for the detection of a stimulus. Other, non shown work includes the investigation of the perception properties of the finger tip [19] and intensive studies of masking and summation properties [88].

Other relevant studies were conducted by ISRAR ET AL. investigating vibrotactile deflection thresholds of hands holding a stylus [104] and a sphere [105], some quite common grip configurations of haptic interfaces. They investigate seven frequencies in the range of 10–500 Hz with an adaptive staircase (1up-3down progression rule) and a 3IFC paradigm and find absolute thresholds of 0.2–0.3 µm at 160 Hz. The studies include the calculation of the mechanical impedance and force perception thresholds as well. BRISBEN ET AL. investigated the perception thresholds of vibrotactile deflections tangential to the skin, a condition becoming more and more important when dealing with tactile feedback on touch screen displays. Whole hand grasps and single digits were investigated with an adaptive staircase (different progression rules) and 2- and 3IFC paradigms. They additionally investigate perception thresholds for 40 and 300 Hz stimuli at different locations on the hand and with different contact areas. Newer studies by GLEESON ET AL. investigate the properties of several stimuli parameters like velocity, acceleration and total deflection [111] on the perception of shear stimuli. They found accuracy of direction perception depending on both speed and total displacement of the stimulus, with accuracy rates grater than

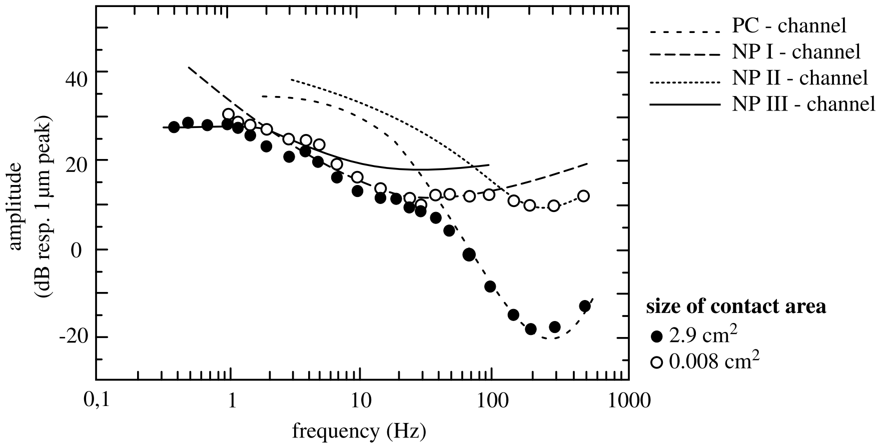

Fig. 2.15 Absolute threshold of tactile perception channels at the thenar eminence with respect to contact size. Measurements were conducted with closed-loop velocity control of the stimuli. To address individual channels, combinations of frequencies, intensities, contact areas and masking effects are employed. The psychometric procedure used converges at a detection probability of $p = 0.75$. Figure is adapted from [110]

95% occurring at tangential displacement of 0.2 mm and a displacement speed of 1 mms^{-1}. The study further includes analysis of priming and learning effects and the application to skin stretch based communication devices.

One of the most important effect on haptic perception originates in the size of the contact area. All of the above mentioned studies show lower perception thresholds for frequencies around 200 Hz with larger contact areas. However, this effects seems to be limited by the minimum area required to arouse mechanoreceptors in the PC channel, which is probably about 3 cm^2, corresponding to a contactor diameter of about 20 mm. When more than one finger is involved in the interaction, [24] did not found a summation effect of thresholds.

Regarding the perception of forces, the corresponding absolute thresholds can be calculated according to Eq. (2.9). There are only a few studies dedicated to the absolute perception of forces. THORNBURY AND MISTRETTA investigate the sensitivity to tactile forces applied by a modified version of von-Frey filaments. They find a significant influence of age on the absolute threshold that is most likely related to the decrease of mechanoreceptor density. Young subjects (mean age 31 years) exhibit absolute thresholds of 140 µN, while older subjects have higher thresholds of about 660 µN, measured with a staircase method, constant stimuli intensities and a 2IFC paradigm. Since the stimuli were applied manually by the experimenter, application dynamics cannot be determined from the study but probably contribute to the very low reported thresholds. ABBINK AND VAN DER HELM investigated absolute force perceptions at the foot with different footwear (socks, sneaker, bowling shoe) for low-frequency stimuli (< 1 Hz) and a static preload of 25 N. They find lowest perception thresholds of 8 N in the sock condition, whereas the perception threshold is

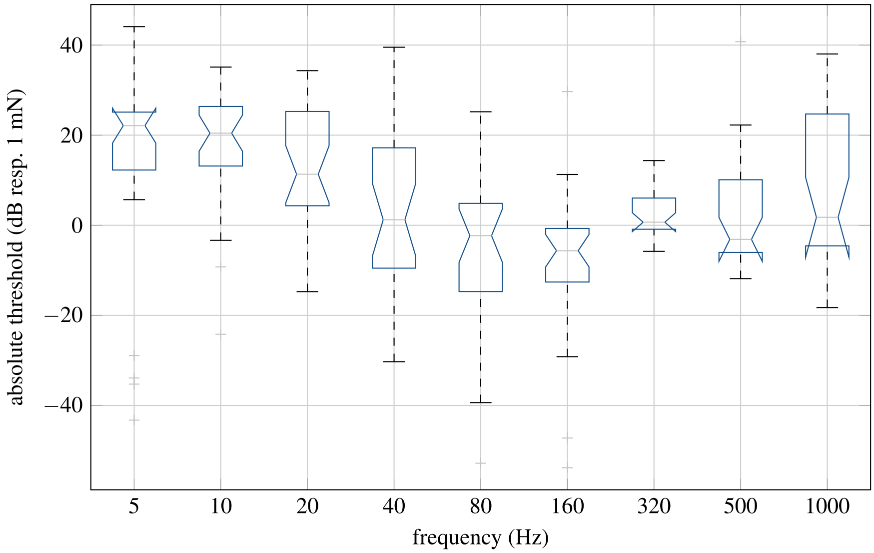

Fig. 2.16 Absolute force perception threshold based on experiments with 27 test persons, measured with a quasistatic preload of 1 N. Thresholds are obtained with an adaptive staircase procedure converging at a detection probability of 0.707 with an 3IFC paradigm. Data is given as boxplot, since not all data for each frequency are normal distributed. The boxplot denotes the median (horizontal line), the interquartile range (IQR, closed box defined by the 0.25- and the 0.75-quantile), data range (dotted line) and outliers (data points with more than 1.5 IQRs from the 0.25- or the 0.75-quantile). The indentation denotes the confidence interval of the median ($\alpha = 0.05$). Data taken from [74, 106]

defined with a detection probability greater than 0.98. Also motivated by the small number of studies, the author of this chapter measured perception thresholds for vibrotactile forces up to 1000 Hz as shown in Fig. 2.16.

In summary, one can find a large number of studies determining absolute thresholds for the perception of stimuli defined by deflections. Less studies are conducted regarding the absolute perception of forces. Table 2.4 summarizes some values of absolute perception thresholds for the human hand.

2.1.3.2 Differential Thresholds

For haptics, several studies furnish evidence about the applicability of Weber's Law as stated in Eq. (2.5). Gescheider et al. [121] as well as Verrillo et al. [122] measure ↪ JNDs of 1 … 3 dB for deflection-defined stimuli with reference stimuli of 5 … 40 dB above absolute threshold for frequency ranges exceeding 250 Hz. The measurements of Gescheider et al. are based on broadband and single frequency stimulus excitation. They show an independence of channels for the JND, whereas no fully constant JND was determined for high reference levels. This is addressed

Table 2.4 Selected absolute thresholds of the human hand

Base item	Threshold	Body part	Value	Source
Static stimuli	Skin deformation	Fingertip	10 μm [a]	[112]
	Two-point threshold	Fingertip	2–3 mm [b]	[6, 112]
	Force	Palm	10–11 mm	[112, 113]
		Fingertip	0.8 mN	[6]
	Pressure	Palm	1.5 mN	[6]
		Fingertip	0.2 N/cm^2	[113]
Dynamic stimuli	Frequency, upper limit	Finger (tactile)	5–10 kHz	[6, 114]
		Whole body (kinaesthetic)	20–30 Hz	[114]
	Maximum sensitivity	Fingertip, palm	At 200–300 Hz [c]	[88]
	Amplitude	Fingertip, palm	0.1–0.2 μm (normal stimulation) at 200–300 Hz [d]	[88]
		Whole hand, grasping	0.2–0.3 μm at 150–200 Hz (tangential stimulation) [e]	[115]
		Sphere, stylus	0.2–0.3 μm at 160 Hz [f]	[104, 105]
	Two-point threshold	Fingertip	0.8 mm [g]	[116]

[a] If movement is permitted, isolated surface structures of 0.85 μm height can be perceived [36, 117]. If surface roughness is to be detected, stimuli as low 0.06 μm are perceived [36]

[b] The two-point threshold decreases, if the two stimuli are presented short after another, a position change of a stimulus can be resolved spatially up to ten times better than the static two-point threshold [112]

[c] The perception threshold is strongly dependent on the vibration frequency, the location of the stimulus and the size of the contact area [88]

[d] Amplitudes larger than 0.1 mm are perceived as annoying at the fingertips [118]. A stimulation with constant frequency and amplitude results in a desensitization, increasing up to a numb feeling which may last several minutes after the end of the stimulation [119, 120]

[e] Whole hand grasping a cylinder with a diameter of 32 mm. Vibrations were created along the cylinder axis

[f] Sphere with a diameter of 2 inches was grasped with the *phalanx distalis* of all fingers, the stylus is taken from a PHANToM haptic interface and held with three fingers

[g] A correct detection probability of at least 0.75 was measured for 12 frequencies ranging from 1 to 560 Hz in 22 subjects

Table 2.5 Relevant parameters and results of studies of dynamic force JNDs. Table based on [74]

Source	Reference stimulus (N)	Stimulus frequency	Interaction condition[a]	JND[b]
[125]	2.25	Not given	Active	10%
[126]	2.5; 3.5	Not given	Active	12%
[127]	Not applicable[c]	Up to 200 Hz (estimated[c])	Active	10%
[128]	0.3; 0.5; 1; 2.5	Quasistatic	Passive	43% ...15%
[129]	1.5	Quasistatic	Passive	10%
[130]	1; 2	100 ... 500 Hz (discrete frequencies)	Passive	23% ...13%

[a] In active conditions, test subjects were required to apply movement by their own, while in passive conditions only the measurement setup exerts forces on the subject
[b] Ordering according to reference force ordering
[c] JNDs are based on an experiment, where subjects could interact freely with a custom haptic interface described in [127]

as *"a near miss to Weber's Law"* by the authors [121], but this observation should not have a significant impact on the design of haptic systems.

Regarding the JND of forces, several studies were conducted with an active exertion of forces by the test person. Jones measures JNDs of about 7% from matching force experiments of the elbow flexor muscles [123], a value that is confirmed by Pang et al. [124]. However, one cannot determine the measurements dynamics from the experimental setup, based on Fig. 1.9 a maximum bandwidth of 10 ... 15 Hz seems to be likely. From other studies evaluating the perception of direction and perception-inspired compression algorithms (Sect. 2.4.4) estimations of the JND for forces can be made. This is summarized in Table 2.5. All studies show JNDs over 10% for reference stimuli well above the absolute threshold and increasing JNDs for reference stimuli near the absolute threshold.

Own studies of the author of this chapter evaluated the JND for dynamic forces in the range from 5 ... 1000 Hz. As reference stimuli, the individual perception threshold and fixed values of 0.25 N and 0.5 N were used. The results are given in Fig. 2.17. They show no channel dependence (despite a significant higher value for the JND at 1000 Hz) and affirm the increasing JND for reference stimuli near the absolute threshold. However, with about 4 ... 8 dB for frequencies less than 1000 Hz the JND in the 0.25 and 0.5 N condition is higher than the previously reported values.

Jones and Hunter investigated the perception of stiffness and viscosity and found JNDs of 23% for stiffness [133] and 34% for viscosity [134] with a matching procedure using both forearms with stimuli generated by linear motors. The JND for stiffness is similar to other studies as reported in [135, 136]. Further differential thresholds for the perception of haptic measures by the human hand are given in Table 2.6.

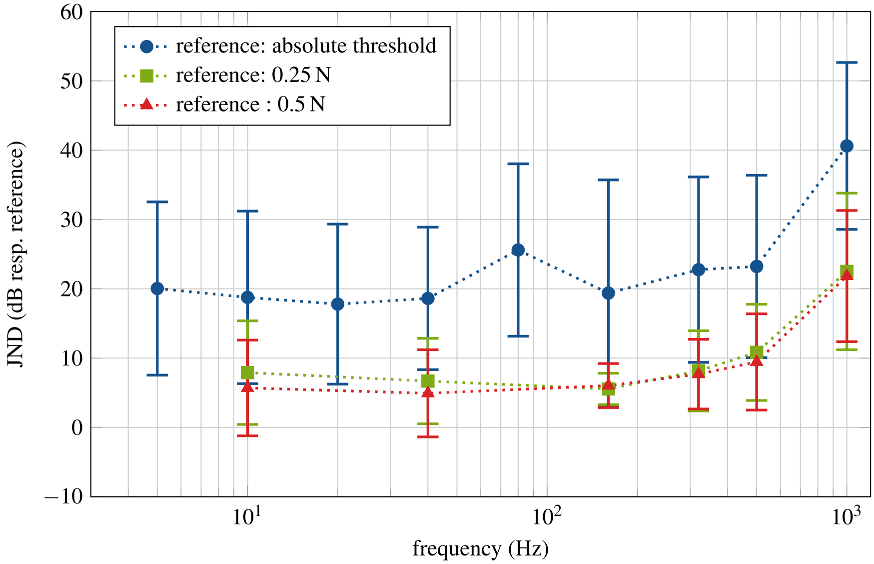

Fig. 2.17 Just Noticeable Differences of dynamic forces JNDs were calculated with an adaptive staircase procedure converging at a detection probability of 0.707 and a 3IFC paradigm from studies conducted with 29 test persons (absolute threshold reference) and 36 test persons (0.25 and 0.5 N reference conditions) respectively. The test setup is described in [131] © Elsevier, all rights reserved, a static pre-load of 1 N was used. Data taken from [74, 132]. © Springer Nature, all rights reserved

2.1.3.3 Object Properties

The properties of arbitrary objects are closely related to the interaction primitives. Typical exploration techniques to detect object properties are dealt with in the following section. Despite the basic perception of form, size, texture, hardness and weight of an object, there are are couple of other properties relevant to the design of haptic systems. BERGMANN TIEST reviews a large number of studies regarding the material properties roughness, compliance, temperature, and slipperiness. The results are relevant for the design of devices to display such properties, the representation of compliance is especially relevant for the interaction with virtual realities. Key points of the analysis are outlined in the following based on [143], whereas primary sources and some other references are cited as well. KLATZKY ET AL. also review the perception of object properties and algorithms to render this properties in engineering applications [144]. The work of SAMUR, summarizing several studies about the perception of object properties, could be of further interest [145].

Roughness Roughness is one of the most studied object properties in haptic perception. The perception of roughness is based on an uneven pressure distribution on the skin surface for static touch conditions and the vibrations arising when stroking a surface or object dynamically. It was shown, that finer textures with

Table 2.6 Selected differential thresholds of the human hand

Base item	Threshold	Body part	Value	Source
Static stimuli	Force	Finger-span	5 … 10%	[136]
	Deflection	Fingertip	10 … 25%	[137]
	Length	Finger-span	3 … 10%	[136]
	Compliance	Finger-span	5 … 15%	[136]
	Pressure	Wrist	4 … 19% [a]	[138]
	Torque	Thumb, index finger	13%	[135, 139]
	Position-resolution (kinaesthetic) [b]	Finger joint	2.5°	[138]
		Wrist, elbow	2°	[138]
		Shoulder	0.8°	[138]
	Force direction	Pen-hold posture [c]	25 … 35°	[140, 141]
Dynamic stimuli	Vibration amplitude at 160 Hz	Fingertip	16%	[142]
	Frequency-resolution	Fingertip (tactile)	8 … 10% [d]	[137]
	Successiveness limen	Mechanoreceptor property	5 ms [e]	[6]

[a] Experiment was made with a reference pressure of 1.8 N/cm^2 at the dorsal side of the wrist. JND increased strongly with reduced contact area: 4.4% at 5.06 cm^2, 18.8% at 1.27 cm^2 [138]
[b] Test subject's limbs were positioned by the experimenter with no active movement involved
[c] A PHANToM haptic interface was used in both studies
[d] The capability to differ stimuli is reduced after 320 Hz [114]
[e] If one has to decide which of two stimuli was applied first, a minimum time of 20 ms has to be between the onset of the two stimuli [6]

particle sizes smaller than 100 μm can only be detected in dynamic touch conditions, while coarser textures can be detected in static conditions, too. Active and passive touch conditions have no effect on the perceived roughness. This is called the *duplex theory of roughness perception* [146]. However, not only sensitive bandwidth and the touch condition have an influence on the human ability to perceive roughness. Other studies found influences of the contact force, other stimuli in the tested set and the friction between surface and skin. Regarding differential thresholds, Knowles et al. found JNDs of 10 … 20% for friction in rotary knobs [147], Provancher et al. recorded JNDs of 19 … 28% for sliding virtual blocks against each other [148].

Scaling experiments showed that roughness can be identified as the opposite to smoothness. In similar experiments, no effect of visual cues was found and a power-function exponent (Eq. (2.8)) of 1.5 was measured. In a nutshell, the perception of roughness appears to be a complex ravel of not only material properties, but also of interaction conditions like friction and contact force. This makes the modeling of roughness challenging, on the other hand, there are a vast number of possibilities to display roughness properties in technical systems [149].

Compliance This property describes the mechanical reaction of an material to an external force. It can be described by the Young's Modulus or—technically more relevant—the stiffness of an object, that combines material and geometric properties of an object as shown further on in Eq. (2.10). When evaluating physical stiffness with the perceived compliance, a power-function exponent of 0.8 was calculated and softness and hardness were identified as opposites. For the perception of softness, cutaneous and kinaesthetic cues are used, while cutaneous information is both necessary and sufficient. Studies by Bergmann Tiest and Kappers determined that soft materials were mostly judged by the stiffness information, i.e. the relationship of material deformation to exerted force, while harder stimuli are judged by the surface deformation [150].
Several other studies show that the perception of the hardness, i.e. the contrary of compliance, of an object is better modeled by the relation of the temporal change of forces compared to the penetration velocity than by the normally employed relation of force to velocity [151]. This has to be considered in the rendering of such objects and is therefore dealt with in Chap. 12. To render a haptic contact perceived as undeformable, necessary stiffnesses from 2.45 Nm^{-1} [138] to 0.2 Nm^{-1} [152] are reported.

Slipperiness Slipperiness is not researched very deeply until now. It is physically strongly related with friction and roughness. The detection of slipperiness is important for the adjustment of grip forces when interacting with objects. While an accurate perception of slipperiness requires some relative movement, micro-slip movements of an grasped objects that are sensed with cutaneous receptors are made responsible for the adjustment of grip forces [153]. Studies show forces just 10% higher than the minimum force needed to prevent slip. The adjustment occurs with a reaction time of $80 \ldots 100\,\mathrm{ms}$, that is faster than a deliberate adjustment [154].

Viscosity Not necessarily an object property, the ratio between shear stress and shear rate is relevant for virtual representation of fluids and visco-elastic materials. Based on real viscous fluids stirred with the finger and a wooden spatula, Weber fractions of about 0.3 were determined for high viscosities with increasing values for low viscosities [155]. Regarding scaling parameters, power function exponents for stirring silicone fluids of 0.42 are reported [83, Chap. 1].

Curvature While curvature itself is not necessarily relevant for the design of haptic systems, the detection capabilities of humans are quite astonishing. In [156] subjects were able to report a curvature with a base-to-peak height of just 90 μm on a strip with the length of 20 mm. However, the researchers suggest a measure of base-to-peak height in relation to half the strip length to generate a robust measure for curvature perception that can be interpreted as the perceivable gradient. This measure leads to a unit-less parameter with a value of 0.09. Differential thresholds are reported to be about 10% for convex curvatures with radii ranging starting from about 3 mm [157]. In the same study, convex curvatures with a radius of 204 mm could discriminated from flat surfaces, for concave curvatures a threshold of 185 mm could be assessed with a detection probability of 0.75.

Temperature Although not only a object property, basic properties of temperature perception are summarized here, partly based on [13]. Humans can detect intensity differences in warming pulses as low as 0.1% (base temperature of 34 °C, warming pulse with base intensity of 6 °C) [158]. Changes of 0.16 °C for warmth and 0.12 °C for cold from a base temperature of 33 °C can be detected at the fingertip and are still lower for the thenar eminence. When skin temperature changes slowly with less than 0.1 $°\mathrm{Cs}^{-1}$, changes of up to 6 °C in a zone of 30–36 °C cannot be detected. More rapid changes will make small changes perceivable. The technical use of temperature perception is limited by a temperature of 44 °C, where damage is done to the human skin [159].

Perceptually more relevant is the thermal energy transfer from skin into the object. Humans are able to discriminate a chance in heat transfer of about 35–45%. Because of different thermal conductivity and specific heat capacity, different materials can be identified by static touch alone. On this heat transfer mechanisms, the modeling, rendering and displaying thermal information is discussed in a number of studies cited in [143]. For technical applications, Jones and Ho discuss known models and the implications for the design of thermal displays [160].

Despite these general properties, there is a vast number of more complex object properties, that arise largely in the interpretation of the user. It is difficult to find clear technological terms for these interpretation. In literature one can find one approach to describe this interpretations: Users are asked to rate objects on different scales called semantic differentials. Based on these ratings, a multi-dimensional scaling procedure will identify similar scales [161]. Regarding surface properties, Hollins showed three general dimensions perceived by an user: rough ↔ smooth, hard ↔ soft and a third, not exactly definable dimension (probably elastic compressibility) [162]. This approach is also successfully used in the evaluation of passive haptic interfaces [163]. The accurate display of surface properties is still a relevant topic in haptic system design. Readers interested in this topic are pointed to the work of Wiertlewski [164] and the results of the Haptex-Project [165].

2.1.3.4 Scaling Parameters

Another important psychophysical measure is the interpretation of the intensity of different stimuli by the user, normally termed scaling. Especially for tactile applications, the perception of the intensity of normal and lateral applied stimuli is of importance. One of the first comparisons of the perception of tangential and normal stimuli was carried out by Biggs and Srinivasan. They found a 1.7 … 3.3 times higher sensitivity for tangential displacements compared to normal stimulation at both the forearm and fingerpad. They conclude, that tangential displacement is the better choice for peak displacement limited actuators, while normal displacement

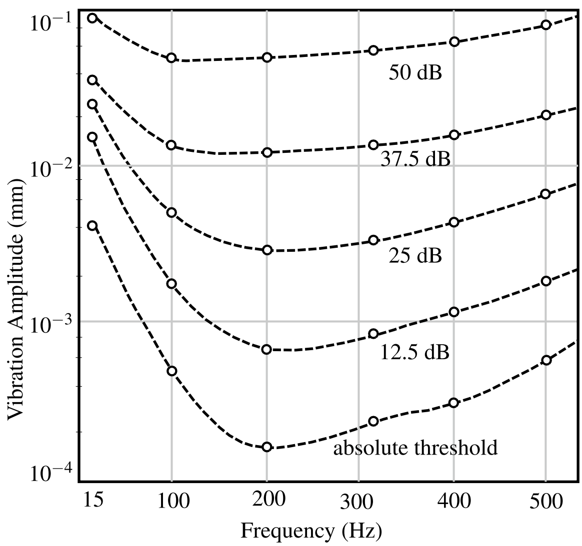

Fig. 2.18 Curves of equal perceived intensity at the fingertip. The lowest curve denotes the measured absolute threshold, while the upper curve is perceived as nuisance. Figure is adapted from [118]

should be chosen for actuators limited in peak forces. One has to note that this not caused by higher sensitivity, but differences in the mechanical impedance for normal and tangential stimuli [166].

Classical psychophysical evaluation of scaling behavior is reported by HUGONY in the last century. Figure 2.18 shows the result as curves of equal perceived intensity, denoting stimulus amplitudes for different frequencies that will be perceived as equal intense by the user. Such curves can be applied to generated targeted intensity changes of complex stimuli: A slight amplitude increase for low-frequency-components will evoke the same perceived intensity than a much larger amplitude change of mid- and high-frequency components. This behavior can be optimized with regard to the energy consumption of the actuators in a haptic system.

The results further imply perception dynamics as high as 50 dB (defined as difference between absolute threshold and nuisance level), that are confirmed by newer studies like [122] stating a dynamic of 55 dB. Other results from the study imply an amplitude JND of 10 ... 25% and a JND of 8 ... 10% for frequency. This goes along well with the above reported results.

2.1.3.5 Some Words About the Quality of Studies About Haptic Perception

Studies of haptic perception are conducted by scientists with various backgrounds. Depending on the formal training and customs in different disciplines, the author experienced a large variety of qualities of haptic perception studies. Based on his own training in measurement and instrumentation and own studies dealing with haptic perception, the following hints are given on how to assess the quality of a perception study for further use in the design of haptic systems.

Measurement Goal and Hypothesis A hypothesis should be stated for each experiment. Hypothesis formulated in terms of well-established psychophysical properties like the ones described above (Sect. 2.1) are preferable for the latter comparability of the study results. Further, external influencing variables should be considered in the hypothesis formulation. In general, one can differentiate dependent, independent, controllable and confounding variables as shown in Table 2.7 for investigations of haptic perception.

Independent variables are addressed in the formulation of the hypothesis and are varied during the experiment. Depending on the hypothesis, known influencing variables can be considered as independent or controllable variable. Controllable variables will have a known effect on the result of the experiment and should therefore be measured or closely watched. Possible means are keeping the test setup at constant temperature, a pre-selection of test subjects based on age, body length and weight etc. Confounding variables will contribute to the measurement error and cannot be completely taken care of.

Measurement Setup and Errors The measurement setup of a haptic perception study should be well fit for the investigated perception parameter or intended result. This means for example, that all parts of the measurement setup should exhibit adequate frequency response, rated ranges and sampling rates for the expected values in the experiment.

The design and construction of the setup should be neat to prevent unwanted effects and errors like for example electromagnetic disturbance by other equipment in the lab. Setups should favorably be fully automated to prevent errors induced by the experimenter.

The setup should be documented including all procedures and measurements of systematic and random errors. Based on a model of the measurement setup and its components, an analysis of systematic error propagation should be conducted as well as a documented calibration of the setup and its components with known input signals and a null signal. Long time stability, reproducibility, external influences and random errors should be analyzed and documented. Application of standardized methods like the ↪ Guide to the Expression of Uncertainty in Measurement (GUM) [167] is preferable. If possible, systematic errors should be corrected.

Measurement Procedure There should be a considerable amount of test persons in a study, a dedicated statistical analysis with less than 15 subjects seems to be questionable and should at least be explained in the study, explicitly addressing the type II error of the experiment design [168]. Larger numbers of 30 and more subjects are probably advisable.

Regarding psychophysical procedures, a previously reported and favorably adaptive procedure should be used. Newer studies should only used non-adaptive procedures in case of non-changeable stimuli (like gratings on real objects). The report of pre-tests and the impact on the design of the final study should be

Table 2.7 Possible variables in haptic perception experiments

Type	Examples
Dependent variables	Psychophysical properties
Independent variables	Contact area, contact force, masking stimuli, other treatments
Controllable variables	Skin moisture, skin temperature, test person's age, systematic errors of the setup
Confounding variables	Fatigue, test person's experience, multimodal interaction, unacquainted factors

discussed in the documentation. Interactions with other sensual modalities like vision and audition should be kept in mind and eventually controlled, for example by ear plugs and masking noise.

Analysis Data sets not included in the analysis should be addressed and the criteria for this decision must be reported. All results should be analyzed statistically and the location parameters of the results should be given (i.e. mean and standard error for normal distributed results, and median and IQR for not normal distributed results). If external parameters are included in the study, an analysis of variance (ANOVA) as well as post-hoc tests for significance of treatment group averages should be conducted and reported. If other analysis tools like for example a confusion matrix are used, effort should be put into a statistical analysis of the significance of the result. Errors of the measurement setup should be addressed in the analysis.

If possible, results should be compared to other studies with similar setups and intention. When large differences occur, a detailed discussion of these differences and suggestions for further studies is advisable. To enable further studies based on the experiment results, test results for all effects (not only the significant ones) should be reported, as they can be used to determine effect sizes (useful for sample size calculations, see [168]) and to conduct meta-studies [169].

If all of the above hints are considered, most conference proceedings would not report results, but only measurement setups and their characterization. However, keeping the criteria for good measurement setups in mind will improve the quality of results and the broaden the usage possibilities of the study results.

2.1.4 Further Aspects of Haptic Perception

Despite the classic psychophysical questions *(detection, discrimination, identification, scaling)*, there are a couple of other aspects relevant for the design of haptic systems. Some of them are discussed briefly in the following.

2.1.4.1 Effects of Multiple Stimulation

When more than one stimulus is applied in close temporal or spatial proximity to the first stimulus, several effects of multiple stimulation are known. The following list is based on VERRILLO [122]:

Masking This effect describes the decline of the detection ability of a stimulus, when an additional, disturbing stimulus, the so-called masker, is present at the same location in temporal proximity. Masking can occur when masker stimuli are present before, while and after the actual stimulus is presented. The masking properties depend on frequency and amplitude of the masker as well as on age of the test person and the receptor channel involved. When the masker is presented right before the test stimulus ($< 1\,\mathrm{s}$), the amount of masking depends on the time offset between masker and stimulus [170, 171], which is specific for each receptor channel. If a dedicated masker is used, specific receptor channels can be addressed. This is an important procedure to investigate properties of individual channels [172]. Masking finds application in the perception-based compression of data streams, for acoustics this is one of the main elements of the MP3-format [173].

Enhancement This effect occurs when a conditioning stimulus causes a stimulus in temporal succession to appear to be of greater intensity.

Summation When two ore more stimuli are presented closely in time, the combination of the sensation magnitude is described as summation.

Suppression This effect is basically a masking effect, when both stimuli are presented at different locations.

For haptics, especially masking effects were investigated, mainly by the group of GESCHEIDER ET AL. [104, 171, 172, 174–177]. Studies of other effects are not known to the author. At the moment, these multiple stimulation effects have to be considered as side-effects in haptic interaction. Except for the analysis of receptor channels, there is no direct use of one known to the author.

2.1.4.2 Linearity of Haptic Perception

Recent studies imply, that the channels of haptic perception do not only have independent thresholds [178], but resemble a linear system. CHOLEWIAK ET AL. investigated spatial displayed gratings and found a necessity for each spatial frequency harmonic to be higher than the perception threshold at that frequency to be perceived by the user [179]. These results allow to consider error margins and detection thresholds independently for each frequency in the design of haptic systems [180].

A first application of this property of haptic perception was presented by ALLERKAMP ET AL. in the design of a haptic system to describe surface properties of textiles: analog to the spectral decomposition of an arbitrary color into red, green and blue, textures were analyzed to be represented by two dedicated vibration

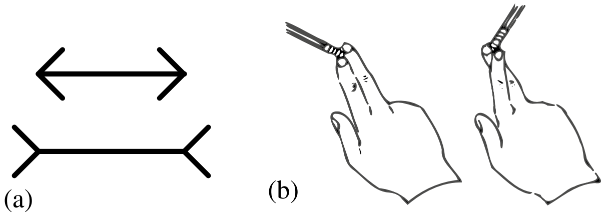

Fig. 2.19 Examples of haptic illusions **a** MÜLLER- LYER-illusion, **b** ARISTOTELES-illusion

frequencies for single receptor types [181]. This approach minimizes hardware and data storage effort to present complex surface properties.

2.1.4.3 Anisotropy of Haptic Perception

Despite the above mentioned differences in the scaling of lateral and tangential stimuli on the skin, there is also an anisotropy of kinaesthetic perception and interaction capabilities [126, 182, 183]. The perception and control of proximal movements (towards the body) is worse than movements in distal direction (away from the body). This property can be of meaning in the ergonomic design of workplaces with haptic interfaces and in tests and evaluations based on Cartesian coordinates.

2.1.4.4 Fooling the Sense of Touch

As well as in acoustics and vision, there are a couple of haptic illusions. They are generated by anatomic properties, neural processing or mis-interpretation of percepts like a conflict of visual and haptic perception [140]. Since many visual illusions can be found in haptics, too, and because of the similar neural processing and interpretation mechanisms, an explanation analogue to the visual system is anticipated [184]. As HAYWARD puts it, "Perceptual illusions have furnished considerable material for study and amusement" [185]: Two examples of basic haptic illusions are given in Fig. 2.19. The MÜLLER- LYER-illusion on the left side is borrowed from visual perception, but can also be proven for haptic stimuli. Both lines are perceived as of different length because of the arrow heads, even if they have the same length. The ARISTOTELES illusion can be reproduced easily by the reader: Touching an object like a pencil with crossed fingers will evoke the illusion of two objects. If a wall is touched instead of an object, a straight wall will be perceived as a corner and vice versa. Further illusions can be found in the works of HAYWARD and LEDERMAN [185, 186].

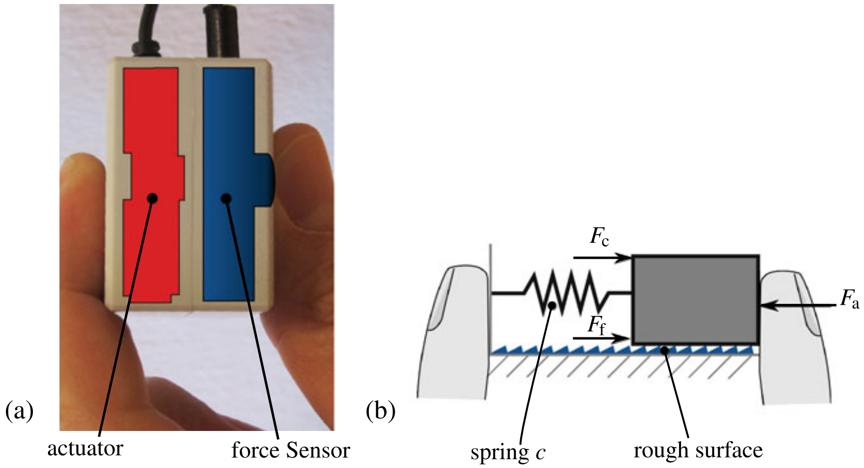

Fig. 2.20 KOOBOH, **a** outer form and internal components, **b** internal system model. Picture courtesy of J. Kildal, *Nokia Research Center*, Espoo, FIN, used with permission

Example: Kooboh

An application of haptic illusions in the design of haptic systems was presented by KILDAL in 2012 [187]. KOOBOH consists of a solid, non-deformable box with an integrated force sensor and a vibration actuator as shown in Fig. 2.20. The control software simulates an internal system model containing a spring connected with a (massless) object sliding on a rough surface.

The user applies a force F_a to the system, normally resulting in a deflection $d = \frac{F_a}{c}$ of the spring c. When the object is moved because of the applied force, a frictional force F_f would be generated depending on the texture of the rough surface and the position of the object. Since the box is non-deformable, the reaction of the (virtual) spring cannot be felt. But because the applied force is measured by the force sensor, the theoretical deflection of the object and the therefrom resulting friction force F_f can be calculated. Depending on the structure of the rough surface, F_f will exhibit periodical, high-frequency contents that can be displayed by the integrated actuator. The user interprets these two contradictory percepts as a fully functional model as shown in Fig. 2.20, efficiently neglecting that the system does not move.

Pseudo-Haptic Feedback

A important technical application of another kind of haptic illusions is the usage of disagreeing information on the visual and the haptic channel. Termed "Pseudo-haptic feedback" it is used in virtual environments to simulate properties like stiffness, texture or mass with limited or distorted haptic feedback and accurate visual feedback [54, 188]. A simple example is given by KIMURA ET AL. in [189] as depicted in Fig. 2.21. A visual representation of a spring is displayed on a mobile phone equipped with a force sensor. The deformation of the visual representation is depending on

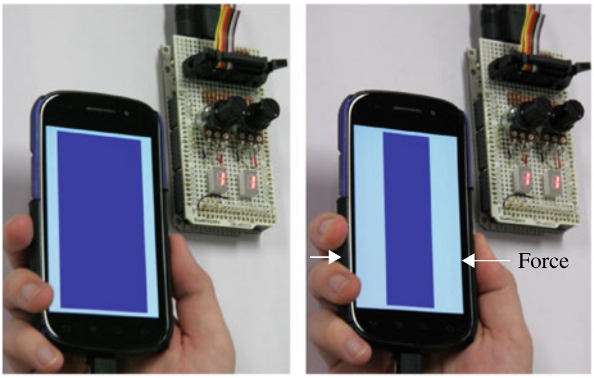

Fig. 2.21 Pseuo-haptic feedback in a mobile application [189] © Springer Nature, all rights reserved. Force exerted on the mobile device by the user is measured with pressure sensors. Based on this force, the deformation on the screen is calculated based on a virtual stiffness, leading to the impression of a compliant device. Pictures courtesy of T. Nojima, University of Electro-Communication, Tokyo, JP

the force applied and the virtual stiffness of the displayed spring. Changing the virtual stiffness leads to a different visual representation and a feeling of different springs—although the user will always press the unchanged mobile phone case.

2.1.4.5 Haptic Icons and Categorized Information

All of the above is based on continuous stimuli and their perception. Another important aspect is the perception of categorized information, that comes to use mainly in communication applications. Probably the most prominent example is the vibration alarm on a smartphone, that can be configured with different patterns for signaling a message or a call. Several groups investigated basic properties of such haptic icons (sometimes also called tactons or hapticons) [190–192]. They found different combinations out of waveform, frequency, pattern and spatial location suitable to create a set of distinguishable haptic icons based on multi-dimensional scaling analysis.

The use of categorized information in haptic systems introduces another measure of human perception, i.e. the information transfer (IT) [193]. This measure describes, how much distinguishable information can be displayed with the haptic signals defined by combinations of the above mentioned signal properties. However, it is no pure measure of perception, but also depends on the haptic system used. Because of that, it qualifies as a evaluation measure for haptic communication systems as detailed in Chap. 13. Reported information transfer ranges from 1.4–1.5 bits for the differentiation of force magnitude and stiffness [135] up to 12 bits for multi-axis systems especially designed for haptic communications of deaf-blind people [171, 194].

2.2 Concepts of Interaction

In daily life, only the least haptic interactions of man with the environment can be classified as solely passive, that are pure passive perception procedures. The most interactions are a combination of motion and perception to implement a prior defined intention. For the design of haptic systems, general agreed on terms are needed to describe intended functions of a system. In this section, some common approaches for this purpose are described. The section ends with a list of motion capabilities of the human locomotor system.

The taxonomy of haptic interaction by Samur as given in Sect. 1.4.2 is one of the possibilities. It was developed for the evaluation of systems interacting with virtual environments and is therefore most suitable for the description of such. Other interactions can be described by combinations of the taxonomy elements as well, but lack some intuition when describing everyday interactions. Stepping a little bit away from the technical basis of Samur's taxonomy and turning towards the functional meaning of haptic interaction for man an its environment, one will find the exploration theory of Lederman and Klatzky outlined in the following section. Further concepts like active and passive touch are described as well as gestures, that are commonly used as input modality on touch screens and other hardware with similar functionality.

2.2.1 *Haptic Exploration of Objects*

One of the most important task of haptic interaction is the exploration of unknown objects to assess their properties and usefulness. Not only tactile information, but also kinaesthetic perception contributes to these assessments. One of the most relevant sources for the evaluation of surfaces is the relative movement between the skin and the object.

In [195], Lederman and Klatzky identify different exploratory procedures that are used to investigate unknown objects. Figure 2.22 shows the six most important procedures [196]. Table 2.8 gives an insight about costs and benefits when assessing certain object properties.

2.2.2 *Active and Passive Touch*

The above described combination of movement action and perception is from such fundamental meaning, that two terms have been established to describe this type of interaction.

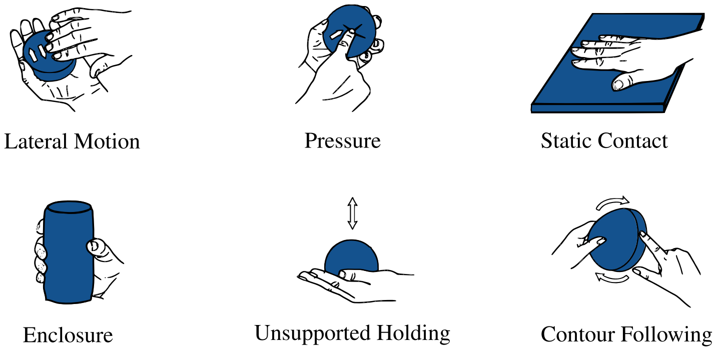

Fig. 2.22 Important exploratory procedures, figure adapted from [196]

Table 2.8 Correlation of exploratory procedures to ascertainable object properties according to [13]. ■ denotes properties that be can be asserted optimally by the exploration technique, □ denotes properties that are asserted in a sufficient way

	Texture	Hardness	Temp.	Weight	Vol.	mF	eF	Duration (s)	Active DoF
Lateral motion	■	□	□					3	2
Pressure	□	■	□					2	1
Static contact	□		■		□	□		<1	0
Unsupported holding				■	□	□		2	2
Enclosure	□			□	■	■		2	1
Contour following	□			□	□	□	■	11	3

Used abbreviations: temp. - temperature, vol. - volume, mF - macroscopic form, eF - exact form

Definition *Active Touch* Active touch describes the interaction with an object, where a relative movement between user and object is controlled by the user.

Definition *Passive Touch* Passive touch describes the interaction with an object, when relative movement is induced by external means, for example by the experimental setup.

Both conditions can be summarized as *dynamic touch*, while the touch of objects without a relative movement is defined as *static touch* [146]. This differentiation is indeed seldom used. Active touch is generally considered superior to passive touch in its performance. Lederman and Klatzky attribute this to the different focus of the observer [196, p. 1439]:

> *Being passively touched tends to focus the observer's attention on his or her subjective bodily sensations, whereas contact resulting from active exploration tends to guide the observer's attention to properties of the external environment.*

Studies show independence of the assessment of material and system properties from the exploration type (active or passive touch condition) [197, 198]. Active touch delivers a better performance for the exploration of geometric properties [196, 199] from a technical view, the implementation of active exploration techniques is a challenge, since transmitted signals have to be synchronized with the relative movement.

2.2.3 Gestures

Gestures are a form of non-verbal communication that are studied in a large number of scientific disciplines like social sciences, history, communication and rhetoric and—quite lately—human-computer-interaction. Concentrating on the latter, one can find gestures when using pointing devices like mice, joysticks and trackballs. More recently, gestures for touch-based devices became more prominent. Some examples are given in Fig. 2.23, for further information see [200] for a taxonomy of gestures in Human-Computer-Interaction. An informative list on all kinds of gestures can be found in the Wikipedia under the reference term "List of Gestures".

Gestures can be used as a robust input means in complex environments, as for example in the car as shown with touch-based gestures in Sect. 14.1 or based on a camera image [201]. For the use in haptic interaction, gestures have further meaning when interacting with virtual environments, as discrete input options in mobile applications, and in connection with specialized haptic interfaces like AIREAL [202], that combines a 3D camera with haptic feedback through an air vortex, or the Ultra-Haptics project, that generates haptic feedback in free air by superposing the signals from a matrix of ultrasound emitters [203]. In 2017 a standard on the usage of gestures in tactile and haptic interaction (ISO 9241-960) was created covering those among other items.

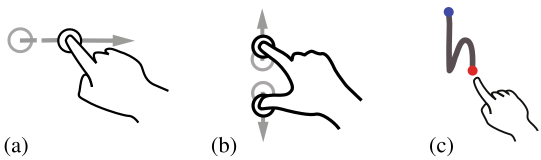

Fig. 2.23 Gesture examples for touch input devices. **a** Horizontal flicker movement, **b** two-finger scaling, **c** input gesture for the letter *h*. Pictures by *Gestureworks*, used with permission

2.2.4 Human Movement Capabilities

Since users will interact with haptic systems, the capabilities of their movement has to be taken into account.

2.2.4.1 Dynamic Properties of the Locomotor System

While anatomy will answer questions regarding the possible movement ranges ([204] for example), there are a few studies dealing with dynamic abilities of humans. TAN ET AL. conducted a study to investigate the maximum controllable force and the average force control resolution [138]. They found maximal controllable forces that could be maintained for at least 5 s in the range of 16–51 N for the joints of the hand and forces in the range of 35–102 N for wrist, elbow and shoulder joints. Forces about half as large as the maximum force could be controlled with an accuracy of 0.7–3.4%. This study is based on just three test persons, but other studies find similar values, for example when grasping a cylindrical grip with forces ranging from 7 N (proximal phalanx of the little finger) to 99 N (tip of the thumb) [205]. AN ET AL. find female's hand strengths in the range of 60–80% of male's hand strengths [206][2].

Regarding velocities, HASSER derives velocities of 60 ... 105 cms^{-1} for tip of the extended index finger [205] and about 17 rads^{-1} for the MCP- and PIP-joints. BROOKS reports maximum velocities of 1.1 ms^{-1} and maximum accelerations of 12.2 ms^{-2} from a survey of 12 experts of telerobotic systems [114].

2.2.4.2 Properties of Interaction with Objects

When touching a surface, users show exploration velocities of about 2 cms^{-1} (with a range of 1 ... 25 cms^{-1}) and contact forces ranging from 0.3 ... 4.5 N [207]. Other studies confirm this range for tapping with a stylus [208] and when evaluating roughness of objects [209]. SMITH ET AL. found average normal forces of 0.49 N–0.64 N for exploring raised and recessed tactile targets on surfaces with the index finger. Recessed targets were explored with slightly larger forces and lower exploring speed (7.67 cms^{-1} compared to 8.6 cms^{-1} for raised targets), increased friction between finger and explored lead to higher tangential forces. While the average tangential force in normal condition was 0.42 N, the tangential force was raised to 0.65 N in the increased friction condition (realized by a sucrose coating of the fingertip) [210].

For minimal invasive surgery procedures with a tool-mediated contact, radial (with respect to the endoscopic tool axis) forces up to 6 N and axial forces up to 16.5 N were measured by RAUSCH ET AL. High forces of about 4 N on average were recorded for tasks involving holding, pressing and pulling of tissue, low forces were

[2] Unfortunately, the number of test subjects involved in the studies is not reported.

used for tasks like laser cutting and coagulation, all measured with a force measuring endoscope operated by medical professionals as reported in [211, 212]. Tasks were carried out with movement frequency components of up to 9.5 Hz, which is in line with the above reported values (Fig. 1.9).

HANNAFORD once created a database with measurements of force and torque for activities of daily living like writing, dialing with a cell phone among others [213].

2.3 Interaction Using Haptic Systems

In this section, interactions Using haptic systems are discussed and the nomenclature for haptic systems is derived from these interactions. The definitions are derived from the general usage in the haptics community and a number of publications by different authors [214–218] as well as logically extended based on the interaction model shown in Fig. 2.24.

While used in a general way until here, the term *haptic systems* will be defined as follows:

> **Definition** *Haptic Systems* Systems interacting with a human user using the means of haptic perception and interaction. Although modalities like temperature and pain belong to the haptic sense, too, *haptic systems* refers only to pure mechanical interaction in this book. In many cases, the term *haptic device* is synonymously used for haptic systems.

In that sense, haptic systems will not only cover the fundamental haptic inputs and outputs, but also the system control instances needed to drive actuators, read out sensors and take care of data processing. This is in accordance to known definitions of mechatronic systems like the one by CELLIER [219]:

> *A system is characterized by the fact that we can say what belongs to it and what does not, and by the fact that we can specify how it interacts with its environment. System definitions can furthermore be hierarchical. We can take the piece from before, cut out a yet smaller part of it and we have a new system.*

The terms *system*, *device* and *component* are not defined clearly on an interdisciplinary basis. Dependent on one's point of view, the same object can be a "device" for a hardware designer, a "system" for a software engineer or just another "component" of another hardware engineer. These terms are therefore also used in different contexts in this book.

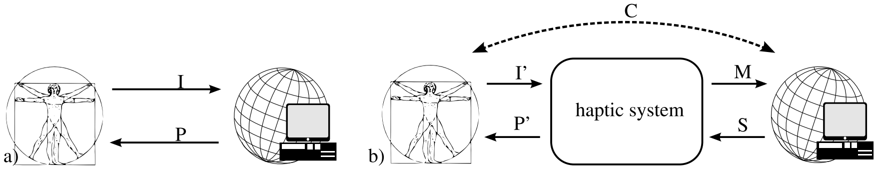

Fig. 2.24 Haptic interaction between humans and environment. **a** Direct haptic interaction, **b** Utilization of haptic systems. The interaction paths are denoted as follows: I—Intention, P—Perception, M—Manipulation, S—Sensing, C—Comanipulation/other senses

Compared to other perception modalities, haptics offers the only bidirectional communication means between the human user and the environment [220, p. 94]. A *user* is defined as

Definition *User* A person interacting (haptically) with a (haptic) system. The user can convey intentions to the system, receiving (haptic) information depending on the *application* of the system. In that sense, a *test person* or *subject* in a psychophysical experiment is a user as well, but not all users can be considered as subjects.

In this book, a haptic system is always considered to have a specific *application* as for example the ones outlined in Sect. 1.5. We therefore also define this term as follows:

Definition *Application* Intended utilization of a haptic system.

One has to keep in mind, that this definition includes ↪ commercial off-the-shelf (COTS) haptic interfaces coupled to a computer with a software program to visualize biochemical components as well as the use of a specially designed haptic display as a physical interface. Especially in this section, the term *application* has therefore to be considered context sensitive.

Figure 2.24 gives a schematic integration of an arbitrary haptic system in the interaction between a human user and a (virtual) environment. Based on this, one can identify typical classes of haptic systems.

2.3.1 *Haptic Displays and General Input Devices*

The probably most basic haptic system shown in Fig. 2.25 is a

> **Definition** *Haptic Display* A haptic display solely addresses the interaction path **P** with actuating functions. Mechanical reactions of the human user have no direct influence on the information displayed by the haptic display, since user actions are not recorded and cannot be provided to the application.

Haptic displays are used to convey information originating in status information of the system incorporating the display. Typical applications are $\hookrightarrow$ Braille row displays and—of course—the vibration alarm in mobile devices. Since the overlap to the next class of systems is somehow fuzzy, for the rest of this book a haptic display is defined as a device that only incorporates actuating functions but no sensory functions (except the internal ones needed for the correct functionality of the actuating part). These type of device is mainly used in communication applications like for example shown in Fig. 1.17, subfigure (a), (c) and (d). Often, a haptic display can be seen as a mechatronic component of a haptic system with additional functionality, for example an *assistive system* described in the next section.

For completeness, also systems addressing only the interaction path **I** can be identified. These are basically general input devices like buttons, keyboards, switches, touch screens and mice, that record intentions of the user mechanically and convey them to an application. Being mechanical components themselves, they naturally exhibit mechanical reactions felt as haptic feedback by the user, but these are normally independent from the application. For example, the haptic feedback from a computer keyboard is the same either for the *F1* key or the *Return* key, while the effects of these intentions are quite different. Therefore, general input devices are defined as devices with a predominant input functionality that can be used in different applications and a subordinated haptic feedback independent from the application and resulting unintended from the real mechanical design of the input device. With the focus on generality, specialized input devices like emergency stop buttons are excluded, since they exhibit a defined haptic feedback to convey the current state of the input device.

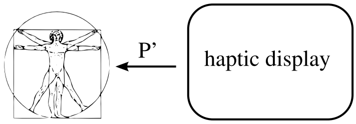

Fig. 2.25 Interaction scheme of a haptic display

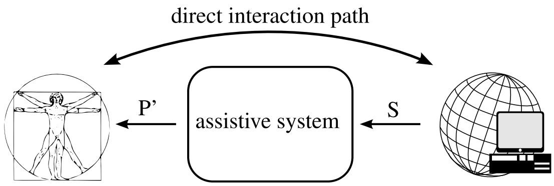

Fig. 2.26 Interaction scheme of an assistive system, that adds haptic feedback to an existing direct interaction

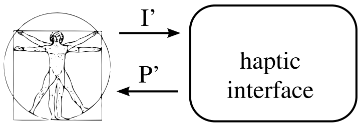

Fig. 2.27 Relevant interaction paths of a haptic interface

2.3.2 *Assistive Systems*

This class of haptic systems shown in Fig. 2.26 is based on haptic displays, but will also include an application dependent sensory function.

> **Definition** *Haptic Assistive System* System that will add haptic information to a natural, non technical mediated haptic interaction on path **P** based on sensory input on path **S**.

Assistive Systems are a main application area for haptic displays. The sensory input of assistive systems is not necessarily of a mechanical kind. However, compared to a haptic display as described above, an assistive system will add to existing, natural haptic interaction (i.e. without any technical means).

2.3.3 *Haptic Interfaces*

If an intention recording function and a *intended* haptic feedback functionality is combined, another class of haptic systems can be defined as shown in Fig. 2.27:

> **Definition** *Haptic Interface* Haptic interfaces address the interaction path **P** with actuating functions, but also record the user's intentions along the interaction path **I** with dedicated sensory functions. These data are fed to the application and evoke commands to the system or visualization under control, depending on the application a mechanical user input can result in direct haptic feedback.

Haptic interfaces are mostly used as universal operating devices to convey interactions with different artificial or real environments. Typical applications with task-specific interfaces include stall-warning sidesticks in aircraft and force-feedback joysticks in consumer applications. Another application is the interaction with virtual environments that is normally achieved with a large number of ↪ COTS haptic interfaces. These can also be used in a variety of other interaction tasks, some applications were outlined in Sect. 1.5. Some ↪ COTS haptic interfaces are shown in Fig. 2.28 as well as an example for a task-specific haptic interface for driving assistance. Other task-specific haptic interfaces are developed for the usage in medical training systems.

In general, ↪ COTS devices support input and output at only a single point in the workspace. The position of this ↪ Tool Center Point (TCP) in the workspace of the device is sent to the application and all haptic feedback is generated with respect to this point. Since the interaction with a single point is somewhat not intuitive, most devices supply contact tools like styluses or pinch grips, that will mediate the feedback to the user. This grip configuration is a relevant design parameter and further addressed in Sect. 3.1.3. Figure 2.29 shows some typical grip situations of ↪ COTS devices with such *tool-mediated contact*.

2.3.3.1 System Structures

To fulfill the request for independent channels for input (user intention) and output (haptic feedback) of the haptic interface and the physical constraint of energy conservation, one can define exact physical representations of the input and output of haptic interfaces. This leads to two fundamental types of haptic systems that are defined by their mechanical inputs and outputs as follows:

Fig. 2.28 Two haptic interfaces, (PHANToM Premium 1.5, © 2022 *3D Systems geomagic Solutions*, Rock Hill, SC, USA) and Accelerator Force Feedback Pedal (AFFP, © 2022 *Continental Automotive*, Hannover, Germany). Both images used with permission

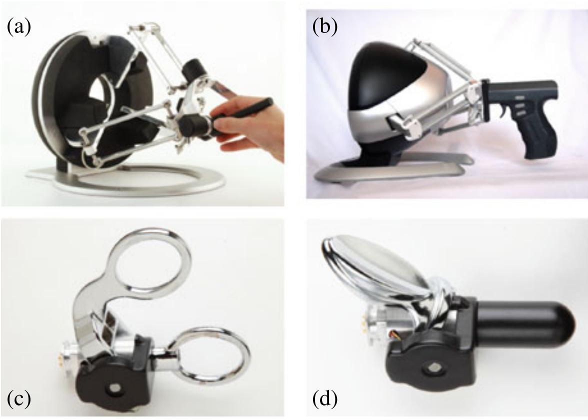

Fig. 2.29 Realizations of tool-mediated contact in commercial haptic interfaces. **a** OMEGA.6 with a stylus interface (*Force Dimension*, Nyon, Switzerland), **b** FALCON with a pistol-like grip for gaming applications (*Novint*, Rockville Centre, NY, USA), **c** and **d** pinch and scissor grip interfaces for the PHANToM PREMIUM © 2022 *3D Systems geomagic Solutions*, (Rock Hill, SC, USA). All images used with permission

Definition *Impedance-Type System* Impedance-type systems (or just *impedance systems*) exhibit a mechanical input in form of a kinematic measure and a mechanical output in form of a force or torque. In case of a haptic interface, the mechanical input (in most cases the position of the ↪ TCP device) is conveyed as an electronic output to be used in other parts of the application.

Definition *Admittance-Type System* Admittance-type systems exhibit a mechanical input in form of a force or a torque, that is conveyed as a electronic output in most cases as well. The mechanical output is given by a kinematic measure, for example deflection, velocity or acceleration.

The principle differentiation of impedance-type and admittance-type of systems is fundamental to haptic systems. It is therefore further detailed in Chap. 6.

2.3.3.2 Force Feedback Devices

The term *force feedback* is often used for the description of haptic interfaces, especially in advertising force-feedback-joysticks, steering wheels and other consumer products. A more detailed analysis of these systems yields the following characteristics for the majority of such systems:

System Structure Because of the output of forces, they resemble impedance-type systems as defined above.

Dynamics Force feedback systems address the whole dynamic range of haptic interaction, but do not convey spatially distributed (tactile) information.

Contact Situation Most force feedback systems do not allow for natural exploration, but will convey information via a tool.

These characteristics show a quite deep level of detail. The only comparable other term with similar detail depth is perhaps *tactile feedback*, mostly defining spatial distributed feedback in the dynamic range of passive interaction (Fig. 1.9). However, these terms are used so widely in technical and non-technical applications with different and not agreed on definitions, that they will not be used in this book in favor of other, clearly defined terms. In that cased, force feedback devices would probably better be described as *impedance type interfaces with tool-mediated haptic feedback*. Since this is a scientific book, the longer term is preferred to a unclear definition.

2.3.4 Manipulators

There is only a limited number of systems from outside the haptic community that can be classified as impedance systems. For admittance systems, one can find haptic interfaces (For example, the Haptic Master interface shown in Fig. 1.14 is an admittance-type interface) as well as mechanical manipulators from other fields. For example, industrial robots are normally designed as admittance systems that can be commanded to a certain position and measure reaction forces if equipped properly. In the here presented nomenclature of haptic system design, such robots can be defined as manipulators:

Definition *Manipulator* Technical system that uses interaction path **M** to manipulate or interact with an object or (remote) environment. Sensing capabilities (interaction path **S**) are used for the internal system control of the manipulator and/or for generating haptic feedback to a user.

Figure 2.30 shows the corresponding interaction scheme.

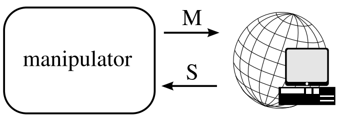

Fig. 2.30 Interaction scheme of a manipulator

2.3.5 Teleoperators

The combination of a haptic interface and a manipulator yields the class of teleoperation systems with the interaction scheme shown in Fig. 2.31.

> **Definition** *Teleoperation Systems* A combined system recording the user intentions on path **I** via the manipulation path **M** to a real environment, measuring interactions on the sensing path **S** and providing haptic feedback to the user via the perception path **P**.

An extension of teleoperators is the class of ↪ telepresence and teleaction (TPTA) systems, that include additional feedback from other senses like vision and/or audition. Both terms are used synonymously sometimes. Teleoperation systems allow a spatial separated interaction of the user with a remote physical environment. The simplest system is archived by coupling a impedance-type haptic interface with an admittance-type manipulator, since inputs and outputs correspond correctly. Often, couplings of impedance-impedance systems are used because of the availability of components, which generates higher demands on the system controller.

2.3.6 Comanipulators

If additional mechanical interaction paths are present, telepresence systems will turn into a class of systems called comanipulator [214]:

> **Definition** *Comanipulation System* Telepresence system with an additional direct mechanical link between user and the environment or object interacted with.

Comanipulator systems are often used in medical applications, since they minimize the technical effort compared to a pure teleoperator because of less moving mass, fewer active ↪ DOF and minimized workspaces, but also induce new challenges for the control and the stability of a system. In an application, the user will move the reference frame of the haptic system.

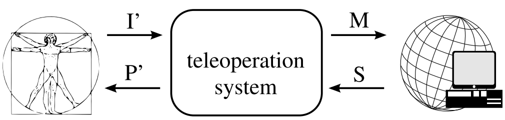

Fig. 2.31 Teleoperation interaction scheme

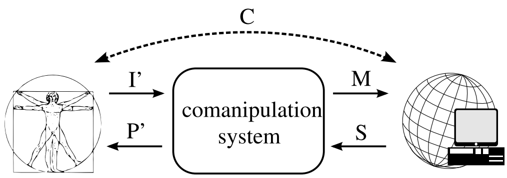

Fig. 2.32 Interaction scheme for comanipulators with an additional direct feedback via comanipulation path C

Compared to the above mentioned assistive systems, comanipulators exhibit a full teleoperational interaction scheme with additional direct feedback, while assistive systems will add additional haptic feedback to a non-technical mediated interaction between user and application. This is shown in Fig. 2.32.

2.3.7 Haptic System Control

To make the above described systems useable in an application, another definition of more technical nature has to be introduced:

Definition *Haptic System Control* The haptic system control is that part of a real system that will not only control the single mechanical and electrical components to ensure proper sensing, manipulating and displaying haptic information, but will also take care of the connection to other parts of the haptic system. This may be for example the connection between a haptic interface and a manipulator or the interface to some virtual reality software.

While the pure control aspects are addressed in Chap. 7, one has also consider other design tools and information structures like Event-Based-Haptics (Sects. 11.3.4, 11.3.4), Pseudo-Haptics (Sect. 2.1.4.4 and the general connection to software (Chap. 12) using a real interface (Chap. 11). In this book and in other sources, one will also find the term *haptic controller* used synonymously for the whole complex of the here-described haptic system control.

2.4 Engineering Conclusions

Based on the above, one can conclude a general structure of the interaction with haptic systems and assign certain attributes to the different input and output channels of a haptic system. This is shown in Fig. 2.33, that extends Fig. 2.24. In the figure, the output channel of the haptic system towards the user is separated in mainly tactile and mainly kinaesthetic sensing channels. This is done with respect to the explanations given in Sect. 1.4.1 and with the knowledge that there are many haptic interfaces that

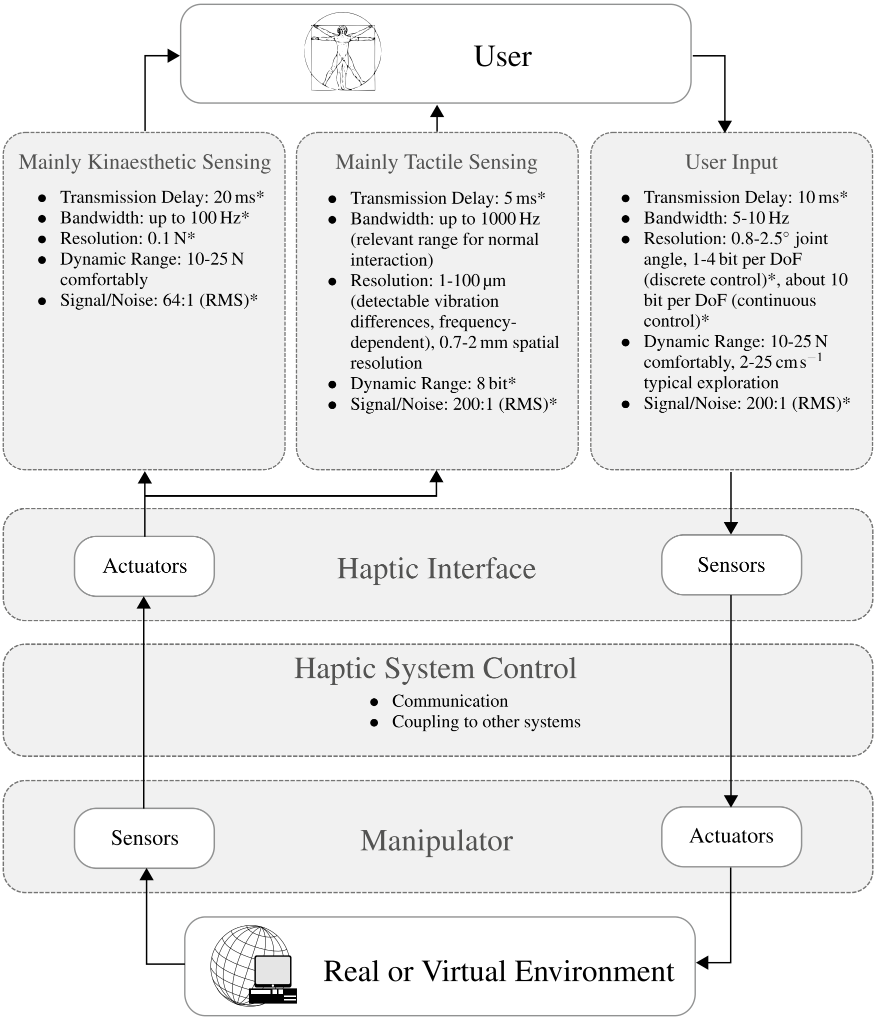

Fig. 2.33 General input and output ports for a haptic system in interaction with the human hand. Figure is based on [6, 221] © Wiley, all rights reserved, values form [221] are based on surveys among experts and are labeled with an asterisk (*), other values are taken from the different sources stated above

will fit in this classification, that will also be used further on in this book occasionally. The parameters given in Fig. 2.33 give an informative basis for the interaction with haptic systems.

In the remaining part of this section, several conclusions for the design of task-specific haptic systems are given based on the properties of haptic interaction.

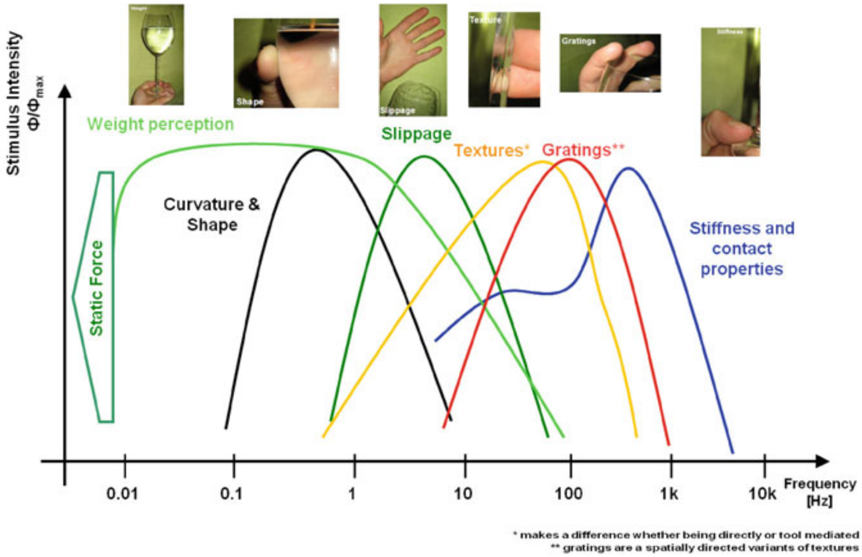

Fig. 2.34 Concept of modalities and their frequency dependency

2.4.1 *A Frequency-Dependent Model of Haptic Properties*

Haptics and especially tactile feedback is a dynamic impression. There are little to no static components. Without exploring scientific findings, a simple impression of the dynamic range covered by haptic and tactile feedback can be estimated by taking a look at different daily interactions (Fig. 2.34).

When handling an object, the first impression which will be explored is its *weight*. There is probably no one who was not caught by surprised at least once lifting an object which in the end was lighter than expected. The impression is usually of comparably low frequency and typically directly linked to the active touch and movement applied to the object.

Exploring an object with the finger to determine its fundamental *shape* is the next interaction-type in terms of its dynamics. When touching objects like that, a global deformation of the finger and a tangential load to its surface are relevant to create such an impression. There have been research performed by HAYWARD showing that indeed the pure inclination of the finger's surface already create an impression of shape. However, still being quite global the dynamic information coded in this property is not very rich.

Dynamics increases when it becomes urgent to react. One of the most critical situations our biology of touch is well prepared for is the detection of *slippage*. Constant control of normal forces to the object prevent it from slipping out of our grasp. Being highly sensitive to shear and stick-slip this capability enables us to gently interact with our surrounding.

When it comes to *slippage textured* surfaces and their dynamics must be mentioned too. Their frequency is of course depending on geometrical properties, however their exploration during active touch typically happens in the range above 100 Hz. Within this sensitive area discrimination capabilities of *textures* are naturally most sensitive, as the vibrotactile sensitivity of the human finger is climbing to its highest level.

Whether *gratings* do differ from *textures* is something which can be discussed endless. The principal excitation of the tactile sensory orchestra may be identical, however *gratings* are more like a dirac pulse, whereas *textures* are more comparable to a continuous signal.

Last but not least, hard contacts and the properties they reveal about an object reflect the most dynamic signal processing a haptic interaction may have. And surprisingly, a strong impact to an object reveals more about its volume and structural properties as any gentle interaction can ever show. Therefore *stiffness* is worth an own set of thoughts in the following section.

2.4.2 Stiffnesses

Already the initial touch of a material gives us information about its haptic properties. A human is able to immediately discriminate, whether he or she is touching a wooden table, a piece of rubber or a concrete wall with his or her finger tip. Besides the acoustic and thermal properties, especially the tactile and kinaesthetic feedback plays a large role. Based on the simplified assumption of a double-sided fixed plate its stiffness k can be identified by the usage of Young's modulus E according to Eq. (2.10) [222].

$$k = 2\,\frac{b\,h^3}{l^3} \cdot E \tag{2.10}$$

Figure 2.35a shows the calculation of stiffnesses for a plate of an edge length of 1 m and a thickness of 40 mm of different materials. In comparison, the stiffnesses of commercially available haptic systems are given in (Fig. 2.35b). It is obvious that these stiffnesses of haptic devices are factors of ten lower than the stiffnesses of concrete, every-day objects like tables and walls. However, stiffness is just <u>one</u> criterion for the design of a good, haptic system and should not be overestimated. The wide range of stiffnesses reported to be needed for the rendering of undeformable surfaces as shown in Sect. 2.1.3 is a strong evidence of the inter-dependency of several different parameters. The comparison above shall make us aware of the fact that a pure reproduction of solid objects can hardly be realized with a single technical system. It rather takes a combination of stiff and dynamic hardware, for especially the dynamic interaction in high frequency areas dominates the quality of haptics, which has extensively been discussed in the last section.

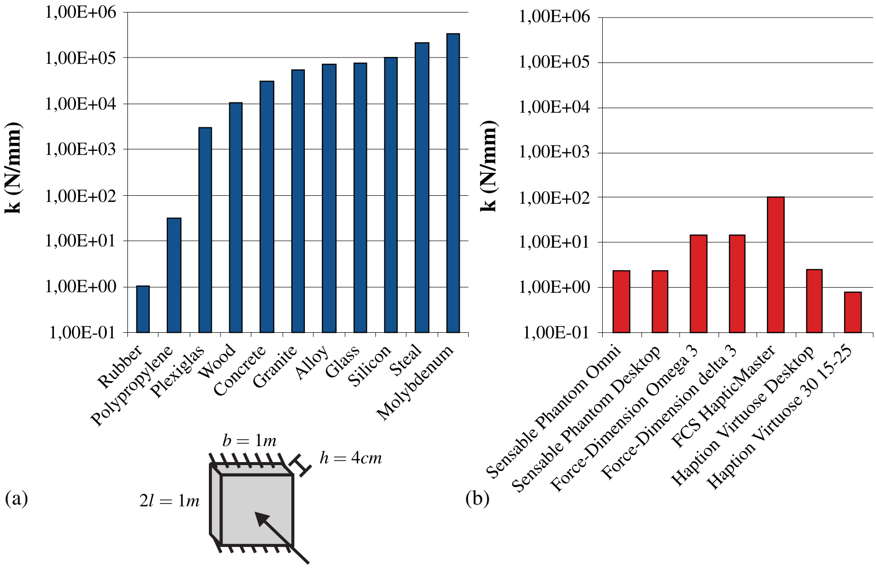

Fig. 2.35 **a** Comparison between stiffnesses of a $1 \times 1 \times 0.04\,\mathrm{m}^3$ plate of different materials and **b** realizable stiffnesses by commercial haptic systems

2.4.3 One Kilohertz—Significance for the Mechanical Design?

As stated above, haptic perception ranges up to a frequency of 10 kHz, whereby the area of highest sensitivity lies between 100 Hz and 1 kHz. This wide range of haptic perception enables us to perceive microstructures on surfaces with the same accuracy as enabling us to identify the point of impact when drumming with our fingers on a table.

For a rough calculation a model according to Fig. 2.36 is considered to be a parallel circuit between a mass m and a spring k. Assuming an identical "virtual" volume V of material and taking the individual density ρ for a qualitative comparison, the border frequency f_b for a step response can be calculated according to Eq. (2.11).

$$f_b = \frac{1}{2\pi}\sqrt{\frac{k}{m}} = \frac{1}{2\pi}\sqrt{\frac{k}{V\rho}} \tag{2.11}$$

Figure 2.36 shows the border frequencies of a selection of materials. Only in case of rubber and soft plastics border frequencies of below 100 Hz appear. Harder plastic material (Plexiglas) and all other materials show border frequencies above 700 Hz. One obvious interpretation would state that any qualitatively good simulation

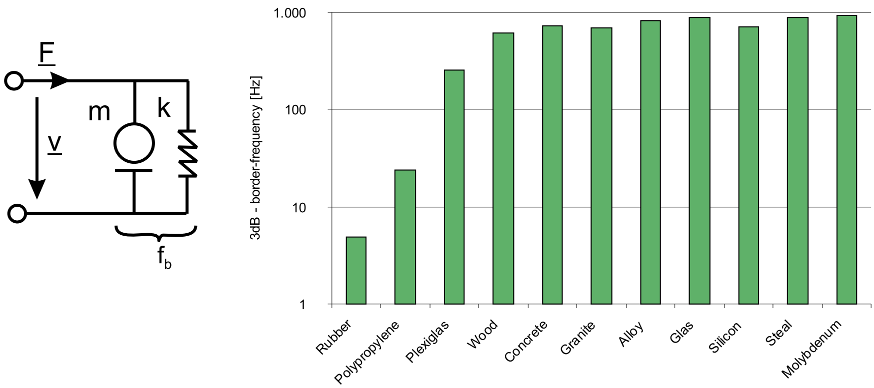

Fig. 2.36 3 dB border frequency f_b of an excitation of a simple mechanical model parametrized as different materials

of such a collision demands at least such bandwidth of dynamics within the signal conditioning elements and the mechanical system.

As a consequence, a frequent recommendation for the design of haptic systems is the transmission of a full bandwidth of 1 kHz (and in some sources even up to 10 kHz). This requirement is valid with respect to software and communications-engineering, as sampling-systems and algorithmic can achieve such frequencies easily today. Considering the mechanical part of the design, we see that dynamics of 1 kHz are enormous, maybe even utopian. Figure 2.37 gives another rough calculation of oscillating force amplitude according to Eq. (2.12).

$$F_0 = \left|\underline{x} \cdot (2\pi f)^2 \cdot m\right| \tag{2.12}$$

The basis of the analysis is a force source generating an output force $\underline{F}_0$. The load of this system is a mass (e.g. a knob) of 10 g (!!). The system does not have any additional load, i.e. it does not have to generate any haptically active force to a user. A periodic oscillation of a frequency f and an amplitude $\underline{x}$ is assumed. With expected amplitudes for the oscillation of 1 mm at 10 Hz a force of approximately 10 mN is necessary. At a frequency of 100 Hz there is already a force of 2–3 N needed. At a frequency of 700 Hz the force already increases to 100 N—and this is what happens when moving a mass of 10 g. Of course in combination with a user-impedance as load the amplitude of the oscillation will decrease in areas of below 100 μm proportionally decreasing the necessary force. But this calculation should make aware of the simple fact that the energetic design and power management of electromechanical systems with application in the area of haptics needs to be done very carefully.

The design of a technical haptic system is always a compromise between bandwidth, stiffness, dynamics of signal conditioning and maximum force-amplitudes. Even with simple systems the design process leads the engineer to the borders of what is physically possible. Therefore it is necessary to have a good model for the

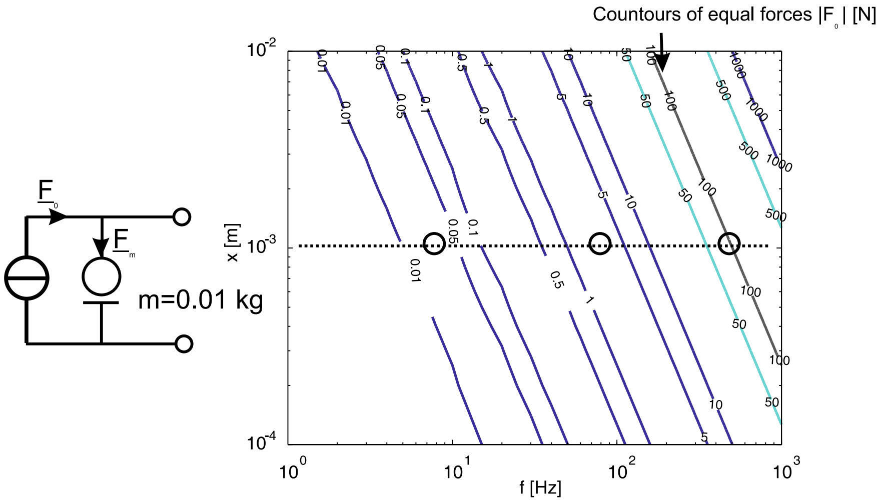

Fig. 2.37 Equipotential line of necessary forces in dependency of amplitude and frequency of the acceleration of a mass with 10 g

user according to his being a load to the mechanical system and according to his or her haptic perception. This model enables the engineer to carry out an optimized design of the technical system, which is the focus of Chap. 3. However there is also the option to use psychophysical knowledge to trick perception by technical means.

2.4.4 Perception-Inspired Concepts for Haptic System Design

At the end of this chapter, two examples shall illustrate the technical importance of an understanding of perception and interaction concepts. The chosen examples present two technical applications that purposeful use unique properties of the haptic sensory channel to design innovative and better haptic systems.

Example: Event-Based-Haptics

Based on the bidirectional view of haptic interactions (Sect. 1.4.2) with a low-frequent kinaesthetic interaction channel and a high-frequent tactile perception channel, KONTARINIS AND HOWE published a new combination of kinaesthetic haptic interfaces with additional sensors and actuators for higher frequencies. Tests included the use in the virtual representation and exploration of objects [223] as well as the use in teleoperation systems.

Based on this work, NIEMEYER ET AL. proposed *Event-Based Haptics* as a concept for increasing realism in virtual-reality applications [224]. In superposing the

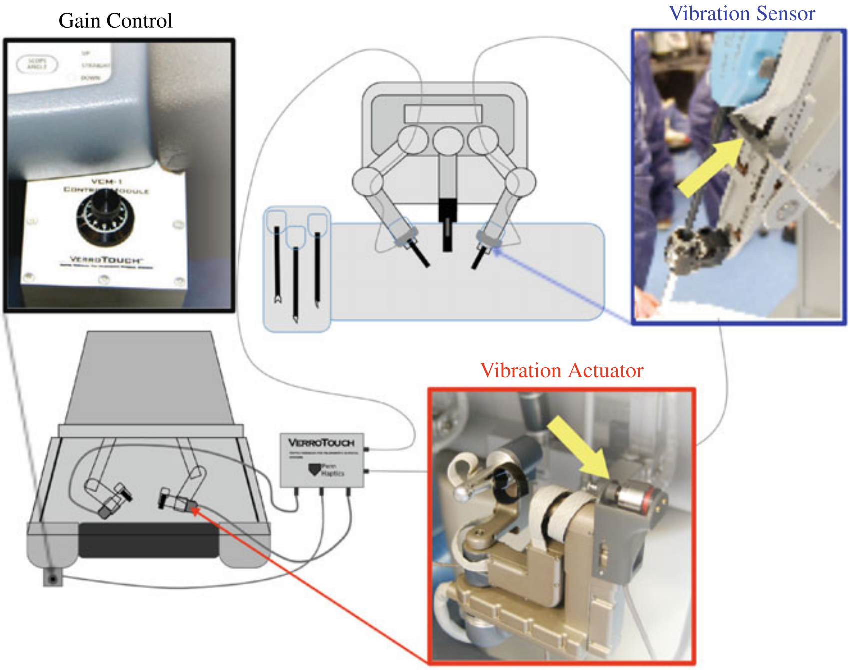

Fig. 2.38 Integration of VerroTouch into the DaVinci Surgical System. Figure adapted from [226] © Springer Nature, all rights reserved

kinaesthetic reactions of a haptic interface with high-bandwidth transient signals for certain events like touching a virtual surface, the haptic quality of this contact situation can be improved considerably [225]. The superposed signals are recorded using accelerometers and played back open-loop if a predefined interaction event takes places.

This concept proved as a valuable tool for the rendering of haptic interactions with virtual environments. Rendering quality is increased with a comparatively small hardware effort in form of additions to (existing) kinaesthetic user interfaces. Technically not an addition to an existing kinaesthetic system, but still based on the Event-Base Haptics approach, the VerroTouch-System by Kuchenbecker et al. was developed as an addition to the DaVinci Surgical System. It adds tactile and auditory feedback based on vibrations measured at the end of the minimal invasive instrument attached to the robot [226]. These vibrations are processed and played back using vibratory motors attached to the DaVinci controls and additional auditory speakers.

The system showed in Fig. 2.38 is able to convey the properties of rough surfaces and contact events with manipulated objects. The augmented interaction was evaluated positively in a study with 11 surgeons [227]. Objective task metrics showed neither an improvement nor impairment of the tested tasks.

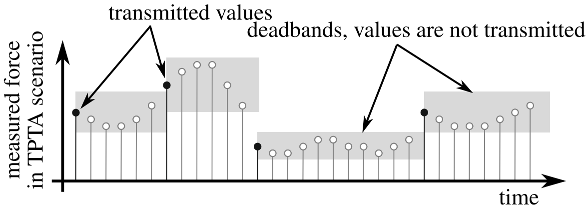

Fig. 2.39 Lossy compression based on the perceptual deadband [127], own illustration

***Example:* Perceptual Deadband Coding**

The *Perceptual Deadband Coding (PD)* is a perception-oriented approach to minimize the amount of haptic data that has to be transmitted in real-time applications such as teleoperation [127, 228]. To achieve his data reduction, new data is only transmitted from the slave to the master side, if the change compared to the preceding data point is greater than the ↪ JND. The Perceptual Deadband Coding is illustrated for the one-dimensional case in Fig. 2.39, but can be extended easily to more-dimensional so-called dead-zones [229].

Recommended Background Reading

[73] **Attention, Perception, and Psychophysics**, Volume 63, Issue 8, 2001. *Special edition about the psychometric function and psychophysical procedures.*

[230] Jones, L. & Tan, H. Z.: **Application of Psychophysical Techniques to Haptic Research**. in IEEE Transactions on Haptics, vol. 6, no. 3, pp. 268-284, July-Sept. 2013. https://doi.org/10.1109/TOH.2012.74.
An expert review and recommendation on psychophysical methods with the focus on human haptic interaction.

[66] Prins, N. & Kingdom, F. A. A.: **Psychophysics: a Practical Introduction**. Academic Press, Maryland Heights, MO, USA, 2010.
Psychophysics textbook with a good overview about modern psychometric procedures and the underlying statistics.

[61] Wickens, T. D.: **Elementary Signal Detection Theory**. Oxford University Press, Oxford, GB, 2002.
Modern and quite entertaining book about modern signal detection theory.

References

1. Ehrenstein WH, Ehrenstein A (1999) Psychophysical methods. In: Modern techniques in neuroscience research, Windhorst U, Johansson H (eds). Springer, Heidelberg, pp 1211–1241. https://doi.org/10.1007/3-540-29491-0
2. Klinke R (2010) Das zentrale Nervensystem - Grundlage bewussten Menschseins. In: Klinke R et al. (eds) Physiologie. Thieme, pp 623–642. ISBN: 978-3137960065
3. Cholewiak RW, Collins AA (1991) Sensory and physiological bases of touch. In: Heller MA, Schiff W (eds) The psychology of touch. Lawrence Erlbaum, London, pp 23–60. 0805807500
4. Treede R-D (2007) Das somatosensorische system. In: Schmidt RF, Lang F (eds), Physiologie des Menschen. Springer, Heidelberg, pp 296–323. https://doi.org/10.1007/978-3-540-32910-7_14
5. Handwerker HO (2006) Somatosensorik. In: Schmidt F, Schaible H-G (eds) Neuro- und Sinnesphysiologie. Springer, Heidelberg. https://doi.org/10.1007/3-540-29491-0
6. Burdea GC (1996) Force and touch feedback for virtual reality. Wiley-Interscience, New York, pp 978–0471021414
7. Dargahi J, Najarian S (2004) Human tactile perception as a standard for artificial ractile sensing - a review. Int J Med Robot Comput Assisted Surg 1(1):23–35. https://doi.org/10.1002/rcs.3
8. Howe RD (1994) Tactile sensing and control of robotic manipulation. Adv Robot 8:245–261. https://doi.org/10.1163/156855394X00356
9. Lederman SJ (1991) Skin and touch. In: Dulbecco R (ed) Encyclopedia of human biology. Academic, Maryland Heights, pp 51–63. ISBN: 978-0122267475
10. Bolanowski SJ (1996) Information processing channels in the sense of touch. In: Franzén O, Johansson R, Terenius L (eds) Somesthesis and the neurobiology of the somatosensory cortex. Birkhäuser, Basel, pp 49–58. ISBN: 978-0817653224. https://doi.org/10.1007/978-3-0348-9016-8_5
11. Bolanowski SJ et al (1988) (2002) Four channels mediate the mechanical aspects of touch. J Acoust Soc Am 84(5):1680–1694. https://doi.org/10.1121/1.397184
12. Bolanowski S, Gescheider G, Verrillo R (1994) Hairy skin: psychophysical channels and their physiological substrates. Somatosens Motor Res 11(3):279–290. https://doi.org/10.3109/08990229409051395
13. Jones L, Lederman S (2006) Human hand function. Oxford University Press, Oxford, p 0195173155
14. Birch AS, Srinivasan MA (1999) Exprerimental determination of the viscoelastic properties of the human fingerpad. Technical report. Massachusetts Institute of Technology, Touch Lab, Cambridge. http://dspace.mit.edu/bitstream/handle/1721.1/4127/RLE-TR-632-41961944.pdf
15. Vallbo Å, Johansson R et al. (1984) Properties of cutaneous mechanoreceptors in the human hand related to touch sensation. Human Neurobiol 3(1):3–14. http://www.ncbi.nlm.nih.gov/pubmed/6330008
16. Seow KC (1988) Physiology of touch, grip and gait. In: Webster JG (ed) Tactile sensors for robotics and medicine. Wiley, New York, pp 13–40. ISBN: 978-0471606079
17. Peters R, Hackeman E, Goldreich D (2009) Diminutive digits discern delicate details: fingertip size and the sex difference in tactile spatial acuity. J Neurosci 29(50):15756. https://doi.org/10.1523/?JNEUROSCI.3684-09.2009
18. Miller LE et al. (2019) Somatosensory cortex efficiently processes touch located beyond the body. Curr Biol 29(24):4276–4283.e5. ISSN: 0960-9822. https://doi.org/10.1016/J.CUB.2019.10.043
19. Gescheider GA et al (2002) A four-channel analysis of the tactile sensitivity of the fingertip: frequency selectivity, spatial summation and temporal summation. Somatosens Motor Res 19:114–124. https://doi.org/10.1080/08990220220131505

20. Israr A, Tan HZ (2006) Frequency and amplitude discrimination along the kinesthetic-cutaneous continuum in the presence of masking stimuli. J Acoust Soc Am 120(5):2789–2800. https://doi.org/10.1121/1.2354022
21. Dudel J (2006) Synaptische Übertragung. Neuro- und Sinnesphysiologie, Schmidt F, Schaible H-G (eds). Springer, Heidelberg. https://doi.org/10.1007/3-540-29491-0
22. Gescheider GA et al (1999) Vibrotactile temporal summation: probability summation or neural integration? Somatosens Motor Res 16:229–242. https://doi.org/10.1080/08990229970483
23. Gescheider GA et al (2005) Spatial summation in the tactile sensory system: probability summation and neural integration. Somatosens Motor Res 22:255–268. https://doi.org/10.1080/08990220500420236
24. King HH, Donlin R, Hannaford B (2010) Perceptual thresholds for single vs. multi-finger haptic interaction. In: IEEE haptics symposium. Waltham, pp 95–99. https://doi.org/10.1109/HAPTIC.2010.5444670
25. Jung J, Ryu J, Choi S (2007) Physical and perceptual characteristics of vibration rendering in mobile device. ACM Trans Appl Percept
26. Verrillo R, Bolanowski S (1986) The effects of skin temperature on the psychophysical responses to vibration on glabrous and hairy skin. J Acoust Soc Am 80:528. https://doi.org/10.1121/1.394047
27. Greenspan JD, Bolanowski SJ (1996) The psychophysics of tactile perception and its peripheral physiological basis. Pain and touch. Kruger L, Friedman MP, Carterette EC (eds). Academic, Maryland Heights. ISBN: 978-0124269101
28. Morioka M, Griffin MJ (2005) Thresholds for the perception of hand-transmitted vibration: dependence on contact area and contact location. Somatosens Motor Res 22:281–297. https://doi.org/10.1080/08990220500420400
29. Hale KS, Stanney KM (2004) Deriving haptic design guidelines from human physiological, psychophysical, and neurological foundations. IEEE Comput Graph Appl 24(2):33–39. https://doi.org/10.1109/MCG.2004.1274059
30. Johnson KO (2001) The roles and functions of cutaneous mechanoreceptors. Curr Opin Neurobiol 11(4):455–461. https://doi.org/10.1016/S0959-4388(00)00234-8
31. Johnson K, Yoshioka T, Vega-Bermudez F (2000) Tactile functions of mechanoreceptive afferents innervating the hand. J Clin Neurophysiol 17(6):539. https://doi.org/10.1097/00004691-200011000-00002
32. Johnson K (2002) Neural Basis of Haptic Perception. Steven's Handbook of Experimental Psychology. Ed. by H. Pashler. Wiley, New York, pp 537–583. https://doi.org/10.1002/0471214426.pas0113
33. Pare M, Carnahan H, Smith A (2002) Magnitude estimation of tangential force applied to the fingerpad. Exper Brain Res 142(3):342–348. https://doi.org/10.1007/s00221-001-0939-y
34. Kuroki S, Watanabe J, Nishida S (2012) Dissociation of vibrotactile frequency discrimination performances for supra-threshold and near-threshold vibrations. In: Isokoski P, Springare J (eds) Haptics: perception, devices, mobility, and communication. Proceedings of the Eurohaptics conference, Tampere, FIN. Springer, Heidelberg, pp 79–84. https://doi.org/10.1007/978-3-642-31404-9_14
35. Mahns D et al (2006) Vibrotactile frequency discrimination in human hairy skin. J Neurophysiol 95(3):1442. https://doi.org/10.1152/jn.00483.2005
36. LaMotte RH, Srinivasan M (1991) Surface microgeometry: tactile perception and neural encoding. In: Franzen O, Westman J (eds) Information processing in the somatosensory system. MacMillan Press, London, pp 49–58. ISBN: 978-0333524930
37. Scheibert J et al. (2004) A novel biomimetic haptic sensor to study the physics of touch. In: Colloque Mécanotransduction. Paris. http://www.lps.ens.fr/~scheibert/MT2004.pdf
38. Edin BB, Abbs JH (1991) Finger movement responses of cutaneous mechanoreceptors in the dorsal skin of the human hand. J Neurophysiol 65(3):657. http://www.humanneuro.physiol.umu.se/PDF-SCIENCE/1991_edin_abbs_DIST.pdf
39. Hollins M (2002) Touch and haptics. In: Pashler H (ed) Steven's handbook of experimental psychology. Wiley, New York, 2002, pp 585–618. ISBN: 978-0471377771. https://doi.org/10.1002/0471214426.pas0114

40. Jones L, Piateski E (2006) Contribution of tactile feedback from the hand to the perception of force. Exper Brain Res 168:289–302. https://doi.org/10.1007/s00221-005-0259-8
41. Fiene J, Kuchenbecker KJ, Niemeyer G (2006) Event-based haptic tapping with grip force compensation. IEEE symposium on haptic interfaces for virtual environment and teleoperator systems. https://doi.org/10.1109/HAPTIC.2006.1627063
42. Libouton X et al (2012) Tactile roughness discrimination of the finger pad relies primarily on vibration sensitive afferents not necessarily located in the hand. Behav Brain Res 229(1):273–279. https://doi.org/10.1016/j.bbr.2012.01.018
43. Clark F, Horch K (1986) Kinesthesia. In: Boff KR, L. Kaufman L, Thomas JP (eds) Handbook of perception and human performance. Wiley-Interscience, New York, pp 13.1–13.61. ISBN: 978-0471829577
44. Jones L (2000) Kinesthetic sensing. MIT Press, Cambridge. http://citeseerx.ist.psu.edu/viewdoc/summary?doi=10.1.1.133.5356
45. Illert M, Kuhtz-Buschbeck JP (2006) Motorisches system. In: Schmidt F, Schaible H-G (eds) Neuro- und Sinnesphysiologie. Springer, Heidelberg. ISBN: 978-3-540-25700-4. https://doi.org/10.1007/3-540-29491-0
46. Smith CU (2000) The biology of sensory systems. Wiley, Chichester, p 445. ISBN: 0-471-89090-1
47. Tan HZ et al. (1993) Manual resolution of compliance when work and force cues are minimized. Advances in robotics, mechatronics and haptic interfaces, pp 99–104. http://citeseerx.ist.psu.edu/viewdoc/download?doi=10.1.1.50.2758&rep=rep1&type=pdf
48. Toffin D et al (2003) Perception and reproduction of force direction in the horizontal plane. J Neurophysiol 90:3040–3053. https://doi.org/10.?1152/?jn.?00271.?2003
49. Darian-Smith I, Johnson K (2004) Thermal sensibility and thermoreceptors. J Investigat Dermatol 69(1):146–153. https://doi.org/10.1111/1523-1747.ep12497936
50. Kruger L, Friedman MP, Carterette EC (eds) (1996) Pain and touch. Academic, Maryland Heights, pp 978–0123992390
51. Draguhn A (2009) Membranpotenzial und Signalübertragung in Zellverbänden. Physiologie, Klinke R et al. (eds). Thieme, pp 60–97. ISBN: 9783137960065
52. Johansson RS, Birznieks I (2004) First spikes in ensembles of human tactile afferents code complex spatial fingertip events. Nat Neurosci 7(2):170–177. https://doi.org/10.1038/nn1177
53. Ernst M, Bülthoff H (2004) Merging the senses into a robust percept. Trends Cognit Sci 8(4):162–169. https://doi.org/10.1016/j.tics.2004.02.002
54. Pusch A, Lécuyer A (2011) Pseudo-haptics: from the theoretical foundations to practical system design guidelines. In: Proceedings of the 13th international conference on multimodal interfaces. ACM, pp 57–64. https://doi.org/10.1145/2070481.2070494
55. Giachritsis C, Wright R, Wing A (2010) The contribution of proprioceptive and cutaneous cues in weight perception: early evidence for maximum-likelihood integration. In: Kappers AML, Bergmann-Tiest WM, van der Helm FC (eds) Haptics: generating and perceiving tangible sensations, LNCS,vol 6191. Proceedings of the Eurohaptics Conference, Amsterdam. Springer, Heidelberg, pp 11–16. https://doi.org/10.1007/978-3-642-14064-8_2
56. Okazaki R, Kajimoto H, Hayward V (2012) Vibrotactile stimulation can affect auditory loudness: a pilot study. In: Isokoski P, Springare J (eds) Haptics: perception, devices, mobility, and communication, LNCS, vol 7282. Proceedings of the Eurohaptics conference, Tampere, FIN. Springer, Heidelberg, pp 103–108. https://doi.org/10.1007/978-3-642-31404-9_18
57. Helbig HB, Ernst MO (2008) Haptic perception in interaction with other senses. In: Grunwald M (ed) Human haptic perception - basics and applications. Birkhäuser, pp 235–249. ISBN: 978-3764376116
58. Fechner GT (1860) Elemente der Psychophysik. Breitkopf und Härtel, Leipzig, pp 978–1271174218
59. Wichmann F, Hill N (2001) The psychometric function: I. Fitting, sampling, and goodness of fit. Percept Psychophys 63(8):1293. https://doi.org/10.3758/BF03194544
60. Harvey LO (1986) Efficient estimation of sensory thresholds. Behav Res Methods 18(6):623–632. https://doi.org/10.1163/156856897X00159

61. Wickens TD (2002) Elementary signal detection theory. Oxford University Press, Oxford, pp 978–0195092509
62. Foster DH, Zychaluk K (2009) Model-free estimation of the psychometric function. Attent Percept Psychophys 71(6):1414–1425. https://doi.org/10.3758/APP.71.6.1414
63. Buus S (2002) Psychophysical methods and other factors that affect the outcome of psychoacoustic measurements. In: Genetics and the function of the auditory system: proceedings of the 19th danavox symposium. Kopenhagen, pp 183–225
64. Hatzfeld C, Werthschützky R (2013) Simulation und Auswahl psychometrischer Verfahren zur Ermittlung von Kennwerten menschlicherWahrnehmung. XXVII. Messtechnisches Symposium des Arbeitskreises der Hochschullehrer für Messtechnik e.V, Knapp W, Gebhardt M (eds). Messtechnik und Sensorik. Aachen: Shaker, Sept. 2013, pp 51–62
65. Otto S, Weinzierl S (2009) Comparative simulations of adaptive psychometric procedures. In: Jahrestagung der Deutschen Gesellschaft für Akustik. Rotterdam, NL: Dt. Ges. für Akustik, pp 1276–1279. ISBN: 9783980865968
66. Prins N, Kingdom FAA (2010) Psychophysics: a practical introduction. Academic, Maryland Heights. ISBN: 978-0-12-373656-7
67. Leek MR (2001) Adaptive procedures in psychophysical research. Percept Psychophys 63(8):1279–1292. https://doi.org/10.3758/BF03194543
68. Levitt H (1971) Transformed up-down methods in psychoacoustics. J Acoust Soc Am 49(2). Suppl 2:467–477. https://doi.org/10.1121/1.1912375
69. Garcia M, Pérez E-A (1998) Forced-choice staircases with fixed step sizes: asymptotic and small-sample properties. Vis Res 38(12):1861–1881. https://doi.org/10.1016/S0042-6989(97)00340-4
70. Taylor M, Creelman C (1967) PEST: efficient estimates on probability functions. J Acoust Soc Am 41(4):782–787. https://doi.org/10.1121/1.1910407
71. King-Smith PE et al (1994) Efficient and unbiased modifications of the quest threshold method: theory, simulations, experimental evaluation and practical implementation. Vis Res 34(7):885–912. https://doi.org/10.1016/0042-6989(94)90039-6
72. Kontsevich L, Tyler C (1999) Bayesian adaptive estimation of psychometric slope and threshold. Vis Res 39(16):2729–2737. https://doi.org/10.1016/S0042-6989(98)00285-5
73. Klein S (2001) Measuring, estimating, and understanding the psychometric function: a commentary. Attent Percept Psychophys 63(8):1421–1455. https://doi.org/10.3758/BF03194552
74. Hatzfeld C (2013) Experimentelle Analyse der menschlichen Kraftwahrnehmung als ingenieurtechnische Entwurfsgrundlage für haptische Systeme. Dissertation, Technische Universität Darmstadt. http://tuprints.ulb.tu-darmstadt.de/3392/. München: Dr. Hut Verlag, 2013. ISBN: 978-3-8439-1033-0
75. Kaernbach C (2001) Adaptive threshold estimation with unforced-choice tasks. Percept Psychophys 63(8):1377–1388. https://doi.org/10.3758/BF03194549
76. Rank M et al. (2012) Masking effects for damping JND. In: Isokoski P, Springare J (eds) Haptics: perception, devices, mobility, and communication, LNCS, vol 7282. Proceedings of the Eurohaptics conference, Tampere, FIN. Springer, Heidelberg, pp 145–150. https://doi.org/10.1007/978-3-642-31404-9_25
77. Macmillan N, Creelman C (2005) Detection theory: a user's guide. Lawrence Erlbaum, London, pp 978–0805842319
78. Weber EH (1905) Tastsinn und Gemeingefühl. Engelmann. ISBN: 9783836402491 (Reprint)
79. Gescheider GA (1997) Psychophysics - the fundamentals. Lawrence Erlbaum, Mahwah, pp 978–0805822816
80. Conner M et al (1988) Individualized optimization of the salt content of white bread for acceptability. J Food Sci 53(2):549–554. https://doi.org/10.1111/j.1365-2621.1988.tb07753.x
81. ISO 20462: photography - psychophysical experimental methods for estimating image quality - Part 3: Quality ruler method. ISO (2012)
82. Garneau CJ, Parkinson MB (2013) Considering just noticeable difference in assessments of physical accommodation for product design. In: Ergonomics ahead-of-print, pp 1–12. http://www.ncbi.nlm.nih.gov/pubmed/24099095

83. Stevens SS (1975) Psychophysics. Stevens G (ed). Transaction Books, Piscataway. ISBN: 978-0887386435
84. Bolanowski SJ, Verrillo RT (1982) Temperature and criterion effects in a somatosensory subsystem: a neurophysiological and psychophysical study. J Neurophysiol 48(3):836–855. http://www.ncbi.nlm.nih.gov/pubmed/7131055
85. Gescheider G et al (1984) Effects of the menstrual cycle on vibrotactile sensitivity. Percept Psychophys 36(6):586–592. https://doi.org/10.3758/BF03207520
86. Green B (1977) The effect of skin temperature on vibrotactile sensitivity. Percept Psychophys 21(3):243–248. https://doi.org/10.3758/BF03214234
87. Frisina R, Gescheider G (1977) Comparison of child and adult vibrotactile thresholds as a function of frequency and duration. Percept Psychophys 22(1):100–103. https://doi.org/10.3758/BF03206086
88. Gescheider GA, Wright JH, Verillo RT (2009) Information-processing channels in the tactile sensory system. Psychology Press, New York, NY, USA, pp 978–1841698960
89. Gescheider GA et al (1994) The effects of aging on information-processing channels in the sense of touch: I. Absolute sensitivity. Somatosens Motor Res 11(4):345–357. https://doi.org/10.3109/08990229409028878
90. Goble A, Collins A, Cholewiak R (1996) Vibrotactile threshold in young and old observers: the effects of spatial summation and the presence of a rigid surround. J Acoust Soc Am 99(4):2256–2269. https://doi.org/10.1121/1.415413
91. Verrillo R (1980) Age related changes in the sensitivity to vibration. J Gerontol 35(2):185–193. https://doi.org/10.1093/geronj/35.2.185
92. Verrillo R (1982) Effects of aging on the suprathreshold responses to vibration. Percept Psychophys 32(1):61–68. https://doi.org/10.3758/BF03204869
93. Goff G et al (1965) Vibration perception in normal man and medical patients. J Neurol Neurosurg Psychiat 28:503–509. https://doi.org/10.1136/jnnp.28.6.503
94. Verrillo R (1979) Comparison of vibrotactile threshold and suprathreshold responses in men and women. Percept Psychophys 26(1):20–24. https://doi.org/10.3758/BF03199857
95. Weinstein S (1968) Intensive and extensive aspects of tactile sensitivity as a function of body part, sex, and laterality. In: First international symposium on the skin senses
96. Henkin R (1974) Sensory changes during the menstrual cycle. In: Ferin M et al. (eds) Biorhythms and human reproduction. Wiley, New York, pp 277–285. ISBN: 978-0471257615. https://www.ncbi.nlm.nih.gov/pubmed/11465979
97. Grunwald M et al (2001) Haptic perception in anorexia nervosa before and after weight gain. J Clin Exper Neuropsychol 23(4):520–529. https://doi.org/10.1076/jcen.23.4.520.1229
98. Verrillo R et al (1998) Effects of hydration on tactile sensation. Somatosens Motor Res 15(2):93–108. https://doi.org/10.1080/08990229870826
99. Greenspan J (1984) A comparison of force and depth of skin indentation upon psychophysical functions of tactile intensity. Somatosens Motor Res 2(1):33–48. http://www.ncbi.nlm.nih.gov/pubmed/6505462
100. Adams M (2011) Project summary nanobiotact. Technical report. EU FP6
101. Dandekar K, Raju B, Srinivasan M (2003) 3-D finite-element models of human and monkey fingertips to investigate the mechanics of tactile sense. J Biomech Eng 125:682. https://doi.org/10.1115/1.1613673
102. Wagner M, Gerling G, Scanlon J (2008) Validation of a 3-D finite element human fingerpad model composed of anatomically accurate tissue layers. In: Haptic interfaces for virtual environment and teleoperator systems, 2008. Symposium on haptics 2008. IEEE, pp 101–105. https://doi.org/10.1109/HAPTICS.2008.4479922
103. Wang Z et al (2012) A 3-D nonhomogeneous FE model of human fingertip based on MRI measurements. IEEE Trans Instrum Meas 61(12):3147–3157. https://doi.org/10.1109/TIM.2012.2205102
104. Israr A, Choi S, Tan HZ (2006) Detection threshold and mechanical impedance of the hand in a pen-hold posture. In: International conference on intelligent robots and systems (IROS). Peking, C, 2006, pp 472–477. https://doi.org/10.1109/IROS.2006.282353

105. Israr A, Choi S, Tan HZ (2007) Mechanical impedance of the hand holding a spherical tool at threshold and suprathreshold stimulation levels. In: Second joint eurohaptics conference and symposium on haptic interfaces for virtual enrivonment and teleoperator systems (World-Haptics conference). Tsukaba. https://doi.org/10.1109/WHC.2007.81
106. Hatzfeld C and Werthschützky R. (2012) Mechanical impedance as coupling parameter of force and deflection perception: experimental evaluation. In: Isokoski P, Springare J (eds) Haptics: perception, devices, mobility, and communication, LNCS, vol 7282. Proceedings of the Eurohaptics conference, Tampere, FIN. Springer, Heidelberg. https://doi.org/10.1007/978-3-642-31401-8_18
107. Dandu D et al. (2019) Spatiotemporal haptic effects from a single actuator via spectral control of cutaneous wave propagation. In: 2019 IEEE world haptics conference, WHC 2019, pp 425–430. https://doi.org/10.1109/WHC.2019.8816149
108. Shao Y, Hayward V, Visell Y (2016) Spatial patterns of cutaneous vibration during whole-hand haptic interactions. Proc Natl Acad Sci USA 113(15):4188–4193. ISSN: 10916490. https://doi.org/10.1073/PNAS.1520866113/-/DCSUPPLEMENTAL. https://www.pnas.org/content/113/15/4188.abstract
109. Hayward V (2011) Is there a 'plenhaptic' function? In: Philos Trans R Soc B: Biol Sci 366(1581):3115–3122. ISSN: 14712970. https://doi.org/10.1098/RSTB.2011.0150. https://royalsocietypublishing.org/doi/abs/10.1098/rstb.2011.0150
110. Gescheider GA, Bolanowski SJ, Hardick KR (2001) The frequency selectivity of information-processing channels in the tactile sensory system. Somatosens Motor Res 18(3):191–201. https://doi.org/10.1080/01421590120072187
111. Gleeson BT, Horschel SK, Provancher WR (2010) Perception of direction for applied tangential skin displacement: effects of speed, displacement and repetition. IEEE Trans Haptics 3(3):177–188. ISSN: 1939-1412. https://doi.org/10.1109/TOH.2010.20
112. Kaczmarek K et al. (1991) Electrotactile and vibrotactile displays for sensory substitution systems. IEEE Trans Biomed Eng 38(1). Dept. of Electr. Eng., Wisconsin University, Madison, pp 1–16. https://doi.org/10.1109/10.68204
113. Shimoga K (1993) A survey of perceptual feedback issues in dexterous telemanipulation part I. Finger force feedback. In: Proceedings of the IEEE virtual reality annual international symposium. Seattle, pp 263–270. https://doi.org/10.1109/VRAIS.1993.380770
114. Brooks TL (1990) Telerobotic response requirements. In: IEEE international conference on systems, man and cybernetics. Los Angeles. https://doi.org/10.1109/ICSMC.1990.142071
115. Brisben AJ, Hsiao SS, Johnson KO (1999) Detection of vibration transmitted through an object grasped in the hand. J Neurophysiol 81:1548–1558. http://jn.physiology.org/content/81/4/1548
116. Kyung K-U et al (2005) Perceptual and biomechanical frequency response of human skin: implication for design of tactile displays. In: First joint Eurohaptics conference and symposium on haptic interfaces for virtual environment and teleoperator systems (WorldHaptics conference). https://doi.org/10.1109/WHC.2005.105
117. Kontarinis DA, Howe RD (1993) Tactile display of contact shape in dextrous telemanipulation. In: ASME winter annual meeting: advances in robotics, mechatronics and haptic interfaces, New Orleans, DSC-vol. 49. Diss:81–88
118. Hugony A (1935) Über die Empfindung von Schwingungen mittels des Taststinns. Zeitschrift für Biologie 96:548–553
119. Caldwell DG, Lawther S, Wardle A (1996) Multi-modal cutaneous tactile feedback. In: Proceedings of the IEEE international conference on intelligent robots and systems. Diss, pp 465–472. https://doi.org/10.1109/IROS.1996.570820
120. Kaczmarek KA, Bach-Y-Rita P (1995) Tactile displays. In: Barfield W, Furness T (eds) Virtual environements and advanced interface design, Diss. Oxford University Press, New York, pp 349–414. ISBN: 978-0195075557
121. Gescheider GA et al (1990) Vibrotactile intensity discrimination measured by three methods. J Acoust Soc Am 87(1):330–338. https://doi.org/10.1121/1.399300

122. Verrillo RT, Gescheider GA (1992) Perception via the sense of touch. In: Summers IR (ed) Tactile aids for the hearing impaired. GB: Whurr, London, pp 1–36. ISBN:978-1-870332-17-0
123. Jones LA (1989) Matching forces: constant errors and differential thresholds. Perception 18(5):681–687. https://doi.org/10.1068/p180681
124. Pang X, Tan H, Durlach N (1991) Manual discrimination of force using active finger motion. Percept Psychophys 49(6):531–540. https://doi.org/10.3758/BF03212187
125. Allin S, Matsuoka Y, Klatzky R (2002) Measuring just noticeable differences for haptic force feedback: implications for rehabilitation. In: Proceedings of the 10th symposium on haptic interfaces for virtual environments and teleoperator systems. Orlando. https://doi.org/10.1109/HAPTIC.2002.998972
126. Dorjgotov E et al. (2008) Force amplitude perception in six orthogonal directions. In: Symposium on haptic interfaces for virtual environments and teleoperator systems. Reno. https://doi.org/10.1109/HAPTICS.2008.4479927
127. Hinterseer P et al (2008) Perception-based data reduction and transmission of haptic data in telepresence and teleaction systems. IEEE Trans Signal Process 56(2):588–597. https://doi.org/10.1109/TSP.2007.906746
128. Höver R et al. (2009) Computationally efficient techniques for data-driven haptic rendering. In: Third joint eurohaptics conference and symposium on haptic interfaces for virtual environment and teleoperator systems (WorldHaptics conference). Salt Lake City, pp 39–44. https://doi.org/10.1109/WHC.2009.4810814
129. Pongrac H et al. (2006) Limitations of human 3D force discrimination. In: Proceedings of human- centered robotics systems. http://citeseerx.ist.psu.edu/viewdoc/download?doi=10.1.1.68.8597&rep=rep1&type=pdf
130. Pongrac H (2008) Vibrotactile perception: examining the coding of vibrations and the just noticeable difference under various conditions. Multimedia Syst 13(4):297–307. https://doi.org/10.1007/s00530-007-0105-x
131. Hatzfeld C, Kern TA, and Werthschützky R (2010) Design and evaluation of a measuring system for human force perception parameters. Sens Actuat: Phys 162(2):202–209. Accepted paper. https://doi.org/10.1016/j.sna.2010.01.026
132. Hatzfeld C, Werthschützky R (2012) Just noticeable differences of low-intensity vibrotactile forces at the fingertip. In: Isokoski P, Springare J (eds) Haptics: perception, devices, mobility, and communication, LNCS, vol 7282. Proceedings of the Eurohaptics conference, Tampere, FIN. Springer, Heidelberg. https://doi.org/10.1007/978-3-642-31404-9_8
133. Jones L, Hunter I (1990) A perceptual analysis of stiffness. Exper Brain Res 79(1):150–156. https://doi.org/10.1007/BF00228884
134. Jones L, Hunter I (1993) A perceptual analysis of viscosity. Exper Brain Res 94(2):343–351. https://doi.org/10.1007/BF00230304
135. Cholewiak SA, Tan HZ, Ebert DS (2008) Haptic identification of stiffnes and force magnitude. In: Symposium on haptic interfaces for virtual environments and teleoperator systems. Reno. https://doi.org/10.1109/HAPTICS.2008.4479918
136. Pang X, Tan H, Durlach N (1992) Manual resolution of length, force and compliance. ASME DSC Adv Robot 42:13–18. https://engineering.purdue.edu/~hongtan/pubs/PDFfiles/C05_Tan_ASME1992.pdf
137. Blume H-J, Boelcke R (1990) Mechanokutane Sprachvermittlung, vol 137. Reihe 10 137. Düsseldorf: VDI-Verl. ISBN: 3-18-143710-7
138. Tan HZ et al. (1994) Human Factors for the design of force-reflecting haptic interfaces. ASME DSC dynamic systems and control 55(1):353–359. http://touchlab.mit.edu/publications/1994_004.pdf
139. Jandura L, Srinivasan M (1994) Experiments on human performance in torque discrimination and control. Dyn Syst Control, ASME, DSC-55 1:369–375. http://www.rle.mit.edu/touchlab/publications/1994_002.pdf
140. Barbagli F et al (2006) Haptic discrimination of force direction and the influence of visual information. ACM Trans Appl Percept (TAP) 3(2):135. https://doi.org/10.1145/1141897.1141901

141. Tan HZ et al. (2006) Force direction discrimination is not influenced by reference force direction. Haptics-e, vol 1, pp 1–6. http://jks-folks.stanford.edu/papers/Haptic-Discrimination.pdf
142. Craig JC (1972) Difference threshold for intensity of tactile stimuli. Percept Psychophys 11(2):150–152. https://doi.org/10.3758/BF03210362
143. Bergmann Tiest WM (2010) Tactual perception of material properties. Vis Res 50(24):2775–2782. https://doi.org/10.1016/j.visres.2010.10.005
144. Klatzky RL, Pawluk D, Peer A (2013) Haptic perception of material properties and implications for applications. Proc IEEE 101:2081–2092. https://doi.org/10.1109/JPROC.2013.2248691
145. Samur E (2010) Systematic evaluation methodology and performance metrcis for haptic interfaces. Dissertation École Polytechnique Fédérale de Lausanne
146. Hollins M, Risner SR (2000) Evidence for the duplex theory of tactile texture perception. Percept Psychophys 62(4):695–705. https://doi.org/10.3758/BF03206916
147. Knowles WB, Sheridan TB (1966) The “FeelâŁž of rotary controls: friction and inertial. Human Fact J Human Fact Ergonom Soc 8(3):209–215. https://doi.org/10.1177/001872086600800303
148. Provancher WR, Sylvester ND (2009) Fingerpad skin stretch increases the perception of virtual friction. IEEE Trans Haptics 2(4):212–223. https://doi.org/10.1109/TOH.2009.34
149. Campion G, Hayward V (2008) On the synthesis of haptic textures. IEEE Trans Robot 24(3):527–536. ISSN:1552-3098. https://doi.org/10.1109/TRO.2008.924255
150. Bergmann Tiest WM, Kappers A (2009) Cues for haptic perception of compliance. IEEE Trans Haptics 2(4):189–199. https://doi.org/10.1109/TOH.2009.16
151. Lawrence DA et al (2000) Rate-hardness: a new performance metric for haptic interfaces. IEEE Trans Robot Autom 16:357–371. https://doi.org/10.1109/70.864228
152. Kwon D-S et al. (2001) Realistic force reflection in a spine biopsy simulator. In: IEEE international conference on robotics and automation, 2001. Proceedings 2001 ICRA, vol. 2. IEEE, pp 1358–1363. https://doi.org/10.1109/ROBOT.2001.932799
153. Cadoret G, Smith AM (1996) Friction, not texture, dictates grip forces used during object manipulation. J Neurophysiol 75(5):1963–1969. http://jn.physiology.org/content/75/5/1963
154. Howe RD (1992) A force-reflecting teleoperated hand system for the study of tactile sensing in precision manipulation. In: 1992 IEEE international conference on robotics and automation, 1992. Proceedings. IEEE, pp 1321–1326. https://doi.org/10.1109/ROBOT.1992.220166
155. Bergmann Tiest WM, Vrijling AC, Kappers AM (2010) Haptic perception of viscosity. In: Haptics: Generating and perceiving tangible sensations. Springer, pp 29–34. https://doi.org/10.1007/978-3-642-14064-8_5
156. Gordon IE, Morison V (1982) The haptic perception of curvature. Percept Psychophys 31(5):446–450. https://doi.org/10.3758/BF03204854
157. Goodwin A, John K, Marceglia A (1991) Tactile discrimination of curvature by humans using only cutaneous information from the fingerpads. Exper Brain Res 86(3):663–672. https://doi.org/10.1007/BF00230540
158. Johnson K et al. (1979) Coding of incremental changes in skin temperature by a population of warm fibers in the monkey: correlation with intensity discrimination in man. J Neurophysiol 42(5):1332–1353. http://www.ncbi.nlm.nih.gov/pubmed/114610
159. Hardy JD, Goodell H, Wolff HG (1951) The influence of skin temperature upon the pain threshold as evoked by thermal radiation. In: Science. https://doi.org/10.1126/science.115.2992.499
160. Jones LA, Ho H-N (2008) Warm or cool, large or small? The challenge of thermal displays. IEEE Trans Haptics 1(1):53–70. https://doi.org/10.1109/TOH.2008.2
161. Borg I, Groenen PJF (2005) Modern multidimensional scaling - theory and applications. Springer, Heidelberg, pp 978–1441920461
162. Hollins M et al (1993) Perceptual dimensions of tactile surface texture: a multidimensional scaling analysis. Attent Percept Psychophys 54(6):697–705. https://doi.org/10.3758/BF03211795

163. Rösler F, Battenberg G, Schüttler F (2009) Subjektive Empfindungen und objektive Charakteristika von Bedienelementen. Automobiltechnische Zeitschrift 4:292–297. https://doi.org/10.1007/BF03222068
164. Wiertlewski M (2013) Reproduction of tactual textures: transducers, mechanics, and signal encoding. Springer. ISBN: 978-1-4471-4840-1
165. Haptex (2007) Grant No. IST-6549, last visited 07.03.2012. European Union. http://haptex.miralab.unige.ch/
166. Biggs J, Srinivasan MA (2002) Tangential versus normal displacements of skin: relative effectiveness for producing tactile sensations. In: 10th symposium on haptic interfaces for virtual environments and teleoperator systems. https://doi.org/10.1109/HAPTIC.2002.998949
167. ISO/IEC Guide 98-3: uncertainty of measurement? Part 3: guide to the expression of uncertainty in measurement. Genf, CH: ISO (2008)
168. Keppel G (1991) Design and analysis: a researcher's handbook. Pearson Education, Old Tappan, pp 978–0135159415
169. Nitsch V, Färber B (2012) A meta-analysis of the effects of haptic interfaces on task performance with teleoperation systems. IEEE Trans Haptics 6:387–398. https://doi.org/10.1109/ToH.2012.62
170. Makous JC, Gescheider GA (1996) Bolanowski SJ (1996) Decay in the effect of vibrotactile masking. J Acoust Soc Am 99(2):1124–1129. https://doi.org/10.1121/1.414597
171. Tan H et al (2003) Temporal masking of multidimensional tactual stimuli. J Acoust Soc Am 116(9). Part 1:3295–3308. https://doi.org/10.1121/1.1623788
172. Gescheider GA, O'Malley MJ, Verrillo RT (1983) Vibrotactile forward masking: evidence for channel independence. The J Acoust Soc Am 74(2):474–485. https://doi.org/10.1121/1.389813
173. Musmann H (2006) Genesis of the MP3 audio coding standard. IEEE Trans Consumer Electron 52(3):1043–1049. https://doi.org/10.1109/TCE.2006.1706505
174. Gescheider GA, Migel N (1995) Some temporal parameters in vibrotactile forward masking. J Acoust Soc Am 98(6):3195–3199. https://doi.org/10.1121/1.413809
175. Gescheider GA et al (1985) Vibrotactile forward masking: psychophysical evidence for a triplex theory of cutaneous mechanoreception. J Acoust Soc Am 78(2):534–543. https://doi.org/10.1121/1.392475
176. Gescheider GA et al (1992) Vibrotactile forward masking as a function of age. J Acoust Soc Am 91(3):1690–1696. https://doi.org/10.1121/1.402448
177. Gescheider GA et al (1995) Vibrotactile forward masking: effects of the amplitude and duration of the masking stimulus. J Acoust Soc Am 98(6):3188–3194. https://doi.org/10.1121/1.413808
178. Bensmaïa S, Hollins M, Yau J (2005) Vibrotactile intensity and frequency information in the pacinian system: a psychophysical model. Attent Percept Psychophys 67(5):828–841. https://doi.org/10.3758/BF03193536
179. Cholewiak SA et al (2010) A frequency-domain analysis of haptic gratings. IEEE Trans Haptics 3:3–14. https://doi.org/10.1109/TOH.2009.36
180. Salisbury C et al (2011) What you can't feel won't hurt you: evaluating haptic hardware using a haptic contrast sensitivity function. IEEE Trans Haptics 4(2):134–146. https://doi.org/10.1109/TOH.2011.5
181. Allerkamp D et al (2007) A vibrotactile approach to tactile rendering. Vis Comput 23(2):97–108. https://doi.org/10.1007/s00371-006-0031-5
182. Acker A (2011) Anwendungspotential von Telepräsenz-und Teleaktionssystemen für die Präzisionsmontage. Dissertation. Technische Universität München, 2011. http://mediatum.ub.tum.de/doc/1007163/1007163.pdf
183. Kappers AML, Koenderink JJ (1999) Haptic perception of spatial relations. Perception 28(6):781–795. https://doi.org/10.1068/p2930
184. Gentaz E, Hatwell Y (2008) Haptic perceptual illusions. In: Grunwald M (ed) Human haptic perception. Birkhäuser, Basel. ISBN: 978-3-7643-7611-6. https://doi.org/10.1007/978-3-7643-7612-3_17

185. Hayward V (2008) A brief taxonomy of tactile illusions and demonstrations that can be done in a hardware store. Brain Res Bull 75(6):742–752. https://doi.org/10.1016/j.brainresbull.2008.01.008
186. Lederman S, Jones L (2011) Tactile and haptic illusions. IEEE Trans Haptics 4(4):273–294. https://doi.org/10.1109/TOH.2011.2
187. Kildal J (2012) Kooboh: variable tangible properties in a handheld haptic-illusion box. In: Isokoski P, Springare J (eds) Haptics: perception, devices, mobility, and communication. Proceedings of the Eurohaptics conference, Tampere, FIN. Springer, Heidelberg, pp 191–194. https://doi.org/10.1007/978-3-642-31404-9_33
188. Lécuyer A (2009) Simulating haptic feedback using vision: a survey of research and applications of pseudo-haptic feedback. Presence: Teleoper Virtual Environ 18(1):39–53. https://doi.org/10.1162/pres.18.1.39
189. Kimura T, Nojima T (2012) Pseudo-haptic feedback on softness induced by grasping motion. In: Haptics: perception, devices, mobility, and communication. Springer, pp 202–205. https://doi.org/10.1007/978-3-642-31404-9_36
190. Brown L, Brewster S, Purchase H (2006) Multidimensional tactons for non-visual information presentation in mobile devices. In: Conference on human-computer interaction with mobile devices and services, pp 231–238. https://doi.org/10.1145/1152215.1152265
191. Enriquez M, MacLean K, Chita C (2006) Haptic phonemes: basic building blocks of haptic communication. In: Proceedings of the 8th international conference on multimodal interfaces (ICMI). ACM, Banff, pp 302–309. https://doi.org/10.1145/1180995.1181053
192. MacLean K, Enriquez M (2003) Perceptual design of haptic icons. In: Proceedings of Euro-Haptics. http://citeseerx.ist.psu.edu/viewdoc/summary?doi=10.1.1.138.6172
193. Tan HZ et al (1999) Information transmission with a multifinger tactual display. Percept Psychophys 61(6):993–1008. https://doi.org/10.3758/BF03207608
194. Tan H (1996) Rabinowitz W (1996) A new multi-finger tactual display. J Acoust Soc Am 99(4):2477–2500. https://doi.org/10.1121/1.415560
195. Lederman SJ, Klatzky RL (1987) Hand movements: a window into haptic object recognition. Cognit Psychol 19(3):342–368. https://doi.org/10.1016/0010-0285(87)90008-9
196. Lederman SJ, Klatzky RL (2009) Haptic perception: a tutorial. Attent Percept Psychophys 71(7):1439. https://doi.org/10.3758/APP.71.7.1439
197. Lederman SJ (1981) The perception of surface roughness by active and passive touch. Bull Psychon Soc 18(5):253–255. https://doi.org/10.3758/BF03333619
198. Li Y et al. (2008) Passive and active kinesthetic perception just noticeable difference for natural frequency of virtual dynamic systems. In: Symposium on haptic interfaces for virtual environments and teleoperator systems. Reno. https://doi.org/10.1109/HAPTICS.2008.4479908
199. Symmons M et al. (2005) Active versus passive touch in three dimensions. In: First joint eurohaptics conference and symposium on haptic interfaces for virtual environment and teleoperator systems (WorldHaptics conference). Pisa, I, 2005. https://doi.org/10.1109/WHC.2005.20
200. Karam M, Schraefel MC (2005) A taxonomy of gestures in human computer interactions. Technical report. University of Southampton, 2005. http://eprints.soton.ac.uk/id/eprint/261149
201. Paek TS, Bahl P, Foehr OH (2011) Interacting with a mobile device within a vehicle using gestures. 20130155237:A1
202. Sodhi R et al (2013) AIREAL: interactive tactile experiences in free air. ACM Trans Graph (TOG) 32(4):134. https://doi.org/10.1145/2461912.2462007
203. Carter T et al. (2013) UltraHaptics: multi-point mid-air haptic feedback for touch surfaces. In: Proceedings of the 26th annual ACM symposium on user interface software and technology. ACM, pp 505–514. https://doi.org/10.1145/2501988.2502018
204. Tillmann BN (2010) Atlas der Anatomie des Menschen. Springer. ISBN: 978-3-642-02679-9
205. Hasser CJ (1995) Force-reflecting anthropomorphic hand masters. Technical report. Report AL/CF-TR-1995- 0110, Armstrong Laboratory. US Air Force. http://oai.dtic.mil/oai/oai?verb=getRecord&metadataPrefix=html&identifier=ADA316017

206. An K, Askew L, Chao E (1986) Biomechanics and functional assessment of upper extremities. Trends in ergonomics/human factors III. Elsevier Science Publishers BV, North-Holland, pp 573–580. http://www.ncbi.nlm.nih.gov/pubmed/18929029
207. Caldwell D, Tsagarakis N, Giesler C (1999) An integrated tactile/shear feedback array for stimulation of finger mechanoreceptor. In: Proceedings of the 1999 IEEE international conference on robotics and automation, vol 1, pp 287–292. https://doi.org/10.1109/ROBOT.1999.769991
208. Pai D, Rizun P (2003) The What: a wireless haptic texture sensor. In: 11th symposium on haptic interfaces for virtual environment and teleoperator systems, pp 3–9. https://doi.org/10.1109/HAPTIC.2003.1191210
209. Tanaka Y et al. (2012) Contact force during active roughness perception. In: Isokoski P, Springare J (eds) Haptics: perception, devices, mobility, and communication, vol 7282. LNCS. Proceedings of the Eurohaptics Conference, Tampere, FIN. Springer, Heidelberg, pp 163–168. https://doi.org/10.1007/978-3-642-31404-9_28
210. Smith AM, Gosselin G, Houde B (2002) Deployment of fingertip forces in tactile exploration. Exper Brain Res 147(2):209–218. https://doi.org/10.1007/s00221-002-1240-4
211. Rausch J et al. (2006) INKOMAN-Analysis of mechanical behaviour of liver tissue during intracorporal interaction. Gemeinsame Jahrestagung der Deutschen, Österreichischen und Schweizerischen Gesellschaften für Biomedizinische Technik 6(9)
212. Rausch J (2005) Analyse der mechanischen Eigenschaften von Lebergewebe bei intrakorporaler Interaktion. Diploma Thesis. Darmstadt: Technische Universität Darmstadt, Institut für Elektromechanische Konstruktionen. http://tubiblio.ulb.tu-darmstadt.de/53792/
213. Redmond B et al. (2010) Haptic characteristics of some activities of daily living. In: 2010 IEEE haptics symposium. IEEE, pp 71–76. https://doi.org/10.1109/HAPTIC.2010.5444674
214. Vander Poorten EEB, Demeester E, Lammertse P (2012) Haptic feedback for medical applications, a survey. In: Actuator conference. Bremen. https://www.radhar.eu/publications/e.-vander-poorten-actuator12-haptic-feedback-for-medical-applications-a-survey
215. Hayward V, Astley OR (1996) Performance measures for haptic interfaces. Robot Res 1:195–207. https://doi.org/10.1007/978-1-4471-0765-1_22
216. Hayward V, MacLean KE (2007) Do it yourself haptics: part I. IEEE Robot Autom Mag 14(4):88–104. https://doi.org/10.1109/M-RA.2007.907921
217. Hayward V, MacLean KE (2007) Do it yourself haptics: part II. IEEE Robot Autom Mag 15:104–119. https://doi.org/10.1109/M-RA.2007.914919
218. Kern T (2006) Haptisches Assistenzsystem für diagnostische und therapeutische Katheterisierungen. PhD thesis. Techische Universität Darmstadt, Institut für Elektromechanische Konstruktionen. http://tuprints.ulb.tu-darmstadt.de/761/
219. Cellier FE (1991) Continuous system modeling. Springer. ISBN: 9780387975023
220. Biggs S, Srinivasan M (2002) Haptic interfaces. In: Stanney K, Hale KS (eds) Handbook of virtual environments. Lawrence Erlbaum, London, pp 93–116. 978-0805832709
221. Ellis S (1994) What are virtual environments? Comput Graph Appl IEEE 14(1):17–22. ISSN: 0272-1716. https://doi.org/10.1109/38.250914
222. Lenk A et al (eds) (2011) Electromechanical systems in microtechnology and mechatronics: electrical, mechanical and acoustic networks, their interactions and applications. Springer, Heidelberg. ISBN: 978-3-642-10806-8
223. Okamura AM, Dennerlein JT, Howe RD (1998) Vibration feedback models for virtual environments. Int Conf Robot Autom. https://doi.org/10.1109/ROBOT.1998.677050
224. Hwang J, Williams M, Niemeyer G (2004) Toward event-based haptics: rendering contact using open-loop force pulse. In: 12th international symposium on haptic interfaces for virtual environment and teleoperator systems. Chicago. https://doi.org/10.1109/HAPTIC.2004.1287174
225. Kuchenbecker KJ, Fiene J, Niemeyer G (2006) Improving contact realism through event-based haptic feedback. IEEE Trans Vis Comput Graph 12(2):219–230. https://doi.org/10.1109/TVCG.2006.32

226. Kuchenbecker K et al. (2010) VerroTouch: high-frequency acceleration feedback for telerobotic surgery. In: Kappers AML, Bergmann-Tiest WM, van der Helm FC (eds) Haptics: generating and perceiving tangible sensations. Proceedings of the Eurohaptics conference, Amsterdam. Springer, Heidelberg, pp 189–196. https://doi.org/10.1007/978-3-642-14064-8_28
227. McMahan W et al (2011) Tool contact acceleration feedback for telerobotic surgery. IEEE Trans Haptics 4(3):210–220. https://doi.org/10.1109/TOH.2011.31
228. Hinterseer P (2009) Compression and transmission of haptic data in telepresence and teleactin systems. Dissertation. Technische Universität München. http://mediatum.ub.tum.de/doc/676484/676484.pdf
229. Steinbach E et al (2011) Haptic data compression and communication. Signal Process Mag, IEEE 28(1):87–96. https://doi.org/10.1109/MSP.2010.938753
230. Jones LA, Tan HZ (2013) Application of psychophysical techniques to haptic research. IEEE Trans Haptics 6(3):268–284. ISSN: 19391412. https://doi.org/10.1109/TOH.2012.74

Chapter 3
The User's Role in Haptic System Design

Thorsten A. Kern, Christian Hatzfeld, and Fady Youssef

Abstract Consequently, a good mechanical design has to consider the user in his or her mechanical properties. The first part of this chapter deals with the discussion of the user as a mechanical *load* on the haptic device. The corresponding model is split into two independent elements depending on the frequency range of the oscillation. Methods and measurement setups for the derivation of mechanical impedance of the user are reviewed and a thorough analysis of impedance for different grip configurations is presented. In the second part of the chapter, the user is considered as the ultimate measure of quality for a haptic system. The relation of psychophysical parameters like the absolute threshold or the JND to engineering quality measures like resolution, errors and reproducibility is described and application depending quality measures like haptic transparency are introduced.

3.1 The User as Mechanical Load

Fady Youssef and Thorsten A. Kern

3.1.1 Mapping of Frequency Ranges onto the User's Mechanical Model

The area of active haptic interaction—movements, made in a conscious and controlled way by the user—is of limited range. Sources concerning the dynamics of human movements differ as outlined in the preceding chapters. The fastest conscious

---

Christian Hatzfeld deceased before the publication of this book.

T. A. Kern (✉) · F. Youssef
Hamburg University of Technology, Eißendorfer Str. 38, 21073 Hamburg, Germany
e-mail: t.a.kern@tuhh.de

F. Youssef
e-mail: f.youssef@tuhh.de

C. Hatzfeld
Technische Universität Darmstadt, Darmstadt, Germany

T. A. Kern et al. (eds.), *Engineering Haptic Devices*, Springer Series on Touch and Haptic Systems, https://doi.org/10.1007/978-3-031-04536-3_3

movement performed by humans is done with their fingers. Movements for typing of up to 8 Hz can be observed.[1] As these values refer to a ten-finger interaction, they have to be modified a bit. However, as the border frequency of a movement lies above the pure number of a repetitive event, an assumption of the upper border frequency of 10 Hz for active, controlled movement covers most cases.

The major part of the spectrum of haptic perception is passive (*passive haptic interaction*, Fig. 1.9). The user does not have any active influence or feedback within this passive frequency range. In fact, the user is able to modify his properties as a mechanical load by e.g. altering the force when holding a knob. But although this change influences the higher frequency range, the change itself happens with lower dynamics within the dynamic range of active haptic interaction. A look at haptic systems addressing tactile and kinaesthetic interaction channels shows that the above modeling has slightly different impacts:

- The output values of kinaesthetic systems $\underline{F}_{\text{out}}$ (Fig. 3.1a) result in two reactions by the user. First, a spontaneous, not directly controllable movement reaction $\underline{v}_{\text{spo}}$ happens as a result of the mechanical properties of the finger tip (depending on the type of grasp, this can be also the complete interior hand and its skin elasticity). Second an additional perception of forces takes place. This perception K[2] is weighted according to the actual situation and results in a conscious reaction of the motor parts of the body. These induced reactions $\underline{v}_{\text{ind}}$ summed up with the spontaneous reactions result in the combined output value $\underline{v}_{\text{out}}$ of the user.
- The movements of tactile devices $\underline{v}_{\text{out}}$ (Fig. 3.1b) and the consciously performed movement of the user $\underline{v}_{\text{ind}}$ result in a combined movement and velocity. This elongation acts on the skin, generating the output value $\underline{F}_{\text{out}}$ as a result of its mechanical properties. This conscious movement $\underline{v}_{\text{ind}}$ sums up to $\underline{v}_{\text{out}}$ in the opposite direction of the original movement, as with opposite movement directions the skin's elongation increases and results in a larger force between user and technical system. Analogously it subtracts with movements in the same direction, as in this case the device (or the user, depending on the point of view) evades the acting force trying to keep deformation low and to perceive just a small haptic feedback. According to this model only the output value $\underline{F}_{\text{out}}$ of the combined movement is perceived and contributes to a willingly induced movement.

If you transfer the model of Fig. 3.1 into an abstract notation, all blocks correspond to the transfer-function $\underline{G}_{\text{Hn}}$. Additionally, it has to be considered that the user's reaction K' is a combined reaction of complex habits and the perception K; therefore a necessity to simplify this branch of the model becomes eminent. For the purpose of device design and requirement specification, the conscious reaction is modeled by a disturbing variable only limited in bandwidth, resulting in a block-diagram according to Fig. 3.2c for kinaesthetic and according to Fig. 3.2d for tactile devices.

---

[1] 8 Hz corresponds to a typing speed of 480 keystrokes per minute. 400 keystrokes are regarded as very good for a professional typist, 300–200 keystrokes are good, 100 keystrokes can be achieved by most laymen.

[2] K, a variable chosen completely arbitrarily, is a helpful construct for the understanding of block-diagrams rather than having a real neurological analogy.

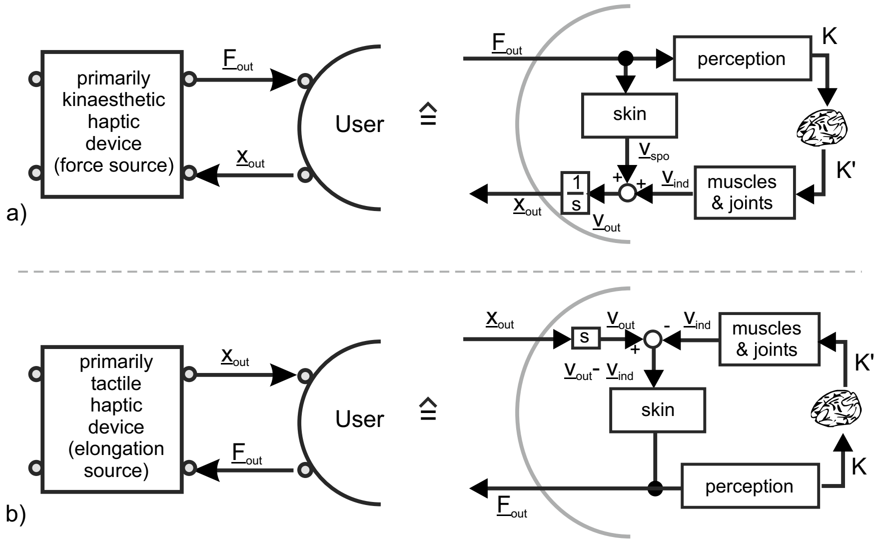

Fig. 3.1 User-models as a block-structure from kinaesthetic (a+c) and tactile (b+d) systems

The transfer function $\underline{G}_{\mathrm{H3}}$ corresponds to the mechanical admittance of the grasp above the border frequency of user interaction f_g.

With regard to the application of the presented models there are two necessary remarks to be considered:

- The notation in Figs. 3.1 and 3.2 for elongations $\underline{x}$ and forces $\underline{F}$ being input and output values of users is just one approach to the description. In fact an *impedance coupling* exists between user and haptic system making it impossible to distinguish between input and output-parameters. However, the decoupled haptic device is designed for being a position or force source. This in fact is the major motivation to define input- and/or output parameters of the user. But there are certain actuators (e.g. ultrasonic devices) which can hardly be defined as being part of either one of these classes. As a consequence, when describing either system, the choice of the leading sign and the direction of arrows should carefully be done!
- The major motivation for this model is the description of a mechanical load for the optimized dimensioning of a haptic system. For guaranteeing the closed-loop control engineering stability of a simulation or a telemanipulation system, further care has to be taken of the frequency range of active haptic interaction below 10 Hz. Stability analysis in this area can either be achieved by more detailed models or by an observation of in- and output values according to their *control-engineering passivity*. Further information on this topic can be found in Chap. 7.

The following sections on user impedance give a practical model for the transfer function $\underline{G}_{\mathrm{H3}}$ used in Fig. 3.2.

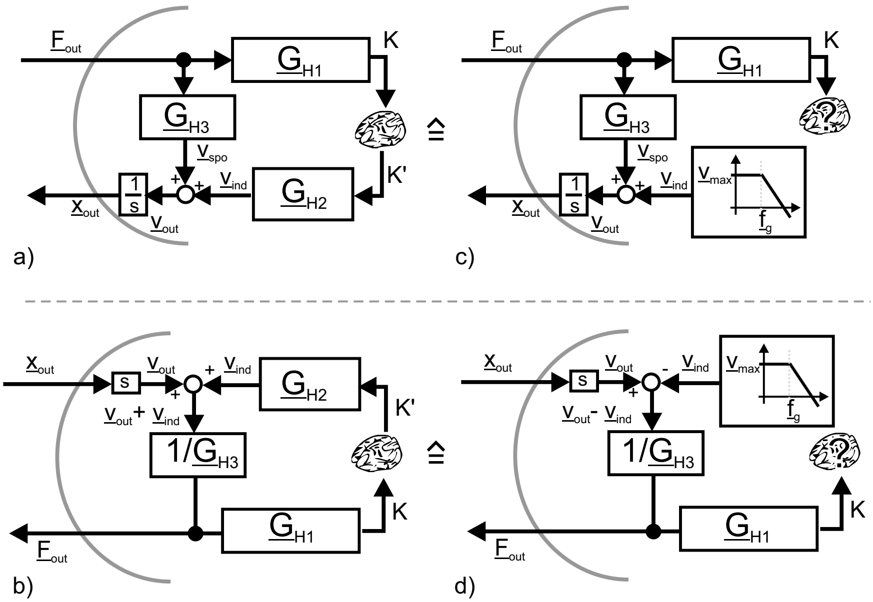

Fig. 3.2 Transformation of the user-models' block-structures in transfer-functions including simplifications of the model for the area of active haptic interaction for kinaesthetic (a+c) and tactile (b+d) systems

3.1.2 Modeling the Mechanical Impedance

The user's reaction as part of any haptic interaction combines a conscious, bandwidth-limited portion—the area of active haptic interaction—and a passive portion, mainly resulting from the mechanical properties of fingers, skin and bones. The influence of this second part stretches across the whole frequency range, but emphasizes the upper area for high frequencies. This section describes the passive part of haptic interaction. The transfer function $\underline{G}_{\text{H3}}$ of Fig. 3.2 is a component of the impedance coupling with force-input and velocity-output and is therefore a mechanical admittance of the human $\underline{Y}_H$ respectively in its reciprocal value the mechanical impedance $\underline{Z}_H$.

$$\underline{G}_{\text{H3}} = \frac{\underline{v}_{\text{spo}}}{\underline{F}_{\text{out}}} = \frac{\underline{v}_{\text{out}} - \underline{v}_{\text{ind}}}{\underline{F}_{\text{out}}} = \underline{Y}_H = \frac{1}{\underline{Z}_H} \tag{3.1}$$

In the following, this mechanical impedance of the user will be specified. The parameter impedance combines all mechanical parameters of an object or system that can be expressed in a linear, time-invariant description, i.e. mass m, compliance k and damping d. High impedance therefore means that an object has at least one of three properties:

1. hard and stiff in the meaning of spring-stiffness
2. large mass in the sense of inertial force
3. sticky and tight in the sense of high friction

In any case a small movement (velocity $\underline{v}$) results in a high force reaction $\underline{F}$ with high impedances. Low impedance means that the object, the mechanics, is accordingly soft and light. Even high velocities result in small counter forces in this case. The human's mechanical impedance is dependent on a number of influence parameters:

- type of grasp being directly influenced by the construction of the handle
- physiological condition
- grasping force being directly influenced by the will of the user
- skin surface properties, for example skin moisture

The quantification of human's mechanical impedance requires taking as many aspects into account as possible. The type of grasp is defined by the mechanical design of the device. Nevertheless a selection of typical grasping situations will give a good overview of typical impedances appearing during human-machine interaction. The user-individual parameters like physiological condition and skin structure can be covered best by the analysis of a large number of people of different conditions. By choosing this approach a span of percentiles can be acquired covering the mechanical impedances typically appearing with human users. The "free will" itself, however, is—similar to the area of active haptic interaction—hard if not impossible to be modeled. The time dependent and unpredictable user impedance dependency on the will can only be compensated if the system is designed to cover all possible impedance couplings of actively influenced touch. Another approach would be to indirectly measure the will to adapt the impedance model of the user within the control loop. Such an indirect measure is, in many typical grasping situations, the force applied between two fingers or even the whole hand holding an object or a handle. In the simplest design the acquisition of such a force can be done by a so called *dead-man-switch*, which in 1988 was already proposed by HANNAFORD for the usage in haptic systems [11]. A dead-man-switch is pressed as long as the user holds the control handle in his or her hand. It detects the release of the handle resulting in a change in impedance from $\underline{Z}_H$ to 0.

3.1.3 Grips and Grasps

There is a nomenclature for different types of grasps shown in Fig. 3.3. The hand is an extremity with 27 bones and 33 muscles. It combines 13 (fingers) respectively 15 (incl. the wrist) degrees-of-freedom.[3] Accordingly the capabilities of man to grasp are extremely versatile.

[3] Thumb: 4 DoF, index finger: 3 DoF, middle finger: 2 DoF (sometimes 3 DoF), ring finger: 2 DoF, small finger: 2 DoF, wrist: 2 DoF. The rotation of the whole hand happens in the forearm and therefore does not count among the degrees of freedom of the hand itself.

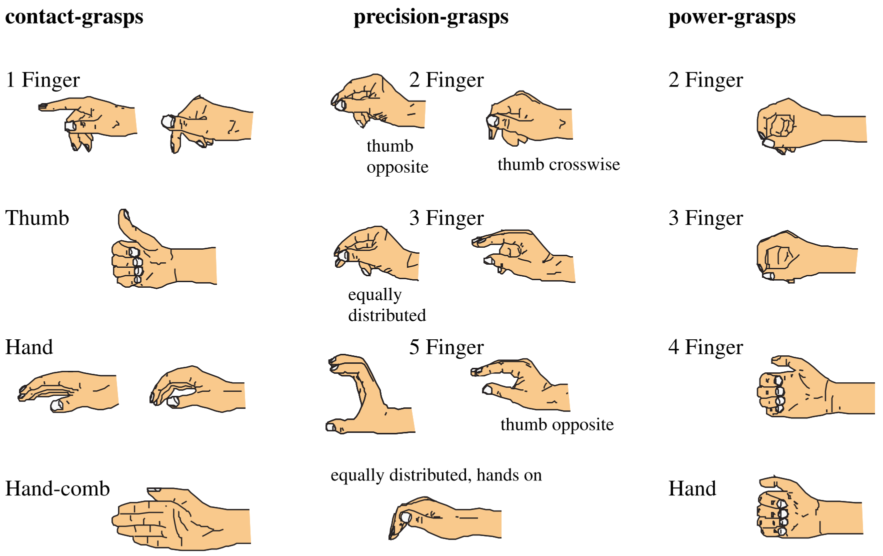

Fig. 3.3 Grip configurations, figure based on [3]

There are three classes of grasps to be distinguished:

- The **contact grasp** describes the touch of an object using the whole hand or major parts of it. Keys and buttons are typically actuated by contact grasps. Even the fingers resting on a keyboard or a piano are called contact grasps. A contact grasp always blocks one direction of movement for an object (which is one half of a degree of freedom). Contact grasps can be regarded as linear only in case of a pre-load high enough. With light touches the point of release and the according lift-off of the object is always nonlinear.
- The **precision grasp** describes the grasping with several fingers. Typically a precision grasp locks at least one degree of freedom of the grasped object by form closure with one finger and a counter bearing—often another finger. Additional degrees of freedom are hindered by friction. Precision grasps vary much in stiffness of coupling between man and machine. At the same time they are the most frequent type of grasping.
- The **power grasp** describes an object with at least one finger and a counter bearing, which may be another finger, but frequently is the whole hand. The power grasp aims at locking the grasped object in all degrees of freedom by a combination of form and force closures. Power grasps are—as the name already implies—the stiffest coupling between humans and machines.

Further discrimination of grasps is made by Feix et al. and documented online [5] with the purpose of reducing the mechanical complexity of anthropomorphic hands [6]. The reported taxonomy could be useful for very specialized task-specific systems. For all classes of grasps, measurements of the human's impedance can be performed. According to the approach presented by Kern [20], the measurement method and the models of user impedance are presented including the corresponding model parameters.

3.1.4 Measurement Setup and Equipment

The acquisition of mechanical impedances is a well-known problem in measurement technology. The principle of measurement is based on an excitation of the system to be measured by an actuator, simultaneously measuring force and velocity responses of the system. For this purpose combined force and acceleration sensors (e.g. the impedance sensor 8001 from *Brüel & Kjær*, Nærum, DK) exist, whereby the charge amplifier of the acceleration sensor includes an integrator to generate velocity signals.

In [28], WIERTLEWSKI AND HAYWARD argue that measurements with impedance heads are prone to measurement errors because of the mechanical construction of the sensor based on [2]. However, errors induced by the construction of the measurement head appear at frequencies larger than 2000 Hz, values that are only seldom used in the design of haptic interfaces. Furthermore, interpersonal variations and calibration of the measurement setup based on a concentrated network parameter approach are used to minimize the errors even for high frequencies in the following.

In general the impedance of organic systems is *nonlinear* and *time-variant*. This non-linearity is a result of a general viscoelastic behavior of tissue resulting from a combined response of relaxation, conditioning, stretching and creeping [9]. These effects can be reproduced by mechanical models with concentrated elements. However, they are dependent on the time-history of excitation to the measured object. It can be expected that measurements based on step excitation are different from those acquired with a sinusoid sweep. Additionally, the absolute time for measurement has some influence on the measures by conditioning. Both effects are systematic measurement errors. Consequently, the models resulting from such measurements are an indication of the technical design process and should always be interpreted with awareness of their variance and errors (Fig. 3.4).

All impedance measures presented here are based on a sinusoid-sweep from upper to lower frequencies. The excitation has been made with a defined force of 2 N amplitude at the sensor. The mechanical impedance of the handle has been measured by calibration measurements and was subtracted from the measured values. The impedance-sensors are limited concerning their dynamic and amplitude resolution, of course. As a consequence, the maximum frequency up to which a model is valid depends on the type of grasp and its handle used during measure. This limitation is a direct result of the amplitude resolution of the sensors and the necessity at high frequencies to have a significant difference between the user's impedance and the handle's impedance for the model to be built on. The presented model-parameters are limited to the acquired frequency range and cannot be applied to lower or higher frequencies. The measurement setup is given in Fig. 3.5.

BOCHEREAU ET AL. [1] introduced a device to record, reproduce and image the fingertip friction. In this study, Frustrated Total Internal Reflection principle (FTIR)

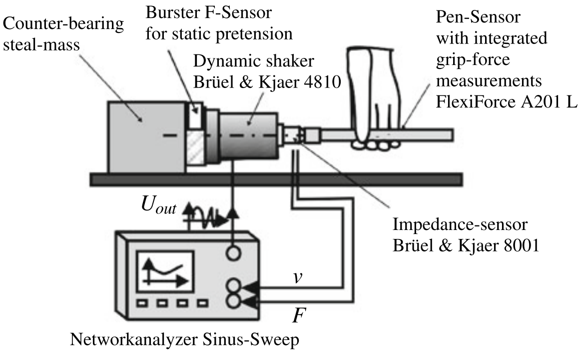

Fig. 3.4 Measurement setup for the acquisition of user impedances according to [20]

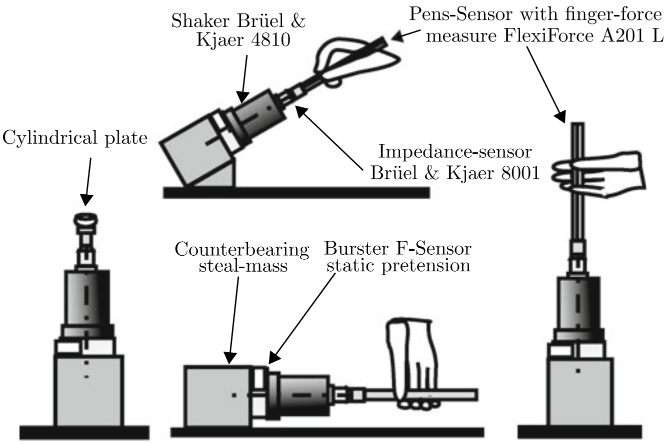

Fig. 3.5 Impedance measurement settings for different grasps

was used to image the evolution of fingertip contact area over time. The device, shown in Fig. 3.6, consists of different parts; one part is designed to record the friction force resulting from the movement of the user's finger over a texture. Three load cells are used in the record phase, in which two are used to compute the normal force and one for the tangential component. The second part of the device is designed to reproduce the friction forces, this is done with the help of a linear electrodynamic motor. The motor is connected to a glass plate, that the motor could vibrate the plate, so that the imaging phase could occur.

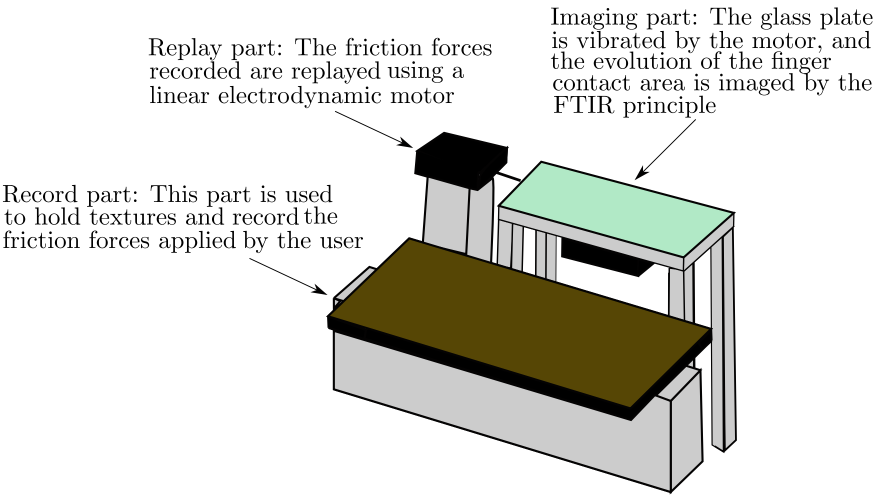

Fig. 3.6 Device to record, replay and image of finger friction movement according to [1]

3.1.5 Models

In order to approximate the human's impedance a number of different approaches were taken in the past (Fig. 3.7). For its description mechanical models based on concentrated linear elements were chosen. They range from models including active user reactions represented by force sources (Fig. 3.7a), to models with just three elements (Fig. 3.7c) and combined models of different design. The advantage of a mechanical model compared to a defined transfer function with a certain degree in enumerator and denominator results from the possibility of interpreting the elements of the model as being a picture of physical reality. Elasticities and dampers connected in circuit with the exciting force can be interpreted as the coupling to the skin. Additionally the mechanical model creates very high rankings by its interconnected elements which allow a much better fit to measurements than free transfer functions.

KERN [20] defined an eight-element model based on the models in Fig. 3.7 for the interpolation of the performed impedance measures. The model can be characterized by three impedance groups typical for many grasping situations (Fig. 3.8).

$\underline{Z}_3$ (Eq. 3.4) models the elasticity and damping of the skin being in direct contact with the handle. $\underline{Z}_1$ (Eq. 3.2) is the central element of the model and describes the mechanical properties of the dominating body parts—frequently fingers. $\underline{Z}_2$ (Eq. 3.3) gives an insight into the mechanical properties of the limbs, frequently hands, and allows to make assumptions about the pre-loads in the joints in a certain grasping situation.

$$\underline{Z}_1 = \frac{s^2 m_2 + k_I + d_I\, s}{s} \tag{3.2}$$

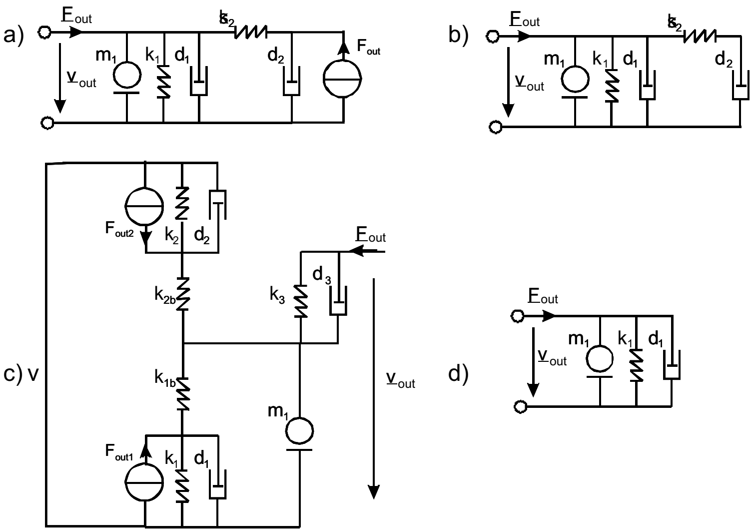

Fig. 3.7 Modeling the user with concentrated elements, **a** [11], **b** [18], **c** [23], **d** [21], own illustrations

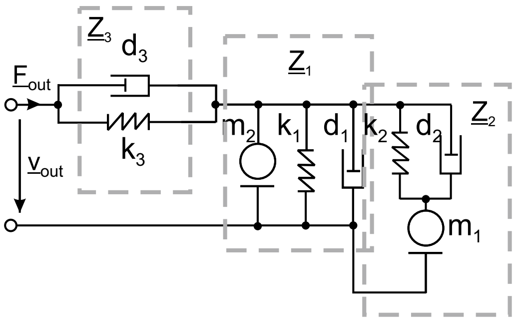

Fig. 3.8 Eight-element model of the user's impedance [20] © Springer Nature, all rights reserved, modeling the passive mechanics for frequencies >20 Hz

$$\underline{Z}_2 = \left(\frac{s}{d_2\, s + k_2} + \frac{1}{s m_1} \right)^{-1} \tag{3.3}$$

$$\underline{Z}_3 = \frac{d_3\, s + k_3}{s} \tag{3.4}$$

$$\underline{Z}_B = Z_1 + Z_2 \tag{3.5}$$

Combined, the model's transformation is given as

$$\underline{Z}_{\mathrm{H}} = \underline{Z}_3 \| \underline{Z}_B \tag{3.6}$$

$$\underline{Z}_{\mathrm{H}} = \left(\frac{s}{d_3\, s + k_3} + \left(\frac{s^2 m_2 + k_1 + d_1\, s}{s} + \left(\frac{s}{d_2\, s + k_2} + \frac{1}{s m_1} \right)^{-1} \right)^{-1} \right)^{-1} \tag{3.7}$$

3.1.6 Modeling Parameters

For above model (Eq. 3.7) the mechanical parameters can be identified by measurement and approximations with real values. For the values presented here approximately 48–194 measurements were made. The automated algorithm combines an evolutionary approximation procedure followed by a curve-fit with optimization based on NEWTON curve fitting, to achieve a final adjustment of the evolutionarily found starting parameters according to the measurement data. The measurements vary according to the mechanical pre-load—the grasping force—to hold and move the control handles. This mechanical pre-load was measured by force sensors integrated into the handles. For each measurement this pre-load could be regarded as being static and was kept by the subjects with a 5% range of the nominal value. As a result the model's parameters could be quantified not only dependent on the grasping situation but also dependent on the grasping force. The results are given in the following section. The display of the mechanical impedance is given in decibel, whereby 6 dB equals a doubling of impedance. The list of model values for each grasping situation is given in Appendix.

3.1.6.1 Precision Grasps

Within the area of precision grasps three types of grasps were analyzed. Holding a measurement cylinder similar to a normal pen in an angle of 30° (Fig. 3.9), we find a weak anti-resonance in the area of around 150–300 Hz. This anti-resonance is dependent on the grasping force and moves from weak forces and high frequencies to large forces and lower frequencies. The general dependency makes sense, as the overall system becomes stiffer (the impedance increases) and the coupling between skin and cylinder becomes more efficient resulting in more masses being moved at higher grasping forces.

The general impedance does not change significantly. if the cylinder is held in a position similar to a máobi Chinese pen (Fig. 3.10). However the dependency on the anti-resonance slightly diminishes compared to the above pen hold posture.

This is completely different to the variant of a pen in a horizontal position held by a three finger grasp (Fig. 3.11). A clear anti-resonance with frequencies between 80 and 150 Hz appears largely dependent in shape and position on the grasping force. All observable effects in precision grasps can hardly be traced back to the change of a single parameter but are always a combination of many parameters' changes.

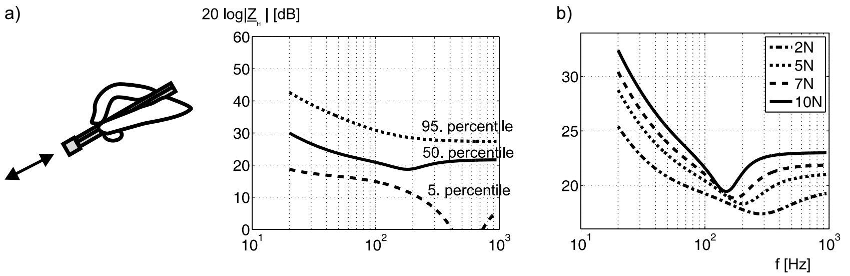

Fig. 3.9 Impedance with percentiles (**a**) and at different force levels (**b**) for a two fingered precision-grasp of a pen-like object held like a pen (Ø10 mm, defined for 20–950 Hz)

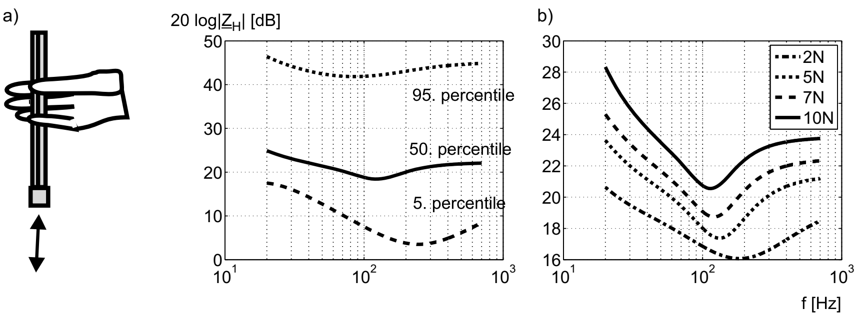

Fig. 3.10 Impedance with percentiles (**a**) and at different force levels (**b**) for a two fingered precision-grasp of a pen-like object held like a "máobi" Chinese pen (Ø10 mm, defined for 20–700 Hz)

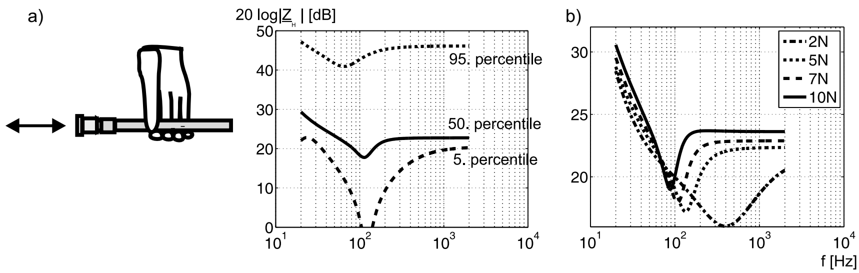

Fig. 3.11 Impedance with percentiles (**a**) and at different force levels (**b**) for a five fingered precision-grasp of a pen-like object in horizontal position (Ø10 mm, defined for 20–2 kHz)

3.1.6.2 One-Finger Contact Grasp

All measurements were done on the index finger. Direction of touch, size of touched object and touch-force normal to the skin were varied within this analysis. Figure 3.12a shows the overview of the results for a touch being analyzed in normal direction. The mean impedance varies between 10 and 20 dB with a resonance in the range

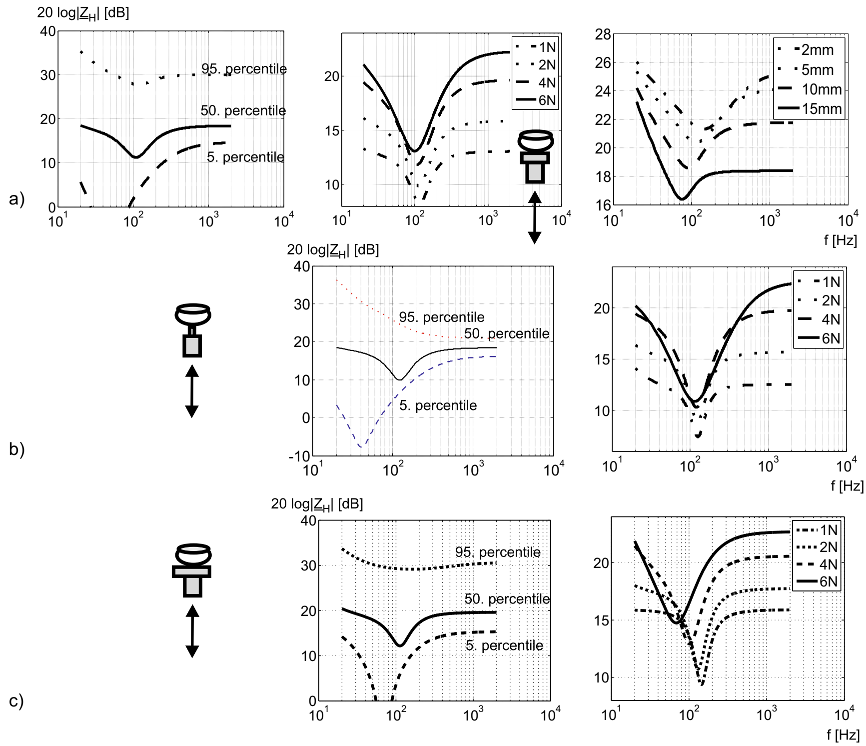

Fig. 3.12 Impedance of finger touch via a cylindrical plate for different contact forces (1–6 N) and in dependency from diameter (**a**), for the smallest plate (Ø 2 mm) and the largest plate (Ø 15 mm) (defined for 20–2 kHz)

of 100 Hz. Throughout all measured diameters of contactor size and forces, no significant dependency of the position of the anti-resonance on touch forces were noted. However, a global increase in impedance is clearly visible. Observing the impedance dependent on contactor size, we can recognize an increase of the anti-resonance frequency. Additionally, it is fascinating to see that the stiffness decreases with an increase of contact area. The increase in resonance is probably a result of less material and therefore less inertia participating in generating the impedance. The increase in stiffness may be a result of smaller pins deforming the skin more deeply and therefore getting nearer to the bone as a stiff mechanical counter bearing.

In comparison, with measurements performed with a single pin of only 2 mm in diameter (Fig. 3.12b), the general characteristic of the force dependency can be reproduced. Looking at the largest contact element of 15 mm, in diameter, we are aware of a movement of the resonance frequency from 150 Hz to lower values down to 80 Hz for an increase in contact force.

In orthogonal direction the skin results differ slightly. Figure 3.13a shows a lateral excitation of the finger pad with an obvious increase of impedance at increased force

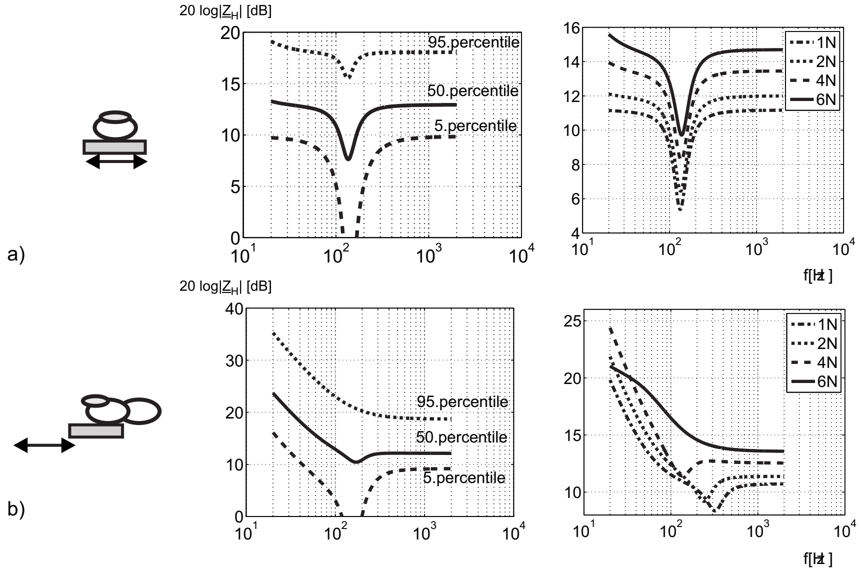

Fig. 3.13 Impedance for finger touch of a plate moving in orthogonal direction to the skin at different force levels (1–6 N) (defined for 20 Hz to 2 kHz). Movement in lateral direction (**a**), distal direction (**b**)

of touch. This rise is mainly a result of an increase of damping parameters and masses. The position of the anti-resonance in frequency domain remains constant at around 150 Hz. The picture changes significantly for the impedance in distal direction (Fig. 3.13b). The impedance still increases, but the resonance moves from high frequencies of around 300 Hz to lower frequencies. Damping increases too, resulting in the anti-resonance being diminished until non-existence.

3.1.6.3 Superordinate Comparison of Grasps

It is interesting to compare the impedances among different types of touch and grasps with each other:

- Almost all raw data and the interpolated models show a decrease of impedance within the lower frequency range of 20 Hz to the maximum of the first anti-resonance. As to precision grasps (Figs. 3.9, 3.10 and 3.11), normal fingertip excitation (Fig. 3.12), the gradient equals 20 dB/decade resembling a dominating pure elongation proportional effect of force response—elasticity—within a low frequency range. Within this low bandwidth-area nonlinear effects of tissue including damping seem to be not very relevant. Looking at this type of interactions we can assume that any interaction including joint rotation of a finger is almost purely elastic in a low frequency range.

- Many models show a clear antiresonance. Its position varies between 200 Hz or even 300 Hz at finger touch analyzed in orthogonal direction (Fig. 3.13). The resonance is a natural effect of any system including a mass and elasticity. Therefore it is not its existence which is relevant for interpretation, but its shape and the position within the frequency range. As to positions, the precision grasps of a cylinder in a pen-like position (Fig. 3.9) and in horizontal position (Fig. 3.11) and the touch of an orthogonal moving plate in distal direction (Fig. 3.13b) and a large plate in normal direction (Fig. 3.13a) have a clear dependence on grasping force. The interpretation is not as obvious as in case one. We assume that the normal touch of the plate shows similarities to the contact situation when touching the rings. Additionally the normal touch is part of the precision grasps mentioned above. In the case of many subjects grasping the horizontal cylinder, it could be observed that the thumb was positioned less orthogonally but more axially to the cylinder, which could excite it primarily in distal direction, thus also contributing to this effect.
- The shape of the anti-resonance is another interesting factor. It can be noted that especially in the analysis of finger grasps and there at orthogonal excitation (Fig. 3.13a), the anti-resonance is very narrow. An interpretation is hard to be formulated. It seems that with grasps and especially touches involving less material the anti-resonance becomes narrower in shape.
- For all measurements, at high frequencies above the anti-resonance, the frequency characteristic becomes linear and constant, which resembles a pure damping effect. This becomes obvious at the pen-hold posture among the precision grasps (Fig. 3.9) and with the lateral displacement in orthogonal direction, (Fig. 3.13a), but is part of any curve and model. Alternatively, inertia could be assumed to dominate the high frequencies, being represented by a linear increase of mechanical impedance. This measured effect is especially relevant, as it confirms common assumptions that for high frequency haptic playback with kinaesthetic devices, the user can be assumed as a damping load.
- A last glance should be taken at the absolute height level and the variance of height of the impedance due to pre-loads. For all grasps it varies in a range (regarding the median curves only) of 20 dB as a maximum. Impedance is higher for power grasps, slightly lower for precision grasps and very much lower for touches, which is immediately obvious. The change in the pre-load for one grasp typically displaces the absolute impedance to higher levels. This displacement varies between 4 and 10 dB.

If speculations should be made on still unknown, not yet analyzed types of touches according to the given data, it should be reasonable to assume the following:

A. **Power grasp** The median impedance should be around 36 dB. Model the impedance with a dominating elasticity effect until an anti-resonance frequency of 80 Hz, not varying much neither in height nor in position of the anti-resonance. Afterward, allow inertia to dominate the model's behavior.
B. **Precision grasp** The median impedance should be around 25 dB. Model the impedance with a dominating elasticity effect until an anti-resonance frequency

of around 200 Hz. The position of the anti-resonance diminishes in an area of 100 Hz due to change in pre-load. Above that anti-resonance let the impedance become dominated by a damping effect. The height of impedance changes in a range of 5 dB by the force of the grasp.

C. **Finger touch** The median impedance should be around 12 dB. Model the impedance with a well balanced elasticity and damping effect until an anti-resonance frequency of around 150 Hz. The position of the anti-resonance is quite constant, with the exception of large contact areas moving in normal and in distal direction. Above that anti-resonance let the impedance become strongly dominated by a damping effect. The absolute height of impedance changes in an area of up to 10 dB depending on the force during touch.

3.1.7 Comparison with Existing Models

For further insight into and qualification of the results, a comparison with published mechanical properties of grasps and touches is presented in this section. There are two independent trends of impedance analysis in the scientific focus: the measurement of mechanical impedance as a side product of psychophysical studies at threshold level, and measurements at higher impedance levels for general haptic interaction. The frequency plots of models and measurements are shown in Fig. 3.14.

In [14] the force detection thresholds for grasping a pen in normal orientation have been analyzed. Figure 3.14a shows an extract of the results compared to the pen-like grasp of a cylinder of the model in Fig. 3.9a. Whereas the general level of

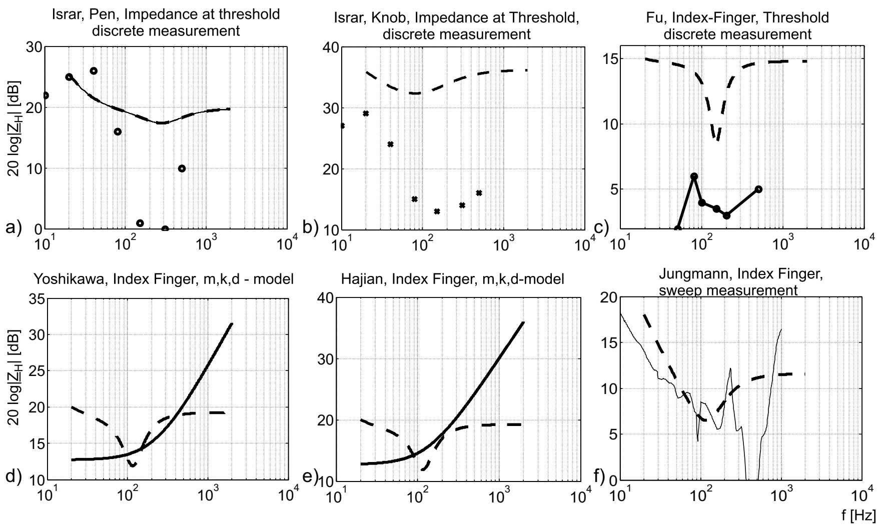

Fig. 3.14 Comparison of the model from Fig. 3.8 with data from similar touches and grasps as published by Israr [14, 15], Fu [8], Yoshikawa [29], Hajian [10], Jungmann [17]

impedance does fit, the dynamic range covered by our model is not as big as described in literature. Analyzing the data as published, we can state that the minimum force measured by ISRAR is ≈60 μN at the point of lowest impedance. A force sensor reliably measuring at this extreme level of sensitivity exceeds the measurement error of our setup and may be the explanation of the difference in the dynamic range covered. In another study [15] the force detection threshold of grasping a sphere with the finger tips was analyzed. The absolute force level of interaction during these measurements was in the range of mN. A comparison (Fig. 3.14b) between our model of touching a sphere and these data show a difference in the range of 10–20 dB. However such small contact forces resemble a large extrapolation of our model data to low forces. The difference can therefore be easily explained by the error resulting from this extrapolation.

FU [8] measured the impedance of the finger tip at a low force of 0.5 N. He advanced an approach published by HAJIAN [10]. A comparison between our model and their data concerning the shape is hardly possible due to the little number of discrete frequencies of this measurement. However the impedance is again 10 dB lower than of our touch model of a five millimeter cylinder at normal oscillations similar to Fig. 3.12. Once more the literature data describe a level of touch force not covered by our measurements and therefore the diagram in Fig. 3.14c is an extrapolation of the model of these low forces.

As a conclusion of this comparison, the model presented here cannot necessarily be applied to measurements done at lower force levels. Publications dealing with touch and grasp at reasonable interaction forces reach nearer to the model parameter estimated by our research. YOSHIKAWA [29] published a study of a three element mechanical model regarding the index finger. The study was based on a time-domain analysis of a mechanical impact generated by a kinaesthetic haptic device. The measured parameters result in a frequency plot (Fig. 3.14d) which is comparable to our model of low frequencies, but does neither show the complexity nor the variability of our model in a high frequency range of above 100 Hz. A similar study in time-domain was performed by HAJIAN [10] with just slightly different results. Measurements available as raw data from JUNGMANN [17] taken in 2002 come quite close to our results, although obtained with different equipment.

Besides these frequency plots, the model's parameters allow a comparison with absolute values published in literature: SERINA [26] made a study on the hysteresis of the finger tips' elongation vs. force curve during tapping experiments. This study identified a value for k for pulp stiffness ranging from 2 N/mm at a maximum tapping-force of 1–7 N/mm at a tapping force of 4 N. This value is about 3–8 times larger than the dominating k_2 in our eight-element model. The results of FU [8] make us assume that there was a systematic error concerning the measurements of SERINA, as the elongation measured at the fingernail does not exclusively correspond to the deformation of the pulp. Therefore the difference in the values of k between our model and their measurements can become reasonable. Last but not least MILNER [22] carried out several studies on the mechanical properties of the finger tip in different loading directions. In the relevant loading situation a value of k ranging from 200 to 500 N/m was identified by him. This is almost perfect within the range of our model's stiffness.

3.1.8 Modeling User's Variability

In order to perform an optimal system and control design, a good modeling of user's variability should be included. The key for a good variability modeling is precise measurments. FU ET AL. [7] performed a variability analysis especially for stylus-based haptic devices. The variability of human arm was studied in two forms: structured and unstructured variability. Structured was defined as the statically defined uncertainties from the paramters of the human arm model used. On the other hand the multiplicative unstructured uncertainties we referred as unstructured variability. Both variability forms are modeled in a way, such that they can be applied directly to a robust stability analysis.

3.1.9 Final Remarks on Impedances

The impedance model as presented here will help with the modeling of haptic perception in high frequency ranges of above 20 Hz. However, it completely ignores any mechanical properties below that frequency range. This is a direct consequence of the general approach to human machine interaction presented in Chap. 2 and has to be considered when using this model.

Another aspect to consider is that the above measurements show a large inter-subject variance of impedances. In extreme cases they span 20 dB meaning nothing else but a factor of 10 between e.g. the 5th and the 95th percentile. Further research on the impedance models will minimize this variance and allow a more precise picture of impedances. But already this database, although not yet completed, allows to identify helpful trends for human load and haptic devices.

3.2 The User as a Measure of Quality

Christian Hatzfeld

SALISBURY ET AL. postulated a very valuable hypothesis for the design of task-specific haptic systems: Their 2011 paper title reads *What You Can't Feel Won't Hurt You: Evaluating Haptic Hardware Using a Haptic Contrast Sensitivity Function* [25]. In this work, they use haptic contrast sensitivity functions (the inverse of the sinusoidal grating detection threshold) to evaluate ↪ COTS devices. With a more general view, the first part of this paper title summarizes the second role of the user and her or his properties in the design of haptic systems: As the instance that determines, whether the presented haptic feedback is good enough or not. In this section, this approach is detailed on three aspects of the system design, i.e. resolutions, errors and the quality of the haptic interaction.

3.2.1 Resolution of Haptic Systems

Resolution is mainly an issue in the selection and design of sensors and actuators, while latter is also influenced by the kinematic structure used in interfaces and manipulators. In general, sensors on the manipulation side have so sense at least as good as the human user is able to perceive after the information is haptically displayed by the haptic interface. On the interface side, sensors have to be at least as accurate as the reproducibility of the human motor capability, to convey the users intention correctly. For the actuating part, the attribution is vice versa: actuators on the manipulating side have to be as accurate as the human motor capability, while the haptic interface has to be as accurate as human perception can resolve.

Unfortunately, this is the worst case for technical development: sensors (on the manipulating side) and actuators (on the interfacing side) have to be as accurate as human perception. Therefore exact readings of *absolute thresholds* are indispensable to determine the necessary resolutions for sensors and actuators, if one wants to build a high-fidelity haptic system. On the other hand, systematic provisions to alter the perception thresholds favourably by changing the contact situation (contact area, contact forces) at the primary interface are possible. This is further detailed in Sect. 5.2.

For applications not involving teleoperation, the requirements are basically the same, but extend to other parts of the system: For the interaction with virtual realities, the software has to supply sufficient discretization of the virtual data (a non-trivial problem, especially if small movements and hard contacts are to be simulated), systems for communication have to supply enough mechanical energy that the perception threshold is surpassed to ensure clear transmission of information. Last, but definitely not least, all errors resulting from digital quantization and other, system inherent noise have to be lower than the absolute perception thresholds of the human user.

3.2.2 Errors and Reproducibility

While resolutions are quite a challenge for the design of haptic systems because of the high sensitivity of human haptic perception, the handling of errors is somewhat easier. The basic assumption about the perception of haptic signals with regard to errors and reproducibility is the following: There is no error, if there is no difference detectable by the user. This property is expressed by the $\hookrightarrow$ JND. *Weber's Law* as stated in Eq. (2.5) facilitates this further: For low references the acceptable error increases due to the increasing differential thresholds. This accommodates the fact, that the absolute errors of technical systems and components usually increase, when the reference values decrease.

For large reference values, this relative resolution of human perception is much smaller than the absolute resolution of technical systems, that is uniformly distributed along the whole nominal range. This has to be taken into account if information are to be conveyed haptically.

3.2.3 Quality of Haptic Interaction

While resolution and errors are pretty much linked directly to perception parameters, the assessment of haptic quality is somewhat more difficult. It is also based on the assumption, that the quality of a haptic interaction is good enough, if all intended information are transmitted correctly to the user and no additional information or errors are perceived. The second part can basically be achieved by considering the above mentioned points regarding errors and resolution. The assessment, if all information is transmitted correctly is more difficult, since the user and the perceived information have to be taken into account. In general, this is only possible if suitable evaluation methods are used, Chap. 13 gives an overview about such methods with respect to the intended application.

Another example for the evaluation of haptic quality is the concept of haptic transparency for teleoperation system. This property describes the ability of a haptic system to convey only the intended information (normally defined as the mechanical impedance of the environment at the manipulator side $\underline{Z}_{\mathrm{e}}$) to the user (in terms of the displayed impedance of the haptic interface $\underline{Z}_{\mathrm{t}}$) without displaying the inherent properties of the haptic system. This definition is further detailed in Sect. 7.5.2. Despite the above said, this property can be tested without a user test, but with considerable effort regarding the mechanical measurement setup.

When further considering haptic perception properties, especially ↪ Just Noticeable Differences, the common binary definition of transparency can be transformed to a nominal value with a lot less requirements on the technical system. This concept was developed by Hatzfeld et al. [12, 13] and is further explained in Sect. 7.5.2.

One should keep in mind, that all of the above mentioned thresholds are generally dependent on frequency and the contact situation in the best case. In the worst case, they are also dependent on the experimental methodology used to obtain them, which will necessarily require a retest of the perception property needed.

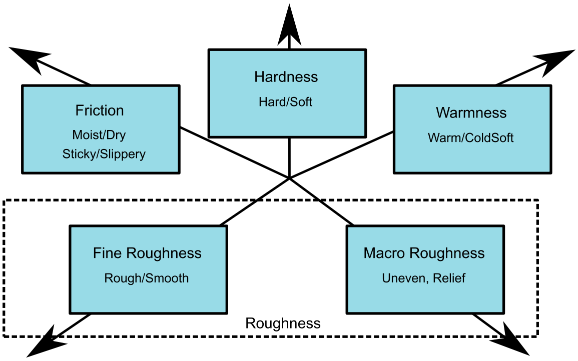

Fig. 3.15 Five psychophysical dimensions of tactile perception for materials and textures, based on OKAMOTO ET AL. [24]

3.2.4 Perceptional Dimensions

All above approaches follow the tendency to describe quality of haptic interaction by perceptional capabilities in a usually physical domain. The inherent assumption is that humans act as sensors for physical properties. Stating this in an explicit way makes it obvious that this can not be true.

This is where *perceptional dimensions* should be considered. All psychophysical fields use this more user-centric approach. And the range for *perceptional dimensions* is wide, from object perception to space perception as nicely summarized by KAPPERS AND BERGMANN TIEST in [19].

However the level of difference between physical and perceptional dimensions is nowhere larger than in the domain of *textures*. OKAMOTO ET AL. identified in a review [24] five dominating tactile dimensions for textures (Fig. 3.15). This triggered systematic research on the discrimination of materials (e.g. [4]) and new quality measures for performance evaluations of texture-rendering devices (e.g. [27]).

Recommended Background Reading

[16] Jones, L. & Lederman, S.: **Human Hand Function**. Oxford University Press, 2006
Extensive Analysis about the human hand including perception and interaction topics.

[6] Feix, T.; Pawlik, R.; Schmiedmayer, H.; Romero, J. & Kragic, D.: **A Comprehensive Grasp Taxonomy** In: Robotics, Science and Systems Conference: Workshop on Understanding the Human Hand for Advancing Robotic Manipulation, 2009.
Thorough Analysis of human grasps, also available online at http://grasp.xief.net/.

References

1. Bochereau S et al (2017) Characterizing and imaging gross and real finger contacts under dynamic loading. IEEE Trans Hapt 10(4):456–465
2. Brownjohn J et al (1980) Errors in mechanical impedance data obtained with impedance heads. J Sound Vibr 73(3):461–468. https://doi.org/10.1016/0022-460X(80)90527-1
3. Bullinger H-J (1978) Einflußfaktoren und Vorgehensweise bei der ergonomischen Arbeitsmittelgestaltung. Universität Stuttgart, Habilitation
4. Culbertson H, Kuchenbecker KJ (2017) Importance of matching physical friction, hardness, and texture in creating realistic haptic virtual surfaces IEEE Trans Hapt 10(1):63–74. ISSN: 19391412. https://doi.org/10.1109/TOH.2016.2598751
5. Feix T (2012) Human grasping database. Letzter Abruf: 20 Mar 2012. http://grasp.xief.net
6. Feix T et al (2009) A comprehensive grasp taxonomy. In: Robotics, science and systems conference: workshop on understanding the human hand for advancing robotic manipulation. http://grasp.xief.net/documents/abstract.pdf
7. Fu MJ, Cavusoglu MC (2012) Human-arm-and-hand-dynamic model with variability analyses for a stylus-based haptic interface. IEEE Trans Syst Man Cybern Part B: Cybern 42(6):1633–1644. ISSN: 10834419. https://doi.org/10.1109/TSMCB.2012.2197387
8. Fu C-Y, Oliver M (2005) Direct measurement of index finger mechanical impedance at low force. In: Eurohaptics conference, 2005 and symposium on haptic interfaces for virtual environment and teleoperator systems. World haptics 2005. First Joint Embedded System & Physical Sciences Research Laboratory, Motorola Labs, USA, pp 657–659. https://doi.org/10.1109/WHC.2005.40
9. Fung Y-C (1993) Biomechanics: mechanical properties of living tissues. 2nd edn. New York [u.a.]: Springer. pp XVIII, 568. ISBN: 0-387-97947-6; 3-540-97947-6
10. Hajian AZ, Howe RD (1997) Identification of the mechanical impedance at the human finger tip. J Biomech Eng 119:109–114. https://doi.org/10.1115/1.2796052
11. Hannaford B, Anderson R (1988) Experimental and simulation studies of hard contact in force reflecting teleoperation. In: Proceedings IEEE International Conference on Robotics & Automation. Jet Propulsion Laboratory, Caltech, Pasadena, CA, USA, pp 584–589. https://doi.org/10.1109/ROBOT.1988.12114
12. Hatzfeld C (2013) Experimentelle Analyse der menschlichen Kraftwahrnehmung als ingenieurtechnische Entwurfsgrundlage für haptische Systeme. Dissertation, Technische Universität Darmstadt. München: Dr. Hut Verlag. http://tuprints.ulb.tu-darmstadt.de/3392/. ISBN: 978-3-8439-1033-0
13. Hatzfeld C, Neupert C, Werthschützky R (2013) Systematic consideration of haptic perception in the design of task-specific haptic systems. Biomed Tech 58. https://doi.org/10.1515/bmt-2013-4227
14. Israr A, Choi S, Tan HZ (2006) Detection threshold and mechanical impedance of the hand in a pen-hold posture. In: International conference on intelligent robots and systems (IROS), Peking, C, pp 472–477. https://doi.org/10.1109/IROS.2006.282353
15. Israr A, Choi S, Tan HZ (2007) Mechanical impedance of the hand holding a spherical tool at threshold and suprathreshold stimulation levels. In: Second joint eurohaptics conference and symposium on haptic interfaces for virtual enrivonment and teleoperator systems (WorldHaptics conference), Tsukaba. https://doi.org/10.1109/WHC.2007.81
16. Jones L, Lederman S (2006) Human hand function. Oxford University Press, Oxford, GB. 0195173155
17. Jungmann M, Schlaak HF (2002) Taktiles Display mit elektrostatischen Polymeraktoren. In: Konferenzband des 47. Internationalen Wissenschaftlichen Kolloquiums, Technische Universität Ilmenau. http://tubiblio.ulb.tu-darmstadt.de/17485/
18. Jungmann M (2004) Entwicklung elektrostatischer Festkörperaktoren mit elastischen Dielektrika für den Einsatz in taktilen Anzeigefeldern. Dissertation. Technische Universität Darmstadt, p 138. http://tuprints.ulb.tu-darmstadt.de/500/

19. Kappers AM, Bergmann Tiest WM (2013) Haptic perception. Wiley Interdisc Rev: Cogn Sci 4(4):357–374. https://doi.org/10.1002/wcs.1238
20. Kern T et al (2006) Study of the influence of varying diameter and grasp-forces on mechanical impedance for the grasp of cylindrical objects. In: Proceedings of the Eurohaptics conference, Paris, F. https://doi.org/10.1007/978-3-540-69057-3_21
21. Kunstmann C (1999) Handhabungssystem mit optimierter Mensch-Maschine-Schnittstelle für die Mikromontage. VDI-Verlag, Düsseldorf. 978-3-642-57024-7
22. Milner TE, Franklin DW (1998) Characterization of Multijoint finger stiffness: dependence on finger posture and force direction. IEEE Trans Biomed Eng 43(11): Diss, 1363–1375. https://doi.org/10.1109/10.725333
23. Oguztoreli MN, Stein RB (1990) Optimal task performance of antagonistic muscles. Biol Cybern 64(2):87–94. https://doi.org/10.1007/BF02331337
24. Okamoto S, Nagano H, Yamada Y (2013) Psychophysical dimensions of tactile perception of textures. IEEE Trans Hapt 6(1):81–93. ISSN: 19391412. https://doi.org/10.1109/TOH.2012.32
25. Salisbury C et al (2011) What you can't feel won't hurt you: evaluating haptic hardware using a haptic contrast sensitivity function. IEEE Trans Hapt 4(2):134–146. https://doi.org/10.1109/TOH.2011.5
26. Serina Elaine R, Mote C, Rempel D (1997) Force response of the fingertip pulp to repeated compression—effects of loading rate, loading angle and anthropometry. J Biomech 30(10):1035–1040. https://doi.org/10.1016/S0021-9290(97)00065-1
27. Strohmeier P, Hornbaek K (2017) Generating haptic textures with a vibrotactile actuator. In: Proceedings of the 2017 CHI conference on human factors in computing systems proceeding, pp 4994–5005. https://doi.org/10.1145/3025453, http://dx.doi.org/10.1145/3025453.3025812
28. Wiertlewski M, Hayward V (2012) Mechanical behavior of the fingertip in the range of frequencies and displacements relevant to touch. J Biomech 45(11):1869–1874. https://doi.org/10.1016/j.jbiomech.2012.05.045
29. Yoshikawa T, Ichinoo Y (2003) Impedance identification of human fingers using virtual task environment. In: Proceedings 2003 IEEE/RSJ International Conference on Intelligent Robots and Systems (IROS 2003), vol 3, pp 3094–3099. https://doi.org/10.1109/IROS.2003.1249632

Chapter 4
Development of Haptic Systems

Thorsten A. Kern and Christian Hatzfeld

Abstract This chapter deals with the general design processes for the development of task-specific haptic systems. Based on known mechatronic development processes like the V-model, a specialized variant for haptic systems is presented, that incorporates a strong focus on the intended interaction and the resulting impacts on the development process. Based on this model, a recommended order of technical decisions in the design process is derived. General design goals of haptic systems are introduced in this chapter as well. These include stability, haptic quality and usability that have to be incorporated in several stages of the design process. A short introduction into different forms of technical descriptions for electromechanical systems, control structures and kinematics is also included in this chapter to provide a common basis for the second part of the book.

4.1 Application of Mechatronic Design Principles to Haptic Systems

Obviously, haptic systems are mechatronic systems, incorporating powerful actuators, sophisticated kinematic structures, specialized sensors and demanding control structures as well as complex software. The development of these parts is normally focus of specialized areas of specialists, i.e. mechanical engineers, robotic specialists, sensor and instrumentation professionals, control and automation engineers and software developers. A haptic system engineer should be at least able to understand the basic tasks and procedures of all of these professions, in addition to the required basic knowledge about psychophysics and neurobiology outlined in the last chapters.

Christian Hatzfeld deceased before the publication of this book.

T. A. Kern (✉)
Hamburg University of Technology, Eißendorfer Str. 38, 21073 Hamburg, Germany
e-mail: t.a.kern@tuhh.de

C. Hatzfeld
Technische Universität Darmstadt, Darmstadt, Germany

T. A. Kern et al. (eds.), *Engineering Haptic Devices*, Springer Series on Touch and Haptic Systems, https://doi.org/10.1007/978-3-031-04536-3_4

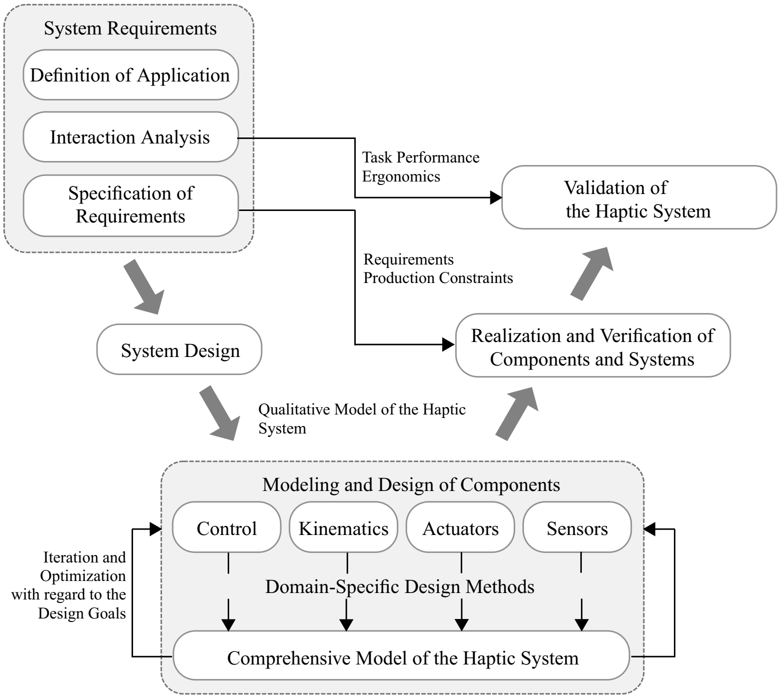

Fig. 4.1 Adaption of the V-model for the design of haptic systems

All of the above mentioned professions use different methods, but generally agree on the same concepts in developing their parts of a haptic system. These can be integrated in some common known development design methods as for example the V- MODEL for the development of mechatronic systems [16]. The model was originally developed for pure software design by the federal republic of Germany, but adapted to other domains as well. For the design of task-specific haptic systems, the authors detailed and extended some phases of the derivation of technical requirements based on [3] (Interaction Analysis) and [4] (Detailed Modeling of Mechatronic Systems). This adapted model is shown in Fig. 4.1. Based on this, five general stages are derived for the design of haptic systems. These stages are the basis for the further structure of this book and therefore detailed in the following sections.

The V- MODEL knows different variations depending on the actual usage and scale of the developed systems. In this case, the above mentioned variation was chosen over existing model variations, to be able to include additional steps in each stage of the V- MODEL. The resulting model is probably nearest to the W- MODEL for the design of adaptronic systems introduced by NATTERMANN AND ANDERL [8], because this model also includes an iteration in the modeling and design stage. It is further based on a comprehensive data management system, that does not only include information about interfaces and dependencies of individual components, but also a simulation model of each part. Since there is no comparable data basis for the design of haptic systems (that probably make use of a wider range of physical actuation and sensing principles than adaptronic systems up to date), the W- MODEL approach is not directly transferable and more iterations in the modeling and design stage have to be accepted.

4.1.1 Stage 1: System Requirements

The first stage is used for the derivation of system requirements. For the design of task-specific haptic systems, a breakdown in three phases seems useful.

Definition of Application As described in Sect. 2.3, each haptic system should be assigned a well-defined application. This definition is the starting point of haptic system design and comes as a probably vague idea from the client ordering a task-specific haptic system and has to be detailed by the development engineer.

Interaction Analysis Based on the detailed application definition, the intended interaction of the user with the haptic system should be analyzed. For this step, the different concepts of interaction shown in Sect. 2.2 will provide useful vocabulary for the description of interactions. Based on this interactions, the intended grip configuration should be chosen and perceptual parameters for this configuration should be acquired, either from known literature or by own psychophysical studies. At least, absolute thresholds and the ↪ JND should be known for the next steps, along with a model of the mechanical impedance of the intended grip configuration.

Another result of this phase are detailed and quantified interaction goals for the application in terms of task performance and ergonomics. Possible categories of these goals are given in Chap. 13. If, for example, a communication system is designed, possible goals could be a certain amount of information transfer (IT) [5] and a decrease of cognitive load in an exemplary application scenario measured by the NASA task-load index [2].

Specification of Requirements Based on the predefined steps, a detailed analysis of technical requirements on the task-specific haptic system can be made. This should include all technical relevant parameter for the whole system and each component (i.e. actuators, sensors, kinematic structures, interfaces, control structure and software design). Chapter 5 provides some helpful clusters depending on different interactions for the derivation of precise requirement definitions.

The result of this stage is at least a detailed requirement list. The necessary steps are detailed in Chap. 5. Further tools for the requirement engineering can be used as well, but are not detailed further in this book.

4.1.2 Stage 2: System Design

In this stage, the general form and principles used in the system and its components have to be decided on. In general, one can find a vast number of different principles for components of haptic systems. During the technical development of haptic systems, the decisions on single components influence each other intensively. However, this influence is not identical between all components. For the engineer it is necessary to proceed in the solution identification for each component, after having gained the knowledge of the requirements for the haptic system. It is obvious that, according to a systematic development process, each solution has to be compared to the specifications concerning its advantages and disadvantages. The recommended procedure of how to deal with the components is the basis of the chapter structure of this section of the book and is summarized once again for completeness:

1. Decision about the control engineering structure of the haptic system based on the evaluation of the application (tactile or kinaesthetic), the impedance in idle state (masses >20 g and friction acceptable) and the maximum impedance (stiffnesses >300 N/m or smaller). This decision is based on the general structures described in Chap. 6 and the control structure of the haptic system described in Chap. 7.
2. Decision about the kinematics based on calculations of the workspace and the expected stiffness as detailed in Chap. 8.
3. Based on the now known mechanical structure, the actuator design can be made. Chapter 9 deals with this topic, starting with a approximate decision about working principles based on performance criteria and detailed information about the common actuation principles for haptic systems.
4. Dependent on the chosen control engineering structure, the force-sensor design can be performed parallel to the actuator design as detailed in Chap. 10.
5. Relatively uncritical for the design is the choice of the kinematic sensors (Chap. 10).
6. The electronic interfaces are subordinate to all the decisions made before (Chap. 11).
7. The software design of the haptic rendering itself, in many aspects, is so independent of prior technical decisions that it can be decoupled in almost all aspects from the rest of the design, when all specifications are made. Chapter 12 summarizes some typical topics for the design of this system component.

Nevertheless it is vital to note that e.g. the kinematics design cannot be realized completely decoupled from the available space for the device and the forces and torques—respectively the actuator. Additionally, kinematics directly influences any measurement technology as even displacement sensors have limitations on resolution and dynamics. The order suggested above for taking decisions has to be understood as being a recommendation for processing the tasks; it does not free the design engineer from the responsibility to keep an overview of the sub-components and their reciprocal influence.

A good possibility to keep track of this influences is the definition of clear interfaces between single components. This definition should include details about the form of energy and data exchanged between the components and be further detailed in the course of the development process to include clear definition of for example voltage levels, mechanical connections, standard interfaces and connectors used etc.

4.1.3 *Stage 3: Modeling and Design of Components*

4.1.3.1 Modeling of Components

Based on the decisions from the preceding stage, the individual components can be modeled and designed. For this, general domain-specific methods and description forms are normally used, which are further described in the following Sect. 4.3. This step will first result in a model of the component, that will include all relevant design parameters that influence the performance and design of the component. Some of these parameters can be chosen almost complete freely (i.e. control and filter parameters), while others will be limited by purchased parts in the system component (one will for example only find sensors with different, but fixed ranges as well as actuators with fixed supply voltages etc.).

4.1.3.2 Comprehensive Model of the Haptic System

In a second step, a more general model of the component should be developed, that exhibits similar interfaces to adjacent components like the ones defined in the preceding Sect. 4.1.2. Furthermore, this model should only include the most relevant design parameters to avoid excessive parameter sets.

When the interfaces of adjacent components match, the models of all components can be combined to a comprehensive model of the haptic system with general haptic input and output definitions (Fig. 2.33) and relevant design parameters for each individual components. Normally, a large number of components is involved in these comprehensive models. For a teleoperation system one can roughly calculate two actuators, two kinematic structures, two positioning sensors for actuator control, one force sensor and the corresponding power and signal processing electronics for *each* ↪ DOF with the resulting modeling and simulation effort.

Even if they are very large, such models are advisable to optimize the haptic system with respect to the below mentioned design goals like stability and haptic quality. Only with a comprehensive model one can evaluate the inter-component influences on these design goals. Based on the descriptions of the system structure given in Chap. 7, the optimization of the comprehensive model will lead to additional requirements on the individual components or modifications of the prior defined interfaces between components. These should also be documented in the requirement list.

One has to keep in mind, that all parameters are prone to errors, especially variances with regard to the nominal value and differences between the real part and the (somewhat) simplified model. During optimization of the comprehensive model, robustness of the results with regard to these errors has to be kept in mind.

4.1.3.3 Optimization of Components

Based on the results of the optimized comprehensive model, the individual components of a haptic system can be further optimized. This step is not only needed, when there is a change of interface definitions and requirements of single components, but is normally also necessary to ensure certain requirements of the system, that are not depending on a single component only. Examples are the overall stiffness of the kinematic structure, the mass of the moving parts of the system and—of course—the tuning parameters of control loops.

For the optimization of components, typical mechatronic approaches and techniques can be used, see for example [4, 9] and Sect. 4.3. Further aspects like standard conformity, security, recycling, wearout, and suitability for production have to be taken into account in this stage, too.

In practice, the three parts of *Stage 3: Modeling and Design of Components* will not be used sequentially, but with several iterations and branches. Experience and intuition of the developer will guide several aspects influencing the success and duration of this stage, especially the selection of meaningful parameters and the depth of modeling of each component. Currently, many software manufacturers work on the combination of different model abstraction levels (i.e. ↪ single input, single output (SISO)-systems, network parameter descriptions, finite element models) into a single CAE-Software with the ability not only to simulate, but also to optimize the model. While this is already possible to a certain amount in commercial software products (for example ANSYS™), the ongoing development in these areas will be very useful for the design of haptic systems.

4.1.4 Stage 4: Realization and Verification of Components and System

Based on the optimization, the components can be manufactured and the haptic system can be assembled. Each manufactured component and the complete haptic system should be tested against the requirements, i.e. a verification should be made. Additionally, other design goals like control stability and transparency (if applicable) should be tested. Due to the above mentioned interaction analysis (see Sect. 5.2 for more details), this step will ensure that the system will generate perceivable haptic signals to the user without any disturbances due to errors. To compare the developed haptic system with others, objective parameters as described in Chap. 13 can be measured.

4.1.5 Stage 5: Validation of the Haptic System

While step 4 will ensure, that the system was developed correctly with respect to the expected functions and the requirements, this step will check if the correct system was developed. This is simply made by testing the evaluation criteria defined in the interaction analysis and comparison with other systems with haptic feedback in a user test.

This development process will ensure, that time-intensive and costly user tests are only conducted in the first and last stages, while all other steps only rely on models and typical engineering tools and process chains. With this detailing of the V- MODEL, the general mechatronic design process is extended in such a way, that the interaction with the human user is incorporated in an optimized way in terms of effort and development duration.

4.2 General Design Goals

There are a couple basic goals for the design of haptic systems, that can be applied with various extend to all classes of applications. They do not lead to rigorous requirements, but it is helpful to keep all of these in mind when designing an haptic system to ensure a successful product.

Stability Stability in the sense of control engineering should be archived by all haptic systems. It affects the safety of a haptic device as well as the task performance of a haptic system and the interactions performed with it. To ensure stability while improving haptic transparency is the main task of the haptic system control. This is further detailed in Chap. 7.

Haptic Quality To ensure a sufficient haptic quality is the second design goal of a haptic system. In general, each system should be able to convey the haptic signals of the human-machine-interaction without conveying the own mechanical properties to the user. For teleoperation systems, one will find the term *haptic transparency* for this preferable behavior. Analogue to the visual transparency of an ideal window, an ideal haptic teleoperation system will let the user feel exactly the same mechanical properties that are exposed to the manipulator of the teleoperation system. Since physical parts of a haptic system exhibit real physical behavior that cannot be neglected, haptic quality is a control task as well to compensate for this real behavior. It is therefore detailed in Chap. 7.

Usability Since haptics is considered as an interaction modality in this book, all usability considerations of human-machine-interfaces should be treated as a design goal. These goals are described in the ISO 9241 standard series[1] and demand *effectiveness* in fulfilling a given task, *efficiency* in handling the system and *user satisfaction* when working with the system.

Usability has therefore be considered in almost all stages of the development process. This includes the selection of suitable grip configurations that prevent fatigue and allow a comfortable usage of the system, the definition of clearly distinguishable haptic icons, that are not annoying when occurring repeatedly and the integration of assistive elements like arm rests. It is advisable to provide for individual adjustment, since this contributes to the usability of a system. This applies to mechanical parts like adjustable arm rests as well as information carrying elements like haptic icons. Methods to assess some of these criteria mentioned are given in Chap. 13 as well as in the standard literature to usability for human-machine-interaction as for example [1].

For the design of haptic systems, the following design principles derived from PREIM's principle for the design of interactive software systems can assist in the development of haptic systems with a higher usability [10]:

- Get information about potential users and their tasks
- Focus on the most important interactions
- Clarify the interaction options
- Show system states and make them distinguishable
- Build an adaptive interface
- Assist users in developing a mental model, i.e. by consistency of different task primitives
- Avoid surprising the user
- Avoid keeping a large of information in the user's memory.

4.3 Technical Descriptions of Parts and System Components

Since the design of haptic systems involves several scientific disciplines, one has to deal with different description languages according to the discipline's culture. This section gives an short introduction into different description languages used in the design of control, kinematics, sensors and actuators. It is not intended to be sufficient, but to give an insight into the usage and the advantages of the different descriptions for components of haptic systems.

---

[1] The ISO 9241 primarily deals with human-computer-interaction in a somewhat limited view of the term "computer" with a strong focus on standard workstations. The general concepts described in the standard series can be transferred to haptics nevertheless, and the ISO 9241-9xx series deals with haptics exclusively.

4.3.1 Single Input—Single Output (SISO) Descriptions

One of the simplest forms of modeling for systems and components are ↪ SISO descriptions. They only consider a single input and a single output with a time dependency, i.e. a time-varying force $F(t)$. The description also includes additional constant parameters and the derivatives with respect to time of the inputs and the outputs. If considering a DC-motor for example, a SISO description would be the relation between the output torque $M_{\text{out}}(t)$ evoked by a current input $i_{\text{in}}(t)$ as shown in Eq. 4.1.

$$\begin{aligned} M_{\text{out}}(t) &= k_{\text{M}} \cdot i_{\text{in}}(t) \\ \Rightarrow h(t) &= \frac{M_{\text{out}}(t)}{i_{\text{in}}(t)} = k_{\text{M}} \end{aligned} \tag{4.1}$$

The output torque is related to the input current by the transfer function $h(t)$. In this case, the transfer function is just the motor constant k_{M} that is calculated from the strength of the magnetic field, the number of poles and windings, and geometric parameters of the rotor amongst others. It is normally given in the data sheet of the motor.

SISO descriptions are mostly given in the LAPLACE-domain, i.e. a transformation of the time-domain transfer function $h(t)$ into the frequency-domain transfer-function $G(s) \bullet\!\!-\!\!\circ\, h(t)$ with the complex LAPLACE operator $s = \sigma + j\omega$. These kind of system descriptions is widely used in control theory to assess stability and the quality of control. However, for the design of complex systems with different components, SISO descriptions have some drawbacks.

- Since only single input and output variables are used, one cannot describe the flow of energy by SISO descriptions accordingly. This is obvious from the above example of a DC-motor: Usable output torque will decrease as the revolution speed of the motor increases, since the amount of energy available is limited by the thermal dissipation capabilities of the motor. This behavior cannot be incorporated in Eq. 4.1, since it involves more than one time-dependent input variable.
- When using SISO descriptions for different components that are arranged in a signal and/or energy transmission chain, one has to adjust the interfaces between components accordingly. This complicates the exchange of single components in the transmission chain. Consider an actuator driving a kinematic structure. The exchange of an electrodynamic principle for a piezoelectric principle will require a new SISO description of the kinematic structure, since a input current to the actuator will evoke different kinds of outputs (a force in the case of the electrodynamic principle and an elongation for the piezoelectric principle).

To overcome these disadvantages, one can extend the SISO description to multiple input and multiple output systems (MIMO). For the description of haptic systems, a special class of MIMO systems is advisable, the description based on network parameters as outlined in the following Sect. 4.3.2.

These drawbacks do not necessarily mean, that SISO descriptions have no application in the modeling of haptic systems: Despite the usage in control design, they are also useful to describe system parts that are not involved in extensive exchange of energy, but primarily in the exchange of information. Consider a force sensor placed on the tip of the manipulator of a haptic system: While the sensor compliance will effect the transmission of mechanical energy from ↪ TCP to the kinematic structure of the manipulator (and should therefore be considered with a more detailed model than a SISO description), the transformation of forces into electrical signals is mainly about information. It is therefore sufficient to use a SISO description for this function of a force sensor.

4.3.2 Network Parameter Description

The description of mechanical, acoustic, fluidic and electrical systems based on lumped network parameters is based on the similar topology of the differential equations in each of these domains. A system is described by several network elements, which are locally and functionally separated from each other and exchange energy via predefined terminals or ports. To describe the exchange of energy, each considered domain exhibits a flow variable in the direct connection of neighboring ports (for example current in the electrical domain and force in translational mechanics) and an effort variable (for example voltage, respectively velocity between two arbitrary ports of the network. Table 4.1 gives the mapping of electrical and translational mechanical elements. Historically, there are two analogies between these domains. The one used here depicts physical conditions best, there is however a single incongruent point: The definition of the mechanical impedance as the quotient of flow variable and effort variable.

Table 4.1 Analogy between electrical and mechanical network descriptions

Electrical domain			Mechanical domain	
Parameter	Symbol		Parameter	Symbol
Voltage	$\underline{u}$	$\leftrightharpoons$	Velocity	$\underline{v}$
Current	$\underline{i}$	$\leftrightharpoons$	Force	$\underline{F}$
Inductivity	L	$\leftrightharpoons$	Compliance	n
Capacity	C	$\leftrightharpoons$	Mass	m
Resistance	R	$\leftrightharpoons$	Viscous damping/friction	$h = \frac{1}{r}$
Impedance	$\underline{Z} = \frac{\underline{u}}{\underline{i}}$	$\leftrightharpoons$	Admittance (mobility)	$\underline{h} = \frac{1}{\underline{Z}}$
Admittance	$\underline{Y} = \frac{1}{\underline{Z}}$	$\leftrightharpoons$	Impedance	$\underline{z} = \frac{\underline{F}}{\underline{v}}$

To couple different domains, loss-less transducers are used. Because they are loss-less, systems in different domains can be transformed into a single network, which can be simulated with an extensive number of simulation techniques known from electrical engineering like for example SPICE. The transducers can be devided in two general classes. The first class called *transformer* links the effort variable of domain A with the effort variable of domain B. A typical example for a transformer is a electrodynamic transducer, that can be described as shown in Eq. 4.2 with the transformer constant $X = \frac{1}{B_0 \cdot l}$:

$$\begin{pmatrix} \underline{v} \\ \underline{F} \end{pmatrix} = \begin{pmatrix} \frac{1}{B_0 \cdot l} & 0 \\ 0 & B_0 \cdot l \end{pmatrix} \cdot \begin{pmatrix} \underline{u} \\ \underline{i} \end{pmatrix} \tag{4.2}$$

B_0 denotes the magnetic flux density in the air gap of the transducer and l denotes the length of the electrical conductor in this magnetic field. Further details about these kind of transducer are given in Chap. 9. If different domain networks are transformed into each other by the means of a transformer, the network topology stays the same and the transformed elements are weighted with the transformer constant. This is shown in Fig. 4.2 on the example of a electrodynamic loudspeaker and applied to electrodynamic actuators in Fig. 4.2.

The other class of transducers is called *gyrator*, coupling the flow variable from domain A with the effort variable form domain B and vice versa. The coupling is described with the transformer constant Y, examples (not shown here) include electrostatic actuators and transducers that change mechanical in fluidic energy. If different domain networks are transformed, the network topology changes, series connections become parallel and vice versa. The single elements change as well, for a gyratory transformation between mechanical and electrical domains an inductor will become a mass and a compliance will turn into a capacitance. A common application for gyratory transformations is the modeling of piezoelectric transducers. This is shown in Chap. 9 in the course of the book.

An advantage of this method is the consideration of influences from other parts in the network, a property that cannot be provided by the representation with SISO transfer functions. On the other side, this method will only work for linear time-invariant systems. Mostly a linearization around a operating point is made to use network representations of electromechanical systems. Some time dependency can be introduced with switches connecting parts of the network at predefined simulation times. Another constrained is the size of the systems and components modeled by the network parameters. If size and wavelength of the flow and effort variables are in similar dimensions as the system itself, the basic assumption of lumped parameters cannot be hold anymore. In that case, distributed forms of lumped parameter networks can be used to incorporate some wave line transmission properties.

In haptics, network parameters are for example used for the description of the mechanical user impedance $\underline{Z}_{\text{user}}$ as shown in Chap. 3, the condensed description of kinematic structures, and the optimization of the mechanical properties of sensors

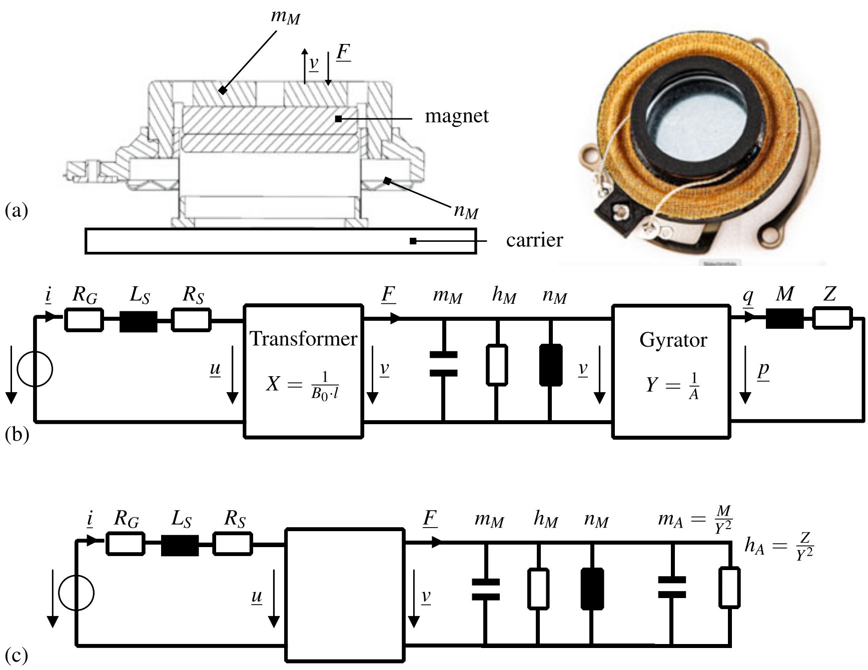

Fig. 4.2 Network model of an electrodynamic exciter–GREWUS Exciter EXR4403L-01A. **a** The system consists out of an electrical system, the electrodynamic transducer with transformatoric constant X, the mechanical parts of the moving parts, the mechanical-acoustic transducer with gyratoric constant Y and the properties of the acoustic system. **b** Shows the corresponding network model and **c** the network model, when acoustic network elements are transformed in equivalent mechanical elements—ignoring for the time-being the dynamics of the carrier this exciter is mounted on or any tactile functionality

and actuators as shown above. Further information about this method can be found in the work of TILMANNS [14, 15] and LENK ET AL. [7], from which all information in this section were taken.

4.3.3 *Finite Element Methods (FEM)*

↪ Finite Element Methods (FEM) are mathematical tools to evaluate ↪ partial differential equations (PDE). Since a lot of physical principles are described by partial differential equations, this technique is used throughout engineering to calculate mechanical, thermal, electromagnetic and acoustic problems [6].

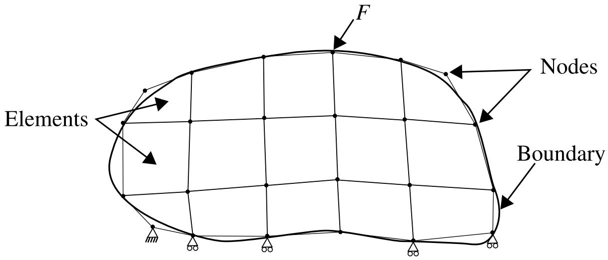

Fig. 4.3 Domain, elements, nodes and boundary conditions of a sample FEM problem formulation

The use of the Finite Element Method requires a discretization of the whole domain, thereby generating several finite elements with finite element nodes as shown in Fig. 4.3. Furthermore, boundary conditions have to be defined for the border of the domain, external loads and effects are included in these boundary conditions.

Put very simple, FE analysis will run through the following steps: To solve the PDE on the chosen domain, first a partial integration is performed on the differential equations multiplied with a test function. This step leads to a weak formulation of the partial differential equation (also called natural formulation), that incorporates the NEUMANN boundary conditions. Discretization is performed on this natural formulation, leading to a set of PDE that has to be solved on each single element of the discretized domain. By assuming a certain type of appropriate shape or interpolation function for the PDE on each element, a large but sparse linear matrix is constructed, that can be solved with direct or iterative solvers depending on the size of the matrix.

There are a lot of commercial software products that will perform FEM in the different engineering fields. They normally include a pre-processor, that takes care of discretization, material parameters and boundary conditions, a solver and a post-processor, that will turn the solver's results into a meaningful output. For the quality of results of FEM the choice of the element types depending on geometry of the considered domain and the kind of analysis and the mathematical solver used is of high importance.

The advantages of the FE method are the treatment of non-linear material properties, the application to complex geometries, and the versatile analysis possibilities that include static, transient and harmonic analysis [6]. The aspect of discretization yields a high computational effort, but also a spatial resolution of the physical value in investigation.

To overcome some disadvantages of FEM there are some extensions to the method: The *combined simulation* maps FE results onto network models that are further used in network based simulations of complex systems [7, 13]. The advantage is the high spatial resolution of the calculation on the required parts only and the resulting higher speed. The data exchange between FE and network model is made by the user. The *coupled simulation* incorporates an automated data exchange between FE and network models at run-time of the simulation. At the moment, many companies work on the integration of this functionality in the program packages for FE and network model analysis to allow for multi-domain simulation of complex systems.

The application of $\hookrightarrow$ finite element model (FEM) in haptics can be found in the design of force sensors (see Chap. 10), the evaluation of thermal behavior of actuators, and the structural strength of mechanical parts.

4.3.4 Description of Kinematic Structures

A description of the pose, i.e. the position and orientation of a rigid body in space, is a basic requirement to deal with kinematic structures and to optimize their properties. If considering Euclidean space, six coordinates are required to describe the pose of a body. This is normally done by defining a fixed reference frame i with an origin O_i and three orthogonal basis vectors $(\mathbf{x}_i, \mathbf{y}_i, \mathbf{z}_i)$. The pose of a body with respect to the reference frame is described by the differences in position and orientation. The difference in position is also called displacement and describes the change of position of the origin O_j of another coordinate frame j that is fixed to the body. The orientation is described by the angle differences between the two sets of basis vectors $(\mathbf{x}_i, \mathbf{y}_i, \mathbf{z}_i)$ and $(\mathbf{x}_j, \mathbf{y}_j, \mathbf{z}_j)$. This rotation of the coordinate frame j with respect to the reference frame i can be described by the rotation matrix ${}^j\mathbf{R}_i$ as given in Eq. (4.3).

$$
{}^j\mathbf{R}_i = \begin{pmatrix} \mathbf{x}_i \cdot \mathbf{x}_j & \mathbf{y}_i \cdot \mathbf{x}_j & \mathbf{z}_i \cdot \mathbf{x}_j \\ \mathbf{x}_i \cdot \mathbf{y}_j & \mathbf{y}_i \cdot \mathbf{y}_j & \mathbf{z}_i \cdot \mathbf{y}_j \\ \mathbf{x}_i \cdot \mathbf{z}_j & \mathbf{y}_i \cdot \mathbf{z}_j & \mathbf{z}_i \cdot \mathbf{z}_j \end{pmatrix} \tag{4.3}
$$

While the rotation matrix contains nine elements, only three parameters are needed to define the orientation of a body in space. Although there are some mathematical constraints on the elements of ${}^j\mathbf{R}_i$ that ensure the equivalence, several minimal representations of rotations can be used to describe the orientation with less parameters (and therefore less computational effort when computing kinematic structures). In this book, only three representations are discussed further, the description by *Euler Angels*, *Fixed Angles* and *Quaternions*.

Euler Angles To minimize the number of elements needed to describe a rotation, the Euler angle notation uses three angles (α, β, γ) that each represent a rotation about the axis of a moving coordinate frame. Since each rotation depends on the prior rotations, the order of rotations has to be given as well. Typical orders are Z-Y-Z and the Z-X-Z rotation shown in Fig. 4.4.
The description by Euler angles exhibits singularities, when the first and last rotations occur about the same axis. This is a drawback when one has to describe several, consecutive rotations and when describing motion, i.e. deriving velocities and accelerations.

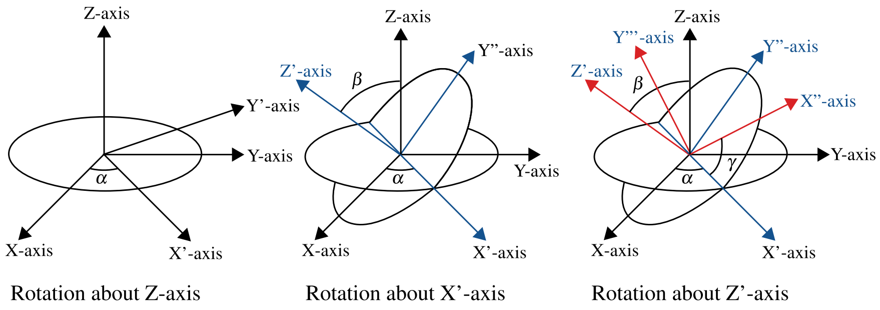

Fig. 4.4 Rotation of a coordinate frame based on Euler Angles (α, β, γ) in Z-X-Z order

Fixed Angles Fixed angle descriptions are basically the same as Euler angle descriptions, the rotation angles (ψ, θ, ϕ) describe however the rotation about the fixed axes of the reference frame. Also known as *yaw* ψ around the $\mathbf{x}_i$-axis, *pitch* θ around the $\mathbf{y}_i$-axis and *roll* ϕ around the $\mathbf{z}_i$-axis, the fixed angles exhibit the same singularity problem as the Euler angles.

Quaternions To overcome this singularity problems, quaternions are used in the description of kinematic structures. Mathematically also known as Hamilton Numbers $\mathbb{H}$, they are an extension of the real number space $\mathbb{R}$. A quaternion ε is defined as

$$\varepsilon = \varepsilon_0 + \varepsilon_1 i + \varepsilon_2 j + \varepsilon_3 k$$

with the scalar components ε_0, ε_1, ε_2 and ε_3 and the operators i, j, and k. The operators fulfill the combination rules shown in Eq. (4.4) and therefore allow associative, commutative and distributive addition as well as associative and distributive multiplication of quaternions.

$$\begin{aligned} &ii = jj = kk = -1 \\ &ij = k, \qquad jk = i, \qquad ki = j \\ &ji = -k, \qquad kj = -i, \qquad ik = -j \end{aligned} \tag{4.4}$$

One can imagine a quaternion as the definition of a vector $(\varepsilon_1, \varepsilon_2, \varepsilon_3)$, that defines the axis the frame is rotated about with the scalar part ϵ_0 defining the amount of rotation. This is shown in Fig. 4.5. By dualization, quaternions can be used to describe the complete pose of a body in space, i.e. rotation and displacement. Further forms of kinematic descriptions as for example the description based on screw theory can be found in [17], on which this section is based primarily and other works like [11, 12].

Fig. 4.5 Rotation of a frame defined by a quaternion

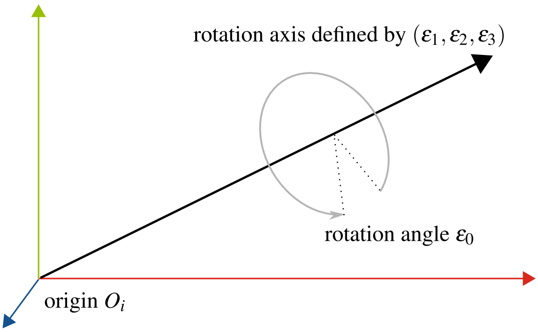

Recommended Background Reading

[4] K. Janschek: **Mechatronic systems design: methods, models, concepts**. Springer, Heidelberg, 2012.
Design methodologies for mechatronic systems that can also be applied to haptic systems.

[6] M. Kaltenbacher: **Numerical simulation of mechatronic sensors and actuators**. Springer, Heidelberg, 2007.
Broad overview about finite element methods and the application to sensors and actuators.

[7] A. Lenk et al. (Eds.): **Electromechanical Systems in Microtechnology and Mechatronics: Electrical, Mechanical and Acoustic Networks, their Interactions and Applications**. Springer, Heidelberg, 2011. ISBN: 978-3-642-10806-8
Introduction to the network element description methodology.

References

1. Boy GA (ed) (2011) The handbook of human-machine interaction—a human-centered approach. Ashgate, Farnham, GB
2. Hart S, Staveland L (1988) Development of NASA-TLX (task load index): results of empirical and theoretical research. Hum Mental Workload 1:139–183. https://doi.org/10.1016/S0166-4115(08)62386-9
3. Hatzfeld C (2013) Experimentelle Analyse der menschlichen Kraftwahrnehmung als ingenieurtechnische Entwurfsgrundlage für haptische Systeme. Dissertation, Technische Universität Darmstadt. München: Dr. Hut Verlag. http://tuprints.ulb.tu-darmstadt.de/3392/. ISBN: 978-3-8439-1033-0
4. Janschek K (2012) Mechatronic systems design: methods, models, concepts. Springer. ISBN: 978-3-642-17531-2
5. Jones L, Tan H (2013) Application of psychophysical techniques to haptic research. IEEE Trans Hapt 6:268–284. https://doi.org/10.1109/TOH.2012.74

6. Kaltenbacher M (2007) Numerical simulation of mechatronic sensors and actuators. Springer. ISBN: 978-3-540-71359-3. https://doi.org/10.1007/978-3-540-71360-9
7. Lenk A et al (eds) Electromechanical systems in microtechnology and mechatronics: electrical, mechanical and acoustic networks, their interactions and applications. Springer, Heidelberg. ISBN: 978-3-642-10806-8
8. Nattermann R, Anderl R (2013) The W-model-using systems engineering for adaptronics. Procedia Comput Sci 16:937–946. https://doi.org/10.1016/j.procs.2013.01.098
9. Pahl G, Wallace K, Blessing L (2007) Engineering design: a systematic approach. Springer. ISBN: 978-3540199175
10. Preim B (1999) Entwicklung interaktiver Systeme. Fallbeispiele und innvoative Anwendungsfelder. Springer, Grundlagen. 978-3540656487
11. Sciavicco L (2000) Modelling and control of robot manipulators. Springer. ISBN: 978-1-4471-0449-0
12. Selig J (2005) Geometric fundamentals of robotics. Springer. ISBN: 978-0-387-27274-0
13. Starke E (2009) Kombinierte simulation—eine weitere Methode zur Optimierung elektromechanischer Systeme. Ph.D. thesis. Technische Universität Dresden. http://tu-dresden.de/die_tu_dresden/fakultaeten/fakultaet_elektrotechnik_und_informationstechnik/ihm/mst/Veroeffentlichungen_MST/Archiv_MST/mst_2010?fis_type=publikation&fis_id=b1847
14. Tilmans H (1996) Equivalent circuit representation of electromechanical transducers: I. Lumpedparameter systems. J Micromech Microeng 6:157. https://doi.org/10.1088/0960-1317/6/1/036
15. Tilmans HA (1997) Equivalent circuit representation of electromechanical transducers: II. Distributedparameter systems. J Micromech Microeng 7(4):285. https://doi.org/10.1088/0960-1317/7/4/005
16. VDI 2206: Entwicklungsmethodik für mechatronische Systeme. Berlin: Verband Deutscher Ingenieure (VDI) (2004). http://www.vdi.de/technik/fachthemen/produkt-und-prozessgestaltung/fachbereiche/produktentwicklung-undmechatronik/themen/rilis-mechatronische-systeme/richtlinie-vdi-2206-entwicklungsmethodik-fuer-mechatronische-systeme/
17. Waldron K, Schmiedeler J (2008) Kinematics. In: Sicilianoand B, Khatib O (eds) Springer handbook of robotics. Springer, pp 9–33. https://doi.org/10.1007/978-3-540-30301-5_2

Part II
Designing Haptic Systems

In the previous chapters, the discussion focused on haptic perception in relation to the human user. In the following chapters, the technical realization of haptic systems will come to the fore. As a result, the general view changes from a user-centered perspective to a device-specific view. More concrete technological issues are explored and more practical help is offered for common challenges in the design process. The chapters in this part are organized according to the classic list of tasks to be accomplished in any technical design process. They begin with more general issues that affect the overall system and then move to specific issues that relate to particular subcomponents. The chapters are intentionally ordered so that those dealing with issues whose range of solutions is severely limited are addressed earlier than those that provide more flexible solutions applicable to many situations. The understanding gained, as well as the methods used to quantify haptic perception, will continue to be used to analyze the quality of technological solutions.

- Chapter 5 The acquisition of requirements for the technical design process is discussed. The design of haptic systems covers a plurality of technological questions. Especially the challenges concerning the high dynamics to be achieved make a systematic approach mandatory for identifying the requirements.

- Chapter 6 After the basic requirements have been identified, a superordinate view of the structure of the system to be built is necessary for which a methodology is given in this chapter. The resulting analysis does not only aim at the decision on the control structure of the device, but also defines the technological sub-problems to be addressed during the following design process.

- Chapter 7 Several issues about the control of haptic systems are discussed, that has to guarantee stability and also haptic quality of new designs.

- Chapter 8 Especially kinaesthetic, but also multidimensional tactile systems have to combine multiple degrees of freedom to fulfill the requirements for certain tasks. This leads to the systematic design of the kinematics of the device. This chapter provides the necessary knowledge on kinematic design and covers specific and sometimes surprising problems of mechanical transfer functions for haptic devices in serial and parallel kinematics.

- Chapter 9 In this most comprehensive chapter of the second part, typical actuator principles with respect to their application in haptic devices are discussed. The sections cover all popular actuation principles in an overview, as well as the details of selected principles for a design from scratch.

- Chapter 10 Especially closed-loop controlled haptic devices need force sensors. Furthermore, telemanipulation systems—besides simulators—are the second most relevant group of high fidelity haptic devices. A haptic telemanipulator requires force sensors at its endeffector, at least. This chapter covers the selection process and the design of force sensors according to the physical principles able to fulfill the specifications of haptic systems.
 For a complete haptic interaction each system requires a position measurement. Technological solutions for this subordinate technological challenge are discussed in this chapter, whereby different positioning- and movement, touch and imaging-sensors are presented.

- Chapter 11 Typically, haptic devices are interfaced with time discrete systems with digital signal processors, may they be controllers for universal interfaces or complete simulation systems. This chapter deals with the interfaces between these computing units and gives insight into the performance of different realizations.

- Chapter 12 When it comes to haptic rendering the simulation of realistic material properties are meanwhile dominating research in software development. The challenges go far beyond the question of textures, but includes tool properties, surface properties and dynamics. This chapter focuses especially on this highly dynamic interface, and compares traditional and advanced methods to create a proper (first contact to a virtual world).

- Chapter 13 This chapter deals with measures and methods for the evaluation of haptic systems. It covers pure system aspects as well as measures for task-performance and the impact on the user.

- Chapter 14 In this chapter, examples of task-specific haptic systems and their development and evaluation are described.

- Chapter 15 Final remarks on all previous chapters are made and the most important recommendations for the design of haptic systems are summarized.

Chapter 5
Identification of Requirements

Jörg Reisinger, Thorsten A. Kern, and Christian Hatzfeld

Abstract In this chapter, the process of requirement definition is described, starting with the definition of the intended application together with the customer. Especially the derivation of technical parameters from the customers expectation and useful tools for this step are discussed. Further, the analysis of the intended interaction and the effects on the requirement identification are discussed. To alleviate the identification of requirements, main requirement groups are derived from the intended type of interaction and presented in five technical solution clusters. A review of relevant standards and guidelines on safety serves as another source of requirements of a haptic systems.

5.1 Definition of Application—The Right Questions to Ask

At the beginning of a technical design process the requirements for the product which, usually, are not clear and unambiguous, have to be identified. Frequently, customers formulate wishes and demands respectively solutions instead of requirements. A typical example is a task of the kind: "to develop a product just like product **P**, but better/cheaper/nicer". If an engineer accepts such a kind of order without getting to the bottom of the original motivation the project will be doomed to failure. Normally, the original wish of the customer concerning the product has to fulfil two classes of requirements:

Christian Hatzfeld deceased before the publication of this book.

J. Reisinger (✉)
Mercedes-Benz Cars Development, Daimler AG, 71059 Sindelfingen, Germany
e-mail: reisinger@haptics.eu

T. A. Kern
Hamburg University of Technology, Eißendorfer Str. 38, 21073 Hamburg, Germany
e-mail: t.a.kern@tuhh.de

C. Hatzfeld
Technische Universität Darmstadt, Darmstadt, Germany

T. A. Kern et al. (eds.), *Engineering Haptic Devices*, Springer Series on Touch and Haptic Systems, https://doi.org/10.1007/978-3-031-04536-3_5

The product shall have

- a certain **function**
- in a distinct **technical** and **market oriented** framework

Phrasing market oriented requirements are manifold yet not in the focus of the following analysis (for details of a general systematic product development see [12, 23]). They may be motivated by an existing product **P** to compete with, but usually they are much more comprehensive and cover questions of budget, time-frame of development, personal resources and qualifications and customers to address.

With regard to the technical framework, the customer typically gives just unspecific details. A statement like “a device shall provide a force on a glove” is not a definition of a requirement but already a solution on the basis of existing knowledge on the part of the customer. The complexity of a real technological solution spans from a single actuator to provide e.g. a vibration to complex kinematics addressing single fingers. Questioning the customer’s original statement, it may even come out, that his intention is e.g. to simulate the force impression when switching the gears of a clutch in a passenger car. The knowledge about the actual application and following that knowledge about the interaction itself allows the developer a much broader approach, leading to a more optimized technical solution.

5.1.1 Experiments with the Customer

The customer formulates requirements—as mentioned before—typically in an inexact instead of a specific way. Additionally, there is the problem of a very unspecific terminology with regard to the design of haptic systems For the description of haptic sensual impressions there are numerous adjectives difficult to quantify, like: rough, soft, smooth, gentle, mild, hard, viscous, as well as others derived from substantives such as: furry, silky, hairy, watery, and sticky which can be compared to real objects. So what could be more obvious than asking the customer to describe his/her haptic impressions by comparisons?

> Ask the customer to describe the intended haptic impression with reference to objects and items in his/her environment. These items should be easily at hand, like e.g. vegetables and fruits which offer a wide spectrum of textures and consistencies for comparison.

Sometimes the customer first needs to develop a certain understanding of the haptic properties of objects and items. This can best be achieved by his/her directly interacting with them. Examples of haptically extreme objects have to be included in a good sample case, too. The evolving technology of 3D printing allows for a very flexible design of such samples.

Provide a sample case including weights and springs of different size, even marbles, fur, leather and silk. Depending on the project, add sandpaper of different granularity. Use these items to explain haptic parameters to the customer and help the customer to optimize the description of the product performance expected!

From practical experience, we can recommend also to take spring balances and letter balances or electronic force sensors with you to customer meetings. Frequently, it is possible to attach a handle directly to the items and ask the customer to pull, until a realistic force is reached. This enables customers of non-technical disciplines to quickly get an impression of the necessary torques and forces.

Take mechanical measurement instruments with you to the customer meetings and allow the customer to touch and use them! This gives him / her a good first impression of the necessary force amplitudes.

In order to give a better impression of texture, mechanical workshops may produce patterns of knurls and grooves of different roughness on metals. Alternatively, sandpaper can be used and, by its defined grade of granularity, can provide a standardized scale to a certain extent.

Use existing materials with scales to describe roughness and simulate the impression of texture.

Recently, different toolkits for haptic prototyping are available. They are specific for certain types of applications, like for example cockpit knobs or texture recording, discrimination and replay. PENN HAPTIC TOOLKIT to record and replay haptic texture properties [5] is one of those systems being conceptually slightly different from the approach done by TU- MÜNCHEN's LMT texture recording and its database [30] at http://zeus.lmt.ei.tum.de/downloads/texture/. Further examples for lo-fi prototyping can be found in [14]. For more sophisticated setups, the usage of a ↪ COTS device and a virtual environment developed with a haptics toolkit could be considered. For vibrotactile feedback specialized prototyping environments like HAPTICLABS.IO are available. With focus on actuator sales, several companies provide a mixture of haptic consulting and actuator customization as a service (*Grewus*, *Nui Lab*, *Actronika*, ...).

Engineering Misconceptions when Asking About Haptics

A normal customer without expertise in the area of haptics will not be able to give statements concerning resolutions or dynamics of the haptic sense. This kind of information has to be derived from the type of interaction and the study of psychophysical knowledge of comparable applications. Therefore, the experience of the developing engineer is still indispensable despite all the systematizations in a technical design process.

> Do not confuse the customer by asking questions about the physical resolution! This is necessarily the knowledge of the haptic engineer. However, learn about the dynamics of the interaction and try to assess the application, e.g. by asking about the frame rate of a simulation, or the maximum number of load changes per seconds of a telemanipulator.

5.1.2 General Design Guidelines

Next to the ideas of the customer and/or user, there are also a number of different guidelines dealing with the design of haptic systems. These guidelines are summarized here very shortly, but a close look in the original references is advisable when applicable to the intended a haptic system.

Usability and Human-Computer-Interaction Guidelines Since all active haptic systems are intended to be used as a human-computer-interface, the applicable guidelines for these systems are also relevant for the design of haptic systems. As mentioned in Sect. 4.2, the ISO 9241-series deals with usability in general, the ISO 9241-9xx standards specifically address haptic systems and should be considered while working on requirement definitions and beyond. As of 2022 the activities of this ISO standardization committee is low, but the former documents still exist and did not outdate in their content. For the use of ↪ COTS devices, MUÑOZ ET AL. introduced a basic guideline for the design of ergonomic haptic interactions, that can be useful for these kind of applications [17].

Design of Haptic Icons The group of BREWSTER works on haptic and auditory icons and did publish several design guidelines for this kind of communication like for example [21]. With the increased availability of high-performance actuators in mobile devices, complex tactile patterns can be realized. The most relevant online resources for inspirations on such patterns was collected by SEIFI and her team, and is arranged at http://hastiseifi.com/VibViz/ according to sensational similarity [28].

HCI for Blind Users SJÖSTRÖM developed guidelines for ↪ virtual systems for blind users in addition to existing guidelines for HCI [29].

Telepresence in Precision Assembly Tasks ACKER investigated the usage of haptic and other feedback in precision assembly tasks [2].

Presence and Performance in Teleoperation Design factors leading to higher presence and improved performance were investigated by DEML [6]. With a strong focus on human factors, a guideline was developed to optimize the human-machine interface [7].

Design of VR and Teleoperation Systems Based on a literature review, a design guide for the development of haptic and multimodal interfaces was developed in [19]. The guide selects guidelines based on an interactive front end. The HAPTICS INDUSTRY FORUM—HIF *www.hapticsif.org* contributed in 2021 an application guide how to introduce and use VR-applications in an industrial context efficiently.

Surface Haptics BASDOGAN ET AL. summarized how artificial haptics generated on actuated but closed surfaces such as touchpanels and touchscreens can be realized [3].

Minimal Invasive Surgery TAVAKOLI ET AL. present the design of a multimodal teleoperated system for minimal invasive surgery and address general questions like control strategies and the effect of time delay [31].

General Benefits of Haptic Systems Based on a meta-study, NITSCH identified several aspects of haptic feedback on task performance measures. Haptic feedback improves working speed, handling accuracy and the amount of force exerted in teleoperation and virtual systems. This holds mainly for kinaesthetic force feedback, vibrotactile feedback predominantly reduces only task completion time [20].

Automotive Haptics The HAPTICS INDUSTRY FORUM—HIF *www.hapticsif.org* released a guideline for the automotive practice of haptic devices and their design with related specifications. It covers a range of car-related HCI topics up to specific technologies used in presence and in the future.

5.2 Interaction Analysis

Based on the demands of a customer and the clarifications obtained in conversation and experiments, a more technical interaction analysis can be performed. The first goal of this step is a technical description of the user with regard to the intended application. Normally, this will include information about the perception thresholds in the chosen grip configuration, information about the movement capabilities, and the mechanical impedance of the user. Naturally, one will not find fixed values for these parameters, but probably only ranges in the best case. In the worst case, own perception studies and impedance measurements have to be conducted.

The second goal of this step is a definition of suitable evaluation parameters and appropriate testing setups. If a reference system (that has to be improved or equipped with haptic feedback in course of the development) is given, reference values of these parameters should be obtained in this stage of the requirement identification as well.

The following steps are advisable for an interaction analysis that will obtain meaningful information for the following requirement specification as stated in Sect. 5.5. They are based on the works of HATZFELD ET AL. [10, 11].

1. Task Analysis Analyze the interaction task as thoroughly as possible. Interaction primitives as described in Sects. 1.4.1 and 2.2 are helpful at this point. Research possible grip configurations suitable for this kind of interactions (3.1.3), if the hand is intended as the primary interface between user and haptic system. Depending on the intended application, other body sites like the torso, the back of the hand or other limbs can be suitable locations for haptic interactions. For the ease of reading, the rest of this section will only mention the hand as primary interface without loss of generality with regard to other body sites.

Take the usage of tools into account (stylus, gripper, etc.) as well as possible restrictions of the manipulator in a teleoperation scenario (see example below). After his, one should have one or more possible interaction configurations, that will be able to convey all interaction primitives needed for the intended usage. If one plans to build a teleoperation, comanipulation or assistive system that adds haptic feedback to interactions that do not already have such, it is probably worthwhile to discuss if all haptic signals have to be measured, transmitted and displayed. Sometimes, the display of categorized haptic information (OK/Not OK, Material A/Material B/Material C etc.) could be sufficient in terms of intended usage of the system, facilitates the technical development, and lowers the cost of the final product.

It is advisable to also have a look on some multimodal aspects of the application as well as other environmental parameters: If a visual channel has to be or can be used, special concepts like pseudo-haptic feedback can be considered in the design of the system. If the system is to be used in a highly distractive environment, robust communication schemes have to be incorporated or an adjustable feedback mode has to be included. These information will help with formulating the system structure and the detailed requirement list.

2. Movement Capabilities Select the one or two most promising grip configurations. Based on these, one should define the maximum and comfortable movement spaces of the user and the typical interaction and maximum exertable forces. Section 2.2.4 gives some values for handling forces and velocity, data for typical movement spaces can be found in applicable standards like ISO 7250 or DIN 33402. These are relevant boundaries for the user input kinematics in terms of workspace and structural load. Interaction forces can be further used to define forces on the slave side of a telemanipulation system (as well as input forces in a virtual system that have to be dealt within the software).

3. Mechanical Impedance Research or measure the mechanical impedance of the selected grip configuration. This impedance is relevant for several control issues like stability (local stability of the haptic interface and overall stability in case of teleoperation systems) and haptic transparency as discussed in Sect. 3.2.

4. Perception Parameters Research or measure relevant perception parameters for the selected grip or body site configuration. Normally, absolute and different thresholds are needed for an estimation of sensor and actuator resolutions as well as tolerable errors. Based on the intended usage, other perception parameters or other interpretations can be meaningful as well. For example, successiveness limens (SL) and two-point-thresholds will affect the design of communication interfaces on all body sites. For an energy-limited system, small JNDs could be beneficial, since they probably will result in a large number of possible transferable information with a small amount of energy.
Keep in mind, that force and deflection thresholds can be calculated from each other by using the mechanical impedance according to Eq. (2.7). If possible, obtain data in more than one dimension to facilitate the requirement definition in the intended ↪ DoF. Be sure to check if there are external conditions, that will influence perception favorably for the technical development. This could be a maximum contact area or a minimum contact force that will lead to higher perception thresholds for the given contact situation. With means of the system developer these conditions can be influenced, for example by the design of the grip or the measurement of a minimum contact force, that has to be applied by the user to make the haptic system functional.

5. Evaluation Criteria Define suitable evaluation criteria regarding the intended task performance. Chapter 13 gives possible criteria depending on the application class of the haptic system. Despite these measures of task performance, measurements of haptic quality (if applicable) and ergonomic measures can be taken into account. The latter will quantify the cost and benefit of a haptically enhanced system compared to a system without haptics. The definition this early in the development allows for the measurement of reference values and eases the final evaluation, since the intended testing procedure of the haptic system can be incorporated in the design process.

A final decision for a grip configuration can either be made based on the values obtained in this interaction analysis in favor of the technical less-demanding option or by conducting user tests considering ergonomic factors like fatigue and task performance, if this is technically possible (for example with ↪ COTS devices). Obviously, this could involve some iterations of the above mentioned points. With this structured approach to interaction, a lot of purposeful information is generated for the derivation of requirements. The approach is illustrated with a short example in the following.

Example: *FLEXMIN Interaction Scheme*

The surgical system FLEXMIN is developed to enhance single port surgery procedures like for example transanal rectum resection [4] with haptic feedback, additional intracorporal mobility compared to rigid instruments and a more ergonomic working posture of the surgeon. Task-analysis as described above was conducted based on an example rectum resection with commercial available, stiff instruments (TEO system, *Karl Storz*, Tuttlingen, Germany) on an anatomical model. Based on the recordings of the surgeon's movements, system constraints like workspace, dexterity, instruments and principal manipulation tasks were identified [16]. This analysis led to the requirements of two manipulators with at least four movement ↪ DoF (positioning in space and rotation along the longitudinal axis) and preferably another DoF for gripping instruments like scissors or forceps.

Based on additional aspects like the request for displaying stiff structures and elements and the available construction space, a parallel kinematic structure was chosen for the intracorporal manipulator already at this point of development [15]. In that case, the ↪ TCP will be at the end of the last part of the lead chain of the parallel mechanism. The movement of this part was chosen as the general form of interaction of the haptic interface used to operate the manipulator [18]. The resulting concept for the haptic interface is shown in Fig. 5.1.

Ergonomic considerations about the surgeon handling two of these interfaces led to a passive linear bearing at the one end of the main kinematic chain of the user interface. On the other end, a parallel delta kinematic structure was chosen to actuate three DoF of the haptic interface. Additional feedback for the rotatory and the grasping DoF is integrated in the grasping part of the user interface. This is shown in Fig. 5.2.

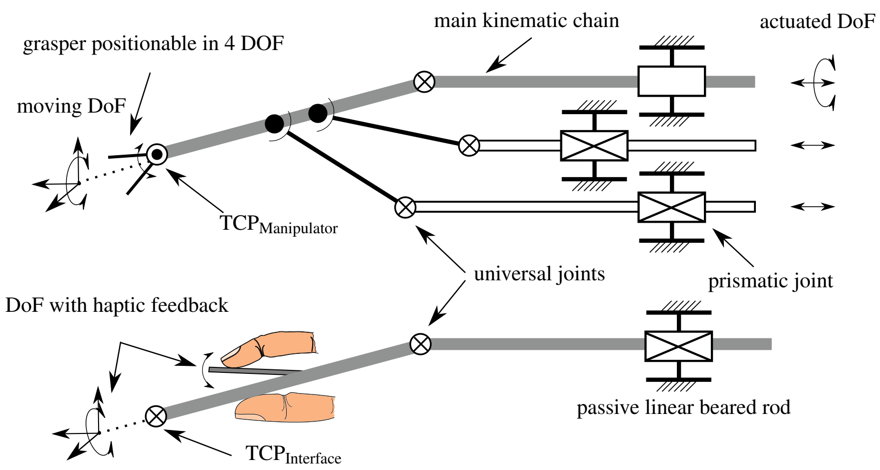

Fig. 5.1 Derivation of the concept of the haptic user interface of FLEXMIN (lower part) from the kinematic structure of the intracorporal manipulator (upper part). Figure adapted from [18]

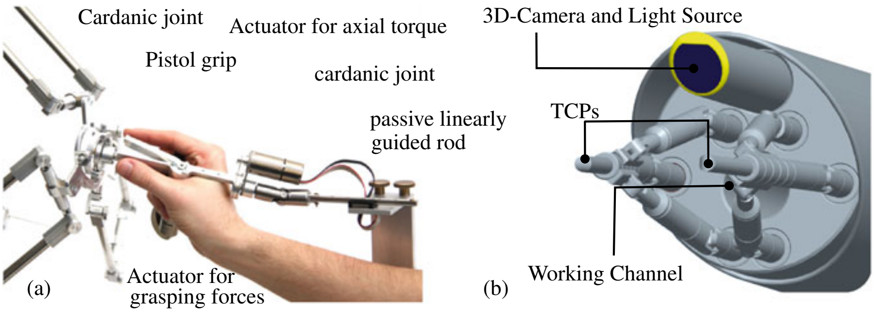

Fig. 5.2 **a** Realization of the haptic user interface of FLEXMIN, **b** Rendering of the intracorporal robot with two manipulator arms, working channel and visual instrumentation. Further information can be found in [15]

5.3 Technical Solution Clusters

After the interaction analysis and the discussion of the customer's expectations towards the haptic system, one should have a in-depth knowledge about the intended function of the haptic system. Based on a quite basic description of this function, general types of haptic systems and the interactions therewith can be identified. Based on these, this section identifies possible technical realizations and summarizes the necessary questions in clusters of possible applications. The list does not claim to be complete, but is the essence of requirement specifications of dozens of developments achieved during the last few years.

The core of the requirements' identification is the definition of the type of haptic interaction. The first question asked should always refer to the type of interaction with the technical system. Is it a simulation of realistic surroundings, the interaction with physically available objects in terms of telepresence; or is the focus of the interaction on the pure communication of abstract information? In the former cases the variants are less versatile than in the latter, as described below. In Fig. 5.3 a decision tree for the identification of clusters of questions is sketched. It is recommended to follow the tree from top to bottom in order to identify the correct application and the corresponding cluster of questions.

Simulation and Telepresence of Objects Does the interaction aim at touching virtual or via telepresence available objects? If this is the case, does the interaction take place directly via fingers, hands or skin, or is a mediator, e.g. a tool the interacting object? Does the user hold a specific tool—a pen, a screw driver, a surgical instrument, a joystick of a plane, in his hands and control one or more other objects with it, or does the user touch a plurality of objects during the interaction with his or her hands? In the case of a tool-interaction the chosen solution can be found in cluster ① "kinaesthetics", in the case of a direct interaction another detail has to be considered.

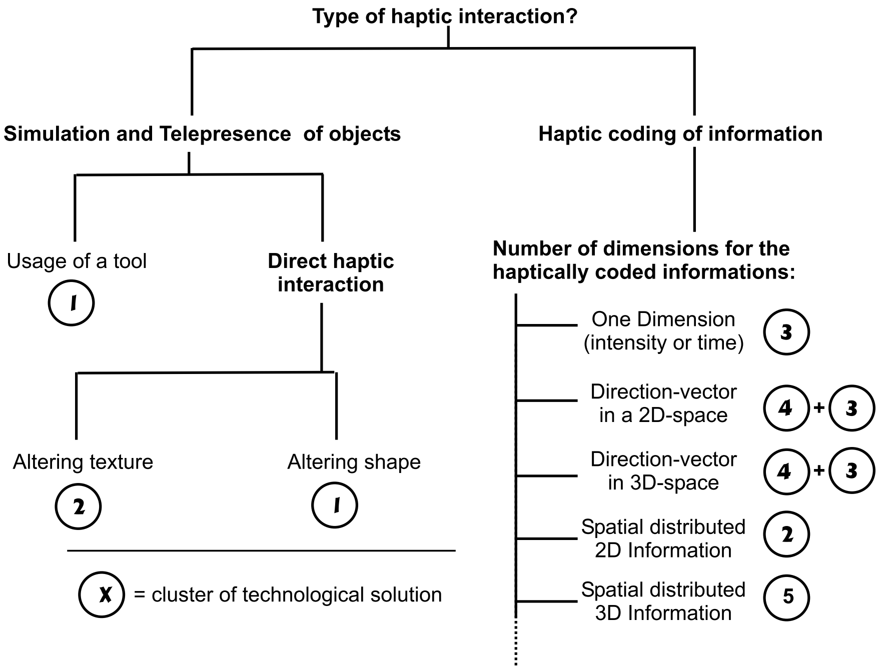

Fig. 5.3 Structure for identifying relevant clusters of questions by analyzing the intended haptic interaction

Direct Haptic Interaction By touching physical objects, the user can notice the differences in all physical attributes of the volume like mass, elasticity, plasticity and inner friction, and their texture. In the case of interacting with shapes, the questions of cluster ① "kinaesthetics" remains relevant, in the case of interacting with textures the questions of cluster ② "surface-tactile" have to be considered. This is not necessarily an alternative decision, however, with the same object interaction, both aspects can be required at the same time or one after the other.

Haptic Coding of Information In the case of abstract, not physical, object- oriented information communication via the haptic sense the question of the dimension of information becomes relevant:

- Does the interaction include a single event which occurs from time to time (e.g. the call of a mobile phone) or is some permanently active information (e.g. a distance to a destination) haptically communicated? These questions are one-dimensional[1] and covered by cluster ③ "vibro-tactile".
- Is the interaction dominated by directional information coding an orientation in a surface (directional movement) or in a space? In this case the questions covered by cluster ④ "vibro-directional" are relevant. In such applications

[1] As the information includes only one parameter.

frequently time respectively distal information is included, also making the questions in cluster ③ become relevant.
- Does the interaction aim at the communication of data distributed within a two-dimensional information layer, like geological maps, road-maps or texts on a page? In these cases the questions of cluster ② "surface-tactile" have to be answered.
- In case there is volumetric information—the electrical field of an atomic bonding or medical data sets—to be haptically transmitted, the questions of cluster ⑤ "omnidimensional" are to be be considered.

In the following sections the questions in the clusters are further discussed and some examples are given for the range of possible solutions to the questions aimed at.

5.3.1 Cluster ① — Kinaesthetic

Cluster ① has to be chosen either when an interaction between fingers and shapes happens directly or when the interaction takes place between tool and object. Both cases are technical problems of multidimensional complexity.[2] Each possible dimension movement corresponds to one degree of freedom of the later technical system. Therefore the questions to be asked are quite straightforward and mainly deal with the requirements for these degrees of freedom of tools and users:

- Which degrees of freedom do the tool/movement show? → rotatory, translatory, combinations[3]
- How large is the volume covered by the movements? → Maximum and minimum values of angles and translations
- How dynamic is the movement? → Identification of maximum and minimum velocities and accelerations. Usually, this question cannot be answered immediately. A close observation of the intended interaction will help and—as far as possible—measurements of movement velocities of instruments and fingers should be made e.g. with the aid of videos,.
- Which forces / torques happen at each degree of freedom[4]? → Definition of maximum and minimum forces and torques.
- What is the maximum dynamics of the forces and torques? → Bandwidth of forces and torques in frequency range, alternatively maximum slope in time-domain

[2] A tool interaction can be a one-dimensional task, but such an assignment concerning the technical complexity can be regarded as an exception.

[3] In the case of a finger movement it has to be noted that not necessarily all movement directions have to be equipped with haptic feedback to provide an adequate interaction capability. Frequently it is even sufficient to provide the grasp-movement with haptic feedback, solely.

[4] Frequently the customer will not be able to specify these values directly. In this case creative variants of the question should be asked, e.g. by identifying the moving masses, or by taking measurements with one's own tools.

("from 0 to $F_{\max}$ in 0.1 s"). Usually, this question cannot be answered directly. Frequently, measurements are difficult and time-consuming, as an influence of the measurement on the interaction has to be eliminated. Therefore it is recommended to do an analysis of the interaction itself and the objects the interaction happens with. If it is soft—something typical of surgical simulation, simple viscoelastic models can be used for interpolating the dynamics. The most critical questions with respect to dynamics often address the initial contact with an object, the collision. In this case especially the stiffness of the object and the velocity of the contact describe the necessary dynamics. But is has to be stated that the resulting high demands are not seldom in conflict with the technical possibilities. In these cases, a splitted concept based on "events" can be considered, where kinaesthetic clues are transmitted in low frequency ranges, and highly dynamic clues are coded in pure vibrations (Chaps. 11 and 12).

5.3.2 Cluster ②—Surface-Tactile

Haptic texture represents the microstructure of a surface. The lateral movement between this microstructure and the finger tip results in shear forces generating the typical haptic impression of different materials. Haptic-bumps on the keyboard-keys J and F are a special form of texture. Another variant of texture are Braille-letters carrying additional abstract information. But there are also more straightforward textures such as the surface of all physical materials[5] Cluster ② has to be chosen when there is a need to present information on any surface via the tactile sense. This can be either coded information on a geological map on a more or less plane surface, but it can also be object specific features like the material itself. The resulting questions for the technical task are:

- Which body parts perform the interaction? → This trivial question has a significant impact, as the body part selected defines the resolution available on user side and consequently the requirements for the size of the texture-generating elements.
- Is the form of the texture-carrying shape subject to changes? If so, how much and in which areas? → If the shape changes a lot, it is likely that the unit providing the texture information has to be adapted to e.g. each finger (e.g. as a pin-array or piezoelectric disc), as the fingers will have to be positioned independently of each other. In this case it may even be necessary to provide a lateral movement between finger and texture-unit to generate shear forces in the skin. In case of the shape being fix, e.g. in the case of a map, a relative movement may happen by the fingers themselves and the texture unit can be designed with less size restrictions.
- How fast does the displayed information change? → Textures change rarely during the simulation of objects and display of maps. This is dramatically different when

[5] Consider: The mechanical stimulus pattern is not the only dimension of haptic textures, especially the thermal conductivity of the surface contributes a lot to the realism of surface-rendering.

e.g. texts or the influences of fluids on textures have to be displayed. The answer to this question has a significant impact on the technical system.

- Which intensity range is covered by the texture? → In the simplest situation the answer can be given by definite displacements and a resolution in bit. Usually, only qualitative values of the properties of objects for interaction are available. These hints have to be complemented by one's own experiments. With regard to the definition of these requirements it is very important to make sure that the planned spatial addressability and maximum intensity change does not exceed the corresponding resolution of the user. A research on the corresponding psychophysical experiments is highly recommended, as otherwise it may not be possible to transmit the intended information density.
- In this category there are numerous established solutions for grounded and wearables devices. BASODGAN ET AL. [3] summarized a relevant state of the art on how to make grounded surfaces smart. See also Chap. 12 for more details on the software-considerations. PACCHIEROTTI ET AL. [22] summarized the state of research on wearable devices for inspirations on surface interaction.

5.3.3 Cluster ③—Vibro-Tactile

Cluster ③ is a solution space for simple one-dimensional technical problems and corresponding questions. It covers independent dimensions of information (e.g. coding an event in a frequency and the importance in the amplitude). In this cluster, distributions of intensity variations and /or time dependent distributions of single events are filed. Technological solutions are usually vibrational motors or tactons, as being used in mobile phones or game-consoles. But even if the technical solution itself seems quite straightforward, the challenge lies in the coding of information with respect to intensity and time and an appropriate mechanical coupling of the device to the user.

- Which mechanical interface for the transmission of haptic information to the user is planned? → More specifically: Is this interface influenced by mechanical limits like housings?
- Which design space is available? → Frequently, vibro-tactile solutions are limited as to the available space at an early stage of the design due to requirements for mobility.
- Which resolution is expected for the planned intensity variation? → The criteria are similar to those of the "surface-tactile" cluster. As the "vibro-tactile" cluster frequently deals with oscillating systems, the dependence of the perception of oscillations on its frequency has to be taken into account. The user's perception is the limiting factor for intensity variations, which themselves are dependent on the mechanical coupling between device and user, too.

5.3.4 Cluster ④—Vibro-Directional

Vibro-tactile systems code one-dimensional information in the form of intensities. It is obvious that by the combination of multiples of such information sources directional information can be transmitted. This may happen two-dimensionally in a plane surface, but also three-dimensionally. Cluster ④deals with such systems. One possible technical solution for directional surface information would be to locate a multitude of active units in the shape of a ring around a body part, e.g. like a belt around the belly. The direction is coded in the activity of single elements. This approach can also be transferred to a volumetric vector, whereby in these cases a large number of units is located on a closed surface, e.g. the upper part of the body. The activity of single elements codes the three dimensional direction as an origin of a normal vector on this surface. In addition to the questions of cluster ③this cluster deals with the following questions:

- What is the intended resolution on the surface/in the space? → As well as before dependent on the body surface used, it is likely that the human perception represents the limit for the achievable resolution. Corresponding literature [9, 32] has to be checked carefully before the technical requirements can be met.
- What number of simultaneously displayed vectors is expected? → The fact that users will be able to identify one direction does not guarantee that with a parallel display of two points the user will perform equally well. Simultaneous display of information frequently results in masking-effects hard to be quantified. Experiments and analysis of the intended application are strongly recommended.
- Which frame of reference is used? → The information displayed is usually embedded in a frame of reference, which is not necessarily identical with the user's frame of reference and his or her body. The user may change his position for example in a vehicle, which results in a loss of the position of the elements fixed to the body and their orientation in the vehicle. It is necessary to be aware of the active frame of reference (local user-oriented, or vehicle-oriented, or maybe even world-oriented) <u>and</u> to provide measurement equipment for identifying changes in user positions and frame of reference. Additionally, it may become necessary to present a haptic reference signal to the user, which calibrates the user's perception to the frame of reference, e.g. a "north"-signal.

5.3.5 Cluster ⑤—Omni-Directional

Cluster ⑤ deals with systems coding real volumetric information. Within such a three-dimensional space each point either includes intensity information (scalar field) or vector information (vector field). The sources of such data are numerous and frequent, may it be medical imaging data, or data of fluid mechanics, of atomic physics, of electrodynamics, or of electromagnetics. Pure systems of haptic interaction with such kinds of data are seldom. Frequently, they are combinations of the clusters "kinaesthetic" and "vibro-tactile" for scalar fields, respectively "kinaesthetic" with six active haptic degrees of freedom for vector fields.[6] Consequently, the specific questions of this cluster add one single aspect to already existing questions of the other clusters:

- Does the intended haptic interaction take place with scalar fields or with vector fields? → For pure vector fields kinaesthetic systems with the corresponding questions for six active degrees of freedom should be considered. In the case of scalar fields, an analysis of vibro-tactile systems in combination with three-dimensional kinaesthetic systems and the corresponding questions should be considered. Then the property of the scalar value corresponds to the dynamics of the coded information.

5.3.6 General Requirement Sources

For any development process there are several questions which always have to be asked. They often refer to the time-frame as well as to the resources available for the development. For haptic devices two specific questions have to be focused on, as they can become quite limiting for the design process due to specific properties of haptic devices:

- Which energy sources are available? → It is not a necessary prerequisite that electrical actuators have to be used for haptic devices, especially in the case of telemanipulation systems. The usage of pneumatic and hydraulic energy sources, especially for tactile devices is a real alternative and should be considered.
- The design, how expensive may it be? → The prices of current kinaesthetic haptic systems reach from 200 EUR of mass-products to 1,500 EUR of medium scale products to devices of 25,000 EUR for small series and 100,000 EUR for individual solutions. These prices only partly result from commercial acquisitiveness, but mostly from the technical requirements and the efforts which have to be taken.

Furthermore, safety is a relevant source of requirements for haptic systems. Because of the importance of this issue, it is dealt within the next section seperately.

5.4 Safety Requirements

Since haptic systems will be in direct contact with human users, safety has to be considered in the development process. As with usability (Sect. 4.2), a consideration

[6] The haptic interaction with objects in a mathematical abstraction always is an interaction with vector fields. In the vectors, forces of surfaces are coded, which themselves are time dependent, e.g. from movements and /or deformations of the objects themselves.

of safety requirements should be made as early in the development process as possible. Furthermore, certain application areas like medicine will require a structured, documented and sometimes certified process for the design of a product which also has to include a dedicated management of risk and safety issues. In this section, some general safety standards that may be applicable for the design of haptic systems are addressed and some methods for the analysis of risks are given.

5.4.1 Safety Standards

Safety standards are issued by the large standard bodies and professional societies like ↪ international Organization for standardization(ISO), the national standard organizations, ↪ institute of Electrical and Electronics Engineers(IEEE), and ↪ International Electrotechnical Commission (IEC) for example. Some relevant standards for the design of haptic systems are listed as follows. Please note that this section will not supersede the study of the relevant standards. For a more detailed view on the general contents of the standards, the websites of the standardizing organizations are recommended.

IEC 61508 This standard termed *Functional Safety of Electrical/Electronic/ Programmable Electronic Safety-related Systems* defines terms and methods to ensure functional safety, i.e. the ability of a system to stay or assume a safe state, when parts of the system fail. The base principle in this standard is the minimization of risk based on the likelihood of a failure occurrence and the severity of the consequences of the failure. Based on predefined values of these categories, a so-called ↪ Safety Integrity Level (SIL) can be defined, that will impose requirements on the safety measures of the system. It has to be noted that the IEC 61508 does not only cover the design process of a product, but also the realization and operational phases of the life-cycle.
The requirements of functional safety impose large challenges on the whole process of designing technical products and should not be underestimated. The application of the rules are estimated to increase costs from 10 to 20 % in the automotive industry for example [27].

ISO 12100 This standard defines terms and methods for machine and plant safety. It can be considered as detailing the above mentioned IEC 61508 for the construction of machines, plants and other equipment. For the design of haptic systems, this standard is probably also useful to assess security requirements for the intended application of the system.

ISO 13485, **ISO 14971**, **IEC 62366**, **IEC 60601** The ISO 13485 standard defines the requirements on the general design and production management for medical devices, while the ISO 14971 standard deals with the application of risk management tools in the development process of medical devices. One has to note that these standards are a good starting point for devices intended for the European market, but further rules and processes of the ↪ Food and Drug Administration

(FDA) have to be considered for products intended for the American market. The IEC 62366 deals with the applicability of usability engineering methods for medical devices. IEC 60601 considers safety and ergonomic requirements on medical devices.

IEEE 830 This standard deals with the requirement specifications of software in general. It can therefore be applied to haptic systems involving considerable amounts of software (as for example haptic training systems). The general principles on requirement definitions (like consistency, traceability, and unambiguousness for example) from this standard can also be applied to the design of technical systems in general.

Since a large number of haptic systems are designed for research purposes and used in closely controlled environments, safety requirements are often considered secondary. One should note however, that industry standards as the ones mentioned above resemble the current state of the art and could therefore provide proven solutions to particular problems.

5.4.2 Definition of Safety Requirements from Risk Analysis

As mentioned above, modern safety standards will not only define certain requirements (like parameters of electrical grounding or automatic shut-down of certain system parts), but have also an impact on the whole design process. To derive requirements for the haptic system, the following steps are advisable during the design process:

1. Assess the relevant safety standards for the intended application and usage of the haptic system. Despite the standards itself, this also includes further regulations and applicable test cases.
2. Define your safety management and development process including project structure, needed certifications, documentation requirements and the life-cycle management.
3. Conduct a risk analysis and derive technical requirements from the results.

Figure 5.4 shows the general risk management flowchart. Based on a risk identification, a risk assessment is made to evaluate the failure occurrence and the severity of the consequences. There are two approaches to identify risks. In a bottom-up-approach, possible failures of single components are identified and possible outcomes are evaluated. This approach can be conducted intuitively, mainly based on the engineering experience of the developer or based on a more conservative approach using check-lists. On the other hand, a top-down-approach can be used by incorporating a $\hookrightarrow$ Fault Tree Analysis (FTA). In that case, an unwanted system state or event is analyzed for the possible reasons. This is done consecutively for these reasons until possible failure reasons on component level are reached. In practice, both approaches should be used to identify all possible risks.

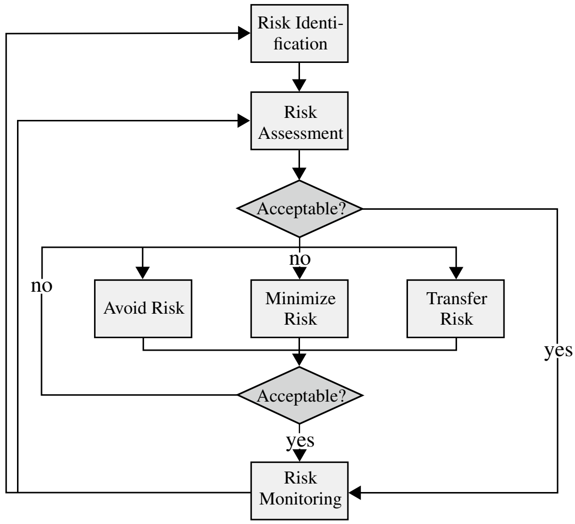

Fig. 5.4 General risk management flowchart

For each identified risk, the failure occurrence and the severity of the consequence has to be evaluated. Especially for hardware components this is a sometimes hideous task, since some occurrences cannot be calculated easily. Based on these values, a risk graph can be created as for example shown in Fig. 5.5. Acceptable risks do not require further actions, but have to be monitored in the further development process. Risks considered to be in the ↪ As Low As Reasonably Practicable (ALARP)—area are considered relevant, but cannot be dealt without an abundant (and therefore not reasonable) effort. Risks in the non-acceptable area have to be analyzed to be at least transferred to the ALARP-area. Please note that the definitions of the different axis in the risk graph and the acceptable, ALARP and non-acceptable area have to be

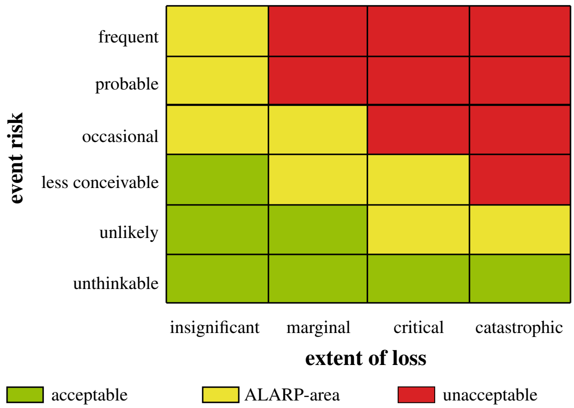

Fig. 5.5 Example of a risk graph

defined for each project or system separately based on the above mentioned standards or company rules.

For each risk, one has three possibilities to deal with the risk, i.e. move it into more acceptable areas of the risk graph:

- First of all, risk can be avoided. If a piezoelectric actuator is used for a tactile application, the user can be exposed to high voltages, if the isolation fails. One can avoid this risk, if no piezoelectric (or other actuator principles) with high voltage demands are used.
- Secondly, the risk can be minimized. In the above mentioned example this could be an additional electrically insulating layer with requirements on breakdown voltage, mechanical endurance and surface texture properties.
- The third possibility is to transfer a risk. This principle is only applicable in a restricted way to the design of haptic interfaces. A possible example would be the assignment of the development of a certain sub-contractor to minimize the technical risks of the development.

After each risk is dealt with, the acceptability has to be evaluated again, i.e. the changes in the risk graph have to be analyzed. Obviously, moving risks into lower-risk regions will consume effort and costs. This considerations can lead to ethical dilemmas, when severe harm to humans has to be weighted against financial risks like damage compensations. For this reason, ↪ ALARP classifications for economical reasons are forbidden by ISO 14971 for medical devices starting with the 2013 edition.

The evolution of risks has to be monitored throughout the whole design and production process of a system. If all steps involved are considered, it is obvious that the design of safe systems will have an significant impact on the overall development costs of a haptic system and a thorough knowledge of all components is needed to find possible risks in the development.

5.5 Requirement Specifications of a Haptic System

The defined application together with the assumption from the customer and the interaction analysis will allow to derive individual requirements for the task-specific haptic system. These system requirements should be complemented with applicable safety and other standards to form a detailed requirement list. This list should not only include a clear description of the intended interactions. Also the intended performance measures (Chap. 13) and as much technical details as possible about the overall system and the included components should be documented. As stated above, the technical solution clusters shown in the preceding Sect. 5.3 will also give possible requirements depending on the intended class of applications.

Table 5.1 Example of a system specification for a haptic device

R/W	Description	Value	Source/Comment
Especially kinaesthetic-motivated parameters			
R	Number of DOFs	2x rot., 1x transl.	Shall give an idea of DOFs, name them!
R	Workspace	$100 \times 50 \times 50\,\text{mm}^3$	Minimum of workspace to be achieved
W	Maximum Workspace	$150 \times 100 \times 100\,\text{mm}^3$	Maximum workspace necessary
R	Maximum force in DOF “name”	5 N	
W	Maximum force in DOF “name”	7 N	Always define a range of forces!
R	Minimum force in DOF “name”	0.2 N	
W	Minimum force in DOF “name”	0.1 N	Always define a range of forces!
R	Maximum dynamics (bandwidth) for DOF “name” in a blocked situation	100 Hz	Shows (among other things) e.g. the maximum dynamics of the driver electronics
W	Maximum dynamics (bandwidth) for DOF “name” in a blocked situation	200 Hz	Shows the bandwidth the customer dreams of
R	Smallest border frequency when movement is blocked	static	There may be applications with pure dynamic movements without a static portion. This makes this question interesting
R	Maximum velocity of movement in idle mode	10 mm/s	This is a question regarding security too, as it defines the mechanical energy stored in the system
R	Maximum bandwidth of the velocity change	10 Hz	The change of velocity, which is the acceleration of the system, has a large influence on the energy the system requires
R	Maximum haptic impedance at the output	10 Ns/m	This is an alternative representation to the independent definition of force and velocity for dynamic (but passive) systems!
R	Minimum haptic impedance at the output	0.01 Ns/m	This is an alternative representation to the independent definition of force and velocity for dynamic (but passive) systems!
R	Smallest position resolution/measurement insecurity for DOF “name”	0.1 mm	Usually measurement of the position is self-evident for haptic interaction
W	Smallest position resolution/measurement insecurity for DOF “name”	0.05 mm	
R	Type of the mechanical interface	Button/pen/none	Is there a handle?
R	Mechanical reference point	Grounded, worn	Has influence on weight, size and energy
R	Direction(s) of the tactile stimulation	Normal to the skin	An alternative would be lateral stimulation or a combination of both
R	Maximum displacement-amplitude of the tactile elements	1 mm	Is especially relevant for pin-displays, but may be also understood as oscillation-amplitude of vibrational elements

(continued)

Table 5.1 (continued)

R/W	Description	Value	Source/Comment
Especially tactile motivated parameters			
R	Minimum amplitude resolution of displacements	Digital (on/off)	May include several levels for the pin to be moved to
R	Highest density of stimulation	2 mm distance from midpoint to midpoint	Varies extremely in dependency from the chosen skin area in contact
R	Maximum geometrical size of stimulation	2 mm diameter	
R	Maximum frequency range of stimulation	100 to 300 Hz	Relevant for tactile actuators only, of course
R	Minimum frequency-resolution	1 Hz	For vibrotactile actuators
R	Maximum force during displacement/stiffness	20 N	Pin-based actuators may not necessarily be stiff. Systems of lower admittance may be used too
R	Connection to the user	Attached to the environment / worn	Necessary to identify, whether there is a relative movement between skin (e.g. finger) and the display
R	Maximum number of fingers simultaneously in contact with the device	1–10	May have an large impact on the design when for example full-hand exploration is required
Digital interface			
R	Minimum resolution of the output data	12 bit	Usually slightly lower than the measurement error of force- and position-measurement
R	Minimum resolution of the input data	12 bit	Usually slightly larger than the resolution of force- and position input-data
R	Frequency of the haptic loop	1000 Hz	Should be at least two times, better would be 10 times, larger than the border frequency of the design. Has influence on the perceived stiffness
W	Other interface-requirements	Use USB/FireWire...	Typically the interface to be used is subject to company politics
R	Interface driver	API	As any other hardware a haptic interface needs an own software driver for abstraction
General parameters			
R	Maximum temperature range for operation	10–50c	May become very relevant for actuator principals with little efficiency in extreme environments (automotive)
R	Maximum volume	$500 \cdot 500 \cdot 200\,\text{mm}^3$	Device-size
R	Weight	1 kg	Especially relevant if the device is worn. This limit will strongly influence the mechanical energy generated
R	Electrical supply	Battery/ 110V/ 230V	Very important, devices were spotted on fairs, which ceased to function due to errors made when considering AC voltages of different countries
R	Maximum power	50 W	Primary power consumption including all losses

Table 5.1 will[7, 8, 9] give an example of such a requirement list with the most relevant technical parameters of a haptic system. However, it is meant to be an orientation and has to be adapted to the specific situation by removing obsolete entries and adding application specific aspects.

Additionally a system specification includes references to other standards and special requirements relating to the product development process. Among others, these are the costs for the individual device, the design-process itself and the number of devices to be manufactured in a certain time-frame. Additionally the time of shipment, visual parameters for the design, and safety-related issues are usually addressed.

5.6 Haptic Design of Mechanical Controls

Chapter 4 described the use of simulation is of advantage regarding development time and effort. The following chapter shows basic relations between technical parameters and subjective behavior of rotary and translatory switches. This chapter is a "how-to" guide regarding how haptic systems could or should feel like, and how ideal haptical designs can be reached. Starting with the rotary switches that describe and explore haptical characteristics, the turnover to the push buttons is done, showing the influences and differences deriving out of the event based perception that plays an important role in the haptical design of devices. The overall content relies on the Dissertation of [24].

5.6.1 Rotary Switches

Typically, rotary devices are described by a torque versus angle description. Due to the remaining shear forces on the finger tips it makes sense to derive these forces as a reference level to get a uniform force level dealing with different knob diameters ($F_{\text{shear}} =$ torque $\div$ ½ diameter). To be clear about what devices we are talking about and furthermore being the standard for rotary devices we use torque instead of shear force. Figure 5.6 shows the structure of a mechanical rotary switch.

A spring-driven tappet is affecting the cam disc with torque. The shapes of the cam disc and the tappet are defining torque over position which are the major parameters defining the haptic behavior of the system. The spring itself is in general "just"

---

[7] R: requirement, W: wish.

[8] The combination of requirements and wishes (R and W) may be used for almost any element of the system specification. It is recommended to make use of this method, but due to clarity in the context of this book this approach of double-questions is aborted here.

[9] A "haptic loop" is a complete cycle including the output of the control-variable (in case of simulators this variable was calculated the time-step before) and the read operation on the measurement value.

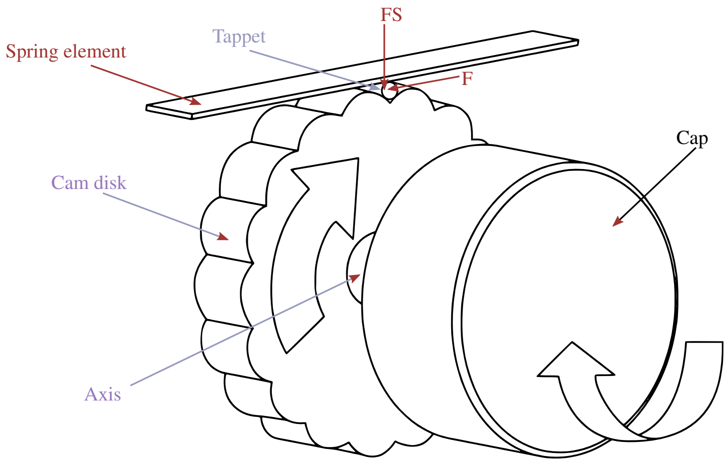

Fig. 5.6 Mechanical setup of a rotary switch [24]

relevant for the overall torque level. Therefore, the main haptical behavior is defined by the cam disc and the tappet while the force level can be adjusted with the spring parameters. Additionally, strongly influencing is the friction and it needs to be considered in a general level not to influence the system negatively. Even the construction of the system influences this particular parameter strongly.

5.6.1.1 Rest Position and Transition Point

The most important issue is the orientation within the torque characteristics. Figure 5.7 shows a simplified characteristic curve without the influence of friction.

The torque versus angle characteristics is not intuitively readable. For example, the rest position of the switch often interpreted to be in a local minimum of the curve. Of course, when looking at the details, the rest position is located in a zero

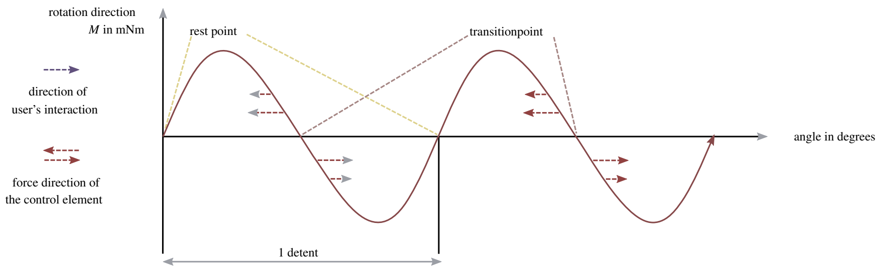

Fig. 5.7 Simplified characteristic curve without friction, showing the basic points for orientation as well as the directions of the user interaction and the force directions

torque position, otherwise it might move due to the remaining forces. Due to the effective direction of movement, resulting out of the torques' sign, a positive torque for example moves the knob to the left/clockwise, while a negative torque moves it to the right/counterclockwise.

Two specific points remain out of this in the zero-crossings of the curve: Thus if both torques, positive and negative, point to a zero-crossing, this point will be stable and become a rest position, where the switch will remain in, until it is forced to move out by external (user) forces. The second type is the opposite. Both torques point away from the zero-crossing, so a little deviation from the zero torque level leads to an increasing torque pulling the knob away from it. That is why it is not a stable position like the rest position, typically actively leading the knob from one stable position to the next and we call it the transition point. This is the typical "changing point" where the user recognizes the physical barrier also called "detent" and its change from one position to the next.

Concluding a rising zero crossing's flange typical is a rest position while a falling flange's zero-crossing is the transition point of the curve.

5.6.2 Friction

While the shape of the curve is relevant for the overall feeling (the "how" the device is moving from one position to the next), the friction is an add-on parameter which affects that overall feeling and the operation of the device. High friction makes the device feel dull and the detents are becoming imprecise, while low friction can cause beating and vibration of the device when snapping into the rest position. Regarding operational issues, a high amount of friction can lead to a sticking of the device at the transition points. Therefore, the remaining spring force becomes too low to move the device out of these positions. This situation can lead to undefined states, where the device remains stuck between two defined positions. Of course, one could cause this to happen intentionally. This may be relevant for security issues and a steep flange may avoid it, at all, unfortunately contrary to a "good feeling".

What happens to the characteristic curve: friction is shifting it vertically, increasing the perceived forces, and because friction is always directing against the control's movement, it causes a hysteresis of the measured curve. In short, low friction has a small hysteresis, and high friction a big hysteresis.

The friction value can be derived from the delta of the hysteresis $F_{\text{friction}} = \frac{1}{2} F_{\text{Hysteresisdelta}}$.

The frictional effects described before can be compared to a static offset as shown in Fig. 5.8, mostly generated by the bearings and additionally, by varying amounts, by the tappet and cam disc.

Even the friction between tappet and cam disc shows some very specific behavior that can help to identify the frictional source in a component. The relation of diameters of the knob and the cam disc or the bearing are quite relevant for the influence of the added friction and can be a possibility to influence it efficiently.

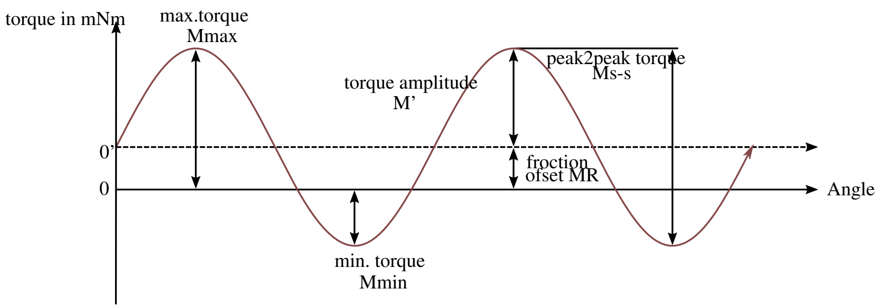

Fig. 5.8 Friction offset of a right turn characteristic curve, without showing a hysteresis

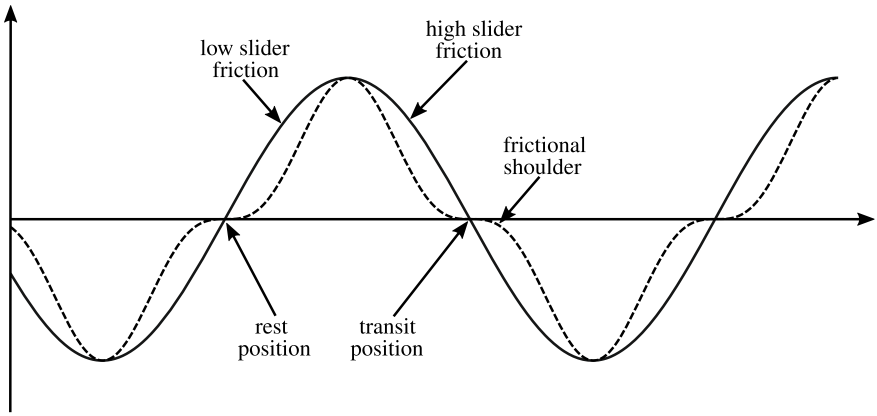

Fig. 5.9 Friction influence caused by slider and cam disc

So how does this friction influence the curve additionally: The friction between tappet and disc is not constantly. While a flat cam disc gradient typically increases the frictional influence, the gradient of the spring plays also an important role. Furthermore, a more compressed spring leads to a higher spring force and a higher friction. Therefore, a steep gradient has comparably low friction.

All the zero crossings, i.e. the rest position and the transition point, typically have a high friction. For the rest position, this is not critical, but for the situation of a standing still in the transition point, as previously described, it is an unwanted thing.

Figure 5.9 shows the impact of this kind of friction, leading to a flatting of the characteristic curve at the zero-crossings, which we call "frictional shoulders". This effect is very practical for identifying the sources of friction during development of devices by measurement.

5.6.2.1 The Integral-Representation

As mentioned before, the intuitive readability of the torque-characteristics is not given. Thus the question if there is an intuitive representation is answered in [26] and [24] describing the integral representation. It shows that the integration of torque-angle characteristics leads to an intuitively readable description. It is possible to describe the behavior of the device as well as a basic mechanical derivation of the cam disc with this principle. The big advantage of this description is the intuitive readability of the "shape". This helps to divide between important and unimportant parameters and indicates the location of problems intuitively. This makes development much more efficient. Equation (5.1) shows the basic mathematical description of the integral representation.

$$I(\varphi) = \int_{\varphi_1}^{\varphi_2} M(\varphi)\,\mathrm{d}\varphi \tag{5.1}$$

To prove the hypothesis, [24] executed several tests. Figure 5.10 shows examples of basic characteristics displayed by a haptic interface to the subjects. The diagrams on the left show the torque representations and those on the right show its associated integral representation. The subjects had to choose the intuitively fitting representation. Significantly, the subjects selected the integral representation. As an example, against all expectations regarding the torque representation the sine (a) and triangle (b) characteristics both feel comparably smooth and more "sine-like", even the triangle a little "weaker" than the sine. The triangle expected to be crisp and sharp, and absolutely did not fulfill any of those expectations.

The integral representation shows a fitting picture: the integrated sine-shape results in cosine and the integrated triangular shaped results in parabolic shapes that are very similar to the sine shape. In addition to this, the area under the triangle is smaller than the sine and its maximum is slightly lower than the sine in integral representation that fully fits to the derived results out of pair comparison studies.

Another Example, the saw tooth shapes expected to be one-sided sharp are fitting well with the integral representation describing the behavior very intuitively. Finally, the square shape leads to a triangular feeling, also represented correctly by the integral.

5.6.2.2 Identification of Parameters for Rotary Haptic Devices

Knowing the integral representation is the basis for identifying relevant parameters, because the transformation helps understanding the perceptional influence. Due to technical reasons, the torque representation is still the describing low-level representation and used for the overall parametrization. The chosen torque parameters shown in Fig. 5.11, which are mainly the rising and falling slope of a rectangular shape.

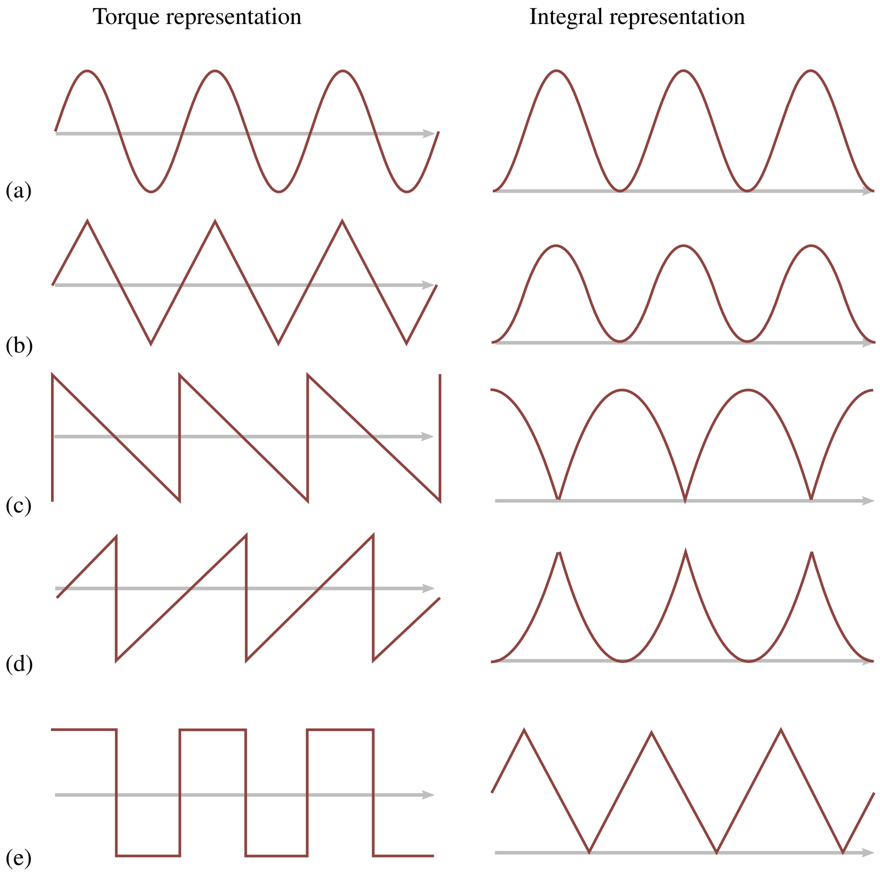

Fig. 5.10 Shapes that were represented by [24] to the subjects to identify the intuitive way to represent haptical feelings graphically

Changing their steepness independently can convert it to the entire shapes shown in Fig. 5.10 that pointed out to be the most relevant ones. The amplitude appeared to be an overall parameter not influencing the character/feeling of the shape. Its influence is the overall force level or resistance, which allows using it to adjust the ease of movement without changing the basic character of the effect.

To identify the parameters and their influence, the different characteristics presented to subjects on the haptic display for rotary switches. Questionnaires as well as pair-comparison tasks helped to identify and quantify the parameters. Figure 5.12 shows the variety of the presented parameters in integral representation. Looking at the rest position, the "width" or "precision" of the device presented quite realistically. Relations to the adjectives shows a steep rising slope at the rest position increases the precision and hardness, while a steep falling slope at the transition point reduces controllability and increases the hardness. The integral representation displays this

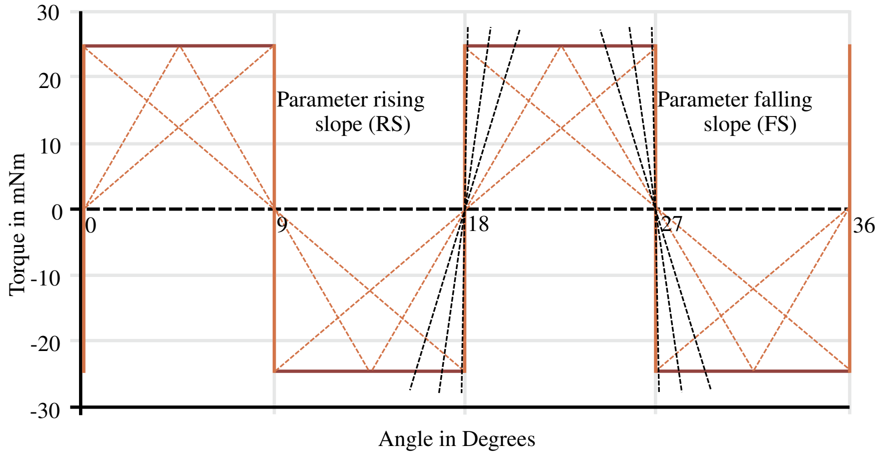

Fig. 5.11 Variation of torque-parameters used for the haptic representations [24]

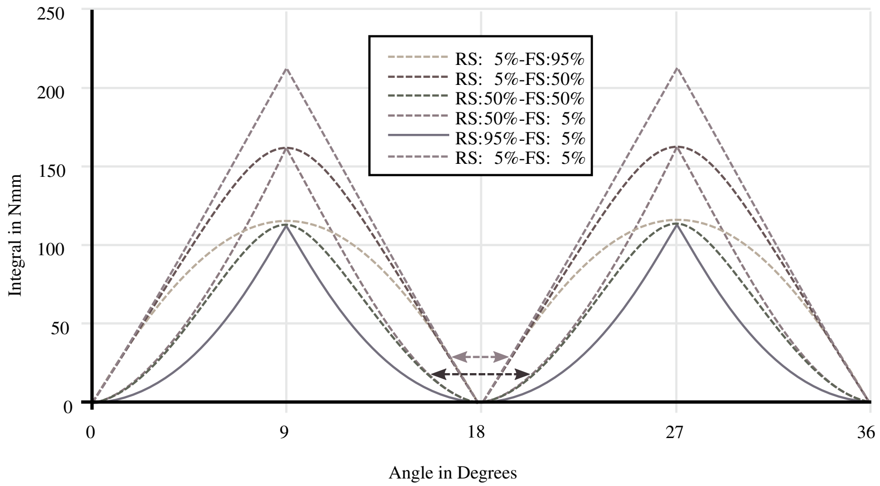

Fig. 5.12 Integral representation of the varied haptic representations [24]

in the width of the rest position, i.e. more precise when it is narrow and less precise when it is wide. Moreover, the transition point is controllable when a round shape leading to the next position given, while it is not controllable when the shape is forming a sharp peak.

Bringing all parameters together, the period that describes the "length" of the detent and the force amplitude, the slopes at the rest position and the transition point are the main parameters of the subjective impression.

Thus, the steepness of the rising slope influences the impression of a precise rest position, where 5% slope was showing the best precision.

The hardness influencing by both flanges. The steeper both are, the harder the impression. Furthermore, the area under the integral representation seems to behave proportionally to the hardness impression. The rising flange of 5% and the falling flange of 50% concluding to be an ideal pairing.

Combining both slope parameters means increasing the precision by the rest position's slope that automatically increases the hardness effect. The falling transition point's slope only affects the hardness.

The falling slope furthermore influences the controllability and the willingness of the device. Thus, a steep falling slope shows a bad controllability of the switch. Explaining it with the hard change of the torque at that point, when the device is working against the user's movement until reaching the transition point. At this position, it suddenly changes its sign suddenly pulling the knob into users moving direction. The steeper the slope the stronger the change. Also, out of a control theories' point of view a very difficult task to handle.

The amplitude of the overall signal is just proportionally influencing the overall impression, but not changing the relations between the adjectives.

The length of the detent influences the signals overall impression also strongly. A reduced angle reduces the influence of the parameters, comparable to a reduction of the resolution because no parameters angles are reducing, not representing flat slopes anymore.

5.6.2.3 Asymmetry

One very specific "trick" is the use of asymmetric characteristics. Figure 5.13 shows the torque representation where the area under the curve is bigger at the left turn than at the right turn by different angles, at all, requiring more energy to overcome. Figure 5.14 shows the integral representation thus the subjective behavior of the device clearly by a curve descending to the right side.

An example of an active electromechanical rotary input device described by Audi patent [25]. The advantage of this specific asymmetric behavior is, it generates the illusion of a descending direction, but using the whole bandwidth of an actuator for every detent. It is not requiring a higher torque bandwidth to decrease the detent's torque between each detent to generate a decreasing impression. Because the asymmetry in energy is providing this feature. Furthermore, the angular range is without any limits, it is possible to descend indefinitely. As mentioned, the classical strategies need a reduction of the torque for each detent, so that the whole range limited by the bandwidth of the actuator and only a part of the overall torque of the motor used to generate the detents torque difference.

An example of passive mechanical haptics would be the Mercedes-Benz Light switches that have been using an asymmetric characteristic in the market since 2012. Describing the use of asymmetry in [8] for creating a haptic barrier between the parking and the driving light sections to make operation more intuitive.

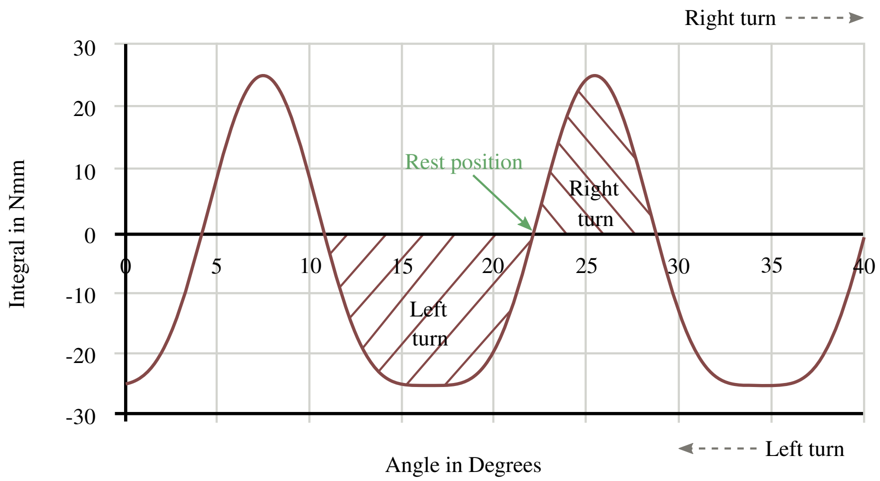

Fig. 5.13 Asymmetric torque characteristic with angular asymmetry [24]

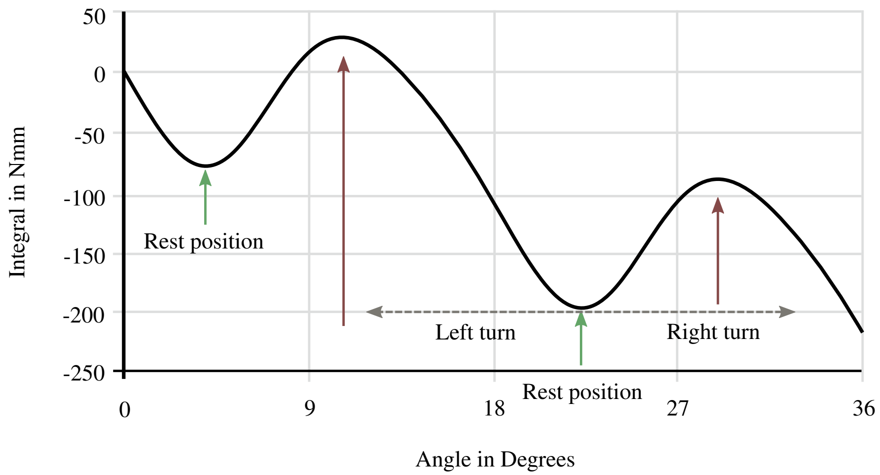

Fig. 5.14 Integral representation that intuitively shows the behavior of the asymmetrically designed control element [24]

5.6.2.4 Construction of the Cam Disc

The basic development of a haptic characteristic using the integral characteristics as an intuitive guide described before. As previously mentioned, the integral relation also serves as a guideline in designing and constructing the mechanical shape of the cam disk and the tappet itself.

Derived out of the basic mathematical description of the Integral representation $\frac{I(\varphi)}{\mathrm{d}\varphi} = M(\varphi)$ the gradient of the cam shape is proportional to the Torque M. We are considering the following elements: the shape of the cam disk, the shape of the tappet, the frictional pairings, and the stiffness and pretension of the spring element. The radius between rotational center and the contact point between the tappet and the cam disk are relevant as well as the radius of the end effector/cap where the finger is grasping.

The gradient at the contact point is nothing more than the derivation of the cam shape, so the relation between shape and force is the required angle α of the shape resulting in the specific force F_{finger} at this point. The gradient angle α of the cam in the contact point calculated as shown in Eq. (5.2). It is a simplified version to explain the basic principle:

$$\alpha = \frac{1}{2}\arcsin\left(2\cdot\frac{F_{\text{finger}}}{c_{\text{spring}}\cdot l_{\text{spring}}+F_{\text{spring0}}}\cdot\frac{r_{\text{finger}}}{r_{\text{cam}}}\right) \tag{5.2}$$

Equation (5.2): calculation of the gradient α at position φ out of the required finger force $F_{\text{finger}}(\varphi)$ at position φ or of course its torque ($M_{\text{finger}}(\varphi) = F_{\text{finger}}(\varphi)\cdot r_{\text{finger}}$)

The parameters of Eq. (5.2) are:

α	Gradient angle of the cam
$F_{\text{finger}}(\varphi)$	wanted force at the finger at position (φ)
M_{finger}	torque at the finger
c_{spring}	spring constant, estimated as constant
l_{spring}	length of the spring; estimated as constant
F_{spring}	spring pre-tension at zero length (l_0)
c_{spring}	spring rate
r_{finger}	radius at finger contact point; estimated as constant
r_{cam}	radius at tappet contact point; estimated as constant, but maybe varying across φ

5.6.2.5 Correction of the Tappet Geometry

The calculations consider a point-contact between tappet and cam with a tappet-diameter of "ZERO" which is quite unrealistic. Especially smaller sized systems are strongly influenced by the tappet. Therefore, the radius of the tappet causes a shift of the contact point as shown in Fig. 5.15.

A very simple principle to consider the influence partly should also show how the correction might take place. Equation (5.3) describes the shift in angular direction to be considered as well. In addition, considering the vertical influence of the shift not described here.

$$s_v = r_{\text{tapped}}\cdot\sin(\alpha) \tag{5.3}$$

Equation (5.3): Correction of the contact point caused by the tappets' radius r_{tappet}

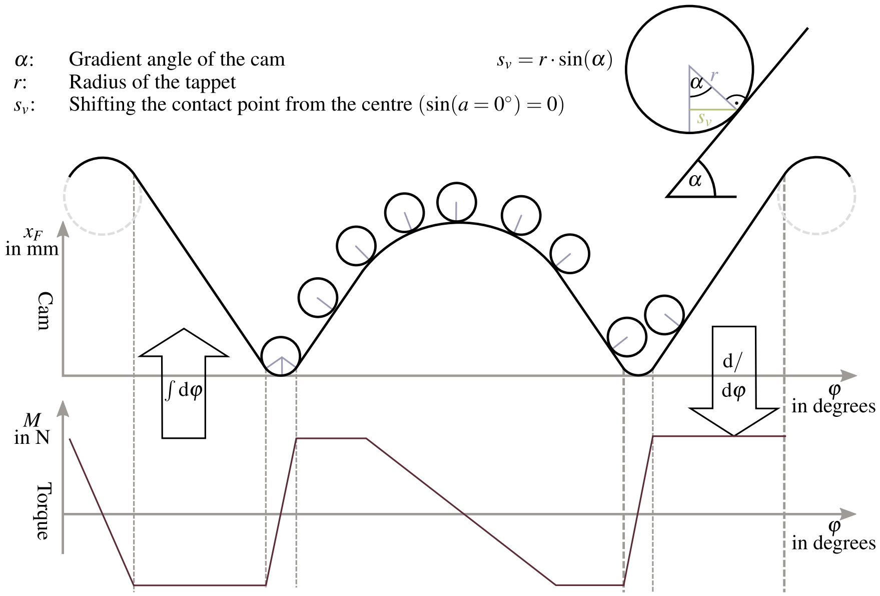

Fig. 5.15 Principle of the tappet's influence on the cam construction and the principle of the relation between gradient of the cam shape and the torque characteristic

5.7 Push Buttons

The second large group of control elements are push buttons. The differences between translatory (push) and rotary controls are quite strong: the linear movement is dominant, characteristic curves of force-travel look different in addition to the behavior, as well as the use case (positioning vs. activating) and the mechanical principle behind it. A closer look at the details indicates that the principles and description are quite different, but anyway are still compatible. The differences appear in the technical ranges and the type of psychophysical stimuli being useful in both domains. Even help understanding (vibrotactile) active haptic systems more clearly.

5.7.1 Characteristic Curve

The typical characteristic curve of push buttons, describing force versus travel (Fig. 5.16), is comparable to the rotary torque versus angle/travel characteristics.

A basic characteristic of the push button is having a single rest position. This rest position needs to be reached by the push button's mechanics on its own, because, due to the cap's geometry, the user cannot typically bring it back there. In principle, the user is positioning the rotary switch to a specific detent. That is why the rotary switch might not return to the same position, it also can move to the next one. This explains why it typically has several zero crossings and transition points. Compared to this, the user can control the push button only in the direction of the push. The device always needs to provide a force working backwards into the direction of the rest position to be able to return to it. Maybe you had already the experience with a hanging button; it is difficult to get the cap returning to the rest position. For this, the force always needs to be positive, or due to friction even higher. So the typical characteristic curve is located in the first quadrant, while the rotary curve typically occupies the first and second, or even all four quadrants.

There is a difference between the measurement points and a typical specification, because the measurement probe first has to approach the cap before the measurement starts. That is why the measurement probe does not see the relevant force until contact. Therefore, the measurement characteristics show a travel until contact at zero-force and no negative forces that would push the button into the rest position while pulling the cap (compare Fig. 5.16). Compared to this, the specification even needs to define this behavior as well, to keep it stable and not jiggling. The origin of Fig. 5.17 shows exactly that behavior where the curve passes the zero level continuing with the same steepness into negative force to generate a stable rest position. In this point, we can see a comparable behavior like the rest position of rotary switches.

5.7.2 The Snap

Looking at the push buttons characteristic its most important parameters are describing the snap and its position. It is the relevant event communicating to the user that his goal, the activation of the function, has been reached.

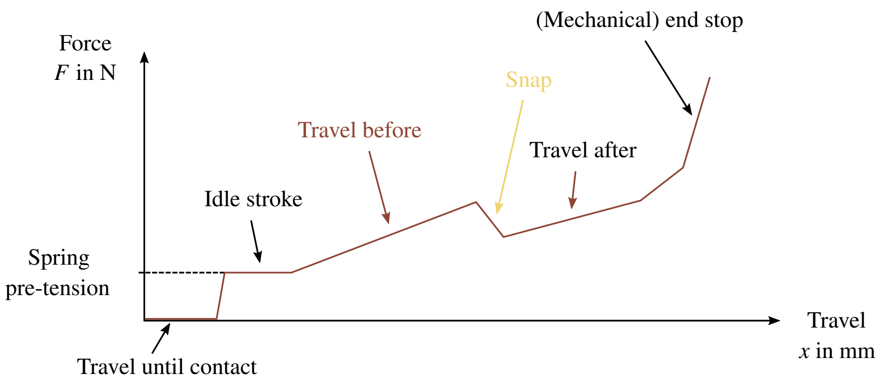

Fig. 5.16 Typical segments of a force-travel characteristic curve of a push button appearing during measurement

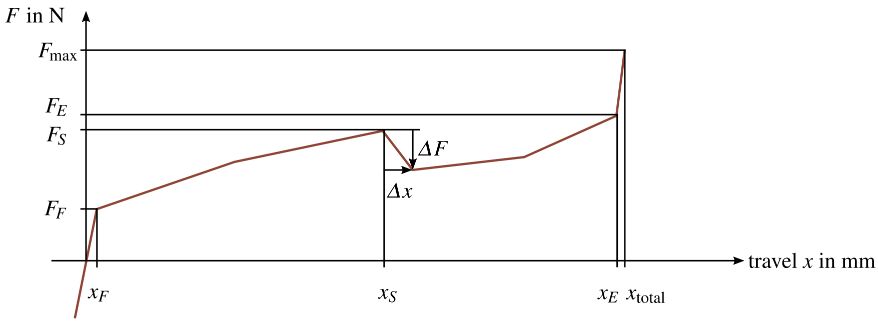

Fig. 5.17 Basic force travel parameters of push buttons without frictional hysteresis

The snap is the falling flange seen in the force-travel depiction. Typically, vertices, also, the snap's ending points, they all refer to the point of origin because of measurement practice. The perceptional point of view shows that considering steepness and height of the flange as a relative definition of the snap is a much better choice. The tolerance ranges can even result in much higher production efficiency, because the factors that affect the overall perception less can be assigned lower tolerance levels.

For example, even if the switching point (F_S/x_S) is moving in $x-$ or $F-$ direction, the snap may remain of the same haptic quality. Therefore, $\Delta F/F_S$ and Δx are the parameters to focus on /to prioritize. Figure 5.17 shows the parameter set.

The tests conducted on the psychophysics of rotary controls repeated for push buttons show that besides the subjective parameter estimation, some further interesting effects presented themselves. While flat and longer snaps showed a comparable rating to the rotary controls, steep and short snaps received a very different rating from the subjects.

F_F/x_F	Spring pre-tension
F_S/x_S	Actuation point
$\mathrm{d}F/\mathrm{d}x$	Snap
F_E/x_E	Start of the mechanical end stop
F_{max}	Maximum force Level
x_{total}	Total travel at F_{max}

5.7.3 *Event-Based Perception*

This observed difference in perception fits perfectly to the phenomenon of event-based perception described in [13] and approves it for the use of linear control elements.

Looking at a measurement, force versus time in Fig. 5.18 shows two haptic events snap and back-snap. Both show a strongly dampened vibration, having the ability to stimulate even Pacinian mechanoreceptors that are sensitive to high vibrotactile

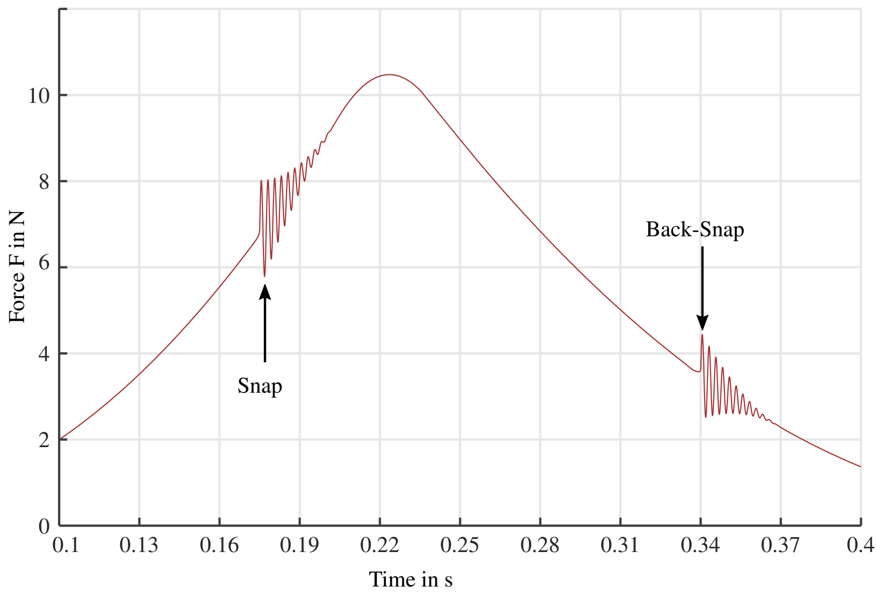

Fig. 5.18 Dynamic snap and back-snap of a push button force versus time

frequencies and acceleration. They may also be able to activate reflexes. In this sense, sharp snaps like micro switches activate a reflex-like perception, just saying "Hi—here was something", while long snaps are perceived to be more explorative, showing greater detail like a shape or resistance, or more visually spoken like a smooth or a long "hill" of the controls behavior showing more detail and catching more attention by exploration.

Concluding, the kind of the snap provides either a reflex-like quick or a detailed shape-like event of different content, speed and mental load.

5.7.4 Relevance of the Probes' Impedance

In conclusion, this event-based perception mechanism shows that the classical approach of the force versus travel description does not show up all information being necessary. Therefore, if vibrations appear within a characteristic curve, an interpretation of those vibrations is essential. Zhou et al. [34] explains an Interaction-based Dynamic Measurement principle (IDM) measuring with a human finger-like probe analyzing the specific vibrations due to subjective impressions. He found that the classical mechanical impedance of the finger is of high importance to allow realistic vibration of the event, lying in the working point. If it deviates, it will appear as a vibration differing from reality. The common impedance range of a probe goes from a stiff static probe to no-probe-influence. The former stiff one suppresses nearly all vibrations, thus only Zero-Hz-Frequencies—such as static forces—remain in the measurement data while the latter contactless one does not affect the device and allows it to vibrate at its natural frequency, for example measuring with a laser vibrometer.

If a probe or human finger were in contact with the device, it will put it out of tune. For this reason, it makes sense to use a probe with a comparable mechanical impedance such as a human finger. More details regarding IDM in Chap 14. A comparable approach with a different goal *Syntouch* is realizing [1]. They are mimicking a human fingertip to quantify surface haptic properties like identification of materials and their haptic dimensions [33]. It includes besides specific mechanical impedances the surfaces' fingerprint to get the system at a realistic working point.

Recommended Background Reading

[13] Kuchenbecker K.J. & Fiene J. & Niemeyer G.: **Improving contact realism through event-based haptic feedback**. In: IEEE Transactions on Visualization and Computer Graphics, vol. 12, no. 2, pp. 219–230, March-April 2006, doi: 10.1109/TVCG.2006.32
A key paper describing the origins of enhancing contact sensations by high-dynamics haptic accelerations. Inspiration for many researchers and still valid in its fundamental approach for many teleoperation-systems.

[20] Nitsch, V. & Färber, B.: **A Meta-Analysis of the Effects of Haptic Interfaces on Task Performance with Teleoperation Systems**. In: IEEE Transactions on Haptics, 2012.
Reviews the effect measures of several evaluation of VR and teleoperation systems. Recommended read for the design of haptic interaction in teleoperation and VR applications.

[14] Magnusson, C. & Brewster, S.: **Guidelines for Haptic Lo-Fi Prototyping**, Workshop, 2008.
Proceedings of a workshop conducted during the HaptiMap project with hints and examples for low-fi prototyping of haptic interfaces.

References

1. http://www.syntouchinc.com
2. Acker A (2011) Anwendungspotential von Telepräsenz-und Teleaktionssystemen für die Präzisionsmontage. Dissertation. Technische Universität München. http://mediatum.ub.tum.de/doc/1007163/1007163.pdf
3. Basdogan C et al (2020) A review of surface haptics: enabling tactile effects on touch surfaces. In: IEEE Transactions on Haptics 13.3, pp 450–470. ISSN: 23294051. https://doi.org/10.1109/TOH.2020.2990712. arXiv: 2004.13864

4. Bhattacharjee HK et al (2011) A novel single-port technique for transanal rectosigmoid resection and colorectal anastomosis on an ex vivo experimental model. In: Surgical endoscopy 25.6, pp 1844–1857. https://doi.org/10.1007/s00464-010-1476-1
5. Culbertson H, López Delgado JJ, Kuchenbecker KJ (2014) One hundred data-driven haptic texture models and open-source methods for rendering on 3D objects. In: IEEE haptics symposium, HAPTICS, pp 319–325. ISSN: 23247355. https://doi.org/10.1109/HAPTICS.2014.6775475
6. Deml B (2004) Telepräsenzsysteme: Gestaltung der Mensch-Maschine-Schnittstelle. Dissertation. Universität der Bundeswehr, München. http://d-nb.info/972737340
7. Deml B (2007) Human factors issues on the design of telepresence systems. In: Presence: Teleoperators and Virtual Environments 16.5, pp 471–487. https://doi.org/10.1162/pres.16.5.471
8. Entenmann V et al (2007) Rotary switch with haptic marking. DE102007039318
9. Erp et al Jv (2004) Vibrotactile waypoint navigation at sea and in the air: two case studies. In: TU-Muenchen (ed), pp 166–173. http://www.eurohaptics.vision.ee.ethz.ch/2004/15f.pdf
10. Hatzfeld C (2013) Experimentelle Analyse der menschlichen Kraftwahrnehmung als ingenieurtechnische Entwurfsgrundlage für haptische Systeme. Dissertation, Technische Universität Darmstadt. http://tuprints.ulb.tu-darmstadt.de/3392/. München: Dr. Hut Verlag. ISBN: 978-3-8439-1033-0
11. Hatzfeld C, Neupert C, Werthschützky R (2013) Systematic consideration of haptic perception in the design of task-specific haptic systems. In: Biomed Tech 58. https://doi.org/10.1515/bmt-2013-4227
12. Janschek K (2012) Mechatronic systems design: methods, models, concepts. Springer. ISBN: 978-3-642-17531-2
13. Kuchenbecker KJ, Fiene J, Niemeyer G (2006) Improving contact realism through event-based haptic feedback. In: IEEE transactions on visualization and computer graphics 12.2, pp 219–230. https://doi.org/10.1109/TVCG.2006.32
14. Magnusson C, Brewster S (2008) Guidelines for haptic Lo-Fi prototyping. Conference Workshop. NordiCHI. http://www.haptimap.org/organized-events/nordichi-2008-workshop.html
15. Matich et al S (2013) A new 4 DOF parallel kinematic structure for use in a single port robotic instrument with haptic feedback. In: Biomed Tech 58, p 1. https://doi.org/10.1515/bmt-2013-4403
16. Matich et al S (2013) Teleoperation system with haptic feedback for single insicion surgery-concept and system design. In: CARS proceedings. Heidelberg
17. Muñoz L, Ponsa P, Casals A (2012) Design and development of a guideline for ergonomic haptic interaction. In: Human-computer systems interaction: backgrounds and applications 2. Springer, pp 15–29. https://doi.org/10.1007/978-3-642-23172-8_2
18. Neupert et al C (2013) New device for ergonomic control of a surgical robot with 4 DOF including haptic feedback. In: Biomed tech 58. https://doi.org/10.1515/bmt-2013-4404
19. Nitsch V (2012) Haptic human-machine interaction in teleoperation systems: implications for the design and effective use of haptic interfaces. Südwestdeutscher Verlag für Hochschulschriften. ISBN: 978-3838132686
20. Nitsch V, Färber B (2012) A meta-analysis of the effects of haptic interfaces on task performance with teleoperation systems. In: IEEE transactions on haptics 6, pp 387–398. https://doi.org/10.1109/ToH.2012.62
21. Oakley et al I (2002) Guidelines for the design of haptic widgets. English. In: People and computers XVI-memorable yet invisible. Springer London, pp 195–211. https://doi.org/10.1007/978-1-4471-0105-5_12
22. Pacchierotti C et al (2017) Wearable haptic systems for the fingertip and the hand: taxonomy, review, and perspectives. In: IEEE transactions on haptics 10.4, pp 580–600. ISSN: 23294051. https://doi.org/10.1109/TOH.2017.2689006
23. Pahl G, Wallace K, Blessing L (2007) Engineering design: a systematic approach. Springer. ISBN: 978-3540199175

24. Reisinger J (2008) Parametrisierung der Haptik von handbetätigten Stellteilen". Dissertation. Technische Universität München. https://mediatum.ub.tum.de/doc/654165/654165.pdf
25. Reisinger J, Mauter G (2006) Aktiver Drehsteller und Verfahren zum Einstellen eines Drehmoments bei einem aktiven Drehsteller. DE102006052653A1, DE102006052653B4
26. Reisinger J et al (2006) Haptical feeling of rotary switches. In: Proceedings of the eurohaptics conference proceedings of eurohaptics 2006 (EHC2006) (July 3-6, 2006). Paris, France, pp 49–55
27. Schloske A (2010) Funktionale Sicherheit und deren praktische Umsetzung nach IEC 61508 und ISO CD 26262. In: Fachverband Elektronik-Design -FED-: Integration und Effizienz-notwendig und möglich : Konferenzband zur 18. FED-Konferenz "Elektronik-Design-Leiterplatten-Baugruppen". http://publica.fraunhofer.de/documents/N-151095.html
28. Seifi H, Zhang K, MacLean KE (2015) VibViz: organizing, visualizing and navigating vibration libraries. In: IEEE world haptics conference, WHC 2015, pp 254–259. https://doi.org/10.1109/WHC.2015.7177722
29. Sjöström C (2002) Non-visual haptic interaction design-guidelines and applications. Dissertation. Lund University. http://lup.lub.lu.se/record/464997
30. Strese M et al (2014) A haptic texture database for tool-mediated texture recognition and classification. In: 2014 IEEE international symposium on haptic, audio and visual environments and games, HAVE 2014-Proceedings, pp 118–123. https://doi.org/10.1109/HAVE.2014.6954342.
31. Tavakoli M et al (2008) Haptics for teleoperated surgical robotic systems. World Scientific Publishing. ISBN: 978-981-281-315-2
32. van Erp J (2005) Vibrotactile spatial acuity on the torso: effects of location and timing parameters. In: First joint eurohaptics conference and symposium on haptic interfaces for virtual environment and teleoperator systems. WHC 2005, pp 80–85. https://doi.org/10.1109/WHC.2005.144.
33. Wettels N et al (2008) Biomimetic tactile sensor array. In: Advanced robotics 22.8, pp 829–849. https://doi.org/10.1163/156855308X314533. https://doi.org/10.1163/156855308X314533
34. Zhou et al W (2014) Interaction-based dynamic measurement of haptic characteristicsof automotive control elements. In: Eurohaptics 2014 (submitted paper). Final contribution and bibliographic data is available from www.springerlink.com

Chapter 6
General System Structures

Alireza Abbasimoshaei and Thorsten A. Kern

Abstract Haptic systems exhibit several basic structures defined by the mechanical in- and outputs, commonly known as impedance or admittance system structures. This chapter describes these structures in open-loop and closed-loop variants and presents commercial realizations as well as common applications of these structures. Based on the different properties of the structures and the intended application, hints for the selection of a suitable structure are given.

When starting the design of haptic devices, the engineer has to deal with the general structures they can be composed of. Haptic devices of similar functionality can consist of very different modules. There are four big classes of possible system designs:

1. “open-loop admittance controlled systems”
2. “closed-loop admittance controlled systems”
3. “open-loop impedance controlled systems”
4. “closed-loop impedance controlled systems”.

6.1 Open-Loop and Closed-Loop Systems

An open-loop system is a system in which there is no feedback. Thus, the noise effects appear in output of the system. Moreover, the input has no reaction to different noises (Fig. 6.1a).

Christian Hatzfeld deceased before the publication of this book.

A. Abbasimoshaei (✉) · T. A. Kern
Hamburg University of Technology, EiÃƒÅ¸endorfer Str. 38, 21073 Hamburg, Germany
e-mail: al.abbasimoshaei@tuhh.de

T. A. Kern
e-mail: t.kern@hapticdevices.eu

T. A. Kern et al. (eds.), *Engineering Haptic Devices*, Springer Series on Touch and Haptic Systems, https://doi.org/10.1007/978-3-031-04536-3_6

But in closed-loop systems, the output influences the input, and the input is changed according to the last output. Thus, in these systems, there is a feedback signal that sends the last output to the input (Fig. 6.1b). So, this system can deal with the noise better.

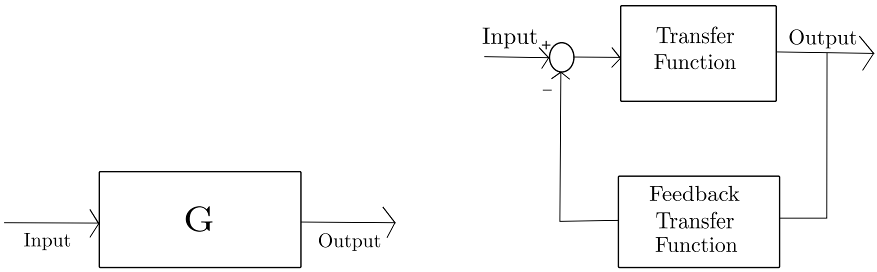

(a) $Open - loopsystemgeneralview$ (b) $Closed - loopsystemgeneralview$

Fig. 6.1 Different loop states

6.2 Open-Loop and Closed-Loop Systems Comparison

The most important difference between these two types of systems is in the usage of the error signal. In closed-loop systems, there is an ability to provide the minimum error. Thus, this system is more precise and independent of the noise. However, the open-loop systems are more simple and easy to implement. They are mostly used in a combination with closed-loop systems.

6.3 Impedance and Admittance Concept

The word impedance is coming from the word “impedire” which means “to hinder something”. Impedance is a kind of resistance in mechanical and electrical systems. In an electric circuit, the current is related to the number of electrons passing the circuit at a certain time. The voltage is the energy that helps them to go through it. But, the resistance in the circuit decreases the speed of the electrons. So when we need more voltage to reach a certain amount of current means that the resistance is bigger and when we reach a smaller current by a certain voltage means that there is a bigger resistance. Thus, resistance (impedance) is directly related to voltage and reverse current. This is the concept of electrical impedance. It is similar to a spring in which force is voltage, spring stiffness is impedance, and the spring displacement is current. In the spring, to reach a certain displacement, when you push it by more

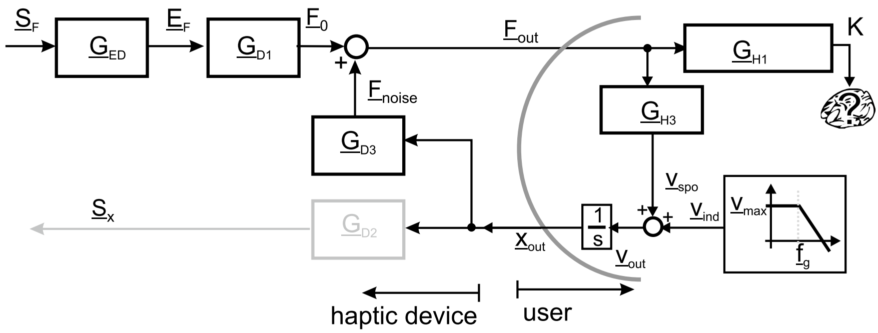

Fig. 6.2 Block-diagram of an open-loop impedance controlled haptic system

force means that the stiffness is bigger and vice versa. This stiffness is the mechanical impedance (Z) that is in the mechanical systems. It is the resistance of the system against force.

Therefore, Impedance controlled systems are based on the transfer characteristics of a mechanical impedance $\underline{Z} = \frac{\underline{F}}{\underline{v}}$ and are typical of the structure of many kinaesthetic devices. They generate a force as output and measure a position as input. Admittance controlled systems instead, are based on the definition of a mechanical admittance $\underline{Y} = \frac{\underline{v}}{\underline{F}}$, describing transfer characteristics with force-input and velocity-output. These systems generate a position change as haptic feedback and get a force reaction from the user as an input source. In the situation of a closed-loop controlled system, this force is measured and used for the correction of the position. This analysis can be regarded as analog in the case of torque and angle replacing force and position for rotary systems. Nevertheless, for readability purposes, the following descriptions concentrate on translational movements and devices only.

6.4 Open-Loop Impedance Controlled Devices

Open-loop impedance controlled systems are based on a quite simple structure (Fig. 6.2). A force signal $\underline{S}_F$ is transferred via a driver $\underline{G}_{ED}$ into a force-proportional energy form $\underline{E}_F$. This energy is then altered into the output force $\underline{F}_0$ by an actuator $\underline{G}_{D1}$. This output force interferes with a disturbing force $\underline{F}_{noise}$. This noise is a result of movements generated by the user $\underline{x}_{out}$ and the mechanical properties of the kinematic design $\underline{G}_{D3}$. Typically, such disturbing forces are friction and inertia. The sum of both forces is the actual output force $\underline{F}_{out}$ of the impedance controller system. Usually, there is an optional part of the system, a sensor $\underline{G}_{D2}$, which measures the movements and the actual position of the haptic system.

Examples: ***Universal Haptic Interfaces***

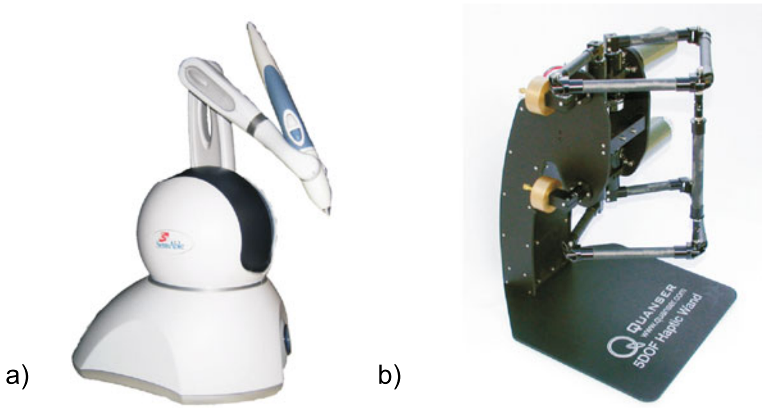

Fig. 6.3 Example of an open-loop impedance controlled system with **a** serial-kinematic (*Geomagic Touch*, *3D Systems geomagic Solutions*) and **b** parallel-kinematic (5 DOF Haptic Wand, *Quanser*) structure. Images courtesy of *3D Systems geomagic Solutions*, Morrisville, NC, USA and *Quanser*, Markham, Ontario, Canada, used with permission

Open-loop impedance controlled systems are the most frequently available devices on the market. As a result of their simple internal design, a few standard components can already be used to build a quite useful design with adequate haptic feedback, if at least some care is taken of the minimization of friction and masses. Among the cheapest designs available on the market today, the *PHANTOM Omni*, recently renamed to *geomagic Touch*, (Fig. 6.3a), connected via Fire-Wire to the control unit, is among the best known. It is frequently used in research projects and for the creative manipulation of 3D-data during modeling and design. In the higher-price segment there are numerous products, e.g. the devices of the company *Quanser* (Markham, Ontario, Canada). These devices are usually equipped with a real-time *MatLab*™(*The MathWorks*, Natick, MA, USA) based control station, adding some flexibility to the modifications of the internal data processing by the end customer. The doubled pantograph-kinematics of the "Haptic Wand" (Fig. 6.3b) allow force feedback in up to five degrees of freedom with three translations and two rotations. Although all these devices may be open-loop impedance controlled, the software usually includes simple dynamic models of the mechanical structures. This allows some compensation of inertial and frictional effects of the kinematics based on the continuous measurement of position and velocities.

6.5 Closed-Loop Impedance Controlled Devices

Closed-loop impedance controlled systems (Fig. 6.4) differ from open-loop impedance controlled systems in such a manner that the output force $\underline{F}_{\text{out}}$ is measured by a force sensor $\underline{G}_{\text{FSense}}$ and is used as a control variable to generate a difference value $\Delta\underline{S}_{\text{F}}$ with the nominal value. An additional component typically is a controller $\underline{G}_{\text{CD}}$ in the control path, optimizing the dynamic properties of the feedback loop. The closed-loop makes it possible to compensate the force $\underline{F}_{\text{noise}}$ resulting from the mechanics of the systems. This has two considerable advantages: On one hand, at idle state the system behaves in a much less frictional and more dynamic way compared to similar open-loop controlled systems. Additionally, as the closed-loop design allows some compensation of inertia and friction, the whole mechanical setup can be designed stiffer. But it has to be noted that part of the maximum output power of actuators will then be used to compensate the frictional force, which makes these devices slightly less powerful than an open-loop design.

Example: **Force Dimension *Delta Series***

Closed-loop impedance controlled systems are usually used in research projects and as special purpose machines. The delta-series of *ForceDimension* (Fig. 6.5) is one example, as it is a commercial system with the option to buy an impedance controlled version. In this variant, force sensors are integrated into the handle, able to measure interaction forces in the directions of the kinematic's degrees of freedom. Closed-loop impedance controlled systems are technologically challenging. On the one hand they have to comply with a minimum of friction and inertia, on the other hand, with little friction, the closed loop tends to become unstable, as an energy exchange between user and device may build up. This is why controllers, typically, monitor the passive behavior of the device. Additionally, the force sensor is a cost-intensive element. In case of the delta-device, the challenge to minimize moving masses has been faced by a parallel-kinematics design.

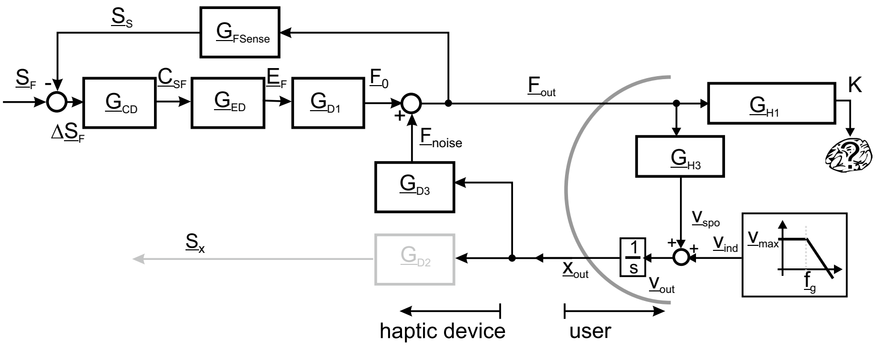

Fig. 6.4 Block-diagram of a closed-loop impedance controlled system with force-feedback

Fig. 6.5 Example of a parallel-kinematic closed-loop impedance controlled system (delta3, *Force Dimension*). Image courtesy of *Force Dimension*, Nyon, Switzerland, used with permission

6.6 Open-Loop Admittance Controlled

Open-loop admittance controlled systems (Fig. 6.6) provide a positional output. Proportionally to the input value $\underline{S}_{\mathrm{x}}$, a control chain with energy converter $\underline{G}_{\mathrm{ED}}$ and kinematics $\underline{G}_{\mathrm{D1}}$ provides a displacement $\underline{x}_0$. This displacement interferes with a disturbance variable $\underline{x}_{\mathrm{noise}}$ which is dependent on the mechanical properties of the kinematics $\underline{G}_{\mathrm{D3}}$ and a direct reaction to the user's input $\underline{F}_{\mathrm{out}}$. In practice an open-loop admittance controlled system typically shows a design which allows to neglect the influence of the disturbance variable. Another optional element of open-loop admittance controlled systems is the measurement of the output force with a force sensor $\underline{F}_{\mathrm{Sense}}$ without closing the control loop.

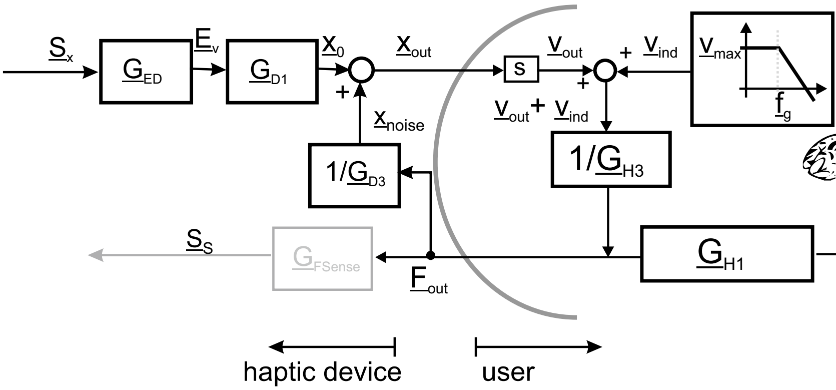

Fig. 6.6 Block-diagram of an open-loop admittance controlled haptic system

Example: Braille Devices

Open-loop admittance controlled systems are used especially in the area of tactile displays. Many tactile displays are based on pin arrays, meaning that they are generating spatially distributed information by lifting and lowering pins out of a matrix. These systems origins are Braille devices (Fig. 6.7) coding letters in a tactile, readable, embossed printing. For actuation of tactile pin-based displays a variety of actuators are used. There are electrodynamic, electromagnetic, thermal, pneumatic, hydraulic and piezoelectric actuators and even ultrasonic actuators with transfer media.

Fig. 6.7 Example of an open-loop admittance controlled system being a Braille row, image by RALF ROLETSCHEK, published under CC BY-SA 3.0

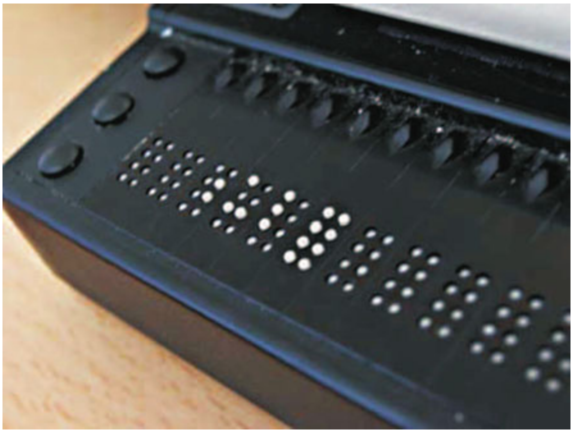

6.7 Closed-Loop Admittance Controlled Devices

Closed-loop admittance controlled devices (Fig. 6.8) provide a positional output and a force input to the controlling element identical to impedance controlled devices. The mandatory measurement of the output force $\underline{F}_{\text{out}}$ is used as control variable $\underline{S}_{\text{S}}$ for calculating the difference $\Delta\underline{S}_{\text{F}}$ with the commanding value $\underline{S}_{\text{F}}$. This difference is then fed through the controller $\underline{G}_{\text{CD}}$ into the control circuit. As a result, the displacement $\underline{x}_{\text{out}}$ is adjusted until an aspired force $\underline{F}_{\text{out}}$ is reached.

A variant of a closed-loop admittance controlled device is shown in Fig. 6.9. Closed-loop admittance controlled devices show considerable advantages for many applications requiring large stiffnesses. However, the force sensors $\underline{G}_{\text{FSense}}$ are quite complex and consequently expensive components, especially when there are numerous degrees of freedom to be controlled. As a variant, the system according to Fig. 6.9 does not use a sensor but just a force-proportional measure, e.g. a current, as control variable. When using e.g. a current with electrodynamic actuators, we can identify even the reaction of the user generating an induction as an additional velocity dependent value.

***Examples*: Universal Haptic Interfaces**

At present, closed-loop admittance controlled systems are the preferred approach to provide high stiffnesses with little loss in dynamic properties. The idea to haptically hide the actual mechanical impedance from the user by closing the control loop makes it possible to build serial kinematics with a large workspace. The FCS HapticMaster (Fig. 6.10a) is such one meter high system with three degrees of freedom and a force of up to 100 N. It includes a force sensor at its handle. The axes are controlled by self-locking actuators. The device's dynamics is impressive, despite its size. However, a damping has to be included in the controller for security reasons resulting in a limitation of bandwidth depending on the actual application.

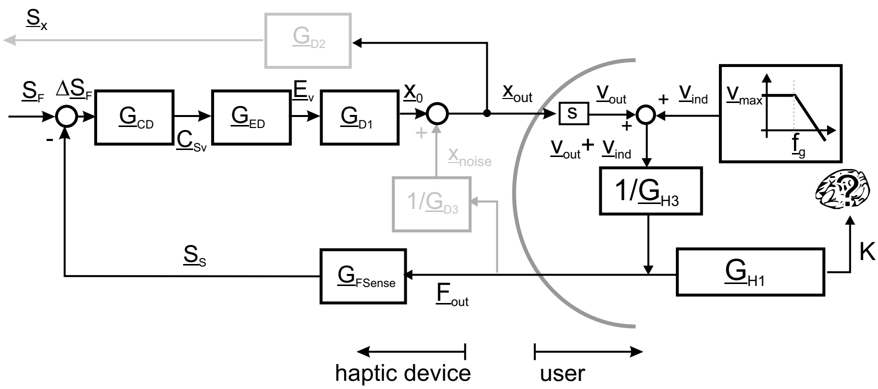

Fig. 6.8 Block-diagram of a closed-loop admittance controlled haptic system with force-feedback loop for control

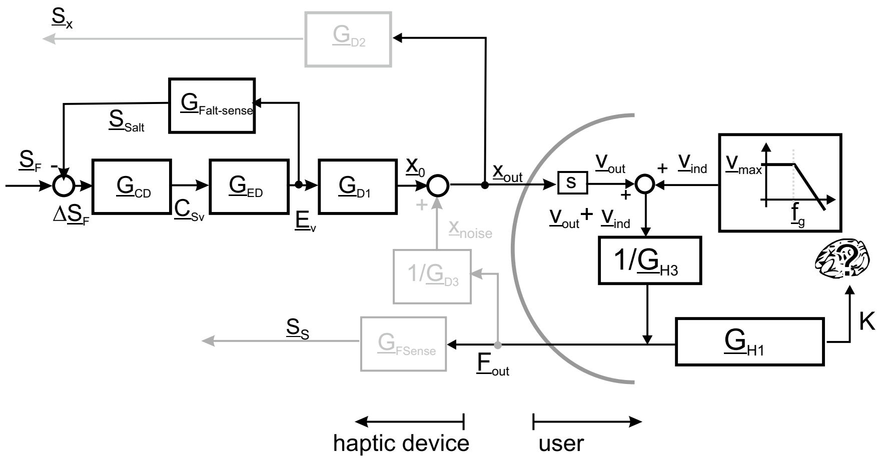

Fig. 6.9 Block-diagram of a closed-loop admittance controlled haptic system with a feedback loop measuring an internal force-proportional value

Fig. 6.10 Examples of closed-loop admittance controlled systems in variants with **a** direct force measurement (*HapticMaster*) and **b** measurement of the actual current (*Virtuose 6D35-45*). Images courtesy of *Moog FCS*, Nieuw-Vennep, the Netherlands and *Haption GmbH*, Aachen, Germany, used with permission

Realizations of the variant of closed-loop admittance controlled devices are the *Virtuose*-systems from *Haption* (Fig. 6.10b). In these devices the current is measured at electrodynamic electronic commutated actuators and fed back as a control value. The devices show impressive qualities for the display of hard contacts, but have limited capabilities in the simulation of soft interactions, e.g. with tissues. Therefore, the application area of such systems is mainly the area of professional simulation of assembly procedures for manufacture preparation.

6.8 Qualitative Comparison of the Internal Structures of Haptic Systems

As the haptic human-machine interaction is based on an impedance coupling, it is always the combination of action and reaction, be it via force or position, which has to be analyzed. In fact, without any knowledge about the internal structure of a device, it is impossible to find out whether the system is open-loop impedance controlled, closed-loop impedance controlled or closed-loop admittance controlled. With experience of the technological borders of the most important parameters like dynamics and maximum force, an engineer can make a well-founded assumption about the internal structure by simply using the device. But concerning the abstract interface of in- and output values, all the devices of the above three classes are absolutely identical to the user as well as to the controlling instance. Despite this fact the technical realizations of haptic systems differ widely in their concrete technical design, of course the parameters influencing this design have to be balanced against each other. Such parameters are:

- Number of components
- Maximum impedance to be achieved at slow motion
- Minimum impedance to be achieved at fast motion
- Force-resolution
- Impedance of mechanical components (e.g. inertia of kinematics)

These parameters and their mapping onto the technical designs are given qualitatively. In Fig. 6.11 the impedance generated by a device in absolute values and the impedance range covered may be one criterion for the performance of a device. Analyzing the systems according to this criterion shows that open-loop admittance controlled systems may have high impedance, which shows smaller variability in tighter borders. Closed-loop admittance controlled systems extend these borders by their ability to modulate the impedance due to the feedback loop. Depending on the design, closed-loop admittance controlled systems vary in the width of this modulation. In the lower area of possible, realizable impedances the open-loop impedance controlled systems follow. They stand out more by simplicity in their design than by large impedance ranges covered. In comparison to the closed-loop admittance controlled systems they gain some impedance width at the lower border of impedances. In order to be able to equally cover lower as well as higher impedances, the choice should be made of closed-loop impedance controlled systems.

Tactile devices

Normally, pure open-loop admittance controlled systems are suitable for tactile devices only, as, with tactile devices, usually there is no active feedback by the user to be measured. The haptic interaction is limited to tensions being coupled to the skin of the user's hands. Such devices show high internal impedance ($\underline{Z}_D$). The dynamics and the resolution concerning the displacement are very high.

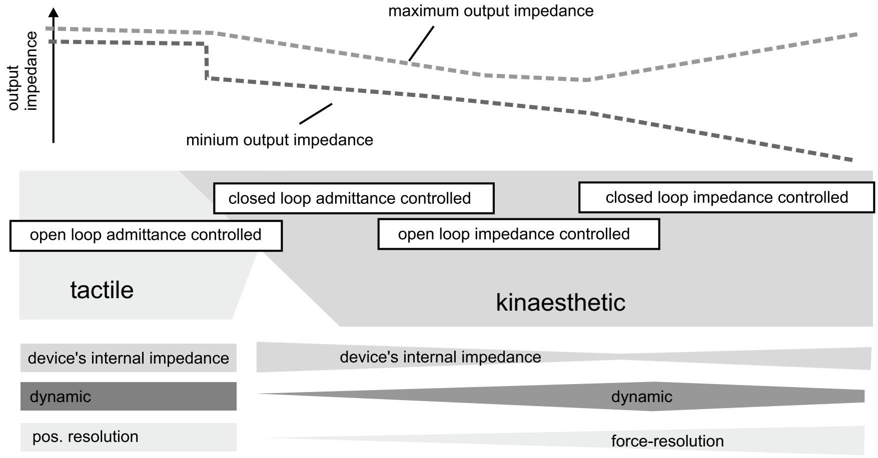

Fig. 6.11 Qualitative comparison of the application areas for different device-structures

Kinaesthetic devices

Can be built with systems allowing a modulation of the displayed impedances. The closed-loop admittance controlled systems excel due to the possibility to use mechanical components with high impedances. The dynamics of these systems are accordingly low (<100 Hz) and the force-resolution is, due to the typical frictions, not trivial when realized. Open-loop impedance controlled systems show a wider dynamic range due to the missing feedback loop with, at the same time, limited dynamic range. Only closed-loop impedance systems allow covering a wide impedance range from lowest to very high impedances, whereby with increasing requirements of force resolution the dynamics of the maximum velocities achieved by the control loop are limited and limitations of the measurement technology become noticeable.

The decision on the design of a haptic system has significant influence on the application range and vice versa. On one hand, it is necessary to identify the requirements to make such a decision. For this purpose, it is necessary to ask the right questions and to have an insight into possible technical realizations of single elements of the above structures. This is the general topic of the second part of this book. On the other hand, it is necessary to formulate an abstract system description of the device. An introduction of how to achieve this is given in the following section.

6.9 How to Choose a Suitable System Structure

The selection of a suitable system structure is one of the first steps in the design of a task-specific haptic systems. Based on the interaction analysis, one should have a sufficient insight into the intended interactions between system and user and should be

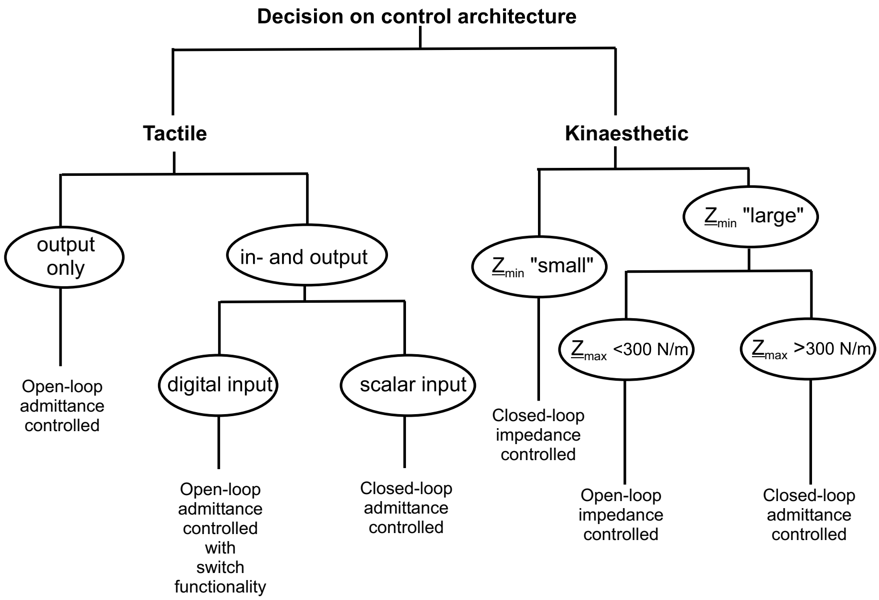

Fig. 6.12 Aid for the decision on the choice of the control structure

able to decide between a mainly tactile and mainly kinesthetic device structure. Based on further criteria like input and output capabilities and the mechanical impedance to be displayed, Fig. 6.12 gives an decision tree for the control structure.

Especially when the application will include an interaction in a multi-modal or virtual environment, further additions to the system structure could be wise to consider, since they promise a large technical simplification while maintaining haptic quality. This includes the approaches of Event-Based-Haptics as well as Pseudo-Haptics (Fig. 6.12).

Chapter 7
Control of Haptic Systems

Alireza Abbasimoshaei, Thomas Opitz, and Oliver Meckel

Abstract Control engineering is an important part for making the system more precise and provide the possibility for the system to reach the desired parameters. This chapter reviews some aspects of the control in haptic systems, including advanced forms of technical descriptions, system stability criteria and measures as well as the design of different control laws in a haptic system. A focus is set on the control of bilateral teleoperation systems including the derivation of control designs that guarantee stability as well as haptic transparency and the handling of time delay in the control loop. The chapter also includes an example for the consideration of thermal properties and non-ideal mechanics in the control of a linear stage made from an EC motor and a ball screw as well as an perception-orientated approach to haptic transparency intended to lower the technical requirements on the control and component design.

The control of technical systems aims a safe and reliable system behavior, and controllable system states. By the depiction as a *system* the analysis is put on an abstracted level which allows covering many different technical systems described by their fundamental physics. On this abstracted level a general analysis of closed loop control issues is possible using several methods and techniques. The resulting procedures are applicable to a various number of system classes. The main purpose of any depiction and analysis of control systems is to achieve high performance, safe system behavior and reliable processes. Of course this also holds for haptic systems. Here stable system behavior and high transparency are the most important control law design goals. The abstract description that shall be used for a closed loop con-

A. Abbasimoshaei (✉)
Hamburg University of Technology, Eißendorfer Str. 38, 21073 Hamburg, Germany
e-mail: al.abbasimoshaei@tuhh.de

T. Opitz
Landgraf-Philipps-Anlage 60a, 64283 Darmstadt, Germany
e-mail: thomas.opitz@opel.com

O. Meckel
Landgraf-Philipps-Anlage 60a, Edit Stein Str. 14, 97957 Wittighausen, Germany
e-mail: oliver.meckel@freenet.de

T. A. Kern et al. (eds.), *Engineering Haptic Devices*, Springer Series on Touch and Haptic Systems, https://doi.org/10.1007/978-3-031-04536-3_7

trol analysis starts with the mathematical formulation of the physical principles the system follows. As mentioned above, systems with different physical principles are covered up by similar mathematical methods. The depiction by differential equations or systems of differential equations proves widely usable for the formulation of various system behaviors. Herein analogies allow transforming this system behavior into the different technical context of a different system, provided that there exists a definite formulation of the system states that are of interest for the closed loop control analysis. The mathematical formulation of the physical principles of the system, also denoted as modeling, is followed by the system analysis including dynamic behavior and its characteristic. With this knowledge, a wide variety of design methods for control systems become applicable. Their main requirements are:

System stability The fundamental requirement for stability in any technical system is the main purpose for closed loop control design. Especially for haptic systems stability is the most important criteria in order to guarantee safe use of the device for the user.

Control quality Tracking behavior of the system states to demanded values every system is faced with external influences also denoted as disturbances which interfere with the demanded system inputs and disrupt the optimal system behavior. To compensate this negative influence a control system is designed.

Dynamic behavior and performance In addition to the first two issues, the need for a certain system dynamic completes this requirements-list. With a view to haptic systems the focus lays on the transmitted mechanical impedance, which determines the achievable grade of transparency.

Besides the quality of the control result tracking the demanded values, the system behavior within the range of changes from these demanded values is focused. Also the control effort which needs to achieve a certain control result is to be investigated. The major challenge for closed loop control law design for haptic systems and other engineering disciplines is to deal with different goals that are often in conflict with each other. Typically a gained solution is never an optimal one, rather a tradeoff between system requirements. In the following Sect. 7.1 basic knowledge of linear and non-linear system description will be given. Section 7.2 gives a short overview about system stability analysis. A recommendation for structuring the control law design process for haptic systems will be given in Sect. 7.3. Subsequently Sect. 7.4 focuses on common system descriptions for haptic systems and shows methods for designing control laws. Closing in Sect. 7.5 a conclusion will be presented.

7.1 System Description

A variety of description methods can be applied for the mathematical formulation of systems with different physical principles. One of the main distinctions is drawn between methods for the description of linear and nonlinear systems, summarized in the following paragraphs. The description based on Single-Input-Single-Output-Systems (SISO) in the LAPLACE domain was already discussed in Sect. 4.3.

7.1.1 Linear State Space Description

Besides the formulation of system characteristics through transfer functions, the description of systems using the state space representation in the time domain allows to deal with arbitrary linear systems too. For Single-Input-Single-Output-Systems, a description using an nth order ordinary differential equation is transformable into a set with n first order ordinary differential equations. In addition to the simplified usage of numerical algorithms for solving this set of differential equations, the major advantage is the applicability to Multi-Input-Multi-Output-Systems (MIMO). A correct and systematic model of their coupled system inputs, system states, and system outputs is comparably easy to achieve. On the contrary to the system description in the LAPLACE domain by transfer functions $G(s)$, the state space representation formulates the system behavior in the time domain. Two sets of equations are necessary for a complete state space system representation. These are denoted as the *system equation*

$$\dot{\mathbf{x}} = \mathbf{A}\mathbf{x} + \mathbf{B}\mathbf{u} \tag{7.1}$$

and the *output equation*

$$\mathbf{y} = \mathbf{C}\mathbf{x} + \mathbf{D}\mathbf{u}. \tag{7.2}$$

The vectors $\mathbf{u}$ and $\mathbf{y}$ describe the multidimensional system input respectively system output. Vector $\mathbf{x}$ denotes the inner system states.

As an example for state space representation the 2nd order mechanical oscillating system as shown in Fig. 7.1 is examined. Assuming the existence of time invariant parameters the description by a 2nd order differential equation is:

$$m\ddot{y} + d\dot{y} + ky = u \tag{7.3}$$

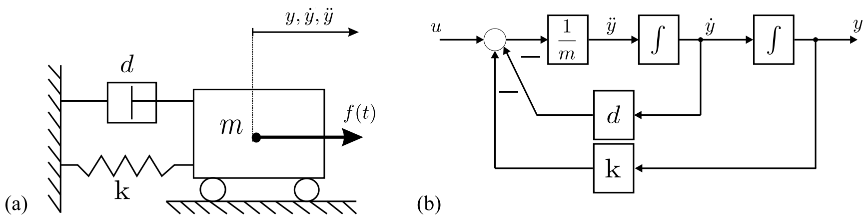

Fig. 7.1 Second order oscillator **a** scheme, **b** block diagram

The transformation of the 2nd order differential Eq. (7.3) into a set of two 1st order differential equation is done by choosing the integrator outputs as system states:

$$\begin{aligned} x_1 &= y \Rightarrow \dot{x}_1 = x_2 \\ x_2 &= \dot{y} \Rightarrow \dot{x}_2 = -\frac{k}{m}x_1 - \frac{d}{m}x_2 + \frac{1}{m}u \end{aligned} \tag{7.4}$$

Thus the system equation for the state space representation is as follows:

$$\begin{bmatrix} \dot{x}_1 \\ \dot{x}_2 \end{bmatrix} = \begin{bmatrix} 0 & 1 \\ -\frac{k}{m} & -\frac{d}{m} \end{bmatrix} \begin{bmatrix} x_1 \\ x_2 \end{bmatrix} + \begin{bmatrix} 0 \\ \frac{1}{m} \end{bmatrix} u \tag{7.5}$$

The general form of the system equation is:

$$\dot{\mathbf{x}} = \mathbf{A}\,\mathbf{x} + \mathbf{B}\,\mathbf{u} \tag{7.6}$$

This set of equations contains the *state space vector* $\mathbf{x}$. Its components describe all inner variables of the process that are of interest and that have not been examined explicitly using a formulation by transfer function. The system output is described by the output equation. In the given example as shown in Fig. 7.1 the system output y is equal to the inner state x_1

$$y = x_1 \tag{7.7}$$

which leads to the vector representation of

$$y = \begin{bmatrix} 1 & 0 \end{bmatrix} \begin{bmatrix} x_1 \\ x_2 \end{bmatrix} \tag{7.8}$$

The general form of the output equation is:

$$\mathbf{y} = \mathbf{C}\,\mathbf{x} + \mathbf{D}\,\mathbf{u} \tag{7.9}$$

which leads to the general state space representation that is applicable for Single or Multi Input and Output systems. The structure of this representation is depicted in Fig. 7.2. Although not mentioned in this example, matrix $\mathbf{D}$ denotes a direct feedthrough which occurs in systems whose output signals y are directly affected by the input signals u without any time delay. Thus these systems show a non-delayed step response. For further explanation on A, B, C and D [38] is recommended. Note that in many teleoperation applications, where long distances between master device and slave device are existing significant time delays occur.

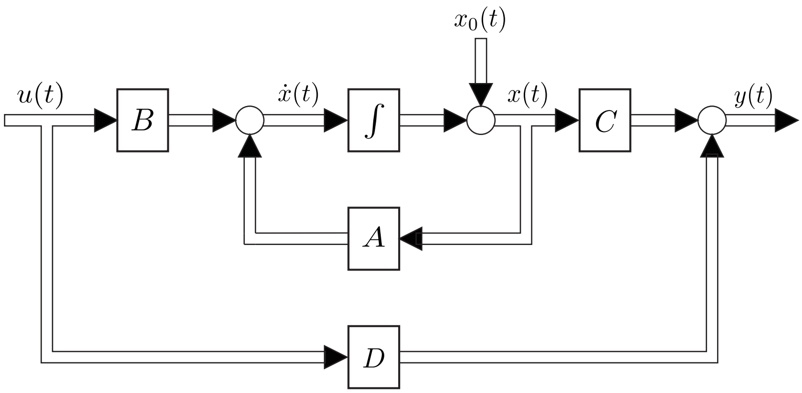

Fig. 7.2 State space description

7.1.2 Nonlinear System Description

A further challenge within the formulation of system behavior is to imply nonlinear effects, especially if a subsequent system analysis and classification is needed. Although a mathematical description of nonlinear system behavior might be found fast, the applicability of certain control design methods is an additional problem. Static non-linearities can be easily described by a serial coupling of a static non-linearity and linear dynamic device to be used as a summarized element for closed loop analysis. Herein two different models are differentiated. Figure 7.3 shows the block diagram consisting of a linear element with arbitrary subsystem dynamics followed by a static non-linearity.

This configuration also known as WIENER-model is described by

$$\tilde{u}(s) = \underline{G}(s) \cdot u(s)$$
$$y(s) = f(\tilde{u}(s)).$$

In comparison, Fig. 7.4 shows the configuration of the HAMMERSTEIN-*model* changing the order of the underlying static non-linearity and the linear dynamic subsystem.

The corresponding mathematical formulation of this model is described by

Fig. 7.3 WIENER-model

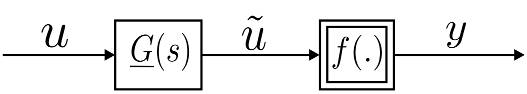

Fig. 7.4 HAMMERSTEIN-model

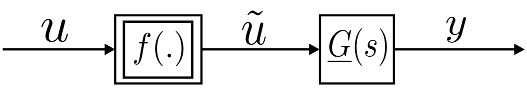

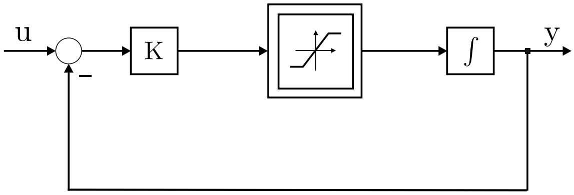

Fig. 7.5 System with internal saturation

$$\tilde{u}(s) = f(u(s))$$
$$y(s) = \underline{G}(s) \cdot \tilde{u}(s).$$

More complex structures appear as soon as the dynamic behavior of a system is affected by non-linearities. Figure 7.5 shows as an example a system with an internal saturation. For this configuration both models cannot be applied as easily as for static non-linearities. In particular if a system description is needed usable for certain methods of system analysis and investigation.

Typical examples for systems showing that kind of nonlinear behavior are electrical motors whose torque current characteristic is affected by saturation effects, and thus whose torque available for acceleration is limited to a maximum value.

This kind of system behavior is one example of how complicated the process of system modeling may become, as ordinary linear system description methods are not applicable to such a case. Nevertheless it is necessary to gain a system formulation in which the system behavior and the system stability can be investigated successfully. To achieve a system description taking various system non-linearities into account, it is recommended to set up a nonlinear state space descriptions. They offer a wide set of tools applicable to the following investigations. Deriving from Eqs. (7.1) and (7.2) the nonlinear system description for single respectively multi input and output systems is as follows:

$$\dot{\mathbf{x}} = \mathbf{f}(x, \mathbf{u}, t)$$
$$\mathbf{y} = \mathbf{g}(x, \mathbf{u}, t).$$

This state space description is most flexible to gain a usable mathematical formulation of a systems behavior consisting of static, dynamic and arbitrarily coupled non-linearities. In the following, these equations serve as a basis for the examples illustrating concepts of stability and control.

7.1.2.1 Common Nonlinearities in Control Systems

In general, a control system can be divided into four parts—plant, actuators, sensors, and controller—as shown in Fig. 7.6. Any of these units can be linear or nonlinear.

Due to centripetal and Coriolis forces, the plant or the physical robot is usually nonlinear. As this type of nonlinearity is continuous, it can be locally approximated

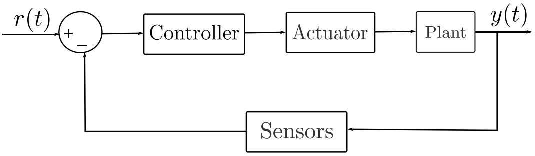

Fig. 7.6 Block diagram of a robotic system

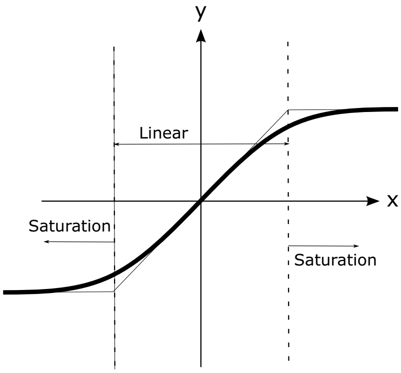

Fig. 7.7 The real and ideal saturation nonlinearity

to be a linear function. In many applications, since the operation range is small, this linearized model is effective and almost accurate.

On the other hand, some nonlinearities (hard nonlinearities) are discontinuous or hard for approximation. Regardless of the operation range, the magnitude and level of their effect on the system's performance define whether to consider them or not. In the following, some of the common nonlinearities will be discussed.

Saturation

In linear control, it is considered that increasing the input to a device results in a proportional increase of the output. However, in real systems, it goes somehow differently. For small inputs, the corresponding output is almost proportional, but when the input increases to a certain level and above that, the output will not increase proportionally or even it may not increase. In other words, the output stays around a maximum value and it can be said that the device is in saturation. The saturation is normally due to the physical limits of the device. For example, the properties of the magnet in a DC motor set the limit to its output torque, the supply voltage limits the output of an operational amplifier, and the length of a spring defines its force limit. The typical real saturation nonlinearity and the ideal saturation function are depicted in Fig. 7.7.

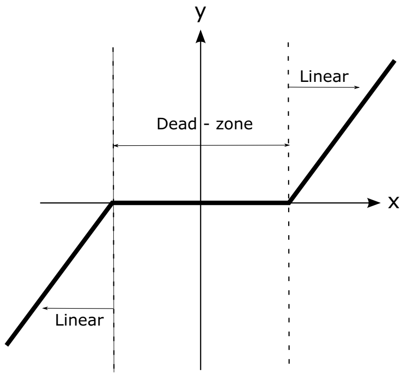

Fig. 7.8 Dead-zone nonlinearity

Since saturation nonlinearity does not change the phase of the input, one can consider it as a variable gain, where the gain decreases when the saturation occurs. The exact effect of saturation on the system performance is rather complicated. Consider a system that is unstable in the linear range, using saturation can limit the system signals, suppresses its divergence, and result in a sustained oscillation. However, it can slow down a linearly stable system since it is a variable and decreases gain as input increases.

Dead-zone

Many practical devices do not respond to the inputs below a certain level. When the input's value is bigger than a threshold, there would be output. The dead-zone nonlinearity can be shown as Fig. 7.8.

One common example is a diode. This electronic element does not pass any current if the input voltage is below its threshold (cut-in voltage), so the output current is almost zero, and if the voltage increases, the diode will behave like an ohmic resistance. Another example can be a DC motor that does not rotate until the input voltage exceeds a minimum level and the produced torque becomes bigger than the static friction on the motor's shaft.

Some possible effects of the dead-zone in a control system are reducing the positioning accuracy, introducing a limit cycle, leading to instability due to zero response in the dead-zone, and reducing chattering of an ideal relay.

Backlash

The clearance of mechanical gears or transmission system results in zero output for a certain range of input (the gap) when the direction of movement is reversed. Consider the gear shown in Fig. 7.9, due to several reasons such as rapid working and

Fig. 7.9 Backlash in gear and the input-output relation

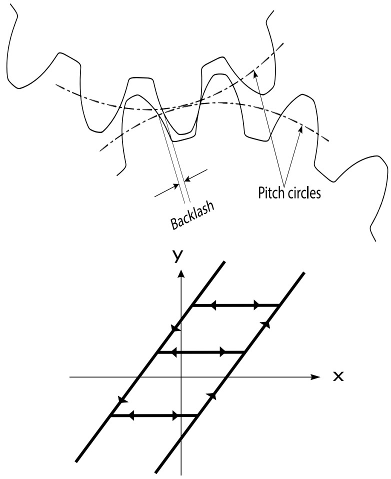

Fig. 7.10 Ideal relay

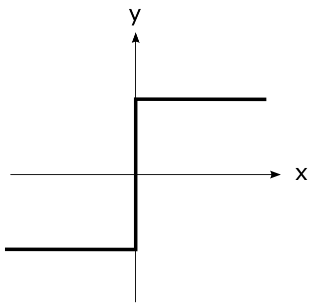

unavoidable manufacturing error, there exists backlash. When the rotating direction of the driving gear changes, the driven gear does not rotate at all until the driving gear makes contact with it. During this period, the rotation of the driven gear is zero. After the establishment of contact, the driven gear will follow the rotation of the driver. Consequently, if the driver performs a periodic rotation, the driven gear's rotation will be a closed path as shown in Fig. 7.9.

The most important characteristic of backlash is its multi-valued nature. It means that the output depends both on the current input value and on its past values. Due to multi-valued nonlinearities like backlash, the system will store energy that can lead to chattering or sustained oscillation or even instability.

Relay or on-off nonlinearity

Consider a saturation with zero linearity range and vertical slope; it is called an ideal relay where the output could be maximum positive, off, or maximum negative (Fig. 7.10).

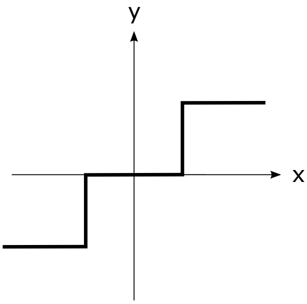

Fig. 7.11 Practical relay

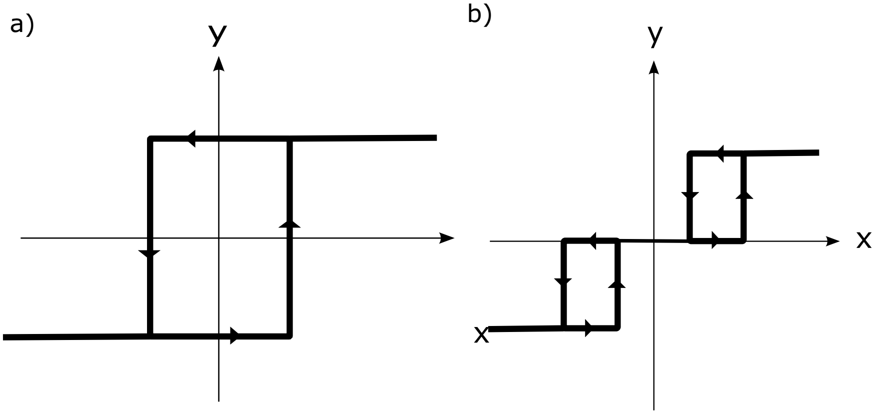

Fig. 7.12 Relay output: **a** no dead-zone **b** significant dead-zone

An example is the temperature control of a domestic heating system using a thermostat. The heating system turns on whenever the temperature is below the set-point and turns off when it is above that. Because of its discontinuous nature, the system will oscillate or chatter around the set-point with high frequency. To reduce the chattering frequency, as shown in Fig. 7.11, practical relays have a definite amount of dead-zone.

Due to the fact that a larger input is needed to close a relay, so, depending on their dead-zone range, a relay can perform as shown in Fig. 7.12.

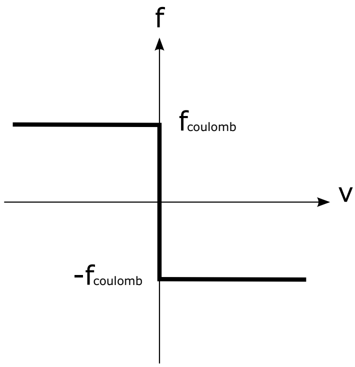

Fig. 7.13 Coulomb friction force as a function of velocity

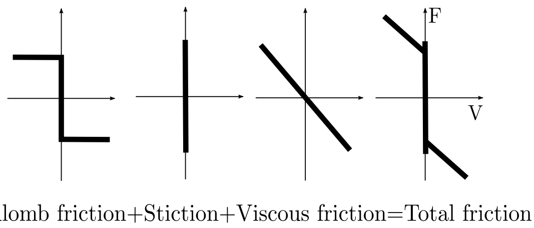

Fig. 7.14 Friction model considering coulomb, stiction, and viscous frictions

Friction

When two mechanical surfaces are sliding or trying to slide, there is a friction force in the opposite direction of moving. The special case is static or coulomb friction. Considering the relative velocity between the two surfaces as the input, the resulting force or the output is shown in Fig. 7.13.

In practice, where commonly there exist stiction and viscous damping as well, the output can be depicted as Fig. 7.14. As shown in this figure stiction force is bigger than coulomb force which makes the total friction a complex nonlinearity.

Dealing with these nonlinearities requires a more sophisticated controller design where two of the well-known and highly efficient control techniques are adaptive control and Sliding Mode Control.

7.1.2.2 Adaptive and Sliding Mode Control (SMC) for Controlling Nonlinearities

Almost all modeled systems contain uncertainties due to intended simplifications such as unmodeled high-order dynamics or linearization of a nonlinear phenomenon, or inaccuracy of the system's parameter. Neglecting the uncertainty results in an adverse effect on the control system. Hence, they should be considered in the controller design. Since linear controller's performance are limited by, for example, waterbed effect, it is needed to deal with nonlinearities by nonlinear controllers. Two well-known and effective approaches to take care of nonlinearity and uncertainty are sliding mode control (SMC) and adaptive control. These two methods will be discussed in the following sections.

Sliding Mode Control

Sliding Mode Control (SMC) is a nonlinear control technique, which presents desirable characteristics such as accuracy, robustness, and fast dynamic response. The design of this controller is done in two parts:

1. A sliding surface, which fulfills the design specifications.
2. A controller law to move the system's states to the designed surface.

This design procedure brings two main advantages: the possibility of having tailored dynamic response, and robustness to nonlinearity, uncertainty, and disturbance. In other words, SMC is capable of controlling a nonlinear process suffering from external disturbance and model uncertainty. For designing the SMC system, a system model could be considered as a nonlinear SISO system as follow:

$$\dot{\mathrm{x}} = \mathrm{f(x, u)} + \mathrm{b(x, t)}u \tag{7.10}$$

$$\mathrm{y} = \mathrm{g(x, t)} \tag{7.11}$$

where u is the scalar input, y is the scalar output, and $x \in R^n$ is the state vector. The ideal controller is the one that y tracks y_d(desired output) and the tracking error $(e = y_d - y)$ tends to a small vicinity of zero after a finite time (transient response).

To design a SMC, the first step is defining the sliding surface as σ(t) in a way that zero error results in $\sigma(t) = 0$, and $\sigma(t)\dot{\sigma}(t) < 0$ fulfils for the rest of the time. A common form of σ(t), which depends on only one parameter is as:

$$\sigma(\mathbf{t}) = (\frac{d}{dt} + \lambda)^{n-1}e(t) \tag{7.12}$$

where $\lambda > 0$ is a constant. For example, in the case of n=3 which is the order of the controller, the sliding surface is:

$$\sigma = \ddot{\mathrm{e}} + 2\lambda\dot{\mathrm{e}} + \lambda^2 e \tag{7.13}$$

The second step is defining a control law that steers the system's states onto the sliding surface, which makes $\sigma = 0$ in finite time. There are some approaches for defining the control law. The two most common ones are standard or the first-order control law and the second-order one will be discussed in the next sections. There is no dependency on the selected approach and SMC allows designing the controller based on an estimation of the original system's dynamics.

First-order SMC

The following formula is one of the most simple SMC controller models. In this model, the control input is a discontinuous function of σ:

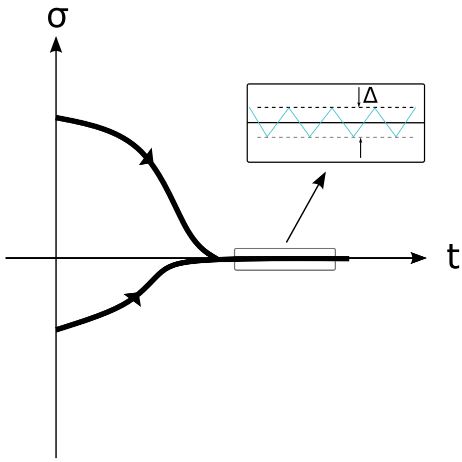

Fig. 7.15 Typical time response of σ variable

$$u = -Usgn(\sigma) \tag{7.14}$$

where sgn(.) is the signum function and $U > 0$ is a sufficiently large constant. Therefore, the control signal is:

$$u = \begin{cases} -U & \sigma < 0 \\ U & \sigma > 0 \end{cases} \tag{7.15}$$

As a result, the σ variable would change typically as shown in Fig. 7.15.
As seen in the Fig. 7.15, the system would do high-frequency chattering in a small vicinity of the desired surface rather than sliding on it. This high-frequency switching could cause oscillation especially in the control of the mechanical systems.

Since this chattering phenomenon is because of the discontinuous sign function, smoothed continuous approximation of it could be rather effective. Two common examples are:

$$sat \quad u = -Usat(\sigma, \varepsilon) = -U\frac{\sigma}{\sigma + \varepsilon} \quad \varepsilon > 0\&\varepsilon \approx 0 \tag{7.16}$$

$$tanh \quad u = -Utanh(\frac{\sigma}{\varepsilon}) \quad \varepsilon > 0\&\varepsilon \approx 0 \tag{7.17}$$

A comparison of the smoothed saturation and the sign function is depicted in Fig. 7.16.
However, smoothing the sign function will result in increasing the tracking error and decreasing the robustness. Another solution could be the usage of the higher-order SMC.

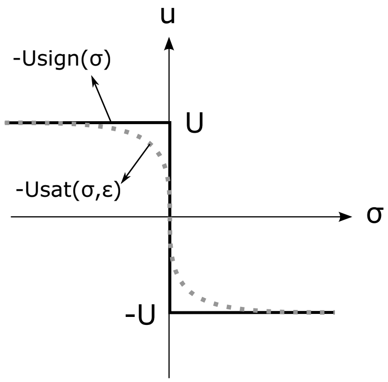

Fig. 7.16 Comparison of sign function and its alternative, smoothed saturation

Second-order SMC

Second-order SMC is capable of the complete elimination of the chattering phenomenon without sacrificing robustness. The first-order SMC steers the system's states in a way that $\sigma(t) = 0$ when the error is zero, while the second-order SMC also forces the derivative of $\sigma(t)$ goes to zero. There exist many well-known functions to generate a second-order sliding mode law such as integral operation sliding surface, PID surface, and super-twisting algorithm. As an example, the super-twisting second-order SMC can be defined as:

$$\begin{cases} u = -V\sqrt{|\sigma|}sgn(\sigma) + w \\ \dot{w} = -Wsgn(\sigma) \end{cases} \tag{7.18}$$

An effective tuning guide for the parameters are:

$$V = \sqrt{U} \quad = 1.1U \tag{7.19}$$

where $U > 0$ is a constant that should be taken sufficiently large. Considering the comparison of the linear PI controller and the super-twisting second-order SMC depicted in Fig. 7.17. This algorithm can be seen as the nonlinear PI controller. It is obvious that the produced control signal by the second-order SMC is continuous. Therefore, the system performs with no chattering.

Adaptive Control

Another approach to the control of a nonlinear system that can improve the system output with uncertainty is the adaptive control method. The basis of this approach is estimating the system's parameters or uncertainties based on measured signals of the system. Therefore, adaptive control lays down in the field of nonlinear control.

This method is useful for a system experiencing a wide range of parameter changes, such as a robotic manipulator designed to manipulate loads of various

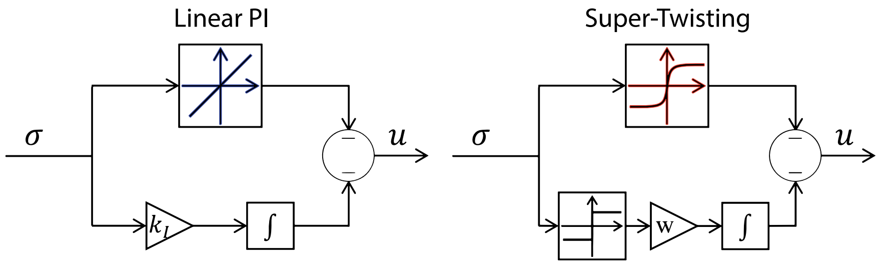

Fig. 7.17 Block diagram of a linear PI controller and the super-twisting SMC

weights. Adaptive control is mainly used in systems where there exists nonlinearity or the variation and uncertainty of its parameters are inevitable. The most important requirement of adaptive control is that parameter adaptation should be done significantly faster than the change of the system parameters. However, in practice, this requirement is often fulfilled since a rapid change of a parameter means that the modeling is not complete and should consider this dynamic behavior theoretically.

There exists another method of controlling nonlinearity and uncertainty, which is the robust control method. Although both methods deal with nonlinearity, there are some differences. In the case of slowly varying parameters, the adaptive control performance is significantly better than the robust control method. The reason is that the adaptive control estimates the varying parameters and redesigns the controller according to these changes. Thus, its performance improves over time, while the robust control method is conservative with consistent performance. Moreover, the robust control requires an estimation of the nonlinearity or uncertainty, while adaptive control can be designed with little or no prior estimation. However, on the other hand, comparing to adaptive control, robust control is capable of dealing with disturbances, fast varying parameters, and unmodeled dynamics. Therefore, a combination of these two methods could be a good solution especially when there is an external part such as rehabilitation systems [1].

As it is mentioned, the superiority of the adaptive control is that the controller learns and adjusts its parameters to enhance the tracking performance. There exist two main methods for this learning and adjustment process: model-reference adaptive control (MRAC) and self-tuning controller (STC). In this book, a brief explanation of the methods is presented to provide an overview of the tools that can be used in the field of haptic.

Model-Reference Adaptive Control

In this method, it is assumed that the structure of the plant's model is known, but some parameters are unknown. A reference model defines the ideal response of the system and the adaptation law adjusts the controller parameters to respond like the reference model (Fig. 7.18).

The reference model should fulfill the expected performance of the system in both time and frequency domain characteristics. Furthermore, by considering the known

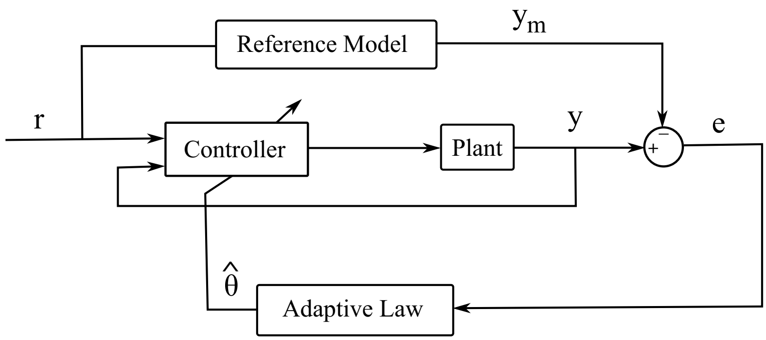

Fig. 7.18 Model-Reference Adaptive Control structure

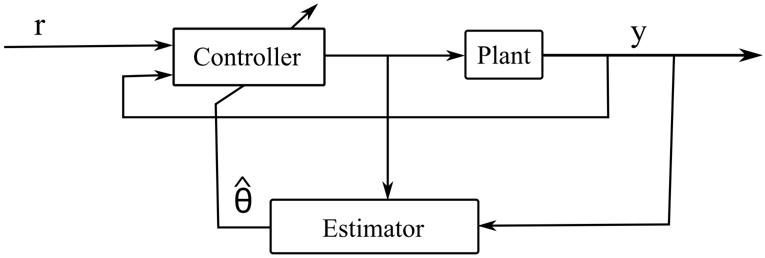

Fig. 7.19 Self-Tuning Controller structure

structure of the plant, its order, and its relative degree, the expected performance could be achievable. In addition, the designed controller should be capable of providing the reference model's performance when the plant's model is exactly known.

Self-Tuning Controller (STC)

In the pole-placement method, where the controller is designed based on the plant's parameters, its parameters could be estimated by using the input-output of the plant (Fig. 7.19). Then, the controller parameters are updated to control the estimated plant.

The adaptation process in this method is different from the MRAC method. MRAC tries to adjust the controller parameters to make the system's response as close as possible to the reference model. However, STC estimates the plant's parameters and adjusts the controller's parameters based on the estimated plant.

Here, the procedure of designing an adaptive controller is explained through an example. In [1], an adaptive law was designed for a sliding mode controlled wearable hand rehabilitation robot to overcome the stiffness variation of the patients' hand. Using the Lyapunov function, not only the stability of the system is guaranteed but also the adaptive law is derived. The Lyapunov function was considered as:

$$V = \frac{1}{2}\sigma^2 + \frac{1}{2}\widetilde{F}^2 \tag{7.20}$$

where σ is the sliding surface and $\widetilde{F} = F_{int} - \widetilde{F}$ is the estimation error of the user's interaction force. Assuming that F_{int} changes slowly, the adaptive law and adaptive controller equation were derived based on the stability criteria of the Lyapunov method, or $\dot{V}$ <0.

7.2 System Stability

As mentioned in above one of the most important goals of the control design is the stabilization of systems or processes during their life cycle, while operative or disabled. Due to the close coupling of haptic systems to a human user via a human machine interface, safety becomes most relevant. Consequently the focus of this chapter lies on system stability and its analysis by using certain methods applicable to many systems. It has to resemble the system's behavior correctly, and has to be aligned with applied investigation technique. For the investigation of systems, subsystems, closed looped systems, and single or multi input output systems, a wide variety of different methods exists. The most important ones shall be introduced in this chapter.

7.2.1 Analysis of Linear System Stability

The stability analysis of linear time invariant systems is easily done by the investigation of the system poles or roots derived from the eigenvalue calculation of the system transfer function $G(s)$. The decisive factor is the sign of the real part of these system poles. A negative sign in this real part indicates a stable eigenvalue; a positive sign denotes an unstable eigenvalue. The correspondence to the system stability becomes obvious while looking at the homogenous part of the solution of the ordinary differential equation describing the system behavior. As example a system shall be described by

$$T\dot{y}(t) + y(t) = Ku(t). \tag{7.21}$$

The homogenous part of the solution $y(t)$ is derived using

$$y_h = e^{\lambda t} \quad \text{with } \lambda = -\frac{1}{T}. \tag{7.22}$$

As it can be seen clearly, the pole $\lambda = -\frac{1}{T}$ has a negative sign only if the time constant T has a positive sign. In this case the homogenous part of $y(t)$ disappears for $t \to \infty$, while it rises beyond each limit exponentially if the pole $\lambda = -\frac{1}{T}$ is unstable. This section will not deal with the basic theoretical background of linear system stability, as these are basics of control theory. Focus of this section is the application of certain stability analysis methods. Herein it will be distinguished between methods for a direct stability analysis of a system or subsystem and techniques of the closed looped stability analysis. For direct stability analysis of linear system the investigation of the poles placement in the complex plane is fundamental. Besides the explicit calculation of the system poles or eigenvalues the ROUTH- HURWITZ *criterion* offers to determine the system stability and the system pole placement with explicit calculation. In many cases this simplifies the stability analysis. For the analysis of the closed loop stability the determination of the closed loop pole placement is also a possible approach. Additional methods leave room for further design aspects and extend the basic stability analysis. Well-known examples of such techniques are

- Root locus method
- NYQUIST's stability criterion.

The applicability of both methods will be discussed in the following without looking at the exact derivation.

7.2.1.1 Root Locus Method

The root locus offers the opportunity to investigate the pole placement in the complex plane depending on certain invariant system parameters. As example of invariant system parameters changing time constants or variable system gains might occur. The gain of the open loop is often of interest within the root locus method for closed loop stability analysis and control design. In Eq. (7.23) G_R denotes the transfer function of the controller, G_S describes the behavior of the system to be controlled.

$$-G_o = G_R G_S \tag{7.23}$$

Using the root locus method, it is possible to apply predefined sketching rules whenever the dependency of the closed loop pole placement on the open loop gain K is of interest. The closed loop transfer function G_g is depicted by Eq. (7.24)

$$G_g = \frac{G_R G_S}{1 + G_R G_S} \tag{7.24}$$

As an example an integrator system with a second order delay (IT_2) described by Eq. (7.25)

$$G_S = \frac{1}{s} \cdot \frac{1}{1+s} \cdot \frac{1}{1+4s} \tag{7.25}$$

is examined. The control transfer function is $G_R = K_R$. Thus we find as open loop transfer function

$$-G_o = G_R G_S = \frac{K_R}{s(1+s)(1+4s)}. \tag{7.26}$$

Fig. 7.20 IT_2 root locus

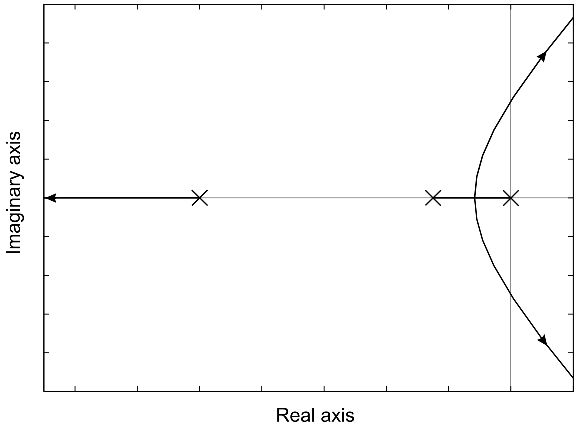

Using the sketching rules which can be found in various examples in literature [37], [48], the root locus graph as shown in Fig. 7.20 is derived. The graph indicates, that small gains K_R lead to a stable closed loop system since all roots have a negative real part. A rising K_R leads to two of the roots crossing the imaginary axis and the closed loop system becomes unstable. This simplified example proves that this method can easily be integrated in a control design process, as it delivers a stability analysis of the closed loop system only processing an examination on the open loop system. This issue is also one of the advantages of the NYQUIST stability criterion. Additionally the definition of the open loop system is sufficient to derive a stability analysis of the system in a closed loop arrangement.

7.2.1.2 NYQUIST's Stability Criterion

This section will concentrate on the simplified NYQUIST stability criterion investigating the open loop frequency response described by

$$-G_o(j\omega) = G_R(j\omega)G_S(j\omega).$$

The NYQUIST stability criterion is based on the characteristic correspondence to amplitude and phase of the frequency response. As example we use the already introduced IT_2-system controlled by a proportional controller $G_R = K_R$. The BODE plot of the frequency response is shown in Fig. 7.21: The stability condition which has to be met is given by the phase of the open loop frequency response, with $\varphi(\omega) > -180°$ in case of the frequency response's amplitude $A(\omega)$ being above 0 dB. As shown in Fig. 7.21, the choice of the controller gain K_R transfers the amplitude graph of the open loop frequency response vertically without affecting the phase of the open loop frequency response. For most applications the specific requirement of a sufficient phase margin φ_R is compulsory. The resulting phase margin is also shown

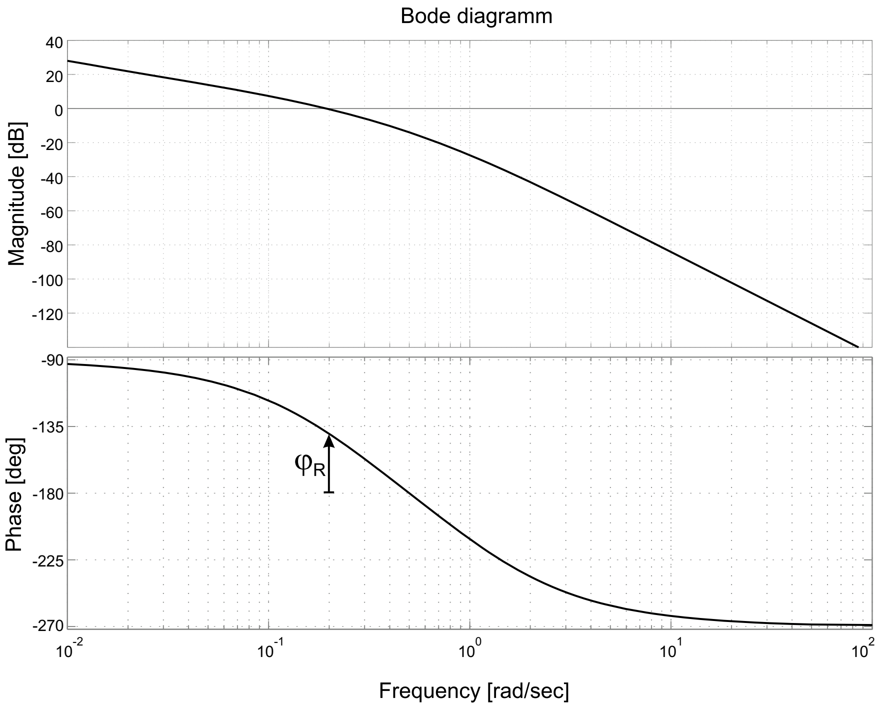

Fig. 7.21 IT_2 frequency response

in Fig. 7.21. All such requirements have to be met in the closed control loop and must be determined to choose the correct control design method. In this simplified example the examined amplitude and phase of the open loop frequency response is dependent on the proportional controller gain K_R, which is sufficient to establish system stability including a certain phase margin. More complex control structures such as PI, $PIDT_n$ or Lead Lag extend the possibilities for control design to meet further requirements.

This section showed the basic principle of the simplified NYQUIST criterion being applicable to stable open loop systems. For an investigation of unstable open loop systems the general form of the NYQUIST criterion must be used, which itself is not introduced in this book. For this basic knowledge it is recommended to consult [37, 48].

7.2.2 Analysis of Non-linear System Stability

The application of all previous approaches for the analysis of system stability is limited to linear time invariant systems. Nearly all real systems show nonlinear effects or consist of nonlinear subsystems. One approach to deal with these nonlinear systems is the linearization in a fixed working point. All further investigations are focused on this point, and the application of the previously presented methods becomes possible. If these methods are not sufficient, extended techniques for stability analysis of nonlinear systems must be applied. The following are examples of representing completely different approaches:

- Principle of the harmonic balance
- Phase plane analysis
- POPOV criterion and circle criterion
- LYAPUNOV's direct method
- System passivity analysis.

Without dealing with the mathematical background or the exact proof the principles and the application of chosen techniques shall be demonstrated. At this point a complete explanation of this topic is too extensive due to the wide variety of the underlying methods. For further detailed explanation, [18–20, 34, 45, 49] are recommended.

7.2.2.1 POPOV criterion

As an preliminary example the analysis of closed loop systems can be done applying the POPOV criterion respectively the circle criterion. Figure 7.22 shows the block diagram of the corresponding closed loop structure of the system that is going to be analyzed.

The bock diagram consists of a linear transfer function $\underline{G}(s)$ with arbitrary dynamics and a static non-linearity $f(.)$. The state space formulation of $\underline{G}(s)$ is as follows:

$$\begin{aligned}\dot{\mathbf{x}} &= \mathbf{A}\mathbf{x} + \mathbf{B}\tilde{u}\\ \mathbf{y} &= \mathbf{C}\mathbf{x}\end{aligned}$$

Thus we find for the closed loop system description:

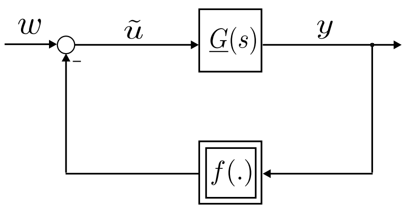

Fig. 7.22 Nonlinear closed loop system

Fig. 7.23 Sector condition

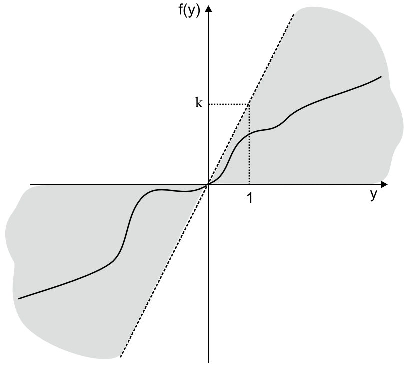

$$\dot{\mathbf{x}} = \mathbf{A}\mathbf{x} - \mathbf{B}f(y)$$
$$\mathbf{y} = \mathbf{C}\mathbf{x}.$$

In case that $f(y) = k \cdot y$ this nonlinear system is reduced to linear system whose stability can be examined with the evaluation of the system's eigenvalues. An arbitrary nonlinear function $f(y)$ the complexity of the problem is extended. So first constraint on $f(y)$ is that it exists only in a determined sector that is limited by a straight line through the origin with a gradient k. Figure 7.23 shows an equivalent example for the nonlinear function $f(y)$. This constraint is depicted by the following equation:

$$0 \leq f(y) \leq ky.$$

The POPOV criterion provides an intuitive handling for the stability analysis of the presented example. The system is asymptotically idle state ($\dot{\mathbf{x}} = \mathbf{x} = \mathbf{0}$) stable if:

- the linear subsystem $\underline{G}(s)$ is asymptotically stable and fully controllable,
- the nonlinear function meets the presented sector condition as shown in Fig. 7.23,
- for an arbitrarily small number $\rho \geq 0$ there exists a positive number α, so that the following inequality is satisfied:

$$\forall \omega \geq 0 \quad \mathrm{Re}[(1 + j\alpha\omega)\underline{G}(j\omega)] + \frac{1}{k} \geq \rho \tag{7.27}$$

Equation (7.27) formulates the condition also know as POPOV *inequality*. With

$$\underline{G}(j\omega) = \mathrm{Re}(\underline{G}(j\omega)) + j\mathrm{Im}(\underline{G}(j\omega)) \tag{7.28}$$

Fig. 7.24 POPOV plot

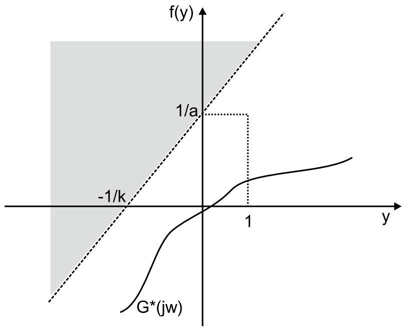

Eq. (7.27) leads to

$$\mathrm{Re}(\underline{G}(j\omega)) - \alpha\omega\mathrm{Im}(\underline{G}(j\omega)) + \frac{1}{k} \geq \rho \tag{7.29}$$

With an additional definition of a related transfer function

$$G^* = \mathrm{Re}(\underline{G}(j\omega)) + j\omega\mathrm{Im}(\underline{G}(j\omega)) \tag{7.30}$$

Eq. (7.29) states that the plot in the complex plane of $\underline{G}^*$, the so called POPOV *plot*, has to be located in a sector with an upper limit described by $y = \frac{1}{\alpha}(x + \frac{1}{k})$. Figure 7.24 shows an example for the POPOV plot of a system in the complex plane constrained by the sector condition. The close relation to the NYQUIST criterion for the stability analysis of linear systems becomes quite obvious here. While the NYQUIST criterion examines the plot of $\underline{G}(j\omega)$ referred to the critical point (-1|0), the location of the POPOV plot is checked for a sector condition defined by a straight line limit.

The application of the POPOV criterion has the excelling advantage, that it is possible to gain a result out of the stability analysis without an exact formulation of the non-linearity within the system. All constraints for the nonlinear subsystem are restraint to the sector condition and the condition to have memoryless transfer behavior. The most complicated aspect within this kind of analysis is how to formulate the considered system structure in a way, that the POPOV criterion can be applied. For completeness the circle criterion shall be mentioned whose sector condition is not represented by a straight line, rather

$$k_1 \leq \frac{f(y)}{y} \leq k_2.$$

defines the new sector condition. For additional explanation on these constraints and the application of the circle criterion it is recommended to consider [34, 45, 49].

7.2.2.2 LYAPUNOV's Direct Method

As second example for stability analysis of nonlinear systems the direct method by LYAPUNOV is introduced. The basic principle is that if both linear and nonlinear stable systems tend to a stable steady state, the complete system energy has to be dissipated continuously. Thus it is possible to gain result from stability analysis while verifying the characteristics of the function representing the state of energy in the system. LYAPUNOV's direct method generalizes this approach to evaluate the system energy by the generation of an artificial scalar function which can describe not only the energy stored within the considered dynamic system, further it is used as an energy like function of a dissipative system. These kinds of functions are called LYAPUNOV functions $V(x)$. For the examination of the system stability the already mentioned state space description of a nonlinear system is used:

$$\dot{\mathrm{x}} = \mathrm{f}(\mathrm{x}, \mathrm{u}, t)$$
$$\mathrm{y} = \mathrm{g}(\mathrm{x}, \mathrm{u}, t).$$

By the definition of LYAPUNOV's theorem the equilibrium at the phase plane origin $\dot{\mathbf{x}} = \mathbf{x} = \mathbf{0}$ is globally, asymptotically stable if

1. a positive definite scalar function $V(\mathbf{x})$ with $\mathbf{x}$ as the system state vector exists, meaning that $V(\mathbf{0}) = 0$ and $V(\mathbf{x}) > 0 \,\forall\, \mathbf{x} \neq \mathbf{0}$,
2. $\dot{V}$ is negative definite, meaning $\dot{V}(\mathbf{x}) \leq 0$,
3. $V(\mathbf{x})$ is not limited, meaning $V(\mathbf{x}) \to \infty$ as $\| x \| \to \infty$.

If these conditions are met in a bounded area at the origin only, the system is locally asymptotically stable.

As a clarifying example the following nonlinear first order system

$$\dot{x} + fx = 0 \tag{7.31}$$

is evaluated. Herein $f(x)$ denotes any continuous function of the same sign as its scalar argument x so that $x \cdot fx > 0$ and $f(0) = 0$. Applying this constraints a LYAPUNOV function candidate can be found described by

$$V = x^2. \tag{7.32}$$

The time derivative of $V(x)$ provides

$$\dot{V} = 2x\dot{x} = -2xf(x). \tag{7.33}$$

Due to the assumed characteristics of $f(x)$ all conditions of LYAPUNOV's direct method are satisfied thus the system has globally asymptotically stable equilibrium at the origin. Although the exact function $f(x)$ is not known, the fact that it exists in the first and third quadrant only is sufficient for $\dot{V}(x)$ to be negative definite. As second example a multi-input multi-output system is examined depicted by its state space formulation

$$\begin{aligned}\dot{x}_1 &= x_2 - x_1(x_1^2 + x_2^2)\\ \dot{x}_2 &= -x_1 - x_2(x_1^2 + x_2^2).\end{aligned}$$

In this example the system has an equilibrium at the origin too. Consequently the following LYAPUNOV function candidate can be found

$$V(x_1, x_2) = x_1^2 + x_2^2. \tag{7.34}$$

Thus the corresponding time derivative is

$$\dot{V}(x_1, x_2) = 2x_1\dot{x_1} + 2x_2\dot{x_2} = -2(x_1^2 + x_2^2)^2. \tag{7.35}$$

Hence $V(x_1, x_2)$ is positive definite and $\dot{V}(x_1, x_2)$ is negative definite. Thus the equilibrium at the origin is globally, asymptotically stable for the system.

A quite difficult aspect when using the LYAPUNOV's direct method is given by how to find LYAPUNOV function candidates. No straight algorithm with a determined solution exists, which is a big disadvantage of this method. SLOTINE [45] proposes several structured approaches to gain LYAPUNOV function candidates namely

- KRASOVSKII's method and
- the variable gradient method.

Besides these SLOTINE provides additional possibilities to involve the system's physical principles in the procedure for the determining of LYAPUNOV function candidates while analyzing more complex nonlinear dynamic systems.

7.2.2.3 Passivity in Dynamic Systems

As another method for the stability analysis of dynamic systems the passivity formalism is introduced within this subsection. Functions can be extended to system combinations by using LYAPUNOV's direct method, and evaluating the dissipation of energy in dynamic systems. The passivity formalism also is based on nonlinear positive definite storage functions $V(\mathbf{x})$ with $V(\mathbf{0} = \mathbf{0})$ representing the overall system energy. The time derivative of this energy determines the system's passivity. As example the general formulation of a system

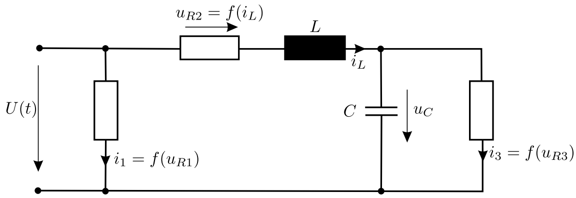

Fig. 7.25 Passivity analysis of an RLC-Network

$$\dot{x} = f(x, u, t)$$
$$y = g(x, u, t).$$

is considered. This system is passive concerning the external supply rate $S = \mathbf{y}^T \mathbf{u}$ if the inequality condition

$$\dot{V}(\mathbf{x}) \leq \mathbf{y}^T \mathbf{u} \tag{7.36}$$

is satisfied. KHALIL distinguishes several cases of system passivity depending on certain system characteristics (*Lossless, Input Strictly Passive, Output Strictly Passive, State Strictly Passive, Strictly Passive*) [34]. If a system is passive concerning the *external supply rate S*, it is stable in the sense of LYAPUNOV.

The combination of passive systems using parallel or feedback structures inherits the passivity from its passive subsystems. With the close relation of system passivity to stability in the sense of LYAPUNOV, the examination of the system stability is possible by verifying the subsystem's passivity. Based on this evaluation it can be concluded that the overall system is passive—always with the assumption that a correct system structure was built.

As an illustrating example the RLC circuit taken from [34] is analyzed in the following. The circuit structure is shown in Fig. 7.25.

The system's state vector is defined by

$$i_L = x_1$$
$$u_C = x_2.$$

The input u represents the supply voltage U, as output y the current i is observed. The resistors are described by the corresponding voltage current characteristics:

$$i_1 = f_1(u_{R1})$$
$$i_3 = f_3(u_{R3})$$

For the resistor which is coupled in series with the inductor the following behavior is assumed

$$U_{R2} = f_2(i_L) = f_2(x_1). \tag{7.37}$$

Thus the nonlinear system is described by the differential equation:

$$
\begin{aligned}
L\dot{x_1} &= u - f_2(x_1) - x_2 \\
C\dot{x_2} &= x_1 - f_3(x_2) \\
y &= x_1 + f_1(u)
\end{aligned}
$$

The presented RLC circuit is passive as long as the condition

$$V(\mathbf{x}(t)) - V(\mathbf{x}(0)) \leq \int_0^t u(\tau)y(\tau)d\tau \tag{7.38}$$

is satisfied. In this example the energy stored in the system is described by the storage function

$$V(\mathbf{x}(t)) = \frac{1}{2}Lx_1^2 + \frac{1}{2}Cx_2^2. \tag{7.39}$$

Equation (7.38) leads to the condition for passivity:

$$\dot{V}(\mathbf{x}(t), u(t)) \leq u(t)y(t) \tag{7.40}$$

which means, that the energy supplied to the system must be equal or higher than the time derivative of the energy function. Using $V(\mathbf{x})$ in the condition for passivity provides

$$
\begin{aligned}
\dot{V}(\mathbf{x}, u(t)) &= Lx_1\dot{x_1} + Cx_2\dot{x}_2 \\
&= x_1\,(u - f_2(x_1) - x_2) + x_2\,(x_1 - f_3(x_2)) \\
&= x_1\,(u - f_2(x_1)) + x_2 f_3(x_2) \\
&= (x_1 + f_1(u))\,u - uf_1(u) - x_1 f_2(x_1) - x_2 f_3(x_2) \\
&= uy - uf_1(u) - x_1 f_2(x_1) - x_2 f_3(x_2)
\end{aligned}
$$

and finally

$$u(t)y(t) = \dot{V}(\mathbf{x}, u(t)) + uf_1(u) + x_1 f_2(x_1) + x_2 f_3(x_2). \tag{7.41}$$

In case that f_1, f_2 and f_3 are passive subsystems, i.e. all functions describing the corresponding characteristics of the resistors exist only in the first and third quadrant, so $\dot{V}(\mathbf{x}, u(t)) \leq u(t)y(t)$ is true, hence the RLC circuit is passive. Any coupling of this passive system to other passive systems in parallel or feedback structures again results in a passive system. For any passivity analysis and stability evaluation this method implements a structured procedure and shows a very high flexibility.

In conclusion it is necessary to mention, that all methods for stability analysis introduced in this section show certain advantages and disadvantages concerning their applicability, information value and complexity, regardless whether linear or nonlinear systems are considered. When a stability analysis is expected to be done, the applicability of a specific method should be checked individually. This section only can give a short overview on the introduced methods and techniques, and does explicitly not claim to be a detailed description due to the limited scope of this section. For any further study the reader is invited to consult the proposed literature.

7.3 Control of Multi-input Systems

There are four types of systems with different inputs and outputs. SISO (single input, single output), SIMO (single input, multiple outputs), MISO (multiple inputs, single output), and MIMO (multiple inputs, multiple outputs). Loop interactions result in unexpected effects from their variables and make these systems complicated.

Many practical systems are multi-input and often nonlinear, such as most of the robotic manipulators, cars, and aircrafts. In these systems, designing a feedback control to fulfill the desired performance and robustness characteristics become more challenging. Here, two control types, position control, and trajectory control will be discussed.

Consider a simple planner robotic manipulator with only two links depicted in Fig. 7.26. The system's dynamic model can be written as:

$$M(q)\ddot{q} + C(q, \dot{q}) + g(q) = \tau \tag{7.42}$$

where $M(q)$ is the inertia matrix of the manipulator, $C(q, \dot{q})$ is the centripetal and Coriolis torques, $g(q)$ is the gravitational torques, and τ is the actuator torques. As can be seen from the above equation, the system is strongly nonlinear (the coriolis and centripetal terms are always nonlinear) with coupled dynamics, which makes it challenging to design a feedback control structure.

As a solution, using high ratio geared actuators can effectively remove the nonlinearity and coupled dynamic difficulties. However, the backlash and friction of the gears, which are hard nonlinearities, adversely affect the performance of the system such as tracking and force control accuracy.

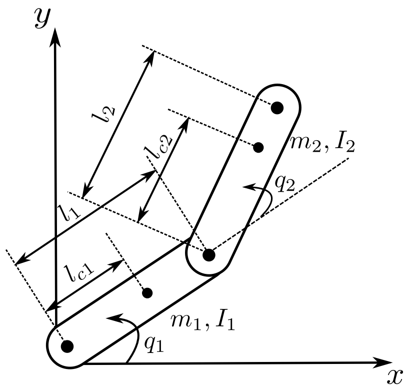

Fig. 7.26 Two-link manipulator

7.3.1 Position Control

Assume that the two-link manipulator is in the horizontal plane, thus $g(p) = 0$, and it is required to move to a defined stationary position i.e. q_d. One can realize that the most simple feedback control law to achieve position control is the joint PD controller, which controls each joint independently based on its position error and its time derivative as:

$$\tau_i = -k_{pi}\tilde{q}_i - k_{di}\dot{q}_i \tag{7.43}$$

where $k_{pi} > 0$, $k_{di} > 0$, $\tilde{q}_i = q_i - q_{di}$ is the position error and $\dot{q}_i$ is the velocity of the ith joint. This control structure can be seen as a spring and damper that are connected to each joint where the neutral position of the springs is the desired position. As a result, the system performs damped oscillation towards the desired position. The stability can be checked by considering the total mechanical energy of the system as Lyapunov function:

$$V = \frac{1}{2}(\dot{q}^T M\dot{q} + \tilde{q}^T K_p\tilde{q}) \tag{7.44}$$

where K_p is the matrix of P controller coefficient, which is diagonal and positive definite. Therefore, the derivative of Lyapunov function can be derived as:

$$\dot{V} = -\dot{q}^T k_d\dot{q} \leq 0 \tag{7.45}$$

where k_d is the matrix of D controller coefficient and the same as k_p, it is diagonal and positive definite as well. As can be seen from the above equation, $\dot{V}$ is the dissipated energy by D controller or the virtual damping. The time response of such a controlled system is almost the same as a damped mass-spring system. However, one should expect a significant variation of time response characteristics of such a highly nonlinear plant with constant controller parameters. Other solutions could be sliding mode control and adaptive control, which are capable of dealing with nonlinearity more effectively.

7.3.2 Trajectory Control

Now consider that the desired position changes with respect to time. Due to the strong nonlinearity of the manipulator in Fig. 7.27 and its equation, the PID-SISO controller structure can't satisfy the desired tracking performance. One solution is to use the general form of the linear controller PID for a MIMO system. In [11], a PID-MIMO control law is tuned based on try and error. The advantage of PID-MIMO over the PID-SISO is that PID-MIMO benefits from the error of all joints to calculate the input of each joint. In other words, K_p and K_d matrices are not diagonal, they are symmetric and positive definite. As a result, the tracking performance significantly improves compared to PID-SISO (PID).

Figure 7.28 depicts the tracking error of the two-linkage robot, which shows that in a multi-input system, utilizing a single-input PID results in significant tracking error.

Other effective control methods could be robust control and adaptive control methods. However, there is a difference in their performance. As mentioned previously, since the nonlinearity of the system is known and modeled, the adaptive control can lead to better performance. In other words, the robust control considers the nonlinearity as uncertainty, which is a much more conservative technique comparing to estimating the nonlinearity in the adaptive control method. Therefore, in this case,

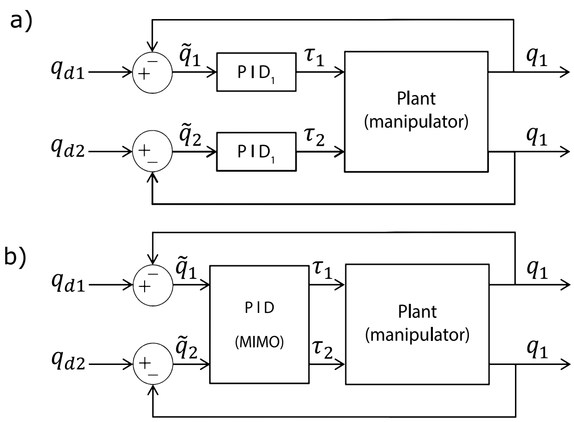

Fig. 7.27 The PID-SISO (PID) controller structure (**a**) and the PID-MIMO controller structure (**b**)

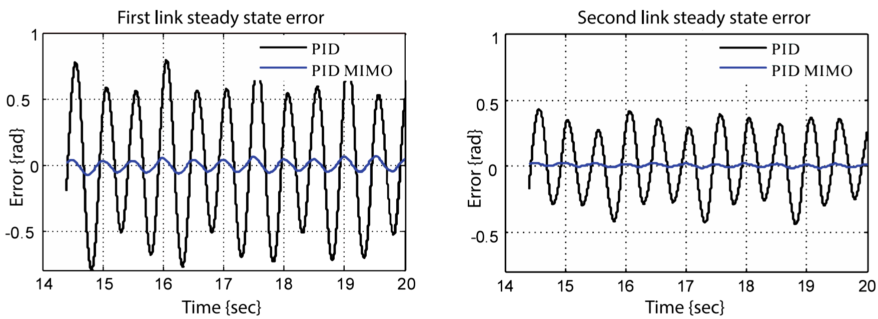

Fig. 7.28 Tracking error comparison of PID and PID-MIMO.png

the adaptive control can result in superior performance. However, considering the haptic or rehabilitation systems, where the robot interacts with an unknown environment or user's command, as discussed in [1] a robust adaptive controller enhances the system performance.

7.4 Control Law Design for Haptic Systems

As introduced in the beginning of this chapter, control design is a fundamental and necessary aspect within the development of haptic systems. Besides the techniques for system description and stability analysis the need for control design and the applicable design rules become obvious. Especially for the control design of a haptic system it is necessary to deal with several aspects and conditions to be satisfied during the design process. The following sections present several control structures and design schemes in order to set up a basic knowledge about the toolbox for analytic control design of haptic systems. This also involves some of the already introduced methods for system formulation and stability analysis, as these form the basis for most control design methods.

7.4.1 Structuring of the Control Design

As introduced in Chap. 6 various different structures of haptic systems exist. Demands on the control of these structures are derived in the following.

Open-loop impedance controlled The user experiences an impression of force which is directly commanded via an open loop based only on a demand value. In Chap. 6 the basic scheme of this structure is shown by Fig. 6.2.

Closed-loop impedance controlled As it can be seen in Fig. 6.4, the user also experiences an impression of force which is fed back to a controller. Here a specific control design will be needed.

Open-loop admittance controlled In this scheme, the user experiences an impression of a defined position. In the open loop arrangement this position again is directly commanded based only on a demand value. Figure 6.6 shows the corresponding structure of this haptic scheme.

Closed-loop admittance controlled This last version as it is depicted in Fig. 6.8 shows its significant difference in the feedback of the force the user applies to the interface. This force is fed back to a demand value. This results in a closed loop arrangement that incorporates the user and his or her transfer characteristics. In difference to the closed loop impedance controlled scheme this structure uses a force as demanded value $\underline{S}_F$ compared with the detected $\underline{S}_S$, but the system output is still a position $\underline{x}_{out}$. This results in the fact that the incorporation of the user into the closed loop behavior is more complex than it is in a closed loop impedance controlled scheme.

All of these structures can be basically implemented in a haptic interaction as shown in Fig. 2.33. From this, all necessary control loops of the overall telemanipulation system become evident:

- On the haptic interface site a control loop is closed incorporating the user which is valid as long as the user's reaction is fed back to the central interface module for any further data processing or control.
- On the process/environment site also, a closed loop exists if measurable process signals (reactions, disturbances) are fed back to the central interface module for data processing or control.
- Underneath these top-level control loops various subsystem control loops exists which have a major impact on the overall system too. As an example, each electrical actuator will most likely be embedded in a cascaded control structure with current, speed and position control.

It becomes obvious that the design of a control system for a telemanipulation system with a haptic interface is complex and versatile. Consequently a generally valid procedure for control design cannot be given. The control structures must be designed step by step involving the following controllers:

1. Design of all controllers for the subsystem actuators
2. Design of a top level controller for the haptic interface
3. Design of a top level controller for the manipulator/VR-environment
4. Design of the system controller that connects interface and manipulator or VR environment.

This strict separation proposed above might not be the only way of structuring the overall system. Depending on the application and functionality, the purpose of the different controller and control levels might be in conflict to each other or simply overlap. Therefore it is recommended to set up the underlying system structure and define all applied control schemes corresponding to their required functionality.

While looking at the control of haptic systems, a similar structure can be established. For both the control of the process manipulation and the haptic display or interface the central interface module will have to generate demand values for force or position, that are going to be followed by the controllers underneath. These demand values derive from a calculation predefined by designed control laws. To gain such control laws a variety of methods and techniques for structural design and optimization can be applied depending on certain requirements. The following subsections give an overview of typical requirements to closed control loop behavior followed by examples for control design.

7.4.2 Requirement Definition

Besides the fundamental need for system stability with sufficient stability margins additional requirements can be set up to achieve a certain system behavior in a closed loop scheme such as dynamic or precision. A quantitative representation of these requirements can be made by the achievement of certain characteristics of the closed loop step response.

Figure 7.29 shows the general form of a typical closed loop step response and its main characteristics. As it can be seen the demanded value is reached and the basic control requirement is satisfied.

Additional characteristics are discussed and listed in Table 7.1. For all mentioned characteristics a quantitative definition of certain requirements is possible. For example the number and amplitude of overshoots shall not extend a defined limit or have a certain frequency spectrum that is of special interest for the control design in haptic systems. As it is analyzed in Chap. 3, the user's impedance shows a significant frequency range which must not be excited within the control loop of the haptic device. Nevertheless a certain cut-off frequency has to be reached to establish a good performance of the dynamic behavior. All these issues are valid for the requirements to the control design of the process manipulation. In addition to the requirements from the step response due to changes of the setpoint value, it is necessary to formulate

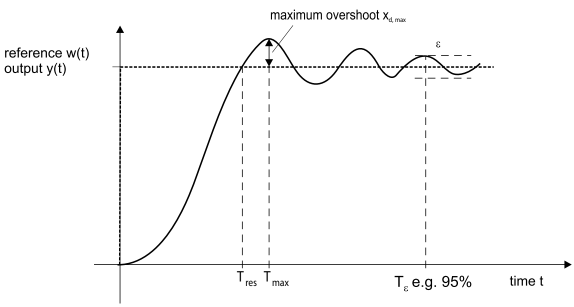

Fig. 7.29 Closed loop step response requirements

Table 7.1 Parameter for control quality requirements

Parameter	Description
$x_{d,max}$	Maximum overshoot
T_{max}	Point of time for $x_{d,max}$
T_ε	Time frame in which the residuum to the demanded value remains within a predefined scope ε
T_{res}	Point of time when the demanded value is reached for the first time

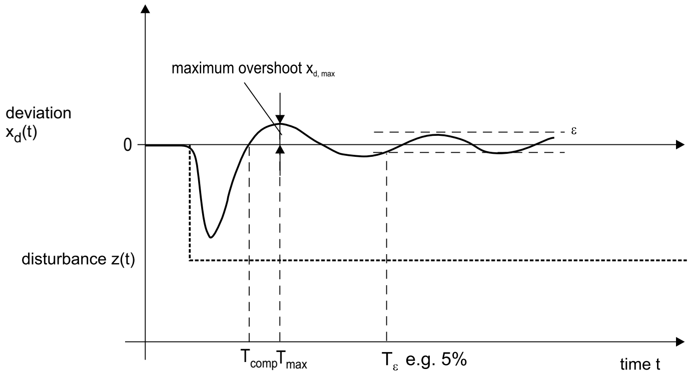

Fig. 7.30 Closed loop disturbance response requirements

requirements concerning the closed loop system behavior considering disturbances originating from the process. Especially when interpreting the user's reaction as disturbance within the overall system description a requirement set up for the disturbance reaction of the control loop has to be established. As it can be seen in Fig. 7.30 similar characteristics exist to determine the disturbance reaction quantitatively and qualitatively. In most cases both the step response behavior and the disturbance reaction cannot satisfy all requirements, as they often come into conflict with each other, which is caused by the limited flexibility of the applied optimization method. Thus it is recommended to estimate the relevance of step response and disturbance reaction in order to choose an optimization approach that is most beneficial. Although determined quantitatively, it is not possible to use all requirements in a predefined optimization method. In most cases an adjustment of requirements is necessary to be made, to apply specific control design and optimization methods. As an example the time T_{res} as depicted above cannot be used directly, and must be transferred into a requirement for the closed loop dynamic characterized by a definite pole placement.

Furthermore simulation techniques and tests offer iteration within the design procedure to gain an optimal control law. However, this very sufficient way of analyzing system behavior and test designed control laws suggests to forget about the analytic system and control design strategy and switch to a trial an error algorithm.

7.4.3 General Control Law Design

This section shall present some possible types of controllers and control structures that might be used in the already discussed control schemes. For optimization of the control parameters several methods exists. They are introduced here. Depending on the underlying system description several approaches to set up controllers and control structures are possible. This section will present the classic PID-control, additional control structures e.g. compensation, state feedback controllers, and observer based state space control.

7.4.3.1 Classic PID-Control

Maybe one of the most frequently used controllers is the parallel combination of a proportional (P), an integrating (I) and a derivative (D) controller. This combination is used in several variants including a P-controller, a PI combination, a PD combination or the complete PID structure. Using the PID structure all advantages of the individual components are combined. The corresponding controller transfer function is described by

$$\underline{G}_R = K_R \left(1 + \frac{1}{T_N s} + T_V s \right). \tag{7.46}$$

Figure 7.31 shows the equivalent block diagram of a PID controller structure. Adjustable parameters in this controller are the proportional gain K_R, the integrator time constant T_N and the derivative time T_V.

With optimized parameter adjustment a wide variety of control tasks can be handled. This configuration offers on the one hand the high dynamic of the proportional controller and on the other, the integrating component guarantees a high precision step response with a residuum $x_d = 0$ for $t \to \infty$. The derivative finally provides an additional degree of freedom that can be used for a certain pole placement of the closed loop system.

As major design techniques the following examples shall be introduced:

Root Locus Method This method has its strength by the determined pole placement for the closed loop system, directly taken into account the dependence on the proportional gain K_R. By a reasonable choice of T_N and T_D the additional system zeros are influenced which affects directly the resulting shape of the root locus and thus the stability behavior. Besides this the overall system dynamic can be designed.

Integral Criterion The second method for the optimization of the closed loop system step response or disturbance reaction is the minimization of an integral criterion. The basic procedure for this method is as the following: The tracking

Fig. 7.31 PID block diagram

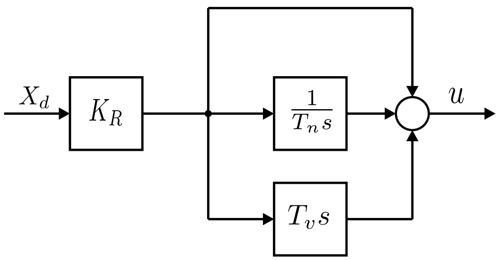

error x_d due to changes of the demanded set point or a process disturbance is integrated (and eventually weighted over time). This time integral will be minimized by adjusting the controller parameters. In case of convergence of this minimization, the result is a set of optimized controller parameters.

For any additional theoretical background concerning controller optimization the reader is invited to consult the literature on control theory and control design [37, 38].

7.4.3.2 Additional Control Structures

In addition to the described PID controller additional control structures extend the influence on the control result without having an impact on the system stability. The following paragraphs therefore shall present and disturbance compensation and a direct feedforward of auxiliary process variables.

Disturbance Compensation

The basic principle of disturbance compensation assumes that if a disturbance on the process is measurable and its influence is known, this knowledge can be used to establish compensation by corresponding evaluation and processing. Figure 7.32 shows a simplified scheme of this additional control structure.

In this scheme a disturbance signal is assumed to affect the closed loop via a disturbance z transfer function $\underline{G}_D$. By measuring the disturbance signal and processing the compensator transfer function $\underline{G}_C$ results in a compensation of the disturbance interference. Assuming an optimal design of the compensator transfer function this interference caused by the disturbance is completely erased. The optimal design of a corresponding compensator transfer function is depicted by

$$\underline{G}_C = -\frac{\underline{G}_D}{\underline{G}_S}. \tag{7.47}$$

Fig. 7.32 Simplified disturbance compensation

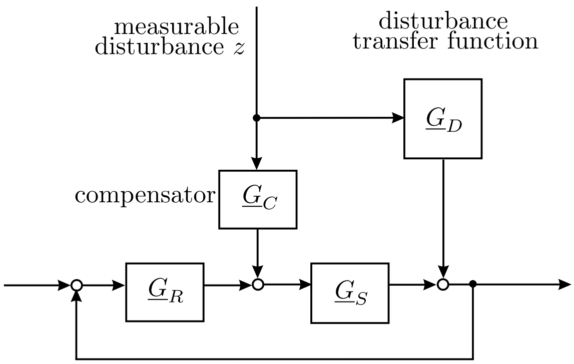

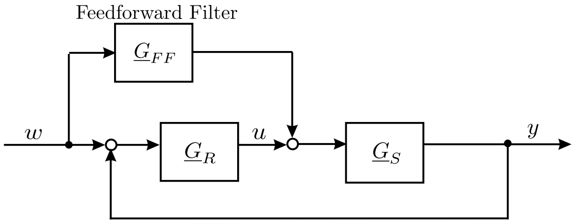

Fig. 7.33 Feedforward of auxiliary input variables

This method assumes that a mathematical and practicable inversion of $\underline{G}_D$ exists. For those cases where this assumption is not valid, the optimal compensator $\underline{G}_K$ must be approximated. Furthermore Fig. 7.32 states clearly, that this additional control structure does not have any influence on the closed loop system stability and can be designed independently. Besides the practicability the additional effort should be taken into account. This effort will definitively increase just by the sensors to measure the disturbance signals and by the additional costs for realization of the compensator.

Auxiliary Input Feedforward

A similar structure compared to the disturbance compensation is the *feedforward* of auxiliary input variables. This principle is based on the knowledge of additional process variables that are used to influence the closed loop system behavior without affecting the system stability. Figure 7.33 shows an example of the feedforward of the demanded setpoint w to the controller signal u using a feedforward filter function $\underline{G}_{FF}$.

7.4.3.3 State Space Control

Corresponding to the techniques for the description of multi-input multi-output systems discussed prior in this chapter, the state space control provides additional features to cover the special characteristics within those systems. As described before, multi-input multi-output systems are preferably depicted as state space models. Using this mathematical formulation enables the developer to implement a control structure that controls the internal system states to demanded values. A big advantage is that the design methods for state space control use an overall approach for control design and optimization instead of a control design step by step for each system state. With this approach it becomes possible to deal with profoundly coupled multi-input multi-output systems with high complexity, and design a state space controller simultaneously. This section will present the fundamental state space control structures. This will cover the *state feedback control* as well as the *observer based state space control*. For further detailed procedures as well as design and optimization methods the reader is referred to [38, 49].

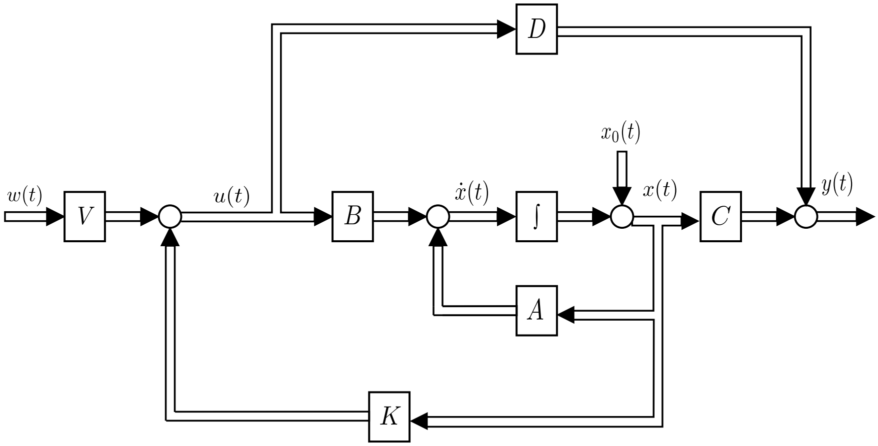

Fig. 7.34 State feedback control

State Feedback Control

As it is shown in Fig. 7.34 this basic structure for state space control uses a feedback of the system states **x**. Similar to the depiction in Fig. 7.2 the considered system is presented in state space description using the matrices **A**, **B**, **C** and **D**. The system states **x** are fed back gained by the matrix **K** to the vector of the demanded values that were filtered by matrix **V**. The results represent the system input vector u. Both matrices **V** and **K** do not have to be square matrices for a state space description is allowed to implement various dimensions for the state vector, the vector for the demanded values and the system input vector.

Observer Based State Space Control

The state space control structure discussed above requires a complete knowledge of all system states, which is nothing else but that they have to be measured and processed to be used in the control algorithm. From a practical point of view this not possible all the time due to technical limits as well as costs and effort. As a result the developer is faced with the challenge to establish a state space control without the complete knowledge of the system states. As a solution those system states that cannot be measured due to technical difficulties or significant cost factors are estimated using a state space observer structure that is shown in Fig. 7.35.

In this structure a system model is calculated in parallel to the real system. As exact as possible this system model is described by the corresponding parameter matrices $\mathbf{A}^*$, $\mathbf{B}^*$, $\mathbf{C}^*$ and $\mathbf{D}^*$. The model input also is represented by the input vector **u**. Thus the model provides an estimation of the real system states $\mathbf{x}^*$ and an estimated system output vector $\mathbf{y}^*$. By comparison of this estimated output vector $\mathbf{y}^*$ with the real output **y**, which is assumed to be measurable, the estimation error is fed back gained by the matrix **L**. This results in a correction of the system state estimation $\mathbf{x}^*$. Any estimation error in the system states or the output vector due to varying initial

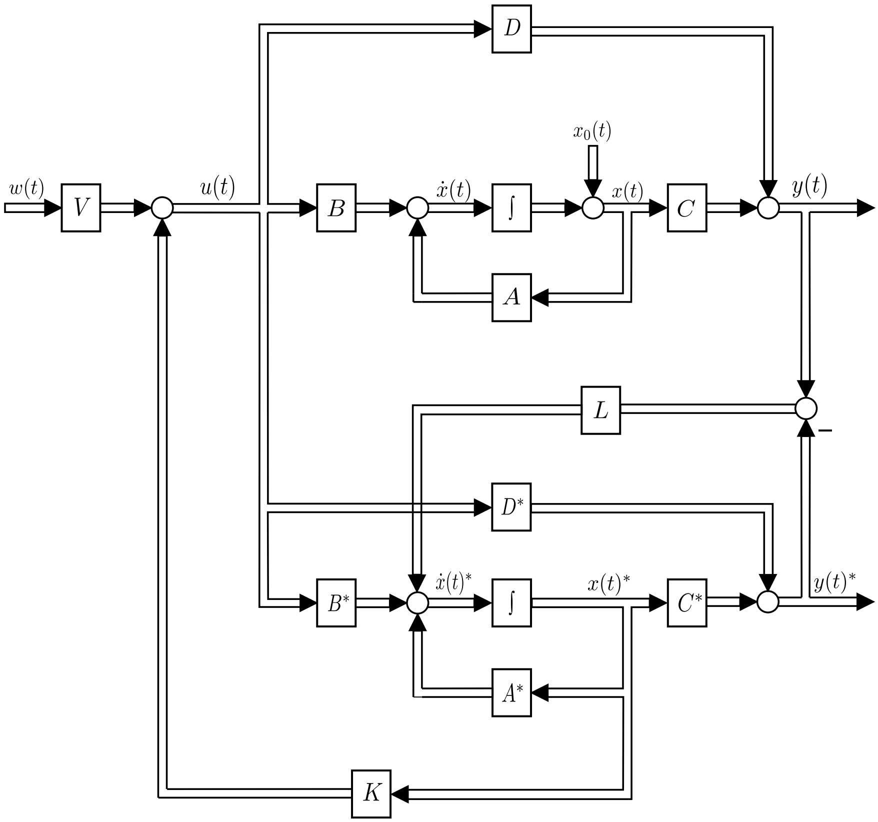

Fig. 7.35 Observer based state space control

states is corrected and the estimated states $\mathbf{x}^*$ are used to be gained by the equivalent matrix $\mathbf{K}$ and fed back for control.

This structure of an observer based state space control uses the LUENBERGER observer. In this configuration all real systems states are assumed not to be measurable thus the state space control refers to estimated values completely. Practically, the feedback of measurable system states is combined with the observer based estimation of additional system states. In [38, 49] examples for observer based state space control structures as well as methods for observer design are discussed in more detail.

Example: Cascade Control of a Linear Drive

As an example for the design of a controller the cascade control of a linear drive build up of an EC motor and a ball screw is considered in this section based on [32]. The consideration includes non-linear effects due to friction, temperature change and a non-linear degree of efficiency of the ball screw.

A schematic representation of the EC motor is given in Fig. 7.36. in which only one phase is illustrated for simplification. The motor is supplied with the voltage u_{DC}.

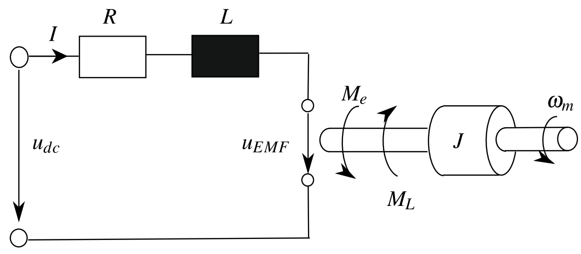

Fig. 7.36 Equivalent circuit of the considered EC-motor with attached ball screw to transform rotary into translational movement

The resistance R and the inductance L represent the stator winding of the motor. The angular speed of the rotor $\underline{\omega}_{\mathrm{M}}$ generates a back electromotive force (back-EMF) u_{EMF}. The mechanical properties of the motor are described by the motor torque $\underline{M}_{\mathrm{e}}$, the load torque $\underline{M}_{\mathrm{L}}$ and the moment of inertia of the rotor J. Mesh analysis yields to the equation for the electrical part of the motor

$$u_{DC} = Ri + L\frac{di}{dt} + u_{EMF} \tag{7.48}$$

which can be written in the frequency domain as

$$\underline{U}_{\mathrm{DC}} - \underline{U}_{\mathrm{EMF}} = \underline{I}(R + sL) \tag{7.49}$$

The back electromotive force U_{EMF} depends on the angular speed of the rotor ω_M, the back-EMF constant k_e and the parameter $F(\phi_e)$ which describes the dependence of the back-EMF of the electrical angle ϕ_e.

$$u_{EMF} = k_e \omega_M F(\phi_e) \tag{7.50}$$

The motor torque M_e generated by the motor current i correlates with the mechanical load M_L and the angular acceleration ω_M of the rotor with the moment of inertia J. It follows:

$$M_e = \frac{i \cdot u_{EMF}}{\omega_M} = ik_e F(\Phi_e) = J\frac{d\omega_M}{dt} + M_L \tag{7.51}$$

In the frequency domain the mechanical properties of the motor are described by

$$M_e - M_L = sJ\omega_M. \tag{7.52}$$

The model takes three different types of non-linearities into account: friction, temperature change and a non-linear efficiency of the ball screw. The friction is modeled as the sum of a static friction K_F and a dynamic friction $k_F \cdot \omega_M$. So the equilibrium of moments of the rotor can now be written as

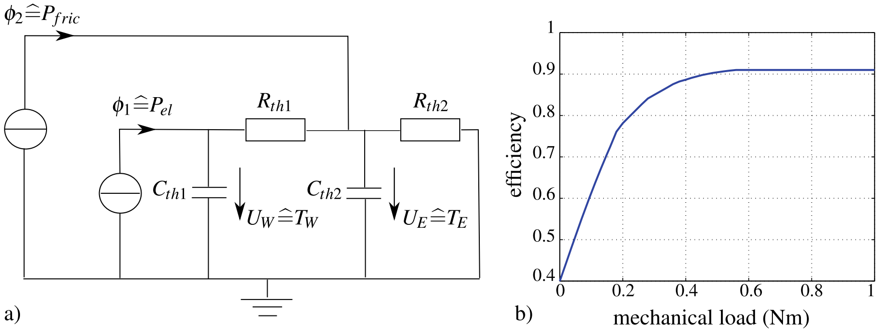

Fig. 7.37 **a** Equivalent thermal circuit of the EC motor, **b** efficiency of the ball screw depending on the mechanical load

$$M_e - M_L - K_F = (k_F + sJ)\omega_M. \tag{7.53}$$

The influence of changes in temperature on motor parameters is modeled by a thermal equivalent circuit shown in Fig. 7.37a. The temperature change of the stator winding T_W can be determined by

$$\Delta T_W = \frac{R_{th1}T_{th2}s + R_{th1}R_{th2}}{T_{th1}T_{th2}s^2 + (T_{th1} + T_{th2})s} P_{el} + \frac{R_{th2}}{T_{th1}T_{th2}s^2 + (T_{th1} + T_{th2} + R_{th2}C_{th1})s + 1} P_{fric}. \tag{7.54}$$

with

$$T_{th1} = R_{th1}C_{th1} \quad \text{and} \quad T_{th2} = R_{th2}C_{th2} \tag{7.55}$$

The resulting resistance of the stator winding R_* and the back-EMF constant k_{e*} can be derived with knowledge of the temperature coefficients α_R, α_k from

$$R_* = R(1 + \alpha_R \Delta T_W), \quad k_{e*} = k_e(1 + \alpha_k \Delta T_W). \tag{7.56}$$

The efficiency of the ball screw depends on the mechanical load of the linear drive. Its qualitative characteristics are shown in Fig. 7.37 (b) and can be included in the model as characteristics in a lookup table. The resulting model can be computed for example in Matlab/Simulink and used for simulation and the design of a controller. In this example a cascade controller is chosen (Fig. 7.38). It contains of an inner loop for current control, a middle loop for velocity control and an outer loop for position control. As controller for the different control loops P- or PI-controllers are used.

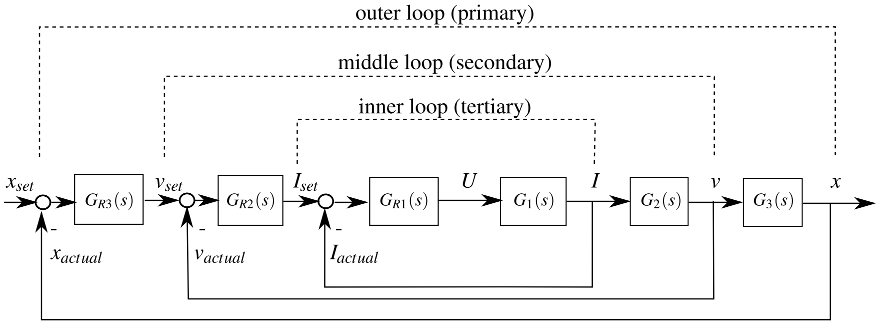

Fig. 7.38 Structure of cascade controller of EC motor

7.5 Control of Teleoperation Systems

In the previous sections an overview on system description and control aspects in general, which can be used for the design of local and global control laws, was given. The focus of this section lies on special methods used for modeling of haptic systems stability analysis of bilateral telemanipulators. In contrary to Sect 7.4 special tools for the development of control laws are presented here, which based upon the two-port hybrid representation of bilateral telemanipulators (Sect. 7.5.1). Subsequently in Sect. 7.5.2 a definition of transparency will be introduced, which can be used to analyze the performance of a haptic system in dependency of the system characteristics and the chosen control law. In Sect. 7.5.3 the general control model for telemanipulators will be introduced to close the gap between the closed loop representation, known from general control theory and used in the Sects. 7.1–7.4, and the two-port hybrid representation. In section Sect. 7.5.4 it will be shown, how a stable and safe operation of the haptic system can be achieved. Furthermore the design of stable control laws in the presence of time-delays will be presented in section Sect. 7.5.5.

7.5.1 Two-Port Representation

In general a haptic system is a bilateral telemanipulator, where a user handles a master device to control a slave device, which is interacting with an environment. A common representation of a bilateral telemanipulator is the general two-port model as shown in Fig. 7.39.

User and environment are represented by one-ports, characterized by their mechanical impedances $\underline{Z}_\mathrm{H}$ and $\underline{Z}_\mathrm{E}$ as they can be seen as passive elements [33], see Chap. 3. The mechanical impedance $\underline{Z}$ is defined by Eq. (7.57)

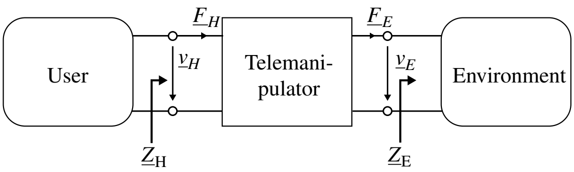

Fig. 7.39 General Two-Port-Model of a telemanipulator

$$\underline{Z} = \frac{\underline{F}}{\underline{v}} \tag{7.57}$$

The user manipulates the master device, which controls the slave device. The slave interacts with the environment. The behavior of the telemanipulator is described by its hybrid matrix **H** [21, 43]. So the coupling of user action and interaction with the environment is described by the following hybrid matrix taking forces and velocities at the master and slave side and the properties of the haptic system into account.

$$\begin{pmatrix} \underline{F}_H \\ -\underline{v}_E \end{pmatrix} = \begin{pmatrix} \underline{h}_{11} & \underline{h}_{12} \\ \underline{h}_{21} & \underline{h}_{22} \end{pmatrix} \cdot \begin{pmatrix} \underline{v}_H \\ \underline{F}_E \end{pmatrix}. \tag{7.58}$$

In this case, the four h-parameters represent

$$\begin{pmatrix} \underline{F}_H \\ -\underline{v}_E \end{pmatrix} = \begin{pmatrix} \text{Master Input Impedance} & \text{Backward Force Gain} \\ \text{Forward Velocity Gain} & \text{Slave Output Admittance} \end{pmatrix} \cdot \begin{pmatrix} \underline{v}_H \\ \underline{F}_E \end{pmatrix} \tag{7.59}$$

Please note that the velocity of the slave v_E is taken into account with a negative sign. This is done to fulfill the convention for general two-ports, where the flow is always flowing into a port. The hybrid two-port representation as shown before is often used to determine stability criteria and to describe performance properties of bilateral telemanipulators. Despite the formulation with force as flow variable (also found in [21, 35], for example), one can also find velocity as flow variable in other two-port-descriptions of bilateral telemanipulators [25] . As long as the coupling is defined by the impedance formulation given in Eq. (7.57), these both variants of the two-port descriptions are interchangeable.

7.5.2 *Transparency*

Beside system stability performance is an important design criterion in the development of haptic systems. The function of a haptic system is to provide a high fidelity force feedback of the contact force at the slave side to the user manipulating the master device of the telemanipulator. One parameter often used to evaluate the haptic sensation presented to the user is transparency. If the user interacts directly with the environment, he experiences a haptic sensation, which is determined by the mechanical impedance $\underline{Z}_E$ of the environment. If the user is coupled to the environment via a telemanipulator system, he experiences a force impression, which is determined by the backward force gain and the mechanical input impedance of the master device. It is desirable that the haptic sensation for the user of the telemanipulator is the same as interacting directly with the environment. Therefore the telemanipulator has to display the mechanical impedance of the environment $\underline{Z}_E$ at the master device. Assume that $h_{12} = h_{21} = 1$, so there's no scaling of velocity or force. Therefore the following conditions have to be hold to reach full transparency.

$$\underline{F}_H = \underline{F}_E \quad \text{and} \quad \underline{v}_H = \underline{v}_E. \tag{7.60}$$

From this follows that for perfect transparency [35]

$$\underline{Z}_H = \underline{Z}_E \tag{7.61}$$

Therefore the force experienced by the user at the master device is

$$\underline{F}_H = \underline{h}_{11}\underline{v}_H + \underline{h}_{12}\underline{F}_E$$

and for the velocity at the slave side holds

$$-\underline{v}_E = \underline{h}_{21}\underline{v}_H + \underline{h}_{22}\underline{F}_E.$$

Therefore the mechanical impedance displayed by the master and felt by the user is described by

$$\underline{Z}_T = \frac{\underline{F}_T}{\underline{v}_T} = \frac{\underline{h}_{11}\underline{v}_H + \underline{h}_{12}\underline{F}_E}{\frac{\underline{v}_E - \underline{h}_{22}\underline{F}_E}{\underline{h}_{21}}} \tag{7.62}$$

By analyzing Eq. (7.62) the conditions for perfect transparency can be derived. To achieve perfect transparency output admittance at the slave side and input impedance at the master side have to be zero. From this follows that for perfect transparency, in the case of no scaling, the matrix has to be in the form

$$\begin{pmatrix} \underline{F}_H \\ \underline{-v}_E \end{pmatrix} = \begin{pmatrix} 0 & -1 \\ 1 & 0 \end{pmatrix} \cdot \begin{pmatrix} \underline{v}_H \\ \underline{F}_E \end{pmatrix}.$$

It is obvious that perfect transparency is in practice not achievable without further actions taken, due to non-zero input impedance $\underline{h}_{11}$ and output admittance $\underline{h}_{22}$ of the manipulator system. If the input impedance would be zero, the user would not feel the mechanical properties of the master device (mass, friction, compliance). An output admittance of zero relates to an ideal stiff slave device.

7.5.2.1 A Perception-Oriented Consideration of Transparency

To obtain a transparent system, the system's engineer has two options: Work on the control structure, as described in the following sections or consider the perception capabilities of the human user in the definition of transparency. The latter is focus of this section, that is based on the more detailed elaborations in [27]. It has to be noted, that this approach still lacks some experimental evaluation.

Up till now, transparency as defined in Eqs. (7.60) and (7.61) is a binary criterion: A system is either transparent if all conditions are fulfilled or is not transparent, if one of the equalities is not given. Despite this formulation, one can define the absolute transparency error $\underline{e}_{\mathrm{T}}$ according to Heredia et al. as shown in Eq. (7.63) [30]

$$\underline{e}_{\mathrm{T}} = \underline{Z}_{\mathrm{H}} - \underline{Z}_{\mathrm{E}} \tag{7.63}$$

and the relative transparency error $\underline{e}'_{\mathrm{T}}$ as shown in Eq. (7.64)

$$\underline{e}'_{\mathrm{T}} = \frac{\underline{Z}_{\mathrm{H}} - \underline{Z}_{\mathrm{E}}}{\underline{Z}_{\mathrm{H}}} \tag{7.64}$$

When analyzed along the whole intended dynamic range and in all relevant ↪ DoF of the haptic system, Eqs. (7.63) and (7.64) allow for the quantitative comparison of different haptic systems and can give insight in the relevant ranges of frequency that have to be optimized for a more transparent system. They also provide the basis for the integration of perception properties in the assessment of transparency.

From the above mentioned definitions of transparency (Eqs. (7.60) and (7.61)) one can conclude, that $\underline{e}_{\mathrm{T}} = \underline{e}'_{\mathrm{T}} \overset{!}{=} 0$ to fulfill the requirement of transparency. On the other hand it is obvious that a human user will not perceive all possible mechanical impedances, since the perception capabilities are limited as shown in Sect. 2.1. To obtain a quantified range for $\underline{e}_{\mathrm{T}}$ and $\underline{e}'_{\mathrm{T}}$, a thought experiment[1] is conducted in the following [46].

Experiment Assumptions

The following assumptions are made for the thought experiment about the user and the teleoperation scenario:

1. Linear behavior of haptic perception as discussed in Sect. 2.1.4.2 is assumed, which holds for a wide range of tool-mediated teleoperation scenarios. Super-threshold perception properties like masking are neglected.
2. For each user there exists a known mechanical impedance $\underline{Z}_{\mathrm{user}}$. This impedance generally depends on external parameters like temperature, contact force as shown in Chap. 3. All of these parameters are assumed to be known and invariant over the

[1] Thought experiments (also *gedankenexperiment*) consider the possible outcomes of a hypothesis without actually performing the experiment, but by applying theoretical considerations. They are conducted when the actual performance of an experiment is not possible or universally valid. Famous thought experiments include for example Schrödinger's Cat to illustrate quantum indeterminacy.

course of the experiment. Further, a set of frequency-dependent sensory thresholds for deflection and forces exists. They are labeled with F_θ and d_θ respectively. Both thresholds can be coupled using the mechanical impedance of the user and $\omega = 2\pi f$ as the angular frequency of the haptic signal as stated in Eq. (7.65) [28].

$$|\underline{Z}_{\text{user}}| = \left|\frac{F_\theta}{j\omega d_\theta}\right| \tag{7.65}$$

3. The user is able to impose an interaction force $\underline{F}_{\text{user,int}}$ or deflection $\underline{d}_{\text{user,int}}$ on the teleoperation system that does not necessarily trigger a sensation event at the contact point. This is for example possible by the movement of an arm, while only the fingertips are in contact with the teleoperation system.
4. The teleoperation system is perfectly transparent, i.e. $|\underline{e}_{\text{T}}| = 0$ for all frequencies. The system is able to read and display forces and deflections reproducible below the absolute thresholds of the user.
5. The environment is considered passive for simplification reasons.

Thought Experiment

For the experiment, an impedance type system is assumed, i.e. the user imposes a deflection on the haptic interface of the teleoperation system and interaction forces measured are displayed to the user. First, we assume an environment impedance $\underline{Z}_{\text{E}} < \underline{Z}_{\text{user}}$. Further evaluation leads to Eq. (7.66).

$$\underline{Z}_{\text{E}} = \frac{\underline{F}_{\text{E}}}{j\omega\underline{d}_{\text{E}}} < \frac{\underline{F}_{\text{user}}}{j\omega\underline{d}_{\text{user}}} = \underline{Z}_{\text{user}} \tag{7.66}$$

For an impedance type system, the user can be modeled as a source of deflection or velocity. In that case, the induced deflection of the teleoperation system equals the deflection of the environment $\underline{d}_{\text{user,int}} = \underline{d}_{\text{H}} = \underline{d}_{\text{E}}$. With Eq. (7.66) this leads to $\underline{F}_{\text{H}} = \underline{F}_{\text{E}} < \underline{F}_{\text{user}}$. Assuming, that the deflection $\underline{d}_{\text{user,int}}$ imposed by the user is smaller as the the user's detection threshold d_θ (assumption no. 3), the resulting amount of force displayed to the user $|\underline{F}_{\text{user}}|$ is smaller than the individual force threshold F_θ according to Eq. (7.65).

This experiment can can extended to admittance type systems easily. Descriptively the result can be interpreted as the environment "evading" manipulation, as for example a slow moving hand in free air: The arm muscles serve as a deflection source moving the hand, but the interaction forces of the air molecules are too small to be detected.

For large environment impedances, the inequalities above are reversed. In that case, the forces or deflections resulting from the interaction are lager than the detection threshold, the user will feel an interaction with the environment.

Experiment Analysis

One can reason that the user impedance will limit the transparency error function from Eq. (7.64) from the experiment. This is done in such a way, that environment impedances lower than the user impedance will be neglected as shown in Eq. (7.67).

$$\underline{e}'_{\mathrm{T}} = \frac{\underline{Z}_{\mathrm{H}} - \max\left(\underline{Z}_{\mathrm{E}}, \underline{Z}_{\mathrm{user}}\right)}{\max\left(\underline{Z}_{\mathrm{E}}, \underline{Z}_{\mathrm{user}}\right)} \tag{7.67}$$

If the user impedance is greater than the environment impedance, the user impedance is used, since the user will not feel any haptic stimuli generated by the lower environment impedance. If the user impedance is smaller than the environment impedance, the environment impedance is used as a reference for the transparency error.

Up till now, only absolute detection thresholds were considered, that describe the detection properties of haptic perception. In a second step, the discrimination properties shall be considered in more detail. It is assumed, that a system is transparent *enough* for a satisfactory usage, if errors are smaller than the differences that can be detected by the user. This difference can be described in a conservative way by the ↪ JND as defined in Sect. 2.1. With that, a limit can be imposed on Eq. (7.67) as given by Eq. (7.68)

$$\underline{e}'_{\mathrm{T}} = \frac{\underline{Z}_{\mathrm{t}} - \max\left(\underline{Z}_{\mathrm{e}}, \underline{Z}_{\mathrm{user}}\right)}{\max\left(\underline{Z}_{\mathrm{e}}, \underline{Z}_{\mathrm{user}}\right)} < c_{\mathrm{JND(z)}} \tag{7.68}$$

This limit $c_{\mathrm{JND(z)}}$ is defined as the JND of an arbitrary mechanical impedance. Although this value is not clearly measurable, it can be either bordered by the JNDs of ideal components like springs, masses and viscous dampers (see Sect. 2.1 for values) or by the JNDs of forces and deflections (since a change in impedance can be detected if the resulting force or deformation for a fixed imposure of deflection or force respectively exceeds the JND). With known values, this leads to a probably sufficient limit of $\left|\underline{e}'_{\mathrm{T}}\right| \leq 3\,\mathrm{dB}$.

With Eq. (7.68) a perception-considering error term of the transparency of haptic teleoperation systems is given. One has to keep in mind the assumptions of the underlying thought experiment and the fact, that experimental evaluation of this approach is still focus of current research activities by the authors.

7.5.3 General Control Model for Teleoperators

In principle a telemanipulator system can be divided into three different layers as shown in Fig. 7.40. The first layer contains the mechanical, electrical and local control properties of the master device. The second layer represents the communication channels between the master and slave and therefore eventually occurring time delays. The third layer describes mechanical, electrical and local control properties of the

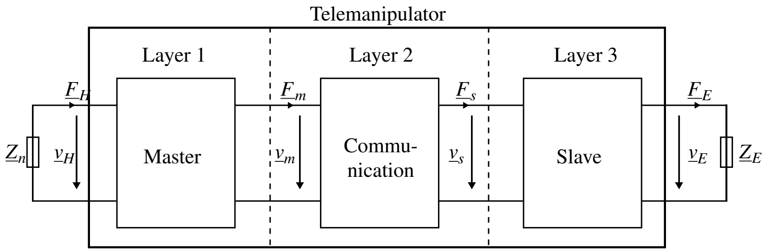

Fig. 7.40 Schematic illustration of a telemanipulator

slave device. As mentioned before the dynamic behavior of a master and accordingly a slave device (first and third layer) is determined by its mechanical and electrical characteristics. Dependent on the type of actuator used in the master device respectively slave device a distinction is made between impedance and admittance devices. Impedance devices receive a force command and apply a force to their environment. On the contrary admittance devices receive a velocity command and behave as a velocity source interacting with the environment (see Chap. 6).

Customarily dominant parameters are the mass and friction of the device. Compliance can be minimized by a well-considered mechanical design. In addition it can be assumed that the dynamic characteristics of the electronic can be disregarded because the mechanical design is dominating the overall performance of the device. A local controller design may extend the usable frequency range of the device and can guarantee a stable operation of the device. In addition it's possible to change the characteristics of the device from impedance behavior to admittance behavior and vice versa [25].

The second layer describes the characteristics of the communication channel. Significant physical values, which have to be transmitted between master and slave manipulator are the values for forces and velocities at the master and slave side. Therefore telemanipulators exhibit at least two and up to four communication channels for transmitting these values. These communication paths may be afflicted with a significant time delay T, which can cause instability of the whole system.

Figure 7.41 shows the system block diagram of a general four-channel architecture bilateral telemanipulator using impedance actuators for master and slave manipulator, for instance electric motors [24, 35]. In total there are four possible combinations of impedance and admittance devices, impedance-impedance, impedance-admittance, admittance-impedance and admittance-admittance.

In this section the impedance-impedance architecture is used due to its common use because of the high hardware availability. The forces of user and environment $\underline{F}_{\mathrm{H}}$ and $\underline{F}_{\mathrm{E}}$ are independent values. The mechanical impedance of user and environment is described by $\underline{Z}_{\mathrm{H}}$ and $\underline{Z}_{\mathrm{E}}$. The communication layer contains of four transmission elements C_1, C_2, C_3 and C_4 for transmitting the contact forces and velocities $\underline{v}_{\mathrm{H}}$, $\underline{F}_{\mathrm{E}}$, $\underline{F}_{\mathrm{H}}$ and $\underline{v}_{\mathrm{E}}$ between master and slave side. $\underline{Z}_{\mathrm{m}}^{-1}$ and $\underline{Z}_{\mathrm{s}}^{-1}$ represent the mechanical

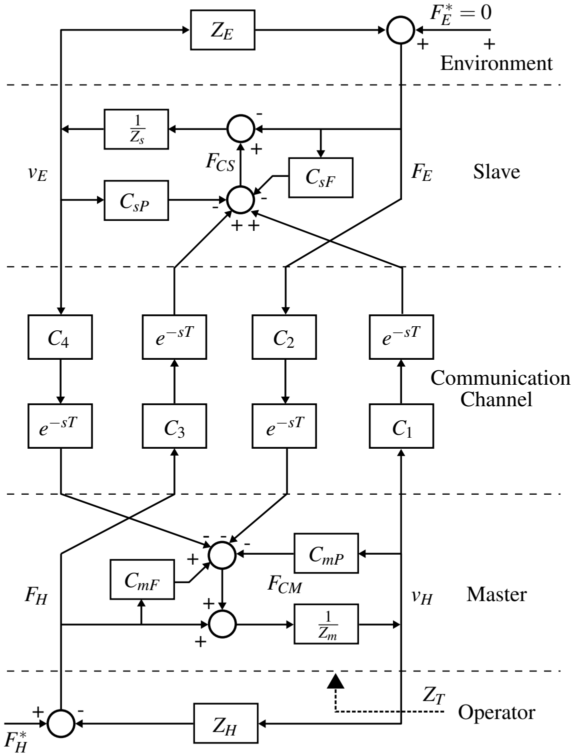

Fig. 7.41 System block diagram of a general telemanipulator in impedance-impedance-architecture as shown in [24]

admittance of master controller and slave manipulator. In addition C_{mP} and C_{sP} are local master and slave position controllers and C_{mF} and C_{sF} are local force controllers.

The dynamics of the four-channel architecture are described by the following equations:

$$\begin{aligned}
\underline{F}_{\mathrm{CM}} &= C_{\mathrm{mF}}\underline{F}_{\mathrm{H}} - C_4 e^{-sT}\underline{v}_{\mathrm{E}} - C_2 e^{-sT}\underline{F}_{\mathrm{E}} - C_{\mathrm{mP}}\underline{v}_{\mathrm{H}} \\
\underline{F}_{\mathrm{CS}} &= C_1 e^{-sT}\underline{v}_{\mathrm{H}} + C_3 e^{-sT}\underline{F}_{\mathrm{H}} - C_{\mathrm{sF}}\underline{F}_{\mathrm{E}} - C_{\mathrm{sP}}\underline{v}_{\mathrm{E}} \\
\underline{Z}_{\mathrm{s}}\underline{v}_{\mathrm{E}} &= \underline{F}_{\mathrm{CS}} - \underline{F}_{\mathrm{E}} \\
\underline{Z}_{\mathrm{m}}\underline{v}_{\mathrm{H}} &= \underline{F}_{\mathrm{CM}} + \underline{F}_{\mathrm{H}}
\end{aligned}$$

So the closed loop dynamics of the telemanipulator are represented by

$$\left(\underline{Z}_{\mathrm{m}} + C_{\mathrm{mP}}\right) \cdot \underline{v}_{\mathrm{H}} + C_4 e^{-sT}\underline{v}_{\mathrm{E}} = (1 + C_{\mathrm{mF}}) \cdot \underline{F}_{\mathrm{H}} - C_2 e^{-sT}\underline{F}_{\mathrm{E}} \tag{7.69}$$

$$-\left(\underline{Z}_{\mathrm{s}} + C_{\mathrm{sP}}\right) \cdot \underline{v}_{\mathrm{E}} + C_1 e^{-sT}\underline{v}_{\mathrm{H}} = (1 + C_{\mathrm{sF}}) \cdot \underline{F}_{\mathrm{E}} - C_3 e^{-sT}\underline{F}_{\mathrm{H}} \tag{7.70}$$

As presented in Sect. 7.5.1 it is common to describe the dynamics of a telemanipulator by two-port representation. In addition several stability analysis methods can be applied on two-port model. From Eqs. (7.69) and (7.69) with (7.58) the following h-parameters can be obtained:

$$\underline{h}_{11} = \frac{(\underline{Z}_{\mathrm{m}} + C_{mP}) \cdot (\underline{Z}_{\mathrm{s}} + C_{sP}) + C_1 C_4 e^{-2sT}}{(1 + C_{mF}) \cdot (\underline{Z}_{\mathrm{s}} + C_{sP}) - C_3 C_4 e^{-2sT}} \tag{7.71}$$

$$\underline{h}_{12} = \frac{C_2(\underline{Z}_{\mathrm{s}} + C_{sP}) e^{-sT} - C_4(1 + C_{sF}) e^{-sT}}{(1 + C_{mF}) \cdot (\underline{Z}_{\mathrm{s}} + C_{sP}) - C_3 C_4 e^{-2sT}} \tag{7.72}$$

$$\underline{h}_{21} = -\frac{C_3(\underline{Z}_{\mathrm{m}} + C_{mP}) e^{-sT} + C_1(1 + C_{mF}) e^{-sT}}{(1 + C_{mF}) \cdot (\underline{Z}_{\mathrm{s}} + C_{sP}) - C_3 C_4 e^{-2sT}} \tag{7.73}$$

$$\underline{h}_{22} = \frac{(1 + C_{sF}) \cdot (1 + C_{mF}) - C_2 C_3 e^{-2sT}}{(1 + C_{mF}) \cdot (\underline{Z}_{\mathrm{s}} + C_{sP}) - C_3 C_4 e^{-2sT}} \tag{7.74}$$

With Eq. (7.62) and Eqs. (7.71)–(7.74) the impedance transmitted to the user $\underline{Z}_{\mathrm{T}}$ is given by Eq. (7.75) [25].

$$\underline{Z}_{\mathrm{T}} = \frac{(\underline{Z}_{\mathrm{m}} + C_{mP}) \cdot (\underline{Z}_{\mathrm{s}} + C_{sP}) + C_1 C_4 e^{-2sT} + \left[(1 + C_{sF}) \cdot (\underline{Z}_{\mathrm{M}} + C_{mP}) + C_1 C_2 e^{-2sT}\right] \cdot \underline{Z}_{\mathrm{E}}}{(1 + C_{mF}) \cdot (\underline{Z}_{\mathrm{s}} + C_{sP}) - C_3 C_4 e^{-2sT} + \left[(1 + C_{sF}) \cdot (1 + C_{mF}) + C_2 C_3 e^{-2sT}\right] \cdot \underline{Z}_{\mathrm{E}}} \tag{7.75}$$

Perfect transparency is achievable, if the time delay T is insignificant. The controllers must hold the following conditions, which are known as the transparency-optimized control law [24, 35]:

$$\begin{aligned} C_1 &= \underline{Z}_{\mathrm{s}} + C_{\mathrm{sP}} \\ C_2 &= 1 + C_{\mathrm{mF}} \\ C_3 &= 1 + C_{\mathrm{sF}} \\ C_4 &= -\left(\underline{Z}_{\mathrm{m}} + C_{\mathrm{mP}}\right) \\ C_2, C_3 &\neq 0 \end{aligned} \tag{7.76}$$

By use of local position and force controllers of master and slave C_{mp}, C_{sp}, C_{mF} and C_{sF}, a perfect transparency can achieved with only three communication-channels. In this case the force feedback from slave to master C_2 can be neglected [24, 26].

The most common control architecture is the forward-flow architecture [21] also known as force feedback or position-force architecture [35], which uses the two channels C_1 and C_2. C_3 and C_4 are set to zero. The position respectively velocity $\underline{v}_{\mathrm{h}}$ at the master manipulator is transmitted to the slave. The slave manipulator feeds back the contact forces between manipulator and environment $\underline{F}_{\mathrm{e}}$. Due to not compensated impedances of master and slave devices perfect transparency is not achievable by telemanipulators build up in the basic forward flow architecture. This architecture has been described and analyzed by many authors [8, 9, 21, 22, 25, 35].

7.5.4 Stability Analysis of Teleoperators

Besides the general stability analysis for dynamic systems from Sect. 7.2, several approaches for stability analysis of haptic devices has been published. Most of them use the two-port-representation introduced in Sect. 7.5.1 for stability analysis and controller design and were derived from classical network theory and communications technology. The subsequent section gives an introduction to the most important of them and also presents methods to guarantee stability of the system under time-delay.

7.5.4.1 Passivity

The concept of passivity for dynamic systems has been introduced in Sect. 7.2.2. Within this subsection the focus is on the application of this concept on the stability analysis of haptic devices. Assume the two-port representation of a telemanipulator as presented in Fig. 7.40. Furthermore, it shall be assumed that the energy stored in the system at time $t = 0$ is $V(t = 0) = 0$. The power P_{in} at the input of the system at a time t is given by the product of the force $F_{\mathrm{H}}(t)$ applied by the user to the master times the master velocity $v_{\mathrm{H}}(t)$.

$$P_{\mathrm{in}} = F_{\mathrm{H}}(t) \cdot v_{\mathrm{H}}(t)$$

Accordingly the power P_{out} at the output of the telemanipulator is given by the contact force of the slave $F_{\mathrm{E}}(t)$ manipulating the environment times the velocity of the slave $v_{\mathrm{E}}(t)$

$$P_{\mathrm{out}} = F_{\mathrm{E}}(t) \cdot v_{\mathrm{E}}(t)$$

Thus the telemanipulator is passive and therefore stable as long as the following inequality is fulfilled.

$$\int_0^t (P_{\mathrm{in}}(\tau) - P_{\mathrm{out}}(\tau)\mathrm{d}\tau) = \int_0^t (F_{\mathrm{H}}(\tau) \cdot v_{\mathrm{H}}(\tau) - F_{\mathrm{E}}(\tau) \cdot v_{\mathrm{E}}(\tau)\mathrm{d}\tau) \geq V(t) \quad (7.77)$$

Alternatively the criterion can be expressed in the form of the time derivative of Eq. (7.77)

$$F_{\mathrm{H}}(t) \cdot v_{\mathrm{H}}(t) - F_{\mathrm{E}}(t) \cdot v_{\mathrm{E}}(t) \geq V(t) \quad (7.78)$$

From Eq. (7.77) respectively Eq. (7.78) it can be seen that the telemanipulator must not generate energy to be passive. Thus a very easy method to receive a stable telemanipulator system is to implement higher damping, but it is decreasing the performance of the system.

Considering the frequency domain passivity of the system can be analyzed by using the immitance matrix of the transfer function [8, 9, 13–15, 40, 42, 43]. A system is passive and hence inherently stable, if the immitance matrix $G(s)$ of the n-port network is positive real. The criteria for positive realness of the immitance matrix, which have to be satisfied, are [7, 29]:

1. $G(s)$ has real elements for real s
2. The elements of $G(s)$ have no poles in $\mathrm{Re}(s) > 0$ and poles on the $j\omega$-axis are simple, and such that the associated residue matrix is non-negative definite Hermitian
3. For any real value of ω such that no element of $G(j\omega)$ has a pole for this value, $G(jw) + G(jw)$ is non-negative definite Hermitian
   For real rational $G(s)$, points 1 and 3 may be replaced by
4. $G(s) + G(s)$ is non-negative definite Hermitian in $\mathrm{Re}(s) > 0$.

User and Environment can be seen as passive [33] Therefore if passivity of the telemanipulator system can be proofed, the whole closed loop of user, telemanipulator and environment can be guaranteed to be passive and hence stable. It has been shown, that a robust (passive) control law and transparency are conflicting objectives in the design of telemanipulators [35]. In many cases the haptic sensation presented to the user can be poor, if a fixed damping value is used to guarantee passivity of the telemanipulator. Thus a new approach by using passivity based control law and improving performance has been done by implementing a passivity observer and passivity controller. The passivity controller increases damping of the system only when needed to guarantee stability. A further benefit from this concept is, that no parameter estimation for the dynamic model of the telemanipulator has to be done and if considered, uncertainties can be compensated [23, 44].

7.5.4.2 Absolute Stability Criterion (Llewellyn)

A stability criterion for linear two-ports has been derived by Llewellyn [12, 29, 36]. His motivation was the investigation of generalized transmission lines and active networks. Later several authors have used the criteria formulated by Llewellyn to analyze the stability of telemanipulators or to design control laws for bilateral teleoperation [3–5, 25]. The criterion is formulated in the frequency domain and it is assumed that the two-port is linear and time-invariant, at least locally [2]. A linear two-port is absolute stable if and only if there exists no set of passive terminations for which the system is unstable.

The following criteria provide both necessary and sufficient conditions for absolute stability for linear two-ports.

1. $G(s)$ has no poles in the right half s-plane, only simple poles on the imaginary axis
2. $\mathrm{Re}(g_{11}) > 0, \mathrm{Re}(g_{22}) > 0$
3. $2\cdot \mathrm{Re}(g_{11})\cdot \mathrm{Re}(g_{22}) \geq |g_{12}g_{21}| + \mathrm{Re}(g_{12}g_{21}) \qquad \forall\omega \geq 0.$

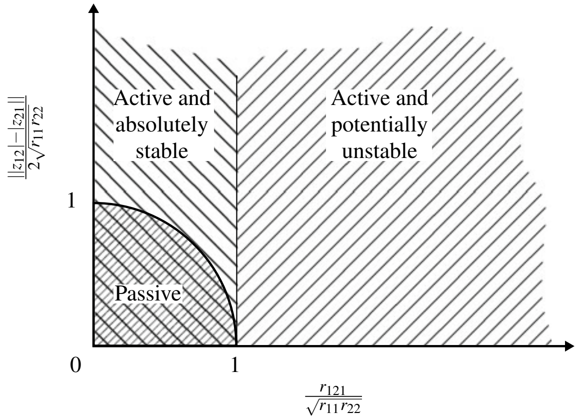

Fig. 7.42 Stability-Activity diagram

The conditions 1 and 2 guarantee passivity of the system when there is no coupling between master and slave. This case occurs, when master or slave are free or clamped. Condition 3 guarantees stability, if master and slave are coupled.

These criteria may be applied to every type of immitance matrix, thus the impedance-matrix, admittance-matrix, hybrid-matrix or inverse hybrid-matrix. If the criteria are fulfilled for one form of immitance matrix they are fulfilled for the other three forms as well. A network for which $h_{21} = -h_{12}$, which is the same as $z_{21} = z_{12}$ holds is said to be reciprocal. In this particular case the tests for passivity and unconditional stability are the same. A passive network will always be absolute stable, but an absolute stable network is not necessarily passive. A two-port which is not unconditional stable is potentially unstable, but this does not mean that it is definitely unstable as shown in Fig. 7.42.

7.5.5 *Effects of Time Delay*

When master and slave are far apart from each other, communication data have to be transmitted over a long distance with significant time-delays, which can lead to instabilities unless the bandwidth of signals entering the communication block is severely limited. Reason for this is a non-passive communication block [8], so energy is generated inside the communication block.

7.5.5.1 Scattering Theory

ANDERSON [8–10] used the scattering theory in order to find a stable control law for bilateral teleoperation systems with time delay. Scattering variables were well known from transmission line theory. The scattering operator S maps effort plus flow into effort minus flow and is defined in terms of an incident wave $F(t) + v(t)$ and a reflected wave $F(t) - v(t)$.

$$F(t) - v(t) = S(t)\,(F(t) + v(t))$$

For LTI systems S can be expressed in the frequency domain as follows:

$$F(s) - v(s) = S(s)\,(F(s) + v(s))$$

In the case of a two-port the scattering matrix can be related to the hybrid matrix $\mathbf{H}(s)$ by loop transformation, which leads to:

$$S(s) = \begin{pmatrix} 1 & 0 \\ 0 & -1 \end{pmatrix} \cdot (\mathbf{H}(s) - 1)\,(\mathbf{H}(s) + 1)^{-1}$$

To ensure passivity of the system the reflected wave must not carry higher energy content than the incident wave. Therefore a system is passive if and only if the norm of its scattering operator $S(s)$ is less than or equal to one [8].

$$\|S(s)\|_{\infty} <\leq 1$$

7.5.5.2 Wave Variables

Wave variables were used by NIEMEYER [40, 42] to design a robust control strategy for bilateral telemanipulation with time-delay. It separates the total power flow into two parts, one the power flowing into the system and the other part representing the power flowing out of the system. Afterward, these two parts are associated with input and output waves. This approach is also valid for non-linear systems. Assume the two-port shown in Fig. 7.43 using $\dot{x}_m$ and F_e as inputs.

Therefore the power flow through the two-port can be written as

$$P(t) = \dot{x}_M^T F_T - \dot{x}_s^T F_S = \frac{1}{2} u_M^T u_T - \frac{1}{2} v_M^T v_T + \frac{1}{2} u_S^T u_S - \frac{1}{2} v_S^T v_S.$$

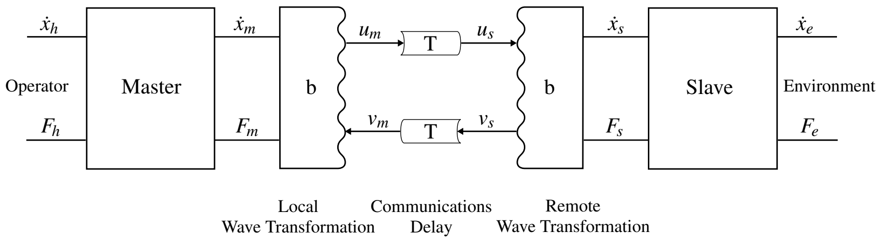

Fig. 7.43 Wave based teleoperator model

Here the vectors $\mathbf{u}_M$ and $\mathbf{u}_S$ are input waves, which increase the power flow into the system. Analog to this $\mathbf{v}_M$ and $\mathbf{v}_S$ are output waves decreasing the power flow into the system. Note that the velocity is denoted here as $\dot{x}$. The transformation from the power variables to wave variables is described by

$$\begin{aligned}
u_M &= \frac{1}{\sqrt{2b}}(F_M + b\dot{x}_M) \\
u_S &= \frac{1}{\sqrt{2b}}(F_S - b\dot{x}_S) \\
v_M &= \frac{1}{\sqrt{2b}}(F_M - b\dot{x}_M) \\
v_S &= \frac{1}{\sqrt{2b}}(F_S + b\dot{x}_S)
\end{aligned}$$

The wave impedance b relates velocity to force and represents an opportunity to tune the behavior of the system. Large b values leads to an increased force feedback at the cost of high inertial forces. Small b values lower any unwanted sensations, so fast movement is possible, but decreases also the force impression of contact forces between slave and environment [41]. The wave variables can be inverted to provide the power variables as a function of the wave variables.

$$\begin{aligned}
F_M &= \sqrt{\frac{b}{2}}(u_M + v_M) \\
F_S &= \sqrt{\frac{b}{2}}(u_S + v_S) \\
\dot{x}_M &= \frac{1}{\sqrt{2b}}(u_M - \dot{x}_M) \\
\dot{x}_S &= -\frac{1}{\sqrt{2b}}(u_S + v_S)
\end{aligned}$$

By transmitting the wave variables instead of the power variables the system remains stable even if the time-delay T is not known [40]. Note that when the actual time-delay T is reduced to zero, transmitting wave variables is identical to transmitting velocity and force.

7.6 Control of Rehabilitation Robots

In this section, some control strategies are explained briefly while avoiding the mathematical formulations. A rehabilitation robot needs to fulfill two requirements to be effective and comfortable. First, high accuracy trajectory tracking is needed to precisely follow the predefined trajectory by the physiotherapist. Second, avoidance of harsh interaction force or torque during the therapy, since the patient usually is not able to control her/his muscles, thus unpredicted movements occur. Therefore, the robot must suppress these undesired interactions in a way that the patient does not experience any harsh force or torque. Some of the strategies to meet the mentioned requirements are discussed in the following sections.

7.6.1 Control Strategies

The first controller choice is the well-known PID controller due to its simple structure and tuning rule. However, due to the highly nonlinear characteristics of rehabilitation robots, PID, fuzzy-PID, or adaptive-PID controllers result in significant undesired overshoot and response delay. Overshoot raises the uncomfortable feeling of the patients and if it is too large, it can cause harm to them. Therefore, a highly robust and stable control structure such as SMC is needed. Many variations of SMC are used in this field such as adaptive SMC, terminal SMC, and super-twisting nonsingular terminal SMC. The main drawback of SMC is the chattering phenomenon due to signum function and high-frequency switching when the system reaches the sliding surface.

In [6], a super-twisting nonsingular terminal sliding mode control (ST-NTSMC) is designed to guarantee the predefined trajectory tracking accuracy of a knee and ankle rehabilitation robot (KARR). As mentioned previously, the super-twisting algorithm eliminates the chattering of SMC while keeping the tracking accuracy. The non-singular terminal SMC is used to enhance the convergence speed and steady-state tracking of the linear-SMC without singularity. In rehabilitation, the goal is to track the predefined joint trajectory by the physiotherapist, while considering the patients' condition such as post-stroke patients who their muscles may move involuntary and exert torques to the robot, that are undesirable and could result in an uncomfortable situation or even worsen the patient's condition. Using admittance control before the ST-NTSMC could suppress this problem. As depicted in Fig. 7.44, instead of feeding the reference trajectory directly to the ST-NTSMC loop, the modified trajectory is used as the input of the SMC loop. This modification is done by measuring the interaction torque and applying it to a dynamic model to calculate the resulting change of the trajectory using equation (7.79).

$$M\ddot{\tilde{x}} + C\dot{\tilde{x}} + K\tilde{x} = \tau_{int} \tag{7.79}$$

where $\tilde{x} = x_r - x_m$,x_r is the predefined trajectory, and x_m is the modified smooth trajectory that ST-NTSMC will follow. The parameters of this dynamic model define the smoothness of the trajectory change. As a result, the predefined trajectory is adjusted in the direction of the interaction torque to eliminate uncomfortable force/torque.

As a result, the system allows deviation from reference trajectory when undesired interaction torque occurred, while accurately tracks the predefined trajectory when there is no interaction torque.

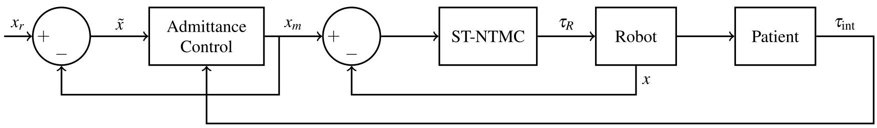

Fig. 7.44 The control structure of the rehabilitation robot [6]

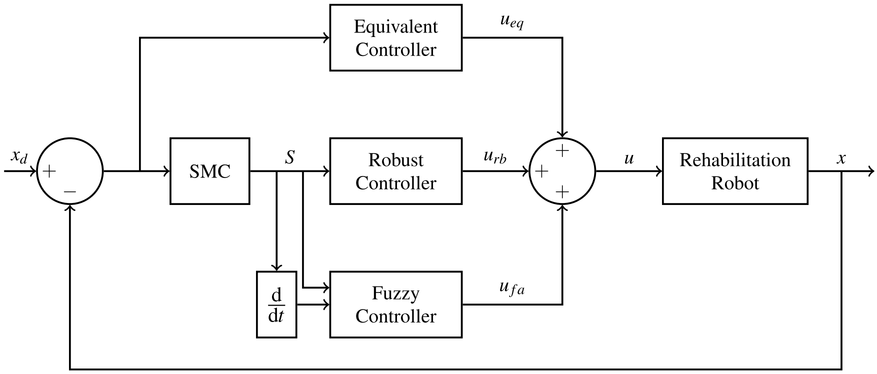

Fig. 7.45 Fuzzy sliding mode controller structure [39]

In [39], a fuzzy SMC is used for a hand rehabilitation robot. In this structure, the fuzzy controller is utilized to reduce the chattering of the SMC. The inputs of the fuzzy controller are S and $\dot{S}$ (sliding surface and its time derivative), and the output (u_{fa}) is a control signal to compensate for the abrupt variation of the SMC's control signal due to sign function and return the sliding variables to the desired surface Fig. 7.45. Experimental results show that the average chattering of the fuzzy SMC is about 25% of the original SMC.

To overcome the variation of the interaction force during the therapy and creating a smooth trajectory tracking performance, in [1], an adaptive law is proposed to estimate the interaction force (Fig. 7.46). The adaptive law is derived in a way that fulfills the Lyapunov stability criterion and is a function of S and robot's physical characteristics.

These are some examples of the control strategies that are used in rehabilitation robots to illustrate the importance of tracking accuracy and the smoothness of the interaction force or torque. The latter is more important and should be considered in the controller design.

7.6.2 *Friction and Backlash Compensation*

The practical systems are not ideal and face with friction (viscous and/or coulomb). In addition, based on the mechanical design and transmission mechanism they could

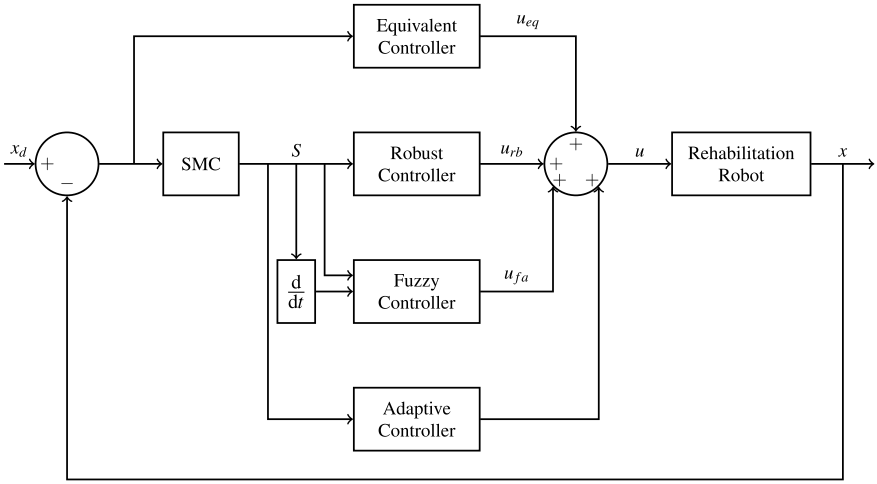

Fig. 7.46 Adaptive fuzzy sliding mode controller structure [1] © Springer Nature, all rights reserved

experience backlash as well. As discussed previously, backlash and coulomb friction are hard nonlinearities and during the controller design should be taken into consideration and suppressed.

In [6], the coulomb friction is considered and modelled as:

$$F(\dot{\theta}) = C\dot{\theta} + F_f sign(\dot{\theta}) \tag{7.80}$$

where C is the viscous friction coefficient and F_f is the coulomb friction. Furthermore, since precise modeling of a nonlinear system is not practical, the model is considered as the nominal model and the total friction is expressed as:

$$F(\dot{\theta}) = C\dot{\theta} + F_f sign(\dot{\theta}) + \Delta F(\dot{\theta}) \tag{7.81}$$

where $\Delta F(\dot{\theta})$ is the uncertainty of friction modeling. Using a robust controller such as ST-NTSMC (or mainly SMC), the system performs robustly with high tracking accuracy. It is important to mention that the accuracy of the nominal model directly affects the performance of the system.

Considering the backlash, the situation is worse since the backlash nonlinearity not only depends on the current condition but also the past condition. In [16, 17] a cable mechanism is used as a motion transmission mechanism. The mechanism is called Bowden-cable transmission where the input-output ($\phi_{in} - \phi_{out}$) relation can be expressed as:

$$\dot{\phi}_{out} = \begin{cases} c_1\dot{\phi}_{in} & \dot{\phi}_{in} > 0 \\ c_2\dot{\phi}_{in} & \dot{\phi}_{in} < 0 \end{cases} \tag{7.82}$$

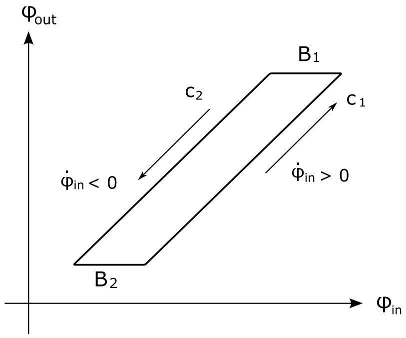

Fig. 7.47 Input-output relation of Bowden-cable transmission

or

$$\dot{\phi}_{out} = \begin{cases} c_1(\phi_{in} - B_1) & \dot{\phi}_{in} > 0 \\ c_2(\phi_{in} + B_2) & \dot{\phi}_{in} < 0 \end{cases} \quad (7.83)$$

Figure 7.47 depicts an example of the input-output relation of this mechanism and illustrates the parameter of equation (7.84).

The nonlinear equation (7.84) is considered as:

$$\phi_{out} = \alpha_{\phi}\phi_{in} + D \quad (7.84)$$

where $\alpha_{\phi} > 0$ is the slope of backlash hysteresis and the dead-zone is considered as the model uncertainty D. Therefore, an adaptive controller is designed to estimate the α_{ϕ} and D by getting the tracking error $(\phi_{in} - \phi_{out})$ as input. Experimental results show that the backlash configuration is either constant or variable (due to the flexibility of the sheaths); the adaptive compensation significantly enhances the tracking accuracy and reduces its error by a factor of five.

Compensating the backlash of this cable transmission mechanism allows putting the actuator(s) away from the joint(s), which reduces the inertia of the rehabilitation robot.

To put it in a nutshell, a robust controller such as SMC is needed for trajectory tracking. Moreover, a control strategy such as adaptive control or admittance control is required to allow the system to perform smoothly in case of undesired interaction force/torque from the patient, which is common for them. In addition, depending on the mechanical design, the friction and/or backlash should be considered and compensated effectively to ensure accurate and smooth tracking. Finally, since there exist uncertainties in the environment and patient interaction, the adaptive control, if designed properly, could significantly enhance the performance of the system.

7.7 Conclusion

The control design for haptic devices faces the developing engineer with a complex manifold challenge. According to the fundamental requirement, to establish a safe reliable and determined influence on all structures, subsystems, or processes the haptic system is composed of, an analytical approach for control system design is not negligible anymore. It provides a wide variety of methods and techniques to be able to cover many issues that arise during this design process. This chapter intends to introduce the fundamental theoretical background. It shows several tasks, functions and aspects the developer will have to focus on, as well as certain methods and techniques that are going to be useful tools for the system's analysis and the process of control design.

Starting with an abstracted view on the overall system, the control design process is based on an investigation and mathematical formulation of the system's behavior. To achieve this a wide variety of methods exists, that can be used for system description depending on the degree of complexity. Besides methods for the description of linear or linearized systems, this chapter introduced techniques for system description to represent nonlinear system behavior. Furthermore the analysis of multi-input multi-output systems is based on the state space description, which is presented here, too. All of these techniques on the one hand are aimed at the mathematical representation of the analyzed systems as exact as possible, on the other hand they need to satisfy the requirement for a system description that further control design procedures are applicable to. These two requirements will lead to a tradeoff between establishing an exact system formulation that can be used in analysis and control design procedures without extending the necessary effort unreasonably.

Within system analysis of haptic systems the overall system stability is the most important aspect that has to be guaranteed and proven to be robust against model uncertainties. The compendium of methods for stability analysis contains techniques that are applicable to linear or nonlinear system behavior, corresponding to their underlying principles that of course limit the usability. The more complex the mathematical formulation of the system becomes, the higher the effort gets for system analysis. This comes in direct conflict to the fact that a stability analysis of a system with a simplified system description can only provide a proof of stability for this simplified model of the real system. Therefore the impact of all simplifying assumptions must be evaluated to guarantee the robustness of the system stability.

The actual objective within establishing a control scheme for haptic systems is the final design of controller and control structures that have to be implemented in the system in various levels to perform various functions. Besides the design of applicable controllers or control structures the optimization of adjustable parameters is also part of this design process As shown in many examples in the literature on control design a comprehensive collection of control design techniques and optimization methods exists, that enable the developer to cover the emerging challenges, and satisfy various requirements within the development of haptic systems as far as automatic control is concerned.

Recommended Background Reading

[25] Hashtrudi-Zaad, K. & Salcudean, S.: **Analysis of control Architectures for Teleoperation Systems with Impedance/Admittance Master and Slave Manipulators**. In: The International Journal of Robotics Research, SAGE Publications, 2001.
Thorough analysis of different control schemes for impedance and admittance type systems.

[31] Hirche, S. & Buss, M.: **Human perceived transparency with time delay** In: Manuel Ferre et al. (eds.), Advances in Telerobotics, Springer, 2007.
Analysis of the effects of time delay on transparency and the perception of compliance and mass.

[47] Tavakoli, M.; Patel, R.; Moallem, M. & Aziminejad, A.: **Haptics for Teleoperated Surgical Robotic Systems** World Scientific Publishing, Shanghai, 2008.
Description and Design of a minimal invasive surgical robot with haptic feedback including an analysis of stability issues and the effect of time delay.

References

1. Abbasimoshaei A, Mohammadimoghaddam M, Kern TA (2020) Adaptive fuzzy sliding mode controller design for a new hand rehabilitation robot. In: International conference on human haptic sensing and touch enabled computer applications. Springer, pp 506–517
2. Adams R, Hannaford B (1999) Stable haptic interaction with virtual environments. IEEE Trans Robot Autom 15(3): 465–474. ISSN: hapt. https://doi.org/10.1109/70.768179
3. Adams R, Klowden D, Hannaford B (2000) Stable haptic interaction using the Excalibur force display. In: IEEE international conference on robotics and automation. Proceedings. ICRA ’00, vol 1, pp 770–775. https://doi.org/10.1109/ROBOT.2000.844144
4. Adams RJ, Hannaford B (1998) A two-port framework for the design of unconditionally stable haptic interfaces. In: 1998 IEEE/RSJ international conference on intelligent robots and systems. Proceedings, vol 2. IEEE, pp 1254–1259. https://doi.org/10.1109/IROS.1998.727471
5. Adams RJ, Hannaford B (2002) Control law design for haptic interfaces to virtual reality. IEEE Trans Control Syst Technol 10(1):3–13. https://doi.org/10.1109/87.974333
6. Almaghout K et al (2020) Design and control of a lower limb rehabilitation robot considering undesirable torques of the patient’s limb. Proc Inst Mech Eng Part H J Eng Med 234(12): 1457–1471
7. Anderson B (1968) A simplified viewpoint of hyperstability. IEEE Trans Autom Control 13(3):292–294. https://doi.org/10.1109/TAC.1968.1098910
8. Anderson R, Spong M (1989) Bilateral control of teleoperators with time delay. IEEE Trans Autom Control 34(5): 494–501. ISSN: 0018-9286. https://doi.org/10.1109/9.24201
9. Anderson RJ, Spong MW (1992) Asymptotic stability for force reflecting teleoperators with time delay. Int J Robot Res 11(2):135–149. https://doi.org/10.1177/027836499201100204
10. Anderson R, Spong MW (1988) Hybrid impedance control of robotic manipulators. IEEE J Robot Autom 4(5):549–556. https://doi.org/10.1109/56.20440
11. Baghli FZ et al (2014) Arm manipulator position control based on multi-input multi-output PID strategy. J Autom Mob Robot Intell Syst 8

12. Bolinder E (1957) Survey of some properties of linear networks. IRE Trans Circuit Theory 4(3): 70–78. ISSN: 0096-2007. https://doi.org/10.1109/TCT.1957.1086385
13. Colgate J (1993) Robust impedance shaping telemanipulation. IEEE Trans Robot Autom 9(4): 374–384. ISSN: 1042-296X. https://doi.org/10.1109/70.246049
14. Colgate J, Brown J (1994) Factors affecting the Z-Width of a haptic display. In: 1994 IEEE international conference on robotics and automation. Proceedings, May 1994, vol 4, pp 3205–3210. https://doi.org/10.1109/ROBOT.1994.351077
15. Colgate J, Stanley M, Brown J (1995) Issues in the haptic display of tool use. In: 1995 IEEE/RSJ international conference on intelligent robots and systems. Human robot interaction and cooperative robots. Proceedings, Aug 1995, vol 3, pp 140–145. https://doi.org/10.1109/IROS.1995.525875
16. Dinh BK et al (2016) Position control using adaptive backlash compensation for Bowden cable transmission in soft wearable exoskeleton. In: 2016 IEEE/RSJ international conference on intelligent robots and systems (IROS). IEEE, pp 5670–5676
17. Dinh BK et al (2017) Adaptive backlash compensation in upper limb soft wearable exoskeletons. Robot Auton Syst 92:173–186
18. Föllinger O (1991) Nichtlineare Regelungen 1. Grundlagen und Harmonische Balance. R. Oldenbourg Verlag GmbH. ISBN: 3-486-21895-6
19. Föllinger O (1970) Nichtlineare Regelungen. 2. Anwendung der Zustandsebene. R. Oldenbourg Verlag GmbH. ISBN: 978-3486218992
20. Föllinger O (1970) Nichtlineare Regelungen. 3. Ljapunow-Theorie und Popow-Kriterium. R. Oldenbourg Verlag GmbH
21. Hannaford B (1989) A design framework for teleoperators with kinesthetic feedback. IEEE Trans Robot Autom 5(4): 426–434. ISSN: 1042-296X. https://doi.org/10.1109/70.88057
22. Hannaford B (1989) Stability and performance tradeoffs in bi-lateral telemanipulation. In: 1989 IEEE international conference on robotics and automation. Proceedings, May 1989, vol 3, pp 1764–1767. https://doi.org/10.1109/ROBOT.1989.100230
23. Hannaford B, Ryu J (2002) Time-domain passivity control of haptic interfaces. IEEE Trans Robot Autom 18(1):1–10. https://doi.org/10.1109/70.988969
24. Hashtrudi-Zaad K, Salcudean S (1999) On the use of local force feedback for transparent teleoperation. In: IEEE international conference on robotics and automation, vol 3, pp 1863–1869. https://doi.org/10.1109/ROBOT.1999.770380
25. Hashtrudi-Zaad K, Salcudean S (2001) Analysis of control architectures for teleoperation systems with impedance/admittance master and slave manipulators. Int J Robot Res 20(6):419–445. https://doi.org/10.1177/02783640122067471
26. Hashtrudi-Zaad K, Salcudean SE (2002) Transparency in time-delayed systems and the effect of local force feedback for transparent teleoperation. IEEE Trans Robot Autom 18(1):108–114. https://doi.org/10.1109/70.988981
27. Hatzfeld C (2013) Experimentelle Analyse der menschlichen Kraftwahrnehmung als ingenieurtechnische Entwurfsgrundlage für haptische Systeme. Dissertation, Technische Universität Darmstadt. http://tuprints.ulb.tu-darmstadt.de/3392/. München: Dr. Hut Verlag. ISBN: 978-3-8439-1033-0
28. Hatzfeld C, Werthschützky R (2012) Mechanical impedance as coupling parameter of force and deflection perception: experimental evaluation. In: Isokoski P, Springare J (eds) Proceedings of the eurohaptics conference haptics: perception, devices, mobility, and communication, Tampere, FIN. LNCS, vol 7282. Springer, Heidelberg. https://doi.org/10.1007/978-3-642-31401-8_18
29. Haykin S (1970) Active network theory. Electrical engineering. Addison-Wesley. ISBN: 978-0201026801
30. Heredia E, Rahman T, Kumar V (1996) Adaptive teleoperation transparency based on impedance modeling. In: SPIE proceedings, vol 2901, pp 2–12. https://doi.org/10.1117/12.26299
31. Hirche S, Buss M (2007) Human perceived transparency with time delay. In: Advances in telerobotics, pp 191–209. https://doi.org/10.1007/978-3-540-71364-7_13

32. Hirsch M (2013) Auswahl und Entwurf eines Positionsreglers unter Berücksichtigung nichtlinearer Effekte für einen parallelkinematischen Mechanismus". Diploma Thesis. Technische Universität Darmstadt
33. Hogan N (1989) Controlling impedance at the man/machine interface. In: IEEE international conference on robotics and automation (ICRA), Scottsdale, AZ, USA, pp 1626–1631. https://doi.org/10.1109/ROBOT.1989.100210
34. Khalil HK (2002) Nonlinear systems. Prentice Hall. ISBN: 0-130-67389-7
35. Lawrence D (1993) Stability and transparency in bilateral teleoperation. IEEE Trans Robot Autom 9(5):624–637. https://doi.org/10.1109/CDC.1992.371336
36. Llewellyn FB (1952) Some fundamental properties of transmission systems. In: Proceedings of the IRE 40.3 , pp 271–283. ISSN: 0096-8390. https://doi.org/10.1109/JRPROC.1952.273783
37. Lunze J (2006) Regelungstechnik 1. Springer, Berlin. ISBN: 3-540-28326-9
38. Lunze J (2005) Lunze J (2005) Regelungstechnik 2. Springer, Berlin. ISBN: 3-540-22177-8
39. Moshaii AA, Moghaddam MM, Niestanak VD (2019) Fuzzy sliding mode control of a wearable rehabilitation robot for wrist and finger. In: Industrial robot: the international journal of robotics research and application
40. Niemeyer G, Slotine J-J (1991) Stable adaptive teleoperation. IEEE J Ocean Eng 16(1): 152–162. ISSN: 0364-9059. https://doi.org/10.1109/48.64895
41. Niemeyer G, Preusche C, Hirzinger G (2008) Telerobotics. In: Siciliano B, Khatib O (eds) Springer handbook of robotics. Springer, Berlin, Heidelberg, pp 741–757. https://doi.org/10.1007/978-3-540-30301-5_32
42. Niemeyer G, Slotine J-J (1998) Towards force-reflecting teleoperation over the internet. In: 1998 IEEE international conference on robotics and automation. Proceedings, vol 3. IEEE, pp 1909–1915. https://doi.org/10.1109/ROBOT.1998.680592
43. Raju G, Verghese G, Sheridan T (1989) Design issues in 2-port network models of bilateral remote manipulation. In: IEEE international conference on robotics and automation (ICRA), Scottsdale, AZ, USA, pp 1316–1321. https://doi.org/10.1109/ROBOT.1989.100162
44. Ryu J-H, Kwon D-S, Hannaford B (2004) Stable teleoperation with time-domain passivity control. In: IEEE Trans Robot Autom 20(2): 365–373. https://doi.org/10.1109/TRA.2004.824689
45. Slotine J-JE, Li W (1991) Applied nonlinear control. Prentice Hall. ISBN: 0-130-40890-5
46. Sorensen RA (1998) Thought experiments. Oxford University Press, Oxford, GB. ISBN: 9780195129137 (Reprint)
47. Tavakoli M et al (2008) Haptics for teleoperated surgical robotic systems. World Scientific Publishing. ISBN: 978-981-281-315-2
48. Unbehauen H (2007) Regelungstechnik I. Vieweg und Teubner. ISBN: 3-834-80230-1
49. Unbehauen H (2007) Regelungstechnik II: Zustandsregelungen, digitale und nichtlineare Regelsysteme. Vieweg und Teubner. ISBN: 3-528-83348-3

Chapter 8
Kinematic Design

Fady Youssef and Sebastian Kassner

Abstract One aspect in haptic devices is the design of the kinematics. The kinematics of a mechanism is the key to implement and accomplish the design goals, like transmitting dynamic feedback in the form of forces or torques, or allowing a sufficient workspace for the user to interact with environment. This chapter introduces the steps of the kinematic design. The chapter consists of five main sections. The first section gives an overview on some basic definitions and the main types of mechanisms. In the second section, the first step in the design, defining the structure of the mechanism, is introduced. This is accompanied with an example. After choosing the most applicable structure for the desired application, the second step takes place, where the kinematic equations are solved. These equations are used to describe the relation between the operating point of the mechanism and the base at any point in time. Different approaches are used to solve those equations depending on the type of the mechanism used. The third and final step in the design process is introduced in the fourth section. This step contains the optimization process of the mechanism in order to achieve a desired operation of the mechanism. Last but not least, the importance of modeling and simulation is discussed in the last section.

8.1 Introduction

The introduction to the topic of kinematic design begins with mentioning the major goals behind the kinematic design. Then, some basic definitions are introduced, followed by a classification of the mechanisms used in haptic interfaces. Finally an introduction to the design steps is given.

F. Youssef (✉)
Hamburg University of Technology, Eißendorfer Str. 38, 21073 Hamburg, Germany
e-mail: f.youssef@tuhh.de

S. Kassner
Knorr-Bremse Systeme für Schienenfahrzeuge GmbH, Moosacher Str. 80, 80809 München, Germany
e-mail: sebastian.kassner@kassner-net.de

T. A. Kern et al. (eds.), *Engineering Haptic Devices*, Springer Series on Touch and Haptic Systems, https://doi.org/10.1007/978-3-031-04536-3_8

8.1.1 Major Design Goals

Kinematics has a big role in haptic devices. It's the mechanical interface between the user and the environment. Different design goals are available depending on the application. In some applications, the goal of the design is to transmit dynamic feedback, e.g. forces or torques, to the user. Other applications require sufficient workspace to ensure the interaction between the user and the environment.

8.1.2 Basic Definitions

In the area of haptic interfaces, some definitions are valid apart from the type of the mechanism used.

Kinematics

Kinematics is the branch in mechanics that studies the motion of points and bodies in space in terms of position, velocity and acceleration without taking into consideration the cause of this motion, e.g forces or torques.

Dynamics

Dynamics, sometimes referred as kinetics, is the branch in mechanics that studies the motion in space with the cause of the motion is considered.

Degree of Freedom

Degrees of freedom are the number of independent motions a body or a mechanism is able to carry out. A free body has 3 DoF in 2D, two translations and one rotation, while in 3D has 6 DoF, three translations and three rotations. Figure 8.1 shows the possible independent motions a body can do in space.

Joints

Joints are used to connect two or more bodies together. Depending on the type of the joint used, the number of allowed relative DoF between the connected bodies is defined. The commonly used joints allow either 1,2 or 3 DoF. Figure 8.2 shows several types of joints.

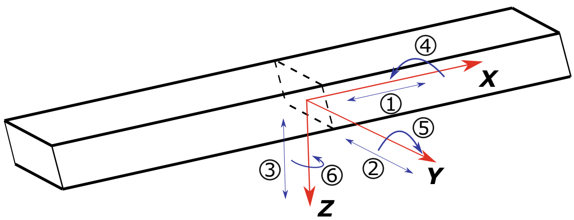

Fig. 8.1 Independent motions of a free body in space. 3 translations and 3 rotations along and about the 3 axes (x, y, z)

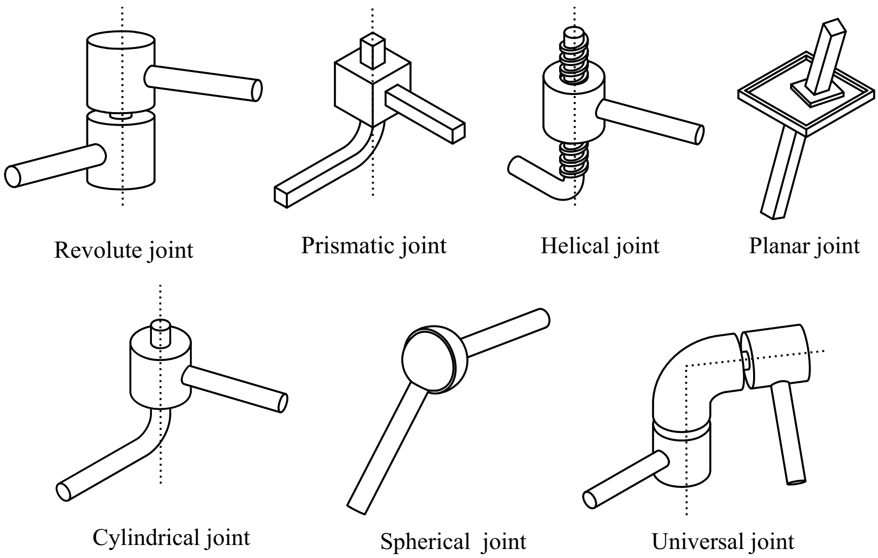

Fig. 8.2 Different types of joints. 1. DoF: Revolute (R), Prismatic (P), Helical (H). 2. DoF: Planar (E), Cylindrical (C), and Universal (U). 3. DoF: Spherical (S)

Active Joints

These are the actuated joints in a mechanism.

Passive Joints

These are the non-actuated joints in a mechanism.

Base

The base is the reference platform of the mechanism. All the calculations are performed relative to this platform. Positions, velocities, and accelerations of any point on the mechanism are given with respect to the base.

Tool Center Point

TCP is the point where the user, or the environment, interacts with the mechanism. Usually it's the end-point of the mechanism.

Workspace

The workspace is the set of all positions in space the TCP can reach.

Singularity

Position in the mechanism's workspace where the mechanism loses the control of one or more DoF. This can be seen in having non-solvable equations. Singularities will be further discussed in Sect. 8.4.2.

Translational Parallel Machine

TPM is a mechanism whose TCP is allowed only to move in Cartesian space (x, y, z).

8.1.3 Classification of Mechanisms

There are three main configurations of mechanisms used in haptic interfaces: Serial, Parallel and Hybrid. This chapter will focus on both serial and parallel mechanisms. Figures 8.3 and 8.4 shows the different configurations of mechanisms used.

Serial Mechanisms

Serial mechanisms are open kinematic chains, in other words there is only one path from the base platform to the TCP. A typical serial mechanism consists of only active joints connected with rods (links). Usually one DoF joints are used. The number of intended DoF of the TCP defines the number of joints in the mechanism. Figure 8.5 shows UR10E from the company *Universal Robots*. The robot has 6 active revolute joints. As can be seen from the figure, there is only one path from the base to the TCP. The joints are connected in series. The advantages of serial mechanism are their simple design, their relatively large workspace and their relatively easy control especially in positioning tasks. On the other hand, the major disadvantage of serial mechanisms is that one actuator carries the load of the all the next actuators. In

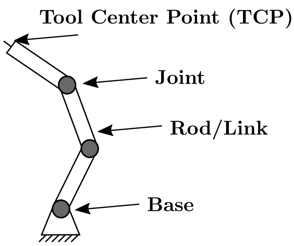

Fig. 8.3 Basic elements of a mechanism

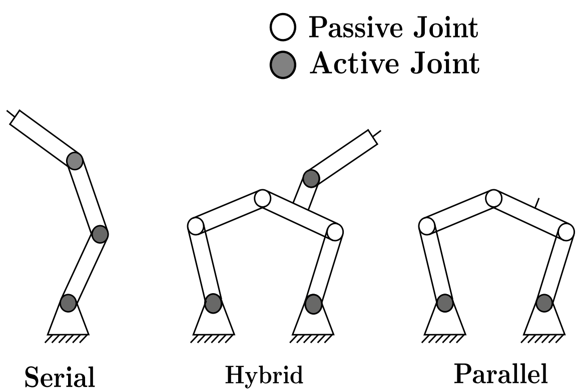

Fig. 8.4 Basic kinematic structures

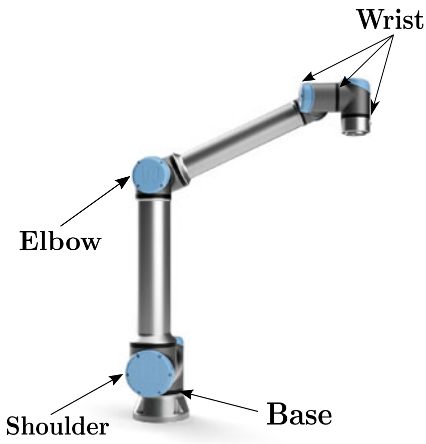

Fig. 8.5 Example of Serial mechanism, UR10E from the company *Universal Robots*

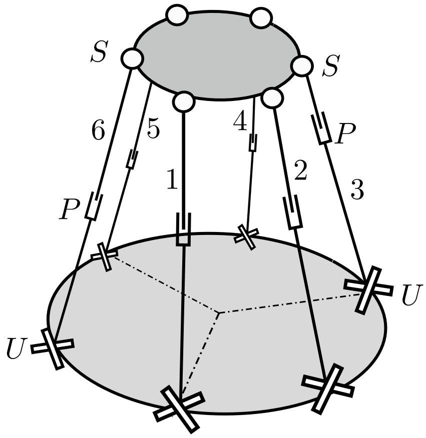

Fig. 8.6 STEWART- GOUGH mechanism

other words, any actuator should overcome its own inertia, the inertia of all the next actuators in the chain, and finally the load acting on the TCP. This drawback affects the dynamic behaviour of serial mechanisms. This drawback can reflect on the mechanism to have an overall low structural stiffness with respect to its own weight.

Parallel Mechanisms

Parallel mechanisms are closed chains mechanisms. In parallel mechanisms, there are at least two paths from the base platform to the TCP. A typical parallel mechanism consists of both active and passive joints. The number of active joints is defined by the intended DoF of the TCP. The most famous parallel mechanism is the STEWART-GOUGH platform Fig. 8.6. Another example of parallel mechanism, OMEGA6 haptic device from the company *Force Dimension*, is shown in Fig. 8.7. OMEGA6 is a pen-shaped force-feedback device. From the figure, one can see that there are three paths

Fig. 8.7 OMEGA6 haptic device, © 2022 *Force Dimension*, used with permission

from the base to the TCP. The main advantage of parallel mechanisms is that the load on the TCP is distributed on multiple kinematic chains, this will lead to a lightweight design, yet a high structural stiffness. The same advantage leads to high transparent transmission of haptic feedback, which is the reason why this configuration is of a great importance in haptic interfaces. On the other hand, the main disadvantages are small workspace and relative complexity of solving the kinematic equations compared to serial mechanisms, in addition to singular positions which is discussed later in this chapter in Sect. 8.4.2.

Hybrid Mechanisms

Hybrid mechanisms are a combination of both serial and parallel mechanisms. It contains both open and closed chains. The most well known example of a hybrid mechanism is the Tricept (Fig. 8.8). It is composed of parallel part that create the translation in the workspace, followed by a serial part in order to create the orientation of the TCP in space [19]. Decoupling the serial part from the parallel part simplifies the design of the mechanism. Hybrid mechanisms stands in between the serial and parallel mechanisms in terms of advantages and disadvantages; they can have a lightweight design compared to pure serial mechanisms and a larger workspace compared to pure parallel mechanisms. In this chapter we will focus on pure serial and pure parallel mechanisms.

8.1.4 Design Steps

Designing the kinematic mechanism of haptic interfaces passes through three steps:

- Defining the structure (Sect. 8.2): In this step, the type of mechanism, the number of appropriate DoF of the joints are defined. This is done based on the application.

Fig. 8.8 TRICEPT T606 parallel kinematic, © 2022 *PKMtricept*, used with permission

- Solving the kinematic equations (Sect. 8.3): In this step the basic foundation for controlling the mechanism is defined. These equations are used later in the last design step.
- Finally dimensioning the mechanism (Sect. 8.4): In this step, the optimization of the mechanism in terms of lengths is done. The optimization process is done based on the intended tasks.

If a serial, a parallel or a hybrid mechanism is suitable for the design of a haptic interface should be decided on a case-by-case basis. All are used in haptic applications.

8.2 Design Step 1: Defining the Mechanism's Structure

The first step in designing the mechanism is the definition of the structure. It leads to the basic configuration of joints, rods and actuators. While the basic structure of the haptic interface is defined in this step, the topological synthesis has to be carried out very thoroughly.

The topological synthesis should be based on an analysis of the specific task. At least the following issues should be addressed:

- Degrees of freedom: In how many DoF should the user interact with the haptic interface? Which DoF are required (e.g. one pure rotatory as in a jog wheel, three to mimic spatial interaction or even six to display three translations and three rotations)?
- Adaption of existing structures: Should the device adapt the structure of the task (e.g. a controlled robot) or of the user (e.g. the user's finger or arm)?

- Workspace: How large is the desired workspace, the TCP has to move in? Are there any restrictions (e.g. areas of the workspace which should not be accessed)?
- Mobility: Is the haptic interface designed as a device which is standing on a fixed place, e.g. on a table, or is designed as a portable device?

The analysis of these requirements lays the foundation for the design of an easy-to-use and ergonomic haptic interface which will be accepted by the user.

8.2.1 Synthesis of Serial Mechanisms

A serial mechanism is not less or more than a sequence of rods and actuators, whereas the actuators can be regarded as driven (active) joints. Whether the actuators are linear or rotary is of no importance for the complexity of the kinematic problem. For the workspace and the orientation of the TCP however this aspect is of highest importance.

A widely used design in serial kinematics is to split the joints into two groups: the first group is responsible for the translation of the TCP, and the second group is responsible for the orientation of the TCP. In Fig. 8.5, one can see that the base, shoulder, and elbow joints are mainly responsible for the translation, while the three joints of the wrist are responsible for the orientation.

If it is not intended to generate a torque as output to the user, the handle attached to this serial mechanism has to be equipped with a passive universal joint. Such a realisation as haptic device can be found in Fig. 8.9, the torques are decoupled from the hand. The handle does not have to be placed exactly in the TCP, as the moments are eliminated by the passive joints. Force vectors can be displaced arbitrarily within space. As a result the hand experiences the same forces like the TCP.

As human beings are equipped with many serial kinematic chains (e.g. arms, legs) the working area of a serial kinematic chain can be understood intuitively. This makes it simple to design a corresponding haptic control unit. This is however not the only criterion and will be further addressed in Sect. 8.4. The design can be done geometrically “with circle and ruler”, however the following should be considered:

- Actuators add inertia and moving masses to the mechanism. In serial mechanisms all actuators are placed in series. This has negative influence on the dynamics of force transmission. Approaches for a dynamic analysis will be discussed later in this chapter in Sect. 8.4.4.
- A simple design criterion could be, to place actuators as near as possible to the base platform of the system and use transmission elements to the points/joints of actuation.

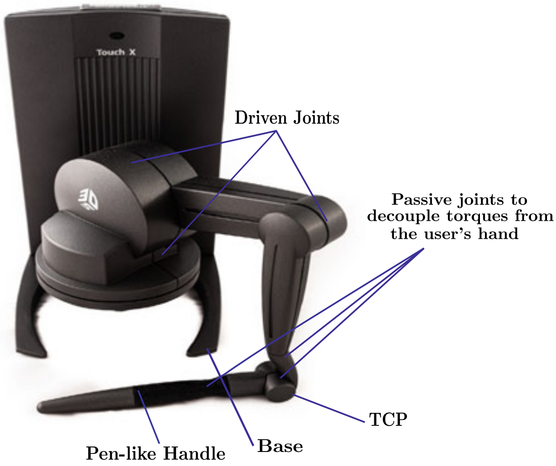

Fig. 8.9 TOUCHX haptic device from the company *3D Systems*

8.2.2 Synthesis of Parallel Mechanisms

The synthesis of a parallel mechanism in general is a less intuitive process than the synthesis of a serial mechanism.

Since a parallel structure comprises several kinematic chains, the fist step is to determine the required number of kinematic chains with respect to the desired degrees of freedom of the mechanism. This can be done using the ratio of the number of chains k and the degrees of freedom F of the mechanism leading to the degree of parallelism [7].

$$P_g = \frac{k}{F} \tag{8.1}$$

A mechanism is considered fully parallel, most common case, if $P_g = 1$. Partially parallel mechanism has $P_g < 1$, while highly parallel mechanism has $P_g > 1$. This means that for a fully parallel mechanism, the number of chains (legs) is equal to the desired number of DoF of the mechanism.

As mentioned earlier, parallel mechanisms consist of both active and passive joints. The relation between the joints (active and passive), and mechanism's DoF is done using the GRUEBLER- KUTZBACH- CHEBYCHEFF mobility criterion:

$$F = \lambda \cdot (n - g - 1) + \sum_{i=1}^{g} f_i - f_{id} + s \tag{8.2}$$

where:

F Mechanism's DoF
λ Spatial factor: 3 for 2D and 6 for 3D mechanisms
n Number of bodies

g Number of joints
f_i DoF of the i joint
f_{id} Sum of identical condition
s Sum of constraints

An identical link is given for example when a rod has universal joints at both of its ends. The rod will be able to rotate around its axis, without violating any constrains. Another example are two coaxial oriented linear joints.

Constraints appear whenever conditions have to be fulfilled to enable the movement. If five joint axes have to be parallel to a (6th) axis to enable a movement, then s = 5. Another example for a passive condition are two driving rods which have to be placed in parallel to enable a motion.

At this stage of the design, Eq. (8.2) can't be applied directly, as n and g aren't known yet. There exists a correlation between the number of chains (legs) k, joints g and elements n is defined according to:

$$n = g - k + 2 \tag{8.3}$$

Assuming spatial mechanism with no identical conditions and no constraints, applying Eqs. (8.3) in (8.2), the total number of joints' DoF to be distributed are:

$$\sum_{i=1}^{g} f_i = F + 6 \cdot (k - 1) \tag{8.4}$$

As a simple rule of thumb:

- Concentrate joint DoF: Universal joints and Spherical joints simplify the design and the transfer characteristics compared to serially placed joints with just one DoF each. Especially the kinematic transfer characteristics are much easier to formulate with concentrated joints.
- Usage of actuators fixed to the frame: With the actuators being fixed to the frame the dynamic properties of the design would be increased, as their mass isn't included in the inertia of the device anymore.
- DoF should be distributed symmetrically: A symmetrical design should be preferred compared to an asymmetrical one. The kinematic transfer functions get significantly simpler.

8.2.2.1 Special Case: Parallel Mechanisms with Pure Translation Motion

An important task of many haptic interfaces is the displaying pure three-dimensional spatial sensation. An example is the interaction with a pen-like tool where only forces in (x, y, z) should be displayed to the user. A special class of 3-DoF parallel mechanisms is used for those applications is TPM. This is achieved by kinematic chains which are blocking one or more rotatory DoF of the TCP and being able to perform translational motion in all directions.

According to CARRICATO [2, 3] two restrictions have to be fulfilled to ensure a parallel kinematic mechanism with pure translational motion:

- Spherical joints shall not be used.
- The axis of rotation of rotatory joints shall not be parallel to the axis of a degree of freedom which should be constrained.

Neglecting over-determined configurations, this results in so-called T5-mechanisms, each comprising four or five rotatory joints. Each joints constrains the rotation of the TCP about one axis. More details are found in [2, 3].

8.2.2.2 Example: DELTA Mechanism

One of the most common topologies to display spatial interaction is the parallel DELTA mechanism (Fig. 8.7). Due to its relevance in the field of haptic interfaces it is used as an example for the topological synthesis. Let us assume the design goal of a parallel kinematic haptic interface for a spatial interaction in (x, y, z). Thus a mechanism with three degrees of freedom is required. Using Eq. (8.1) for a fully parallel mechanism $P_g = 1$ on $F = 3$ haptic degrees of freedom leads to a mechanism with $k = 3$ kinematic chains or legs.

In a second step we have to determine the the required joint degrees of freedom using GRUEBLER'S formula (Eq. (8.2)). This leads to the sum of $\sum_{i=1}^{g} f_i = 15$ joint degrees of freedom.

Regarding an equal behavior in all spatial directions it is self-evident to distribute the 15 joint degrees of freedom with five degrees in each leg. This leads to the topologies in Table 8.1. The topologies are denominated according to the joints in one leg starting from the base of the mechanism to the TCP, e.g. a UUP mechanism comprises of a universal joint, followed by another universal joint, and finally one prismatic joint. The selection of an appropriate topology then can be carried on by a systematic reduction of the 3-DoF topologies in Table 8.1. The reduction is based on the following criteria:

- Functionality as a TPM: Criteria like the number of R-joints or the existence of a S-joint eliminate a large number of topologies.
- Position of actuators: Rotatory, linear or piston actuators (e.g. in a hydraulic system) act as R-, P- or C-joints. When having topologies with an U-joint attached to the base platform this would lead to actuators which are located within the kinematic chain. The required acceleration to move the actuators with relatively high masses then would inhibit that the dynamic advantages of a parallel mechanism have the fullest effect.
- Number of joints: A concentration of two R-joints into one U-joint and a R- and P-joint in into a C-joint respectively simplifies the mechanisms geometry and thereby its kinematic equations.

Table 8.1 Topologies for 3-DoF mechanisms with 5 DoF in each leg

Joints per leg	Topologies
1 × 1 DoF, 2 × 2 DoF	UUP, UPU, PUU, UUR, URU, RUU, CUP, CPU, CUR, CRU, RCU, UCP, UPC, PCU, UCR,URC, RUC, CCP, CPC, PCC, CCR, CRC, RCC
2 × 1 DoF, 1 × 3 DoF	SPP, SRR, SPR, SRP, PSP, RSP, PSR, RSR, PPS, RRS, RPS, PRS
3 × 1 DoF, 1 × 2 DoF	RRRU. RRUR, RURR, URRR, RRPU, RRUP, RURP, URRP, RPRU, RPUR, RUPR, RUPR, URPR, PRRU, PRUR, PURR, UPRR, RPPU, RPUP, RUPP, URPP, PRPU, PRUP, PURP, UPRP, PPPU, PPUP, PUPP, UPPP, RRRC, RRCR, RCRR, CRRR, RRPC, RRCP, RCRP, CRRP, RPRC, RPCR, RCPR, CRPR, PRRC, PRCR, PCRR, CPRR, RPPC, RPCP, RCPP, PRPC, PCRP, PPPC,PPCP, PCPP, CPPP
5 × 1 DoF	32 iterations of P- and R-joints

Taking into account the above mentioned criteria, the remaining configurations are: UPU, PUU, CUR, CRU, RUU and RUC (Fig. 8.10). Table 8.2 shows the eliminated topologies based on the different criteria. Looking carefully at these topologies in Fig. 8.10, one recognizes that only RUU and RUC have rotatory joint attached to the base platform. Thus these are the only two topologies that can be reasonably driven by a rotatory electrical motor. What makes the RUU (DELTA) mechanism special is that there are only joints with rotatory degrees of freedom within the kinematic chains. All forces and torques are converted into rotatory motion and there is no chance for the mechanism to cant. DELTA mechanisms have singular positions within the workspace. This has to be considered when dimensioning the mechanism Sect. 8.4. The RUU/DELTA was introduced in 1988 by Clavel [4]. Besides acting as a spatial haptic interface (Fig. 8.7), the mechanism is kind of widely used in robotic applications (e.g. pick-and-place tasks). In these devices with mainly kinaesthetic feedback, a mechanical mechanism is used to link the user and the feedback generating actuators. Furthermore the user's input commands are often given by moving a mechanical mechanism.

8.3 Design Step 2: Kinematic Equations

The second step in designing a mechanism is finding the relation between the base and the TCP at any point in time. This is done by solving the kinematic equations. There are two main types of kinematic equations; forward kinematic and inverse kinematic. Before addressing the kinematic equations, some basic definitions should be introduced.

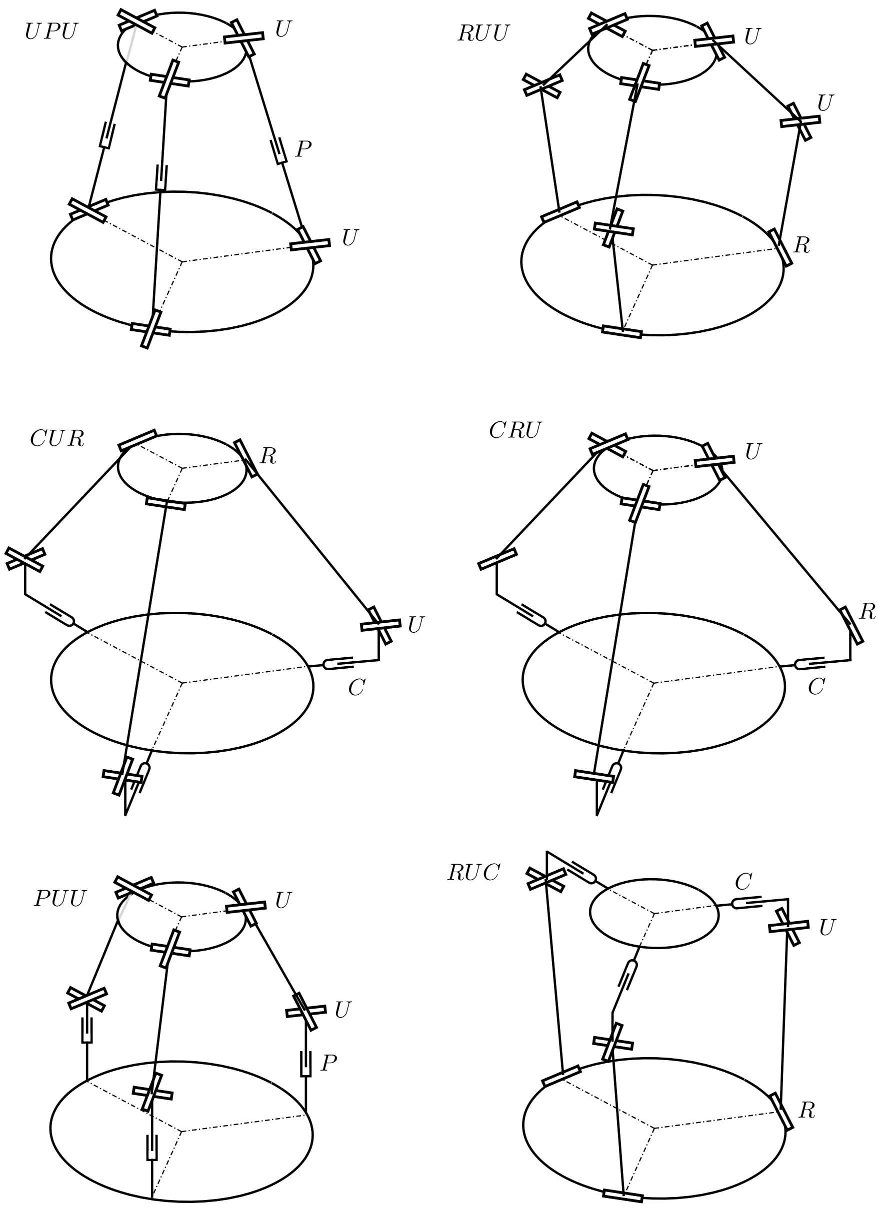

Fig. 8.10 Possible TPM mechanisms

Table 8.2 Eliminated topologies, sorted by the distribution of the 5 DoF in each leg

Elimination criterion	5 × 1 DoF	3 × 1 DoF, 1 × 2 DoF	2 × 1 DoF, 1 × 3 DoF	1 × 1 DoF, 2 × 2 DoF
No TPM	RRRRP, RRPRR, RRPPR, RRPPP, RPRRR, RPRRP, RPRPR, RPRPP, RPPRR, RPPRP, RPPPR, RPPPP, PRRRR, PRRRP, PRRPR, PRRPP, PRPRR, PRPRP, PRPPR, PPRRP, PPRPR, PPRPP, PPPRR, PPPRP, PPPPR, PPPPP, PRPPP	RPPU, RPUP, RUPP, URPU, PURP, UPRP, PPPU, PPUP, UPP, UPPP, RRPC, RRCP, RCRP, CRRP, RPRC, RPCR, RCPR, CRPR, PRRC, PRCR, PCRR, CPRR, RPPC, RPCP, RCPP, CRPP, PRPC, PRCP, PCRP, CPRP, PPPC, PPCP, PCPP, CPPP	SPP, SRR, SPR, SRP, PSP, RSP, PSR, RSR, PPS, RRS, RPS, PRS	CUP, CPU, RCU, UCP, UPC, PCU, PUC, UCR, CCP, CPC, PCC, CCR, CRC, RCC
High number of joints	RRRRR, RRRPR, RRPRP, PPRRR	RRRU, RRUR, RURR, RRPU, RRUP, RURP, RPRU, RPUR,RURP, PRRU, PRUR, PURR, UPRR, RRRC, RRCR, RCRR, CRRR		
Base joint can’t be used as an actuator		URRR, URRP, URPR		UUP, UUR, URU, URC

Forward Kinematics

Forward kinematics is defined as giving the joints’ angles/positions $q = (q_1, q_2, \ldots, q_n)$ as input and calculating the pose (position and orientation) $p = (p_1, p_2, \ldots, p_m)$ of the TCP.

$$p = f(q)$$

In serial kinematics, solving the forward kinematics is usually done analytically. On the other hand, for parallel mechanisms the direct kinematic problem can only be solved numerically. However, there are exceptions that can be seen later in this chapter.

An important application of the forward kinematic problem is the calculation of a input command in impedance controlled devices.

Inverse Kinematics

Inverse kinematics is the opposite to the forward kinematics. The pose of the TCP is given, and the joints' angles/positions are calculated.

$$q = f^{-1}(p)$$

Geometric, algebraic, and numerical methods are used to solve the inverse kinematics problem. The method used depends on the type of mechanism. Numerical methods can be applied to any type of mechanisms. Inverse kinematics in parallel mechanisms is usually easier to calculate compared to serial mechanisms.

In admittance controlled devices, inverse kinematics is used to calculate the required evasive movement in order to regulate a desired contact force between user and the haptic interface.

Coordinate Frames

Coordinate frame i, Fig. 8.11, or simply frame i, is composed of an origin O_i and three mutually orthogonal base vectors $(\hat{x}_i, \hat{y}_i, \hat{z}_i)$, that is fixed to a particular body [22]. The pose of each body (rod) in a mechanism is always expressed relative to another body. In other words, the pose can be expressed as the relation between two frames, each frame is stick to one body. The pose consists of two parts, position and rotation (orientation). In a mechanism, the most two important frames are the tool and base frames. The pose of the TCP, or any frame inside the mechanism, is usually given relative to the base frame.

Position Vector

Position vector is the vector connecting the origins of two frames. The 3×1 position vector of frame j relative to frame i is given as:

$${}^{i}p_j = \begin{bmatrix} {}^{i}p_j{}^{x} \\ {}^{i}p_j{}^{y} \\ {}^{i}p_j{}^{z} \end{bmatrix}$$

The components of this vector are the Cartesian coordinates of O_j in frame i. This gives the translation between the two origins.

Rotation Matrix

Orientation of frame j relative to frame i is expressed using rotation matrix. A rotation matrix is 3×3. It is composed as follows:

$${}^{i}R_j = \begin{bmatrix} \hat{x}_j \cdot \hat{x}_i & \hat{y}_j \cdot \hat{x}_i & \hat{z}_j \cdot \hat{x}_i \\ \hat{x}_j \cdot \hat{y}_i & \hat{y}_j \cdot \hat{y}_i & \hat{z}_j \cdot \hat{y}_i \\ \hat{x}_j \cdot \hat{z}_i & \hat{y}_j \cdot \hat{z}_i & \hat{z}_j \cdot \hat{z}_i \end{bmatrix}$$

For example, a simple rotation of frame j around $\hat{z}_i$ only by an angle θ (Fig. 8.12) gives the following rotation matrix:

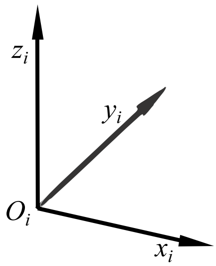

Fig. 8.11 Example of an arbitrary coordinate frame

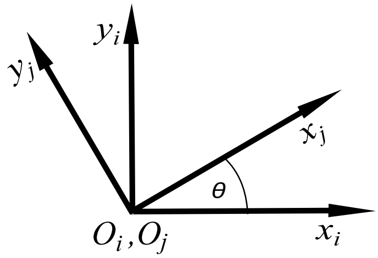

Fig. 8.12 Simple rotation of one frame around an axis of another frame

$$
{}^{i}R_j = \begin{bmatrix} \cos\theta & -\sin\theta & 0 \\ \sin\theta & \cos\theta & 0 \\ 0 & 0 & 1 \end{bmatrix}
$$

The different representations of multiple rotations can be found in [22].

Homogeneous Transformation Matrix

With homogeneous transformations, position vectors and rotation matrices are combined together in a compact notation. Homogeneous transformation matrix is a 4×4 matrix, and is given as follows:

$$
{}^{i}T_j = \begin{bmatrix} {}^{i}R_j & {}^{i}p_j \\ 0 & 1 \end{bmatrix}
$$

The matrix ${}^{i}T_j$ transforms vectors from frame j to coordinate frame i. Its inverse ${}^{j}T_i = {}^{i}T_j{}^{-1}$ transforms vectors from coordinate frame i to frame j.

Remarks:

- Matrix multiplications are associative, but they are not commutative. Thus the order for multiplication is highly important for the calculations, and specially in the forward kinematics.
- The numbers (0, 1) in the last row of the matrix guarantee that rotations and translations do not influence each other. With this feature a simple algorithm can perform

rotations and translations with a single matrix multiplication. This increases the clarity of an implementation and may be one reason why homogeneous coordinate transformations are widespread within robotics and even virtual reality programming.

8.3.1 Solving Kinematic Equations in Serial Mechanisms

In order to solve the forward kinematic equations in serial mechanisms, the DH convention is used. This convention was introduced by JACQUES DENAVIT and RICHARD HARTENBERG in 1955.

Denavit-Hartenberg Convention

In [5, 10, 22] the different variants of the DH convention, proximal and distal, are well differentiated. The convention is based on attaching frames to each link in the mechanism and performing two translations and two rotations to jump from one frame to the next one. Regardless the variant used, there are common steps as follow:

1. Defining and attaching a coordinate frame on each link (rod) according to the variant used, starting from the base to the TCP. The frames should be oriented in such way that frame *i + 1* can be reached from frame *i* after performing the four operations, two translations and two rotations.
2. Composing the DH-table using the DH-parameters (θ, d, a, α). These parameters represent the four operations (e.g. Table 8.4).
3. Formulation of the homogeneous transformation matrix ${}^{i}T_{i+1}$ that relates frame *i+1* to frame *i*. Each transformation matrix represents a row in the DH-table.
4. Multiplying all the transformation matrices to calculate the total transformation matrix that relates the TCP to the base, ${}^{base}T_{TCP}$.

$$
{}^{base}T_{TCP} = {}^{base}T_1 . {}^{1}T_2 . \ldots . {}^{n-1}T_n . {}^{n}T_{TCP} \tag{8.5}
$$

${}^{base}T_{TCP}$ gives the pose of the TCP in the base frame. The matrix is function of the active joints' values and the dimensions of the links. Substituting with the actuators angles/positions gives the TCP pose in result to the given set of values.

Inverse Kinematics in Serial Mechanisms

There are multiple approaches to solve the inverse kinematics problem in serial mechanisms. Generally, the inverse kinematics problem is nonlinear. A lot of questions rise when solving the inverse kinematics such as, whether there is a solution at all or the existence of multiple solutions. The two main approaches are closed-form and numerical solutions.

Pieper [20] introduced an approach to solve the inverse kinematics (closed-form) of a six DoF serial manipulator, where three axes meet at one point.

8.3.1.1 Example: UR10E

UR10E (Fig. 8.5) is one example of serial mechanisms used in haptic interfaces. The forward kinematics will be discussed in this part. The proximal variant (Modified DH convention) is used in this analysis. In the proximal variant:

- The frames start from the base as frame 0.
- The total number of frames is $n + 1$, where is n the number of links.
- The definition of the four parameters are different than in the classic convention as seen in Table 8.3.
- The transformation matrix relating any two frames $i - 1$ and i is given as follows:

$$
{}^{i-1}T_i = \begin{bmatrix} \cos\theta_i & -\sin\theta_i & 0 & a_{i-1} \\ \sin\theta_i \cos\alpha_{i-1} & \cos\theta_i \cos\alpha_{i-1} & -\sin\alpha_{i-1} & -d_i \sin\alpha_{i-1} \\ \sin\theta_i \sin\alpha_{i-1} & \cos\theta_i \sin\alpha_{i-1} & \cos\alpha_{i-1} & d_i \cos\alpha_{i-1} \\ 0 & 0 & 0 & 1 \end{bmatrix} \tag{8.6}
$$

The robotic arm has six revolute DoF, so we have a total seven frames and total of six rows of the DH-table (Table 8.4). The frames are given in Fig. 8.13. The next step is formulating the six transformation matrices as follow:

Table 8.3 Definitions of Modified DH parameters

Parameter	Description
a_{i-1}	Distance from Z_{i-1} to Z_i along X_{i-1}
α_{i-1}	Angle from Z_{i-1} to Z_i about X_{i-1}
d_i	Distance from X_{i-1} to X_i along Z_i
θ_i	Angle from X_{i-1} to X_i about Z_i

Table 8.4 DH Table of UR10E

$\boldsymbol{i}$	$\boldsymbol{a_{i-1}}$ (m)	$\boldsymbol{\alpha_{i-1}}$ (rad)	$\boldsymbol{d_i}$ (m)	$\boldsymbol{\theta_i}$ (rad)
1	0	0	$d_1 = 0.1807$	θ_1
2	0	$\pi/2$	0	θ_2
3	$a_2 = -0.6127$	0	0	θ_3
4	$a_3 = -0.57155$	0	$d_4 = 0.17415$	θ_4
5	0	$\pi/2$	$d_5 = 0.11985$	θ_5
6	0	$-\pi/2$	$d_6 = 0.11655$	θ_6

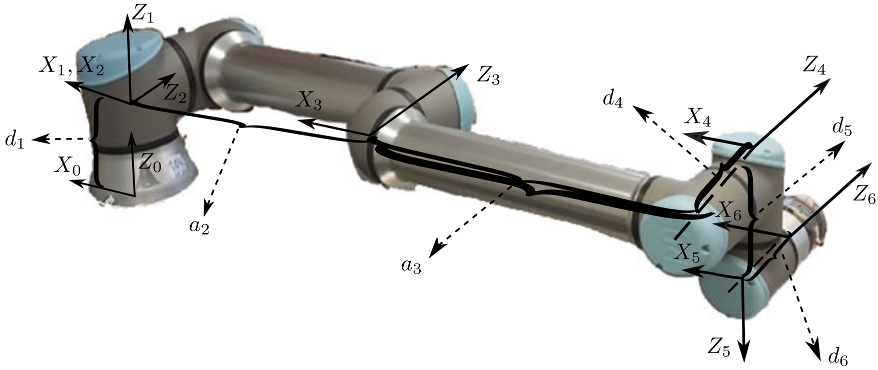

Fig. 8.13 Coordinate frames of UR10E according to modified DH convention

$$
{}^{0}T_1 = \begin{bmatrix} \cos\theta_1 & -\sin\theta_1 & 0 & 0 \\ \sin\theta_1 & \cos\theta_1 & 0 & 0 \\ 0 & 0 & 1 & d_1 \\ 0 & 0 & 0 & 1 \end{bmatrix}
$$

$$
{}^{1}T_2 = \begin{bmatrix} \cos\theta_2 & -\sin\theta_2 & 0 & 0 \\ 0 & 0 & -1 & 0 \\ \sin\theta_2 & \cos\theta_2 & 0 & 0 \\ 0 & 0 & 0 & 1 \end{bmatrix}
$$

$$
\vdots
$$

$$
{}^{5}T_6 = \begin{bmatrix} \cos\theta_6 & -\sin\theta_2 & 0 & 0 \\ 0 & 0 & -1 & d_6 \\ -\sin\theta_2 & -\cos\theta_2 & 0 & 0 \\ 0 & 0 & 0 & 1 \end{bmatrix}
$$

The total transformation matrix is given as follows:

$$
{}^{0}T_6 = {}^{0}T_1.{}^{1}T_2.{}^{2}T_3.{}^{3}T_4.{}^{4}T_5.{}^{5}T_6 \tag{8.7}
$$

The closed-form approach to solve the inverse kinematics of this robot is discussed in details in [11]. The numerical approach will be discussed later in this chapter in Sect. 8.5.3.

8.3.2 Solving Kinematic Equations in Parallel Mechanisms

Solving kinematic equations in parallel mechanisms is somehow different compared to serial mechanisms. The main goal remains the same, to get the relation between the pose of the TCP and the values of the joints' angles/positions. The presence of both active and passive joints adds complexity to the kinematic equations. Also, if the joints aren't distributed equally on all chains (legs), the kinematics gets more complicated.

Forward Kinematics

In contrast to serial mechanisms, for parallel mechanisms the direct kinematic problem can only be solved numerically. However, there are exceptions as can bee seen later. As mentioned earlier, the STEWART- GOUGH platform (Fig. 8.6) is one of the most famous parallel mechanisms. Solving the forward kinematics of this platform may end with 40 possible solutions [21] and [16]. Many approaches were introduced to solve the kinematics problem in general, like elimination [9], interval analysis [14], continuation [21]. Recently, other algorithms were introduced to cope with the real-time constraints, such as, using Neural networks [18], or using the information from the inverse kinematics and the small changes in the motion of the TCP [24].

Inverse Kinematics

The procedure of calculating the inverse kinematic problem can be split up into the following three steps:

1. Formulation of closed vector chains for each leg, starting at the coordinate system enclosing the TCP and going back to the reference coordinate system, usually the base.
2. Splitting the vector chains in all Cartesian movement directions of the individual leg.
3. Solving the resulting system of equations according to the TCP coordinates.

8.3.2.1 Example: RUU/DELTA Mechanism

TPM is a special case in parallel mechanisms. Solving the forward and inverse kinematics is somehow not complicated. One example of TPM is the RUU/DELTA mechanism.

Forward Kinematics

Figure 8.14 shows the necessary dimensions and angles to derive the kinematic equations. It is desired to express all these equations with respect to the world frame in the middle of the base platform. The x axis points towards the first leg. A local frame $(x_{A_i}, y_{A_i}, z_{A_i})$ with the origin A_i is fixed at the first joint of the i^{th} leg. This local coordinate system is rotated by $\phi_i = (i-1) \cdot 120$ degrees, with $i = 1, 2, 3$

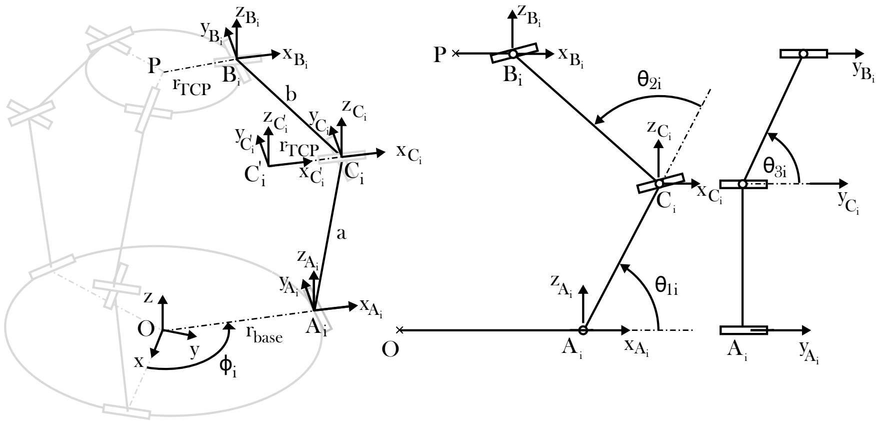

Fig. 8.14 Coordinate frames of DELTA mechanism according to [23]

with respect to the world frame. The transformation between the base frame and the A_i frame is as follows:

$$
{}^{base}T_{A_i} = \begin{bmatrix} \cos(-\phi_i) & \sin(-\phi_i) & 0 & 0 \\ -\sin(-\phi_i) & \cos(-\phi_i) & 0 & 0 \\ 0 & 0 & 1 & 0 \\ 0 & 0 & 0 & 1 \end{bmatrix} \cdot \begin{bmatrix} 1 & 0 & 0 & r_{base} \\ 0 & 1 & 0 & 0 \\ 0 & 0 & 1 & 0 \\ 0 & 0 & 0 & 1 \end{bmatrix} \tag{8.8}
$$

$$
{}^{base}T_{A_i} = \begin{bmatrix} \cos(-\phi_i) & \sin(-\phi_i) & 0 & r_{base} \cdot \cos(-\phi_i) \\ -\sin(-\phi_i) & \cos(-\phi_i) & 0 & -r_{base} \cdot \sin(-\phi_i) \\ 0 & 0 & 1 & 0 \\ 0 & 0 & 0 & 1 \end{bmatrix} \tag{8.9}
$$

The transformation is a rotation around the z axis in the world frame by angle $-\phi_i$ and then a translation in the x_i direction by distance r_{base}.

Another frame is attached to the point C_i. This frame has the same orientation as the A_i frame, the relative position is dependent on the angle θ_{1i}. The transformation between these two frames is:

$$
{}^{A_i}T_{C_i} = \begin{bmatrix} 1 & 0 & 0 & a \cdot \cos\theta_{1i} \\ 0 & 1 & 0 & 0 \\ 0 & 0 & 1 & a \cdot \sin\theta_{1i} \\ 0 & 0 & 0 & 1 \end{bmatrix} \tag{8.10}
$$

As mentioned above the forward kinematic problem in general cannot be solved for parallel kinematic mechanisms. In case of the DELTA mechanism it is different. Here the method of trilateration can be applied. This approach is based on the fact that, if looking at one leg, all points B_i are on the surface of a sphere with radius b and the center point C_i. The surface is given by sphere equation:

$$(x - x_{C_i})^2 + (y - y_{C_i})^2 + (z - z_{C_i})^2 = b^2 \tag{8.11}$$

with the center coordinates $(x_{C_i}, y_{C_i}, z_{C_i})$ of the sphere.

In order to use the trilateration method more easily, a virtual frame C_i' will be placed with a distance of $-r_{TCP}$ along the x axis of frame C_i. The transformation between the two frames is:

$$^{C_i}T_{C_i'} = \begin{bmatrix} 1 & 0 & 0 & -r_{TCP} \\ 0 & 1 & 0 & 0 \\ 0 & 0 & 1 & 0 \\ 0 & 0 & 0 & 1 \end{bmatrix} \tag{8.12}$$

As mentioned before, the usage of homogeneous transformation matrices gives the ability to jump from one frame to another. The same idea could be used in expressing compound transformations. For example, the transformation between the base frame and the C_i' can be expressed as jumping from the base frame to frame A_i, then jump from frame A_i to frame C_i and finally a jump from frame C_i to frame C_i'.This compound transformation can be expressed as follows:

$$^{base}T_{C_i'} = {}^{base}T_{A_i} \cdot {}^{A_i}T_{C_i} \cdot {}^{C_i}T_{C_i'} \tag{8.13}$$

The reason behind attaching the virtual frame C_i' is that, considering three spheres with radius b and center C_i', the three sphere surfaces of the three legs intersect in the point P, which is the solution of the forward kinematics. Additionally, the other two angles of each leg, θ_{2i} and θ_{3i}, aren't known. The equation of the three spheres can be formulated as follows:

The solution of the set of equations leads to two points of intersection of the spheres, only one of them is geometrically meaningful.

Inverse Kinematics

The DELTA mechanism is especially known from impedance-controlled devices. In this mode of operation the inverse kinematics problem is not needed. However it is a very useful tool in the design process to determine the available workspace which is shown later in Sect. 8.4.

A frame is attached to the TCP at point P with the same orientation as the base frame. Three other frames are attached to each point B_i with the same orientation as the frames at A_i and C_i. To solve the inverse kinematics of each leg, we can use the following compound transformation:

$$^{base}T_{TCP} = {}^{base}T_{A_i} \cdot {}^{A_i}T_{C_i} \cdot {}^{C_i}T_{B_i} \cdot {}^{B_i}T_{TCP} \tag{8.14}$$

where:

$$
{}^{base}T_{TCP} = \begin{bmatrix} 1 & 0 & 0 & x_P \\ 0 & 1 & 0 & y_P \\ 0 & 0 & 1 & z_P \\ 0 & 0 & 0 & 1 \end{bmatrix} \quad {}^{C_i}T_{B_i} = \begin{bmatrix} 1 & 0 & 0 & b \cdot \sin\theta_{3i} \cdot \cos(\theta_{1i} + \theta_{2i}) \\ 0 & 1 & 0 & b \cdot \cos\theta_{3i} \\ 0 & 0 & 1 & b \cdot \sin\theta_{3i} \cdot \sin(\theta_{1i} + \theta_{2i}) \\ 0 & 0 & 0 & 1 \end{bmatrix}
$$

$$
{}^{B_i}T_{TCP} = \begin{bmatrix} \cos(\phi_i) & \sin(\phi_i) & 0 & r_{TCP} \cdot \cos(\phi_i) \\ -\sin(\phi_i) & \cos(\phi_i) & 0 & -r_{TCP} \cdot \sin(\phi_i) \\ 0 & 0 & 1 & 0 \\ 0 & 0 & 0 & 1 \end{bmatrix} \tag{8.15}
$$

The unknown matrices are ${}^{A_i}T_{C_i}$ and ${}^{C_i}T_{B_i}$, that are function of the three unknown angles, θ_{1i},θ_{2i}, and θ_{3i}. In order to solve for the angles, all the known matrices should be on one side and the unknown should be on the other side. We get:

$$
{}^{base}T_{A_i}{}^{-1} \cdot {}^{base}T_{TCP} \cdot {}^{B_i}T_{TCP}{}^{-1} = {}^{A_i}T_{C_i} \cdot {}^{C_i}T_{B_i} \tag{8.16}
$$

Multiplying the two matrices on the right hand side give:

$$
{}^{A_i}T_{B_i} = \begin{bmatrix} 1 & 0 & 0 & a \cdot \cos\theta_{1i} + b \cdot \sin\theta_{3i} \cdot \cos(\theta_{1i} + \theta_{2i}) \\ 0 & 1 & 0 & b \cdot \cos\theta_{3i} \\ 0 & 0 & 1 & a \cdot \sin\theta_{1i} + b \cdot \sin\theta_{3i} \cdot \sin(\theta_{1i} + \theta_{2i}) \\ 0 & 0 & 0 & 1 \end{bmatrix} = \begin{bmatrix} 1 & 0 & 0 & x_{B_i} \\ 0 & 1 & 0 & y_{B_i} \\ 0 & 0 & 1 & z_{B_i} \\ 0 & 0 & 0 & 1 \end{bmatrix} \tag{8.17}
$$

This leads to, according to [23]:

$$
\theta_{3i} = \arccos \frac{y_{B_i}}{b} \tag{8.18}
$$

$$
\theta_{2i} = \arccos \frac{x_{B_i}{}^2 + y_{B_i}{}^2 + z_{B_i}{}^2 - a^2 - b^2}{2ab \sin\theta_{3i}} \tag{8.19}
$$

$$
\theta_{1i} = \arctan \frac{x_{B_i} - b \sin\theta_{3i} \cos(\theta_{1i} + \theta_{2i})}{z_{B_i} - b \sin\theta_{3i} \sin(\theta_{1i} + \theta_{2i})} \tag{8.20}
$$

Equations (8.18)–(8.20) are the solution to the inverse kinematic equation for each leg.

8.4 Design Step 3: Dimensioning a Haptic Kinematic

The last step in the design is dimensioning. Optimizing the dimensions of the mechanism, lengths of the rods/links defined in step 1 (Sect. 8.2), affects the workspace of the mechanism, the transmission of forces/torques, and the velocities. The goal of the optimization is to reach a specific optimum performance. This may be a maximized workspace with homogeneous transfer characteristics of forces from the TCP to the actuators. Dimensioning procedure in parallel mechanisms is usually more complicated compared to that in serial mechanisms. According to MERLET, parallel mechanisms with well designed dimensions can perform better than one with better suited topology but worse dimensions [15]. An important parameter in haptic interfaces is the impedance. In order to calculate the impedance of the system, the values of the velocities and the forces have to be known. In this part of the chapter, an introduction will be given on how the dimensioning procedure is performed.

Jacobian Matrix

In both the forward and inverse kinematic problems, the vectors q and p are linked via the mechanism's gearing properties. Those properties are represented by the Jacobian matrix J. For the mechanism's kinematics, the Jacobian matrix represents the transmission matrix of the first order. It carries all information regarding dimensions and transmission properties. J is defined by the partial derivative of TCP coordinates with respect to the joints' coordinates. However, generally, the Jacobian could be calculated for any frame in the mechanism, but usually the TCP frame is the important frame to be considered. The size of the matrix is $m \times n$, where m is the number of TCP coordinates and n is the number of joints' coordinates. For example, the TCP of UR10E robot has $m = 6$ $(x_p, y_p, z_p, \alpha_p, \beta_p, \gamma_p)$ and $n = 6$ $(\theta_1, \theta_2, \theta_3, \theta_4, \theta_5, \theta_6)$. So the Jacobian matrix of this mechanism consists of m rows and n columns:

$$J = \begin{bmatrix} \frac{\partial x_p}{\partial \theta_1} & \frac{\partial x_p}{\partial \theta_2} & \frac{\partial x_p}{\partial \theta_3} & \frac{\partial x_p}{\partial \theta_4} & \frac{\partial x_p}{\partial \theta_5} & \frac{\partial x_p}{\partial \theta_6} \\ \frac{\partial y_p}{\partial \theta_1} & \frac{\partial y_p}{\partial \theta_2} & \frac{\partial y_p}{\partial \theta_3} & \frac{\partial y_p}{\partial \theta_4} & \frac{\partial y_p}{\partial \theta_5} & \frac{\partial y_p}{\partial \theta_6} \\ \frac{\partial z_p}{\partial \theta_1} & \frac{\partial z_p}{\partial \theta_2} & \frac{\partial z_p}{\partial \theta_3} & \frac{\partial z_p}{\partial \theta_4} & \frac{\partial z_p}{\partial \theta_5} & \frac{\partial z_p}{\partial \theta_6} \\ \frac{\partial \alpha_p}{\partial \theta_1} & \frac{\partial \alpha_p}{\partial \theta_2} & \frac{\partial \alpha_p}{\partial \theta_3} & \frac{\partial \alpha_p}{\partial \theta_4} & \frac{\partial \alpha_p}{\partial \theta_5} & \frac{\partial \alpha_p}{\partial \theta_6} \\ \frac{\partial \beta_p}{\partial \theta_1} & \frac{\partial \beta_p}{\partial \theta_2} & \frac{\partial \beta_p}{\partial \theta_3} & \frac{\partial \beta_p}{\partial \theta_4} & \frac{\partial \beta_p}{\partial \theta_5} & \frac{\partial \beta_p}{\partial \theta_6} \\ \frac{\partial \gamma_p}{\partial \theta_1} & \frac{\partial \gamma_p}{\partial \theta_2} & \frac{\partial \gamma_p}{\partial \theta_3} & \frac{\partial \gamma_p}{\partial \theta_4} & \frac{\partial \gamma_p}{\partial \theta_5} & \frac{\partial \gamma_p}{\partial \theta_6} \end{bmatrix} \tag{8.21}$$

More details are found in [12].

The Jacobian matrix is used to express various relations between the inputs and outputs of a mechanism, such as the relation between the velocities of the joints compared to the velocity of the TCP, and the relation between the torques applied to the joints and the forces on the TCP. These relations are discussed later in this section.

8.4.1 Workspace

The dimensions of the mechanism affect the workspace. To perform an optimization the following steps should be taken:

1. Definition of parameters and their span of values (e.g. rod lengths)
2. Analytical or numerical description of the optimization problem
3. Mathematical optimization, e.g. via a gradient approach or evolutionary algorithms

These steps are discussed and covered in [8, 17]. The key challenge is the formal description of the optimum. This process should be done using a computer software which will be discussed later in Sect. 8.5. Within the optimization process, the measurement value for an optimum has to be determined by scanning the complete workspace and optimizing relevant parameters of the mechanism between each scanning process. In [1] several optimizations are given using the singular values of the Jacobian matrix as a measure.

8.4.2 Isotropy and Singular Positions

The dimensioning process continues by taking into account the best desirable working points of the TCP inside the workspace and what positions should be avoided.

Isotropy describes the optimum working points in the workspace, these are the configurations where the servo transmissions are highly coupled, meaning that the error between the input and the output is minimised.

On the other hand, singularities are the configurations that should be avoided. In singular positions, the control of one or more of the mechanism's DoF are lost. If a mechanism approaches a singular position its transmission or gear ratio changes quickly until the mechanism is locked in the singular position. Singularities are divided into two main types [5].

Workspace-Boundary Singularities

This type of singularity occurs when the mechanism is fully stretched to the edge of the workspace. This applies to all types of mechanisms.

Workspace-Interior Singularities

This type occurs inside the workspace. In serial mechanisms, one of these singularities happens especially in six DoF mechanisms where the axes of the last three joints (wrist) intersect in on point. Usually this happens when two axes are coincident.

Figure 8.15 shows examples of both types of singular positions. The key to analyze the isotropy and singularity is based on the properties of the Jacobian matrix. A key performance index which is derived from the Jacobian matrix is the condition number κ.

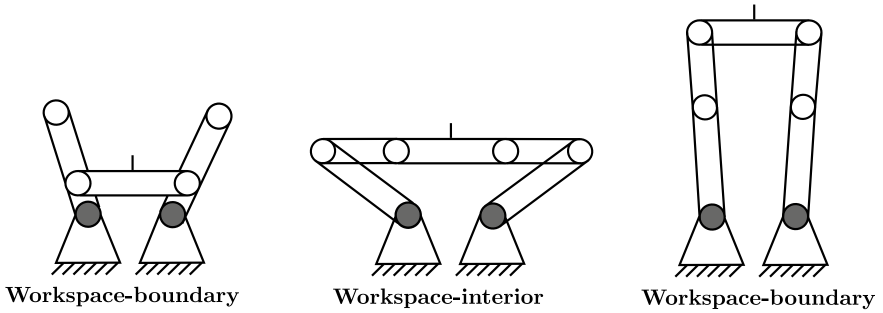

Fig. 8.15 Different singular positions

The Conditioning Number

The kinematic transmission behavior is rated by the singular values σ_i of the inverse Jacobian matrix J^{-1}. In general the singular values of a matrix **A** are defined as:

$$\sigma_i(A) = \sqrt{\lambda_i(A^T A)} \tag{8.22}$$

The role of the singular values can be shown by GOLUB'S method of singular value decomposition [6]. It is based on the fact that for a real $m \times n$ matrix **A**, with $m \geq n$, and rank r can be fractioned in the following product:

$$A = U \cdot \Sigma \cdot V^T \tag{8.23}$$

Where U consists of n orthonormalized eignevectors of the n largest eignevalues of AA^T and V consists of the orthonormalized eigenvectors of $A^T A$. Σ is a $m \times n$ diagonal matrix as follows:

$$\boldsymbol{\Sigma} = \left(\begin{array}{ccc|c} \sigma_1 & & & \vdots \\ & \ddots & & \cdots 0 \cdots \\ & & \sigma_r & \vdots \\ \hline & \vdots & & \\ \cdots & 0 & \cdots & \cdots 0 \cdots \\ & \vdots & & \vdots \end{array}\right) \tag{8.24}$$

Where $\sigma_1 \geq \cdots \geq \sigma_r > 0$. The conditioning number is defined as:

$$\kappa = \frac{\sigma_{max}}{\sigma_{min}} \tag{8.25}$$

As a function of the Jacobian matrix κ changes with respect to the mechanism's position. The conditioning number can reach values from $\frac{1}{\kappa} = 0 \cdots 1$.

The goal is to have a highly isotropic transmission, which means a conditioning number of 1. On the other hand, singular positions should be avoided. In terms of the Jacobian matrix, the rank of the matrix decreases in the singular position. This will translated into a conditioning number of ∞ or $\frac{1}{\kappa} = 0$.
For the two types of singularities introduced earlier, the loss of rank of the Jacobian matrix is characterized by:

- Workspace-boundary singularity: $\det(J) = 0$
- Workspace-interior singularity: $\det(J^{-1}) = 0$.

Optimization Criteria

Besides the analysis of isotropy and singular positions, another aspect one has to take care of in the design process is the transmission of force and speed.

Recalling Eq. (8.35), to limit the maximal required force and torque and thereby limit also the size of the used actuators, it is important to reach a good transmission of forces and torques even in cases of a disadvantageous σ_i. We can derive the criterion as follows:

$$\sigma_{min}(J^{-1}) \rightarrow max \tag{8.26}$$

For maximizing the speed transmission, the criterion could be as follows:

$$\sigma_{max}(J^{-1}) \rightarrow min \tag{8.27}$$

Table 8.5 sums up various design optimization criteria.

One major drawback of Eq. (8.25) is that it rates the mechanism for Jacobian matrix or position. The pure optimization of $1/\kappa$ would in fact lead to one single position where the mechanism reaches high isotropy. However one cannot draw the conclusion that the whole workspace in total has an optimized transmission behavior.

Table 8.5 Summary of optimization criteria

Design aspect	Criterion
Force transmission	σ_{min} $(\mathbf{J}) \rightarrow$ max
No singular positions	σ_{min} $(\mathbf{J}) \rightarrow$ max
High stiffness	σ_{min} $(\mathbf{J}) \rightarrow$ max
Speed transmission	σ_{max} $(\mathbf{J}) \rightarrow$ min
Isotropy	$\frac{\sigma_{min}(\mathbf{J})}{\sigma_{max}(\mathbf{J})} \rightarrow$ max

What is needed is a measure to rate $1/\kappa$ of a whole workspace. This measure is provided by the global conditioning index as in [15].

$$\upsilon = \frac{\int_W \frac{1}{\kappa} dW}{\int_W dW} \tag{8.28}$$

The global conditioning index can be optimized using computer algorithms.

8.4.3 Velocities

The velocities of the joints and those of the TCP are related with the Jacobian matrix of the mechanism:

$$dp = J \cdot dq \tag{8.29}$$

Equation (8.29) gives the output velocity of the TCP with respect to the joints' velocities. The same idea could be done to get the desired joints' velocities in order to have a required velocity of the TCP:

$$dq = J^{-1} \cdot dp \tag{8.30}$$

The optimization process should involve the desired velocities of the TCP, this will affect the motors used to drive the joints.

8.4.4 Dynamics

For the design and operation of haptic interfaces there is another equation of high importance related to the transformation of forces and torques by a mechanism. In order to express the dynamics of a mechanism, the equations of motion of the links are to calculated. The goal is to find the required torques/forces on the joints. CRAIG [5] divided the approaches to calculate the equations of motions into: Iterative (numerical) and closed form (analytical).

Iterative Approach: NEWTON-EULER Dynamics Algorithm

One example of iterative methods is the NEWTON- EULER dynamics algorithm. This algorithm is split into parts, outward and inward iterations. The algorithm is as follows:

1. Outward iterations are computed to calculate the velocities and accelerations (linear and rotational) of the center of mass of each link/rod in the mechanism. The iterations start with the first link and ends with the last link.

2. Using the calculated velocities and accelerations of each link, the forces and the torques acting on the link are calculated using the NEWTON- EULER equations. This step occurs along with the outward iterations.
3. Finally the torques/forces on each joint are calculated using the inward iterations. These iterations start with the final link and move back to the first link.

The usage of a numerical approach can be applied to any robot. It only needs the inertia tensors of each link, position vectors that connect the links with each other and the rotation matrices between each two links. On the other hand, sometimes the information about the gravity and the non-inertial effects are important. A closed form equation should be introduced in that case.

Closed Form Approach

Closed form approaches express the dynamics of a mechanism in more detail. There are a lot of methods that can be used to express the equations of motion analytically. Two of these methods are discussed in this chapter: NEWTON- EULER equation and Lagrangian dynamic formulation.

The general form of a NEWTON- EULER equation for a link is as follows:

$$\tau = M(\theta)\ddot{\theta} + V(\theta, \dot{\theta}) + G(\theta) \tag{8.31}$$

where:

- τ Vector of torques applied on the joints
- M Mass matrix of the mechanism
- V Vector includes the Coriolis and centrifugal terms
- G Vector includes the gravitational terms

Another method that is widely used is the Lagrangian dynamic formulation. The NEWTON- EULER equation is considered a force balance approach, while, on the other hand, Lagrangian formulation is considered as an energy approach. This method uses the energy of the system to express the equations of motions.

A scalar function called the Lagrangian (L) is defined as:

$$L(\theta, \dot{\theta}) = k(\theta, \dot{\theta}) - u(\theta) \tag{8.32}$$

where:

- L Lagrangian function
- k Sum of the kinetic energy of the mechanism
- u Sum of the potential energy of the mechanism

The equations of motion are given as follow:

$$\tau = \frac{d}{dt}\frac{\partial L}{\partial \dot{\theta}} - \frac{\partial L}{\partial \theta} \tag{8.33}$$

The number of equations of motion obtained using the Lagrangian dynamics formulation depends on the number of the generalized coordinates. The generalized coordinates are the parameters needed to express the configuration of a mechanism. In our case the joints' values are the generalized coordinates. This means that the Lagrangian function L should be expressed only in terms of the generalized coordinates.

The equations showed (8.31) and (8.33) include only the forces as a result of rigid body mechanics, the most important factor that isn't included is friction. There are multiple ways to model friction forces; the two most important models are viscous friction and Coulomb friction. An additional part F_f is added to Eq. (8.31) to model the friction:

$$\tau = M(\theta)\ddot{\theta} + V(\theta, \dot{\theta}) + G(\theta) + F_f(\theta, \dot{\theta}) \tag{8.34}$$

Equations (8.31) and (8.33) give the same output. Also, both of them are expressed in terms of the joints' positions, velocities, accelerations or, in other words, in the joint space. In order to express the forces on the TCP, the Jacobian matrix can be used as follows:

$$\tau = J^T(\theta) \cdot F \tag{8.35}$$

Combining Eqs. (8.31) and (8.35) results to:

$$J^{-T}\tau = J^{-T}M(\theta)\ddot{\theta} + J^{-T}V(\theta, \dot{\theta}) + J^{-T}G(\theta) \tag{8.36}$$

Which results to:

$$F = J^{-T}M(\theta)\ddot{\theta} + J^{-T}V(\theta, \dot{\theta}) + J^{-T}G(\theta) \tag{8.37}$$

Other methods are available to express the equations of motion of mechanisms. Malvezzi et al. [13] made a qualitative comparison between three approaches to express the dynamics of a serial mechanism. The dynamics in serial mechanisms gets complicated with the increase in number of links, however, it's not as complicated as the case of parallel mechanisms.

8.4.4.1 Example: Equations of Motion of 2-DoF Serial Mechanism

To show how obtaining the equations of motion is complicated, a simple mechanism will be discussed. Figure 8.16 shows a 2-DoF serial mechanism. The mechanism is simplified such as the masses m_1 and m_2 are considered to be point masses at the end of each link and the links are considered massless. Also the friction forces aren't taken into consideration. The equations of motion are obtained using the Lagrange dynamic formulation. The generalized coordinates of this mechanism are θ_1 and θ_2. Recalling Eq. (8.33), the two equations of motion are as follows:

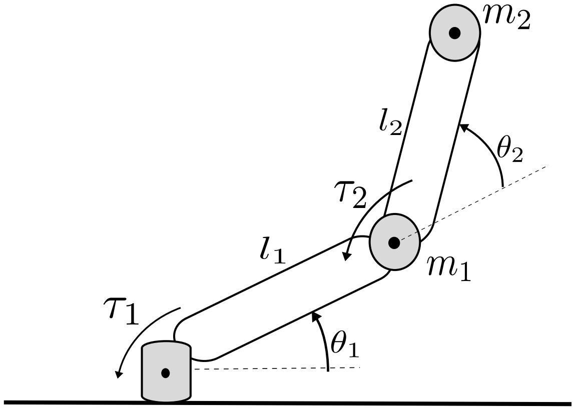

Fig. 8.16 2-DoF serial mechanism

$$\tau_1 = \frac{d}{dt}\frac{\partial L}{\partial \dot{\theta}_1} - \frac{\partial L}{\partial \theta_1} \tag{8.38}$$

$$\tau_2 = \frac{d}{dt}\frac{\partial L}{\partial \dot{\theta}_2} - \frac{\partial L}{\partial \theta_2} \tag{8.39}$$

Where each equation represents the torque on each motor that creates the motion of each angle.

The total kinetic energy of the mechanism is:

$$k_{Total} = k_{m_1} + k_{m_2} = \frac{1}{2} \cdot m_1 \cdot (v_{m_1})^2 + \frac{1}{2} \cdot m_2 \cdot (v_{m_2})^2 \tag{8.40}$$

$$v_{m_1}{}^2 = (l_1 \cdot \dot{\theta}_1)^2$$

To get v_{m_2}, one can obtain first the position of m_2 in Cartesian space and convert it to the joint space:

$$x_{m_2} = l_1 \cdot \cos\theta_1 + l_2 \cdot \cos(\theta_1 + \theta_2)$$

$$y_{m_2} = l_1 \cdot \sin\theta_1 + l_2 \cdot \sin(\theta_1 + \theta_2)$$

$$v_{m_2}{}^2 = (\dot{x}_{m_2})^2 + (\dot{y}_{m_2})^2$$

This leads to:

$$\begin{aligned} v_{m_2}{}^2 = {} & l_1{}^2\dot{\theta}_1{}^2 + (\dot{\theta}_1 + \dot{\theta}_2)^2 l_2{}^2 \\ & + 2\dot{\theta}_1 l_1 l_2 (\dot{\theta}_1 + \dot{\theta}_2)[\sin\theta_1 \sin(\theta_1 + \theta_2) + \cos\theta_1 \cos(\theta_1 + \theta_2)] \end{aligned}$$

Using the angle addition trigonometric function, v_{m_2} is given as follows:

$$v_{m_2}{}^2 = l_1{}^2\dot{\theta}_1{}^2 + (\dot{\theta}_1 + \dot{\theta}_2)^2 l_2{}^2 + 2\dot{\theta}_1 l_1 l_2(\dot{\theta}_1 + \dot{\theta}_2)[\cos\theta_2]$$

The total kinetic energy of the mechanism is:

$$k_{Total} = \frac{1}{2}\cdot m_1 \cdot (l_1 \cdot \dot{\theta}_1)^2 + \frac{1}{2}\cdot m_2 \cdot l_1{}^2\dot{\theta}_1{}^2 + (\dot{\theta}_1 + \dot{\theta}_2)^2 l_2{}^2 + 2\dot{\theta}_1 l_1 l_2(\dot{\theta}_1 + \dot{\theta}_2)[\cos\theta_2]$$

The potential energy of the mechanism is:

$$u_{Total} = m_1 \cdot g \cdot y_{m_1} + m_2 \cdot g \cdot y_{m_2} \tag{8.41}$$

$$u_{Total} = m_1 \cdot g \cdot l_1 \sin\theta_1 + m_2 \cdot g \cdot [l_1 \sin\theta_1 + l_2 \sin(\theta_1 + \theta_2)]$$

Hence, the Lagrangian function L is defined as:

$$L = k_{Total} - u_{Total} \tag{8.42}$$

The torques to be applied on the joints, recalling Eqs. (8.38) and (8.39), are as follow:

$$\begin{aligned}\tau_1 = {} & (m_1 + m_2)l_1^2\ddot{\theta}_1 + m_2 l_2^2(\ddot{\theta}_1 + \ddot{\theta}_2) + m_2 l_1 l_2 \cos\theta_2(2\ddot{\theta}_1 + \ddot{\theta}_2) - m_2 l_1 l_2 \sin\theta_2\dot{\theta}_2^2 \\ & - 2m_2 l_1 l_2 \sin\theta_2\dot{\theta}_1\dot{\theta}_2 + m_2 l_2 g \cos(\theta_1 + \theta_2) + (m_1 + m_2)l_1 g \cos\theta_1\end{aligned} \tag{8.43}$$

$$\tau_2 = m_2 l_2[(\ddot{\theta}_1 + \ddot{\theta}_2)l_2 + l_1 \cos\theta_2\ddot{\theta}_1 + l_1 \sin\theta_2\dot{\theta}_1^2 + g\cos(\theta_1 + \theta_2)] \tag{8.44}$$

Or in matrix form like Eq. (8.34):

$$\begin{aligned}\begin{bmatrix}\tau_1\\ \tau_2\end{bmatrix} = {} & \begin{bmatrix}(m_1 + m_2)l_1^2 + m_2 l_2^2 + 2m_2 l_1 l_2 \cos\theta_2 & m_2 l_2^2 + m_2 l_1 l_2 \cos\theta_2 \\ m_2 l_2{}^2 + m_2 l_1 l_2 \cos\theta_2 & m_2 l_2{}^2\end{bmatrix}\begin{bmatrix}\ddot{\theta}_1\\ \ddot{\theta}_2\end{bmatrix} + \\ & \begin{bmatrix}-m_2 l_1 l_2 \sin\theta_2\dot{\theta}_2^2 - 2m_2 l_1 l_2 \sin\theta_2\dot{\theta}_1\dot{\theta}_2 \\ m_2 l_1 l_2 \sin\theta_2\dot{\theta}_1^2\end{bmatrix} + \begin{bmatrix}m_2 l_2 g\cos(\theta_1 + \theta_2) + (m_1 + m_2)l_1 g\cos\theta_1 \\ m_2 l_2 g \cos(\theta_1 + \theta_2)\end{bmatrix}\end{aligned} \tag{8.45}$$

As mentioned earlier, the torque equations are expressed in joint space. In order to express the forces acting on the TCP, the Jacobian matrix is to be used. The Jacobian matrix of this mechanism is:

$$J = \begin{bmatrix}\frac{\partial x}{\partial\theta_1} & \frac{\partial x}{\partial\theta_2} \\ \frac{\partial y}{\partial\theta_1} & \frac{\partial y}{\partial\theta_2}\end{bmatrix} = \begin{bmatrix}-l_1 \sin\theta_1 - l_2 \sin(\theta_1 + \theta_2) & -l_2 \sin(\theta_1 + \theta_2) \\ l_1 \cos\theta_1 + l_2 \cos(\theta_1 + \theta_2) & l_2 \cos(\theta_1 + \theta_2)\end{bmatrix} \tag{8.46}$$

recalling Eq. (8.36), J^{-T} is expressed as:

$$J^{-T} = \frac{1}{l_1 l_2 \sin\theta_2} \begin{bmatrix} l_2 \cos(\theta_1+\theta_2) & -l_1\cos\theta_1 - l_2\cos(\theta_1+\theta_2) \\ l_2 \sin(\theta_1+\theta_2) & -l_1\sin\theta_1 - l_2\sin(\theta_1+\theta_2) \end{bmatrix} \tag{8.47}$$

Recalling Eq. (8.37):

$$J^{-T} M(\theta) = \frac{1}{l_1 l_2 \sin\theta_2} \begin{bmatrix} M'_{11} & M'_{12} \\ M'_{21} & M'_{22} \end{bmatrix} \tag{8.48}$$

Where:

$$\begin{aligned} M'_{11} = {} & (m_1+m_2) l_1^2 l_2 \cos(\theta_1+\theta_2) + m_2 l_1 l_2^2 \cos\theta_2 \cos(\theta_1+\theta_2) \\ & - m_2 l_1 l_2^2 \cos\theta_1 - m_2 l_1^2 l_2 \cos\theta_1 \cos\theta_2 \end{aligned} \tag{8.49}$$

$$M'_{12} = m_2 l_1 l_2^2 (\cos\theta_2 \cos(\theta_1+\theta_2) - \cos\theta_1) \tag{8.50}$$

$$\begin{aligned} M'_{21} = {} & (m_1+m_2) l_1^2 l_2 \sin(\theta_1+\theta_2) + m_2 l_1 l_2^2 \cos\theta_2 \sin(\theta_1+\theta_2) \\ & - m_2 l_1 l_2^2 \sin\theta_1 - m_2 l_1^2 l_2 \sin\theta_1 \cos\theta_2 \end{aligned} \tag{8.51}$$

$$M'_{22} = m_2 l_1 l_2^2 (\cos\theta_2 \sin(\theta_1+\theta_2) - \sin\theta_1) \tag{8.52}$$

Accordingly:

$$J^{-T} V(\theta, \dot{\theta}_1) = \frac{1}{l_1 l_2 \sin\theta_2} \begin{bmatrix} V'_1 \\ V'_2 \end{bmatrix} \tag{8.53}$$

Where:

$$V'_1 = -m_2 l_1 l_2^2 \sin\theta_2 \cos(\theta_1+\theta_2)(\dot{\theta}_1+\dot{\theta}_2)^2 - m_2 l_1^2 l_2 \cos\theta_1 \sin\theta_2 \dot{\theta}_1^2 \tag{8.54}$$

$$V'_2 = -m_2 l_1 l_2^2 \sin\theta_2 \sin(\theta_1+\theta_2)(\dot{\theta}_1+\dot{\theta}_2)^2 - m_2 l_1^2 l_2 \sin\theta_1 \sin\theta_2 \dot{\theta}_1^2 \tag{8.55}$$

And:

$$J^{-T} G(\theta) = \frac{1}{l_1 l_2 \sin\theta_2} \begin{bmatrix} G'_1 \\ G'_2 \end{bmatrix} \tag{8.56}$$

Where:

$$G'_1 = m_1 l_1 l_2 g \cos\theta_1 \cos(\theta_1+\theta_2) \tag{8.57}$$

$$G'_2 = (m_1+m_2) l_1 l_2 g \cos\theta_1 \sin(\theta_1+\theta_2) - m_2 l_1 l_2 g \sin\theta_1 \cos(\theta_1+\theta_2) \tag{8.58}$$

If we assume from Eq. (8.37), that $F = [F_x \; F_y]^T$, this leads to the force acting on the TCP in x- and y-direction:

$$F_x = \frac{1}{l_1 l_2 \sin\theta_2}[\, M'_{11}\ddot{\theta}_1 + M'_{12}\ddot{\theta}_2 + V'_1 + G'_1] \tag{8.59}$$

$$F_y = \frac{1}{l_1 l_2 \sin\theta_2}[\, M'_{21}\ddot{\theta}_1 + M'_{22}\ddot{\theta}_2 + V'_2 + G'_2] \tag{8.60}$$

Equations (8.59) and (8.60) express the forces with respect to the angular accelerations of the joints $\ddot{\theta}$. The same forces could be expressed with respect to the accelerations of the Cartesian variables $\ddot{X}$. The general form is found in [5]:

$$F = M_x(\theta)\ddot{X} + V_x(\theta, \dot{\theta}) + G_x(\theta) \tag{8.61}$$

Where:

$$M_x = J^{-T}(\theta)M(\theta)J^{-1}(\theta) \tag{8.62}$$

$$V_x = J^{-T}(\theta)(V(\theta, \dot{\theta}) - M(\theta)J^{-1}(\theta)\dot{J}(\theta)\dot{\theta}) \tag{8.63}$$

$$G_x = J^{-T}(\theta)G(\theta) \tag{8.64}$$

From this example:

- Although the mechanism is just a simple 2-DoF planar one, the equations of motion are already complicated. The equations get more complicated as the number of DoF increases. This issue is somehow solved by obtaining the equations of motion by a computer-based algorithm. This is the reason, why the role of simulation is so important (Sect. 8.5).
- Looking at the equation of τ_1, it can be seen that the required torque on the first joint contains many terms depending on both angles (θ_1 and θ_2). This explains the statement related to serial mechanisms in particular that each joint is responsible for the dynamics of the following links.

8.5 Role of Simulation

The design steps of kinematic mechanisms are introduced in the previous sections. The example introduced in Sect. 8.4.4.1 shows how complex the equations of motion are. This complexity, not only in the equations of motion, but rather in the whole dimensioning process, is the reason behind using computer-based simulations.

Figure 8.17 shows a block diagram of the usage of kinematic mechanisms in a general application. Taking a pick-and-place application, the goal of the manipulator is to follow a certain trajectory in Cartesian space. The desired trajectory is the input in our case.

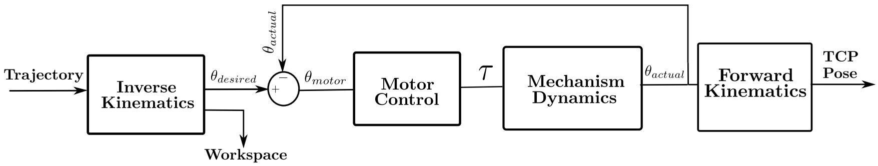

Fig. 8.17 Block diagram of the usage of a kinematic mechanism in a general application

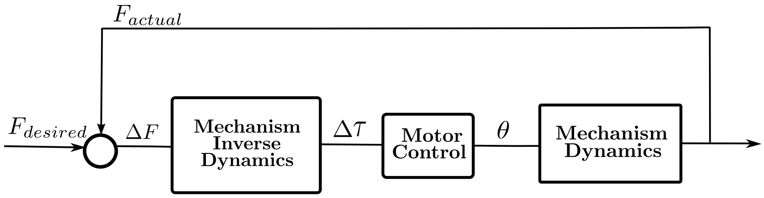

Fig. 8.18 Block diagram of the usage of a kinematic mechanism in a haptic application

Next comes the role of the inverse kinematics to transfer the desired trajectory into desired joint angles. Generally, inverse kinematics has another importance, that is the definition of the manipulator workspace. Any point inside the workspace has a solution for the inverse kinematics equations of the mechanism.

The desired angles are subtracted from the actual joint angles and the difference is fed to the control block. For the scope of this chapter, the control block isn't discussed. What is important for this chapter, is that the output of this block is the torques applied to the motors.

The torques are the inputs to the manipulator dynamics block, that contains the equations of motion of the manipulator. The output of this block are the actual angles of the joints. The actual joints angles complete the feedback loop to the desired angles summation point.

The actual angles can be also used to get the pose of the TCP using the forward kinematics of the manipulator.

For haptic applications, the general diagram in Fig. 8.17 doesn't perfectly match. In haptic applications, sometimes, the goal isn't to follow a specific trajectory, but rather to have a desired force on the TCP, as shown in Fig. 8.18.

The desired forces are subtracted from the actual forces sensed on the TCP. The difference is fed to the control block. The output of the control block are the torques applied on the motors.

The torques are fed to the manipulator dynamics block. This block doesn't only contain the mechanism dynamics, but also the dynamics of the user are modeled. The simplest model of the user is a mass-spring-damper system. The outputs of the this block are the actual forces on the TCP.

8.5.1 Example of Software Used in Simulation

There are many software on the market that model and simulate the kinematics of haptic interfaces. For haptic interfaces, the inverse kinematics is of high importance and it limits the software to be used. Generally, all the software have many features in common:

- Model the kinematic mechanism, apart from the programming language used or the way of modeling, whether using programming scripts or blocks.
- Model the environment of the application with all the external inputs.
- Visualize and simulate the movement of the mechanism inside the environment during performing a predefined application.

Comparing between different software isn't the scope of this chapter. We will focus in this secion on Matlab® and its offered toolboxes to give only an example on how the modeling and simulation are implemented. The example shown in Sect. 8.4.4.1 will be discussed in terms of optimizing the workspace and how the kinematic and dynamic equations are solved.

8.5.2 Optimizing the Workspace

As mentioned earlier, any point inside the workspace has a solution for the inverse kinematics of the mechanism. Referring to the example in Sect. 8.4.4.1, the workspace depends on the lengths of the two links and the limits of the two revolute joints. Figure 8.19 shows the workspace of the mechanism with two different combinations of link lengths. In both combinations the limits of the joints are as follow:

$$0^\circ \leq \theta_1 \leq 90^\circ$$

$$0^\circ \leq \theta_2 \leq 90^\circ$$

The lengths in the first combination are ($l_1 = l_2 = 10\,\text{cm}$), where in the second combination the lengths are ($l_1 = l_2 = 20\,\text{cm}$). For more complex mechanisms, more variables will be included in the optimization process. One has to keep in mind that by changing the lengths, the dynamics of the mechanism change as well. This will be discussed in the following sections.

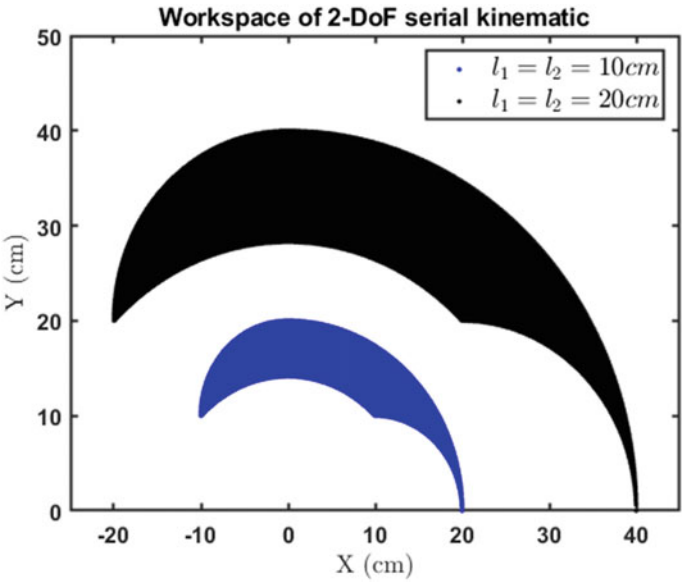

Fig. 8.19 Workspace of 2-DoF mechanism with different combinations of link lengths

8.5.3 Solving Kinematic and Dynamic Equations

In Matlab® there are many ways to model the kinematic equations. One way is to model the mechanism as a rigid-body tree. This is done by defining all the links/legs, and the joints. The rigid-body tree approach supports serial mechanisms, however, parallel mechanisms aren't directly supported.

In haptic applications, another approach is more applicable. As mentioned earlier in Fig. 8.18, the goal is to maintain certain forces on the TCP. This can be modeled using Simulink® and Simscape Multibody™ toolbox.

Generally, forward and inverse kinematics equations, Jacobian matrix and equations of motion could be modeled using Matlab or Simulink, such that the optimization criteria listed in Table 8.5 could be implemented.

In Simscape Multibody™ toolbox, the designer has the option to either import the mechanism from a CAD software, or to use the predefined model blocks in the toolbox. The toolbox offers variety of joints and sensors. Figure 8.20 shows a simple modeling of our 2-DoF mechanism. The two links (l_1 and l_2) and the two masses (m_1 and m_2) are modeled using the predefined blocks, frames are attached to the each end of the links and the masses. The revolute joints connect the frames and constraint the motion in the specified direction only, rotation about the z-axis. The solver of the toolbox solves the kinematic equations defined by connection of the

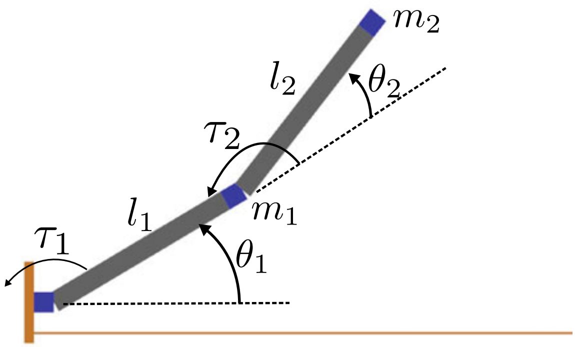

Fig. 8.20 Simscape Multibody™ model of 2-DoF serial mechanism

blocks, and singular positions are also detected. Modeling the mechanism using the toolbox solves the equations of motion. The torques applied on the joints and the joints' values are sensed using predefined sensors in the joint block. Applying Eq. (8.35), the forces on the TCP are calculated.

As mentioned earlier, changing the lengths of the links affects the dynamics of the mechanism. Consider the two link length combinations used in Sect. 8.5.2 and the masses (m_1 and m_2) are set to be 0.1 kg.

A simplified haptic scenario is when the user is obliged to follow a certain trajectory. An example of such trajectory could be that θ_1 is fixed, and the input to θ_2 is in the form of a sine wave. To simulate the torques applied to the joints and the result forces on the TCP for both combinations, the trajectory of the simplified scenario is applied to the joints. Fig. 8.21 shows the required torques on the joints for both combinations of lengths. From Fig. 8.21, it can be seen that the τ_1 is higher than τ_2 in both length combinations. The reason behind it, as mentioned earlier, in serial mechanisms one actuator carries the load of all the following actuators. Subsequently, the forces on the TCP can be calculated using Eq. (8.35). The forces are represented in Fig. 8.22.

The Simulink® model of this simplified scenario is shown in Fig. 8.23. The model consists of two main subsystems; the first contains the model of the mechanism: links, masses, joints, and the environment. The second subsystem contains the Jacobian matrix of the mechanism in order to calculate the forces on the TCP. Generally, more subsystems are added that contain, for example, the controller. From the values represented in Figs. 8.21 and 8.22, one can decide on the driver, the motors in this example, that will be able to apply the required torques to the joints.

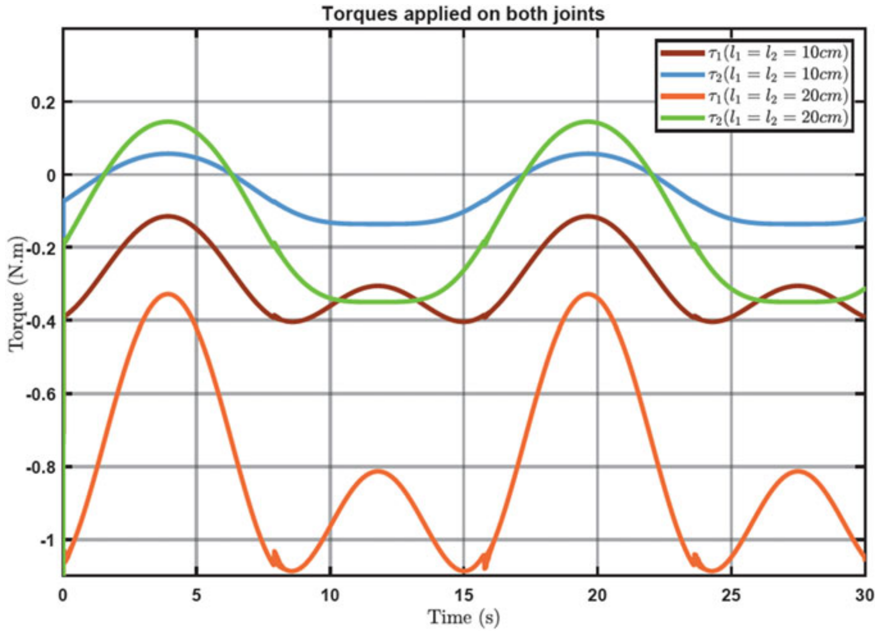

Fig. 8.21 Torques on both joints

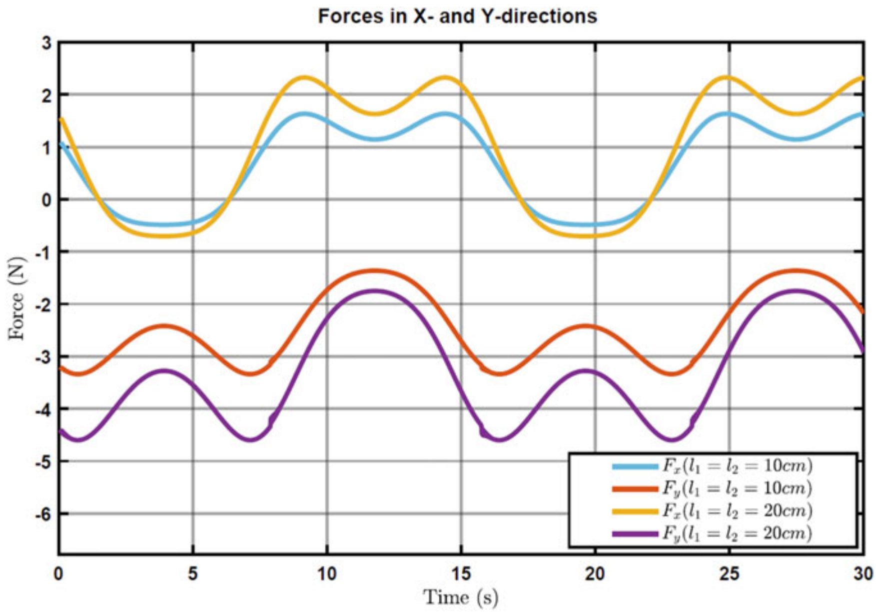

Fig. 8.22 Forces on the TCP

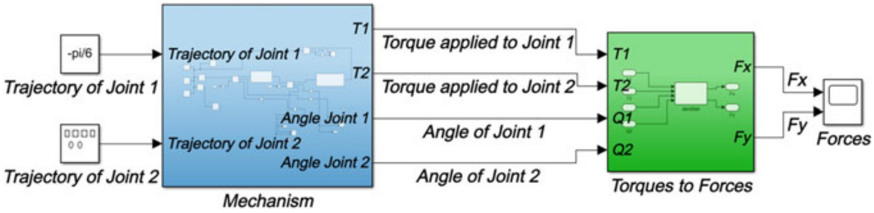

Fig. 8.23 Simulink® model of the mechanism in a simplified haptic scenario

References

1. Bleicher F (2003) Parallelkinematische Werkzeugmaschinen. Verlag, NWV-Neuer Wiss. 3708301188, 9783708301181
2. Carricato M, Parenti-Castelli V (2002) Singularity-free fully-isotropic translational parallel mechanisms. Int J Robot Res 21(2):161–174. https://doi.org/10.1177/027836402760475360
3. Carricato M, Parenti-Castelli V (2003) A family of 3-DOF translational parallel manipulators. J Mech Des 125 (2):302–307. https://doi.org/10.1115/1.1563635
4. Clavel, R. (1988). DELTA, a fast robot with parallel geometry. In C. W. Burckhardt (ed.), Proc of the 18th International Symposium on Industrial Robots (p./pp. 91–100), New York: Springer-Verlag
5. Craig JJ (2005) Introduction to robotics: mechanics and control. Pearson Prentice Hall. ISBN: 9789702607724
6. Golub GH, Reinsch C (1971) Singular value decomposition and least squares solutions. Springer, pp 134–151. https://doi.org/10.1007/978-3-662-39778-7_10
7. Husty M et al (2013) Kinematik und robotik. Springer. ISBN: 3642590292, 9783642590290
8. Kirchner J (2001) Mehrkriterielle optimierung von parallelkinematiken. Verlag Wiss, Scripten
9. Lee T-Y, Shim J-K (2003) Improved dialytic elimination algorithm for the forward kinematics of the general Stewart-Gough platform. In: Mechanism and machine theory, vol 38, no 6, pp 563–577. https://doi.org/10.1016/S0094-114X(03)00009-0
10. Lipkin, H. "A Note on Denavit-Hartenberg Notation in Robotics." Proceedings of the ASME 2005 International Design Engineering Technical Conferences and Computers and Information in Engineering Conference. Vol 7: 29th Mechanisms and Robotics Conference, Parts A and B. Long Beach, California, USA. September 24–28, 2005. pp. 921–926. ASME. https://doi.org/10.1115/DETC2005-85460
11. Q. Liu, D. Yang, W. Hao and Y. Wei, Research on Kinematic Modeling and Analysis Methods of UR Robot, (2018) IEEE 4th Information Technology and Mechatronics Engineering Conference (ITOEC), 2018, pp. 159–164, https://doi.org/10.1109/ITOEC.2018.8740681
12. López M et al (2006) Delta robot: inverse, direct, and intermediate Jacobians. In: Proceedings of the institution of mechanical engineers, Part C: Journal of mechanical engineering science, vol 220, no 1 (2006), pp 103–109. https://doi.org/10.1243/095440606X78263
13. Malvezzi, F., Orsino, R.M.M., Coelho, T.A.H. (2019). Lagrange's, Maggi's and Kane's Equations Applied to the Dynamic Modelling of Serial Manipulator. In: Fleury, A., Rade, D., Kurka, P. (eds) Proceedings of DINAME 2017. DINAME 2017. Lecture Notes in Mechanical Engineering(). Springer, Cham. https://doi.org/10.1007/978-3-319-91217-2_20
14. Merlet J-P (2004) Solving the forward kinematics of a Gough-type parallel manipulator with interval analysis. Int J Robot Res 23(3):221–235. https://doi.org/10.1177/0278364904039806
15. Merlet J-P (2005) Parallel robots, vol 128. Springer Science & Business Media. ISBN: 9781402041327
16. Mourrain B (1993) The 40 "generic" positions of a parallel robot. In: Proceedings of the 1993 international symposium on Symbolic and algebraic computation, pp 173–182

17. Neugebauer R (2006) Parallelkinematische Maschinen: Entwurf, Konstruktion. Anwendung. Springer, Berlin, Heidelberg, New York. ISBN 103-540-20991-3
18. Parikh PJ, Lam SS (2009) Solving the forward kinematics problem in parallel manipulators using an iterative artificial neural network strategy. Int J Adv Manuf Technol 40(5):595–606. https://doi.org/10.1007/s00170-007-1360-x
19. Pham P (2009) Design of hybrid-kinematic mechanisms for machine tools. EPFL. https://doi.org/10.5075/epfl-thesis-4314
20. Pieper DL (1969) The kinematics of manipulators under computer control. Stanford University
21. Raghavan M (1991) The Stewart platform of general geometry has 40 configurations. In: vol 97768, Proceedings of the ASME 1991 Design Technical Conferences. 17th Design Automation Conference: Vol 2 Computer-Aided Design, Mechanical Systems Simulation, and Analysis, Mechanisms, and Robotics. Miami, Florida, USA. September 22–25, 1991. pp. 397–402. ASME. https://doi.org/10.1115/1.2919188
22. Siciliano B, Khatib O, Kröger T (2008) Springer handbook of robotics, vol 200. Springer. https://doi.org/10.1007/978-3-540-30301-5
23. Tsai L-W, Joshi S (2002) Kinematic analysis of 3-DOF position mechanisms for use in hybrid kinematic machines. J Mech Des 124(2):245–253. https://doi.org/10.1115/1.1468860
24. Wang Y (2006) “An incremental method for forward kinematics of parallel manipulators." 2006 IEEE Conference on Robotics, Automation and Mechatronics, pp 1–5. https://doi.org/10.1109/RAMECH.2006.252629

Chapter 9
Actuator Design

Thorsten A. Kern, Henry Haus, Marc Matysek, and Stephanie Sindlinger

Abstract Actuators are the most important elements of any haptic device. Their selection or design significantly influences the quality of the haptic impression. This chapter deals with commonly used actuators, organized according to their physical principle of operation. It focuses on the electrodynamic, electromagnetic, electrostatic and piezoelectric actuator principles. Each actuator type is discussed in terms of its main physical principles, with examples of sizing and one or more applications. Other, less frequently used actuator principles are mentioned in several examples. The preceding chapters focused on the basics of control engineering and kinematic design. They covered topics of structuring and fundamental character. This and the following chapters deal with the design of technical components as parts of haptic devices. Experience teaches us that actuators for haptic applications can rarely be found "off-the-shelf". Their requirements always include some outstanding features in rotational frequency, power-density, working point, or geometry. These specialities make it necessary and helpful for users to be aware of the capabilities and possibilities for modifying existing actuators. Hence this chapter addresses both groups of readers: the users who want to choose a certain actuator and the mechanical engineer who intends to design a specific actuator for a certain device from scratch.

T. A. Kern (✉)
Hamburg University of Technology, Hamburg, Germany
e-mail: t.a.kern@tuhh.de

H. Haus
Darmstadt University of Technology, Institute for Electromechanical Design, Merckstr. 25, 64283 Darmstadt, Germany
e-mail: henry.haus@gmx.de

M. Matysek
Continental Automotive GmbH, VDO-Str. 1, 64832 Babenhausen, Germany
e-mail: mark.matysek@continental-corporation.com

S. Sindlinger
Roche Diabetes Care GmbH, Sandhofer Strasse 116, 68305 Mannheim, Germany
e-mail: stephanie.sindlinger@roche.com

T. A. Kern et al. (eds.), *Engineering Haptic Devices*, Springer Series on Touch and Haptic Systems, https://doi.org/10.1007/978-3-031-04536-3_9

9.1 General Facts About Actuator Design

Thorsten A. Kern

Before a final selection of actuators is made, the appropriate kinematics and the control-engineering structure, according to the previous chapters, should have been fixed. However, in order to handle these questions in a reasonable way, some basic understanding about actuators is mandatory. Especially the available energy densities, forces and displacements should be estimated correctly for the intended haptic application. This section provides some suggestions and guidelines to help and preselect appropriate actuators according to typical requirements.

9.1.1 Overview of Actuator Principles

There are a certain number of approaches to transform an arbitrary energy source into mechanical energy. Each of these approaches is one actuation principle. The best known and most frequently used principles are:

Electrodynamic principle A force, so called LORENTZ-force, acting upon a conductor conducting current.
Electromagnetic principle A force, acting upon a magnetic circuit to minimize the enclosed energy.
Piezoelectric principle A force, created by the atomic structure of a crystal due to applied voltage.
Capacitive principle A force, resulting from charges trying to minimize the energy in a capacitor.
Magnetorheological principle Viscosity change within a fluid resulting from particles trying to minimize the energy contained within a magnetic circuit.
Electrochemical principle Displacement of or pressure within a closed system, whereby a substance emits or bounds a gas and consequently changes its volume due to the application of electrical energy.
Thermal principle Change of length of a material due to controlled temperature changes, making use of the material's coefficient of thermal expansion.
Shape-memory alloy Sudden change of an object's shape switching between two crystal structures when exposed to relatively small temperature changes.

Each of these principles is used in different embodiments. They mainly differ in the exact effective direction of e.g. a force vector[1] or a building principle.[2] As a consequence a wide-spread terminology exists for naming actuators. The major terms are given here:

[1] The electromagnet principle for instance is divided into magnetic actuators and actuators according to the reluctance principle; the piezoelectric principle is subdivided into three versions depending on the relative orientation of electrical field and movement direction.

[2] E.g. resonance drives versus direct drives.

Electric motor The most general term of all. It may describe any electromechanic transformer. However, in most cases it refers to an actuator rotating continuously whose currents are commutated (mechanically or electronically), or which is equipped with a multiphase alternating current unit. Typically, it is a synchronous motor, a drive with a magnetic rotor moving synchronously to the rotating electromagnetic field. In a more general understanding the term includes hysteresis motors and squirrel-cage rotors/induction-machines, too. But the latter has not yet reached any relevance for haptic systems.

EC-motor Specific embodiment of the synchronous motor and very common to haptic applications. Motor according to the electromagnetic or electrodynamic principle with an electronic control unit for the rotating field (electronic-commutated, electronically commutated).

DC-motor In a general sense any motor operated with a DC-voltage. However in a more specific form a motor with a stationary stator-field and a alternating rotor-field. Used among haptic applications because of its cheapness and simplicity. This is an actuator according to the electromagnetic or electrodynamic principle with a mechanical control unit for the rotating field using switching contacts (mechanically commutated).

Resonance actuator Generic term for a whole class of actuators with very different actuation principles. The term describes an actuator containing one component which is driven in its mechanical resonance mode (or nearby its resonance mode). Typically, parts of this component make an elliptic oscillation driving a second component in small steps via a frictional coupling. As a result of the high frequency, the movement of the second component seems uninterrupted. The term is most frequently applied to piezoelectric actuators.

Ultrasonic actuator Resonance-actuator performing steps at a frequency within ultrasonic ranges (>15 kHz). These actuators are built almost always according to the piezoelectric principle.

Voice-coil-actuator Translational drive according to the electrodynamic principle. Mainly consisting of a conductor wrapped around a cylinder. The cylinder itself is placed in a magnetic circuit, resulting in a Lorentz-force when a current is applied to the conductor. There are two major embodiments, either with a "moving coil", another variant with a "moving magnet".

Shaker/Exciter A specific form of a voice-coil-actuator with an elastic suspension between the coil and the magnetic circuit. When current is applied to the coil an equilibrium condition between the suspension's spring and the Lorentz-force is achieved at a specific dynamic displacement. With an alternating current a wide range of frequencies can be addressed. Actuators according to this structure are frequently used for fast and dynamic movements of masses. Whereas the origins can be found in vibration testing (this is where its name comes from), this actuator-type is meanwhile regularly used to create surface-haptics on touch-surfaces or vibrational-feedback in mobile-devices.

Plunger-type magnet Actuator according to the electromagnetic principle. A rod made of ferromagnetic material is pulled into a magnetic circuit equipped with a coil. These actuators have very nonlinear force-displacement characteristics, but can create high forces with comparably little power required.

Stepper-motor Generic term for all actuation principles moving forward step by step. In contrast to the resonance-drives no component of a stepper-motor is driven in resonance mode. Their step-frequency is below any resonance of the system and may vary. These actuators may even be used in a "microstep mode", interpolating movement between so called "full-steps", which are original to their mechanical design. The term is most frequently used for rotatory drives. Especially for those working according to the reluctance-principle or another electromagnetic actuation principle.

Pneumatic and Hydraulic These actuation principles do not have a direct electric input value. They transform pressure and volume-flow into displacement and force. The media for pressure transmission is air in case of pneumatics and a fluid, typically oil, in case of hydraulics. Usually, the pressure itself is generated via actuators, e.g. electrical actuators attached to a compressor, and controlled via electrical valves.

Bending-actuator Actuator with an active layer, frequently made of a piezoelectric material—attached to a passive mechanical substrate. By actuating the active layer, mechanical tensions between this layer and the substrate build up, resulting in a bending movement of the whole actuator.

Piezoelectric stack A larger number of piezoelectric layers mechanically connected in series. Small displacements of each layer sum up to a large usable displacement of the whole actuator.

Piezoelectric motor/drive Generic term for all drives according to the piezoelectric principle. It frequently refers to drives moving a rotor or translator with a frictional coupling. However, this movement does not need to happen in resonance mode.

Capacitive actuator Actuator according to the capacitive principle and frequently used in microtechnology. Usually equipped with a comb-like structure of electrode-pairs, generating forces in millinewton range with micrometers of displacement.

Shape-memory wire Wire on the basis of shape-memory alloys capable to shorten in the range of percents ($\approx 8\%$ of its total length) when changing its temperature (e.g. by controlling a current flowing through the wire. The current heats up the wire according to its thermal loss at the wire's electrical resistance).

Surface-wave actuators Generic term for a group of actuators generating high-frequency waves in mechanical structures or exciting the resonance-modes of structures. This actuator is frequently based on piezoelectric principles and is used for the generation of haptic textures.

Each of the above actuation principles can be found in tactile and/or kinaesthetic systems. To simplify the decision process for a new design, all actuators can be grouped into classes. Most of the physical working principles can be grouped either into "self-locking" or "free-wheeling" systems.[3] These groups are identical to:

- Positional-sources (x) respectively angular-sources (α) with high mechanical impedance
- Force-sources (F) respectively torque-sources (M) with low mechanical impedance

According to the basic structures of haptic systems (Chap. 6) it is likely that both classes are used within different haptic systems. The correlation between basic structures of haptic systems and actuators is depicted in Table 9.1. This table shows a tendency towards typical applications. However actuators can be "impedance-matched" to a certain application. This happens by adding mechanical elements (springs, dampers) in series to the actuator. By this it is possible to use any actuator for any basic structure of haptic systems, trading in advantages for disadvantages which may be justified by the specific application and its requirements.

9.1.2 Actuator Selection Aid Based on Its Dynamics

Different actuator designs according to the same physical principle still cover wide performance ranges regarding their achievable displacements or forces. Based on the author's experience, these properties are put into relation to the dynamical ranges relevant for haptic applications. In Fig. 9.1 the most important actuation principles are visualized in squares scaled according to their achievable displacements (a)[4] and typical output forces and torques (b). The area covered by a specific version of an actuator is typically smaller than the area shown here. The diagram should be read in such a way that e.g. for haptic applications, . electromagnetic linear actuators exist, providing a displacement up to 5 mm at $\approx$ 50 Hz. These designs are not necessarily the same actuators which are able to provide $\approx$200 N, as with electromagnetic systems the effectively available force increases with smaller maximum displacement (Sect. 9.4). The diagrams in Fig. 9.1 visualize the bandwidths of realization-possibilities according to a certain actuation principle and document the preferred dynamic range of their application. Using the diagrams, we have to keep in mind

[3] This is—of course—a simplification. An actuator is supposed to be considered to have an internal impedance $\underline{z}$ and a source-capability, e.g. a force $\underline{F}$ or velocity $\underline{v}$. The combination of both make the impedance-range actuators can address in dependency of Frequency f. This is similar to all other sources, may it be electrical with a certain Wattage at a certain voltage up to a threshold of current, or may it be hydraulic where a certain flow can be provided up to a certain pressure. However for the sake of simplification and as a matter of fact, actuators can be considered first of all and within a certain operational range *ideal* sources.

[4] For continuously rotating principles all displacements are regarded as unlimited.

Table 9.1 Typical application areas for actuator principles in haptic systems

Control-type		Admittance		Impedance	
Type	Actuator	Closed-l	Open-l	Open-l	Closed-l
Rot.	Electric motor[a]	X	X	(X)[b]	–
Rot. and Transl.	EC-motor	–	–	X	X
Rot and Transl.	DC-motor	–	–	X	X
Rot and Transl.	Resonance-actuator	X	X	(X)	–
Rot and Transl.	Ultrasonic-actuator	X	X	(X)	–
Transl.	Voice-Coil	–	–	X	X
Transl.	Exciter	X	X	–	–
Transl.	Plunger-type magnet	X	–	–	–
Rot. (and transl.)	Stepper-motor	X	X	–	–
Transl. (and rot.)	Pneumatic	(X)	X	X	(X)
Transl. (and rot.)	Hydraulic	–	X	–	X
Transl.	Bending-actuator	–	X	–	–
Transl.	Piezo-stack	(X)	X	–	–
Transl. and rot.	Piezo-actuator	X	X	X	(X)
Transl.	Capacitive	–	(X)	–	–
Transl.	Shape-memory	–	(X)	–	(X)
Transl.	Surface wave	–	(X)	–	

X: is frequently used by many groups and even commercialized
(X): some designs, especially in research
-: very rare to almost none, an if it is used, it is only in the context of research)
Type: Gives an idea about which actuator design (translatory or rotatory) is used more often. If the actuator is unusual but does exist, the marker is set into brackets
Annotations:
[a] in the meaning of a mechanically commutated drive with a power between 10–100 W
[b] by high frequency vibrations of the commutation

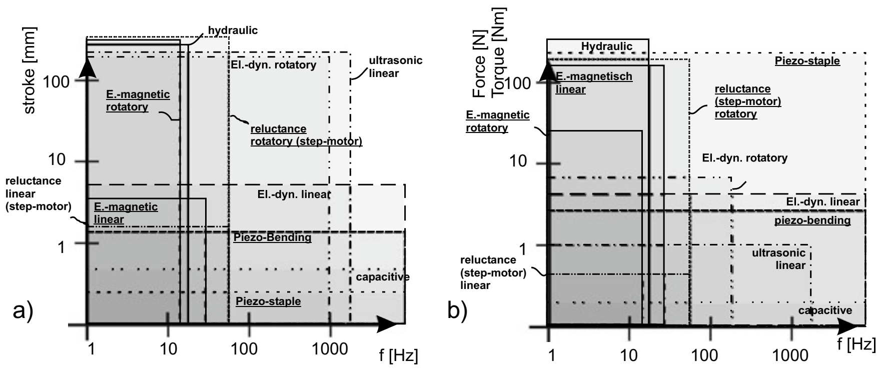

Fig. 9.1 Order of the actuator principles according to the achievable displacement (**a**) and forces resp. torques (**b**) in dependency from their dynamics. Further information can be found in [1]

that the borders are fluent and have to be regarded in the context of the application and the actuator's individual design.

9.1.3 Gears

In general machine engineering the usage of gears is a matter of choice for adapting actuators to their load and vice versa. Gears are available in many variants. A simple lever can be a gear; complex kinematics according to Chap. 8 are a strongly nonlinear gear. For haptic applications specialized gear designs are discussed for specific actuation principles in the corresponding chapters. However, there is one general aspect of the application of gears with relevance to the design of haptic systems which has to be discussed independently: the scaling of impedances.

There is no principal objection to the use of gears for the design of haptic systems. Each gear (Fig. 9.2) may it be rotatory/rotatory (gearwheel or frictional wheel), translatory/translatory (lever with small displacements), rotatory/translatory (rope/cable/capstan) has a transmission "tr". This transmission ratio scales forces

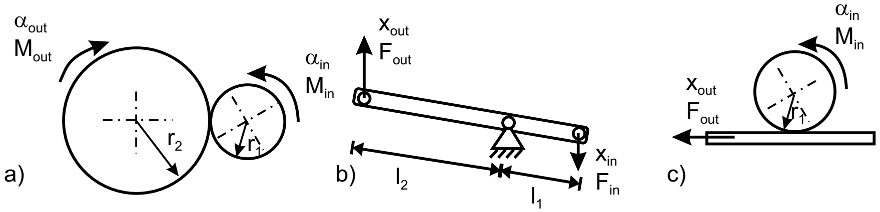

Fig. 9.2 Simple gear design with wheels (**a**), a lever (**b**) and a cable, rope or belt (**c**)

and torques neglecting loss due to friction according to

$$\frac{F_{\text{out}}}{F_{\text{in}}} = tr = \frac{l_2}{l_1}, \tag{9.1}$$

$$\frac{M_{\text{out}}}{M_{\text{in}}} = tr = \frac{r_2}{r_1}, \tag{9.2}$$

$$\frac{F_{\text{out}}}{M_{\text{in}}} = tr = \frac{1}{2\pi\, r_1}, \tag{9.3}$$

and displacements respectively angles according to

$$\frac{x_{\text{in}}}{x_{\text{out}}} = tr = \frac{l_2}{l_1}, \tag{9.4}$$

$$\frac{\alpha_{\text{in}}}{\alpha_{\text{out}}} = tr = \frac{r_2}{r_1}, \tag{9.5}$$

$$\frac{\alpha_{\text{in}}}{x_{\text{out}}} = tr = \frac{1}{2\pi\, r_1}. \tag{9.6}$$

The velocities and angular velocities scale to the differential of above equations. Assuming the impedance of the actuator $\underline{Z}_{\text{transl}} = \frac{F}{\underline{v}}$ resp. $\underline{Z}_{\text{rot}} = \frac{M}{\underline{\alpha'}}$, one consequence of the load-condition of a driven impedance $\underline{Z}_{\text{out}}$ from the perspective of the motor is:

$$\underline{Z}_{\text{transl}} = \frac{\underline{F}_{\text{in}}}{\underline{v}_{\text{in}}} = \frac{\underline{F}_{\text{out}}}{\underline{v}_{\text{out}}} \frac{1}{tr^2} = \underline{Z}_{\text{transl out}} \frac{1}{tr^2} \tag{9.7}$$

$$\underline{Z}_{\text{rot}} = \frac{\underline{M}_{\text{in}}}{\underline{\alpha'}} = \frac{\underline{M}_{\text{out}}}{\underline{\alpha'}} \frac{1}{tr^2} = \underline{Z}_{\text{rot out}} \frac{1}{tr^2} \tag{9.8}$$

The transmission-ratio tr is quadratic for the calculation of impedances. From the perspective of an actuator, the driven impedance of a system is getting small with a gear showing transmission-ratios larger than one. This is favourable for the actuating system (and the original reason for the application of gears). For haptic applications, especially for impedance controlled ones, the opposite case has to be considered. In an idle situation and with a transmission ratio larger than one[5] the perceived mechanical impedance of a system $\underline{Z}_{\text{out}}$ increases to the power of two with the transmission-ratio. Another aspect makes this fact even more critical, as the increase of output force changes only in a linear way with the transmission ratio, whereas e.g. a motor's unwanted moment of inertia is felt to increase quadratically.

[5] Which is the normal case, as typically the fast movement of an actuator is transmitted into a slower movement of the mechanism.

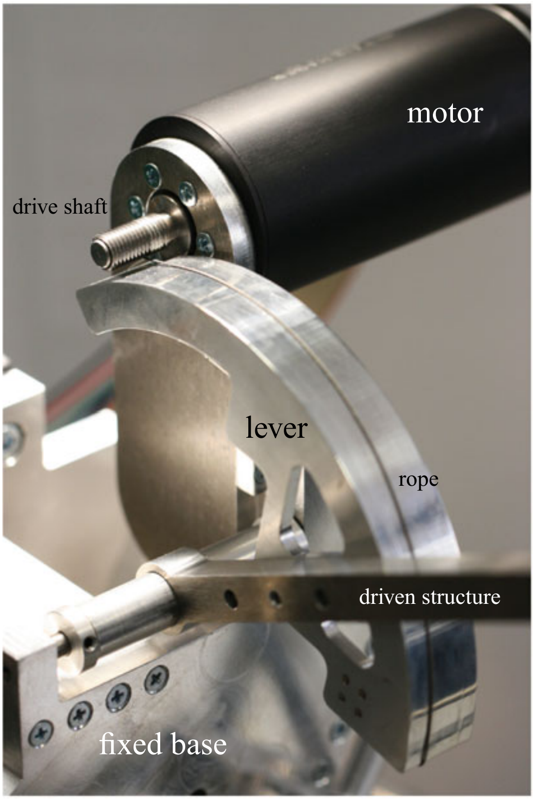

Fig. 9.3 Rope-based gear as widely used in haptic interfaces. The driven structure is connected to a lever, on which the driving rope is running. The driving rope is wound around the driving shaft of the motor. The number of revolutions around the shaft is determined by the amount of torque to be transmitted via the gear, threads are used to minimize friction and wearout between individual turns of the driving rope

This effect is obvious to anyone who has ever tried to rotate a gear-motor with a high transmission ratio (e.g. $tr > 100$) at its output. The inertia and internal frictions upscaled by the gear are identical to a self-locking of the actuator.

As a consequence, the usage of gears with force-controlled haptic systems makes sense only for transmission ratios of 1–20 (with emphasis on the lower transmission ratios between 3–6). For higher transmission ratios, designs according to Fig. 9.2c and Eq. (9.6) based on ropes or belts proved valid. They are used in many commercial systems, as with the aid of the definition $tr = \frac{1}{2\pi\, r_1}$ and the included factor 2π a comparably high transmission ratio can be achieved easily. In combination with rotatory actuators (typically EC-drives) with low internal impedances this design shows very impressive dynamic properties. Figure 9.3 shows an example for the application of such a gear to drive a delta mechanism [2].

Recently, a new type of gear came into view of several researchers [3]. The Twisted-String-Actuator (TSA) is based on a relatively small motor with large rotation speed that twists a string or a set of strings. Because of the twisting, the strings contract and provide pulling forces in the range of several ten newtons that can be transferred via bowden cables. Applications especially include exoskeletons as for example presented in [4] and other devices that are weight-sensitive.

Some advice may be given here out of practical experience: wheel-based gears are applicable for haptic systems but tend to generate unsteady and waving output torques due to their toothing. By a careful mechanical design, this unsteadiness can be reduced. The mechanical backlash should be minimized (which is typically accompanied by an increase in friction) for example by material combinations with at least one soft material. At least one gear should have spur/straight gearing, whereas the other one can keep involute gearing.

9.2 Electrodynamic Actuators

Thorsten A. Kern

Electrodynamic actuators are the most frequently used type of drives for haptic applications. This popularity is a result of the direct proportion between their output value (force or torque) from their input values (the electrical current). In case of kinaesthetic applications they are typically used as open-loop controlled force sources. In tactile applications these very dynamic actuators are frequently used as oscillators or exciters to move a mass and by the inertia and system-reaction create a buzz-feeling. They can be found equally as much in form of rotary or translational actuators. Depending on the design either the electrical coil or the magnet is the moving component of the actuator, whereas the other part is fixed to the device. This section gives a short introduction to the mathematical basics of electrodynamic systems. Afterward some design variants are discussed in more details. The final subsection deals with the drive electronics necessary to control electrodynamic systems.

9.2.1 The Electrodynamic Effect and Its Influencing Variables

Electrodynamic actuators are based on the LORENTZ-force

$$\mathbf{F}_{\text{Lorentz}} = \mathbf{i} \cdot l \times \mathbf{B}, \tag{9.9}$$

acting upon moving charges in a magnetic field. The LORENTZ-Force is dependent on the current $\mathbf{i}$, the magnetic induction $\mathbf{B}$ such as the length of the conductor l, which is typically formed as a coil. This subsection deals with optimization of each parameter for the maximization of the generated output force F_{Lorentz}. Any electrodynamic actuator is made of three components:

- generator of the magnetic field (another coil, or most frequently a permanent magnet)
- magnetic flux conductor (steel circuit, soft- or hard-magnetic core)
- electrical conductor (frequently formed as a coil or a more complex winding)

After a shallow look at Eq. (9.9) a recommendation for the maximization of the output force could be to simply increase the current **i** in the conductor. However with a given and limited available space for the conductor's length l (coil's cross section), and a flux density **B** with an upper border (0.8 to 1.4 T), the effectiveness of this change has to be put into question. This can be shown with a simple calculation example.

9.2.1.1 Efficiency Factor of Electrodynamic Actuators

For example a straight-forward design of an electrodynamic actuator similar to the AVN 20–10 (Fig. 9.4) is analyzed. It contains a wound coil with a permanent-magnet in a ferromagnetic core. The electrical power loss P_{el} of this electrodynamic system is generated mainly in a small moving coil with a pure ohmic resistance $R_{\mathrm{coil}} = 3.5\,\Omega$ and a nominal current $i = 0.78$ A:

$$P_{\mathrm{el}} = R_{\mathrm{coil}}\, i^2 = 3.5\,\Omega \cdot 0.78\,\mathrm{A}^2 = 2.13\,\mathrm{W}. \tag{9.10}$$

With this electrical power loss, and at a flux density $\mathbf{B} = 1.2$ T, and with an orthogonal conductor orientation, and a conductor length within the air gap $l = 1.58$ m, the actuator itself generates the force

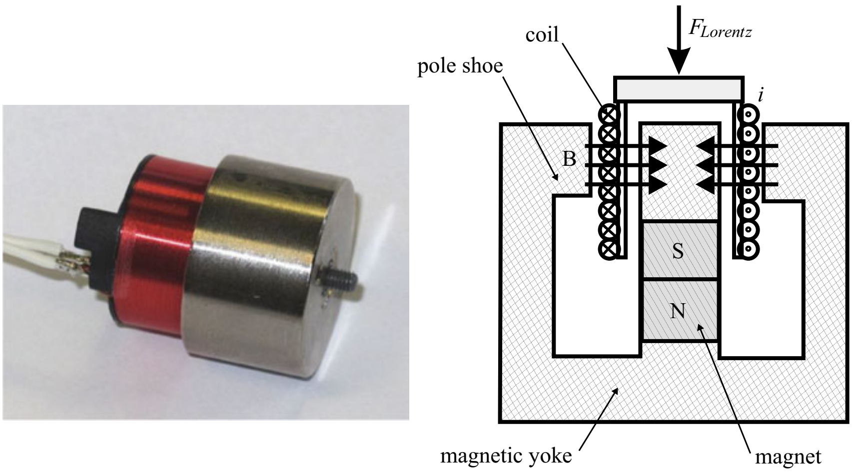

Fig. 9.4 Moving-coil actuator and corresponding functional elements

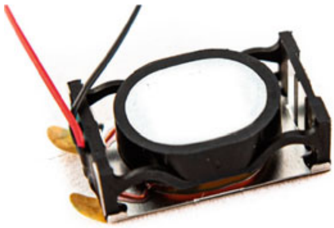
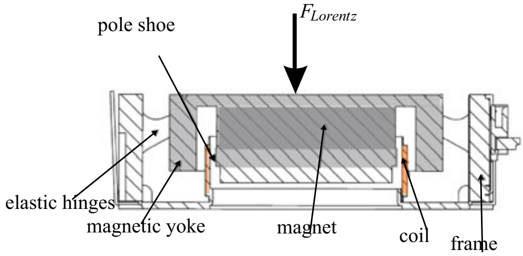

Fig. 9.5 Actuator as an exciter, moving mass-type actuator with fixed coil, GREWUS Exciter EXS241408WA

$$F_{\text{Lorentz}} = i\, l\, B = 0.78\,\text{A} \cdot 1.58\,\text{m} \cdot 1.2\,\text{T} = 1.48\,\text{N}\,. \tag{9.11}$$

Assuming the system being driven in idle mode—working against the coil's own mass of $m = 8.8$ g only—being accelerated from idleness, and performing a displacement of $x = 10$ mm, above electrical power P_{el} is needed for a period of

$$t = \sqrt{2\,\frac{x}{a}} = \sqrt{2\,\frac{x\,m}{F}} = 0.011\,s \tag{9.12}$$

seconds. The electrical energy loss sums up to

$$W_{\text{el}} = P_{\text{el}} \cdot t = 23,4\,mJ. \tag{9.13}$$

This gives an efficiency factor of $\frac{W_{\text{mech}}}{W_{\text{el}}+W_{\text{mech}}} = 38\%$ for idle mode and continuous acceleration. And this is a valid working point leading to exciter-type actuators (Fig. 9.5) whose efficiency and primary application in mobile applications derive from a highly dynamic movement.

Assuming now that such an actuator shall generate a force of 1 N against a finger tip for a period of e.g. two seconds, an electrical power of $W_{\text{el}} = 2.13\,\text{W} \cdot 2\text{s} = 4.26\,\text{J}$ is needed. This would be identical to an efficiency factor well below 1%. And indeed the efficiency factor of electrodynamic actuators in haptic applications lies in the area of low percentages due to the common requirement to generate quite static forces without much movement. This simple calculation points to one major challenge with electrodynamic actuators: The electrical power lost due to heat transmission extends the mechanically generated power by far. Consequently during the design of electrodynamic actuators the thermal management of energy losses is key.

9.2.1.2 Minimization of the Power Loss

Typical designs of electrodynamic actuators either have a wound conductor which in itself is self-supportive, or which is wound on a coil-carrier (Fig. 9.6). The available

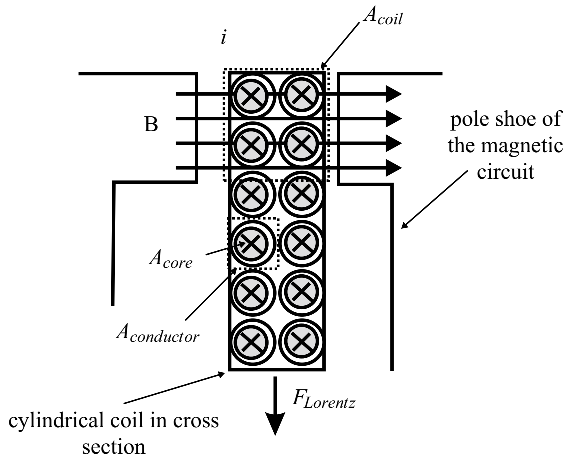

Fig. 9.6 Cross-section through a cylindrical electrodynamic actuator according to the moving coil principle

space for the electrical coil within the homogenous magnetic flux is limited (A_{Coil}). The number of coil-turns $N_{\text{Conductor}}$ is limited too within this area due to the cross-sectional surface a single turn needs $A_{Conductor}$. This cross-sectional surface is always more than the actual cross-section of the conductor, as the winding will have gaps in between single turns (Eq. (9.15)). Additionally the actual conducting core with the cross sectional surface A_{Core} will be smaller than the cross-section of the conductor itself due to its isolation. Both parameters describing the geometrical losses in cross sections which are available within tables of technical handbooks [5] and are assumed as factors $k \geq 1$ according to Eq. (9.14). The length l of the conductor can be easily calculated by multiplication with the numbers of turns and the mean circumference $Circ$ of the coil (Eq. (9.16)).

The choice of the conductor's diameter influences the resistance of the coil via the conducting area A_{Core}. The specific length-based resistance R_{spezf} of a conductor is given according to Eq. (9.17). Big conducting diameters with large cross-sections A_{Core} allow coils able to conduct high currents at low voltages but—due to the limited volume available—few windings. Small diameters limit the necessary currents at high voltages and carry more windings. By a careful choice of wire-diameter the winding can be adjusted as a load to the corresponding source to drain the maximum available power.

The power loss P_{Loss} (Eq. (9.18)) acceptable within a given winding is limited. This limit is defined by the generated heat being able to dissipate. As a rule of thumb a standard copper winding can carry (if able to dissipated heat to one side) $4\frac{A}{mm^2}$ continuously. In case of printed-circuit-boards (PCBs) the current-density for copper can be increased to even $20-40\frac{A}{mm^2}$ due to the very good thermal coupling between copper and environment. The real technical solution is dependent on the time of continuous operation, the thermal capacity resulting from the volume of the actuator and the materials it consists of, and a potential cooling system. A calculation of heat transmission is specific to the technical solution and can not be solved in general within this book. But the dependency of LORENTZ-force on power loss can be formulated:

$$A_{\text{Conductor}} = k \cdot A_{\text{Core}} \tag{9.14}$$

$$N_{\text{Conductor}} = \frac{A_{\text{Coil}}}{A_{\text{Conductor}}} \tag{9.15}$$

$$l_{\text{Conductor}} = N_{\text{Conductor}} \cdot Circ \tag{9.16}$$

$$R_{\text{spezf.}} = \frac{l_{\text{Conductor}}\,\rho}{A_{\text{Conductor}}} \tag{9.17}$$

$$P_{\text{Loss}} = i^2 \cdot R_{\text{Coil}} \tag{9.18}$$

From Eq. (9.18) follows

$$i = \sqrt{\frac{P_{\text{Loss}}}{R_{\text{Coil}}}} \tag{9.19}$$

With Eq. (9.17) there is

$$i = \sqrt{\frac{P_{\text{Loss}}\,A_{\text{Core}}}{\rho\,l_{\text{Conductor}}}} \tag{9.20}$$

put into Eq. (9.9) (keeping the direction of current flow $\mathbf{e}_i$) there is

$$F_{\text{Lorenz}} = \sqrt{\frac{P_{\text{Loss}}\,A_{\text{Core}}\,l_{\text{Conductor}}}{\rho}}\,\mathbf{e}_i \times \mathbf{B} \tag{9.21}$$

by considering Eqs. (9.15)–(9.16) the result is

$$F_{\text{Lorenz}} = \sqrt{\frac{P_{\text{Loss}}\,A_{\text{Coil}}\,N\,\text{Circ}}{\rho\,k}}\,\mathbf{e}_i \times \mathbf{B} \tag{9.22}$$

The Eqs. (9.15)–(9.18) put into Eq. (9.9) gives a precise picture of the influence values on the LORENTZ-force (Eq. (9.22)). The level of Lorentz-force is given by the power loss P_{Loss} acceptable within the coil. If there is room for modifications to the geometrical design of the actuator, the cross-sectional area of the coil and the circumference of the winding should be maximized. Additional a choice of alternative materials (e.g. alloy instead of copper) may minimize the electrical resistance. Furthermore the filling-factor k should be reduced. One approach could be the use of wires with a rectangular cross section to avoid empty spaces between the single turns.

The question for the maximum current itself is only relevant in combination with the voltage available and in the context of adjusting the electrical load to a specific electric source. In this case for i_{Source} and u_{Source} the corresponding coil-resistance has to be chosen according to Eq. (9.23).

$$P_{\text{Source}} = u_{\text{Source}} \cdot i_{\text{Source}} = i^2_{\text{Source}} \cdot R_{\text{Coil}}$$
$$R_{\text{Coil}} = \frac{P_{\text{Source}}}{i^2_{\text{Source}}} \tag{9.23}$$

Surprisingly from the perspective of a realistic design an increase in current is not necessarily the preferred option to increase the LORENTZ-force according to Eq. (9.22). The possibility to optimize P_{Loss} by adding cooling, or to analyze the temporal pattern of on- and off-times is much more relevant. Additionally the flux-density **B** has a—compared to all other influence factors—quadratically higher influence on the maximum force.

9.2.1.3 Maximization of the Magnetic Flux-Density

For the optimization of electrodynamic actuators a maximization of the flux density **B** is necessary within the area where the conducting coils are located. This place is usually called air-gap and resembles an interruption of the otherwise closed ferromagnetic core conducting the magnetic flux. The magnetic flux density is influenced by

- the choice of ferromagnetic material for the magnetic core,
- the field winding/exciter winding of the static magnetic field, and
- the geometrical design of the magnetic core.

In the context of this book some basic design criteria for magnetic circuits are given. For an advanced discussion and optimization process source [6] is recommended.

Basics for the Calculation of Magnetic Circuits

Calculating magnetic circuits show several parallels to the calculation of electrical networks. As shown in Table 9.2 several analogies between electrical and magnetic variables can be defined.

The direct analogy to the magnetic flux ϕ is the electrical current I. Please note that this is an aid for thinking and not a mathematical reality, although it is very common. The actual direct analogy for the current I would be a time dependent magnetic flux $\frac{d\phi}{dt}$, which is usually not defined with an own variable name. The great exception with this model is the magnetomotive force Θ, which resembles the sum of all magnetic voltages V identical to a rotation within an electrical network. Or another way to say it: It is the source of potential difference in a magnetic network. Nevertheless it is treated differently, as many applications require generating a magnetomotive force Θ to be generated by a certain number of winding-turns N and a current I, often referred to as ampere turns. The coupling between field- and flux-variables is given by the permittivity ε in case of electrical values and by the permeability μ in case

Table 9.2 Analogies between electric and magnetic values

Description	Electric	Magnetic
Flux differential flux	Charge Q (Coulomb = As) Current $I = \frac{dQ}{dt}$ (A)	Magnetic flux ϕ (Weber = Vs)
Flux-value	Dielectric flux density D (C/m^2) $Q = \int_A \mathbf{D} d\mathbf{A}$ Current density J (A/m^2) $I = \int_A \mathbf{J} d\mathbf{A}$	Flux density B (Tesla = Vs/m^2) $\phi = \int_A \mathbf{B} d\mathbf{A}$
El.-mag. coupling formerly	Voltage U (V) Electromotive force (e.m.f.)	Current linkage Θ (A) Magnetomotive force (m.m.f.)
Induction-laws	$U = -N \frac{d\phi}{dt}$ $U = -N \int \mathbf{B} dA \frac{d}{dt}$	$\Theta = N \frac{dQ}{dt}$ $\Theta = N\, I = V$ (N = turns)
Field-values	El. field strength E (V/m)	Magn. field strength H (A/m)
Differential-values	Voltage U (V) $U = \int_a^b \mathbf{E} d\mathbf{s}$	Magnetic voltage V (A) $V = \int_a^b \mathbf{H} d\mathbf{l}$
Mesh-equations	$U_{\text{ges}} = \sum_i U_i$	$\Theta = \sum_i V_i$
Resistances	El. resistance R (Ω) $R = \frac{U}{I}$	Magn. resistance R_m (A/Vs) reluctance $R_m = \frac{V}{\phi}$
Coupling factors	Permittivity $\varepsilon = \varepsilon_0\, \varepsilon_r$ ($\varepsilon_0 = 8{,}854 \cdot 10^{-12}$ C/Vm)	Permeability $\mu = \mu_0\, \mu_r$ ($\mu_0 = 1,256 \cdot 10^{-6}$ Vs/Am)
Coupling between field- and flux-values	$\mathbf{D} = \varepsilon\, \mathbf{E}$	$\mathbf{B} = \mu\, \mathbf{H}$
Power (W)	$P_{\text{el}} = U \cdot I$	$P_{\text{mag}} = V \cdot \phi = \Theta \cdot \phi$
Energy (J)	$W_{\text{el}} = P_{\text{el}}\, t$	$W_{\text{mag}} = P_{\text{mag}}\, t = \phi\, V\, t$ $W_{\text{mag}} = \sum_n H_n\, l_n \cdot B_n\, A_n$

of magnetic values. It is obvious that the field-constants ε_0 differs from μ_0 by the factor 10^6. This is the main reason for the electromagnetic effect being the preferred physical realization of actuators in macroscopic systems.[6]

However above dependencies although valid consider linearity. The electrical permittivity can be regarded as quite constant (Sect. 9.5) even for complex actuator designs, and can be approximated as linear around an operating point. The permeability μ_r of typical flux-conducting materials however shows a strong nonlinear relationship, the materials are reaching saturation. The level of magnetic flux has to be limited to prevent saturation-effects in the design of magnetic core.

[6] In micro-mechanical systems the energy-density relative to the volume becomes more important. The manufacture of miniaturized plates for capacitive actuators is much easier to realize with batch processes than the manufacture of miniaturized magnetic circuits.

Magnetic Circuits

For the maximization of the magnetic flux density it is necessary to either analyze the magnetic circuit mathematical-analytically and/or do a numerical simulation of it. For the simulation of magnetic fields common CAD and FEM products are available.[7] For classification of the mathematical problem three solution levels exist: stationary, quasi-stationary, and dynamic magnetic fields. With stationary magnetic fields there is no time dependent change of the magnetic circuit. A steady state of flux density is assumed. With quasi-stationary field the induction is being considered resulting from changes within the current generating the magnetic field or a linearized change within the geometry of the magnetic circuit (e.g. a movement of an anchor). Dynamic magnetic fields consider additional effects covering the dynamic properties of moving mechanical components up to the change of the geometry of the magnetic circuit and the air gaps during operation. By dealing with electrodynamic actuators the analysis of static magnetic circuits is sufficient for a first dimensioning. The relevant dynamic drawbacks for electrodynamic actuators are presented in Sect. 9.2.1.4.

There are two principle possibilities to generate the magnetic flux densities within the volume of a conducting coil:

1. Generation via winded conductors with another coil (exciter winding)
2. Generation via a permanent magnet

Both approaches show specific pros and cons: With a winded conductor the flux density $B = \mu\,(N\,I - H_{Fe}\,l_{Fe})$ can be raised without any theoretical limit. In practical application the flux-conducting material will reach saturation (Fig. 9.7) actually limiting the achievable maximum flux density. Additionally the ohmic resistance of the winding will generate electrical power losses, which will have to be dissipated in addition to the losses resulting from the electrodynamic principle itself (Sect. 9.2.1.1). Abandoning any flux-conducting material and using exciter-windings with extremely low electrical resistance extraordinary high field-densities can be reached.[8] Till now, such a technological effort for haptic devices is not made yet.

Building a magnetic circuit with a permanent magnet, the practical border for the flux density is given by the remanence flux density B_r of the magnetic material. Such a magnet can be compared to a source providing a certain magnetic power. The flux density—being the relevant quality for electrodynamic actuators—is not independent from the magnetic load attached to the permanent magnet. Additionally the relevant properties of the magnetic material are temperature-dependent, and wrong use of specific magnet-materials may harm its magnetic properties.[9]

Nevertheless modern permanent-magnetic materials made of "rare earths" are the preferred source to generate static magnetic fields for electrodynamic actuators. The

[7] For the very beginning there are several free or open software-projects available for electrical and magnetic field simulation, e.g. for rotatory or planar systems a program from David Meeker named "FEMM" www.femm.info.

[8] MRI systems for medical imaging generate field densities of 2 T and more within air gaps of up to 1 m diameter by the use of supra-conducting coils and almost no magnetic circuit at all.

[9] E.g. when removing AlNiCo magnets out of their magnetic circuit after magnetization, they may drop below their coercive field strength actually losing performance.

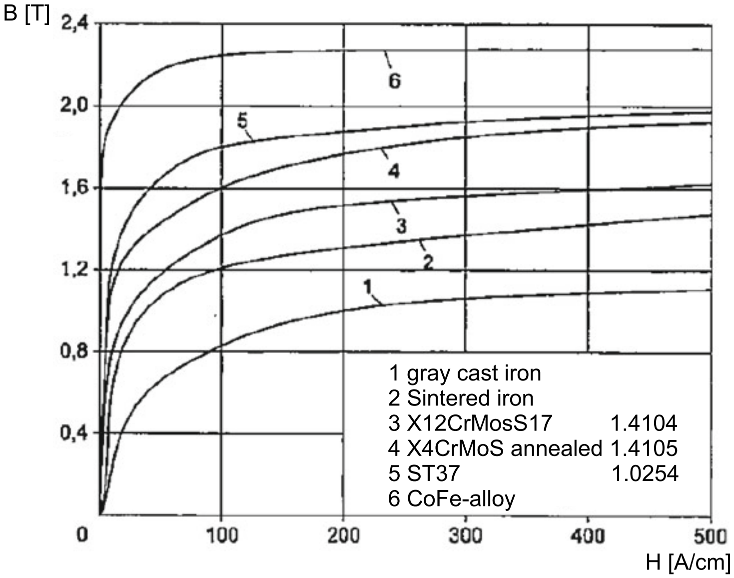

Fig. 9.7 Saturation curve of typical magnetic materials [6] © Springer Nature, all rights reserved

following section gives some basics on the calculation for simple magnetic circuits. In extension to what is shown here a more precise analytical calculation is possible [6]. However it is recommended to use simulation tools early within the design process. Especially leakage fields are a great challenge for the design of magnetic circuits. And especially beginners should develop a feeling for the look of these fields with the aid of simulation tools.

Direct Current Magnetic Field

Figure 9.8a shows a magnetic circuit out of iron with a cross section A and an air-gap with the length ξ_G ($G =$ Gap). The magnetic circuit has a winding with N turns conducting a current I. The medium length of the magnetic circuit is l_{Fe}. For calculation the circuit can be transformed into a magnetic equivalent network (Fig. 9.8b). According to the analogies defined in Table 9.2 the magnetic induction generates a magnetomotive force Θ as a differential value. In combination with two magnetic resistances of the iron circuit R_{mFe} and the air gap R_{mG} a magnetic flux ϕ can be identified.

For the calculation of the flux density B in the air gap, it is assumed that this magnetic flux ϕ is identical to the flux within the iron part of the circuit. Leakage fields are disregarded in this example.[10]

[10] Considering leakage fields would be identical to a parallel connection of additional magnetic resistors to the resistance of the air gap.

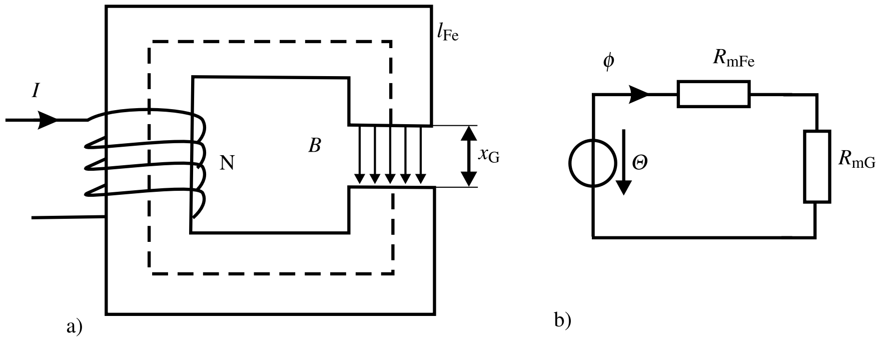

Fig. 9.8 Magnetic field generation B via a current-conducting coil with N turns (**a**), and derived equivalent circuit representation (**b**)

$$B = \frac{\phi}{A}$$

The magnetic resistance of materials and surfaces are dependent on the geometry and can be found in special tables [6]. For the magnetic resistance of a cylinder of the length l and the diameter d a resistance according to Eq. (9.24) is given.

$$R_m = \frac{4\,l}{\mu\,\pi\,d^2} \tag{9.24}$$

For the magnetic circuit the magnetic resistances $R_{m\mathrm{Fe}}$ and $R_{m\mathrm{G}}$ can be regarded as known or at least calculable. The magnetic flux is given by

$$\phi = \frac{\Theta}{R_{m\mathrm{Fe}} + R_{m\mathrm{G}}}, \tag{9.25}$$

and the flux density by

$$B = \frac{\Theta}{(R_{m\mathrm{Fe}} + R_{m\mathrm{G}})\,A}. \tag{9.26}$$

Using this procedure a clever approximation of the magnetic resistances of any complex network of magnetic circuits can be made. In this specific case of a simple horseshoe-formed magnet an alternative approach can be chosen. Assuming that the magnetic flux density in the air-gap is identical to the flux density in the iron (no leakage fields, see above) the flux-density B is given by:

$$B = \mu_0 \mu_r\, H \tag{9.27}$$

Assuming that μ_r is given either as a factor or with a characteristic curve (like in Fig. 9.7) only the magnetomotive force Θ within the iron has to be calculated. With

$$\Theta = H_{\mathrm{Fe}}\, l_{\mathrm{Fe}} + H_{\mathrm{G}}\, \xi_G = \frac{B}{\mu_0 \mu_r}\, l_{\mathrm{Fe}} + \frac{B}{\mu_0}\, \xi_G \tag{9.28}$$

the flux density

$$B = \Theta\, \frac{1}{\frac{l_{\mathrm{Fe}}}{\mu_0 \mu_r} + \frac{\xi_G}{\mu_0}}, \tag{9.29}$$

results and can be written down immediately. The generalized model of a coil in a magnetic circuit is that of an ideal magnetic voltage source.

Permanent Magnets Generating the Magnetic Field

As stated earlier the typical approach to generate the magnetic field within an electrodynamic actuator is by using a permanent magnet. Permanent magnets are not just some ideal flux- or field-sources. Therefore some basic understanding of magnet technology will be necessary.

As a simple approach a magnet is a source of energy which is proportional to the volume of the magnet. Magnets are being made out of different magnetic materials (Table 9.3) differing in the maximum achievable flux density (remanence flux density B_r), the maximum field-strengths (coercive field strength $H_{c\,B}$ and $H_{c\,J}$)), and their energy density BH_{max}, such as the temperature coefficient. Additionally identical materials are differentiated according to being isotropic or anisotropic. With isotropic magnets its substance is made of homogeneous material which can be magnetized in one preferred direction. With anisotropic material a magnetic powder was mixed with a binding material (e.g. epoxy) and formed via a casting or injection-molding process. Latter approach enables almost unlimited freedom for the magnet's geometry and a very large influence concerning the pole-distribution on the magnet. However anisotropic magnets are characterized by slightly worse characteristic values in energy density such as maximum field-strengths and flux densities.

Figure 9.9 shows the second quadrant of the B-H-characteristic curve (only this quadrant is relevant for an application of a magnet within an actuator) of different magnetic materials. The remanence flux density B_r equals the flux density with

Table 9.3 Magnetic properties of permanent-magnet materials [6] © Springer Nature, all rights reserved

Material	B_r (T)	$H_{c\,B}$ (kA/m)	$(BH)_{max}$ (kJ/m^3)
AlNiCo (isotrop)	0,5 ... 0.,9	10 ... 100	3 ... 20
AlNiCo (anisotrop)	0,8 ... 1,3	50 ... 150	30 ... 70
Hard ferrite (isotrop)	0,2 ... 0,25	120 ... 140	7 ... 9
Hard ferrite (anisotrop)	0,36 ... 0,41	170 ... 270	25 ... 32
SmCo (anisotrop)	0,8 ... 1,12	650 ... 820	160 ... 260
NdFeB (anisotrop)	1,0 ... 1,47	790 ... 1100	200 ... 415

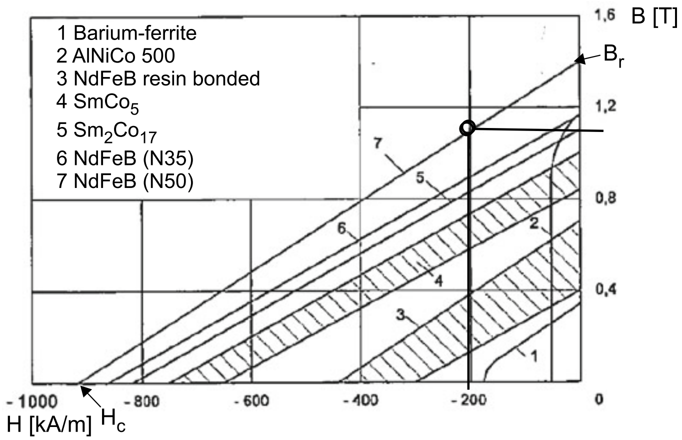

Fig. 9.9 Demagnetization curves of different permanent-magnet materials [6] © Springer Nature, all rights reserved

short-circuit pole shoes (a magnet being surrounded by ideal iron as magnetic circuit). When there is an air gap within the magnetic circuit (or even by the magnetic resistance of the real magnetic circuit material itself), a magnetic field strength H appears as a load. As a reaction an operation point is reached, which is shown here as an example on a curve of NdFeB for a flux-density of $\approx$200 kA/m. The actually available flux density at the poles is decreased accordingly. As electrodynamic actuators for haptic applications face high requirements according to their energy density, there are almost no alternatives to the usage of magnet materials based on rare earths (NdFeB, SmCo). This is very accommodating for the design of the magnetic circuit, as nonlinear effects near the coercive field strength such as with AlNiCo or Barium-ferrite are of no relevance.[11] Rare earth magnets allow an approximation of their B/H-curve with a linear equation, providing a very nice relationship for their magnetic resistance (Fig. 9.10c):

$$R_{\mathrm{Mag}} = \frac{V}{\phi} = \frac{H_c\, l_{\mathrm{Mag}}}{B_r\, A} \tag{9.30}$$

Equation 9.30 and Fig. 9.10c reveal the actual mental model of a permanent magnet in a circuit: At their working-point, they can be considered linear non-ideal magnetic voltage source $V = H_c\, l_{\mathrm{Mag}}$ with an internal resistance R_{Mag}.

[11] The small coercive field strength of these materials e.g. result in the effect, that a magnet magnetized within a magnetic circuit does not reach its flux density anymore once removed and even after re-assembly into the circuit again. This happens due to the temporary increase of the air gap, which is identical to an increase of the magnetic load to the magnet beyond the coercive field strength. Additionally the temperature-dependency of the coercive field strength and of the remanence flux density is critical. Temperatures just below the freezing point may result in a demagnetization of the magnet.

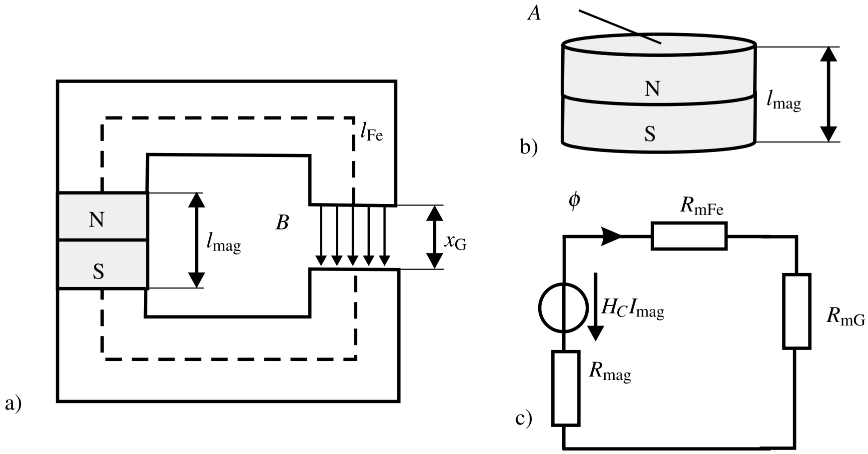

Fig. 9.10 Magnetic field generation B via permanent magnets (**a**), derived equivalent circuit (**b**), and dimensions of the magnet (**c**)

With this knowledge the magnetic circuit of Fig. 9.10a and the corresponding equivalent circuit (Fig. 9.10b) can be calculated identical to an electrically excited magnetic circuit.

The flux density within the iron is once again given by

$$B = \frac{\phi}{A} \tag{9.31}$$

For the given magnetic circuit the resistances $R_{m\mathrm{Fe}}$ and $R_{m\mathrm{G}}$ are assumed as known or calculable. From Eq. (9.30) the magnetic resistance of the permanent magnet is known. The source within the equivalent circuit is defined by the coercive field strength and the length of the magnets $H_c\, l_{\mathrm{Mag}}$. These considerations result in

$$\phi = \frac{H_c\, l_{\mathrm{Mag}}}{R_{m\mathrm{Fe}} + R_{m\mathrm{G}} + R_{\mathrm{Mag}}}, \tag{9.32}$$

and the flux density

$$B = \frac{H_c\, l_{\mathrm{Mag}}}{(R_{m\mathrm{Fe}} + R_{m\mathrm{G}} + R_{\mathrm{Mag}})\, A}. \tag{9.33}$$

Slightly rearranged and R_{Mag} included gives

$$B = \frac{B_r\, H_c\, \frac{l_{\mathrm{Mag}}}{A}}{(R_{m\mathrm{Fe}} + R_{m\mathrm{G}})\, B_R + H_c\, \frac{l_{\mathrm{Mag}}}{A}}. \tag{9.34}$$

Equation (9.34) states by the factor $B_r\ H_c\ \frac{l_{\text{Mag}}}{A}$ that it is frequently very helpful for achieving a maximum flux density B in the air gap to increase the length of a magnet with at the same time minimized cross-sectional area of the magnetic circuit—which is of course limited by the working distance within the air gap and the saturation field strengths of the magnetic circuit.

9.2.1.4 Additional Effects in Electrodynamic Actuator

To do a complete characterization of an electrodynamic actuator there are at least three more effects, whose influences will be sketched within the following paragraphs.

Induction

For a complete description of an electrodynamic actuator the *dynamic* properties needs to be considered next to the geometrical design of its magnetic circuit and the mechanical design of its winding and the considerations concerning electrical power losses. For this analysis the electrodynamic actuator is regarded as a bipolar transformer (Fig. 9.11).

A current $\underline{i}_0$ generates via the proportional constant $B\,l$ a force $\underline{F}_0$, which moves the mechanical loads attached to the actuator. The movement itself results in a velocity $\underline{v}_0$ which is transformed via the induction law and the proportional constant to an induced voltage $\underline{u}_1$. By measurement of $\underline{u}_1$ and a current source the rotational velocity or the movement velocity v can be measured, with a voltage source the measurement of $\underline{i}_0$ provides a force- or torque-proportional signal. This is the approach taken by the variant of admittance controlled devices as a control value (Sect. 6.7).

The induction itself is a measurable effect, but should not be overestimated. Typically electrodynamic actuators are used as direct drives at small rotational or translational velocities in haptic systems. Typical coupling factors with rotatory drives are—depending on the size of the actuators—in an area between 100 to 10 $\frac{\text{revolutions}}{s\,V}$. At a rotational speed which is already fast for direct drives of 10 Hz, induced voltage amplitude $|\underline{u}_1|$ of 0.1–1 V can be achieved. This is around 1–5% of the control voltage's amplitude.

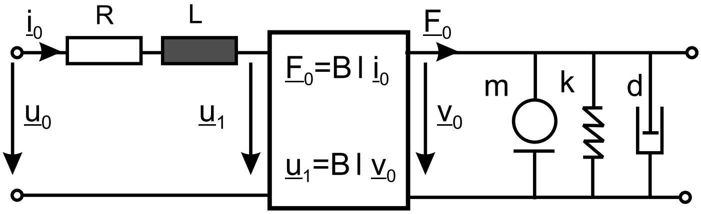

Fig. 9.11 Electrical and mechanical equivalent circuit of an electrodynamic actuator as being a transformer

Electrical Time Constant

Another aspect resulting from the model according to Fig. 9.11 is the electrical transfer characteristics. Typical inductances L of electrodynamic actuators lie in the area of 0.1–2 mH. The ohmic resistance of the windings is largely depending on the actual design, but as a rule of thumb values between 10–100 Ω can be assumed. The step-response of the electrical transfer system $\frac{\underline{i}_0}{\underline{u}_0}$ shows a time-constant $\tau = \frac{L}{R} = 10-30\,\mu\text{s}$ and lies within a frequency range $\gg$10 kHz, which is clearly above the relevant dynamic area of haptics.

Field Response

A factor which can not so easily be neglected when using electrodynamic actuators for high forces is the feedback of the magnetic field generated by the electromagnetic winding on the static magnetic field. Taking the actuator from the example at the beginning (Fig. 9.4) positive currents generate a field of opposite direction to the field generated by the magnet. This influence can be considered by substitution of both field sources. Depending on the direction of current this field either enforces or weakens the static field. With awkward dimensioning this can result in a directional variance of the actuator properties. The problem is not the potential damage to the magnet, modern magnetic materials are sufficiently stable, but a variation of the magnetic flux density available within the air gap. An intended application of this effect within an actuator can be found in an example according to Fig. 9.52.

A deeper discussion about electrodynamic actuators based on concentrated elements can be found in [7].

9.2.2 *Actual Actuator Design*

As stated earlier electrodynamic actuators are composed of three basic components: coil/winding, magnetic circuit, and magnetic exciter. The following section describes a procedure for the design of electrodynamic actuators based on these basic components. As the common principle for excitation a permanent magnet is assumed.

9.2.2.1 Actuator Topology

The most fundamental question for the design of an electrodynamic actuator is its topology. Usually it is known whether the system shall perform rotary or translation movements. Afterward the components magnetic circuit, the location of magnets, pole-shoes and the coil itself can be varied systematically. A few quite common structures are shown in Fig. 9.13 for translational actuators, and in Fig. 9.12 for rotatory actuators. For the design of electrodynamic actuators in any case the question should be asked, whether the coil or the magnetic circuit shall move. By this variation apparently complex geometrical arrangements can be simplified drastically. Anyway

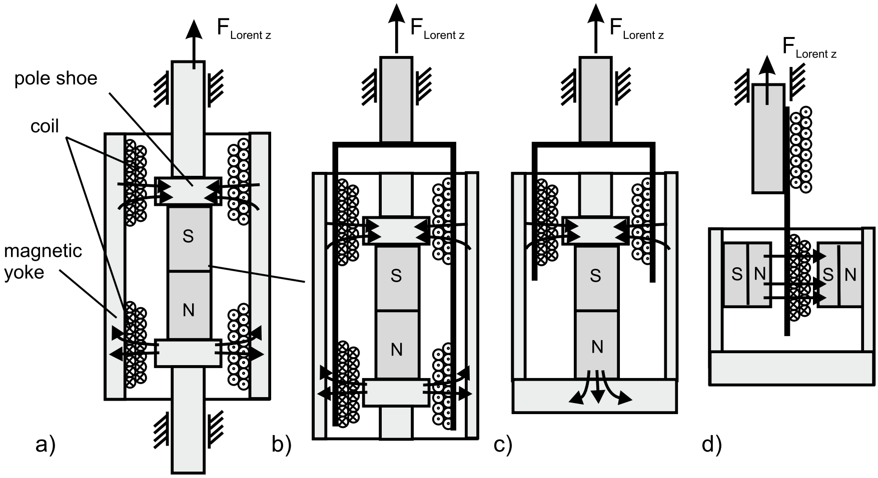

Fig. 9.12 Variants of electrodynamic actuators for translational movement with moving magnets (**a**), moving coils (**b**), as plunger-type (**c**), and as flat-coil (**d**)

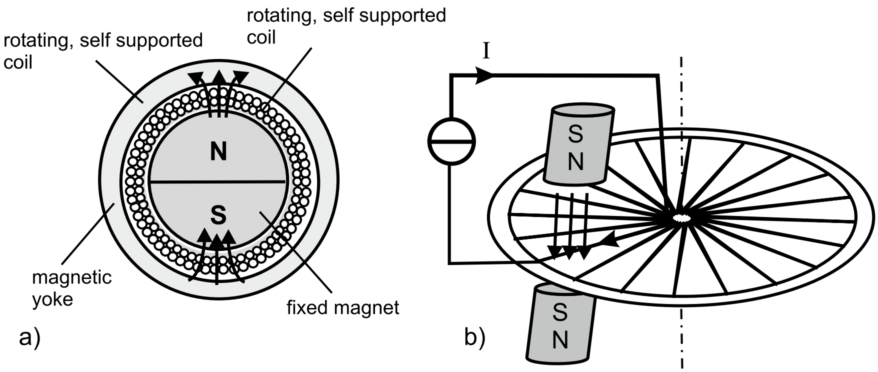

Fig. 9.13 Variants of electrodynamic actuators for rotatory movements with self-supportive winding (**a**), and with disc-winding

it has to be considered that a moving magnet has more mass and can typically be moved less dynamically than a coil. On the other hand there is no contact- or commutating problem to be solved with non-moving windings.

Moving Coils

Electrodynamic actuators according to the principle of moving coils with a fixed magnetic circuit are named "moving coil" in the case of a linear movement and "iron-less rotor" in the case of a rotatory actuator. They always combine few moving masses and as a result high dynamics. The translatory version shows displacements of a few millimeters, and is used especially within audio applications as loudspeaker. Actuators according to the principle of "moving coils" have two disadvantages:

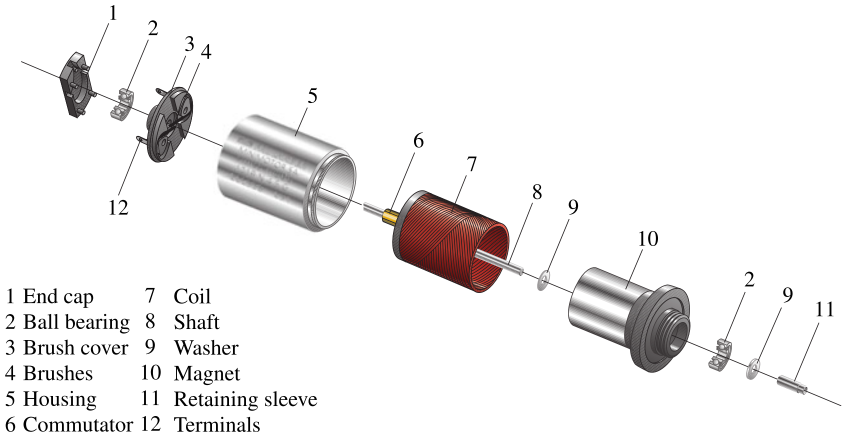

Fig. 9.14 Design of an electrodynamic actuator with self-supportive winding according to the FAULHABER-principle. Picture courtesy of *Dr. Fritz Faulhaber GmbH*, Schöneich, Germany, used with permission

- As the coil is moving, the electrical contact is subject to mechanical stresses. Especially with high displacements the contact has to be mechanically robust.
- If there is the idea to design moving coils as pure force sources with large displacements, always only a small area of the conducting coil is within the air-gap and therefore contributes to the force generation. With large displacements moving coils show an even lower efficiency factor. This can be compensated by switching the active coil areas, which again results in the necessity to have more contacts.

A similar situation happens with rotatory systems. Based on the electrodynamic principle there are two types of windings applicable to rotatory servo-systems: the *Faulhaber* and the *Maxon*-winding of the manufacturers with identical names. These actuators are also known as "iron-less" motors. Both winding principles allow the manufacture of self-supportive coils. A diagonal placement of conductors and a baking process after winding generates a structure sufficiently stable for the centrifugal forces during operation. The baked coils are connected with the rotating axis via a disk. The complete rotor (Fig. 9.14) is build of these three components. By the very small inertia of the rotor such actuators show impressive dynamic properties. The geometrical design allows placing the tubular winding around a fixed, diametral-magnetized magnet. This enables another volume reduction compared to conventional actuators as its housing has to close the magnetic circuit only instead of providing additional space for magnets.

Within the self-supportive winding there are areas of parallel lying conductors combined to poles.[12] With moving coils there is always the need for a specialized

[12] The *Faulhaber* and the *Maxon* excel by a very clever winding technique. On a rotating cylinder respectively a flatly pressed rectangular winding poles can be combined by contacting closely located areas of an otherwise continuous wire.

contactor, either via contact rings, or electronic commutation or via mechanical switching. Depending on the number of poles all coils are contacted at several points. In case of mechanical switching these contacts are placed on the axis of the rotor and connected via brushes with the fixed part of the actuator named "stator". This design enables a continuous movement of the rotor, whereas a change of the current flow is made purely mechanically by the sliding of the brushes on the contact areas of the poles on the axis. This mechanical commutation is a switching procedure with an inductance placed in parallel.

As such an actuator can be connected directly to a direct current source, they are known as "DC-drives". As stated within Sect. 9.1 the term "DC-drive" is not only limited to actuators according to the electrodynamic principle but is also frequently applied to actuators following the electromagnetic principle (Sect. 9.4).

Moving Magnet

In case of *translatory* (Fig. 9.12a) systems actuators according to the principle of a moving magnet are designed to provide large displacements with compact windings. The moving part of the actuator is composed almost completely of magnetic material. The polarity direction of this material may vary in its exact orientation. Actuators according to this principle are able to provide large power, but are expensive due to the quantity of magnet material necessary. Additionally the moving magnet is heavy; the dynamics of the actuator is therefore smaller than in the case of a moving coil. Nevertheless some very successful designs exists. A special form-factor can be found with the TAPTICENGINE (Fig. 9.15) specialized for a very slim design at a still comparably large accelerated mass. The translator followed a moving-magnet-design with poles facing each other forcing the magnetic flux to exit through the airgap with coils wound flat on a magnetic back iron. The whole translator is spring-balanced and can operate in a wide frequency range with a clear resonance defined by the spring k and the moving-mass m: $f_r = \frac{1}{2\pi}\sqrt{\frac{k}{m}}$. A related design but more straightforward as built on rotational symmetry is shown in Fig. 9.16 called HAPCOILONE manufactured and sold by the French company ACTRONIKA. Due to the large moving mass, a combined damper and spring-element and some very reasonable coiling such system allows a wide-bandwidth at an excellent power-level.

In case of a *rotatory* system a design with moving magnet is comparable to a design with moving coil. Figure 9.17 shows such a drive. The windings fixed to the stator are placed around a diametral magnetized magnet. It rotates on an axis, which frequently additionally moves the magnetic circuit too. Providing the right current feed to the coil the orientation of the rotor has to be measured. For this purpose sensors based on the Hall-effect or optical code wheels are used.

Electrodynamic actuators with moving magnet are known as EC-drives (electronic-commutated). This term is not exclusive to electrodynamic actuators, as there are electronic-commutated electromagnetic drives too. EC-drives—whether they are electrodynamic or electromagnetic—combined with the corresponding driver electronics are frequently known as servo-drives. Typically a servo-drive is an actuator able to follow a predefined movement path. Servo-drives are rarely used for haptic

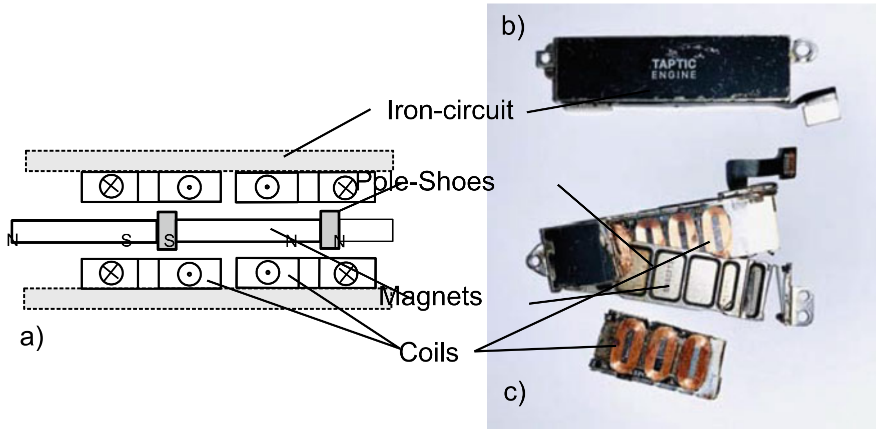

Fig. 9.15 TAPTICENGINE as used in mobile devices of the company APPLE. Flat electrodynamic actuator with moving magnet on a translator. Figure shows principle sketch (**a**), assembled unit (**b**) and disassembled unit with lower translator with spring and upper body forming the magnetic back iron visible (**c**)

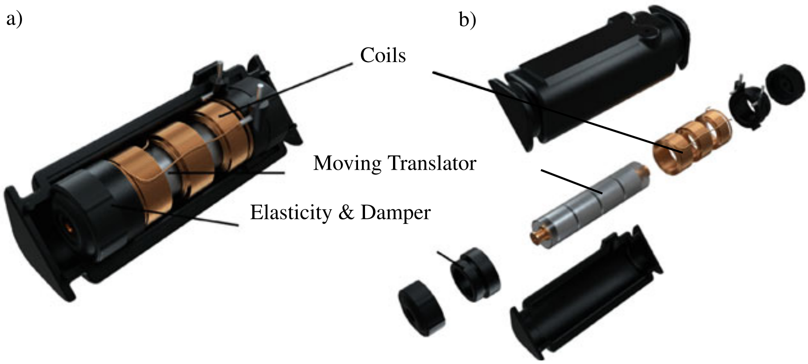

Fig. 9.16 Exciter-concept HAPCOILONE by the company ACTRONIKA with moving-magnet design for high-performance haptic applications, ©2022 *actronika*, used with permission

devices. However the usage of EC-drives for haptic application is very frequent, but then they are equipped with specialized driver electronics.

9.2.2.2 Commutation in the Context of Haptic Systems

If continuous rotations are required, there is the need to switch the direction of the current flow. This process is called *commutation*. This necessary commutation of the current for rotating actuators has a big influence upon the quality of force- respective torque-output.

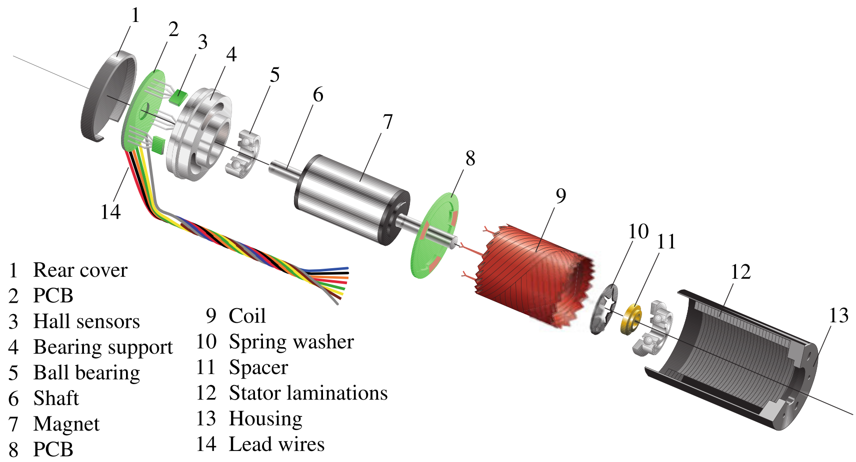

Fig. 9.17 Components of a EC-drive. Pictures courtesy of *Dr. Fritz Faulhaber GmbH*, Schöneich, Germany, used with permission

Mechanically Commutating Actuators

With mechanically commutating actuators the current flow is interrupted suddenly. Two effects of switching contacts appear: The voltage at the contact point increases, sparks may become visible—an effect which is called electrical brush sparking. Additionally the remaining current flow induces a current within the switched-off part of the winding which itself results in a measurable torque. Depending on the size of the motor, this torque can be felt when interacting with a haptic system and has to be considered in the design.

The current- and torque changes can be reduced by the inclusion of resistors and capacitors into the coil. However this results into high masses of the rotor and worse dynamic properties. Beside that a full compensation is impossible. Nevertheless mechanically commutating actuators are in use for inexpensive haptic systems. The GEOMAGIC TOUCH from *geomagic* and the FALCON from *Novint* use such actuators.

Electronic Commutated Electrodynamic Actuators

Electronic commutated electrodynamic actuators differ from mechanically commutated actuators by the measurement technology used as a basis for switching currents. There are four typical designs for this technology:

- In sensor-less designs (Fig. 9.18a) an induced voltage is measured within a coil. At zero-crossing point one pole is excited with a voltage after an interpolated 30° phase delay dependent on the actual revolution speed of the rotor. In combination of measurement of the inductance followed by a switched voltage, a continuous rotation with batch-wise excitation is realized. This procedure can not be applied to low rotation speeds, as the induced voltage becomes too low and accordingly the switching point can hardly be interpolated. Additionally the concept of using

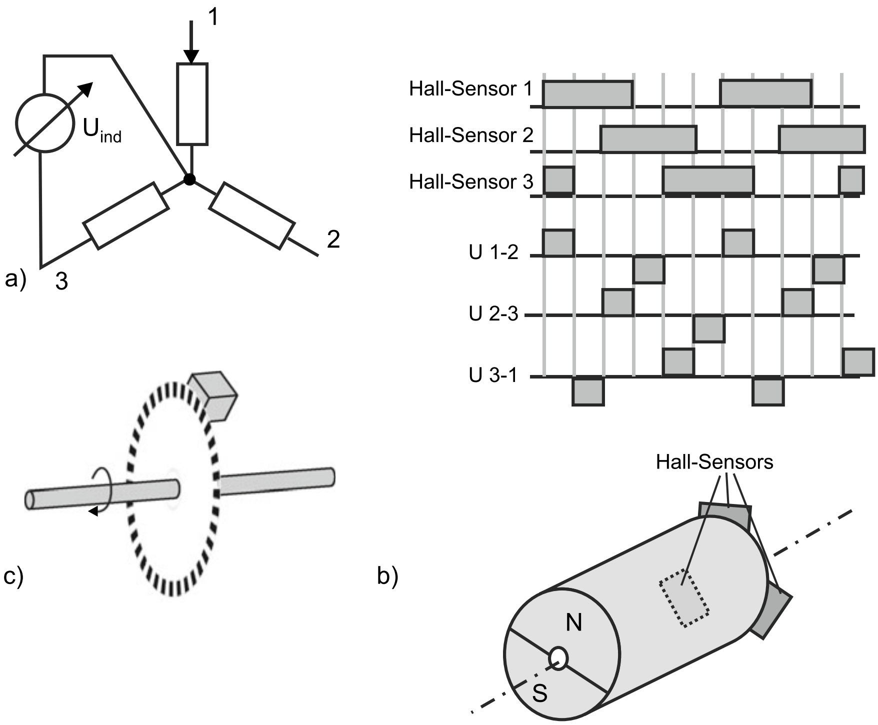

Fig. 9.18 Technologies for different commutation methods: sensor-less (**a**), block-commutation (**b**) and optical code-wheel (**c**)

one to two coils for torque generation results in a high torque variations at the output of up to 20%, making this approach not useful for haptic systems.

- Block-commutating procedures (Fig. 9.18b) are based on the usage of simple hall-switches or field-plates for position detection of the rotor. Three sensors located at 120° angular phase shift allow the detection of six different rotor positions. Reducing positioning information to six orientations per revolution makes this approach equally inappropriate for haptic applications, as the torque varies in a range of $>15\%$ for one revolution.
- Sinus-commutating procedures with analogue hall-sensors are based on the measurement of the rotor position by at least two sensors. They are placed with an angle of either 120° or 90° at the front of the rotor. They provide voltages in an angular phase shift according to their geometrical position. By analyzing the polarity and the absolute height of the voltages absolute positioning information can be obtained and used for commutating the windings. If the phase lag between both sensor signals is identical to the phase lag between the poles of the winding a direct control of current-drivers can be performed without the need for a digitization or a specific calculation step.

- Sinus-commutating with digital code-wheels (Fig. 9.18c) are based on the measurement of rotor position by the use of—usually optical—code discs. By reflective or transmissive measurement the rotor position is sampled with high resolution. This relative positioning information can be used for position measurement after an initial calibration. Depending on the code-wheels resolution a very smooth sinusoid commutation can be achieved with this method.

The sinus-commutating methods are the preferred solutions used for haptic applications due to the little torque variations and their applicability for slow revolution speeds typical to direct drives.

9.2.3 Actuator Electronics

Electrodynamic actuators require some specific electrical circuits. In the following section the general requirements on these electronics are formulated.

9.2.3.1 Driver Electronics

Driver electronics are electrical circuits transforming a signal of low power (several volts, some milli-ampere) into a voltage- or current level appropriate to drive an actuator. For electrodynamic actuators in haptic applications driver electronics have to provide a current in a dynamic range from static up to several kilohertz. This paragraph describes general concepts and approaches for such circuits.

Topology of Electric Sources

Driver electronics for actuators—independently from the actuation principle they are used for—are classified according to the flow of electrical energy (Fig. 9.19). There are four classes of driver electronics:

- 1-quadrant controllers are capable of generating positive output currents and voltages. An actuator driven by them is able to move in one direction. These controller use only the first quadrant according to Fig. 9.16a.
- Switched 1-quadrant controllers are capable of a direction change by the input of a logical signal. They are working within the 1st and 3rd quadrant according to Fig. 9.19a. The switching point is a nonlinear step in their characteristic curve.
- Real 2-quadrant controllers are capable of providing a characteristic curve which is steady around the zero point. They function in the 1st and 3rd quadrant according to Fig. 9.19a, but are not capable to conduct currents and voltages with opposite directions.
- 4-quadrant controllers function within all four quadrants of Fig. 9.19a. They are able to control currents and voltages in any combination of directions. Four-quadrant controllers allow energy recovery by induced currents to an energy storage, which is especially relevant for mobile applications.

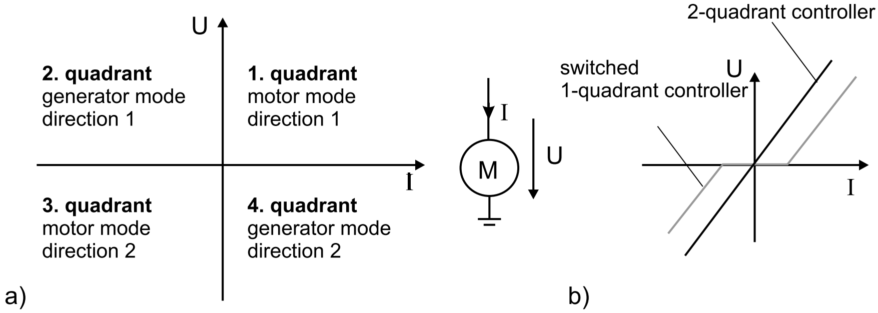

Fig. 9.19 Visualization of the four quadrants of an electric driver, formed by the directions of current and voltage

For haptic application the switched 1-quadrant controller is frequently met, as many haptic systems do not have the necessity to control the device near the voltage- or current-zero point. However for systems with high dynamics and low impedance the 2-quadrant and the 4-quadrant controller are relevant, as the unsteadiness near the zero-point is perceivable with high quality applications.

Pulse-Width-Modulation and H-Bridges

With the exception of some telemanipulators, the sources controlling the actuators are always digital processors. As actuators need an analogue voltage or current to generate forces and torques some transformer between digital signals and analogue control value is necessary. There are two typical realizations of these transformers:

1. Usage of a digital-analog converter (D/A-converter)
2. Usage of a ↪ Pulse-Width-Modulation (PWM)

The use of D/A-converters as external components or integrated within a micro-controller is not covered further in this book, as it is, if necessary to use, extremely simple. It just requires some additional efforts in circuit layout. Latter results in it being not used much for the control of actuators.

With electrodynamic actuators the method of choice are driver electronics based on PWM (Fig. 9.20a). With the PWM a digital output of a controller is switched with a high frequency (>10 kHz[13]). The period of the PWM is given by the frequency. The program controls the duty cycle between on- and off-times. Typically one byte is available to provide a resolution of 256 steps within this period. After filtering the

[13] Typical frequencies lie in between 20–50 kHz. However especially within automotive technology for driving LEDs, PWMs for current drivers with frequencies below 1 kHz are in application. Frequencies within this range are not applicable to haptic devices, as the switching in the control value may be transmitted by the actuator and will therefore be perceivable especially in static conditions. Typical device designs show mechanical low-pass characteristics even at frequencies in the area of 200 Hz already. However due to the sensitivity of tactile perception in an area of 100–200 Hz, increased attention has to be paid on any switched signal within the transmission chain.

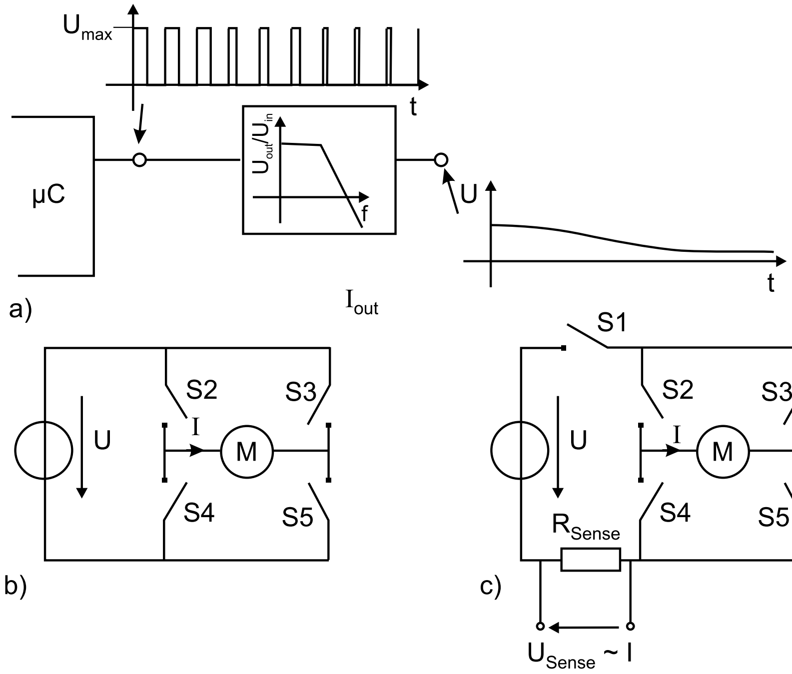

Fig. 9.20 Principle of puls-width-modulation (PWM) at a digital μC-output (**a**), h-bride circuit principle (**b**), and extended h-bridge with PWM (S1) and current measurement at (R_{Sense}) (**c**)

PWM, either via an electrical low-pass or via the mechanical transfer-characteristics of an actuator, a smoothed output signal becomes available.

Pulse-width-modulation is frequently used in the combination with H-bridges (Fig. 9.20b). The term H-bridge results from the H-like shape of the motor surrounded by four switches. The H-bridge provides two operation modes for two directions of movement and two operation modes for braking. If according to Fig. 9.20b the two switches S2 and S5 are on, the current I will flow through the motor in positive direction. If instead switches S3 and S4 are switched on, the current I will flow through the motor in negative direction. One additional digital signal acting upon the H-bridge will change the direction of movement of the motor. This is the typical procedure with switched 1-quadrant controllers. Additional switching-states are given by switching the groups S2 and S3 respectively S4 and S5. Both states results in short-circuit of the actuator and stops its movement. Other states like simultaneously switching S2 and S4 respectively S3 and S5 results in short-circuit of the supply voltage, typically destroying the integrated circuit of the driver.

To combine the H-bridge with a PWM either switch-groups S2 and S5 can be switched according to the timing of the PWM, or additional switches S1 (Fig. 9.20c) can be placed in series to the H-bridge modulating the supply voltage U. In a practical realization latter is the preferred design, as the timing of the switches S2 to S5 is very critical to prevent likely short circuits of the supply voltage. The effort to perform this timing between the switching is usually higher than the costs of another switch in series. The practical realization of H-bridges is done via field-effect transistors. The discrete design of H-bridges is possible, but not easy. Especially the timing between switching events, the prevention of short-circuits, and the protection of the electronics against induced currents is not trivial. There are numerous integrated circuits available at the market which already include appropriate protective circuitry and provide only a minimum of necessary control lines. The ICs L6205 (2A), L293 (2.8A) and VNH 35P30 (30A) are some examples common with test-bed developments. For EC drives there are specific ICs performing the timing for the field-effect transistors and reducing the number of necessary PWMs from the microcontroller. The IR213xx series switches three channels with one external half-bridge per channel built up from N-MOS transistors with a secure timing for the switching events.

The PWM described above with an H-bridge equals a controlled voltage source. For electrodynamic systems such a control is frequently sufficient to generate an acceptable haptic perception. Nevertheless for highly dynamic haptic systems a counter induction (Sect. 9.2.1.4) due to movement has to be expected, resulting in a variation of the current within the coils generating an uncontrolled change of the LORENTZ-force. Additionally the power-loss within the coils (Sect. 9.2.1.1) may increase the actuator's internal temperature resulting in a change of conductivity of the conductor's material. The increasing resistance with increasing temperatures of the conductor results in less current flow at a constant voltage source. An electrodynamic actuator made of copper as conductive material would generate a reduced force when operated. With higher requirements on the quality of haptic output a controlled current should be considered. In case of a PWM a resistor with low resistance (R_{Sense} in Fig. 9.20c) has to be integrated, generating a current-proportional voltage U_{Sense}, which itself can be measured with an A/D input of the controller. The control circuit is closed within the microcontroller. However the A/D transformation and the closing of the control circuit can be challenging for state of the art electronics with highly-dynamic systems with border frequencies of some kilohertz. Therefore analog circuits should be considered for closed-loop current controls too.

Haptic Driver ICs

Meanwhile for standard applications using excentric rotating mass (ERM) motors or linear resonant actuators (LRA) such as the engines shown in Fig. 9.15 or Fig. 9.16 integrated circuits with additional value exists. TEXAS INSTRUMENTS (TI) for example offers the *DRV2605* driver circuit with included PWM, controlled by an I2C protocol. It includes already some basic tactile patterns and by this offers a simple extension to any microcontroller to create basic patterns without loading the computing needs onto the main unit. And it even goes beyond that. For example with focus on industrial applications MAXIM released the *MAX11811*, a driver combining resistive touchscreen measurement with haptic actuation. Almost all major manufacturers of integrated circuits meanwhile offer such drivers, which—for standard applications—makes it easy to create some level of haptic output especially for touchscreen-type of applications.

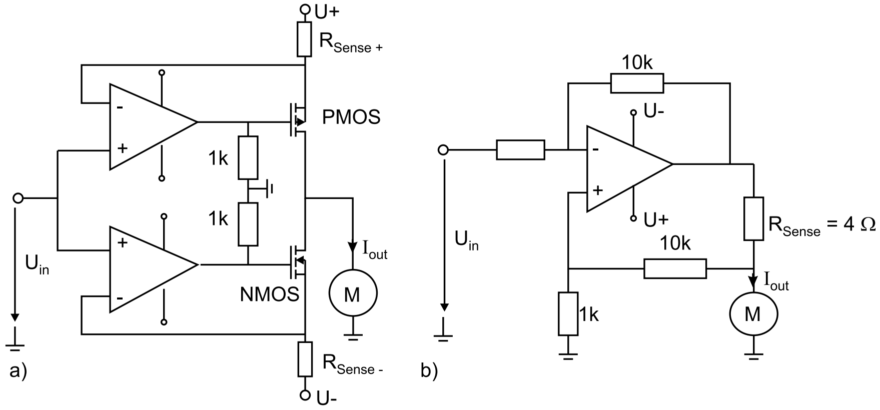

Fig. 9.21 Discrete closed-loop current control [8] © Springer Nature, all rights reserved (**a**), and closed-loop current control with a power-operational-amplifier (**b**)

Analogue Current Sources

Analogue current sources are—to make it simple—controlled resistors within the current path of the actuator. It should be noted that with the wide and easy access to PWMs this technology is not common anymore. However in terms of tactile performance, those sources are still a gold-standard as no high-frequency-component is involved into the signal generation. Their resistance is dynamically adjusted to provide the wished current flow. Identical to classical resistors analogue current sources transform the energy which is not used within the actuator into heat. Consequently in comparison to the switched H-bridges they are generating a lot of power loss. By the use of a discrete current control (Fig. 9.21a) analogue current sources for almost any output currents can be built by the choice of one to two field-effect-transistor (FET). For heat dissipation they are required to be attached to adequate cooling elements. There are only little requirements on the operational amplifiers themselves. They control the FET within its linear range proportional to the current-proportional-voltage generated at R_{Sense}. Depending on the quadrant used within operational mode (1 or 3) either the N-MOS transistors or the P-MOS transistor is conductive. An alternative to such discrete designs is the use of power-amplifiers (e.g. LM675, Fig. 9.21b). It contains fewer components and is therefore less dangerous to make errors. Realized as non-inverting or inverting operational amplifier with a resistor for measurement R_{Sense}, they can be regarded as a voltage controlled current source.

9.2.3.2 Monitoring Temperature

Resulting from the low efficiency factor and the high dissipative energy from electrodynamic actuators it is useful to monitor the temperature nearby the coils. Instead of including a measuring resistor PT100 nearby the coil, another approach monitors the electrical resistance of the windings themselves. Depending on the material of the windings (e.g. cooper, Cu) the conductivity changes proportional to the coil's temperature. With copper this factor is 0.39% per Kelvin temperature change. As any driver electronics either works with a known and controlled voltage or current, measurement of the other component immediately provides all information to calculate resistance and consequently the actual coil temperature.

9.2.4 Examples for Electrodynamic Actuators in Haptic Devices

Electrodynamic actuators are most frequently used as exciters for tactile systems also named linear-resonant-actuators (LRA) , or as force and torque sources within kinaesthetic systems. Especially EC-drives can be found in the products of *Quanser*, *ForceDimension*, *Immersion*, and *SensAble/geomagic*. Mechanically commutated electrodynamic actuators are used within less expensive devices, like the Phantom Omni or the Novint Falcon.

9.2.4.1 Cross-Coil System as Rotary Actuator

Beside self supportive coils electrodynamic actuators according the design of cross coils are one possibility to generate defined torques. Continental VDO developed a haptic rotary actuator device being a central control element for automotive applications (Fig. 9.22). It contains a diametral magnetized NdFeB-magnet. The magnet is surrounded by a magnetic circuit. The field-lines reach from the magnet to the magnetic circuit. The coils surround the magnet in an angular phase of 90°, and the electrodynamic active winding section lies in the air-gap between magnetic circuit and magnet. The rotary position control is made via two hall-sensors placed in a 90° position. The actuator is able to generate a ripple-free torque of $\approx$25 mNm at a geometrical diameter of 50 mm, which is additionally increased by an attached gear to $\approx$100 mNm torque output.

9.2.4.2 Reconfigurable Keypad—HapKeys

Although the design shows similarities to Fig. 9.16, this design was built for kinaesthetic feedback. The electrodynamic linear actuators building the basis of this device are equipped with friction type bearings, and moving magnets with pole-shoes within cylindrically wound fixed coils as shown in Fig. 9.23. The coils have an inner diameter of 5.5 mm and an outer diameter of 8 mm. The magnetic circuit is decoupled from other nearby elements within the actuator-array. It is made of a tube with a wall thickness of 0.7 mm of a cobalt-iron alloy with very high saturation flux density. Each actuator is able to generate 1 N in continuous operation mode.

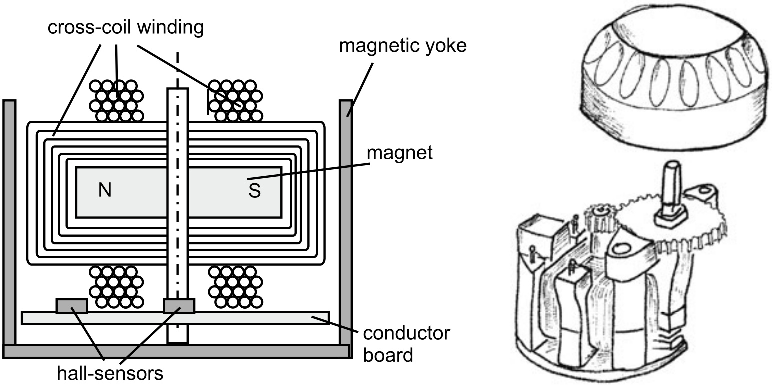

Fig. 9.22 Electrodynamic cross-coil system with moving magnet as haptic rotary actuator

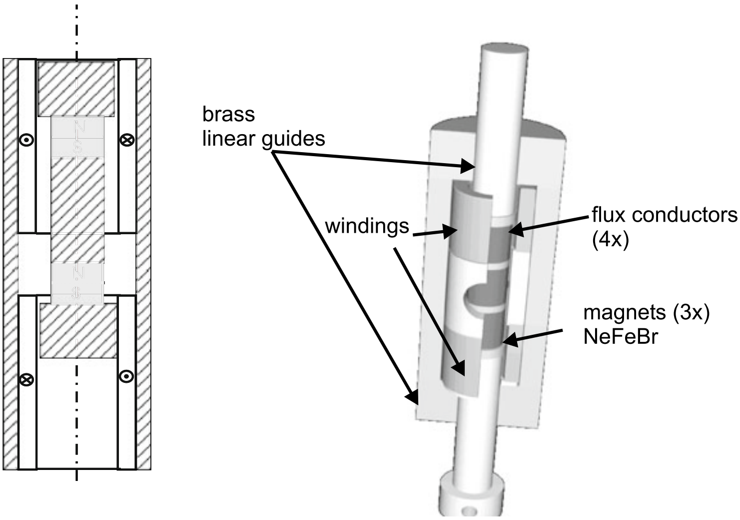

Fig. 9.23 Electrodynamic linear actuator with moving magnet [9]

9.2.5 Conclusion About the Design of Electrodynamic Actuators

Electrodynamic actuators are the preferred actuators used for kinaesthetic impedance-controlled haptic devices due to their proportional correlation between the control value "current" and the output-values "force" or "torque". The market of DC -and EC-drives offers a wide variety of solutions, making it possible to find a good compromise between haptic quality and price for many applications. Most suppliers of such components offer advice on how to dimension and select a specific model based on the mechanical, electrical and thermal properties as for example shown in [10].

If there are special requirements to be fulfilled, the design, development, and start of operation of special electrodynamic actuator variants are quite easy. The challenges by thermal and magnetic design are manageable, as long as some basic considerations are not forgotten. The examples of special haptic systems seen in the preceding section prove this impressively. Just driver electronics applicable to haptic systems and its requirements are still an exceptional component within the catalogs of manufactures from automation-technology. They must either be paid expensively or be built by oneself. Therefore commercial manufacturers of haptic devices, e.g. *Quanser*, offer their haptic-applicable driver electronics independent from the own systems for sale.

For the design of low-impedance haptic systems currently no real alternative to electrodynamic systems exists. Other actuation principles which are discussed within this book need a closed-loop control to overcome their inner friction and nonlinear force/torque-transmission. This always requires some kind of measurement technology such as additional sensors or the measurement of inner actuator states. The efforts connected with this are still a big advantage for electrodynamic actuators, which is gained by a low efficiency factor and as a consequence the relatively low energy density per actuator-volume.

9.3 Piezoelectric Actuators

Stephanie Sindlinger and Marc Matysek

Next to the very frequently found electrodynamic actuators, the past few years piezoelectric actuators were used for a number of device designs. Especially their dynamic properties in resonance mode allow an application for haptics, which is very different from the common positioning application they are used for. As variable impedance a wide spectrum of stiffnesses can be realized. The following chapter gives the calculation basics for the design of piezoelectric actuators. It describes the design variants and their application in haptic systems. Beside specific designs for tactile and kinaesthetic devices approaches for the control of the actuators and tools for their dimensioning are presented.

9.3.1 The Piezoelectric Effect

The piezoelectric effect was discovered by Jacques and Pierre Curie first. The term is derived from the Greek word “piedein—piezo” = “to press” [11].

Figure 9.24 shows a scheme of a quartz crystal (chemical: SiO2). With force acting upon the crystal mechanical displacements of the charge-centers can be observed

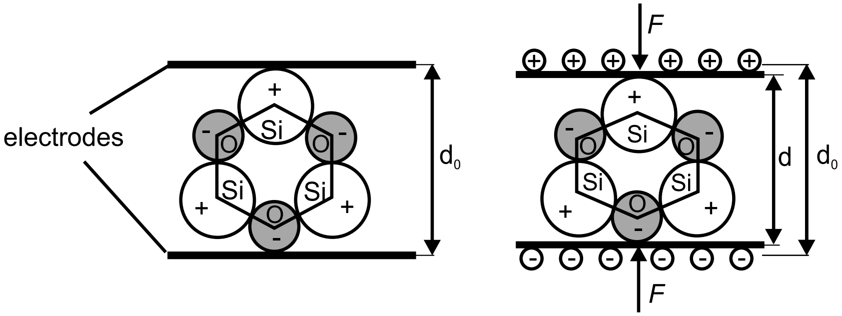

Fig. 9.24 Crystal structure of quarz in initial state and under pressure

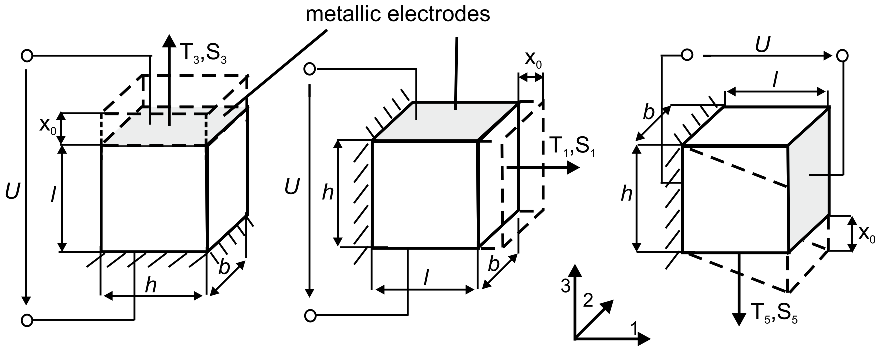

Fig. 9.25 Effects during applied voltage: longitudinal effect (left), transversal effect (center), shear effect (right)

within the structure, resulting in microscopic dipoles within its elementary cells. All microscopic dipoles sum up to a macroscopic measurable voltage. This effect is called "reciprocal piezoelectric effect". It can be reversed to the "direct piezoelectric effect". If a voltage is applied on a piezoelectric material a mechanical deformation happens along the crystal's orientation, which is proportional to the field strength in the material [12].

Piezoelectric materials are anisotropic—direction dependent—in their properties. Consequently the effect depends on the direction of the electrical field applied, and on the angle between the direction of the intended movement and the plane of polarization. For the description of these anisotropic properties the directions are labeled with indices. The index is defined by a Cartesian space with the axes being numbered with 1, 2 and 3. The plane of polarization of the piezoelectric material is typically orientated on direction 3. The shear at the axes is labeled with indices 4, 5 and 6.

Among all possible combinations, there are three major effects (Fig. 9.25), commonly used for piezoelectric applications: longitudinal- , transversal- and shear-effect.

The *longitudinal effect* acts in the same direction as the applied field and the corresponding field strength E_3. As a consequence the resulting mechanical tensions T_3 and strains S_3 lie within plane 3 too. With the *transversal effect* mechanical actions show normal to the electrical field. As a result from a voltage U_3 with the electrical field strength E_3 the mechanical tensions T_1 and strains S_1 appear. The *shear-effect* happens with the electrical voltage U applied along plane 1 orthogonal to the polarization plane. The resulting mechanical tensions appears tangential to the polarization—in the direction of shear—and are labeled with the directional index 5.

9.3.1.1 Basic Piezoelectric Equations

The piezoelectric effect can be described most easily by state equations:

$$P = e \cdot T \tag{9.35}$$

and

$$S = d \cdot E \tag{9.36}$$

with

with	P	=	direction of polarization (in C/m^2)
	S	=	deformation (non-dimensional)
	E	=	electrical field strength (in V/m)
	T	=	mechanical tension (in N/m^2)

The piezoelectric coefficients are

- the piezoelectric coefficient of tension (also: coefficient of force) e (reaction of the mechanical tension on the electrical field)

$$e_{ij,k} = \frac{\partial T_{ij}}{\partial E_k} \partial \tag{9.37}$$

- and the piezoelectric coefficient of strain (also: coefficient of charge) d (reaction of the strain on the electrical field)

$$d_{ij,k} = \frac{\partial \varepsilon_{ij}}{\partial E_k} \partial \tag{9.38}$$

The correlation of both piezoelectric coefficients is defined by the elastic constants C_{ijlm}

$$e_{ij,k} = \sum_{lm} \left(C_{ijlm} \cdot d_{lm,k} \right) \tag{9.39}$$

Usually the tensors shown in the equation above are noted as matrix In this format, matrices result of six components identical to the defined axes. The matrix shown below describes the concatenation of the dielectrical displacement D, the mechanical strain S, the mechanical tension T, and the electrical field strength E.

This matrix can be simplified for the specific cases of a longitudinal and a transversal actuator. For a longitudinal actuator with electrical contact in direction 3 the following equations are the result.

	T_1	T_2	T_3	T_4	T_5	T_6	E_1	E_1	E_3
D_1	0	0	0	0	d_{15}	0	ε_{11}	0	0
D_2	0	0	0	d_{15}	0	0	0	ε_{11}	0
D_3	d_{31}	d_{31}	d_{33}	0	0	0	0	0	ε_{11}
S_1	s_{11}	s_{12}	s_{13}	0	0	0	0	0	d_{31}
S_2	s_{12}	s_{11}	s_{13}	0	0	0	0	0	d_{31}
S_3	s_{13}	s_{13}	s_{33}	0	0	0	0	0	d_{33}
S_4	0	0	0	s_{44}	0	0	0	d_{15}	0
S_5	0	0	0	0	s_{44}	0	d_{15}	0	0
S_6	0	0	0	0	0	$2(s_{11} - s_{12})$	0	0	0

$$D_3 = \varepsilon_{33}^T E_3 + d_{31} T_1 \tag{9.40}$$

$$S_3 = d_{31} E_3 + s_{11}^E T_1. \tag{9.41}$$

Accordingly for a transversal actuator the correlation

$$D_3 = \varepsilon_{33}^T E_3 + d_{33} T_3 \tag{9.42}$$

$$S_3 = d_{33} E_3 + s_{33}^E T_3 \tag{9.43}$$

with
D_3 = dielectric displacement in C/m^2 — D = 0: open-ended
E_3 = field-strength in V/m — E = 0: short-cut
S_1, S_3 = $\Delta L/L$ = strains, dimensionless — S = 0: mech. short-cut
T_1, T_3 = mechanical tensions N/m^2 — T = 0: idle mode
ε_{33}^T = relative dielectricity constant at mechanical tension = 0
d_{31}, d_{33} = piezoelectric charge constant in C/N
s_{11}^E, s_{33}^E = elasticity constant at field strength = 0

becomes valid.

Therefore the calculation of piezoelectric coefficients simplifies into some handy equations: The charge constant d can be calculated for the electrical short-circuit—which is $E = 0$— to

$$d_{E=0} = \frac{D}{T} \tag{9.44}$$

and for the mechanical idle situation—which is $T = 0$—to

$$d_{T=0} = \frac{S}{E}. \tag{9.45}$$

The piezoelectric tension constant is defined as

$$g = \frac{d}{\varepsilon^T}. \tag{9.46}$$

The coupling factor k is given by Eq. (9.47). It is a quantity for the energy transformation and consequently for the strength of the piezoelectric effect. It is used for comparison among different piezoelectric materials. However note that it is not identical to the efficiency factor, as it does not include any energy losses.

$$k = \frac{converted\ energy}{absorbed\ energy}. \tag{9.47}$$

A complete description of the piezoelectric effect, a continuative mathematical discussion, and values for piezoelectric constants can be found in literature, such as [7, 13, 14].

9.3.1.2 Piezoelectric Materials

Till 1944 the piezoelectric effect was observed with monocrystals only. These were quartz, turmalin, lithiumniobat, potassium- and ammonium-hydrogen-phosphat (KDP, ADP), and potassium sodium tartrate [12]. With all these materials the direction of the spontaneous polarization is given by the direction of the crystal lattice [11]. The most frequently used material was quartz.

The development of polarization methods made it possible to retrospectively polarize ceramics by the application of a constant exterior electrical field in 1946. By this approach "piezoelectric ceramics" (also "piezoceramics") were invented. By this development of polycrystalline materials with piezoelectric properties the whole group of piezoelectric materials got an increased attention and technical significance. Today the most frequently used materials are e.g. barium titanate (MaTiO3) or lead zirconate titanate (PZT) [12]. C 82 is a piezoelectric ceramic suitable for actuator design due to its high *k-factor*. However as all piezoelectric ceramic materials it shows reduced long term stability compared to quartz. Additionally it has a pyroelectric effect which is a charge increase due to temperature changes of the material [7]. Since the 1960s the semi-crystalline synthetic material polyvinylidene fluoride (PVDF) is known. Compared to the materials mentioned before, PVDF excels by its high elasticity and reduced thickness (6–9 μm).

Table 9.4 shows different piezoelectric materials with their specific values.

Looking at these values PZT is most suitable for actuator design due to its high coupling factor with large piezoelectric charge modulus and still a high Curie temperature . The Curie temperature represents the temperature at which the piezoelectric properties from the corresponding material are lost permanently. The value of the curie temperature depends on the material (Table 9.4).